1999 Shuttle Small Payloads Symposium

Proceedings of a conference held at
U.S. Naval Academy
Annapolis, Maryland
September 13–15, 1999

The NASA STI Program Office ... in Profile

Since its founding, NASA has been dedicated to the advancement of aeronautics and space science. The NASA Scientific and Technical Information (STI) Program Office plays a key part in helping NASA maintain this important role.

The NASA STI Program Office is operated by Langley Research Center, the lead center for NASA's scientific and technical information. The NASA STI Program Office provides access to the NASA STI Database, the largest collection of aeronautical and space science STI in the world. The Program Office is also NASA's institutional mechanism for disseminating the results of its research and development activities. These results are published by NASA in the NASA STI Report Series, which includes the following report types:

- TECHNICAL PUBLICATION. Reports of completed research or a major significant phase of research that present the results of NASA programs and include extensive data or theoretical analysis. Includes compilations of significant scientific and technical data and information deemed to be of continuing reference value. NASA's counterpart of peer-reviewed formal professional papers but has less stringent limitations on manuscript length and extent of graphic presentations.

- TECHNICAL MEMORANDUM. Scientific and technical findings that are preliminary or of specialized interest, e.g., quick release reports, working papers, and bibliographies that contain minimal annotation. Does not contain extensive analysis.

- CONTRACTOR REPORT. Scientific and technical findings by NASA-sponsored contractors and grantees.

- CONFERENCE PUBLICATION. Collected papers from scientific and technical conferences, symposia, seminars, or other meetings sponsored or cosponsored by NASA.

- SPECIAL PUBLICATION. Scientific, technical, or historical information from NASA programs, projects, and mission, often concerned with subjects having substantial public interest.

- TECHNICAL TRANSLATION. English-language translations of foreign scientific and technical material pertinent to NASA's mission.

Specialized services that complement the STI Program Office's diverse offerings include creating custom thesauri, building customized databases, organizing and publishing research results . . . even providing videos.

For more information about the NASA STI Program Office, see the following:

- Access the NASA STI Program Home Page at http://www.sti.nasa.gov/STI-homepage.html

- E-mail your question via the Internet to help@sti.nasa.gov

- Fax your question to the NASA Access Help Desk at (301) 621-0134

- Telephone the NASA Access Help Desk at (301) 621-0390

- Write to:
  NASA Access Help Desk
  NASA Center for AeroSpace Information
  7121 Standard Drive
  Hanover, MD 21076–1320

1999 Shuttle Small Payloads Symposium

Edited by:
Gerard Daelemans
NASA Goddard Space Flight Center
Greenbelt, Maryland

Frances L. Mosier
Swales Aerospace
Beltsville, Maryland

Available from:

CONTENTS

CONTENTS (CONTINUED)

CONTENTS (CONTINUED)

CONTENTS (CONTINUED)

SPACE SHUTTLE PROGRAM MANIFEST PROCESS & FLIGHT OPPORTUNITIES FOR SMALL PAYLOADS

Richard M. Swalin and Anne E. Sweet
NASA Johnson Space Center

ABSTRACT

The Space Shuttle Program has, since the early flights, exerted great effort to maximize the cargo complement for each individual mission. Historically, because of the capabilities of the Space Shuttle, there have almost always been opportunities to fly what are termed secondary payloads on every mission. However, with the challenges associated with assembling the International Space Station, accommodations for secondary payloads are significantly limited. In an attempt to deal with this situation, the Space Shuttle Program has developed techniques that will identify and utilize flight opportunities, as well as policies that may create opportunities.

INTRODUCTION

The Space Shuttle is a unique national asset providing dependable access to space. Each Shuttle flight is prepared and executed carefully, utilizing the talents of thousands of dedicated individuals throughout the Shuttle and customer communities. The Space Shuttle Program has the responsibility of maximizing the science and technological return of each flight. Over the history of the Space Shuttle Program, a broad spectrum of payloads has been flown. They have ranged from small boxes weighing less than a pound to large complex payloads that consume most of the Shuttle's cargo bay and weigh over 40,000 pounds. The establishment of various categories of payloads as related to their respective Shuttle services is used as a manifesting tool and creates a mechanism by which the Shuttle's resources are exploited to the fullest extent possible.

The categories of payloads have historically been identified in two major classifications – Primary and Secondary – intended to establish the significance of Shuttle services required. This paper will focus only on the secondary, or small payloads that are accommodated in the Space Shuttle cargo bay. Typically cargo bay small payloads are of a size that is less than one quarter of the Space Shuttle cargo bay (less than fifteen feet in length) and usually weigh less than 6000 pounds. Examples include side-wall or cross-bay mounted Hitchhiker class and Get-Away-Special carrier payloads.

The ability of NASA to sponsor and support a substantial number of small cargo bay payloads has enabled the Shuttle Program to take advantage of surplus services on any given mission. Even though the Space Shuttle Program has been extremely successful in providing opportunities for small cargo bay payloads in the past, the forecast of opportunities in the next several years is limited. Because of the complexity and resource requirements for assembling the International Space Station, there has been a growing backlog of science and research technology payloads. To mitigate this situation, the Space Shuttle Program has, for some time, been pursuing two efforts. One is to develop techniques for identifying and developing strategies for utilizing mission specific Shuttle capabilities in excess of the respective International Space Station requirements. The second is to identify appropriate rationale for justifying additional Shuttle flights for science and research missions not related to the International Space Station.

IDENTIFYING PAYLOAD OPPORTUNITIES IN CONJUNCTION WITH INTERNATIONAL SPACE STATION ASSEMBLY AND UTILIZATION ACTIVITIES

For those flights which are related to the International Space Station, the complexity of the operational requirements, the size of assembly elements, and the limitations of the docked environment make it difficult to accommodate small cargo bay payloads. However, the Space Shuttle Program continues to diligently search for opportunities to fly small payloads in conjunction with International Space Station activities. As a part of the normal manifest planning process, opportunities can be identified for payloads that are in the early development phases. However, the Space Shuttle Program is also striving to create a process that allows more mature payloads to take advantage of late opportunities in a cargo manifest that may develop due to unexpected delays or replanning of International Space Station cargo complements.

The analyses performed by the Space Shuttle Program in support of our normal flight assessment process and of the International Space Station Design Analysis Cycles contain preliminary information that can be used to ascertain potential small payload opportunities. Because these opportunities will be fewer and farther between, we have developed a more formal process for identifying the unused resources. The relevant information can be depicted in a manner that allows for a quick determination of mission specific performance margin and available cargo bay real estate as shown in table 1. This allows the identification of the flights on which side-wall attach hardware (sill mounted beams) and/or cross-bay structures can potentially be accommodated. With this information, the Space Shuttle Program and its user community can then be queried to determine if development or readiness preparation strategies would be prudent or advantageous. Final determination of the mission specific complement is dependent on many factors. However, early identification of potential opportunities allows the Space Shuttle Program and its non-International Space Station users to develop long term strategies to better plan and posture ourselves to take advantage of opportunities that arise.

JUSTIFYING ADDITIONAL SHUTTLE SCIENCE & RESEARCH MISSIONS

As is readily understood from our previous discussion, the numbers of opportunities that can be identified today are limited. This leads to a situation that makes it extremely difficult on the science and research technology community to develop long term strategies and lobby for resources to support their endeavors. This has long been a concern of the Space Shuttle Program. In our effort to mitigate this problem, we have attempted to develop concepts that would allow the creation of new science and research missions. Although not all concepts have been successful, we have gained ground each time and, we believe, have built a successful plan using previous lessons learned.

A concept that was not implemented, but from which useful techniques were developed, was that of the 'Stand-By Research' mission. Earlier this year the Space Shuttle Program in conjunction with the Office of Space Flight developed a concept to identify a candidate cargo, initiate documentation and analyses, and proceed to a program integration milestone approximately ten (10) months from flight. At that point, the mission would march in place until a flight opportunity appeared. However, flight opportunities resulting from unexpected events in the International Space Station assembly process would be difficult to identify early enough to orderly prepare, even on this shortened template. Secondly, the fact that the cargo could be held in limbo for an extended period of time was not a prudent utilization of resources. Thus, the 'Stand-by Research' mission concept was dropped. However, developing a scheme for implementing the concept proved useful.

With lessons learned in hand, the Space Shuttle Program, in conjunction with the Office of Space Flight, developed a different proposal. This proposal took advantage of existing manifested flights to the International Space Station, titled 'Launch-on-Need' missions, for which no specific cargo had been identified. Due to the success-oriented nature of the International Space Station assembly sequence and the anticipated need for additional flights, these missions were placed on the manifest in target timeframes to acknowledge this perceived need. To avoid showing a delay in the Station's completion for flights that

may not be needed, the flights were manifested on a vehicle that is not currently configured to dock with the International Space Station, OV-102 – Columbia. Applying the scheme for our 'Stand-by Research' mission to the International Space Station 'Launch-on-Need' flights, we could essentially identify the 'Launch-on-Need' cargo as being 'stand-by' cargo. This would allow the Space Shuttle Program to identify the Columbia flights as research missions and manifest existing payloads that were lacking an opportunity to fly. The reality of an implemented 'Launch-on-Need' flight to the International Space Station would be fulfilled by one of the other vehicles anyway, thus assuring the fulfillment of the research missions assigned to OV-102.

The Space Shuttle Program strongly embraces the need to continue to fly science and research technology missions on the Shuttle. We believe that there is an on-going desire for short-term science and research technology in low earth orbit. We in the Space Shuttle Program are committed to ensuring that those opportunities are there today and will continue to be there in the future.

Table 1. Example of weight and volume opportunity matrix as of 7/1/99

	Flight		STS-102		STS-100		STS-104		STS-105		STS-107		STS-106	
	Cargo		ISS-5A.1		ISS-6A		ISS-7A		ISS-7A.1		SH-DM		ISS-UF1	
	Crew Size		5		7		5		7		6		5	
	Available MLE		0		0		7		0		0		37	
Bay	Item	WT kg (lb)	Port	Star.	Port	Star.	Port	Star.	Port	Star.	Port	Star.	Port	Star.
	Middeck/MLE	23 (50)	0		0		7		0		0		37	
1	Side wall on OV-102	230 (500)	0	0	0	0	0	0	0	0	0	0	0	0
2	GAS Beam/side	320 (700)	0	0	0	0	0	0	0	0	1	1	0	
3	GAS Beam/side	320 (700)	1	1	1	1	1	0	1	1	1	0	1	1
4	GAS Beam/side	320 (700)	1	0	0	0	0	0	0	0	0	0	1	1
5	GAS Beam/side	320 (700)	0	0	0	0	0	0	0	0	0	0		0
6	GAS Beam/side	320 (700)	0	0	0	0	0	0	0	0	0	0		0
7	GAS Beam/side	320 (700)	0	0	0	0	0	0	0	0	0	0	0	0
8	GAS Beam/side	320 (700)	0	0	0	0	1	1	0	0	0	0	0	0
9	APC/ICAPC	230 (500)	0	0	0	0	1	1	0	0	0		0	0
10	APC/ICAPC	230 (500)	0	0	0	0	1	0	0	0	0		0	0
11	APC/ICAPC	230 (500)	0	0	0	0	0	0	0	0	0	0	0	0
12	APC/ICAPC	230 (500)	0	0	0	0	0	0	0	0	0	0	0	0
13	GAS Beam/side	455 (1000)	1	1	1	1	1	1	1	1		0	1	1
Total weight kg (lb)			1,860 (4,100)		1,545 (3,400)		2,700 (5,950)		1,545 (3,400)		950 (2100)		3,020 (6,650)	
Available APM kg (lb)			760 (1,670)		540 (1,200)		430 (950)		680 (1500)		0 (0)		5,900 (13,000)	
Planning Potential kg (lb)			**760 (1,670)**		**540 (1,200)**		**430 (950)**		**680 (1500)**		**0 (0)**		**3,020 (6,650)**	

ACRONYMS

APC	Adaptive Payload Carrier
APM	Ascent Performance Margin
GAS	Get-Away-Special
ICAPC	Increased Capacity Adaptive Payload Carrier
ISS	International Space Station
Kg	Kilograms
Lb	Pounds
MLE	Middeck Locker Equivalent
OV	Orbiter vehicle
SH-DM	SpaceHab Double Module
Star	Starboard
STS	Space Transportation System
UF	Utilization Flight
WT	Weight

PAYLOAD DOCUMENTATION ENHANCEMENT PROJECT

Betty G. Brown
Customer and Flight Integration
Space Shuttle Program

ABSTRACT

In late 1998, the Space Shuttle Program recognized a need to revitalize its payload accommodations documentation. As a result, a payload documentation enhancement project was initiated to review and update payload documentation and improve the accessibility to that documentation by the Space Shuttle user community.

INTRODUCTION

The foundation of the Space Shuttle program design requirements are found in the NTS 07700 (Volume XIV, Payload Accommodations) series of documents. The cornerstone of the payload document community is found in Volume XIV, Payload Accommodations, of that series. Volume XIV describes the capabilities of the Space Shuttle system to accommodate payloads. It reflects the baseline Space Shuttle system as it is presently configured and is the official source of Space Shuttle vehicle capabilities to deliver payloads to orbit and return them to Earth, as well as the services that the Space Shuttle provides to payloads and the means by which payloads can avail themselves of these services. Volume XIV also contained the official set of standard interface provisions between the Orbiter and payloads. The original document contained an introductory document with 10 appendixes aligned along technical disciplines. Appendixes 1 through 10 contain system description and design data concerning accommodations and interface requirements. The appendixes are: Contamination Environment, Thermal, Electrical Power and Avionics, Structures and Mechanics, Ground Operations, Mission Planning and Flight Design, Extravehicular Activities, Payload Deployment and Retrieval System, Intravehicular Activies, and Integration Hardware.

Payload customers in search of information on flying on the Shuttle and the physical accommodations of the Shuttle were introduced to these documents which then referenced a small mountain of additional documents. Potential customers in search of the rudimentary requirements were often delivered a carton of documents to read. Although the documents have been in an electronic library for several years, this library was not accessible outside of the NASA community.

PROJECT PLAN

In early 1999, the Manager of the Space Shuttle Program Integration authorized a team of NASA and United Space Alliance from JSC and KSC to review the technical data, update it, and determine a document architecture that would make it easier for the payload customer to access and search for information.

The team recommended an introductory document and set of user guides aligned by payloads types; specifically, attached payloads, deployable/retrievable payloads, small payloads, and middeck payloads. These user guides, patterned after our own internal "Standard Integration Plan Blank Books" and some of the expendable launch vehicle user guides, will contain all information pertinent to a particular class of payload.

The second part of the plan is to have this information available on an Internet web site. The site will have a query and search system. If the user guides referenced other documents, that document would be hyperlinked to the site. The information will be characterized such that it is considered "public domain"; thus it will not be necessary for the potential customer to obtain permission to "surf" the web site. However, access to payload specific documentation will continue to be limited.

NSTS 07700, Volume XIV, Payload Accommodations, remains at the top of the official payload documentation tree. This document will be expanded to contain some of the policy and general requirements that were previously in the technical appendixes. By a query and hyperlink system, the web user will be able to access the information that is pertinent to them.

For example, a middeck payload customer would be routed to only the information relevant to a middeck user, e.g., thermal middeck accommodations. The engineer who is interested in all thermal payload data would be routed to all thermal data.

The web site will contain an overview of Shuttle capabilities, history, and payload accommodations. The Internet user will be introduced to the payload integration process with information beginning with how to make a request for a flight assignment and proceeding to the preparation for launch process. Engineering product definitions and typical schedules will be provided. Documents that are referenced will be hyperlinked to enable the web user to easily obtain the required data. Throughout the web site, there will be definitions, acronyms explained and personal contact information.

The third part of the plan is the development of a compact disk (CD) that takes advantage of today's multimedia capabilities. This CD will have high level introductory information for flying on the Shuttle. The CD will be a documentary-like overview of Shuttle processes and accommodations. It will contain background music, animation, and video clips of actual Shuttle events. The emphasis of the CD will be on the unique capabilities and dependability of the Shuttle. It can either be presented at first contact meetings or sent to potential customers. The CD can either standalone or work in conjunction with the web site.

The long-term goal is to have a web site query system that will allow the customer to build their unique payload integration documentation. The payload integration documentation would evolve from a narrative type document to a data-submittal type document that could be electronically maintained and updated. The integration plans that contain the requirements of the payload and Shuttle accommodations will be based on a "fill-in-the-blank" type scenario. The negotiation of requirements and accommodations can be initiated electronically and the agreement developed and potentially approved via electronic means.

SUMMARY

The Space Shuttle Program has been on the cutting edge of technology development but in the area of documentation, the program has fallen into the government red tape trap and projects the image of a huge bureaucracy with unwieldy requirements. After flying for over 17 years and for over 95 missions, the Space Shuttle Program should be able to trim its documentation down to basic essential information and provide it in a concise manner without the lacy trim of "motherhood and policy". The responsibility should not be on the potential customer to ferret out information but on the Space Shuttle Program to present in a format that is accessible, succinct, and usable. This documentation enhancement plan is to alleviate the customer of the burden of searching pages of documents for bits of information. It is the Space Shuttle Program's intent to present payload accommodation information in a professional and crisp manner that projects a positive image of the Space Shuttle Program and NASA.

SHUTTLE HITCHHIKER EXPERIMENT LAUNCHER SYSTEM (SHELS)

Mr. Gerry Daelemans
NASA Goddard Space Flight Center
Mail Code 870.G
Greenbelt, MD 20771
301-286-2193
gerry.daelemans.1@gsfc.nasa.gov

ABSTRACT

NASA's Goddard Space Flight Center Shuttle Small Payloads Project (SSPP), in partnership with the United States Air Force and NASA's Explorer Program, is developing a Shuttle based launch system called SHELS (Shuttle Hitchhiker Experiment Launcher System), which shall be capable of launching up to a 400 pound spacecraft from the Shuttle cargo bay. SHELS consists of a Marman band clamp push-plate ejection system mounted to a launch structure; the launch structure is mounted to one Orbiter sidewall adapter beam. Avionics mounted to the adapter beam will interface with Orbiter electrical services and provide optional umbilical services and ejection circuitry. SHELS provides an array of manifesting possibilities to a wide range of satellites.

INTRODUCTION

In 1984, the NASA Headquarters Office of Space Flight (OSF) established the Shuttle Small Payloads Project (SSPP) at the Goddard Space Flight Center to develop and operate carrier systems for low-cost and quick reaction accommodations of secondary payloads on the NASA Space Transportation System (STS). These carrier systems range from the more complex such as the Hitchhiker (HH) carrier system to the self-contained Get Away Special (GAS) carrier system. To date, SSPP has flown over 285 cargo-bay payloads aboard the Space Shuttle.

Utilizing modular hardware components, HH payloads may vary in weight and size from a few hundred pounds up to 5500 pounds; the former requiring the mounting provisions of a single adapter beam and the latter requiring a full cross-bay bridge. HH payloads use Orbiter power and data services and provide experimenters with real-time command and telemetry link to a control center located at Goddard.

Over the years, SSPP has developed adjunct systems to the HH carrier providing additional accommodations and manifesting possibilities to a wide variety of Orbiter users. The recently developed Hitchhiker-Jr. Carrier system, using a Hitchhiker Remote Interface Unit (HRIU) in a single five-cubic-foot canister, receives Orbiter power and is commanded by and sends telemetry to the crew controlled Payload General Support Computer (PGSC) laptop. Additionally, SSPP has developed a small launcher system capable of ejecting 150-pound satellites (or other experiments) from either a canister or a cross-bay bridge pallet.

More recently, SSPP has begun development of the SHELS launcher system. Both the NASA Explorer Program Office and the U.S. Air Force Space Test Program (STP) Office are funding the SHELS development effort. SHELS shall be capable of ejecting up to a 400-pound spacecraft and will provide the option of power and data umbilical services. The Explorer Program Office wants a launch system provided that is compatible with its University Explorer (UNEX) class missions while the U.S. Air Force STP Office has targeted SHELS for a number of its small satellites. It is anticipated that other users will step forward as the SHELS system becomes operational sometime in the 2001 time frame.

SYSTEM OVERVIEW

Taking advantage of an array of existing modular components and Orbiter power and data services, the SHELS system development effort requires little in the way of new electrical hardware design. The bulk of the design effort is an ejection mechanism and launch structure. As shown in Figure 1, with existing hardware shaded, the SHELS system components include: the HH avionics and its mounting plate; the Hitchhiker Ejection System Electronics (HESE); the Satellite Interface Box (SIB); the SHELS support structure; and ejection system. For those spacecraft that do not require umbilical service, the SIB is not required.

As seen in Figure 2, the HH avionics provides the interface to Orbiter power and data services and crew controlled Standard Switch Panel (SSP) switches. For umbilical users, power and data command/telemetry signals are routed to the spacecraft via the HH avionics and SIB. The SIB provides signal isolation protection to the HH avionics circuitry. The SSP switches are routed via the HH avionics to the HESE, which contain the PRE-ARM, ARM, and FIRE relays. These relays and their status provide safety inhibit and monitor functions necessary to prevent accidental spacecraft ejection and other related hazards.

The SHELS launch structure is a monolithic investment cast structure, which is cast from A356-T6 strength class 10 aluminum alloy, and mounts directly to the sidewall adapter beam. The SHELS ejection system mounts to the top of the launch structure and uses a Marman band clamp mechanism approximately 17 inches in diameter. The ejection system push plate design accommodates the mounting of the umbilical power and signal connectors. The SHELS ejection dynamics do not impart any significant tip-off or rotation about the satellite's ejection axis. A mission unique thermal shroud will surround the payload and mount to the support structure.

With its ability to be mounted to the Orbiter sidewall, the SHELS design allows for ease of manifesting and requires little in the way of Orbiter resources.

Satellite
Adapter Beam (2)
HESE
PIB
HH Avionics
Ejection System
Cast Support Structure
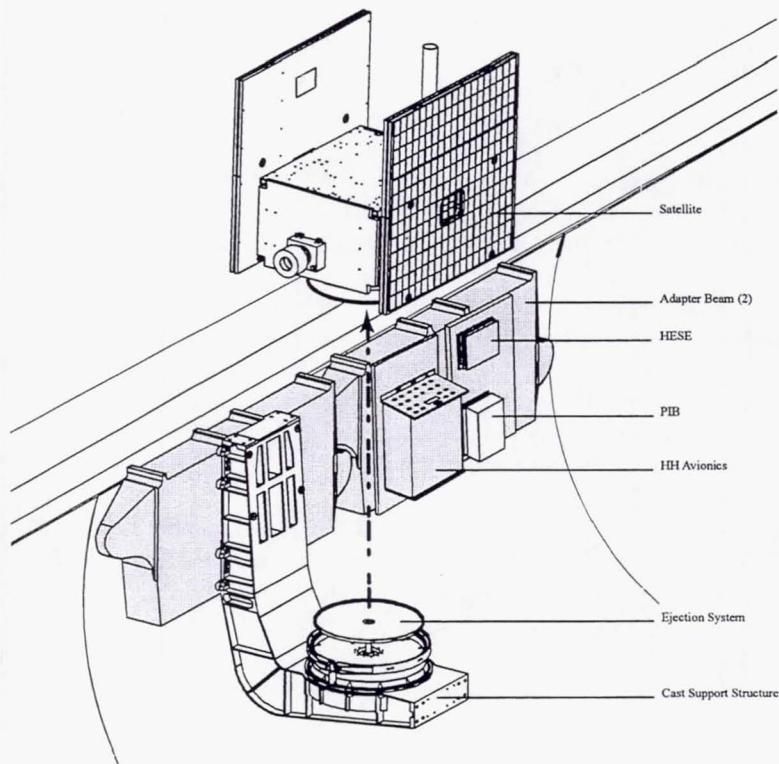
Figure 1. SHELS with Existing Hardware (Thermal Shroud Not Shown)
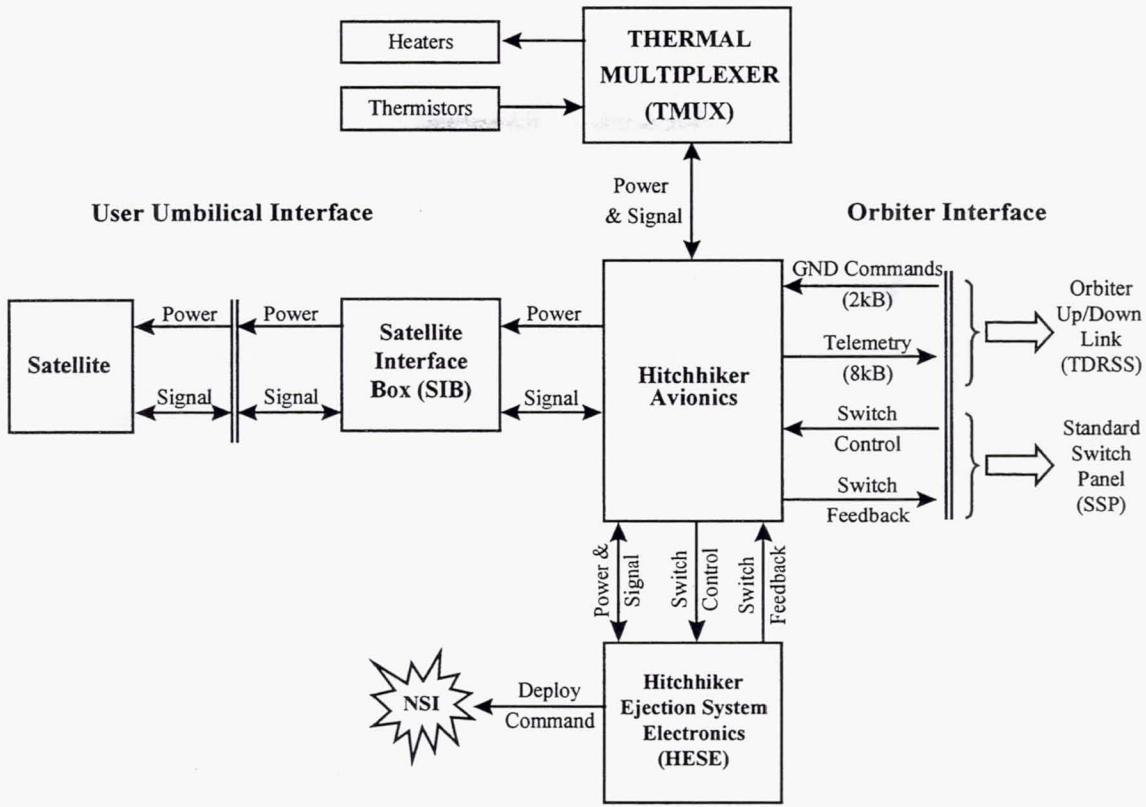
Figure 2. SHELS Electrical Functional Block Diagram

ACCOMMODATIONS

The SHELS system is being designed to accommodate up to a 400-pound satellite with a center of gravity (CG) no more than 24 inches above the ejection system separation plane. The satellite CG must be within .25 inches of the ejection system centerline.

While the structure must meet all load and frequency requirements of accommodating a 400-pound satellite with a 24-inch CG offset, what remains to be determined is the Orbiter capabilities of accommodating such loads. The weak link in the SHELS system is the three bolts that attach the adapter beam to the Orbiter sidewall. It is expected that the Orbiter capability shall vary from one cargo bay location to another as the loading on these three bolts is highly dependant on the cargo bay payload complement. A coupled loads analysis to be run in '00 shall provide loads data that will determine actual SHELS system capabilities with respect to payload mass and CG.

Allowable satellite envelope is currently being defined; its constraints are driven by complex geometry. The payload envelope is constrained in the vertically (Orbiter Z axis) by the cargo bay door envelope. The payload envelope constraints in the X and Y axes are generally limited by the clearances between the payload and the cast structure and the payload and the thermal shroud. The largest rectangular-shaped satellite that would fit within the current payload envelope is 36 x 25 x 46 inches in the X, Y, and Z axes, respectively.

The ejection velocity is expected to be between 1.5 ft/sec and 4.0 ft/sec. There is no capability to spin-up a payload prior to ejection. The design shall preclude tip off rates that would result in colliding the payload with the thermal shroud; at this time there has been no analysis to determine a tip off rate.

Payload customers are required to withstand applied loads of 11 g's in the X, Y, and Z axes simultaneously with safety margins of 1.25 on yield and 1.4 on ultimate. These load factors are applied at the center of mass of the ejected payload.

Thermal shroud survival heaters shall supply a maximum of 280 Watts power at 28VDC. Heat is radiated to the payload.

The electrical umbilical shall provide a power and a signal interface connector to the payload. Total power available is 280 Watts at 28VDC divided among four circuits rated at 2.5 Amps maximum each. The signal interface shall provide 1200 baud asynchronous command and telemetry, three analog 0-5 volt signal inputs, three digital 28 Volt bi-level signals and a minute pulse.

MECHANICAL SYSTEMS OVERVIEW

The SHELS mechanical system consists of a launch structure, ejection system, and mission unique thermal shroud. The system is designed to accommodate a wide range of spacecraft and provide a cost effective user friendly launch system with minimum integration. The entire system is being modeled in Pro-Engineer™. Figure 3 shows a 3-D view of the SHELS launch structure and the ejection system.

Launch Structure

The SHELS launch structure is a premium quality, aerospace, structural casting with a riveted stress-skin panel for increased torsional capability. The casting material is aluminum alloy A356-T6 strength class 10, fabricated with rapid prototype casting techniques. Investment castings traditionally have been fabricated by the lost wax method, requiring tooling to produce an injection molded, near net shape, wax pattern. Once produced, the wax patterns are processed by bonding preformed wax gates and risers to facilitate casting. Then the pattern is invested, or dropped, in a stucco solution of fractured ceramic and water. The stucco encapsulates the entire wax pattern with ceramic approximately .25 inch thick per side producing a casting shell. The shell is dried at room temperature then heated or de-waxed in an autoclave in order to melt and pour off the wax from within the shell. Hence the term lost wax method. The shell is then fired in a furnace and filled with the desired molten alloy. When the casting cools and solidifies the shell is broken away, the gates and risers are removed and finished. The casting is then annealed, straightened, solution treated to T6 condition, and inspected. The inspection process includes dimensional and non-destructive evaluation (liquid penetrant and x-ray).

The rapid prototype technique varies from the lost wax method by substituting a precision crafted wooden pattern for the wax pattern. The wooden pattern is then gated, invested, dried, and burned out in a furnace at the ignition temperature of the wood. After pattern burnout, the shell is cooled, flushed, and inspected to insure that the shell is free of debris. The shell is then processed in the same manner as a traditional investment casting.

The rapid prototype casting method may appear labor intensive but the wooden patterns are produced direct from a solid CAD-CAM model and routed to shape by CNC routers and conventional woodworking techniques. The routed sections are then assembled, filleted, and inspected to prepare them for foundry processing. This method foregoes the need for injection molding tools and provides engineers with incredibly complex structures priced competitively with conventional structures at quantities of one.

Goddard has successfully developed and flown numerous structural castings and one satellite that was entirely investment cast. The castings have proven cost and weight efficient and structurally robust. Cast structures provide 100% joint efficiency and allow designers to produce complex and compact structures previously inaccessible or incapable of fabrication by welding, riveting, or machining. This advantage allows designers to selectively localize material at key structural points and use cross-sectional inertias to their maximum advantage. In addition, high efficiency structural forms previously costly to fabricate, such as isogrid and geodesically stiffened lattice, become cost competitive when cast.

Castings offer an additional cost advantage by reducing designing, drafting, and checking. Fewer parts translate directly to project savings.
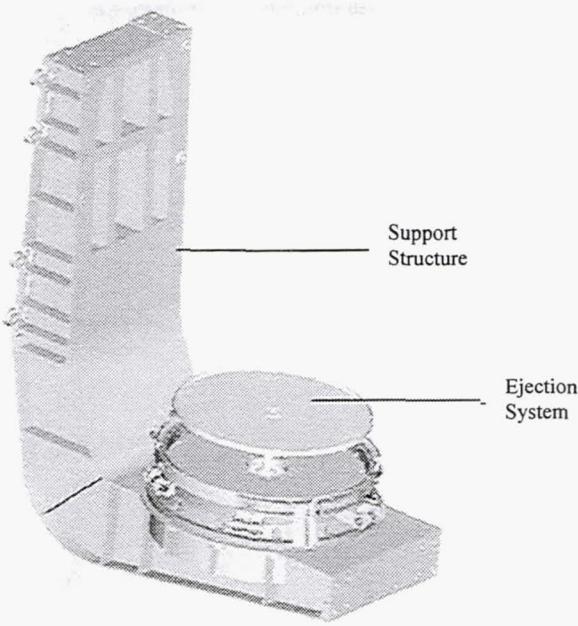
Figure 3. Cast Aluminum Structure in 3D

Ejection System

The SHELS ejection system consists of a strap and shoe Marman band, ejection base and center mounted compression spring/push plate assembly. The thermally isolated ejection system is mounted to the SHELS launch structure, which provides the structural interface to the adapter beam.

The Marman band consists of two stainless steel tension straps and ten shoes which are loosely riveted to the strap. Trunnions are riveted to the ends of each strap and provide a swiveled attach point for the separation bolts which tension the system. The aluminum and titanium shoes have 20° ramp angles and low friction hard coatings applied to all surfaces. The titanium shoes are located under each of the end trunnions due to the higher local loads produced at these locations. When the separation bolts are preloaded, the shoes clamp the system by riding up matching ramps on the ejection base flange and payload interface plate flange. Each of the separation bolts will also have a bolt force sensor to monitor band tension during assembly, testing, and under various environmental conditions. The Marman band will be pull tested to worst case conditions to verify no gapping occurs at the interface. A 1.25 test factor will be used.

The Marman band is released by redundant, NSI actuated, bolt cutters. A nominal separation of the payload from the ejection base will occur if only one of the bolt cutters functions. When the separation bolts are cut, the Marman band snaps off the flange interfaces and is held in a retracted position by six torsion spring assemblies. Once the Marman band has snapped off the flanges, a centrally located compression spring is free to push the payload away from the ejection base. A guide shaft riding in a set of linear ball bearings guides the push plate during the stroke of the spring. The linear bearings provide a low friction, tightly controlled ejection with low tip off imparted to the payload. A line of balls in each linear bearing also rides in a "V" groove cut down the length of the guide shaft. This arrangement prevents the spring from imparting a rotational input into the payload during ejection. Ejection velocity may be tailored to the payload requirements by placing different size compression springs in the adjustable spring housing. Presently the maximum ejection velocity for a 400-pound payload is 4 ft/sec with a maximum 5 in stroke.

As an optional capability, the ejection system allows for the mounting of two internal or two external low force umbilical connectors. The connectors provide power and telemetry to the payload while it is in the Orbiter bay prior

11

to ejection. The two internal umbilical connectors would be mounted on adjustable brackets on the ejection base plate right next to the compression spring assembly. The two external umbilical connectors would be mounted to brackets attached to the outside diameter of the ejection base.

Electrical Systems

The flight electrical segment provides the interface with the Orbiter for power, command and telemetry, both ground and crew. The electrical system is illustrated in Figure 2.

Functional Overview

For a typical mission, shortly after orbit insertion, the crew will activate the HH avionics from the SSP. Once activated, command (2 Kbps) and telemetry (8 Kbps) processing is controlled from the Advanced Carrier Customer Equipment Support System (ACCESS) located in the Payload Operations and Control Center (POCC) at Goddard. Communication of the commands and telemetry occurs through the Tracking and Data Relay Satellite System (TDRSS) and associated ground network.

The initial setup of the HH avionics includes health checks, survival heater activation, and then experiment power on, as necessary. As the deployment window approaches, the satellite will be deactivated. Then the HESE will be activated via ground commanding and operated by the crew to deploy the satellite. Once deployed, satellite commanding will be conducted from the experimenter's ground station.

At mission's end, the HH avionics power distribution system is deactivated from the ground, then the crew will deactivate the HH avionics from the SSP in preparation for the return home.

Carrier Electrical Description

The HH avionics interfaces to the Orbiter to provide electrical services to the experiments. These services include: hardwire switching and displays to the HESE electronics for satellite deployment, real-time command (uplink at 2 Kbps) and telemetry (downlink at 8 Kbps), and electrical power distribution. For SHELS, the satellite power interface will be limited to 280W.

The thermal multiplexer (TMUX) acts as a power distribution unit. It uses a single avionics power port and distributes up to 400W to multiple, thermostatically-controlled heater circuits. The TMUX multiplexes the local heater circuit temperature data, monitored by thermistors, for transport to the ground processing system.

The SIB is used to isolate the satellite from the HH avionics. The SIB uses one power and signal port on the avionics to interface with the satellite. Side A of the power port (280W) is fused and diode isolated from the avionics power system. Side B is used to power the signal isolation interface electronics located in the SIB. The isolated signal interfaces currently identified are 1200 baud asynchronous command and telemetry, three 0-5 V Analog telemetry inputs, three +28V bi-level / pulse outputs, and one Mission Elapsed Time Minute pulse (METMIN) output.

The umbilical interface is only required by an experimenter who wishes to use the power/signal interface with the HH avionics. This interface design uses the NEA Electronics™ proprietary 'soft' release connector technology at the satellite interface to the ejection system. Currently there are two umbilical connectors located within the ejection system pedestal assembly. One connector is primarily dedicated to power, the other is dedicated to signal.

HESE provides the required number of (safety) inhibits and controls to prevent inadvertent satellite deployment. The crew uses three switches on the SSP to sequence the HESE through the deployment sequence. The HESE is only powered during the deployment sequence.

Two NASA Standard Initiators (NSI), each with a booster cartridge, are integrated into two HH-designed bolt cutter assemblies. These bolt cutters sever two bolts to release the Marman band clamping the satellite to the ejection system structure. The function of the NSI's is achieved through the operation of the HESE.

12

Advanced Carrier Customer Equipment Support System (ACCESS) (not shown) provides the ground data handling between the customer's ground hardware and the Orbiter data network.

Thermal Systems

The thermal design of the SHELS casting and ejection system shall be consistent from mission to mission. This design is passive and is composed of various surface finishes including multi-layer insulation (MLI).

The thermal design of the shroud shall vary from mission to mission and be driven by the particular thermal requirements of the satellite. The maximum thermostatically controlled heater power available to the shroud is 280W. Other passive thermal controls shall vary on a case-by-case basis.

The MLI shall incorporate alternating layers of Kapton™ and Dacron™ netting with an outer layer of beta cloth for durability.

The casting shall be directly mounted to the Adapter beam allowing the casting to closely follow the temperature of the beam. By mounting this way, the thermal stresses induced in the casting shall be reduced. Conversely, the ejection system and satellite shall be isolated from the casting to the maximum extent possible. MLI shall be attached to the thermal shroud as necessary to maintain the satellite at its safety and non-operational limits and to decrease the amount of shroud heater power loss.

To qualify the design, the casting and ejection system shall go through thermal vacuum testing.

A geometric model shall b developed using VIEW 386 and SSPTA 386. A thermal math model shall be developed in SINDA85.

STRUCTURAL VERIFICATION

Analysis

A finite element model of the SHELS launch structure has been created for static and dynamic analysis. The pre and post processor used for creation of the model and visualization of the results is FEMAP, version 5.0, a product of Enterprise Software Products, Inc. The finite element solver used for static and normal modes analysis is UAI/NASTRAN, version 20, a product of Universal Analytics, Inc.

The quasi-static design loads used for analysis are 11 g's applied simultaneously in three orthogonal axes. All positive/negative combinations are evaluated, for a total of eight load cases. The design loads are based on the loads used for traditional HH payloads mounted to the Orbiter sidewall. The design case is a payload that weighs 400 pounds and has a CG 24 inches above the separation plane. Detailed stress analysis is ongoing.

Several iterations were made in the design of the launch structure to increase its stiffness and raise the fundamental frequency. Through experience with other sidewall mounted payloads, it was determined that the frequency should be well above 21 Hz, if possible, to avoid excessively high loads that could result from certain landing forcing functions in the coupled loads analysis. The final design of the launch structure has a fundamental frequency of 29 Hz. Plots of the first two mode shapes are shown in Figures 4 and 5. The finite element model of the support structure will be coupled with a model of the adapter beam for assessment of the stresses in the adapter beam. The adapter beam has previously been qualified to carry two 400-pound canisters. The analysis will determine whether any additional qualification testing will be required for the adapter beam.

A preliminary coupled loads study will be performed using the all-up SHELS math model, which will consist of the math models of the launch structure and the adapter beam, with a lumped mass representing the payload. This preliminary study will give an indication of the expected loads and interface forces. The study will use the current Orbiter math model and forcing functions.

Updated Orbiter math model and forcing functions are currently being developed. A significant reduction in the loads predictions for sidewall payloads is anticipated with the update. Therefore, a complete coupled loads analysis of SHELS in every potential Orbiter bay location will be performed after the release of the updated Orbiter model. This analysis will determine payload manifesting options by establishing payload weight and CG envelopes for each Orbiter bay location.

Testing

The SHELS launch structure, including the ejection system, will be qualified through a series of structural tests. Testing will include modal survey, static loads, random vibration, and functional and gravity negation.

Modal Survey

A modal survey will be performed for verification of the math model. The test configuration will consist of the SHELS launch structure attached to a representation of the adapter beam interface. The ejection system and a mass mockup of the payload will be attached to the support structure. All major structural modes below 50 Hz will be identified. The math model will be correlated with the frequencies and mode shapes measured in the test. Payloads shall have a fundamental frequency of at least 50 Hz or a modal survey will be necessary for the payload.

Output Set: Mode 1 28.78033 Hz
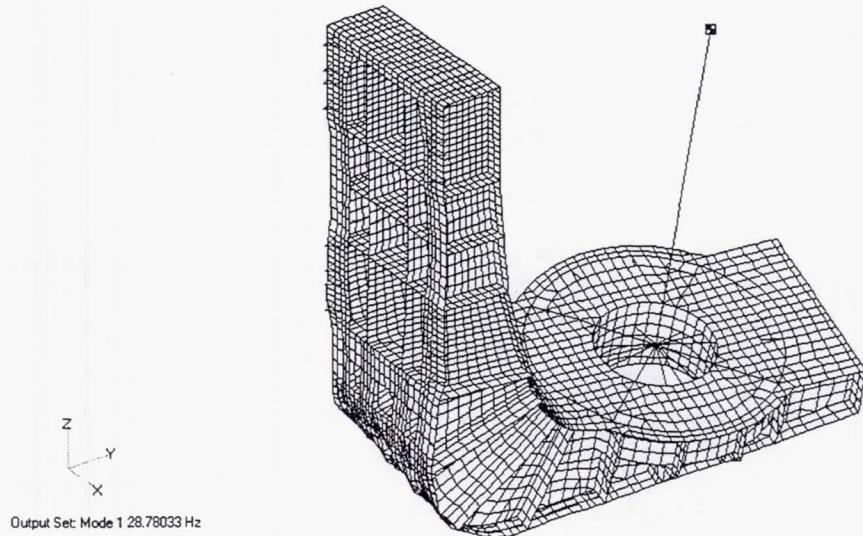
Figure 4. SELS Launch Structure — Mode 1

Z
.....Y
X

Output Set: Mode 2 28.95739 Hz
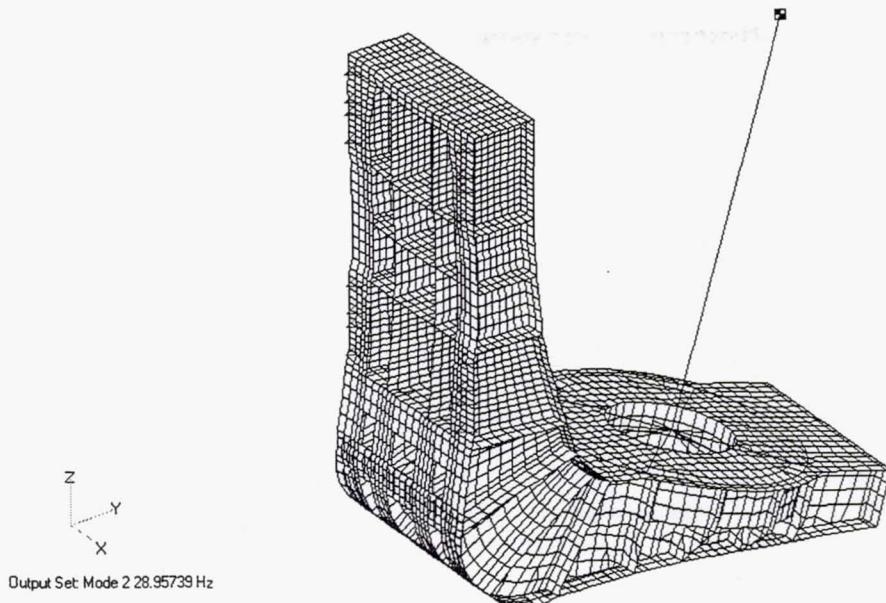
Figure 5. SHELS Launch Structure — Mode 2

Static Loads Testing

A static loads test will be performed for strength qualification of the SHELS launch structure. Qualification of the launch structure and of the ejection system will be accomplished simultaneously. The load vectors for the test will be determined analytically. A test factor of 1.25 will be applied to the design loads.

The static loads test will consist of a series of three pull tests applying combined axial, shear, and moment loads to the Marman band interface. Marman band preload will differ for each pull test to account for the different mass properties (weight and CG) of future satellites. Data from these tests will validate the friction and stiffness parameters used in the basic Marman band preload equations. Successful completion of these tests will allow the specific mass properties of each payload and the predicted accelerations for that mission to determine band preload. A lighter payload, for example, can use a lower band preload, which decreases shock loading during band separation

Random Vibration Testing

Random vibration testing will be performed on the ejection system to qualify the design. The system will be subjected to random vibration in all three axes. The test input levels will envelope the maximum expected flight levels plus 3 dB and the recommended minimum workmanship levels. The maximum expected flight levels will be determined from a random base drive analysis.

Functional & Gravity Negation Testing

A large number of functional tests are planned for the ejection system to assure that the band will release from the interface flanges under varying conditions and system configurations. Several functional tests, including functional tests after each pull test, are planned: they will use different separation bolt preloads; single and double bolt cutter firings; and hot and cold temperature extremes. Some functional test will include the low force separation connectors. Gravity negation tests will also be performed to determine the amount of rotational tip off imparted to the payload by the ejection system during separation. The test will be performed with a payload mass simulator that

15

has been connected with cables over a set of pulleys to a counter weight that balances the system. The cable is connected to the mass simulator at a very low-friction ball joint that is positioned at the CG of the simulator. The low-friction ball joint allows the mass simulator to rotate when external load is applied to the system as if it were in a zero-gravity environment. A series of tests will be performed with varied conditions and configurations to determine worst case tip off rotations. These tests will help to establish design criteria for the thermal shroud and provide important information to payload attitude control systems.

FUTURE ENHANCEMENTS

To increase SHELS manifesting possibilities, it is advantageous to reduce SHELS from a two-beam configuration to a one-beam configuration as shown in Figure 6 and further minimize need for Orbiter services.

By expanding the functionality of the SIB, replacing the HH avionics with a single PGSC crew controlled HRIU, and adding two additional mounting plates to the SHELS casting adapter beam, it is possible to package SHELS on one adapter beam (Figure 7). Umbilical power and data services are now maintained via the PGSC, HRIU expanded SIB [Multipurpose Interface Box (MPIB)] configuration.

This new SHELS configuration eliminates Orbiter services required of a ground controlled payload. This configuration also enables the crew to power SHELS components, survival thermal shroud heaters not withstanding, just before satellite ejection, further reducing the need for Orbiter power services.
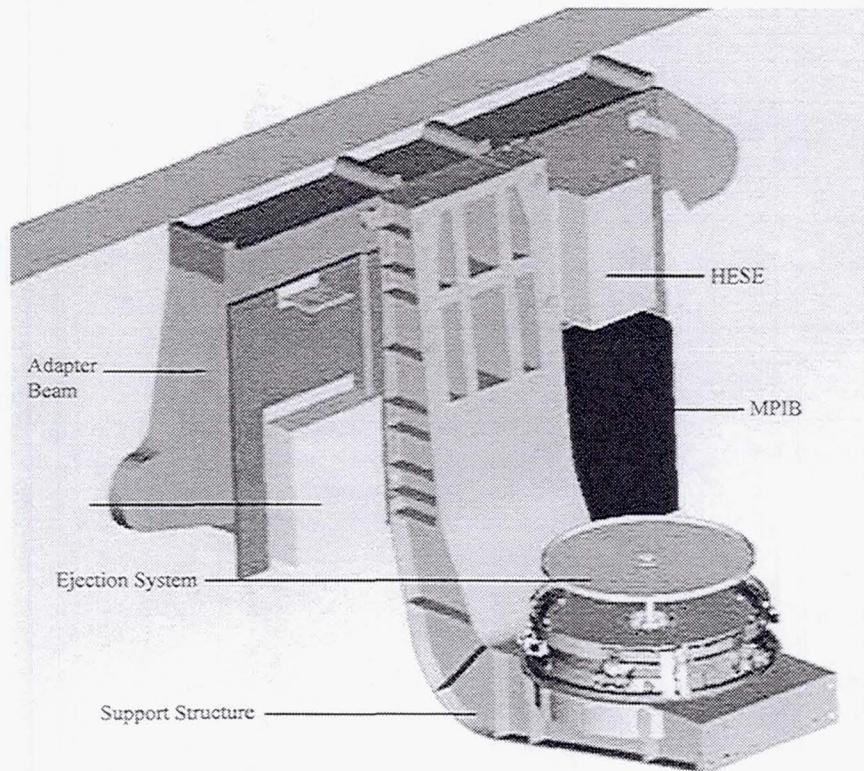
Figure 6. SHELS Configured for One Sidewall Adapter Beam
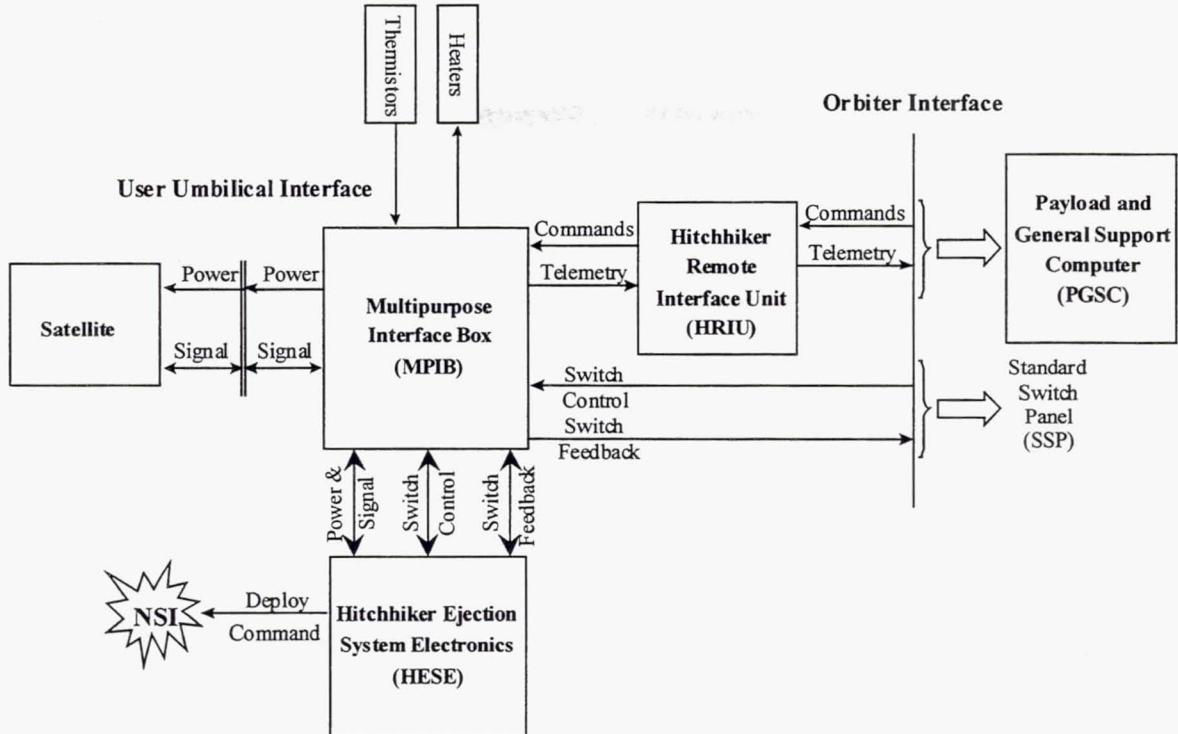
Figure 7. SHELS Electrical Functional Block Diagram for One Sidewall Adapter Beam

17

Page intentionally left blank

Hitchhiker On Space Station

Gerard Daelemans
NASA Goddard Space Flight Center
(301) 286-2193

Theodore Goldsmith
Swales Aerospace Inc.
(301) 902-4536

ABSTRACT

The NASA/GSFC Shuttle Small Payloads Projects Office (SSPPO) has been studying the feasibility of migrating Hitchhiker customers past present and future to the International Space Station via a "Hitchhiker like" carrier system. SSPPO has been tasked to make the most use of existing hardware and software systems and infrastructure in its study of an ISS based carrier system.
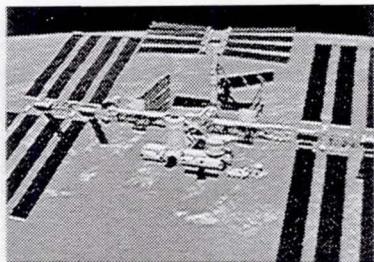
This paper summarizes the results of the SSPPO Hitchhiker on International Space Station (ISS) study. Included are a number of "Hitchhiker like" carrier system concepts that take advantage of the various ISS attached payload accommodation sites. Emphasis will be given to a HH concept that attaches to the Japanese Experiment Module - Exposed Facility (JEM-EF).

ISS HITCHHIKER STUDY OBJECTIVES

The objectives of the Hitchhiker on ISS study were to examine the potential for using existing or modified Shuttle Hitchhiker flight and ground systems, facilities, personnel, and general low-cost, quick reaction approach to support smaller scientific payloads on Space Station. Any such implementation should avoid duplicating any already planned ISS capabilities and allow for easy transition of existing Shuttle Hitchhiker customers to ISS.

EXISTING PLANNED SPACE STATION EXTERNAL PAYLOAD ACCOMMODATIONS

Existing plans for Space Station external payload accommodations were examined in detail in order to determine the most promising possibilities for complementary use of Hitchhiker derived systems and implementation approach. The current plans are summarized as follows:

The ISS has attachment latches (the Payload Attach System (PAS)) located on the main truss. Two are located on the nominal top (zenith - space facing) side of the starboard (S3) truss and a second pair are located on the bottom (nadir - earth facing) side. An additional set (upper and lower) of latches is located on the port side (P3) of the truss. The S3 locations are planned for scientific payloads while the P3 locations are initially planned for temporary storage and handling of non-operating payloads and other equipment but may eventually be used for operating payloads. Each electrically operated latch has a remotely operated connector providing 120vdc power, MIL 1553 data and command signals, and a fiber optic high rate data line which can be used periodically for scheduled downlink of accumulated data.

The truss mounts can handle payloads up to 11,000 lb. (5000Kg) up to 15 x 7.5 x 10 feet (4.6 x 2.3 x 3.0 m) in size.

JEM-EF   ELM-ES
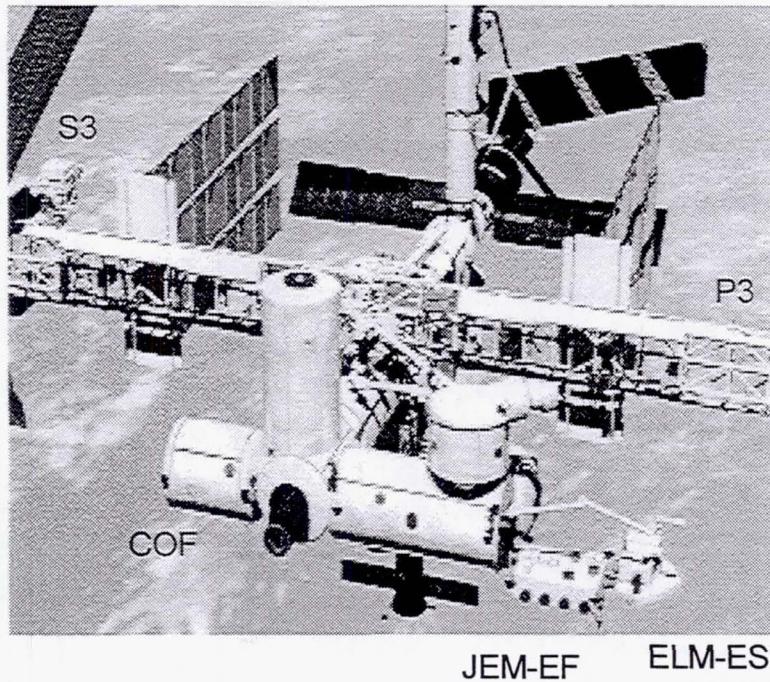
ISS Payload Accommodations

The EXPRESS Pallet being developed by the Brazilian Space Agency is designed to mount to the truss. Each pallet can accommodate six pallet adapters while occupying one truss mount. The adapters are flat plates with a grid hole mounting arrangement for payload equipment up to 500 lb (227 Kg) and 34 x 46 x 49 inches (.9 x 1.2 x 1.3 m) in size. Adapters are provided with electrical accommodations including MIL 1553, 120vdc and 28vdc power, and an ethernet connection to a multiplexer which feeds the fiber optic system.

The European Columbus Orbiting Facility (COF) will have four external mounting positions for accommodating payloads on adapter plates similar to EXPRESS.
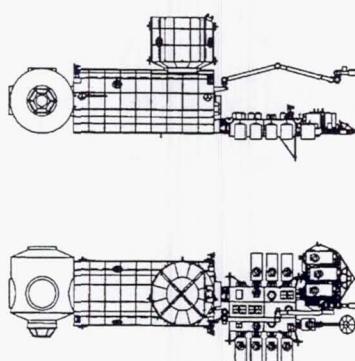
The Japanese Experiment Module - Exposed Facility (JEM-EF) is a "back porch" attaching to the Japanese pressurized module and has ten electrically operated latches for attaching payloads in various orientations. Two of the positions can handle 5500 lb (2500Kg) and the remaining eight can handle 1100 lb (500 Kg) with sizes of 72 x 40 x 31 inches (1.8 x 1.0 x .8 m). Electrical accommodations vary somewhat with mounting position and include 120vdc power, MIL 1553, and ethernet. Unlike the other mounts, JEM-EF provides fluid cooling. JEM has a manipulator arm with tool driving capability.

Various Shuttle "logistics" carriers are planned to transport payloads to and from station including the Brazilian Unpressurized Logistics Carrier (ULC), and Japanese Experiment Logistics Module - Exposed Section (ELM-ES). The Japanese H2 expendable launcher may also be used to launch JEM payloads and to destructively reenter payloads after their operational period if intact return is not required.

Payloads are installed and removed using extensive robotics including various "manipulator arms" similar to the Shuttle RMS. For ISS, new grasping and tool driving capabilities are being developed.

In addition to the four truss mounts, two COF adapter positions and five JEM-EF positions are assigned to NASA use.

ISS HITCHHIKER JEM-EF PAYLOAD BUS

The Hitchhiker carrier proposed for use with JEM-EF consists of a rectangular box structure. A Payload Interface Unit (PIU) on one end provides for latching to the JEM-EF platform and includes power, data, and fluid interfaces. A second latch interface on the side of the structure is used for attaching the structure to the upload carrier during Shuttle missions to and from ISS. A pair of grapple fixtures are also provided to allow the structure to be handed off between the Shuttle and Station or JEM RMS arms during installation maneuvers. Depending on the exact configuration of the latch it is possible that only one grapple fixture will be required.
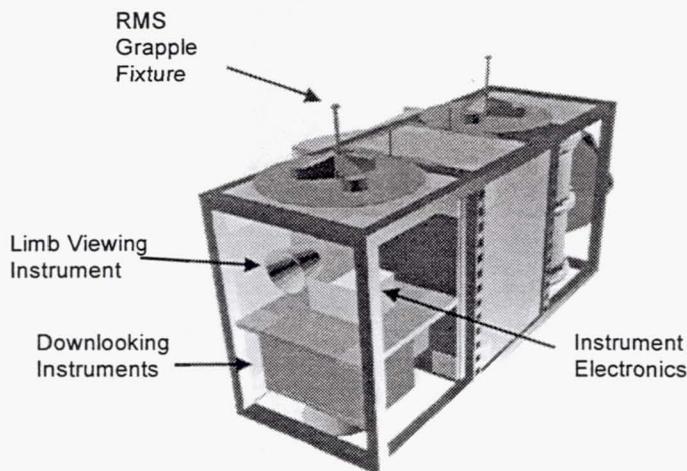
ISS Hitchhiker JEM-EF Carrier

The structure is provided with adjustable shelves for accommodating various size instruments and instrument electronics boxes. Hitchhiker-type canisters may also be used to house instruments. Outer skins on the structure provide thermal treatment and can have aperture holes as required. In addition to multilayer insulation blankets or other thermal surfaces, thermostatically controlled louvers may be used to provide thermal control of the payload. High dissipation payloads may require use of the JEM fluid loop system for heat removal.

A power distribution system provides individually switched and current limited power for up to four instruments. Power is 120vdc but converters can be installed to provide limited amounts of 28vdc power if necessary.

A data system in the bus provides simple, easy to use, Hitchhiker type electrical interfaces for up to four instruments. The use of the Hitchhiker interface allows easy modification of existing instruments for flight on ISS and allows dual use of new instruments if desired. Instruments may connect to a local MIL-1553 bus or a local ethernet 10 Base T bus in addition to the Hitchhiker interfaces. A data storage system may also be provided depending on instrument requirements.

OTHER ISS HITCHHIKER ACTIVITIES

The Hitchhiker Program is also investigating the use of existing or modified Shuttle Hitchhiker equipment to support Shuttle launch or return of ISS payload equipment. This includes side-mount (GAS Beam) or cross-bay (MPESS) equipment. The Program is also interested in supporting investigations which require both Shuttle and ISS support such as phased development of flight instrumentation. In addition, the Program is developing a database of ISS payload related documentation for support of investigators. A CAD system for supporting payload accommodations studies, proposal development, and field-of-view studies is also under development.

ISS HITCHHIKER INTEGRATION AND OPERATIONS PLAN

The ISS Hitchhiker Program will share GSFC resources, facilities, and personnel with the continuing Shuttle Hitchhiker Program. GSFC will provide interface management (including support for documentation, interface engineering, safety, launch and flight operations planning, and crew training) and perform instrument to carrier integration and checkout at GSFC in a manner similar to the Shuttle Hitchhiker Program. GSFC will also provide a control center for operating and monitoring the carrier systems and providing general support to investigators as required. Because ISS Hitchhiker payloads will operate for much longer periods than Shuttle Hitchhiker, it is anticipated that most investigators will want their own control center facilities to operate their instruments and acquire data during missions. These facilities will communicate directly with the ISS Payload Center at MSFC or NASDA.

ISS HITCHHIKER PROGRAMMATICS

It is anticipated that future science flight opportunities announced by the NASA Offices of Earth and Space Science will include the option of proposing missions for flight on the ISS JEM-EF. Submitters can incorporate ISS Hitchhiker into their proposals. We expect that recurring standard Hitchhiker integration and operations activities will be provided at no cost to proposers in a manner similar to the existing Shuttle Hitchhiker services. However, because flight hardware will be utilized for a much longer period by ISS Hitchhiker users there may be a use fee. In addition, optional, non-standard, hardware or services will be priced on a case-by-case basis. The Hitchhiker Program is planning to support experimenter proposal development and feasibility work regarding ISS JEM Hitchhiker at no cost to the proposer. If a selected proposal utilizes ISS, existing NASA Headquarters and JSC procedures will handle ISS and Shuttle manifesting.

CONCLUSION

The U.S. assigned external payload space on JEM-EF represents approximately one-quarter of all the ISS external payload space available for use by U.S. investigators and is therefore an extremely valuable national resource. By providing simple, Hitchhiker style hardware and management interfaces for small payloads, the ISS Hitchhiker enables competitive, cost-effective science payloads to be proposed and flown using this resource.

ADDITIONAL INFORMATION

For additional Hitchhiker information call Gerry Daelemans at (301) 286-2193 or consult the ISS Hitchhiker web site at http://ssppiss.gsfc.nasa.gov or the Shuttle Hitchhiker web site at http://sspp.gsfc.nasa.gov.

JEM-EF
PIA Attach Fitting
ISS HH
Payload

**JEM-EF Platform
with payloads**

JEM Payload

crawl
space
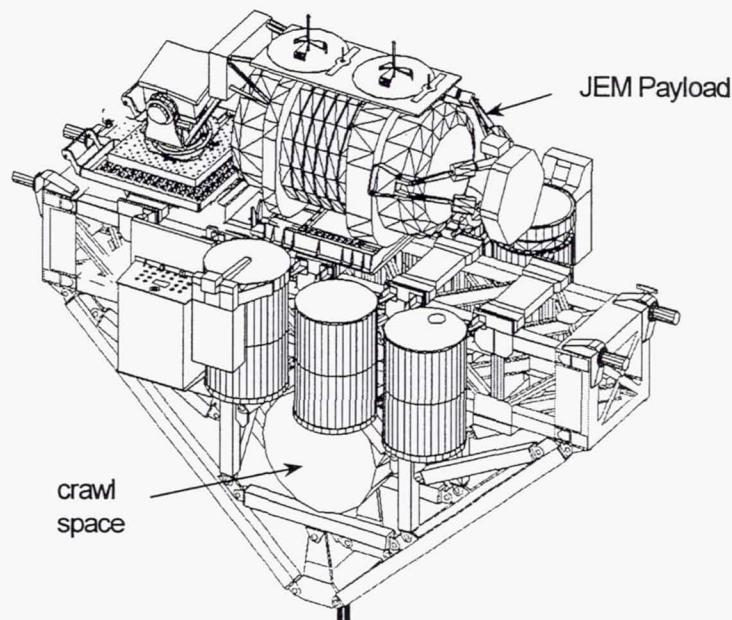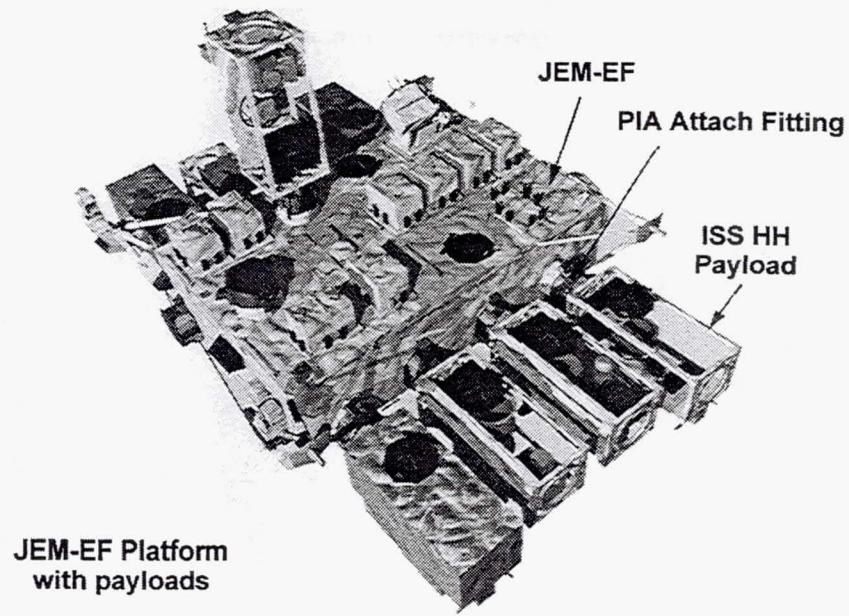
Shuttle Hitchhiker Carrier Modified for JEM Payloads

Page intentionally left blank

SPACE EXPERIMENT MODULE (SEM)

Charles L. Brodell
NASA Wallops Island Flight Facility
Mail Code 546.W
Wallops Island, VA

Space Experiment Module (SEM)

The Space Experiment Module (SEM) Program is an education initiative sponsored by the National Aeronautics and Space Administration (NASA) Shuttle Small Payloads Project. The program provides nationwide educational access to space for Kindergarten through University level students. The SEM program focuses on the science of zero-gravity and microgravity. Within the program, NASA provides small containers or "modules" for students to fly experiments on the Space Shuttle. The experiments are created, designed, built, and implemented by students with teacher and/or mentor guidance. Student experiment modules are flown in a "carrier" which resides in the cargo bay of the Space Shuttle. The carrier supplies power to, and the mean to control and collect data from each experiment.

Overview

The Space Experiment Module (SEM) Carrier System is a self-contained assembly of engineered subsystems which function together to provide structural support, power, experiment command and data storage capabilities. The carrier system is a five cubic foot 'canister' containing ten experiment modules.

The small, enclosed module (pictured right) can contain approximately 300 cubic inches (4.9 L) of experiment apparatus weighing up to 6 lb. (2.7 Kg.). Experiments may be active (uses carrier supplier power) or passive (non-powered). Students may design active experiments 'on paper' using NASA supplied software and databases. Passive experiments are generally packed in NASA-provided "Space Capsules". Experiment design must adhere to safety standards.

The Space Capsules used to contain passive test articles are clear, sealable polycarbonate vials, 1.0 inch in diameter and 3.0 inches in depth. Space Capsules are packed in special formed foam layers during integration.

The active experiment container uses the "Module Cover" as the Experiment Mounting Plate. The free space available for experiment apparatus in the Module experiment compartment is the "Experiment Envelope". The Envelope is a precisely defined volume outlined on the inboard surface of the Experiment Mounting Plate and extends 3.25 inches below the inboard surface.

The software required for active experimentation is accessible through the World Wide Web [filename semxx.zip (xx is the version number) at the File Transfer Protocol site on http://sspp.gsfc.nasa.gov]. The software application helps the experimenter describe the experiment; enter power consumption, parts, materials, and timeline; and
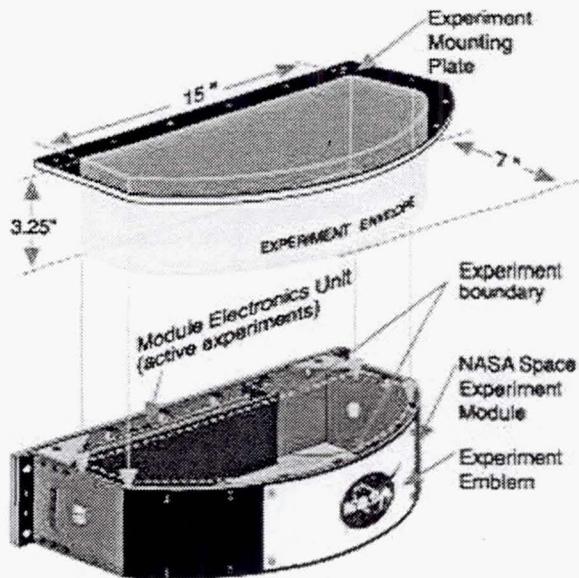
control and command data. The software may be used to analyze the data for SEM compatibility and "post-flight" reports.

The active modules are powered by one 12-Volt battery independent of the Shuttle power supply. Each powered module has an integrated programmable control circuit board or "Module Electronic Unit" (MEU) for data sampling and storage. The MEU processes the student-devised flight operations timeline. A "Ground Module Electronic Unit" is provided to selected active experimenters for development and testing of their active experiment.

Experiments selected to participate will receive a hardware package to support the construction and development of the selected experiment. The hardware package contents are determined by the proposed experiment design.

Experiments are required to be shipped to NASA approximately four months prior to the scheduled flight. The SEM canister is generally installed three months prior to launch in the Space Shuttle cargo bay.

During the early state of the Shuttle flight, astronauts activate the SEM canister via the Payload and General Support Computer. For active experiments (using battery power) the MEU's carry out their unique programmed timeline defined by the experimenter's.

Participation in flight integration and post-flight de-integration is conditional and coordinated through the program. Students and teachers are invited at their expense to attend the launch at Kennedy Space Center.

Following Shuttle spaceflight of the SEM carrier, the experiment hardware or space capsules and the active inflight data from the MEU's is returned to the student experimenters. Experimenters are requested to provide NASA a copy of their post-flight data analysis and reports. NASA archives the results and are available on the website at:

http://sspp.gsfc.nasa.gov/sem/history/history.html

Experimenter groups are awarded a "Flight Certificate" which includes a SEM sticker flown on the Shuttle Mission.

SEM Flight History

A variety of SEM experiments have flown on Shuttle missions since 1996. Students of all ages have enjoyed the experience of exploring the space environment. A history of SEM flight can be viewed at the above website.

SEM-01 STS-80 Space Shuttle Columbia
Launch date: November 19, 1996

SEM-02 STS-85 Space Shuttle Discovery
Launch date: August 7, 1997

SEM-03 STS-91 Space Shuttle Discovery
Launch date: June 2, 1998

SEM-04 STS-95 Space Shuttle Discovery
Launch date: October 29, 1998

SEM-05 STS-91 Space Shuttle Discovery
Launch date: June 2, 1998

SEM-06 STS-101 Space Shuttle Atlantis
Scheduled for Launch: December 2, 1999

SEM-07 STS-88 Space Shuttle Endeavor
Launch date: December 4, 1998

For more information on experiment names and types, that have flown or are scheduled to fly, view the SEM history page at the above web address or the "What's New" section at:

http://sspp.gsfc.nasa.gov/sem/new.html

Getting Started

Submitting a proposal for a SEM experiment offers students an excellent opportunity to explore space and interact with the NASA Space Transportation System (STS) or Space Shuttle program. Instruction for submitting an application can be found in the "How To Participate" section at: **http://sspp.gsfc.nasa.gov/sem**

SEM Support Structure
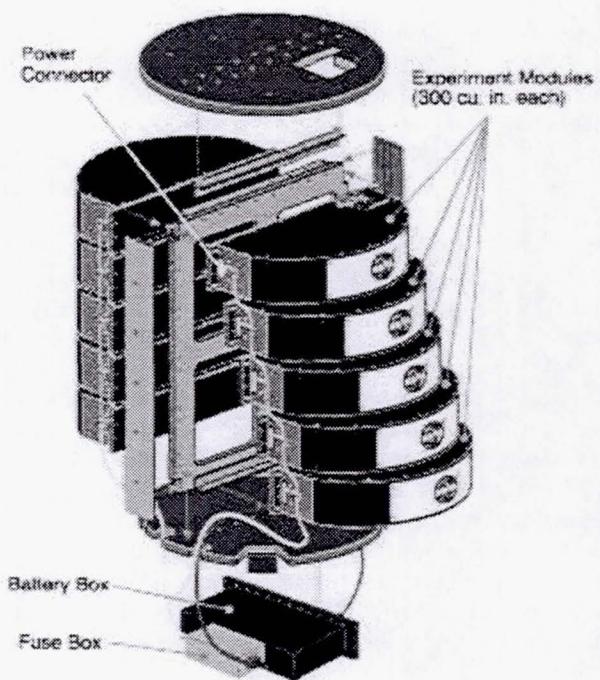
The SEM Support Structure is the structural backbone of the SEM subsystems housed within the GAS canister. It serves as the mounting frame for the Power Subsystem components and ten modules.

Additional Information

Applications for participation in the SEM program are accepted on a continuous basis. For additional information or questions, please contact the following:

Charles L. Brodell
SEM Mission Manager
Phone: (757)824-1827
FAX: (757)824-2145
Charles.L.Brodell.1@
gsfc.nasa.gov

Barbara Justis
Technical Liaison
Phone (757)824-1732
FAX: (757)824-2145
Barbara.J.Justis.1@
gsfc.nasa.gov

For written correspondence, send your request to:

Code 870.W
Shuttle Small Payloads Project
Goddard Space Flight Center
Wallops Island Flight Facility

ANALYSIS OF THREE-DIMENSIONAL ROLLER PERFORMANCE IN A MICRO-g ENVIRONMENT

B. Roberts[†], L. Shook[*], L. Hossaini[*], and R. Cohen[‡]

Space Systems Laboratory
University of Maryland

ABSTRACT

Approximately 960 hours of extravehicular activity (EVA), or spacewalks, are planned for the construction of the International Space Station over the next six years. This is over two-and-a-half times the total number of EVA hours accumulated by the National Aeronautics and Space Administration (NASA) in the past 35 years of U.S. spaceflight. Therefore, it is advantageous to explore ways to assist astronauts in being more efficient while working in space. The Space Systems Laboratory at the University of Maryland is investigating ways of improving conventional ratcheting tools that do not work effectively in confined spaces and have been seen to exhibit other limitations that restrict their use during EVA. By replacing the traditional ratchet mechanism with a NASA/Goddard Space Flight Center-developed three-dimensional (3-D) sprag and roller mechanism, ratcheting tools can be made more efficient. In October of 1998, a 3-D roller mechanism was flown on space shuttle mission STS-95 as part of the Space Experiment Module program. The goal of the experiment was to quantify the roller's performance when operating for an extended period in a micro-g environment. This paper discusses the design of the experiment, as well as the results obtained.

INTRODUCTION

As space exploration continues, more and more extravehicular activity (EVA) will be needed to expand and strengthen the foothold we have established in space, both in orbit and beyond. Starting in December 1998 with the first spacewalk of the International Space Station (ISS) era and continuing through the completion of the ISS in 2004, approximately 960 hours of EVA will be performed to assemble the station (ref. 1). This is over two-and-a-half times the 377 hours of spacewalks that the National Aeronautics and Space Administration (NASA) has conducted since 1965 (ref. 2). This increased need has led both engineers and designers to try to improve the efficiency of the tools and systems that astronauts use for EVA in space. In doing so, it is hoped that astronauts can get the most out of the limited time and currently available resources while working in space. Turning this interest toward tools, it can be seen that simply adapting tools designed for 1-g environments will not be sufficient for an intensive EVA program, such as that planned for ISS construction. By researching improvements to tools commonly used in a micro-g environment, it should be possible to limit astronaut fatigue and improve overall efficiency.

The Space Systems Laboratory (SSL) has been investigating a new type of wrench for use in space. This was done by incorporating the three-dimensional (3-D) sprag and roller technology developed by NASA/Goddard Space Flight Center (GSFC) in place of the ratchet mechanism found in existing wrenches. To further this research, a group of graduate and undergraduate students at the University of Maryland designed an experiment to evaluate the 3-D sprag and roller mechanism. This paper will discuss the on-orbit testing of the mechanism, flown on space shuttle mission STS-95 as part of the Space Experiment Module (SEM) program.

[†] NASA Graduate Student Researchers Program Fellow
[*] Graduate Research Assistant
[‡] Research Engineer

BACKGROUND

Space Systems Laboratory

The SSL was founded in 1975 at the Massachusetts Institute of Technology. It then moved in 1990 to the University of Maryland, where its Neutral Buoyancy Research Facility, the only neutral buoyancy facility in the world located on a college campus, was completed in 1992. Over the past 24 years, the SSL has conducted research into ways to make human beings more productive while working in space and developed advanced techniques for neutral buoyancy simulation of space activities. This research has included studies of the ways the human body works in space, quantification of human abilities in orbit, and the design of tools and telerobotic systems to help astronauts work in space. The SSL currently has three faculty members, 12 full-time staff members, 20 graduate students, and approximately 30 undergraduate students.

Overrunning Clutches

Overrunning, or one-way, clutches are used in rotating mechanical systems when torque must be transmitted in only one direction or when the driven member is to be permitted to "overrun" the driver. Ratchet, roller, and sprag clutches are three types of overrunning clutches that automatically engage to transmit torque by relative rotation in one direction and automatically disengage for overrunning by relative rotation in the other direction.

The first type of overrunning clutch developed was the simple ratchet and pawl mechanism, originally used in clocks, dating back to 1162. Unfortunately, the geometry of this type of clutch constrains it to stopping at a limited number of positions and limits the torque that can be applied.

The next step in one-way clutch evolution was the roller clutch, referred to as a two-dimensional (2-D) roller clutch and shown in Figure 1. It has one race that provides a cylindrical race surface and another race that has a series of wedge-shaped friction surfaces spaced about its circumference. The rollers are installed between these concentric races at the wedge-shaped friction surfaces. Engagement and disengagement are determined by the direction of relative rotation. Relative rotation in one direction causes the rollers to roll up the wedge surface and wedge between the races, engaging the clutch and providing a solid link for the transmission of torque. Rotation in the other direction causes the rollers to roll down the wedge surface, disengaging the clutch for overrunning. This increases the amount of torque the clutch can transmit over that of a ratchet clutch and gives the clutch a nearly infinite number of stop positions.

The final step in perfecting the one-way clutch was the development of the sprag clutch, referred to as a 2-D sprag clutch and shown in Figure 2. It has a cylindrical outer and inner race and a series of specially contoured and processed sprags installed in the annular space between the concentric races.
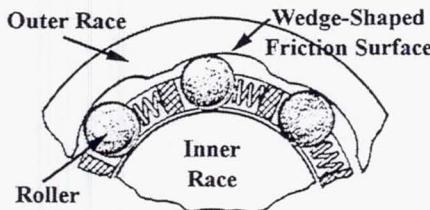
Figure 1: Two-Dimensional Roller Clutch   Figure 2: Two-Dimensional Sprag Clutch
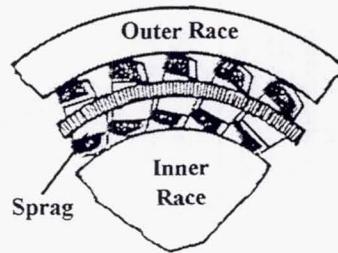
Each sprag is designed with a geometry that makes its two diagonals of different length, as shown in Figure 3. One direction of relative rotation between the races causes the sprags to rotate so that the longest diagonal is in contact with the two races. The length of this diagonal is greater than the annular distance between the races, so the sprags are wedged between the races, providing a solid connection for the transmission of torque. Relative rotation between the races in the opposite direction

causes the sprags to rotate so that the shortest diagonal is in contact with the two races. Its effective length is such that the clutch is disengaged and free to overrun.

NASA/GSFC was having problems with traditional 2-D sprags while using them in joint brakes for robots. They were attempting to use sprags with large contact angles to increase the frictional holding force, but the sprags kept slipping. In addition, lubricants required to get the 2-D sprags to unlock were off-gassing in a vacuum environment. The solution was to replace the concentric, cylindrical surfaces of the inner and outer races with grooves, into which the tapered periphery of a 3-D sprag (ref. 3) fits, as shown in Figure 4. Locking occurs as a result of the wedging action between the tapered periphery of the 3-D sprag and the grooved race.
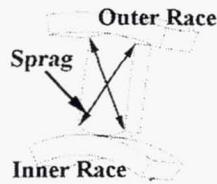
Figure 3: Two-Dimensional Sprag and Races   Figure 4: GSFC Three-Dimensional Sprag and Races
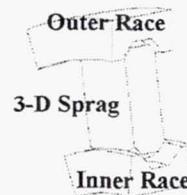
The benefits of 3-D sprags over their 2-D counterparts are that they:
- require no lubricants, thus preventing possible slipping in thermal vacuum
- create four point contacts (two between the outer taper of the 3-D sprag and the outer grooved race and two between the inner taper of the 3-D sprag and the inner grooved race) instead of the two line contacts of the 2-D sprag, thus:
  - allowing loose tolerances
  - doubling the number of contact points
  - increasing the locking efficiency
  - allowing larger contact angles, which reduce the level of sprag-to-race contact stress.

Ratchet Wrenches

Ratchet mechanisms have been in use in hand tools since 1847 (ref. 4), and the design has changed very little in the subsequent 150 years. Although the design functions well for use on Earth, as demonstrated by its longevity, it is not ideally suited for use by a space-suited astronaut. Typical problems encountered with traditional ratchet wrenches in space are:
- limited functionality in confined spaces
- high backdrive torque resulting in loosening when tightening is desired
- inability to control high-inertia interfaces
- lubricant evaporation
- user fatigue during repetitive throws of the wrench.

"Ratchetless" Wrench

Based on the previous discussion of the limitations of ratchet wrenches and the evolution of one-way clutches, it seems logical that wrenches should follow the same progression. Attempts have been made to create a "ratchetless" wrench using rollers or sprags (ref. 5), but all have failed due to high contact stresses. During the development of 3-D sprag and roller prototypes, the idea evolved to replace the traditional ratchet mechanism with 3-D sprags and rollers (ref. 6) because they have a lower contact stress than their 2-D counterparts.

The roller mechanism in the wrench uses three pairs of 3-D rollers installed between concentric races, as shown in Figure 5. Each pair is made up of two rollers (labeled A and B), that are connected by a spring. The spring pushes the A and B rollers apart, wedging them between the races, engaging both rollers. A moveable pin is placed between each A/B roller pair. When a pin contacts a roller, it pushes that roller out of the wedged position between the races, thus disengaging that roller. These three pins, which are constrained to move together, can be locked in one of three positions: center, rotated clockwise (CW),

or rotated counterclockwise (CCW). When the pins are in the center position, they do not contact either the A or B rollers; all of the rollers remain engaged, allowing the mechanism to apply torque in both directions. Moving the pins from the center position in the CW direction disengages the A rollers of all three pairs. This allows torque to be transmitted in the CCW direction. When the pins are moved in the CCW direction, all of the B rollers are disengaged, and torque can now be transmitted in the CW direction.
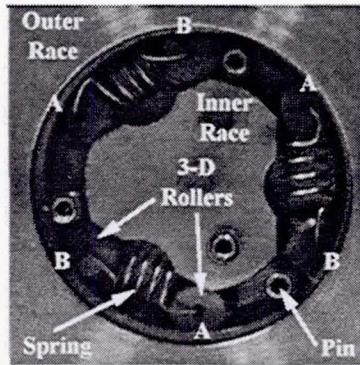
Figure 5: Three-Dimensional Roller Mechanism (pre-flight)

When used in place of the traditional ratchet mechanism, 3-D sprags and rollers result in a wrench that has the following advantages over the traditional ratchet wrench:
- ability to operate down to arbitrarily short backthrows
- low backdrive torque
- ability to apply torque in the clockwise or counterclockwise direction, or to lock out all motion and transmit torque in both directions
- no lubrication requirement, thereby extending on-orbit lifetime
- a compact, simple design
- a higher maximum torque than the equivalently sized ratchet wrench
- a lower perceived mental workload for the EVA subject using the wrench.

SPACE EXPERIMENT MODULE FLIGHT EXPERIMENT

Experiment Design

A 3-D roller mechanism was flown as part of the SEM program in the cargo bay of space shuttle mission STS-95 from October 29 until November 7, 1998. Twenty-one seconds of backdrive and applied torque data were collected every 2 hours. The objective of the experiment was to see how the mechanism operated during seven days in a micro-g environment. The inner and outer races of the mechanism were made of 455 stainless steel. The rollers were made of D7 tool steel and coated with a 0.0001" thick layer of titanium nitride to prevent galling.

At the beginning of a data run, a motor first turned the 3-D roller mechanism in the backdrive direction, free-spinning the mechanism. The motor then reversed, causing the rollers to lock, the motor to stall, and torque to be applied. It then reversed again and continued to free-spin the mechanism. Torque data were collected as the mechanism moved in both the backdrive and applied torque directions. A potentiometer was used to verify that the motor was turning during the backdrive portion and that the roller mechanism did not slip when locked in the applied torque direction. Two thermistors were located inside the module—one on the torque sensor to determine the temperature of the environment inside the module and one on the motor to determine its temperature. The experiment mounting plate onto which these parts were mounted is shown in Figure 6.
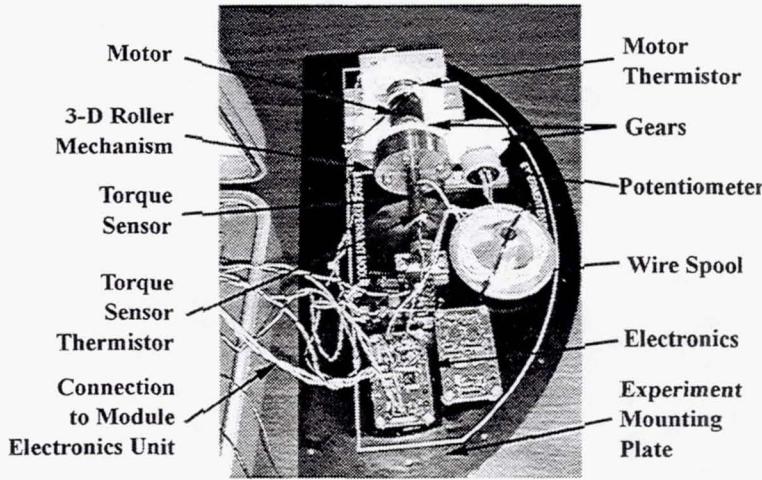
Figure 6: Three-Dimensional Roller Experiment Mounting Plate

Experiment Operation

The experiment operated as follows. The motor turned the 3-D roller mechanism in the backdrive direction for 2 minutes and 49 seconds. Then, for 1 second, it reversed, causing the rollers to lock and the motor to stall, applying 30 inch-pound-force (in-lbf) of torque. It reversed again and continued to free-spin the mechanism for 10 seconds. Twenty-one seconds of backdrive and applied torque data were collected every 2 hours. This consisted of 10 seconds of backdrive torque data before the motor stalled, 1 second of applied torque data while the motor was stalled, and 10 seconds of backdrive torque data after the motor reversed. Position data from the potentiometer and temperature data from both of the thermistors were collected the entire time that torque data were being collected. A sample data run, typical of those that occurred every 2 hours, 10 minutes, and 54 seconds, is summarized in Table 1. A total of 70 data runs were recorded, with all data collected at 5 Hz.

Table 1: Three-Dimensional Roller Experiment Sample Data Run

Time	Event
T = 0m : 0s	Turn on the electronics
T = + 0m : 1s	Turn on the motor
T = + 2m : 40s	Collect torque data
T = + 2m : 50s	Reverse motor
T = + 2m : 51s	Reverse motor again (toward the original direction)
T = + 3m : 1s	Stop collecting data
T = + 3m : 2s	Turn off motor and electronics

Just as with every SEM experiment, the roller experiment had an integrated programmable control circuit board, or module electronics unit (MEU), that provided power, preprogrammed sequencing of the experiment operation, data acquisition, and storage of experiment data. A timeline based on the 70 data runs was generated using a C computer program and stored on the MEU.

Integration, Launch, and On-Orbit Operation

After installation of the experiment's equipment in SEM position 8, the 3-D roller SEM (which was designated experiment 0051), along with seven others, was integrated into the SEM carrier system, as shown in Figure 7. This was then placed into a Get Away Special (GAS) canister, shown in Figure 8. After integration into the GAS canister, the experiment was shipped

the Kennedy Space Center, installed on the Spartan flight support structure, and loaded into the cargo bay of *Discovery* (see Figure 9).
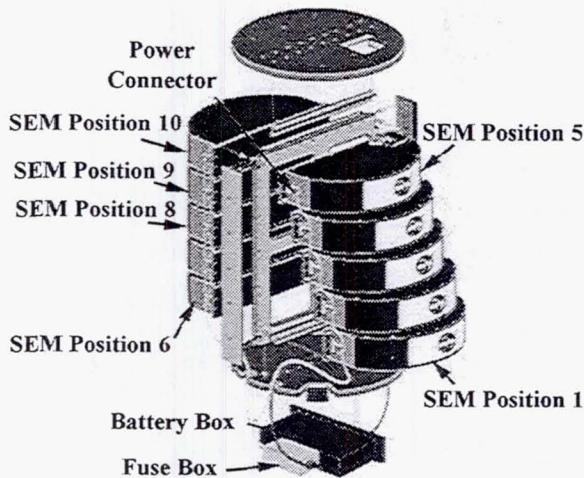
Figure 7: SEM Carrier System (adapted from ref. 7)

Figure 8: Integration of SEM-04 into a GAS Canister (NASA Photo)
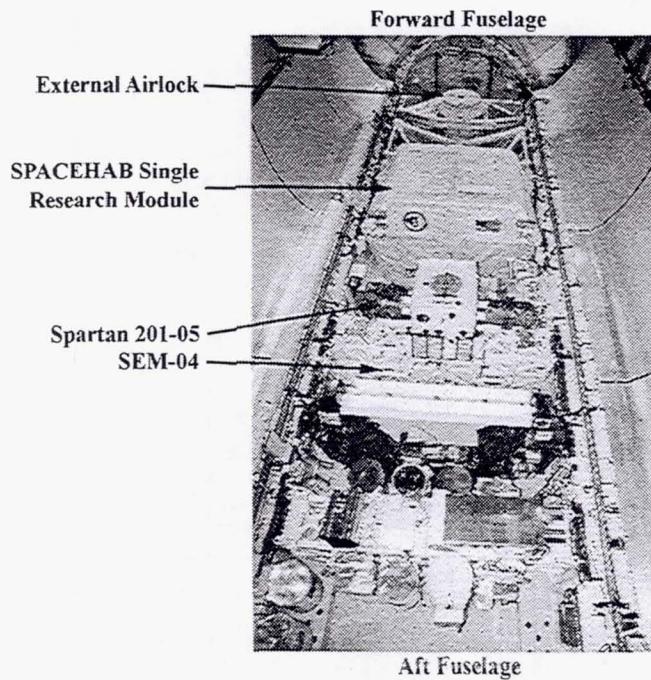
Figure 9: Photo of STS-95 Cargo Bay Layout (NASA Photo)

Launch of STS-95 occurred on October 29, 1998, at 2:19 p.m. EST. SEM-04 was activated at 6 hours, 25 minutes, and 40 seconds after launch (at 8:45 p.m. EST). The timeline ran for 6 days, 6 hours, 45 minutes, and 5 seconds. The experiment stopped running and data collection ceased on November 5 at 3:30 a.m. EST. SEM-04 was deactivated on November 5 at 4:03 p.m. EST (7 days, 1 hour, 43 minutes, and 50 seconds after launch). STS-95 landed on November 7, 1998, at 12:04 p.m. EST, and the experiment was returned to the SSL on December 16, 1998.

Results

The first data run (data run 1) and the final data run (data run 70) are shown in Figures 10 and 11, respectively. The data from the torque sensor are shown as voltages. Backdrive torque is the lower data and applied torque is the data at 5 volts that was chopped off by the electronics. Zero applied torque occurs somewhere in between these two rages.
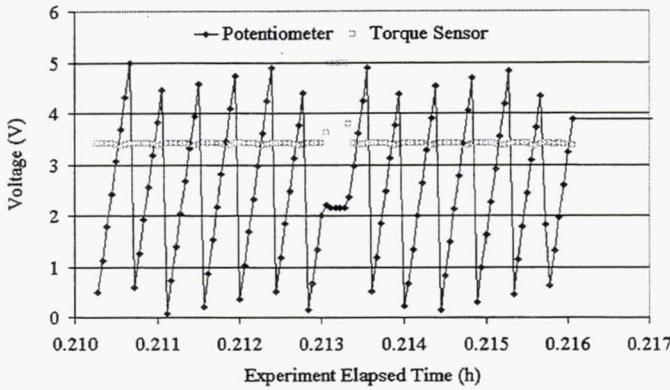
Figure 10: Data Run 1
(started at 12 minutes, 37 seconds)
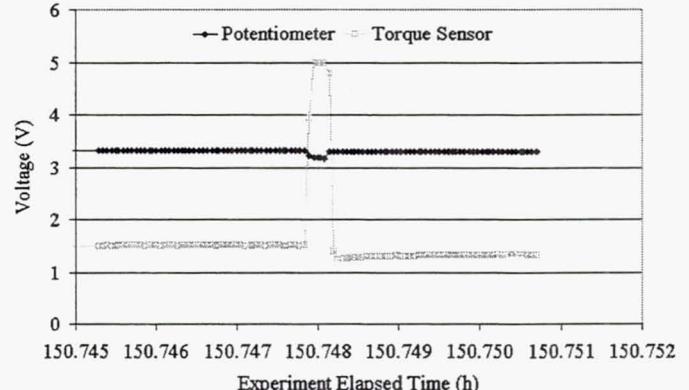
Figure 11: Data Run 70
(started at 6 days, 6 hours, 44 minutes, 43 seconds)

It appears from these plots and an analysis of the rest of the data that the backdrive torque, both during the 10 seconds prior to the mechanism locking and during the 10 seconds following, is relatively consistent over a given data run. As can be seen from Figure 11, the mechanism seized in the backdrive direction toward the end of the mission, as is evident from the flat potentiometer data. In reviewing the torque and potentiometer data over the entire experiment (Figure 12), it can be seen that the mechanism stopped working in the backdrive direction during the 33rd data run (Figure 13). This data run began at 2 days, 21 hours, 58 minutes, and 44 seconds. In data run 33, the potentiometer data show that the mechanism appears to have seized at 2 days, 22 hours, 1 minute, and 32 seconds, during the first backdrive portion. After this event, the potentiometer data flatten out, since the mechanism can no longer move in the backdrive direction. When the motor reverses 2.3 seconds later, the mechanism can be seen to operate correctly in the applied torque direction. The motor reverses again, and the backdrive direction is still shown to be seized. An oscillation in the backdrive torque can be seen in data run 33 prior to the mechanism seizing. The same oscillation can also be seen slightly in data run 1 (Figure 10) and the amplitude of this oscillation increased when the rest of the data runs prior to data run 33 were analyzed. The 34th through 70th data runs show that the mechanism still operated properly in the applied torque direction.
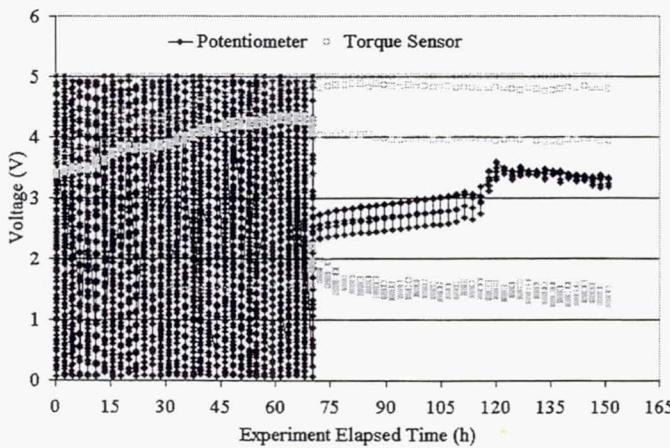
Figure 12: Three-Dimensional Roller Experiment Data
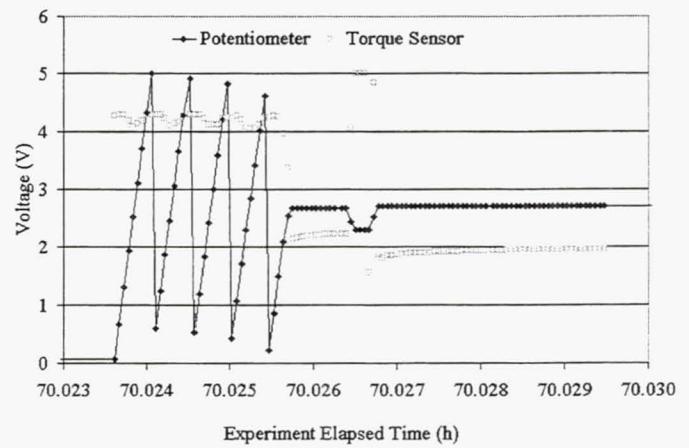
Figure 13: Data Run 33
(started at 2 days, 22 hours, 1 minute, 25 seconds)

After opening up the mechanism, it appears as if one of the rollers came out of the groove and got wedged between the outer race and the side of the inner race, as shown in Figure 14. This is exactly the type of behavior that was observed during preflight tests.
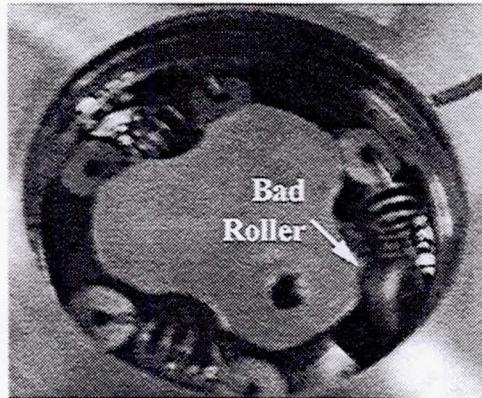
Figure 14: Three-Dimensional Roller Mechanism (postflight)

The temperature data collected on the surface of the motor, when compared with the temperature in the rest of the 3-D roller SEM and other SEMs, indicate that the motor began heating after the 33rd data run. This can be seen in Figure 15, suggesting a stalled motor and/or a seized mechanism. The temperature measurements collected by NASA (ref. 8) were done inside another SEM at position 9 and on the outside of the SEMs in positions 5 and 6.
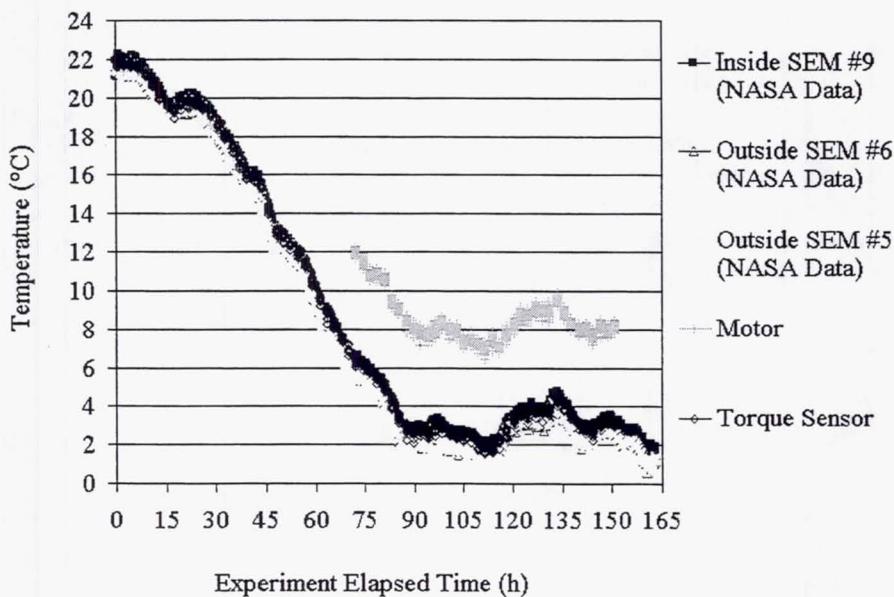
Figure 15: SEM-04 Temperature Data

The battery usage profile collected by NASA for SEM-04, as shown in Figure 16, indicates discharge spikes corresponding to the motor turning on. Not every cycle was captured by NASA's MEU, because battery data were only collected every 5 minutes. Therefore, the timing was sometimes out of phase with the data runs. Comparing the battery discharage voltage over the entire mission further corroborates the conclusion that the motor stalled in the backdrive direction. This is indicated by the increased discharge voltages that occur after the 33rd data run, as compared with those before that run.
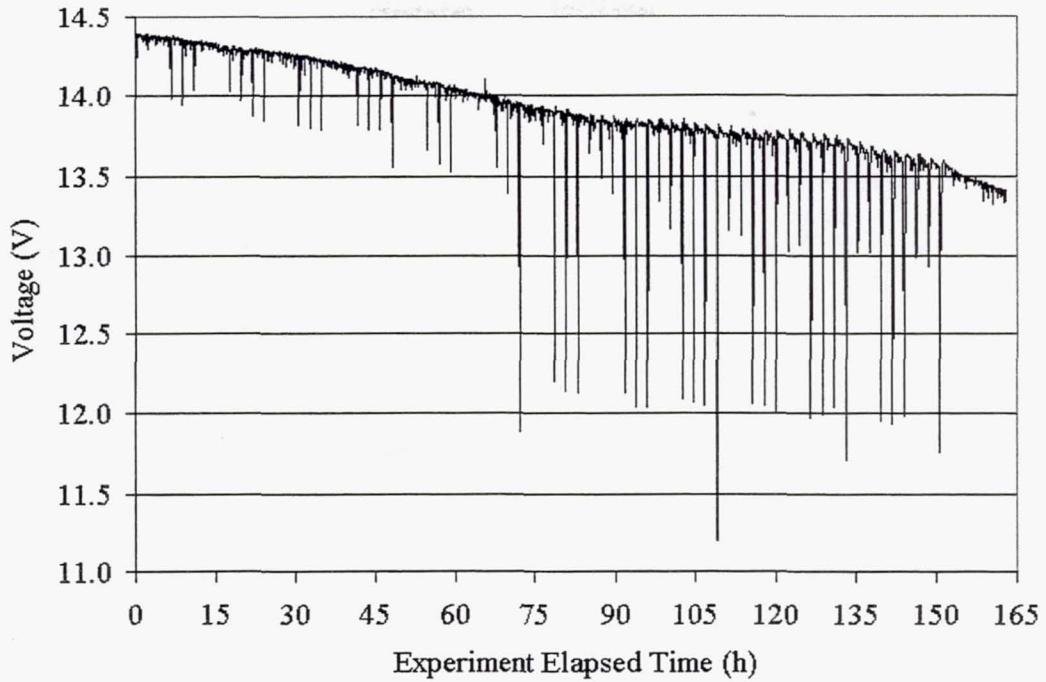
Figure 16: SEM-04 Battery Data

Before the mechanism seized in data run 33, the backdrive torque decreased (high voltage corresponds to lower backdrive torque). This can be seen in Figure 17, which plots the average backdrive torque for each of the 70 data runs.
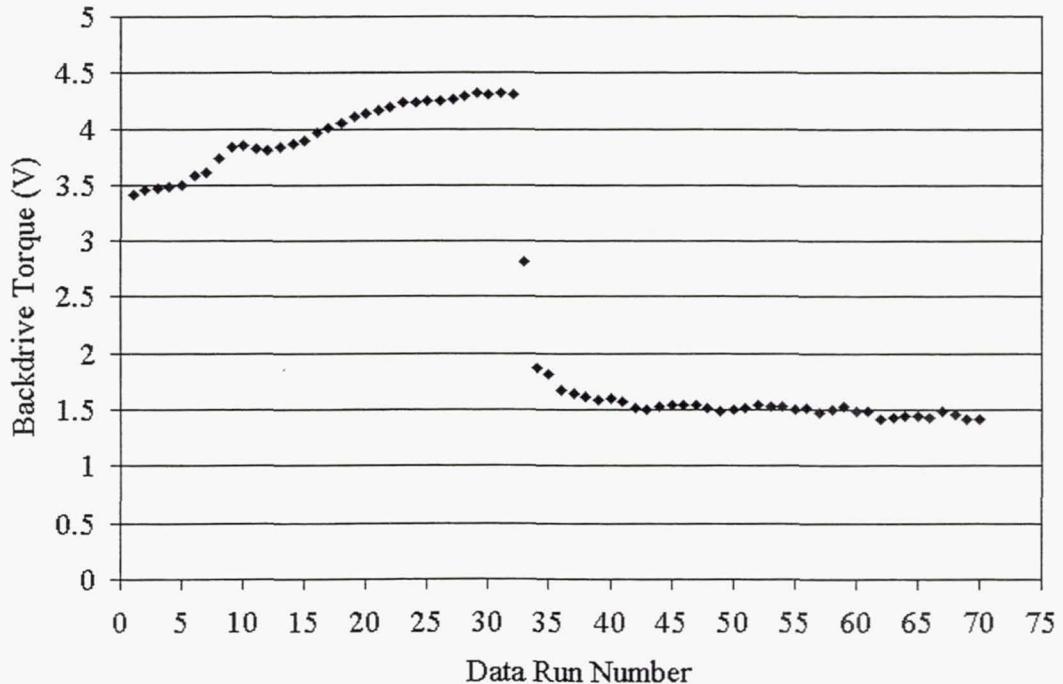
Figure 17: 3-D Roller Experiment Backdrive Torque for Each Data Run

LESSONS LEARNED AND FUTURE PLANS

One set of data that would have been helpful in the analysis is torque collected when nothing was moving. The motor spun the mechanism in the backdrive direction for 2 minutes and 39 seconds before torque data were collected. Before the motor was activated, an entry should have been made in the timeline to collect zero torque data during each data run. In addition, the required delivery date of the experiment was moved up by one month, which prevented an intensive series of ground tests of the mechanism. If the experiment is flown again, a series of ground tests should be run to collect baseline data and to catch potential problems with the operation of the mechanism early enough to make modifications. Because of the problem with the roller coming out of the groove, the inner hub has been redesigned with deeper grooves, which provide more metal above and below the rollers, helping to prevent them from coming out of the inner race. It is the hope of the team that the redesigned 3-D roller mechanism will refly on a future shuttle flight.

Using the technology discussed in this paper, an EVA wrench has been built using 3-D rollers in place of the ratchet. This wrench has been verified in two different simulations of the weightless environment of space—the KC-135A Reduced-Gravity Flying Laboratory and the NASA/Johnson Space Center's Neutral Buoyancy Laboratory (NBL). However, both of these simulations have limitations. Although the KC-135A is a good simulation of the "free-fall" feeling of spaceflight, it is limited in duration to around 25 seconds at a time. The NBL provides a good long-duration simulation of the weightlessness that an astronaut will feel, but because the wrench is not neutrally buoyant, its true performance in a weightless environment cannot be measured. The SEM experiment quantified the roller mechanism's performance when operating for an extended period in a micro-g environment. By using a combination of these results, it is hoped to further prepare the 3-D sprag and roller technology for extensive use in aerospace mechanisms and EVA tools by space-qualifying its geometry.

For a complete summary of the development and evaluation of the roller wrench, see reference 9 or visit http://wrench.ssl.umd.edu

SYMBOLS AND ABBREVIATIONS

2-D	two-dimensional	ISS	International Space Station
3-D	three-dimensional	MEU	module electronics unit
CCW	counterclockwise	NASA	National Aeronautics and Space Administration
CW	clockwise	NBL	Neutral Buoyancy Laboratory
EVA	extravehicular activity	SEM	Shuttle Experiment Module
GAS	Get Away Special	SSL	Space Systems Laboratory
GSFC	Goddard Space Flight Center	STS	Space Transportation System
in-lbf	inch-pound-force		

REFERENCES

1. International Space Station—EVA, Internet WWW page, http://shuttle.nasa.gov/station/eva/index.html
2. Portree, David S. F., and Robert C. Treviño, *Walking to Olympus: An EVA Chronology*, Monographs in Aerospace History Series #7, NASA History Office, October 1997.
3. Vranish, J. M., "Three-Dimensional Roller Locking Sprags," U.S. Patent 5,482,144, January 1996.
4. Avery, Z. W., "Ratchet-Wrench," U.S. Patent 5,009, March 1847.
5. Kutzler, James, W., "Lashless Socket Drive," U.S. Patent 4,457,41, July 1984.
6. Wade, Michael O., and James W. Poland, Jr., "Using a 3-D Sprag in Ratcheting Tools," Goddard Space Flight Center Technologies Review, Case No. GSC 13,802, September 1996.
7. SEM Support Structure System Description, Internet WWW page, http://sspp.gsfc.nasa.gov/sem/experimenter/descriptions/support.html
8. McCaughey, K., SEM: Mission 04 Post Flight EDR #04 Data Processing, Orbital Sciences Corporation Report, December 1998.
9. Roberts, B., "Evaluation of a Three-Dimensional Roller Clutch Reversible Hand Socket Wrench for Extravehicular Activity," Master of Science Thesis, University of Maryland at College Park, August 1999.

THE EFFECTS OF MICROGRAVITY AND EXTREME TEMPERATURES ON MOLD

Wiletha Davis
West Richland Elementary School

PREFACE

To begin this presentation I would like to give you some information regarding our school.

Our district is in a small rural community in Southern Illinois. It is located in the village of Noble, which has a population of 700 people. We are primarily a farming community. The district enrollment is approximately 500 students, K-12. The K-6 building, in which I teach grade 5, has an enrollment of just under 300 students.

The launch day of the STS-95 was a memorable one for our community and school. The entire day was spent with each grade level participating in activities commemorating the occasion. The classrooms and hallways were decorated in space motif. My class launched air propulsion rockets, and grade 6 launched solid fuel model rockets. Parents and the news media visited the school to watch the activities.

As the time of the shuttle launch approached, all 300 students, teachers, administrators, regional superintendent, parents, and the news media were all packed into the cafeteria to watch the launch on a big screen TV. At the moment of lift-off, a huge cheer erupted in the room.

This project was something the students and members of the community will never, ever forget. I can't begin to count the number of people who have stopped me on the street, in stores, or in church to tell me how much they appreciate the positive media coverage this project has brought to our community.

One of my 5th grade girls said it best in an interview with a TV reporter. I quote: "You live in this little town where nothing ever happens. Then someone tells you that something of yours is going up on the space shuttle. There are no words to describe it."

INTRODUCTION

This experiment from beginning to culmination involved two grade levels. It was initially started by the 5th grade class in March 1998. This class, consisting of 40 students, are now 7th graders. It was completed by the 5th graders who are currently 6th graders, consisting of 30 students. The students, with the supervision of the teacher, Wiletha Davis, planned and executed the experiment.

METHOD

This experiment was chosen because we had recently studied different plant forms in science. Its adaptability to involve all students was a major factor in the decision.

EXPERIMENT

We contaminated five slices of bread by rubbing them against different items. We chose bread with no preservatives. We felt preservatives would retard the growth of mold.

Contaminates

We used houseplants to contaminate two slices of bread. These were a Peace Lily and a Pathos vine. A moldy orange was used. One slice was rubbed on the grass in the lawn; another, on the bathroom floor.

The purpose was to determine if different varieties of mold could be grown.

Material

Each contaminated slice of bread was put into a plastic sandwich bag away from the sunlight. Daily inspections were made by the students in order to detect any mold growth. After a few days a few specks of mold were visible. Soon the different colors were detected. The students were amazed at the colors they saw.

We chose potato dextrose agar in slant tubes as a growing medium for the mold. This particular type of agar was chosen because it has a longer shelf life. We planned to isolate each variety in an individual tube.

A sterile metal pick was the device used to isolate the colors onto the agar. The students touched the pick on the mold and then swiped it across the agar. They isolated gray, black, white, and yellow mold. The students checked the progress of the experiment daily. They identified the varieties that were growing as Rhizopus, Penicillin, and Aspergillus.

Problem

The plans were to simply transfer the mold from our tubes to the vials supplied by NASA. However, the necks of our tubes were too small for the agar to slip through. Also, the vials supplied by NASA were smaller than ours. It would not slip out of the tubes. The only thing we could do was to break the necks off our tubes. After we did that, we put the mold in vials. They were mailed to NASA in June.

CULMINATION

Return

Our project was hand delivered back to us by Barbara Justis on December 22, 1998. Ms. Justis explained each part of the container. She very carefully explained each step of unpacking the experiment. The 5th and 6th grade classes helped her to unpack it. They were very appreciative to be a part of this. This enabled them to better visualize how it flew on the shuttle.

Upon investigation we saw there was a significant growth in 1 of the vials, 15 vials had some growth, and nothing was detected in 6 vials. Microscopic investigation revealed no changes or unusual fruiting.

As part of our project we were simultaneously growing more tubes of mold in our classroom. Our purpose was to compare mold cultures with that which grew in space. Upon microscopic comparison, no changes were noted.

Completion

New mold growth was started from cultures that flew in space. That growth was observed and monitored. Microscopic comparisons were made between cultures grown in the classroom and the ones grown from the mold that flew in space. Microscopic investigation revealed longer strands of mold and larger fruiting.

Benefits

This experiment was very beneficial in many ways. The students were taught to think about types of mold and their growth. They learned how to conduct a scientific experiment. They learned how to use a microscope, the importance of microscopic investigation, and the use of scientific tools.

The students learned that to answer one question can also lead to more questions.

What kind of results would one see from a second generation of mold flying in space?

I have a display of our experiment.

GADGET STUDENT EXPERIMENTS ON SEM
A RETROSPECTIVE LOOK AT THE EXPERIMENTS OF
FLIGHTS STS-80, STS-85, AND STS-95

Lynne F. Zielinski
Physics Teacher, Glenbrook North High School

Jonathan Donenberg, Saif Choudhury, Paul Jung, Marc Landeweer
Students, Glenbrook North High School

ABSTRACT

Students from the Glenbrook Aerospace Development Get-away Experiment Team (GADGET) of Glenbrook North High School in Northbrook, Illinois have flown both passive and active SEM experiments aboard shuttle missions STS-80, STS-85, and STS-95. This paper discusses the four active experiments, over sixty-five passive experiments, and their results. Also described are the lessons GADGET has learned through the successes, failures, and real-world problem solving associated with the process of designing, building, analyzing, and disseminating experiment information.

The payloads to be discussed are multi-disciplinary, involving teachers and students in grades 2-12. The disciplines participating in these experiments include science, art, english, broadcasting, applied technology, history, humanities, and computer science. On STS-80, one active Surface Tension I and forty-four passive experiment payloads were flown. The STS-85 mission flew the active experiments, Mosquito, Surface Tension I, Surface Tension II, and Crystal Growth, and twenty-two passive experiments. The Surface Tension I experiment flew for a third time on the STS-95 mission.

Additionally, in an endeavor to bring the promise and excitement of the space program into the classroom, GADGET has developed an outreach program that involves schools in and out of our state. GADGET program strategies used to effectively accomplish this outreach will also be presented.

INTRODUCTION

The Glenbrook Aerospace Development Get-away Experiment Team, known as GADGET, is a student organization native to Glenbrook North High School in Northbrook, Illinois. Founded in 1994, GADGET allows students to design, construct, test, and eventually fly SEM experiments aboard the Space Shuttle. Students are encouraged to create multidisciplinary experiments with gravity as the independent variable. GADGET experiments are comprised of many elements from multiple disciplines including physics, biology, applied technology, education, computer sciences, broadcasting, and the fine arts.

Since its inception, GADGET has flown four active SEM experiments aboard shuttle flights STS-80, STS-85, and STS-95. Through a student outreach program, GADGET has fostered interest and involvement among students from local elementary and middle schools. Through successes and failures, GADGET encourages real-world problem solving in the design, construction, and analysis of experiments.

There are three main sections that make up this paper. The first presents GADGET's active experiments. Here, information is provided about each of the four active experiments. The experiments are sequenced relative to its associated flight. Along with a description of each experiment are the lessons learned, successes, and failures. Two other sections are also presented within this paper, one on the outreach program with its passive experiments and the final section presenting future plans for SEM experiments.

ACTIVE EXPERIMENTS

STS-80

On STS-80, GADGET sent one active experiment, Surface Tension I, and forty-four passive experiment tubes. The active site of the experiment was a rectangular, aluminum box lined with six different types of paper. Six syringes were used to inject paints and dyes into the box through one of its faces. Three of the syringes contained primary color acrylic paints, while the other three contained less viscous secondary colored dyes. Upon activation of the apparatus, a small motor releases a spring pulled plexiglas block, allowing the syringes to introduce the paints and dyes into the aluminum container. The paints, free from gravitational influence, collide with each other and the paper on the inside faces of the box. After deintegration, the box would be opened and the visual patterns on the interior analyzed both scientifically and artistically in order to better understand the behavior of paints and dyes in microgravity.
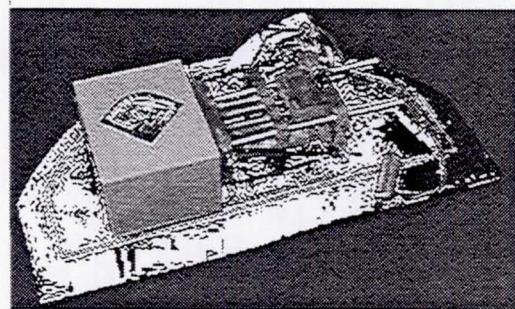
Surface Tension experiment on SEM plate.

Unfortunately, one factor precluded the successful execution of the experiment aboard STS-80. Due to an unforeseen stripping of the plastic gear inside the motor – whose purpose was to release the plexiglas block so injection could occur – the motor seized-up and only a partial firing occurred. Inside the box, some evidence of firing was present but not definitive enough to draw conclusions from.

Through the failure of Surface Tension I, the GADGET experimenters were able to learn a great deal about real-world engineering. Though the malfunction in the apparatus was unexpected, it allowed the experiment designers to reevaluate some of their mechanism's basic components. Specifically, the problem with the plastic gears was easily corrected by replacing the plastic-geared motor with a metal-geared one. The quick analysis of the problem also led to a quick turnaround in the experiment – only forty-eight hours after receiving the experiment back from NASA, GADGET was able to replace the faulty motor and send the apparatus back to fly on STS-85 as a back-up experiment.

STS-85

Four active experiments flew aboard STS-85. These were the Mosquito, Surface Tension II, Crystal Growth, and Surface Tension I experiments. The first three listed flew together on one plate while the fourth was contained on a separate plate.

The Mosquito experiment involved determining the viability of raising mosquito larvae in a microgravity environment. The experiment required the designers to learn not only about the engineering sciences, but also about the biological sciences. The artificial environment was composed of an acrylic tube containing mosquito eggs. During the course of the experiment, water and food were to be injected into the tube. After a given

Mosquito experiment (front), Surface Tension II experiment (rear), and Crystal Growth experiment (small tube laying on top) on SEM plate.

amount of time, a biological preservative/fixative would be used to preserve the mosquitoes for ground-based analysis. This experiment met with difficulty; air bled into the lines connecting the water and fixative syringes through the acrylic tube. This caused the pumps to fail in siphoning the syringes' contents correctly. During the construction of the experiment plate, the project encountered several problems. Originally, an alcohol solution was used to sterilize the acrylic tube. Unfortunately, the alcohol solution dissolved the tube, causing a breakdown

in its structure, creating cracks and splits. The alcohol was replaced with hydrogen peroxide, a substance found to be non-corrosive in small concentrations, as a sterilizing agent. The apparatus was reconstructed, but the group failed to discover a mistake in the electrical wiring before sending in the experiment. Due to time constraints, the mechanism was finished and sent before proper testing could be completed. From these errors, GADGET students learned of the importance of ground-based testing, as well as the importance of comprehensive research.

Surface Tension II, which ran on the same SEM plate as the Mosquito experiment, was designed to create a sculpture in a microgravity environment. The apparatus model was similar to Surface Tension I in that spring-loaded syringes were used to inject a caulk-like material into a small box. Unfortunately, this material hardened prematurely due to the near nine month wait for flight. Consequently, the failure of the experiment to perform was due not to any direct engineering flaw, but instead to the unanticipated hardening of the fluid during the near nine month wait for flight. Long wait periods for SEM experiments is an inherent danger for all experiments and must be considered in detail by experiment designers. From this experiment, an important lesson was learned about timing. The GADGET experimenters working on the Surface Tension II experiment realized that when designing a mechanical apparatus, one must take into consideration not only its primary purpose, but also the environment under which it will operate and the physical and chemical properties of its components.

The Crystal Growth experiment, which ran on the same SEM plate as the Mosquito and Surface Tension II experiments, was designed and built by students at Parma High School in Parma, Ohio as part of GADGET's outreach program. This experiment deals with the growth of lysozyme crystals which are a form of protein found in human tears. The shape of a protein can help scientists ascertain its structure and the structures of the molecules composing it. A protein's shape and its function are inextricably linked. The shapes of proteins are most accurately visualized through crystallography and more perfect crystals lead to more conclusive results. Therefore, the focus of this experiment is to create a perfect crystal. Experiments have shown that crystals grow with fewer flaws in space than on Earth, but the forces of re-entry into the atmosphere are enough to destroy any near-perfect crystal structure. For this reason, Parma students proposed to grow lysozyme crystals in an agarose gel. The gel should support the crystals and maintain their nearly perfect shapes. Agarose buffer gel, containing 50 mg of lysozyme, was separated from a 5 percent buffered solution of sodium chloride ($NaCl$) by a parafilm barrier. A nichrome wire was embedded in the barrier.

During the flight, a problem arose with the experimental procedure. The aqueous sodium chloride proved problematic in the presence of the copper-lined connectors. An oxidation-reduction reaction occurred as a result of the interaction between the copper and the sodium chloride. The reaction interfered with the formation of the crystals. Despite this unanticipated result, the experimental design proved otherwise successful.

The Surface Tension I experiment, modified from its original STS-80 form, flew as a back-up experiment on its own SEM plate for STS-85. This revised version of the experiment included a new motor with metal gears, but was intended to run in exactly the same manner as on the previous flight. Unfortunately, the experiment failed again. Due to prolonged stress over the nearly nine month wait prior to flight, the motor mount bent under the pressure of the springs, which were supposed to drive the syringes. The springs meant for driving the syringes put prolonged stress on the motor mount, which gradually bent over the course of the near nine month time span that the experiment spent waiting for launch. Thus, the motor was not able to properly rotate and inject the paints and dyes into the box. From the failure of Surface Tension I, GADGET learned about the concept of redundancy in engineering and in supporting mounting plates with additional strength.

STS-95

In hopes of rectifying previous errors and malfunctions, the Surface Tension I experiment flew for a third time aboard STS-95 as a back-up experiment. In order to ensure a successful execution of the experiment, a significant number of test runs were performed and modifications were made from the original STS-80 apparatus. A steel support was added to hold the motor mount in an effort to combat the force of the high-tension springs that had caused the earlier malfunction. Sealing caps inside the box were replaced with grease plugs to hole the paints in their syringes. Due in no small measure to these changes in design, the Surface Tension I experiment operated as designed. The Surface Tension I experiment was truly a multidisciplinary endeavor. The Glenbrook North art classes made paintings of predicted patterns. Applied technology students built the apparatus. Broadcasting

students documented the process and created video programs. The physics classes made scientific predictions of how the paints and dyes would interact in space. The members of the project team themselves learned a great deal about engineering an experiment model from conception to post-flight analysis.

GADGET COMMUNITY OUTREACH

Another aspect of GADGET is its community outreach program. Through the outreach program, GADGET is able to accomplish many goals. The outreach program offers opportunities to high school and grade school students to create their own passive experiments. GADGET students conduct presentations to teachers and students about the program, experimental results, and describing the passive experiment process. Subsequently, GADGET members work with teachers and students on designing viable scientific experiments for the passive tube. Working with passives also require GADGET members to train teachers in incorporating the passive experiments into their science curricula.

Presentations generally include topics concerning the passive experimental process, such as integration, deintegration, and data analysis. Other important scientific topics are explained, such as the scientific method and the significance of variables. The experiments themselves are not complicated, but the research and analytical processes are valuable tools in science education and instruction.

The presentations are followed by a brainstorming session, in which the students are given a chance to propose possible future experiments. Of the proposals, the teachers and students pick the most promising experiment ideas. The teachers will base a short-term curriculum around the proposals, while the students work on developing the experiments using the scientific method. Though passive tubes have their limitations, the program is valuable insofar as it allows young students to conduct their own research. Grade school students are encouraged to be both creative and realistic with their designs. Though for the students, the process focuses on obtaining results, the goals of the teachers are more complex. The teachers are most interested in how students craft their hypotheses; the process spotlights how well the students understand and synthesize information taught to them regarding variables and conditions that their experiments will experience in space.

The STS-80 popcorn experiment exemplifies the general passive experiment procedure undergone by grade school students. The students from Seth Paine Elementary School participating in the experiment were required to first examine the general differences between space and Earth. They then hypothesized how those changes would effect the popcorn seeds. The result of their research is outlined in Table 1 below. The subsequent questions needed to form hypotheses are listed in Table 2. Though result of their work appears simple, it displays evidence of sound scientific reasoning on the part of 2nd grade students. Thus, even though there were no discernable "results" to speak of, the effects of the outreach program can still be considered successful in that they clearly teach the scientific method to grade school students.

Table 1 – Results of environmental research from Seth Paine Elementary School students on the passive popcorn experiment.

	EARTH AND SPACE COMPARISIONS FOR POPCORN	
	On Earth	**In Space**
Temperature	5 to 50 degrees Celsius	Fluctuates wildly (-160 to 100 degrees Celsius). During Launch – 5 to 65 degrees Celsius
Gravity	Average gravity is 1 g	Microgravity means the gravitational effects are near zero in space. During launch its around 2 to 3 g's
Radiation	Minimal	Effects of cosmic rays, gamma rays, x-rays and ultraviolet rays are much greater in space
Sound	Low decibel level	High decibel level during launch
Vibration	Little perceptible vibrations	Strong vibration during launch

Table 2 – Questions used to develop hypotheses from Seth Paine Elementary School students for passive popcorn experiment.

Hypotheses For The Popcorn Experiment	
Primary Hypotheses	**Secondary Hypotheses**
Will the kernels' color be different?	Will the popcorn smell different?
Will the popcorn taste differently?	Will the kernels pop bigger? Smaller?
Will the kernels be shaped differently?	Will the number of kernels popped be greater, less, or equal?
	Will they grow differently if planted?
	Will the space plant be healthier?
	Will it pop at a different temperature?
	Will it pop at a different rate?
	Will the seeds germinate?
	Will germination time change?

Elementary school students are generally concrete thinkers; they do not understand what they cannot directly sense. Abstract concepts, such as space and time, are more difficult to grasp. The passive experiments combine concrete and abstract elements in order to create a science curriculum of greater depth. Of significance to the teachers is the manner in which students learn more about the abstract components of science. Clearly, the GADGET outreach program is successful in guiding students through the basics of the scientific method, holding their attention with the abstract idea of space, all the while teaching them to perform like true scientists.

PASSIVE EXPERIMENTS

Through its outreach program, GADGET has allowed elementary, junior high, and high school students to design their own inactive experiments to fly on an SEM plate. A number of these small tubes can be placed on one SEM plate, making these passive experiments an ideal way to allow multiple groups of students to get involved with the SEM program.

STS-80

The primary purpose of involving elementary school students in the design and production of passive experiments is to foster interest in the scientific process and the space program without becoming involved in the complications of designing an active experiment. A further purpose is to give high school students the opportunity to use their scientific knowledge, work with younger students, create and present information, and develop scientific techniques. Schools with projects on STS-80 included Seth Paine Elementary School, Lake Zurich, Illinois; Parma High School, Parma, Ohio; and Glenbrook North High School, Northbrook, Illinois. The passive experiments aboard STS-80 are listed in Table 3.
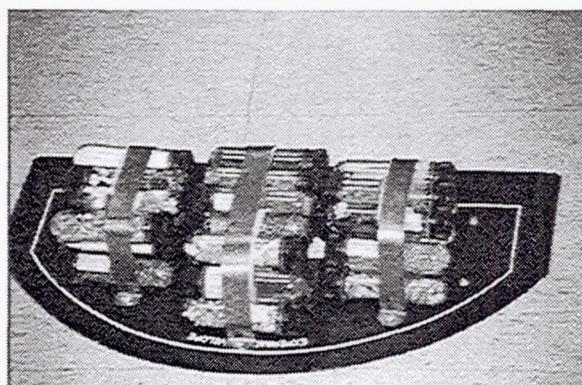
Passive experiment configuration on SEM plate.

Table 3 – Passive experiments flown on STS-80 along with their results.

Tube Contents	Results	Program
Gak^{tm}*	Material coated sides of tube – When opened the material peeled from the wall and formed a lump	Seth Paine Elementary School
Haploid yeast strain	Viability reduced	Parma High School
Vegetable seeds	Plants grew taller than ground controls yielding larger fruit Germinated plants showed no differences in growth	Seth Paine Elementary School
Tree seeds	Did not germinate	Glenbrook North High School
Hair, feathers, fur	Some color change in blonde and gray hair samples occurred	Glenbrook North High School
Layered, colored sand	Layers mixed together	Seth Paine Elementary School
Brine shrimp	No change detected	Seth Paine Elementary School
Magnet in salt water	No change detected	Glenbrook North High School
Wire coil and iron filings	Iron filings moved to the outer layers of the tube	Glenbrook North High School
Colored Modeling clay – 2 spheres of same size	No change detected	Seth Paine Elementary School
Crayon markings and paper	Flecks of colored wax dots on paper	Seth Paine Elementary School
Printing toner	No change detected	Seth Paine Elementary School
Mosquito eggs	Some eggs hatched prematurely – no eggs survived due to dehydration	Glenbrook North High School
Popcorn	No change detected	Seth Paine Elementary School Glenbrook North High School
Grass seeds	Grew fastener than ground controls	Seth Paine Elementary School
Flower seeds	Grew faster than ground controls	Seth Paine Elementary School
Film with paperclip	Developed film produced image of paperclip due to radiation	Glenbrook North High School

- Gak^{TM} is a registered a trademark of Nickelodeon

Some of the STS-80 passive experiments are noteworthy. Second graders from Seth Paine Elementary School sent a tube filled with layered, colored sand. The tube came back with the colors thoroughly mixed due to the vibration of launch. Other tubes contained various vegetable seeds that were planted outside and tended by the students in a garden alongside Earth-based control seeds in a comparative "space-garden." The seeds from the passive tube grew plants of greater yield than those sprouted from the Earth-based control seeds. The Seth Paine students believed that exposure to the extremely cold temperatures of space, referred to as the "long winter" effect, allowed the seeds in the tube to emerge from the flight better preserved than their ground-based counterparts. Fifth graders from Seth Paine placed about half of a passive tube with Gak ^{TM}. Upon return, it was noticed that the material had completely lined the interior of the passive tube. When opened, the material immediately pealed from the tube walls and reformed into a lump. The fifth grade students have no explanation for this, but they have a lot of ideas.

The Parma High School students designed a more extensive and complex passive experiment. In this experiment, Parma students sent yeast in a passive tube in an attempt to examine the effects of microgravity on the viability of specific strains of the bacteria. Upon return, the Parma students observed a reduced viability of the haploid yeast strain. Some yeast growth in the tube was also observed, suggesting that yeast can grow even in extreme conditions.

GADGET was able to send twenty-two more passive tubes aboard STS-85. The schools involved from Northbrook, Illinois were Glenbrook North High School, Northbrook Junior High School, and Wood Oaks Junior High School. Additionally, experiments from Seth Paine Elementary School in Lake Zurich, Illinois, and Appleton High School in Appleton, Wisconsin were flown. The experiments and their results are outlined in Table 4 below.

Table 4 – Passive experiments flown on STS-85 along with their results.

Tube Contents	Results	Program
Popcorn	No change when popped	Appleton High School, Glenbrook North High School
Brine shrimp	No change detected	Seth Paine Elementary School
Vegetable seeds	Space plants grew taller, faster, and produced larger fruit compared with ground controls	Northbrook Junior High School, Seth Paine Elementary School, Appleton High School
Flower and wild flower seeds	Accelerated Growth	Glenbrook North High School, Seth Paine Elementary School
Saltwater	No change detected	Seth Paine Elementary School
Film	Film was exposed due to radiation	Seth Paine Elementary School
Jelly beans	No change detected	Seth Paine Elementary School
Tree seeds	No apparent change in seedlings – seedlings did not survive	Glenbrook North High School, Seth Paine Elementary School
Human Hair	Darkening of blonde hair	Glenbrook North High School
Yeast	50% of yeast was viable	Seth Paine Elementary School
Water bears	No change detected	Glenbrook North High School
Lichen	No change detected	Glenbrook North High School
Pond water	No change detected	Seth Paine Elementary School
Rain water	No change detected	Seth Pane Elementary School
Mosquito eggs	Pre-hatching occurred some eggs were viable and grew to adult	Glenbrook North High School
Baking soda	No change detected	Seth Paine Elementary School
Balloon	No change detected	Seth Paine Elementary School
Various adhesive tapes on paper	No change detected	Seth Paine Elementary School
Light bulb	No change detected	Seth Paine Elementary School
Different kinds of ink on paper	No change detected	Seth Paine Elementary School
Gravel	No change detected	Seth Paine Elementary School
Foam	No change detected	Wood Oaks Junior High School
Wisconsin Fast plant	Accelerated Growth	Wood Oaks Junior High School

One particular passive experiment of note was the passive mosquito experiment. The mosquito eggs unexpectedly suffered from "pre-hatching." Mosquito eggs are supposed to hatch when liquid water is available; pre-hatching is the condition when the eggs mistake the presence of humidity within the tube with actual liquid water and hatch prematurely. Subsequently, most of the mosquitoes hatched and died during the flight. A small percentage of the eggs hatched and grew to the adult phase.

FUTURE PLANS

GADGET is in the process of designing a number of new and innovative SEM experiments, as well as revising old experiments, in order to continue its success in student-oriented microgravity research and

experimentation. These experiments include Aeroponics, 3-D Resonance, Tornado, Plant Root Growth, and Environmental Studies along with the revised versions of the Surface Tension and Mosquito experiments.

Currently, Aeroponics is the only experiment near readiness for a flight. Aeroponics is a technique used to grow plants without the use of soil. It is similar to hydroponics in that a nutrient solution is used to grow plants. It is different in that the solution is sprayed onto the plant's root system rather than immersing the roots in the solution as the hydroponic technique does. Aeroponics may be a solution to the food production problem of long-duration space missions. As stays in space get longer, the feasibility of sending supply ships becomes questionable. Astronauts will need a continuous supply of food. An aeroponic farming method may be the solution. Unfortunately, the inherent limitations of space habitats make conventional farming practices impractical. The water supply is limited and microgravity makes fluids behave differently. Aeroponics sidesteps many of these limitations by using minimal quantities of water, no soil, and less space than conventional agriculture. Aeroponics is proven to grow plants with less waste, utilizing fewer resources. In the GADGET experiment, the seeds are held in place by artificial supports instead of soil. Germination occurs when a nutrient solution is sprayed onto six corn seeds in the growth chamber. Humidity and sequenced spraying will encourage plant growth throughout the mission. At mission close, a fixative will be sprayed into the chamber to preserve the plants for study.

Another project slated for a future flight is the Three-Dimensional Resonance project. The project intends to observe the effects of harmonic resonant frequencies on fluids in a microgravity environment. Substances of all types often vibrate when stimulated at their resonant frequency. Many non-solid substances have been observed to form symmetric shapes while resonating. On Earth, however, the effects of gravity can dampen or overcome the delicate effects of the resonance. This experiment will melt a petroleum-based substance encapsulated in a same density sodium silicate solution in microgravity. Sound waves at predetermined resonance frequencies will be applied to the fluids and allowed to cool while under the effects of the sound waves. Upon return, the solid material's shape will be analyzed to determine the substance's physical arrangement and how it resonated in a gravity-free environment.

The Tornado experiment is designed to look at the effects of microgravity on the vortex produced by spinning water. It is believed that vortices created without gravity will be different from those created on Earth. This is due to fluid viscosity differences associated with the conservation of angular momentum and Newton's law of inertia.

The Plant Root Growth experiment is designed to look at how magnetic fields may effect the direction of the growth of plant roots. This experiment will grow two sets of seeds. One set will be grown in a magnetic field while the other will act as a control.

The Environmental Studies experiment will look at measuring the temperature, accelerations, magnetic fields, and humidity of the environment that SEM experiments experience. This experiment will measure these quantities and store the information on a computer hard drive for analysis upon return to Earth.

Ongoing experiments will also be flown in the future, with modifications. These include Surface Tension I and the Mosquito experiments. Surface Tension I will most likely be extended so that data can be collected over a wide range of fluid viscosities and paper textures. The Mosquito experiment will run in a similar fashion to its original format, except that peroxide will be replaced by a liquid chlorine solution. This change, along with other structural modifications will lead to a successful execution of the experiment.

CONCLUSION

The Glenbrook Aerospace Development Get-away Experiment Team has been and continues to be successful in its goal to foster and facilitate interest in space, engineering, science, art, and journalism through problem solving and the creativity of imagination. The value of being involved in an educational program like GADGET is not strictly limited to science reasoning, however. Most of the organization's members have academic focuses beyond science. Project ideas often arise under non-scientific circumstances. For example, the

Surface Tension experiments were conceived to combine the traditionally separate fields of art with physics. Similarly, the 3-D Resonance experiment was prompted by the project members' study of acoustics in music.

GADGET strives to move beyond the classroom by allowing its members to gain hands-on experience in real-life scientific problem solving, writing, and public speaking. The projects often lead the members to an interaction with scientists and professional organizations as well as interactions with people outside of science. For instance, GADGET members associated with the Aeroponics experiment are mentored by scientists at Aeroponics International in Colorado. The Mosquito group is mentored by Dr. Robert Novak from the University of Illinois. The Surface Tension students work with a spectrum of people including artists, art teachers, and applied technology people. The 3-D Resonance experimenters work with LavaWorld, Inc., the manufacturers of the LavaLite lamp.

GADGET has undertaken a big responsibility by using high school students as the primary engineers and technicians in developing its experiments. Working through and developing the experiments is a process worthwhile to the students' education whether they fly or not and whether the experiments are successful or not. While GADGET will help prepare students for careers in science, engineering, business, and space exploration, it will also provide them with skills necessary in all walks of life. As consultants, GADGET students act as mentors to grade school students, encouraging them to participate in microgravity science through its outreach program. This program has achieved its two-fold goal of carrying out passive experiments and expanding the scientific horizons of grade school students. GADGET's success in both passive and active experiments, as well as with its community outreach program, are all products of the tremendous work and dedication of its member students. In alignment of these achievements, the GADGET program motto holds true and steadfast: "The Sky is *NOT* the Limit!"

THE GROWTH AND DEVELOPMENT OF MOSQUITOES IN A MICROGRAVITY ENVIRONMENT

Lynne F. Zielinski
Physics Teacher, Glenbrook North High School

Kevin Haworth, Jason Georgacakis and Kurt Landeweer
Students, Glenbrook North High School

ABSTRACT

The mosquito growth and development experiment is a cooperative effort spearheaded by four secondary students from the Glenbrook Aerospace Development Get-away Experiment Team (GADGET) at Glenbrook North High School in Northbrook, Illinois. The experiment has now existed for three and a half years. To date, the experiment has been flown, in both passive and active forms in SEMs aboard STS-80 and STS-85. The experiment has three phases. Each phase has the purpose of determining the effect of microgravity on the life cycle of mosquitoes. The initial goals, beyond retrieval of scientific data, are to teach scientific method and scientific process while peaking the interest of secondary students in various scientific fields. This paper presents an overview of this experiment, the results after the first two flights, and lessons learned.

The experiment will use three phases to determine which characteristics of insect development are effected. Phase I is a passive experiment whose purpose is to determine the effects that microgravity may have upon mosquito eggs. Phase I was flown aboard STS-80 and STS-85. Phase II is an active experiment which focuses on the actual biological processes of the mosquito egg, larva, and pupa. Phase II flew on STS-85. Phase III of the experiment requires an extended duration of time in a microgravity environment. For that reason, it would need to take place aboard the International Space Station or a minimum fourteen day shuttle mission. This final phase of the experiment is currently being developed.

INTRODUCTION

Insects are an essential part of any ecosystem. To ensure that ecosystems can be created in microgravity or low-gravity environments, like those present on small moons, tests need to be run. This experiment will determine how the growth and development of insects, represented by mosquitoes, will be effected. Mosquitoes represent an excellent insect for testing these effects. They go through an aquatic and aerial phase which is representative of many types of insects. More importantly however, they prove to be one of the hardiest invertebrates and can remain dormant for several months in the egg stage – a necessary condition for a SEM experiment due to the four to six month integration period prior to a flight.

All phases of this experiment lend valuable information to medical entomologists working on abating mosquitoes and to biologists working on a sustained environment in areas that experience less than one g-force. The experiment in all phases emphasizes the idea of process rather than product. The experiment's successes and failures helped in redesigning the mosquito experiment to make it simpler and more efficient. They also provide valuable ideas for changes which can be applied to future SEM experiment configurations and construction. Multiple educational lessons were also learned and will be discussed in this paper.

The mosquito life cycle has four main phases: egg, larval, pupal, and adult. In the initial stage, the adult female lays eggs in a moist environment that will eventually become flooded with water. Once the area becomes flooded and the eggs are submerged, they hatch into larvae. There are four subcategories of the larval stage: first

instar, second instar, third instar, and fourth instar. A molting represents each instar. Molting occurs when the larvae have grown too big for their exoskeleton. The growth is due to the ingestion of food. Most types of mosquito larvae can survive months with no food. When this does happen, the larvae cease development and remains at its current stage in the life cycle. In the controlled environment, the larvae will eat ground fish food. After the fourth instar, the larvae enter the pupal stage where a complete metamorphosis occurs. After the metamorphosis is complete, adult mosquitoes will hatch from the pupal casing and emerge as adult flies. From here, male and female mosquitoes will mate. The females will lay eggs in a moist area renewing the cycle.

Certain problems arise in the life cycle of the mosquito that put constraints on how a microgravity experiment can be run. While the mosquitoes are still eggs, they are highly sensitive to humidity levels. Each different species of mosquito hatches at different humidity levels. The three species used in this experiment are Aedes triseriatus, Aedes albopictus, and Aedes aegypti bora bora. Aedes triseriatus is the hardiest. All of them will hatch before they are submerged in water if the humidity is high enough. When this occurs, it is called pre-hatching. The eggs are no longer viable and the larvae die almost immediately. Another problem faced by the eggs is temperature. Once temperatures are greater than 50 degrees Celsius or less than –10 degrees Celsius the eggs are no longer viable.

PHASE I

Flights

Phase I flew aboard STS-80 and STS-85. The experiment tubes were part of a passive GADGET SEM plate on each flight.

Procedure

Phase I of the experiment is passive. It involves placing mosquito eggs in a space-safe test tube along with but slightly separated from a humidity control system. On STS-80, the humidity control system was a moistened piece of paper towel 2 by 6 cm (0.79 by 2.36 inches). Because of the dryness of the paper when it returned, a piece of cellu-cotton 8.89 by 8.89 cm (3.5 by 3.5 inches) replaced the paper towel on STS-85. The mosquito eggs which were laid on germination paper were placed into the test tube and were sealed by NASA with a sealant around the lip of the test tube cap. The amount of saturated cellu-cotton used was based off of the standard level employed by entomologists for mosquito colonies. A control with identical specifications was made. For the STS-85 flight, the germination paper and eggs were dipped in rubbing alcohol and then air dried to prevent fungal growth.

Testing

No testing was done on the passive experiments for either of the two flights. On future flights testing will be done for humidity levels and fungal growth.

Materials

1. Sterile space-safe test tubes (provided by NASA).
2. Germination paper with mosquito eggs. There should be 250 or more eggs per test tube.
3. A. Paper Towel: 2 by 6 cm (0.79 by 2.36 inches). Used in STS-80 experiment.
   B. Cellu-Cotton: 8.89 by 8.89 cm (3.5 by 3.5 inches). Used in STS-85 experiment.
   C. Filter paper cut into 1 by 4 cm and 1 by 2 cm pieces. Because of current testing, the exact amount to be used on the next flight is unknown.
4. Sealant. (Provided by NASA)
5. Isopropyl alcohol.
6. Deionized water.

Hypotheses

It is not believed that the eggs will be effected by the space environment. As cited earlier, if the temperature exceeds the range of –10 to 50 degrees Celsius the eggs will be adversely affected. Temperature is the predicted principle deterrent of viability. The other important factor in determining the eggs viability is radiation. On the SEM, it is unknown how much radiation the eggs will receive and its effects.

Results and Analysis

On both of the flights, the humidity was maintained initially. However, when the STS-80 experiment returned, the test tube contained no humidity. This significantly increases the difficulty of rearing the eggs. It is known that the moisture was present for some time because pre-hatching occurred. An accurate method of counting and rearing the surviving mosquito eggs was not done scientifically and no mosquitoes survived.

The eggs returned from the STS-85 experiment were still moist. Upon return, the eggs were divided into two groups. One was reared at Glenbrook North High School and the other at the Medical Entomology Laboratory at the University of Illinois by Dr. Robert Novak. The results from the Glenbrook group were not encouraging. The rate of viability (the eggs that could possibly be hatched) was 43.24 percent (48 eggs out of 111 were still intact). The number of eggs that did hatch from all the eggs was 9 out of 48 potentially viable eggs. These figures were higher compared to the control kept at Glenbrook North High School. The Glenbrook Control had 33.51 percent viable eggs. Both of these numbers are much lower than the control kept at the Medical Entomology Laboratory. The Medical Entomology Laboratory Control had nearly 95 percent of the eggs viable, of which, 97.37 percent hatched. This data implies that eggs can be reared after being in the microgravity environment. If the design is reworked, the survival rate of the eggs in the microgravity environment could be near 90 percent.

Since the Glenbrook Control and the Space Group were similar in number of eggs viable and they were packed identically, it can be induced that if the method of packing was upgraded to Medical Entomology Laboratory standards, the viability and hatching percentages should come near the Medical Entomology Laboratory results. However, it should be noted that the Medical Entomology Laboratory eggs were placed in a nutrient broth to help increase the hatching rate. Working in conjunction with the Medical Entomology Laboratory, it was hypothesized that the viability rate of the eggs would be high enough to warrant Phase II.

Lessons Learned

1. When the STS-80 test tube was received after deintegration, it was noticed that no moisture was present. The amount of water present upon the return of the STS-85 tube was difficult to measure. Therefore on future flights, methods will need to be adopted to address this issue of humidity control. Current humidity tests involve placing eggs in the flight tubes and using different amounts of saturated filter paper with the eggs. Filter paper is being used instead of cellu-cotton because of the greater ease in measuring how much water is actually in the test tube. The filter paper will be cut 1 cm by 4 cm and 1 cm by 2 cm. Each test will examine how many completely saturated pieces of paper can be used before condensation is found on the sides of the test tube or pre-hatching occurs. To prevent moisture leaks, a sealant will be applied around the lip of the test tube and cap.

2. During integration, the warmth of the environment and the moisture in the tube creates a breeding ground for mold and fungus. To prevent this, the germination paper and eggs were dipped in alcohol for the STS-85 flight. This will also be done with materials used on future flights.

3. As mentioned earlier, filter paper is being used because the amount of water can be measured more accurately as can the amount of paper available to absorb condensation. The need to measure all the aspects of the experiment more accurately is a necessity. This includes the count of viable versus non-viable eggs.

51

4.   The students who led the experiment neglected to keep accurate documentation of their work. This has led to lapses in data in certain areas. Beginning with the testing for the next flight, a highly detailed documentation process has been implemented.

PHASE II

Flights

Phase II flew aboard STS-85 on the GADGET SEM plate.

Procedure

Phase II is an active experiment. In this experiment, the mosquito eggs are housed in a chamber which is 3.18 cm (1.25 inch) in diameter and 15.2 cm   (6 inch) in length. One end of the growth chamber is cut at a 45° angle and capped with plexiglas to help concentrate water in one area of the growth chamber. The other end of the growth chamber is capped with an expandable rubber plug. In a manner similar to the Phase I experiment, the humidity of the growth chamber needed to be maintained and moistened cellu-cotton was used. Once the SEM plate is activated, heaters turn on to warm up the chamber and the water that will be used to flood the chamber. The flooding will hatch the mosquito eggs.

Approximately one hour after the heaters are turned on, the water is injected from a 60 mL syringe by using a model airplane fuel pump. Flexible silicone tubing is used to connect the syringe and pump. From the pump, tubing runs to one of the four inlet/outlet valves on the growth chamber. The inlet valves are placed in holes drilled into the tube and fixed in place with silicone sealant. To prevent an over pressurization of the chamber, there is another valve with tubing going to the back side of the syringe. In order to prevent the water from spilling out the back end of the syringe, the plunger is cut so that it does not protrude out of the back of the syringe. A rubber plug is inserted to retain any water that may pass out of an outlet valve.
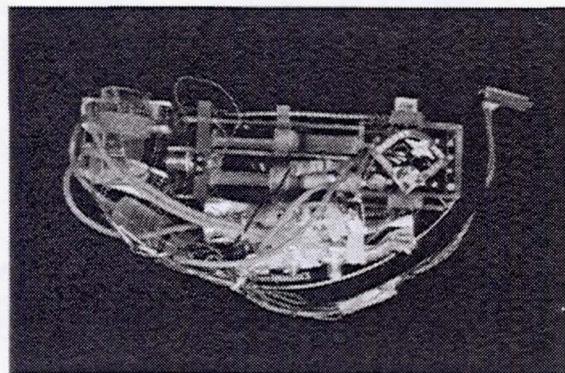
The Mosquito experiment is located in the curved part of the SEM plate.

The water fills approximately one quarter of the chamber. The SEM 60 watt-hour power restriction forces the power to the heater to be switched off and on over the period of ten days. To prevent the tube from becoming overheated, the heater is connected to a relay circuit with a thermoster. The relay is designed to go on when the temperature drops below 23.89° C (75 ° F). This promotes the most rapid growth and development of the mosquitoes. The circuit was built at Glenbrook North High School by students. To help retain the heat, the growth chamber is cloaked in a space blanket which also helps to avert the SEM plate in acting as a heat synch. Once the eggs hatch, the larvae are able to eat rabbit chow pellets. The eggs and pellets are kept in place inside the chamber with non-toxic double-sided tape. Once submerged, the rabbit chow pellets breakdown into small enough pieces for the larvae to consume.

Once the mission has come to a close, the chamber is flooded with a fixative. This ceases the development of the mosquitoes in its stage of development and preserves them for later Earth-based studies.

Testing

This experiment was tested for its two main systems prior to the STS-85 launch. One set of tests was run to determine if the heaters would prevent the water from freezing. To perform this test, a heater was placed around the growth chamber, which was two-thirds filled with water. The entire unit was placed in a freezer overnight and the heater was given electricity. After the first test, the water was frozen. The heater and relay were then adjusted and the test rerun. After twelve hours in the freezer, the water was not frozen. The heater had, in

fact, kept the water warm. Due to the time constraints in building the experiment, longer duration freeze tests were not performed.

Another set of tests was run on the injection system. In this test, the amount of force the pump could produce on the water was performed. The idea was to determine if the pump could pull the water out of the syringe. Early testing proved that alone, the pump did not produce enough force to move the plunger of the syringe. After multiple tries at adjusting the injection system, including giving the plunger an initial push, it was found that the best method employed putting lubricant on the plunger. The reduced friction was enough to allow the plunger to force the water into the chamber after the pump was turned on.

Materials

1. Growth Chamber.
   A. 3.81 cm (1.5 inch) diameter clear plexiglas tube 15.24 cm (6 inches) long.
   B. Clear plexiglas sheet 5.08 by 6.35 cm (2 by 2.5 inches).
2. Expandable rubber plug 3.18 to 3.5 cm.
3. Inlet valves (6).
4. Silicone Sealant.
5. Flexible Silicone Tubing.
6. Model Airplane Fuel Pumps (2).
7. 60 mL Syringe.
8. Lubricant.
9. Rubber Stopper.
10. Heater with circuit to keep temperature at $23.89^{\uparrow}$ C.
11. Space Blanket (NASA provided).
12. Mosquito Eggs.
13. Rabbit Chow Pellets.
14. Water
15. Fixative

Hypothesis

There are many areas of concern in the Phase II experiment. Beginning with the start of the mosquito life-cycle, it is predicted that the eggs will hatch. This is based off of the results of Phase I. From here it is predicted that if the mosquitoes cannot locate food and air they will not progress beyond the first or second instar. It is hypothesized that the larvae will have a difficult time locating food and air because it is known on Earth that the larvae use gravity as a directional guide. In the microgravity environment, the directional guide disappears and there is no specific place where the food or air will be located. Another hypothesis predicts that if the larvae are able to locate food and air and progress to the pupal stage, then the imaginal clusters will not be in their correct position for metamorphosis. The imaginal clusters migrate through the mosquito's body during the larval and pupal stage. It is believed that the migration will not occur correctly in the absence of gravity. With the incorrect positioning of the clusters, it is believed that the mosquito will abort its development. If it is not aborted, then the adult mosquito will exhibit severe mutations.

Results and Analysis

Due to unforeseen mechanical errors, the water did not inject into the chamber at the start of the experiment. This prevented the eggs from hatching and developing. This and other faults are discussed in the Lessons Learned section below.

Lessons Learned

1. The design of the water injection system used was poor. It has several weaknesses. The first was the power of the pump. As mentioned earlier, due to time constraints, the testing and adjusting of the pump so that it could move the plunger and water did not permit the study of what would happen to

the system after several weeks or longer of waiting prior to activation. What apparently happened on the flight was the bleeding of air into the system. Air pockets were observed in many portions of the tubing. These pockets caused the pump to lose a great deal of efficiency and thus, its ability to move the water. Another factor which could have caused the failure was a washing out of the lubricant. It is possible for the lubricant to be diluted or eroded, thus making it impossible for the pump to move the water – even at full strength.

2. A new system has been designed to ensure injection for a future flight. The system places a solenoid where the pump was in the original injection system. A plunger is still used, but instead of a rubber plug, a spring is inserted into the back of the syringe and a metal covering is placed over the back and sealed to prevent water leakage. As water enters the syringe, the spring is compressed. Once the syringe is full, the solenoid is closed. This system has been tested and has plenty of force to move the water. It has also been left for a week and a half without leaking. The bleeding of air into the tubing will not be a factor in this system. This same method of fluid injection can be used for the fixative.

3. As mentioned in Phase I, the prevention of fungus is a problem. It turned into a large problem for the Phase II experiment. When the experiment was returned after deintegration, large pieces of fungus could be seen easily. A 100 percent effective means of eliminating the fungus is still being sought. On STS-85, the germination paper was put in isopropyl alcohol and then dried. The same was done with the cellu-cotton and rabbit chow pellets. To sterilize the syringe, tubing, pumps, and chamber, alcohol was passed through the system. An immediate problem arose from this. When alcohol comes into contact with plexiglas, it causes stress fractures. This destroyed the initial growth chamber and brings up the point of creating a back-up experiment beside the control and space experiment in case of such an accident. After recreating the chamber with new materials, hydrogen peroxide was used to flush out the chamber followed by deionized water. On future flights, a light chlorine solution will replace the hydrogen peroxide as a sterilizer.

4. In order to maintain the correct temperature, an electrical circuit needed to be created. The circuit was created by a student and teacher at Glenbrook North High School. The relay circuit built was fairly complex. As such, there were many places where a small error could be made that would short the circuit. To help prevent this, the circuit was turned on at room temperature and then placed in a refrigerator. From this point it was witnessed that the circuit did switch on and off properly. However, when the experiment returned, the circuitry was one of the items analyzed. It appeared after examination that the circuit may have had some faulty points. The circuit was not post-tested however. For future flights, the circuit will be replaced with a heater/circuit that is professionally manufactured with preset specifications. This will eliminate all need to attempt to create a complex circuit.

5. One of the largest constraints on any active SEM experiment is the 60 watt-hour power limit. To cope with this, the SEM timeline was programmed to turn the power to the heater on and off. The main problem with this was that while the heater was off, the temperature of the SEM plate could drop, and would not be detected by the thermister. Or, the temperature could rise when the heater is given power. If this type of event occurred, the heater would never be used. A new method of heating has yet to be determined. The best ideas use insulation, such as a space blanket, to prevent the temperature fluctuations.

6. After running ground tests growing the mosquitoes in the growth chamber, it was determined that a larger amount of water was needed than originally planned for. To solve this problem for future flights, a new design using two syringes filled with water and a T-valve will be used to connect them both to the solenoid.

7. The final change that needs to be made has already been mentioned but needs to be said again. A better system of documentation needs to be maintained. Once the experiment becomes active, there

is much more reason to document how it will be done. There are many more parts, systems, and data to remember.

Phase III

Flights

It is hoped that phase III will someday fly on a long duration mission like that of the International Space Station or a fourteen day or longer Shuttle mission.

Procedure

The final phase of the experiment is still very much on the drafting board. Initially, it operates like the Phase II experiment. However, a wire screen is inserted in the growth chamber which leads to a chamber which allows the adults to fly freely in. The screen will keep the water from entering into this chamber. When the adults emerge from the growth chamber, they can fit though the screen to remove themselves from the water. Connected to this part of the chamber is a tube lined with fly paper. The fly paper will catch any mosquitoes who cannot control flight and bounce into the tubing. On the opposite end of the tubing will be an attractant chamber with pheromones and imitation nectar. These substances will attract the adults, tempting them to fly across the tube. The specifics of the rest of the experiment have yet to be worked out.

Testing

No testing has been done yet.

Materials

1. Same parts as used in Phase II.
2. Imitation Nectar.
3. Pheromones
4. Fly Paper
5. Screening

Hypotheses

If the mosquitoes are able to develop into adults, it is hypothesized that they can sustain controlled flight. This is believed to be true because just as astronauts may have difficulty getting their bearings in a microgravity environment, they eventually adjust. It is believed that the mosquitoes will also adjust.

CONCLUSION

There are many intangible, immeasurable lessons learned beyond the scientific elements and facts associated with the creation of an SEM experiment. Students have greatly improved their communication, presentation, and technical skills. The communication and presentation skills learned include both writing and public speaking. The students learned how to write sophisticated science papers. Technical writing skills have been enriched to the point where students can convert the complex language of science and the technical aspects of their experiment into a simpler, every-day language understood by anyone. As part of the outreach program, students had to present their experiments to others. This places the student in the position of being able to clearly define, express, and defend their thoughts and ideas.

Beyond the communication skills, the students learned how to deal with technical problems. This enhanced the normally acquired skill level of typical high school students. Skills gained include dealing with the circuitry, building the apparatus, controlling the temperature, and rearing mosquitoes. The students learned the problem solving skills associated with the determination of where to seek help and how they could acquire the needed information. They also learned team building skills and how to work effectively with their peers and mentors.

With all the successes and failures associated with this experiment, it has been learned by the students, their teachers, classmates, and fellow community members that the process rather than the product is the most important lesson learned. The experiment has served as a real-world problem that has taught many people to pool their talents and achieve their goals. With all the scientific data retrieved and skills gained, this experiment, in all its phases, is a success. The enticement of space made this project happen and once again proved that *The Sky is NOT the Limit!*

SURFACE TENSION: THE ART OF SCIENCE

Lynne F. Zielinski
Physics Teacher, Glenbrook North High School

Vince Pinelli
Broadcasting Teacher, Glenbrook North High School

Kevin Haworth, Patrick Kearney, and Keun Young Lee
Students, Glenbrook North High School

ABSTRACT

The Surface Tension Experiment is a veteran of three Space Shuttle SEM missions. It is the work of students and teachers involved with the Glenbrook Aerospace Development Get-away Experiment Team (GADGET) of Glenbrook North High School in Northbrook, Illinois. The students and teachers come from many disciplines including applied technology, computer sciences, graphic and illustrative arts, broadcasting, humanities, and various fields of science.

The Surface Tension Experiment used paints and dyes to study the art of fluid interactions in a microgravity environment. Experimental data revealed both expected and unexpected results. As in all good science inquiry the results raised more questions than answers. This paper will look at the results and the educational lessons which have been learned through the successes and failures of this experiment.

The areas of fluid studies being explored include: cohesion, adhesion, surface tension, capillarity, and viscosity. The art aspects that are important include the properties of paints and paper, color mixing, and the elements and principles of design. Using scientific reasoning and artistic curiosity, the patterns formed on different surfaces by the color coded immiscible and non-immiscible fluids may be predicted. The uniqueness of the experiment allows for a mechanical production of a painting in space whose results could only be created in a microgravity environment. The permanent visual documentation of liquid behavior provides tangible results and raises philosophical questions; Are the results of this experiment art? Through the mixing of different viscosity paints and dyes, this experiment unlocks the imagination by studying the mysteries of art and science. Through the reactions of fluids in a microgravity environment, science uses art to explain the art of science.

INTRODUCTION

The main focus of this experiment is to determine how paints and dyes interact with themselves, each other, and different surfaces. To study these interactions from a science perspective, the properties of viscosity, surface tension, adhesion, and cohesion need tot be understood. From the art perspective, color mixing, absorbency, and the elements and principles of design are the main concern.

Viscosity is a fluid property which measures how resistant a fluid is to flow. For example, glue is highly viscous while motor oil has a low viscosity. If a fluid has high viscosity, it has high cohesion. Cohesion is the interaction of high and low viscosity fluids with each other. High viscosity fluids prefer to stick to its own molecules than to flow. If a fluid has low viscosity, then it has low cohesion because the fluid would prefer to flow than to stick to itself.

The molecular bonds within a liquid are responsible for different viscosities. If two liquids of different viscosities come into contact and are able to mix, then the resulting fluid will have a viscosity different than either of the two original fluids. If two liquids are unable to mix and they bounce off of one another or one liquid completely engulfs the other, their properties remain unchanged and surface tension is the dominant force.

Surface tension is defined as the way in which liquids travel or behave due to the strong attraction of its molecules to each other. This attraction acts like a thin skin across the liquid's surface holding it together. In the microgravity environment, surface tension is what gives a drop of water it's spherical shape. The Surface Tension experiment is designed to help in the understanding of how the paints and dyes will interact with each other.

When any low viscosity fluid subject to flow is located on a boundary layer where it comes in contact with a dissimilar fluid or solid, it can exhibit a different property. If, for example, a water droplet is surrounded by air, each water molecule is subject to attractive and repulsive forces from nearby molecules. If the interior forces within the droplet are greater, surface tension dominates. If attraction between molecules of different fluids is greater, cohesion dominates. If attraction between molecules of fluids and solids are greater, adhesion dominates. Adhesion is a property which determines how easily a liquid clings to a surface. It includes how fluids of high s and low viscosity will interact with different surfaces.

Students and teachers in several disciplines are currently studying the results of GADGET's Surface Tension experiment. After two unsuccessful attempts, the experiment was successful on its third try and functioned in the manner designed. Experimental data revealed both expected and unexpected results. As in all good science inquiry, the results raised more questions than provided answers. This experiment proved to be an avenue for unlocking the imagination and reinforcing scientific method strategies. Through the reactions of fluids in a microgravity environment, science uses art to explain the art of science.

EXPERIMENT DESCRIPTION

This experiment uses six syringes to inject three primary color paints and three secondary color dyes into a metal box lined with six different types of absorbent and non-absorbent papers. A motor releases an acrylic block pulled by springs. The acrylic block pushes the paints and dyes out of the six syringes and into the paper lined box. The paints, free from gravitational influence, collide with each other and the paper on the inside faces of the box.

Concept drawing of how fluids are injected into the box.

The experiment used acrylic paints and water-based dyes, which have different viscosities. The higher viscosity paints were primary colors: red, blue, and yellow. Piggy backed on top of the paint syringes were the less viscous dyes. The secondary colors used were orange, magenta, and green. The three different color dyes are immiscible and can mix with each other. The three paints will behave similarly. Meanwhile, viscosity prevents the dyes from mixing with the paints. They are considered non-immiscible fluids.

Surface Tension experiment on SEM plate.

The papers were arranged inside the metal box so that the side opposite the syringes was a non-absorbent material: a foam core board. The other five sides were covered with various absorbent water color and art papers. The papers in the box were arranged so that the maximum interaction of the paints and dyes would occur between the surfaces and each other.

PURPOSE

Due to the multi-disciplinary nature of this experiment, there are many purposes which address the scientific and artistic aspects of its design. The purpose of this experiment is to:

1) determine the mixing characteristics of color coded immiscible and non-immiscible fluids.
2) determine the ability of immiscible and non-immiscible fluids to bond to various absorbent papers.
3) study the structural characteristics of immiscible and non-immiscible fluids when dried in microgravity.
4) study the surface tension, cohesive, and adhesive properties of immiscible and non-immiscible fluids when bonded to absorbent and non-absorbent surfaces and with each other.
5) use Newtonian physics of trajectory and projectile motion to map and create a computer simulation of the route taken, mass lost, and energy used in the rebounding of the various fluid projectiles.
6) study the dynamics of fluid viscosity when immiscible and non-immiscible fluids meet.
7) predict the patterns formed on the different surfaces by color coded immiscible and non-immiscible fluids.
8) mechanically produce a painting in space whose results and effects could only be created in a microgravity environment.
9) produce a permanent visual documentation of how liquids of different viscosities react in a microgravity environment.

HYPOTHESES

The hypotheses from a science perspective associated with this experiment include:

1) Surface tension fluid dynamics will dominate over capillary action.
2) Fluid mass loss will be greatest when the fluid strikes the papers at near normal angles and minimal at oblique angles.
3) Fluid energy loss will be minimal, showing many impacts for each fluid droplet.
4) Fluid trajectories will show angles consistent with Newtonian physics.
5) Fluid trajectories will be straight lines and not curved.
6) Capillary absorption will be circular on both absorbent and non-absorbent materials
7) Immiscible fluids will not mix and blend colors. Instead they will create spiral or helical mixing patterns.
8) Non-immiscible fluids will not mix. When they adhere to each other they will demonstrate surface tension dominance. When they adhere to absorbent paper, capillary action will dominate.
9) Non-immiscible fluids with the least viscosity will surround the more viscous fluids when they meet.
10) Non-absorbed fluids will create both hemisphere and crater-like shapes.
11) Only circular markings will be made if fluid is traveling at a low velocity.
12) Fourier analysis can be successfully completed on the product.
13) Van der Waals forces and laminar flows can be determined.

The hypotheses from the art perspective were more intangible and creative. Art students made their predictions through the media of painting, graphic design, and computer animations. Most students depicted hundreds of colored dots of varying size all over the canvas. Few had the paint concentrated on the "back" wall like that of the actual results. Discussions were held at various points in the student development of the finished product. At one point, some physics students were brought into the art classes to act as "experts" in leading a discussion on how fluids behave in the microgravity environment. Benefits were gleaned by both groups of students.

HISTORICAL BACKGROUND

The Surface Tension experiment was conceived in 1995 while brainstorming experiment ideas for experiments to fly in the NASA Get-Away Special Canister (GAS Can). Teachers and students, from different disciplines, gathered together to design and build the experiment. This multi-disciplinary experiment eventually involved teachers and students associated with applied technology, graphic and illustrative arts, life skills, computer sciences, radio and television broadcasting, and physics. While at a the 1995 Shuttle Small Payloads Symposia, an opportunity arose to fly the experiment in a Space Experiment Module (SEM).

The Surface Tension experiment has been flown on three NASA SEM flights. The first two flights aboard Columbia on STS-80 and Discovery on STS-85 were unsuccessful. Problem solving skills and the process of redesigning the experiment were excellent learning opportunities for the students. The third flight opportunity, on Discovery STS-95, operated successfully. Both expected and unexpected results were achieved.

STS – 80

The experiment motor on the Columbia flight used plastic gears. Due either to the stresses during ground tests or the pressure of the spring launching mechanism, the gears became stripped. The motor was replaced with metal gears for the next flight opportunity.

The experiment appeared to have a partial release because the acrylic block which pushes the paints into the box was noticed to be at an angle during deintegration. Upon opening the experiment box, it appeared that some fluid had been release. It is interesting that of the two impacts shown on the back wall, one produced a splatter pattern and drip indicating a definite gravitational influence. The second impact shows three near perfect circles indicating that they may have been released in microgravity. There is no definitive way to determine whether any of the fluid release occurred in microgravity
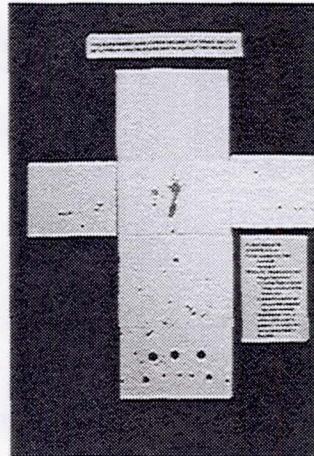
Results of STS-80 partial release.

STS – 85

An opportunity arose for the modified Surface Tension experiment to be flown as a back-up experiment on this mission. The wait for the launch of the Discovery mission was approximately nine months from when the experiment was loaded to launch. As a result of this long wait time, the motor mount bent under the pressure of the springs, driving the release mechanism into the acrylic block. The release mechanism was rendered inoperative. Thus, the motor was not able to properly rotate and inject the paints and dyes into the box.

In order to ensure a successful execution of the experiment for a future flight, a number of test runs were performed and modifications were made from the original STS-80 apparatus. A steel support was added to hold the motor mount in an effort to combat the force of the high-tension springs that had caused the earlier malfunction. Sealing caps inside the box were replaced with grease plugs to hole the paints in their syringes after determining that they might inhibit the flow of the paints into the box.

STS – 95

In the hopes of flying the experiment for viable results, it was brought to Goddard Space Flight Center and demonstrated to NASA engineers. It was loaded and left as a back-up experiment in case a scheduled active experiment had a problem and could not fly. GADGET was fortunate that the experiment had the opportunity to fly this historic mission. The experiment operated successfully: firing while in the microgravity environment.
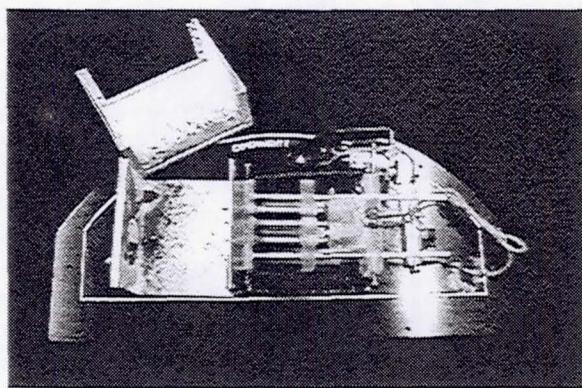
Interior view after successful firing on STS-95.

PRELIMINARY RESULTS

After studying the ground tests and the original hypotheses, several predictions were made by students. Below are some of these predictions and the associated results.

Prediction 1: The fluids would bounce around inside the box covering all of the walls with circular marks. Note: Art students created splatter paintings that served as a visual prediction of what they thought the result would look like. Only one student came close to the actual result.

Result: The fluids did not cover the walls of the box. The dyes appear to have hit the back wall first and splattered in a pattern similar to ground test experiments. However, the acrylic paints, being more viscous, struck the wall and stuck to it without splattering due to strong adhesion forces.

Prediction 2: Most paint and dye markings would be circular.

Result: Some perfect circular markings were found on top of the paint on the back wall of the box. The colors of these circles are brownish. This is not a primary or secondary color originally injected into the box. The brownish color was probably created by the mixing of two secondary dyes which must have floated around inside the box before finally resting on the back wall.
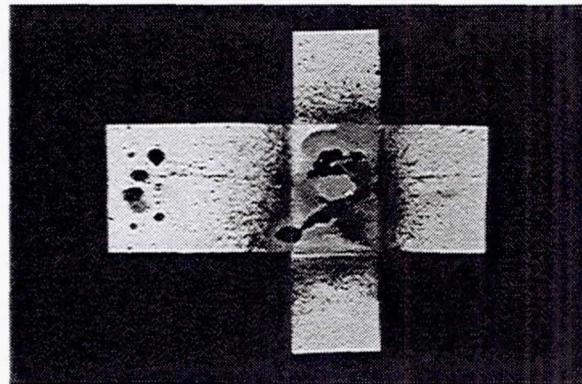
Layout view after successful firing on STS-95.

Prediction 3: The paint and dye imprints would be absorbed into the papers creating two-dimensional circular marks on the papers.

Result: Some circles were imprinted. Initially it was thought that all paints and dyes were hemispherically placed on the back non-absorbent wall. Most of the paints had a three dimensional quality to them, looking something like a "frozen lava lamp." All paints appeared to have an oblong appearance which GADGET attributes to the firing of a Shuttle maneuvering jet while the paints were drying. Other causes may have moved the paint during orbit or landing.
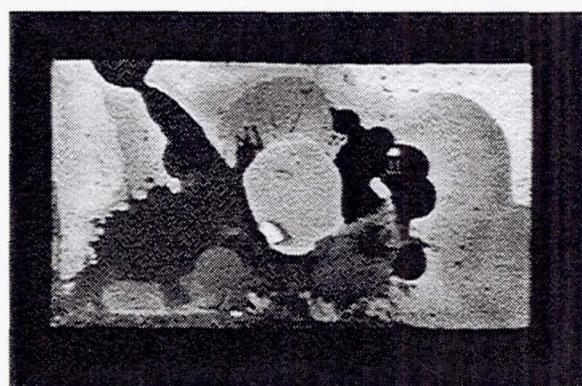
Back wall of experiment box from STS-95 flight.

Prediction 4;   The sealing caps attached to the syringes would be found "stuck" somewhere in the box.

Result: Two of the sealing caps were "stuck" to the paint on the back wall and one on the bottom of the box. One of the caps on the back wall appears to have been moved while the paints were drying. GADGET believes that the movement was caused by a Shuttle maneuvering jet. However, because of the direction, it would have had to of been a different maneuvering jet fire than the one that moved the drying paints.

Prediction 5:   The paints and dyes would not mix with each other as non-immisible fluids.

Result: There is no indication of the paints and dyes mixing.

Prediction 6:   There would be no splatter marks on the back wall.

Result: Inconclusive result. There appears to be no splattering of the paints. However, the dye marks are covered by the paint and it cannot be determined if they exhibited a splatter pattern. However from the side panels, it appears that some splattering did occur from the dyes.

Prediction 7:   The motion of some drops of paints or dyes will be trackball to additionally verify Newton's First Law of Motion.

Result: At this time it is difficult to track any one particular paint or dye mark. Students are trying to figure out a method of verifying this hypothesis.

Prediction 8:   Immiscible fluids would swirl and not blend in color.

Result: Inconclusive result. It appears that in at least one case this did not occur and the dyes blended creating a brownish color. It is not apparent whether the blending occurred while the dyes floated together or through the capillary action experienced after striking the absorbent paper. The paints showed no such mixing or blending.

Prediction 9:   Adhesion and high viscosity will cause the paints to be attracted to the low absorbency foam board.

Result: The adhesion of the paints to only the foam core board is in agreement with this prediction.

UNANTICIPATED RESULTS

While it was thought that some paints and dyes would adhere to the syringes, it was unexpected that the red and blue paints would create three-dimensional hills. Even more unexpected was that the blue paint's hill appeared to be dripping up and not straight outward like the red hill. GADGET believes that the paints showed this phenomena because they were more viscous than the dyes which did not exhibit this behavior. The creation of the upward drip is a mystery at this time.

QUESTIONS RAINED

The results of this experiment are so vast that more questions were asked than answers provided. Students have a lot more data to analyze and understand before this experiment is considered complete. The following are some questions that have been raised as a result of this experiment and its results:

Are the results of this experiment art?

What is art?

Should the results of this experiment be considered "art"?

What could this experiment mean to the art world?

Can this be considered 'art' from a scientific perspective?

Can science produce art?

Is this the Art of Science or the Science of Art?

Is there a way to track the motion of any one of the droplets?

Why were the hills formed?

Why are there fewer perfect circles than expected?

Is there a way to repeat the experiment to see what hit the back wall first?

Do the results show that the paints and dyes work in microgravity differently than they do on Earth?

What would happen if glass balls or some other material were left inside the box?

What would happen if deflectors were placed in the path of the fluids as they were being injected?

Can science use art to explain the reactions of liquids in a microgravity environment?

What could the value of this "first mechanically produced painting in space" be to the sciences?

How should the results (paints/dyes on paper) be displayed?

How might this experiment and the results improve an understanding or further collaboration involving science and art?

Could the speed at which the fluids are traveling be reduced to be able to lessen the splattering of dyes so more opportunities to study mixing could take place?

How is this experiment different from the ground tests? Why?

Can media used in art benefit science experiments?

Could the acrylic paint serve as a glue with lightweight beads floating or suspended in the box during flight?

Can further insight be gained as to how liquids react in a microgravity environment by looking at how or when the acrylic paint hits the wall? Can this be accomplished by adding glass beads which are allowed to float freely in microgravity prior to the syringes ejecting the paint? Then, look at where and what beads stick under what paint color or on top of what paint color.

CONCLUSION

Through the Surface Tension experiment, students have become aware of the interelatedness and dependency between academic disciplines. There are many lessons to be learned from the successes and failures of such real-world experiments. They include being sure that adequate testing of experimental apparatus has occurred, redundancy, strength of materials, and proper documentation of data. The more intangible lessons learned include persistence, dedication, and creativity. In combination, these lessons lead to success.

By being involved with GADGET, students realize that scientists alone can not make an experiment successful. It takes administrators, money manages, artists, advertisers, historians, writers, and many others. It is only when all the academic disciplines work together that a project like the Surface Tension experiment can be successfully completed. A multi-disciplinary group of students, with guidance from teachers, mentors, and volunteer community members need to work together to design and build experiments that could one day fly aboard the Space Shuttle. After all, *The sky is NOT the Limit!*

Page intentionally left blank

TOYING AROUND WITH SILLY PUTTY AND BUBBLE SOLUTION
Oakcrest High School
Mays Landing, New Jersey

Norma Boakes
Interdisciplinary Math/Science Instructor
Grades 9 - 12

ABSTRACT

Students at Oakcrest High School, as part of a new interdisciplinary math and science class, ran a Space Experiment Module (S.E.M.) experiment during the 1998-1999 school year. The experiments, entitled Silly Putty Longevity and Adaptability Testing (S.P.L.A.T.) and Bubble Lab Adds Science and Technology (B.L.A.S.T.), contained silly putty and bubble solution in 22 small vials. Within the time that the experiment was assembled, submitted, flew, and returned to Oakcrest, my students were in charge of answering a basic question, "What effect would micro-gravity have on the substances' physical characteristics?" By utilizing what they learned about the scientific method and many of the math and science skills covered in class, students created and conducted pre-flight and post-flight testing, as well as came to their own conclusions about what had happened.

The paper you are about to read will tell you how this was done, what purpose the experiment served as an educational tool, and the positive effects the experiment had on the math and science curriculums.

BACKGROUND

Last year, Oakcrest High School decided to implement a new program that would link a math and science class together. This interdisciplinary approach, which has become popular among many schools, is meant to help students realize and explore the connections between two related subjects. Our Integrated Math I classes with Inclusion were chosen to pilot this new program. This non-college prep, basic skills course covers numerical operations, as well as basic Algebra and Geometry concepts. The class is made up of mainly ninth grade students and about 10% special education students. The science class to be linked to Integrated Math I was our General Science class. This class is similar in that it is meant for ninth grade non-college prep students and contains special education students, as well. The topics taught in this class include the basics of earth and space science as well as such topics as electricity, storms, work, etc.

To make the interdisciplinary aspect of the two classes work, the classes were scheduled in two-period blocks of time consisting of two 40-minute classes. Students were then scheduled so that they would have science and math in back to back periods. By having this set up, we were able to get 80 minutes of time together with groups of about 50 students and a total of three to four teachers including at least one math, science, and special education teacher. Once everything was scheduled, we had two interdisciplinary math/science teams set up. (There were a few students that did not have what we called "cross-over" having only the math or science portion of the program, but this did not really cause any major difficulties.)

SPACE EXPERIMENT MODULE (S.E.M.) EXPERIMENTS

Purpose

To begin our math/science program, we decided that the best way to get things going was to have projects for each marking period that would link the two classes for team projects. One of the major units to be covered was space, so the S.E.M. project was a perfect opportunity. With the help of the N.A.S.A. program I attended over the summer, entitled N.A.S.A. Educational Workshop for Math, Science, and Technology teachers (N.E.W.M.A.S.T.), I submitted the proposal for S.P.L.A.T. and B.L.A.S.T. I struggled for a while on what to do, since there were many options you had when writing an experiment. My choice was to go with a passive experiment that required no external source of energy. Then, I was faced with what to put in the small vials that would be placed in this passive experiment.

Why choose silly putty and bubble solution? That's what everyone always asks. Well, I wanted something basic that any student at any level would be able to understand and be familiar with. It was also safe to handle and very inexpensive. (In fact, with just a few phone calls a toy company happily donated all the supplies we needed!) To be honest what was more important than what was in the vials was what the students would do with it. My hidden purpose was to have students work through the scientific process. What better way to teach something so basic, yet so important to science (and math for that matter), then to have students actually participate in it? As well, as you will soon see, with a little thought and creativity we were able to integrate many of the skills we normally teach or review in our math and science classes. What needs to be kept in mind, as I did when designing this experiment, is that what your doing does not have to be complex to be meaningful.

Shown above are the contents of our experiment. There were two half circle layers, one with vials of bubble solution and the other with silly putty. Both envelopes fit inside the metal envelope shown on the left.

Preparation

Now that the experiment was written and accepted, my colleagues and I had to make this S.E.M. unit happen. The 22 vials, half filled with silly putty and the others filled with bubble solution, were the first to be prepared and sent to N.A.S.A. In addition, sets of control samples were also prepared in identical vials. (In this way, students would be able to see if just time in a sealed container in a normal environment might have some effect on the substances.)

Once the experiment was sent, we now had to determine the structure of our S.E.M. unit. Since the idea was to give students first hand experience with the scientific method and how experimentation is structured, we decided on setting up research teams. With the scheduling set up I described earlier, we had two different groups of about 50 students to break into teams. It was decided that there would be 5 or 6 students in each team and that each student in the group would get a specific job, although everyone was involved in the actual experimenting. The jobs included leader, checker, supplier, note-taker, and associate members. (Since we had students with no "cross-over", who would only be with us for half of the time, we created associate members so that these students could be involved as well.) This set up worked great. Besides

the grouping being a realistic job situation and students were able to work co-operatively to solve a real problem.

Experimentation Stages

With our research teams in place, we were ready to plan the experimentation stages. We designated four main stages: *introduction and planning, pre-flight testing, post-flight testing, and analyzing data*. Within each stage, students worked in their designated research teams. Each group was responsible for completing each of these stages.

To keep things organized and to keep track of team progress, each group was given a team binder. Within this binder is a list of each team member's duties, sections for each stage of experimentation, and all lab sheets needed. (This turned out to be an excellent tool for evaluating understanding and progress!)

Stage 1: Introduction and Planning

One of our team leaders shares her enthusiasm as she sits with her research team.

At the start of the school year, this stage was used to orient students to their research teams and let them know what their responsibilities were. In addition, since we did most of the experiment planning during the summer, we needed to talk to the students about what the S.E.M. was and what our experiment was all about.

Once the students were given the background they needed and we explained the details of the S.E.M. and our experiment, students were given the first and most important task, to complete the beginning steps of the scientific method. They had to state the problem, define the hypothesis for both B.L.A.S.T. and S.P.L.A.T., determine what factors would have an effect on the experiment in a space environment, and find ways to test these factors. (This was all done on a prepared lab sheet.) With the students' input, we were then able to set up the experimentation.

Stage 2: Pre-flight Testing

It was now time to set up labs to do pre-flight testing. With the original vials already sent to NASA we chose to use regular samples of silly putty and bubble solution to experiment with. This data was referred to as "baseline data". This data would then be compared later with the space and control samples.

Using the factors that students identified for each of the substances, we set up lab days for both B.L.A.S.T. (bubble solution) and S.P.L.A.T. (silly putty). Stations for each factor were created with all the equipment they needed at each station. Students were then given a set amount of time at each station to do the experimenting. In each team binder we placed a lab sheet for each station and instructions on how to complete the labs. (Remember that the lab sheets can be used later as an evaluation tool.) Teachers were then assigned to specific stations to give students assistance where necessary.

I have given many of the details of the experimentation to try to illustrate the rich connections that we were able to make with such a simple experiment. Students busily

worked on calculations (such as ratios, proportions, utilizing formulas, and averaging), took measurements, discussed experimenting techniques, utilized their science skills, etc. Not only did they utilize and review important math and science concepts, but they also learned how to work in co-operative teams. The best part is that they had fun while doing it!

B.L.A.S.T. –

The chosen factors that students wanted to test were bubbles' diameter, color, last-ability, traveling distance, average number created, and density. So, armed with a bottle of bubble solution and extra wands, students began learning some of the characteristics of bubbles.

In the bubble diameter station students simply blew bubbles onto a desk. Using the imprint the bubble made on the surface they measured their diameter using a ruler. By averaging a set of trials, students determined the average diameter of a bubble.

A team member carefully pours the bubble solution into a cylinder to determine it's mass.

At the density station, students used mass and volume to calculate the density of their solution. They first had to find mass by measuring a beaker without and then with liquid. They then used a graduated cylinder to determine volume. Finally, these numbers could be used to calculate the density.

Another station was quite simple: color. Here, students observed solution in glass containers. Using color samples, they decided how to describe the substance and it's color.

Last-ability refers to the ability of a bubble to last once it is created. Using three different size bubbles (small, medium, and large) and a guide to judge the type of bubble, students had to use a stop watch to time the bubble lasting time from the moment it left the wand until it popped. For each size bubble, teams did three trials then averaged their results.

One student chooses to practice her bubble making style.

One of the more difficult labs was determining the average number of bubbles created with the dip of a wand. We decided on using a fan as a wind source and marking a distance to place the wand when creating bubbles with the wind from the fan. Students then determined a method to calculate the number of bubbles created. The difficulty was getting an accurate count. Students had fun with it though and used several different ways to come up with a realistic value.

The last station was traveling distance. Here students had to determine if the size of the bubble effected how far it traveled. To make this possible, we used a stationary fan, a large ruler taped to the floor, and a clear area for observing. Once the wand was dipped and placed in front of the fan, students observed each of the bubble types and determined distance traveled using the

ruler. Each size was observed three times then averaged. Once this was complete, students used the data to answer the question posed.

S.P.L.A.T. -

For silly putty, students wanted to investigate its color, stretch, "breaking-point", density, bounce, "pressure-point", imprint, and general observations. Each area had samples of silly putty to work with.

The color lab allowed students to identify a specific color for the silly putty. Many students felt that the color would be effected over time. As well, we were given three non-traditional colors so the identification would be helpful later in the experimentation.

The stretch lab was just as the name applies. Here students determined a way to see how far silly putty is really capable of stretching. Students rolled the putty into a cylinder shape of a specific diameter. Two students held the ends, and they began to walk at a slow, steady pace away from each other. When the silly putty began to droop in the middle, the students stopped and the distance it had stretched was calculated.

"Breaking-point" was tested using a similar method. The silly putty was shaped into a cylinder shape, two students held the ends, and then they began to stretch it as before. The only difference is that they kept going until the silly putty broke apart. Students then calculated that distance.

The density lab was where students determined the mass and volume of the silly putty, then used the density formula (D=M/V). To determine mass, the sample was weighed on a scale. For volume, students used the displacement method to determine the sample's volume. The two values were then used to calculate density.
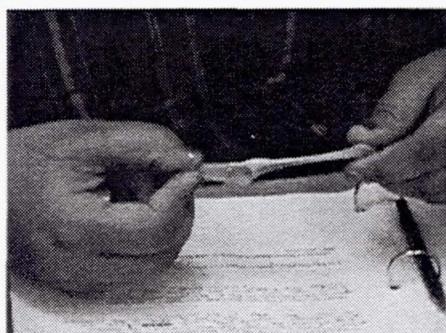
A students works with the silly putty to determine some of its' characteristics.

"Pressure-point" is what my students considered the point at which silly putty could no longer hold its' form under pressure. Students formed the silly putty into a cube, then placed wax paper on top. By stacking small weights on top of the putty, students were able to determine when silly putty would begin to lose its' form. Students used a number of trials in most cases, then averaged the results.

Something I think most of us did when we were children was use silly putty to lift images off of printed materials such as comic strips. This was the imprint lab. Students used the silly putty to check such things as ability to transfer an image, what materials worked better than others did, etc. To help make answers consistent among groups, a lab sheet was created to rate the silly putty on a set scale.

Under general observations, students simply worked with the silly putty to answer a number of simple questions. They looked for things like its' ability to hold its' shape, its' texture, and how it compared to other substances such as play dough or clay. (I was very surprised to find out that many students had never played with silly putty, so this lab helped them to get a chance to play and talk about it.)

Stage 3: Post-Flight Testing

The final stage of the experiment was done with the "space" samples that had returned from the Space Experiment Module and those that had been set aside as "control" samples (mentioned earlier).

The experimentation was done just as it was done before. Students used the same labs to collect data and analyze the samples. The only difference is that they had to be very careful with the samples since they could not be replaced! To keep the "space" samples from getting mixed up with the "control" samples (which we had fewer of), specific teams were picked to work with "control" samples. However, only the teachers knew who those teams were.

Two of my students help me to extract the "space" sample from the vial.

Stage 4: Analyzing Experiment Data

With both pre-flight and post-flight testing complete, students could now use the data collected to answer their hypothesis. To help students organize their data, after each of the testing stages, students were asked to transfer their data onto a summary sheet. (The summary sheet helped students refer to their data as well as help us to determine if any experiments needed to be repeated or finished.) So in this stage, in each of the team binders were summary sheets from both testing stages to compare. The final step to this was to have students fill out a table that would combine the data from the "baseline" set (normal, every day samples), "space", and "control" samples. They actually had two tables, one for silly putty and one for the bubble solution. (The groups that had the control samples were revealed at this point and shared their data with the other groups to complete the table.)

Team members work on their final calculations.

With their data tables complete, teams could now look at the data to determine what significant changes occurred. Set up in teams, we let students decide how to analyze their data and make their own conclusions. We helped the process by giving suggestions, answering questions, and bringing their attention to important areas.

To conclude the project, teams were asked to turn in a "lab report" consisting of their data tables, written conclusions under each experimentation category that included their reasoning, and an overall statement about what had happened to the two substances. I have to admit that this was challenging for my students, but at the same time, very worthwhile. Students struggled with how to analyze their data and how to write their conclusions based on their analysis. With team-to-teacher discussions, however, they began to find ways to make their data meaningful.

It was not the details of the stage that is important here, but the learning that took place. Students learned how to look at a large set of data and make it meaningful, write concise statements about what they determined, have mathematical/ scientific discussions, and problem solve.

EXTENSION ACTIVITIES

The experiments we did with S.P.L.A.T. and B.L.A.S.T. were a great learning experience in the classroom, but we didn't end it there. Since students had had a lot of questions about space and space travel, we did a number of things to enhance what we were doing.

One way we did this was by educating students about NASA and their purpose. They had a particular interest in the STS-88 mission that contained our experiment, so we spent some time talking about the International Space Station mission, viewing a film on the history of space flight, and learning more about the space shuttle. NASA also invited the teachers involved in the program to see the STS-88 Endeavor Mission lift off from Kennedy Space Flight Center, so a small group of us did just that. With the wealth of photos, footage, and information we had gotten, we returned to our classes and shared in the experience.

Our group that traveled to Wallops Flight Facility pose with the SEM paying particular attention to our experiment (2nd envelope going downward within the open SEM)

Another extension was taking a small group of students to Wallops Flight Facility in Virginia to pick up our experiment. Again, NASA invited a small group to watch our experiment be disseminated from the Space Experiment Module. With financial assistance from our school, we were able to take four students to the NASA site. This was very exciting for the students. They not only got to be the first to see our experiment, but they were able to speak with some of the scientists and tour the facilities. As well, they participated in a launch simulation at the Control Center there. Our students were then able to come back and share this experience with the school and community.

One last extension worth mentioning is the cumulative project we decided on to end our unit on space. Our project was to run a Space Week celebration. During this week, we ran daily labs dealing with such space topics as the constellations, planets, meteorites, and laser mapping (all of which were developed from free materials I had received from NASA's educational resources). In addition we held a Space Week open house where members of the community, faculty, and students could come and see all the work we had done throughout the year and showcase some of the activities we had done. We had student volunteers run the labs and talk about their experiences. Highlights of the night also included borrowed meteorite and lunar samples from NASA and a star gazing activity run by a local astronomer.

CURRICULAR IMPACT

I must take a moment to share with you what changes have occurred as a result of the SEM project. First, and most obvious, is the value it has to enhance what we already do in the classroom. With this project we were able to make students active participants in the scientific method, practice math and science skills they had learned, work cooperatively, and communicate

effectively with each other. We also added to our curriculum. Never before have we covered as much about space and our universe. We had also never done such large scale cooperative labs.

Totally unexpected was the tremendous impact this kind of project had on the overall atmosphere of the class. Judging from three years experience teaching this specific course, I witnessed a turn around in student behavior. I was often plagued with discipline problems in a non-college freshmen level class, but not this year. In fact, I had only a handful of small incidents. Much of this stemmed from having students work cooperatively throughout the school year. I also noticed that students were more interested in what we were doing. Students became more inquisitive, felt more comfortable asking and answering questions, and helped each other when they were having difficulty. Students also told me that they were having fun. (Little did they know they were gaining valuable skills and information at the same time!) The best change that I noticed was that students were telling classmates and family about what they were doing. I got lots of phone calls and positive comments from other students. I was thrilled to see that students felt so good about what they were doing.

If you're still not sure what the SEM project can do for you, let me share some results I discovered while evaluating our new interdisciplinary curriculum this year. The most dramatic results were found via a survey I did with all of the classes involved. After tallying the results, I found a number of interesting things. For one, over 50% of the students reported doing better in math this year. This is great considering that 57% of this same group reported getting a C or lower in their math class last year. As well, 87% of students felt what they did in math class was worthwhile and meaningful. In addition, I asked about what activities they liked best. 35% of students picked the space experiment! While doing the survey, I thought it might also be valuable to see how the grades compared to last year. Here I also saw an improvement. There was a 5% improvement in grades. Particularly, special education students did exceeding well, improving their grades by 40%. (Also, no special education students earned lower than a C this year.) To make sure it wasn't just coincidence I looked back to previous years. This was still the best improvement I had seen.

I am compelled to mention yet another positive result of the SEM project, the large amount of positive "press" we received. When I say "press" I am referring to articles and interviews. We had 5 major articles written during the school year and had our local TV station come for two visits. With this "press", we were able to convey to the community what good things were going on in the classroom. It also gave the students pride in what they're doing and let parents know that what their children were doing was challenging and valuable.

On a more personal note, the SEM project impacted me as an educator. I had never before written a grant. Since I was doing this new interdisciplinary program I thought I might give it a try, so that I could enhance what I planned on doing. Well, I can proudly report that I received two mini-grants totally almost $900 to run Space Week and over $700 from my school district to add some basic astronomy to the curriculum next year. I was also recently informed that I will be receiving the Space Week International Teacher Award for my accomplishments with the Space Week activity I ran. I must give credit to NASA, NEWMAST, and the SEM program for helping to expand my horizons and encourage me to do more with what I teach.

CONCLUSION

I hope I have inspired you to consider the space experiment in your classroom! It truly has far reaching benefits. It can be done in many subjects. We chose to use it in our math and science curriculums, but it could easily be extended into other subjects. You may also want to consider doing an interdisciplinary approach and teaming with other teachers and their students. However you chose to use the experiment, it will certainly be a worthwhile endeavor.

Don't be afraid to take the chance. When I first heard of the experiment, I thought, "Could I do this with my students? Will it be too complicated to plan? What do I do?" I have to

stress that your idea doesn't have to start out complex. Even the simplest of things can have value! The main thing is to try it. I must admit that it was tricky at first when deciding on what exactly to experiment with and setting up the details of the lab work, but it was worth the time and effort. Also, use your students as a source. Most of the experiment ideas and set up came from discussions we had with our students. As well, contact the closest NASA Educational Resource Center. There are lots of free materials and experienced people to help you there. Remember that the sky's the limit, well, not any more!

Page intentionally left blank

RAD: The Space Shuttle Radiation Environment And Its Effect on High Sensitivity Film

(STS-85/STS-91 SEM Experiment)

Authors:

Alexandra Moody, Student, Honors Biology Class - Middleton High School
Margaret Spigner, Teacher, Honors Biology Class - Middleton High School
James H. Nicholson, CAN DO Project Principal Investigator - Medical University of South Carolina
Thomas J. O'Brien, CAN DO Project Chief Engineer - Medical University of South Carolina
Carol A. Tempel, CAN DO Project Coordinator - Charleston County School District

ABSTRACT

The "RAD" (Radiation Assay Device) SEM experiment consists of two parts: a set of passive radiation dosimeters and several rolls of high speed color photographic film. The experimental package was flown on two separate high inclination shuttle missions, STS-85 (57°) and STS-91 (51°). The goal was to accurately measure the amount and type of radiation exposure to a typical payload in low earth orbit and to evaluate the possible effect on commercial sensitized photographic products that might be used in a small shuttle payload for research documentation.

BACKGROUND

The radiation environment of low Earth orbit has been studied throughout the space age, primarily from the point of view of health and safety. Space flight, and to a lesser extent atmospheric airplane flight, does expose the body to higher levels of radiation than would be the case at sea level. Although the space shuttle flies outside of the radiation shield of the atmosphere, it is operating within the magnetosphere, which is the earth's most important radiation barrier. During periods of low solar activity, the orbital radiation environment is considered an acceptable health risk for the relatively short duration of a shuttle mission. Higher inclination missions would be expected to show somewhat increased radiation levels since the shuttle is operating nearer to the poles where the magnetosphere is weakest.
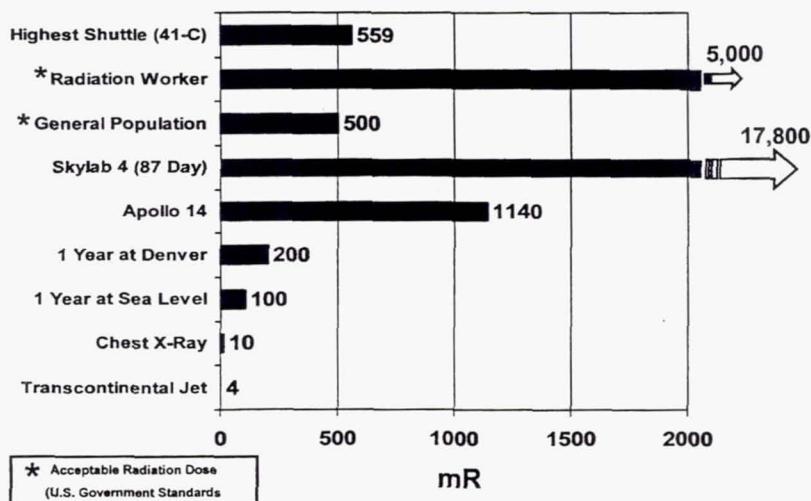
Figure 1. Radiation exposure for different conditions

Generally speaking, a typical shuttle mission should expose the crew to a radiation dose similar to living one year in the mountains. Shuttle mission STS-41C recorded the highest dose with the crew getting an exposure during their eight-day mission that was slightly higher that the U.S. government acceptable radiation dose for the general population for one year. Even this dose is only a tenth of the acceptable one-year dose for a worker in the radiation industry. A longer duration mission such as Skylab or Mir can expose the crew to doses many times the limit, but since it is a one time exposure, the health risks are considered acceptable. The greatest fear is a major solar flare which can expose a protected crew to doses up to 100 REM (100,00 mR) per hour. The radiation levels on a high inclination flight during a quiet solar period were not expected to significantly effect film shielded within the substantial physical structure of the payload and assembly. Practical experience with less sensitive films in previous payloads such as G324 (GeoCam) had shown no noticeable problems.

Experimental Design

Both the passive radiation dosimeters and the photographic film were carefully matched to control samples, which were treated identically in every respect except for the space flight itself. A sample of film from the same emulsion batch was processed immediately after purchase to serve as a control for any fogging due to normal film aging during the eighteen-month experimental period. Another control film sample was stored in normal room conditions at sea level. This sample was processed at the same time as the space-flown sample. The primary film selected was Kodak Royal Gold 1000 high-speed color negative film. Samples of several other popular commercial high-speed transparency and negative films were also flown but without full controls.

The radiation dosimeters were custom made by R. Craig Yoder, Ph.D. and Mark Salasky at Landauer Inc. Two pair of dosimeters were produced, one pair to serve as a ground control and one pair to serve as a mission sample. Each pair of dosimeters consists of an Optically Stimulated Luminescence (OSL) package and a Neutrak 144 package.

The OSL detector consists of specially prepared sapphire (al_2O_3) powder bonded to a clear styrene film base. Luminescence is used to measure the radiation dose received. The OSL detector measures primarily low Linear Energy Transfer (LET) radiation such as electrons and photons. The package contains 15 detectors, some of which are encased by a 1 mm thick aluminum attenuator. The attenuator acts as a filter to separate low energy x ray and electron dose from the dose due to high-energy photons and electrons.

The Neutrak 144 particle track detectors assess dose from high LET radiation made up principally of protons, helium nuclei, and to a lesser extent, heavy ions. Eleven Neutrak 144 detectors are included in each package. Each detector is a

Figure 2 – RAD, dosimeters and flight package

piece of allyl diglycol carbonate plastic also known by the trade name CR-39. High LET radiation disrupts the chemical bonds at the locations where they strike. After exposure the detector is etched in a caustic bath, which causes the radiation-damaged sites to become visible as pits or tracks. The number of tracks under microscopic examination is directly correlated to radiation dose.

The expectation was that a typical shuttle mission would show radiation levels somewhat higher than the ground control but at doses of minimal physiological effect and below the sensitivity threshold of the film products.

DOSIMETER RESULTS

Upon return of the payload, the radiation dosimeters were returned to the manufacturer for analysis. The passive dosimeter results for the space-flown film showed dosages of low LET radiation approximately twice that of control levels (68.2 vs. 145.6 mR) and dosages of high LET (higher energy) radiation that were many times greater than control (8.4 vs. 126 mR). The average control total dosage was <100 mR and the average payload dosage >250 mR. This result was consistent with previously published data and showed that STS-85 had a fairly typical radiation environment compared to other shuttle missions. The total exposure of 272 mR applied to the crew represents the equivalent of approximately 18-month normal background radiation living at the elevation of Denver Colorado.

Mean Radiation Dosage
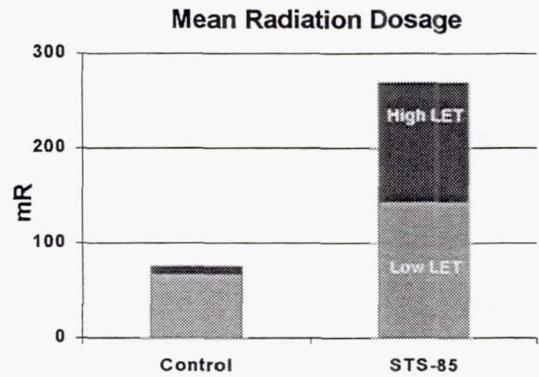
Figure 3. Dosimeter result for STS-85

FILM RESULT

Surprisingly however, the ISO 1000 color negative film showed a level of fogging not only obvious to the naked eye but also significant enough to seriously degrade any images recorded. The question was how to reconcile the low radiation levels as shown on the dosimeters with the dramatic fogging of the film.

Figure 4. Film samples
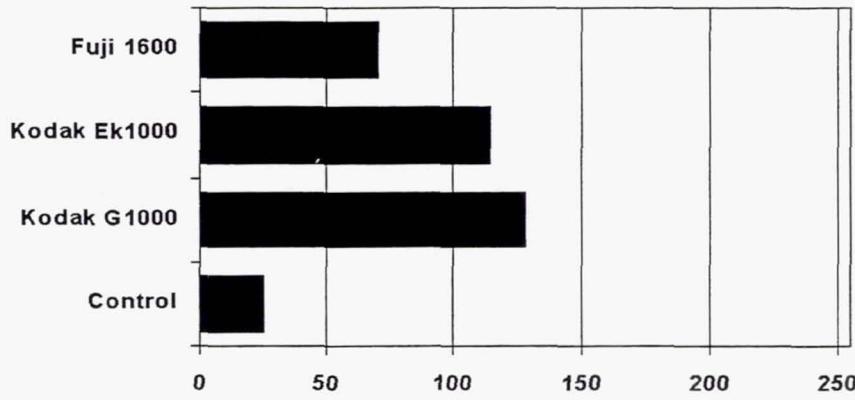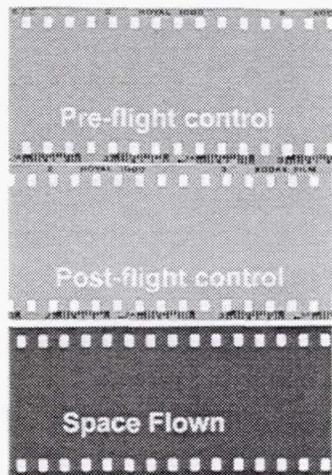
Figure 5. Results by film type

The fog density level was consistent on each roll of the Kodak Royal Gold 1000 film flown. The pattern of fogging was even showing no evidence of shadowing. A re-flight on STS-91 demonstrated a similar although less dramatic result. Over film types flown showed varying degrees of fog density which did not correlate directly to film sensitivity or manufacturer. Fujicolor Super HG 1600 (ISO1600), the most sensitive film flown, actually showed a significantly lower density than either of the ISO 1000 films. A roll of Fujichrome Provia ISO 400 color transparency film showed no significant damage. The results indicate that ISO alone cannot serve as a reliable indicator of the likelihood of film damage due to radiation. Actual testing of samples should be used to verify film suitability before use in a payload.

The degree of fogging on the primary test film was so unexpectedly high that it raised the question whether it was due to radiation alone. Long storage times, the dry nitrogen atmosphere and possible heat exposure were other possible factors.

77

VERYFYING THE FILM RESULTS

A separate experiment was designed to establish whether the observed film result was consistent with the STS-85 background radiation levels shown by the dosimeters. Since the film and dosimeters were carried in the same experimental housing, the radiation exposures to each should be identical. The long standing Can Do Project's Business-Education Partnership with the Medical University of South Carolina made accurate testing possible. Dr. Don Fry of the M.U.S.C. Department of Radiology set up a test to expose film samples to measured x-ray radiation doses. The films were exposed to doses of 328 mR (closest possible match to the flight dose of 272 mR), 1186 mR and 4650 mR using a standard hospital x-ray unit. The test and control film samples were also compared to film exposed to a standard airport security x-ray machine (dosage unknown). The film samples were then processed under controlled conditions. The film was digitally scanned and measured by computer densitometry using the facilities of the M.U.S.C. Department of Pathology Image Analysis Core Facility.
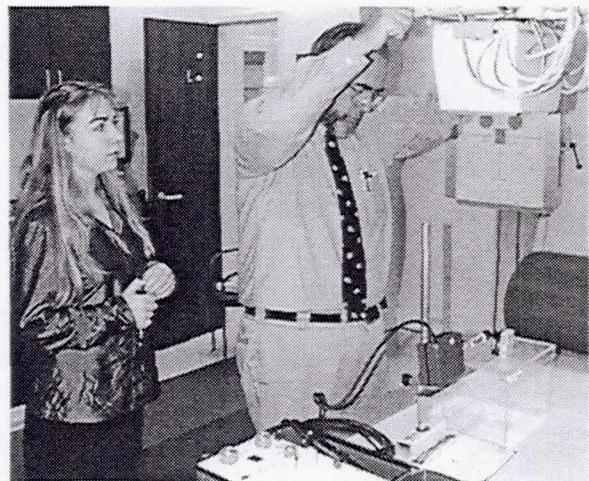
Figure 6. The author and Dr. Fry x-ray the film
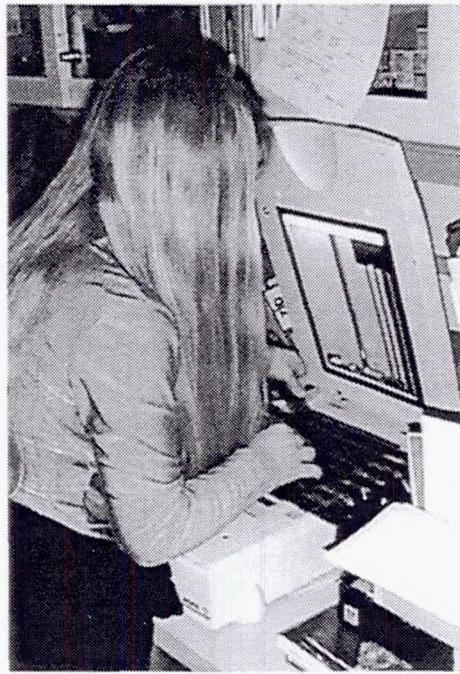
Figure 7. Scanning the film
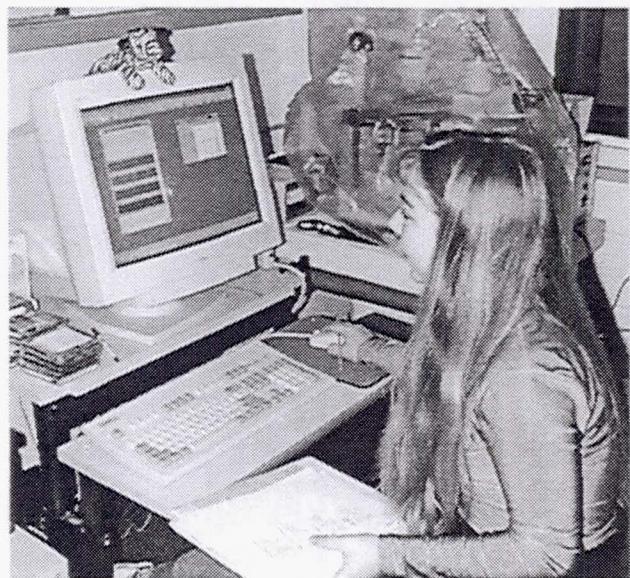
Figure 8. Computerized densitometry

The results indicated that the shuttle mission had a far greater effect on film than multiple passes through an airport security check. A single pass through an airport machine approximately equals the normal background fogging of the film during eighteen months aging. The shuttle flown film density was somewhat

higher but similar to the density from an equivalent medical x-ray dosage (based on the dosimeter results from the same flight).
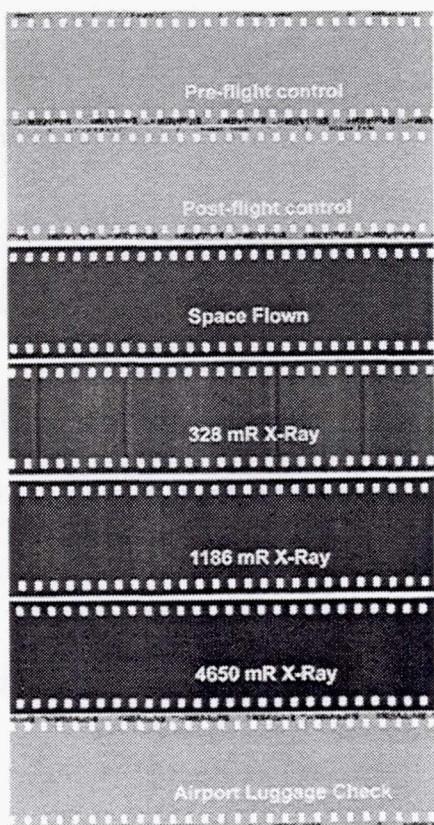
Figure 9. Test and flight films
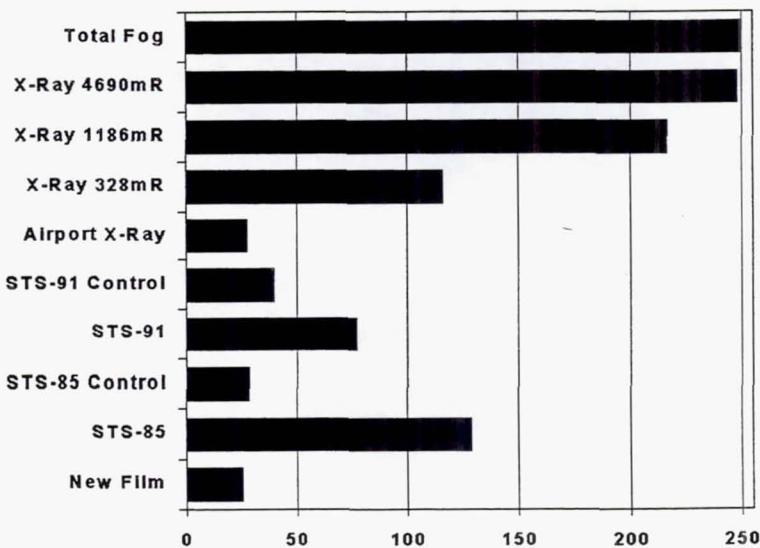
Figure 10. Density values measured by computerized denitometry for test and space flown film

TEST RESULTS

The comparison between the x-ray samples and the STS-85 film samples showed a density level that was consistent although the space-flown film showed a slightly higher density even though the measured radiation level was slightly lower. The x-rayed film showed distinct patterns (shadowing) that were not evident in the space sample. This is a result of the "point source" nature of the clinical x-ray machine as opposed to the diffuse source of natural radiation. The density on the flight sample is very likely enhanced by the unintentional film sensitization caused by prolonged exposure to a dry inert gas atmosphere (a process similar to that employed by astronomers to increase emulsion sensitivity for long exposures to dim light). Such sensitization would show the most effect on slow long time exposures, which characterizes the background radiation.

CONCLUSIONS

Modern high-speed film emulsions are extremely sensitive to exposure to the high-energy form of radiation experienced in low earth orbit. The payload structure does not provide sufficient shielding to block this high LET radiation. These results indicate that high-speed photographic films are possibly not suitable for image recording in space shuttle payloads without special shielding. Preference should be given to lower sensitivity films where possible and testing should be used to verify the choice of material.
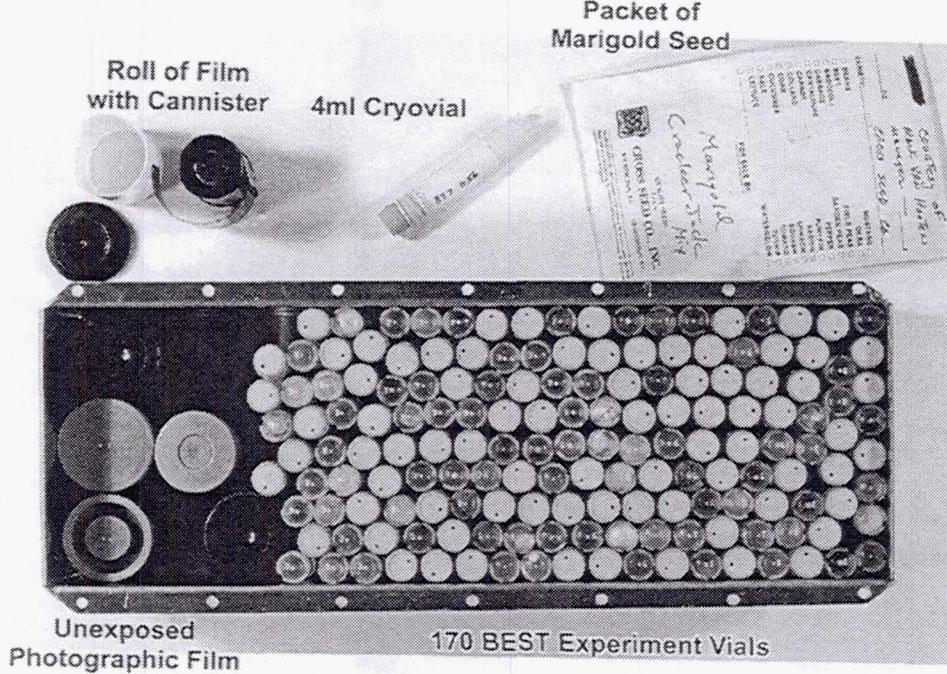
Figure 11. The SEM passive experiment housing showing the film and other contents. The RAD dosimeter package is shown above.

REFERENCES

Brehm, Peter, **Introduction to Densitometry**, Graphic Communications Association, 1990

Lujan, Barbara F. and White, Ronald J, **Human Physiology in Space**, National Space Biomedical Research Institute, http://www.nsbri.org/, 1999

Travis, Elizabeth Latorre, **Primer of Medical Radiobiology**, Year Book Medical Publishers, Chicago, 1975

POLY: Resurrection in Space

An Active Biological Experiment to Measure Plant Revival Using Chlorophyll Fluorescence

(STS-85 SEM Experiment)

Authors:
Haley Chamberlain, Student, Advanced Placement Biology, Wando High School
Ruth Truluck, Teacher, Advanced Placement Biology - Wando High School
James H. Nicholson, CAN DO Project Principal Investigator - Medical University of South Carolina
Thomas J. O'Brien, CAN DO Project Chief Engineer - Medical University of South Carolina
Carol A. Tempel, CAN DO Project Coordinator - Charleston County School District

Introduction

One difficult challenge facing small payload experimenters is to design an active biological experiment that works. The long and often unpredictable pre-flight storage period makes it difficult to find a suitably hardy living specimen that can survive a long period of complete dormancy and still produce useful data during the short time period of a shuttle flight. **BARI**, the CAN DO Project's first attempt at an active biological experiment to grow bacteria cultures in space was largely spoiled by an unexpectedly long flight delay and resulting storage period. The mechanism worked perfectly but the bacteria growth was severely inhibited by the dehydration of the culture media. This led to an effort to find a more stable specimen.

Polypodium polypodioides – The Resurrection Fern

A middle school science class taught by Ms. Rie Cowan originally nominated the common Resurrection Fern as a possible experiment. Resurrection Fern *(Polypodium polypodioides)* is a common sight on rough tree bark and rocks throughout forests of South Carolina and the Southeastern United States. Students gathered the sample flown on STS-85 from a backyard on Seabrook Island, South Carolina.

A true epiphyte, the fern uses the trees only for physical support and gathers all nutrition from the air, not through the roots. When water is available, the fern fronds unroll, become green and produce spores. In times of dryness, they curl up and turn brown. They can remain in this dormant state for prolonged periods and still "green-up" in a matter of hours after a rain. This ability to "resurrect" from a state that appears dead and dried out to the casual observer gives the plant its name.
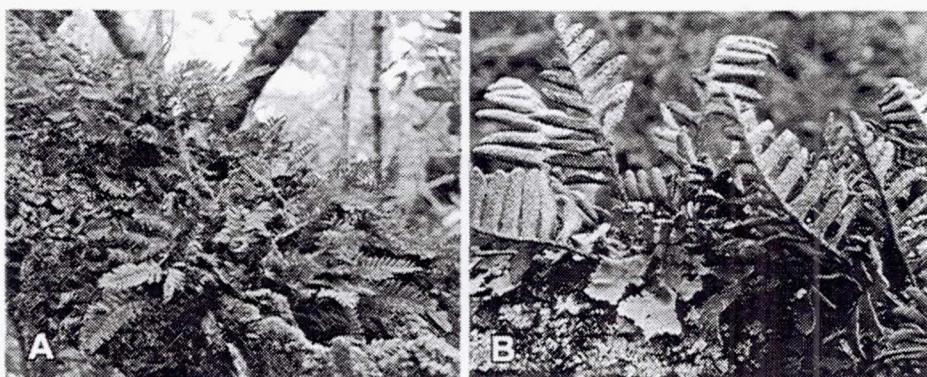
Figure 1. Resurrection Fern in the wild. (A) Growing on a tree (B) Close-up

Experimental Design

The design involves two separate steps: one to provide water, carbon dioxide and light to stimulate revival and two, to measure the return of biological activity.
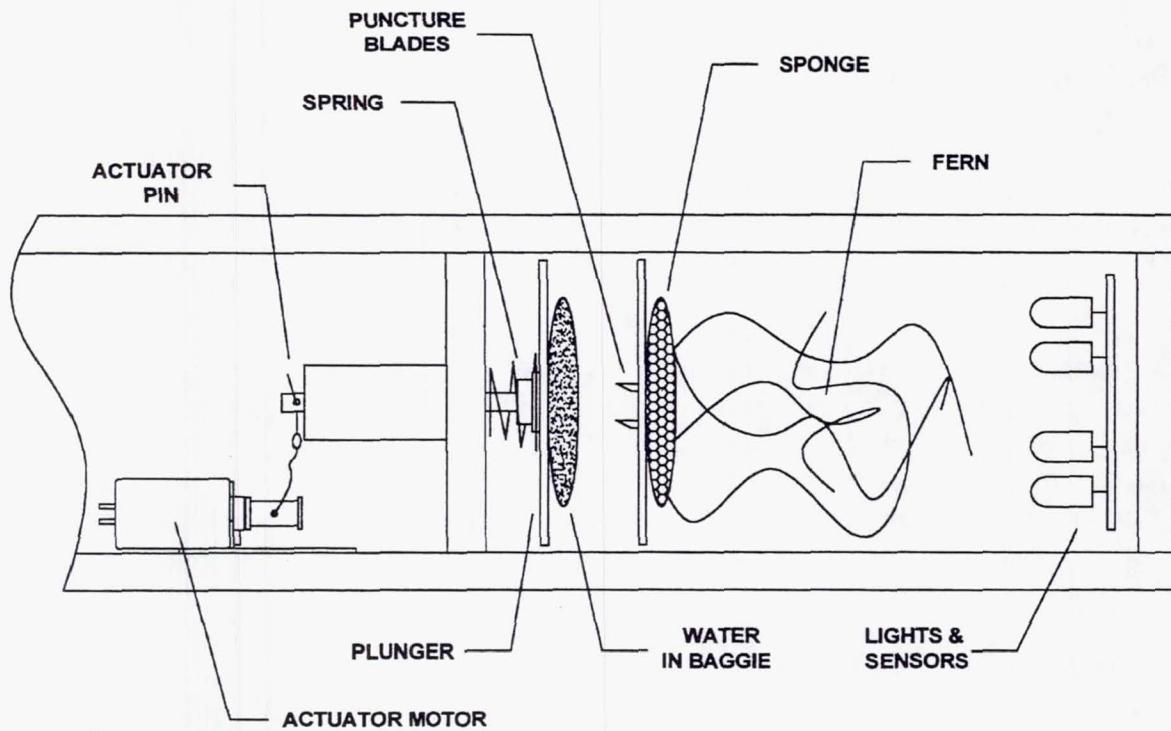
Figure 2. Poly housing and automatic mechanism

The SEM timeline software was used to control the mechanism and to gather measurements at the proper interval. A simple mechanism was designed to use a spring-loaded plunger to push a "seal-a-meal" plastic pouch of water onto sharp razor points. The water was then absorbed into a gauze pad to which the specimen was attached. A ground-up
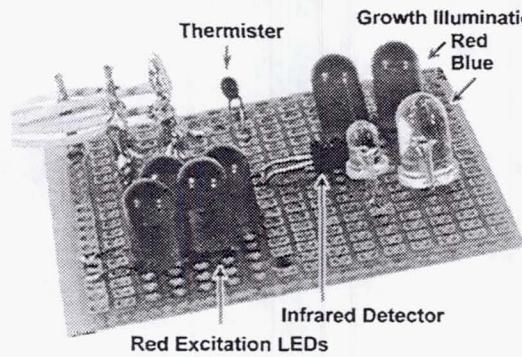
Figure 3. LED lamps and detectors

Alka-Seltzer tablet that was sprinkled onto the gauze pad provided carbon dioxide, automatically activating in the presence of water. The SEM time line software then energized a bank of high output blue LEDs to provide several hours light for a period of plant growth stimulation. Plant biological activity was monitored through the measurement of chlorophyll fluorescence. Light energy absorbed by plant chlorophyll is used first to produce chemical energy available to the plant. The capacity for photochemistry is limited however, and excess energy is often dissipated by re-emission, mostly as heat. A smaller but measurable amount is given off as red and near-infrared light. This fluorescence can be induced by a brief exposure to red light allowing a measurement of active chlorophyll levels. Red LEDs

were activated for a brief excitation period followed by an immediate measurement using a phototransistor to look for any induced fluorescence. Baseline fluorescence measurements were made before and after plant activation without red light excitation to check for any autofluorescence. A series of measurements with red excitation were made before and after the plant growth interval and then after a two day latent period (without growth light) to see if the chlorophyll levels would drop back towards baseline. This measurement was followed by another period with growth light provided to check for a recovery in chlorophyll activity.

A. The apparatus

B. Water dispensing

C. CO_2 generation

D. Blue LED growth stimulation

E. Red LED fluorescence excitation

F. Chlorophyll fluorescence measurement
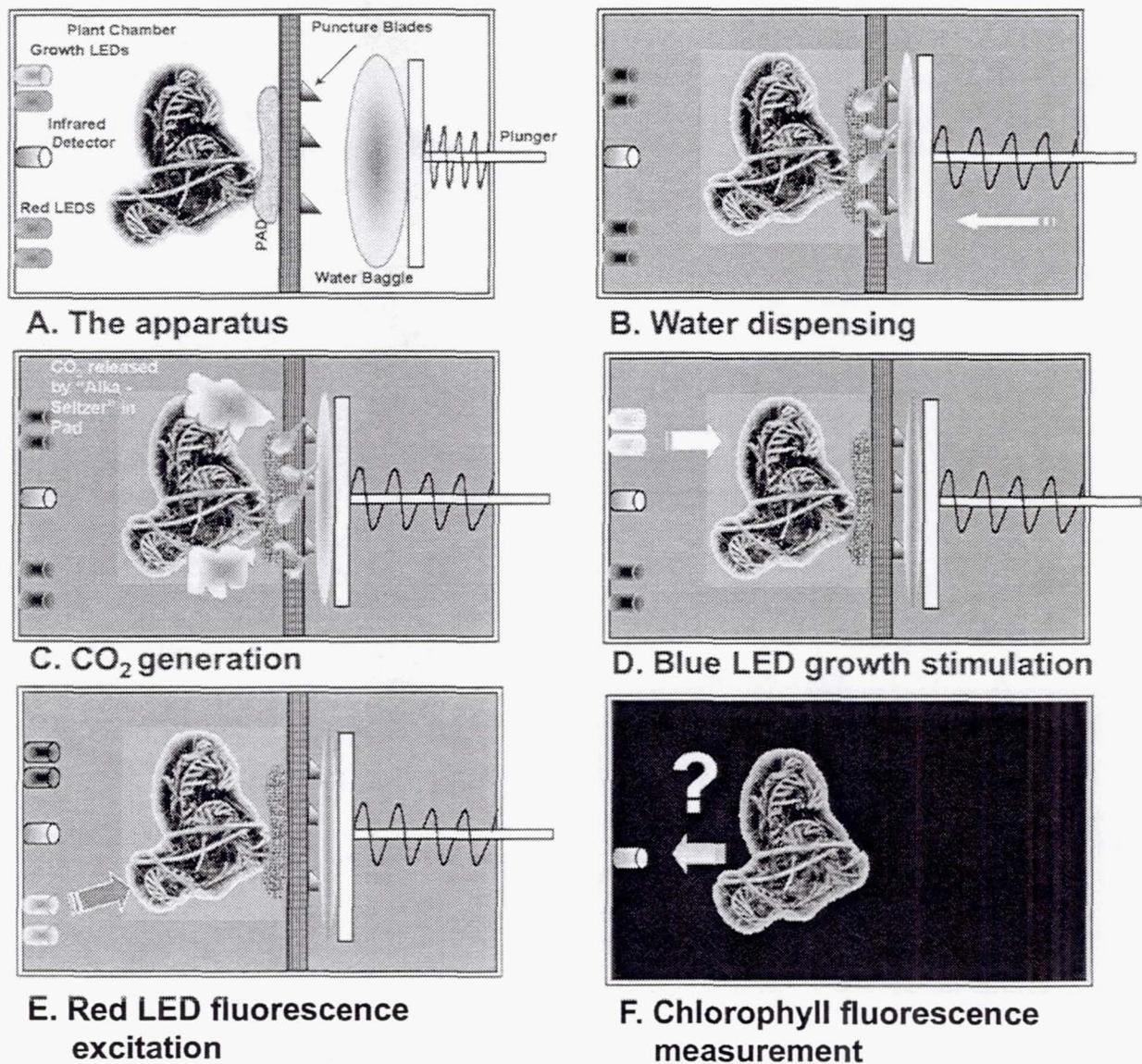
Figure 4. The individual experimental steps conducted under the control of the SEM timeline software program

MEASUREMENT OF BIOLOGICAL ACTIVITY

The apparatus to provide the necessary water, CO_2 and light to the plant is fairly simple in concept. The more difficult challenge was to design a simple and reliable method to measure the physiological activity level to verify successful revitalization. Various methods including photography and 0_2 measurement were considered and rejected because of size, weight, complexity, and cost. Measuring chlorophyll production showed the most promise. Chlorophyll is produced in all green plants during biologically active periods, but it breaks down quickly in plants that are dead or are shut down into completely dormant states. A rise in chlorophyll levels is a sure indicator of active plant metabolism.

Chlorophyll actively absorbs light energy to drive the photochemical process in the plant cells. It converts some of the light energy into chemical energy that then becomes available to the plant. The capacity of this photochemistry to absorb energy is limited and excess energy has to be removed. Most excess energy is re-emitted as heat but a small amount is given off in the form of red light. This fluorescence can be measured to show chlorophyll activity.

RESULTS
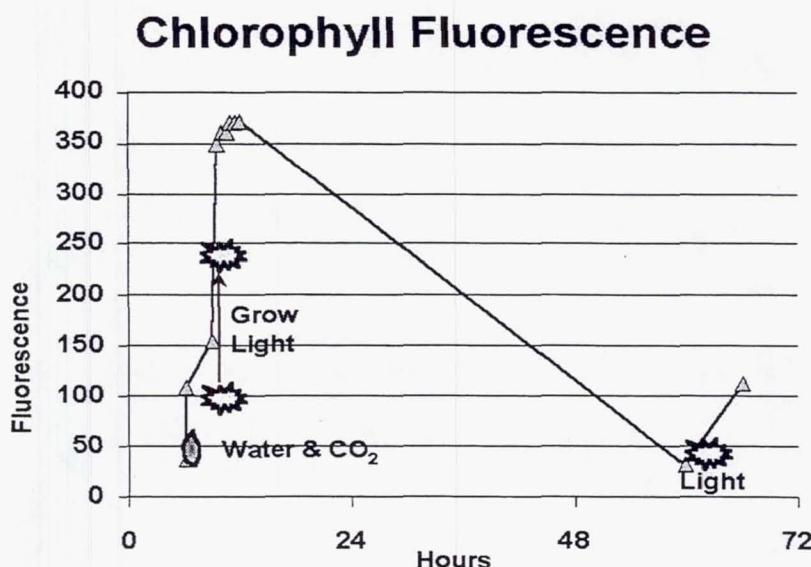
Figure 5. Fluorescence Vs Timeline showing the rise in chlorophyll signal after stimulation by light and water

As can be seen in the graph, chlorophyll fluorescence dramatically increased after each period of growth light activation and returned to baseline after a two-day dormant period. This result matches the expected biological behavior of the plant and demonstrates rapid revival of the Resurrection Fern after a long dormant interval. It also demonstrates the potential value of chlorophyll fluorescence as a method to monitor plant activity, which could be applied to other biological experiments. *POLY* proved to be a hardy space traveler and exhibited regeneration patterns unaltered by its orbital adventure.

RAD (radiation experiment)
SOUSA (sound recorder)

Control Electronics

OPIE
(paint drying experiment)

POLY
(Resurrection Fern experiment)
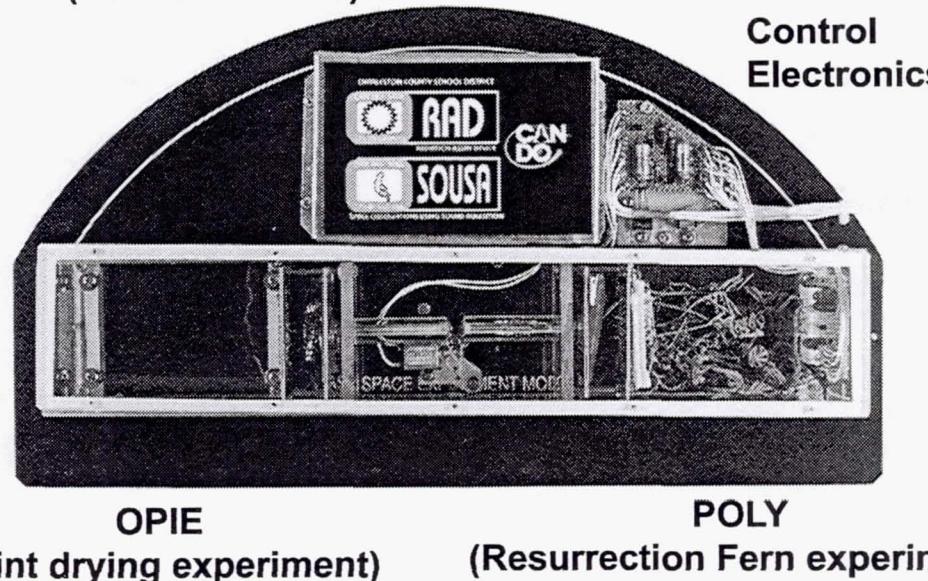
Figure 6. SEM Module with 3 active (POLY, OPIE, and SOUSA) and one passive (RAD) experiment. Note the clear acrylic chamber within which OPIE and POLY share a common activation motor in the center section. The motor pulls a pin releasing a spring activator for each experiment. In the righthand section of the chamber the Resurrection Fern sample can be seen.

REFERENCE

Anderson, Donald B., **Plant Physiology**, 2nd. Edition, D. Van Norstrand Company Inc., Princeton, NJ, 1958

Jones, David L., **Encyclopedia of Ferns**, Vol. 1, Timber Press Inc., 1992

Lellinger, David B., and Evans, A. Murray, **A Field Manual of the Ferns and Fern-Allies of the United States and Canada**, Smithsonian Institute Press, 1985

Lichtenthaler, Hartmut L., **Applications of Chlorophyll Fluorescence: In Photosynthesis Research, Stress Physiology, Hydrobiology and Remote Sensing**, Kluwer Academic Publishers, 1988

Page intentionally left blank

SEPARATION OF IMMISCIBLE FLUIDS IN MICROGRAVITY
AND
EFFECTS OF MICROGRAVITY ON CRUSTACEANS FLOWN IN DIAPAUSE

NORFOLK PUBLIC SCHOOLS
Joy W. Young
NORSTAR Project
Norfolk Public Schools Science and Technology Advanced Research Project

ABSTRACT

The Norfolk Public Schools Science Technology Advanced Research (NORSTAR) experiment flew aboard the Space Shuttle Discovery, STS-91, June 2, 1998. The experiment was flown as part of a Space Experiment Module (SEM). The main objective of the NORSTAR SEM was to encourage the interest of high school students in design, testing and analysis of a space investigation that had scientific significance. This paper describes the two NORSTAR SEM experiments: separation of immiscible fluids in microgravity; effects of microgravity on small crustaceans flown in diapause stage of development.

INTRODUCTION

The NORSTAR program is an extended day science elective for gifted students, grades 9-12. NORSTAR students flew an acoustics experiment Get-Away-Special in 1994 and a preliminary immiscible fluids SEM experiment in 1996. The SEM program has provided NORSTAR students with the opportunity to experience hands-on, real time scienctific investigation . It has also put them in contact with NASA mentors who have provided the expertise and inspiration to motivate high school students.

Immiscible Fluids Experiment

This experiment was designed to observe the behavior (displacement) of immiscible fluids in a microgravity environment. The separation of oil and colored water was videotaped for 2 hours in space. This experiment was flown previously in November 1996. However, we programmed the motor incorrectly so that it continued to mix the fluids for the duration of the experiment which resulted in no separation. We did observe differences in that a vortex formed in the oil/water mixture at a lower motor speed in microgravity than on earth. The experiment was reprogrammed for the second flight.
The students saw the potential values of this basic experiment to be:

- the pharmaceutical industry may benefit in preparing medications in space
- the food processing industry may benefit in developing better salad dressings and other foods containing significant amounts of oil and water for use in space colonies
- the manufacturers of lubricants may find alternative lubricants that do not separate in microgravity.

Crustaceans in Microgravity Experiment

This experiment was designed to observe the development of small crustacean's (Daphnia, Brine Shrimp and Triops) eggs after they had been exposed to microgravity. The eggs were flown in a state of

diapause (suspended animation). On their return to earth, their development into adults was observed and compared to eggs from the same batch which remained on earth.

The students saw the potential values of this experiment to be:

- new insights into developmental biology
- altering animal development under microgravity conditions
- possible effects of microgravity on primary food chain organisms grown in space for long-term space travel.

EXPERIMENTAL DESIGN

Immiscible Fluids Experiment

An acrylic container was filled with a mixture consisting of 50% colored salt water (to lower the freezing point in space) and 50% canola oil (chosen because it is a pure oil with only one surface tension measurement). To ensure that the liquids were equally distributed within the container a teflon coated magnetic stir bar mixed the liquids at the beginning of the experiment in microgravity. An electric motor turned a magnet outside the container to activate the stir bar for three minutes. The motor was then turned off and separation was recorded by a Hi 8 video camera for a 2 hour period.

Crustaceans in Microgravity Experiment

The eggs were packed in a state of diapause in a sealed acrylic container attached to the experiment baseplate. Daphnia, Brine Shrimp and Triops are small crustacean species that are able to remain in the diapause stage for 9 months or more as a survival strategy in the event of prolonged drought in their natural habitat. When rehydrated they revert to their natural state, hatching, feeding and reproducing. After the SEM flight both samples (earth and microgravity) were placed in their respective growth media under the same conditions of light and temperature. Observations were made on a daily basis of the number hatching, activity, size and longevity.

EXPERIMENTAL RESULTS

Immiscible Fluids Experiment

On earth, when oil and water were mixed the oil floated on the water surface due to density differences. During the first few seconds in microgravity the water formed one large sphere in the center of the acrylic container surrounded by the oil. Several small spheres of water were also observed dispersed in the oil surrounding the main water sphere. During the next 6 minutes the small water spheres moved through the oil towards the central water sphere and coalesced with it (Fig. 1). After 17 minutes the large water sphere dropped to the bottom of the container out of view of the camera.
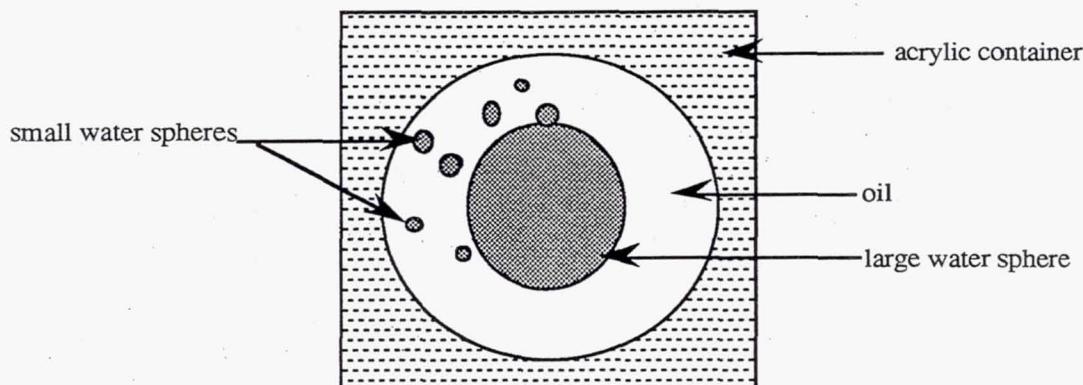
Fig. 1 Separation of immiscible fluids in microgravity

Crustaceans in Microgravity Experiment

These results are qualitative based on student observation using daily journal entries and basic measuring equipment. The Brine Shrimp and Daphnia were difficult to observe due to their small size so all counts were estimated. The space Brine Shrimp did not orient themselves toward the light as did the earth Brine Shrimp. Space Brine Shrimp did not grow as quickly but eventually reached much larger size than any of the earth colony. The space Daphnia were larger, more numerous and more active than the earth Daphnia. Their life spans were the same. The space Triops also did not grow as quickly and more hatched than the earth Triops. Numbers hatched in both groups were minimal and no accurate comparison could be made.

DISCUSSION OF EXPERIMENTAL RESULTS

Immiscible Fluids Experiment

We theorize that in microgravity, where density with its weight component has less effect, the oil has greater adhesiveness to the acrylic container than cohesiveness to its own molecules and therefore moves to the acrylic container's inner surface. The water, having greater cohesiveness to its own molecules than to the acrylic surface, formed a sphere in the center of the container, surrounded by the oil. The Apollo-Soyuz Test Project (ASTP) which flew in July 1975 included a Liquid Spreading Demonstration which showed similar results (ref. 1). The surface tension between the molecules of water and oil caused the small water spheres to move towards the large water sphere. The surface area of one large sphere of water is less than that of several small spheres and surface tension energy will try to minimize surface area causing the spheres to coalesce. This being so, might other mixtures separate over time in microgravity due to differing surface tension forces? These results may bear further investigation using more sophisticated equipment and mathematical analysis than high school students can provide. We intend to devise other experiments in the areas of capillarity, chromotography and diffusion to further investigate the surface tension phenomenon.

Crustaceans in Microgravity Experiment

Qualitative observations showed that the crustaceans flown in space hatched out in greater numbers than those that remained on earth. The space crustaceans also were slower growing, lived longer, were more active and dispersed more throughout their media than those which remained on earth. This was an interesting experiment which afforded the students the chance to gather and record observations but yielded no statistically significant data.

CONCLUSION

The SEM program has offered a unique opportunity to NORSTAR students to experience scientific investigation. As a result of the SEM program a group of inner city, gifted and talented students were motivated to plan as a team, design, construct and analyze an actual space experiment. All this was made possible by the continued cooperation between NASA and Norfolk Public Schools. We are looking forward to future SEM opportunities.

REFERENCES

1. Page, Lou., and Thornton Page. Apollo-Soyuz Pamphlet no. 8: Zero-G Technology. U.S. Government Printing Office. Washington, D.C. 1997, p9.

THE GET AWAY SPECIAL PROGRAM: YEAR 2000 AND BEYOND

David A. Wilcox
NASA Goddard Space Flight Center

ABSTRACT

The Get Away Special Program flew its first payload in 1982. Since then, 157 payloads have flown on the STS. As the GAS program approaches the new millennium, interest in flying the low-cost access to space continues. Many changes are in store, or are already underway, that will impact the GAS user community in the coming years. This presentation will briefly outline some of those changes and other external impacts to the GAS Program.

INTRODUCTION

The Get Away Special Program, or GAS, has been in place since the early days of the Space Shuttle Program. The fundamental premise behind the program remains the same today as it was in 1982 when the first GAS payload was flown on STS-4:

- Enable low-cost access to space
- Encourage the use of space by all researchers; educational organizations to private companies and foreign organizations
- Research and development on concepts that might lead to prime experiments
- Generate enthusiasm amongst the educational community and foster space education

For more information on the fundamental aspects of the Get Away Special, technical information summaries, flight history, available reference documentation, and other information about the program, the NASA Goddard Space Flight Center (GSFC) maintains an extensive web site at: http://www.wff.nasa.gov/~sspp/gas/gas.html

CURRENT STATUS

To date 157 GAS payloads have flown on a total of 35 STS missions. On average approximately 10-11 GAS payloads have been flown per year. (See Figure 1) Most recently 16 GAS payloads were flown in 1998 on 5 missions. Other than the years 1987 and 1988 when the Shuttle Program was recovering from Challenger, only 1990 went by without a GAS flight. This year the GAS program faces only it's second operational year without a single flight opportunity, due primarily to the International Space Station assembly. Nevertheless, there continues to be much interest in the program from long-standing customers and new customers as well. There are 440 GAS reservations on file

today. The GAS project team maintains an "active" list of payloads to denote customers who are actively submitting documentation and working with NASA. Currently, there are 30 payloads on this active list, representing a diverse group of organizations from high schools and universities across the country to international organizations like the Canadian Space Agency (CSA) and the European Space Agency (ESA).

IMPACT OF ISS ASSEMBLY ON GAS

As NASA moves further into the assembly sequence of the International Space Station, the opportunities for small payloads like GAS enter an era with a greater degree of uncertainty. Although opportunities in the GAS program has always been based on available weight and volume margin in the cargo bay, the missions identified for ISS have a greater degree of variability in their parameters. In addition, the Shuttle Program is shortening its templates for standard processing of missions. This includes the preparation of the Orbiter and all of the systems that comprise the STS, as well as delivery and installation of cargo elements. The combination of these two factors will result in the GAS customer and NASA's GAS project team having less time to react to flight opportunities. Another new consideration presented by the ISS missions involves the environmental conditions experienced by the payloads mounted in the cargo bay. The Orbiter will be docked with the ISS elements for long periods of time and the orientation of the ISS-Orbiter configuration could potentially produce some severe temperature extremes for cargo bay payloads. Until the larger ISS solar arrays are installed, the ISS will be orbiting in a configuration that maximizes the effect of the smaller arrays. This happens to orient the Orbiter such that payloads on the sidewall of the cargo bay could be in direct sunlight for extremely long periods of time. There is the possibility that portions of the ISS could end up shadowing the cargo bay in some locations. In order to know the predicted thermal conditions for a given payload, extensive modeling will be required on a mission-by-mission basis. As further ISS missions fly, it is expected that further data will become available to the GAS project team that will enable us to determine the severity of the thermal issue.

CHANGES TO GAS AFFECTING THE CUSTOMER

There are many changes going on within the NASA community. Some are with regard to shifts in focus; for example, towards greater efforts in the area of educational outreach. Within the Shuttle Small Payloads Project (SSPP), this was a driving force in the development of the Space Experiment Module (SEM) Program. Other changes involve updates to hardware, documentation, and policy. The following sections briefly describe some of the changes that will be affecting GAS customers in the coming months and years.

Changes to CFR (Policy)

The GAS Program is governed by federal law. The Code of Federal Regulations (14 CFR 1214.9 and 1214.10) has always held the requirements for eligibility, classification and

flight priority. When the program was introduced, three classes were formed: Class I (Educational), Class II (Commercial/Private/Foreign), and Class III (US Government) The flight assignment priority was then established as II, I, II, III. The Class II payloads were given stronger emphasis at the time because it was felt that educational and government experiments would have many other opportunities within other programs to fly. Figure 2 shows historically how many payloads have flown from each class.

With NASA placing greater emphasis on the opportunity to use GAS as a tool for fostering educational outreach, the NASA Administrator recently directed that the policy be revisited. The resulting changes, which are yet to be implemented, will further emphasize the Class I educational payloads. The existing policy is in the process of being revoked. It is expected that the new policy will be placed into effect sometime in 2000. Until that time, however, the program will not be on hold and will be governed by the new classification and priority rotation established during the review of the existing policy (Reference 2). Five classes will now comprise the queue system: Class I (US Educational), Class II (US Government), Class III (US Commercial), Class IV (International Educational), and Class V (International Government/Industry). The flight assignment priority will be established such that every other payload will be from Class I, in other words as follows: I, II, I, III, I, IV, I, V.

GAS Hardware Upgrades

NASA is in the process of upgrading some of the GAS hardware that has been in service since the inception of the program. The lower end plate of the GAS canister, known as the Instrumented Electronics Plate (IEP), contains the electronics that provide control of the payload power. The components that comprise this system, including the GAS Control Decoder (GCD) are being upgraded to a digital interface to the crew laptop, or PGSC. The functions and services provided to the customer will essentially remain the same; however, the GAS team will be provided with some housekeeping data that was not previously available. It is conceivable that this additional data, including temperature, pressure, and more accurate relay status information, could be made available post-flight to GAS customers.

Changes to GAS Safety Requirements

The basic safety certification process for GAS payloads, as it is presented to the customer, will not be much different than it has been in the past. GSFC continues to be the advocate for the GAS customers in obtaining safety approval for flight aboard the STS.

The primary focus of recent changes in documentation and requirements for safety involves emphasis on improved communications; both between the GAS project team and the customer, and between GSFC and the Shuttle Program centers, Johnson Space Center (JSC) and Kennedy Space Center (KSC). In the coming months, customers will be seeing improved safety help documentation, including a more clearly defined schedule

of required documentation within the approval process. A Memorandum of Agreement (MOA) is being established between the three NASA centers that are involved with processing GAS safety that will streamline the process and provide a smoother flow of information between all parties.

GAS Documentation

The GAS Experimenters Handbook, last updated in 1995, has remained essentially the same since early in the program's history. The GAS safety manuals and guidelines have been through several iterations over the years. With the increasing availability and convenience of the Internet as a media tool, a revision to the handbook at this time will be centered around providing an on-line users guide, with available hard-copy versions. Safety reference documentation will be integrated within the handbook to emphasize the importance of safety within a project's development.

Changes Within Goddard Space Flight Center

GSFC has undergone some organizational changes within the last two years that have had an impact on GAS. As part of an initiative to redefine the role of Wallops Flight Facility (WFF) as part of GSFC, project management and engineering support to the GAS Program began transitioning to WFF in late 1997. By the year 2000, most of the functions for the GAS and SEM programs will be performed at WFF. For GAS customers this means that some familiar names and faces have and will be changing. However, with GSFC's ever increasing commitment to being a customer-focused organization, it is our desire that any organizational impacts within the Center not affect the level of assistance offered to the GAS customer.

SUMMARY

Despite the changes summarized in this paper, the GAS Program continues to receive the support from NASA Headquarters as a viable method of providing low-cost access to space for a diverse user community. It is the hope of the GSFC GAS project team that our customers continue to find the program a worthwhile endeavor.

REFERENCES

1. NASA 14 CFR 1214.9, Use of Small Self-Contained Payloads
2. Memo from J. Rothenberg, Code M AA for Space Flight, to the NASA Administrator, *Review of the NASA Small Self-Contained Payloads (SSCP) Program*, dated September 16, 1998.

Figure 1: GAS Payloads Flown (By Year)
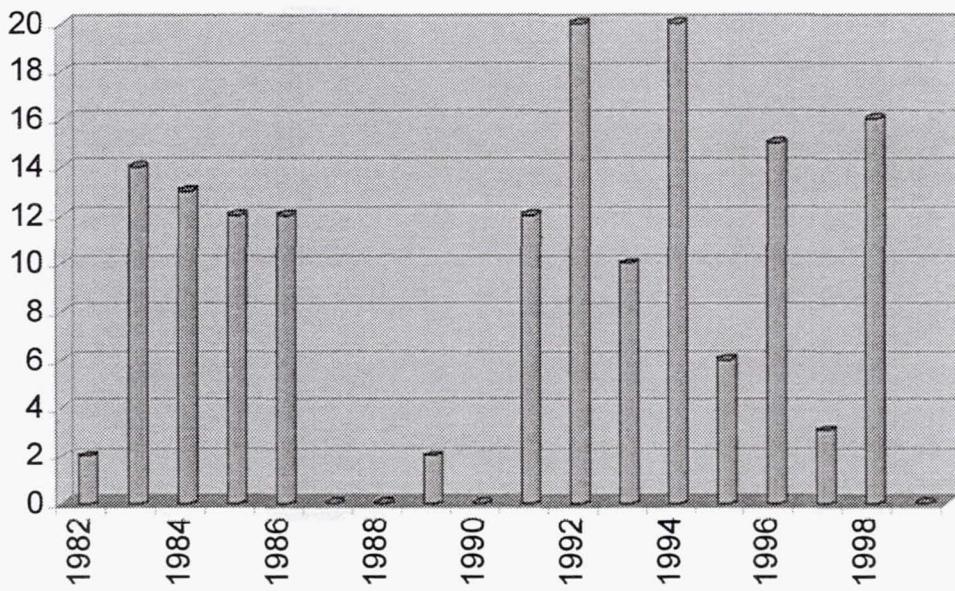
Figure 2: GAS Payloads Flown (By Class)
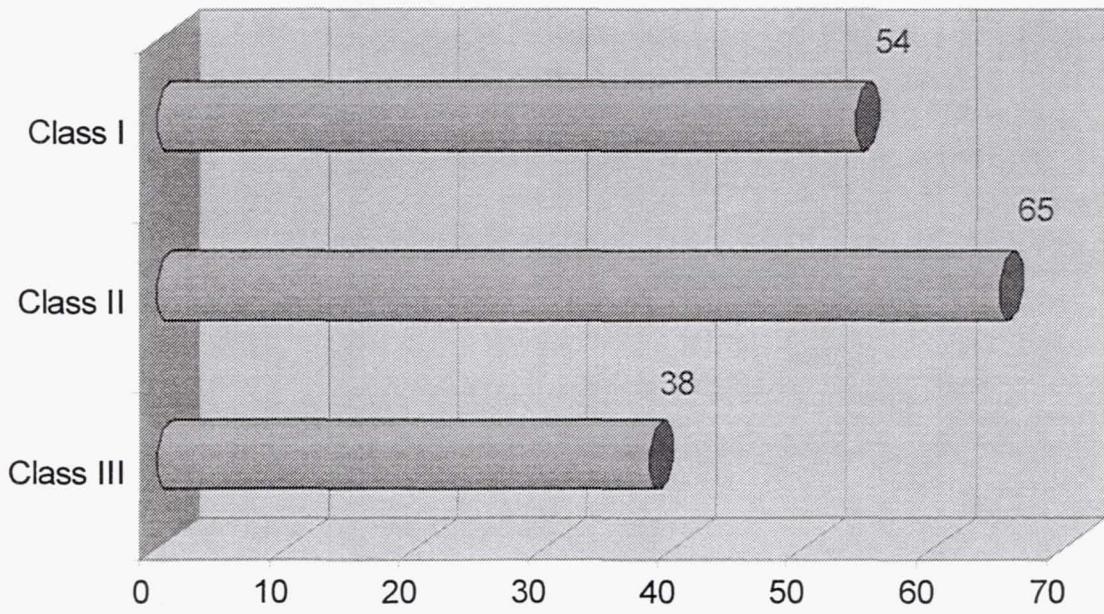
Page intentionally left blank

EFFECT OF GRAVITATIONAL ACCELERATION
ON CARDIAC DIASTOLIC FUNCTION

The Hearts In Space Project, 1985 to 1999
NASA Get Away Special Payloads G-572 (STS-85)[1] and G-779 (STS-95)[2]

Principal Investigators:

Thomas E. Bennett, Ph.D., Department of Biology, Bellarmine College, Louisville, KY
George M. Pantalos, Ph.D., Departments of Surgery and Bioengineering, University of Utah,
        Salt Lake City, UT
M. Keith Sharp, Sc.D., Department of Bioengineering, University of Utah, Salt Lake City, UT

Principal Student Investigators:

Bellarmine College: Thomas Schurfranz
University of Utah: Scott Everett, Kevin Gillars, Sean O'Leary, Rich Lorange, Stewart Woodruff
Utah State University: Mark Lemon (Dr. Jan Sojka, faculty advisor)

Introduction

After nearly 14 years of development, the Hearts In Space experiment has completed two orbital flight opportunities on board the Space Shuttle Discovery. The first opportunity was the 12 day flight of the STS-85 mission in August 1997 and the second opportunity was the 9 day flight of the STS-95 mission in October/November 1998. The experiment, which is a collaborative effort between students and faculty at Bellarmine College (Louisville, KY), the University of Utah (Salt Lake City), and Utah State University (Logan) to study the effects of gravity on cardiac function, has been a qualified success as some, but not all, of the data collection was achieved. All of the temperature surveillance data, vital to monitoring the environment and function of the experiment, was collected for both missions. Failures in the power distribution circuitry of the experiment has limited the amount of blood pressure and blood flow data acquired on both flights. However, the hemodynamic data that has been collected lends strong support to the hypothesis that the gravitationally dependent, intraventricular hydrostatic pressure difference contributes to the filling process of the heart and that its absence in weightlessness may result in reduced cardiac filling and ejection with each heart beat.

Project History

This project began in 1985 with a contest for high school students called Project Challenge sponsored by Kentucky Tomorrow Foundation. Students submitted descriptions of experiments to be judged for inclusion in a NASA Get Away Special canister. One winner, who enrolled at Bellarmine College, proposed to investigate the function of a total artificial heart in microgravity. Advice was sought from the Artificial Heart Laboratory at the University of Utah and a partnership began with their faculty and students. Several years later faculty and students at Utah State University joined the team bringing their expertise in GAS canister development. Thus began an interdisciplinary, intercollegiate partnership dubbed the Hearts in Space project. Dozens of students from the three institutions have participated in the design and development of the Hearts in Space experiment. Numerous other individuals, corporations, and institutions have provided materials, instrumentation, technical advice, support services, and monetary grants to the project over the past 14 years.

Scientific Background

The investigation of cardiovascular adaptation to space flight has seen substantial advancement in the last several years. In-flight echocardiographic measurements of astronaut cardiac function on the Space Shuttle have documented an initial increase, followed by a progressive reduction in both left ventricular volume index and stroke volume index with a compensatory increase in heart rate to maintain cardiac output. To date, the reduced cardiac size and stroke volume have been presumed to be the consequence of the reduction in circulating fluid volume within a few days after orbital insertion. However, no specific mechanism for the reduced stroke volume has been identified. This investigation used a hydraulic simulator of the cardiovascular system to examine the possibility that the observed reduction in stroke volume may, in part, be related to fluid physics effects (i.e. hydrostatic pressure) on heart function.

Many factors influence the filling of the heart during diastole. These factors include (1) the atrial pressure, (2) the inertia of the blood as it enters the ventricle, (3) the transmural pressure difference, (4) the myocardial compliance including myofibril passive, elastic recoil, and (5) the gravitational acceleration-dependent hydrostatic pressure difference that exists in the ventricle due to its size and anatomic orientation. This pressure gradient, which can be estimated to be 6660 dynes/cm^2 ($\approx$ 5 mm Hg) in an average adult, acts to augment the diastolic filling of the heart. The team of investigators have hypothesized that the absence of this contribution to the ventricular filling process in the microgravity environment of space flight may account, in part, for physiological factors that would act to reduce cardiac filling and consequently result in a reduced stroke volume.

Payload Development

The first functional circulatory simulator (phase 1 design) was flown aboard NASA's KC-135 aircraft in August 1992. The circulatory components (wt 160-lb) were laid out in a horizontal configuration (Figure 1) with the artificial heart mounted so that it could operate in either a 45° anatomic orientation or in a 0° horizontal (null-G) orientation. The heart controller, data recorder, and other support instrumentation were mounted in a 5-foot tall equipment chassis (wt 440-lb). The results from the flights demonstrated that a hydraulic circulatory model would function during the 20-second interval of microgravity provided by the parabolic trajectory of the airplane and that the data collected

established preliminary proof of concept. Over the next five years, a total of fourteen experiments on board the NASA KC-135 aircraft along with numerous ground tests, including shake table testing and cold room testing, would be needed to develop a self-contained, fully automated, orbital version of the experiment that met the size, weight, and safety requirements for a Get Away Special canister.

Payload Description

The final experimental apparatus (Figure 2), which was affectionately called 'Art Heart', consisted of a pneumatically actuated, elliptical artificial ventricle (UTAH-100 human version left ventricle) connected to a closed-loop, vascular simulator circuit with adjustable compliance and resistance elements to create physiologic pressure and flow conditions (Figure 3). A 40% glycerin in water solution was used in the simulator circuit to simulate the viscosity of whole blood in the 20° C to 40° C temperature range. The ventricle was powered by a miniaturized controller originally developed for use with clinical artificial heart recipients. Ventricular instrumentation included high-fidelity, acceleration-insensitive, catheter-tip pressure transducers in the apex and base to determine the instantaneous ventricular pressures and ΔP_{LV} across the left ventricle ($LVP_{apex} - LVP_{base}$). The ventricle was also instrumented with pressure transducers immediately upstream of the inflow valve in an artificial atrium and downstream of the outflow valve, and an ultrasonic transit-time flow probe downstream of the outflow valve. Acceleration was sensed by a miniature accelerometer and the temperature was monitored at three key locations in the experiment and digitally recorded on an ambient temperature-recording unit. A heating element was incorporated into the hydraulic circuit to establish and maintain the temperature in the operational range of 20° to 40° C. The experiment was wrapped in a thermal-insulating blanket of Nomex® felt with a Beta cloth cover. A bi-directional roller pump was used to inject or withdraw fluid from the hydraulic circuit to create different preload conditions for the artificial ventricle. The experiment was microprocessor controlled with analog signals stored on a seven-channel FM data tape recorder that could provide up to three hours of continuous recording. Power for the experiment was provided by an array of alkaline batteries in a sealed battery box (Figure 4).

Payload Operation

The experiment flight plan called for GAS Control Decoder (GDC) Relay A to be activated (hot) by a baroswitch to initiate the temperature monitoring portion of the experiment about two minutes into the launch phase at an altitude of 70,000 feet. The temperature monitoring is continuous throughout the mission until GDC Relay A deactivation (latent) just prior to planned re-entry. Orbital operation of the experiment is initiated by a crewmember as early as possible into the mission by the activation of GDC Relay B (hot). Initially the control algorithm checks the temperature of the experiment. If the temperature is below the pre-set value of 20° C, a heating cycle is started using the heating elements in the fluid circuit. The artificial heart is turned on every ten minutes during the heating cycle for a few beats to circulate the fluid and distribute the heat around the simulator fluid circuit. Performance of the experimental protocol is initiated once the minimum operational temperature has been established. By experimentally varying the circulating fluid volume in the hydraulic circuit, ventricular function can be determined for varying preload pressures at a regulated, afterload (aortic) pressure of 95 mm Hg. This variation in preload condition will permit the construction of a ventricular function curve for the microgravity environment to be compared to a ventricular function curve constructed from data recorded pre-flight in the 1-G environment. If the proposed hypothesis is true, there will be a parallel shift to the right of the ventricular function curve of approximately 2 mm Hg for the microgravity condition.

Mission STS-85: Orbital Flight of G-572, August 7-19, 1997

Integration and Launch Activities

The successful completion of pre-launch preparations or integration required extraordinary effort by the team members and supporting organizations to overcome critical technical problems that arose in the final days of preparation. A uniquely customized, factory-modified circuit board for the flow probe shorted out during integration and had to be rebuilt and replaced. Integration, which began in April 1997, could not be successfully completed until a second trip to the Kennedy Space Center in May. Fortunately, NASA's re-scheduling of STS-83 to July moved the launch date for STS-85 back by one month, permitting enough time to complete the integration process on the Hearts In Space experiment while staying assigned to the STS-85 mission. Over 100 family, friends, and supporters of the Hearts in Space project traveled to KSC to watch the launch of Shuttle Discovery on August 7, 1997. Many more individuals followed the launch on NASA Select TV back at the three campuses. There was quite a bit of media coverage about Hearts in Space throughout Kentucky, Utah, Florida, and surrounding states.

First Orbital Flight Results

Early post-flight evaluation during de-integration of the experiment indicated that the experiment did function as planned and withstood the flight in good condition. Valuable temperature data was recorded throughout the mission which, when examined in detail, revealed further evidence that the experiment had performed as planned (Figure 5). However, the primary data tape recorder failed to receive sufficient power to operate shortly after the experimental protocol was initiated. Therefore only a limited amount of the pressure and flow data needed to test the hypothesis was recorded. The data that was acquired was analyzed and resulted in one data point to the right of the plot of the 1-G cardiac performance data recorded prior to launch (Figure 6). Although not statistically significant this single data point does fall within the predicted area and thus supports the hypothesis that gravitational effects help to fill the heart in 1-G.

Once the experiment returned to the laboratory, it was possible to determine that the data recorder stopped operating due to the failure of a connection in the electrical pathway that carried power from the batteries sealed in the back of the experiment to the primary data recorder. It was also detected that a key battery may have been at lower than nominal voltage and that there was a previously unrecognized cold temperature sensitivity of certain electronic components. These problems were corrected by: (1) improving the procedure for securing all electrical connectors, (2) re-testing all batteries under loaded conditions before sealing the battery box, and (3) based on the temperature data, requesting that the experiment be turned on during the first 6 hours of flight when the temperature of the entire experiment would be above 20° C.

Encouraged by the performance of the experiment and the data obtained during the first orbital flight, preparations were initiated for a second shuttle flight to acquire the rest of the needed pressure and flow data. An assignment to re-fly the experiment as G-779 on STS-95 in October/November 1998 was received in April 1998. Thanks to a generous grant from Jewish Hospital Heart and Lung Institute in Louisville, KY covering the launch fee, shipping costs, travel expenses and other items, we were able to rapidly accept a flight manifest on what was to become an historic flight.

Mission STS-95: Orbital Flight of G-779, October 29-November 7, 1998

Integration and Launch Activities

Pre-launch integration activities went fairly quickly the second time. The only slowdown was caused by the need to disassemble a fuse housing within the battery box so the safety engineer could visually inspect each fuse. Since there were no major design modifications performed after the first flight and all mechanical and electrical components were the same, getting re-certified for flight was almost routine. The presence of Senator John Glenn as Payload Specialist 2 on this flight made this launch very media intense and added an extra air of excitement. One drawback was the very limited number of launch passes available to family and friends. Nevertheless, another large contingent of Hearts in Space supporters was on hand to witness a most spectacular launch of the shuttle Discovery. The media coverage for our project was impressive with both Louisville and Salt Lake City television crews live at KSC. Riding the coattails of Astronaut Glenn, caused Hearts in Space (as well as all the other payloads on board) to be mentioned on several national news broadcasts.

Second Orbital Flight Results

Post-flight inspection during de-integration of the payload indicated that the experiment once again arrived back from the flight in good condition. The tape counter indicated that it had advanced during the flight although not as much as we anticipated. An analysis of the digital temperature recording unit revealed three channels of temperature data throughout the duration of the orbital mission (Figure 7) which indicates normal operation. When testing the voltages of each battery it was discovered that most of them were still at full charge instead of being drained as expected. A protocol restart signal was given to see if the payload would begin to run; but nothing happened. We had good batteries but no voltage to the computer that initiates and runs the control algorithm. Upon disassembly back at the laboratory a blown capacitor was discovered on the main power distribution circuit board. When a new capacitor was soldered in replacing the bad one, the system responded to activation of GDC relay B and began operation normally. Thus the premature shutdown of the experiment in orbit was due to the failure of that capacitor. The reason why the capacitor blew out is still unknown.

Since the tape recorder had advanced during the flight, a detailed analysis of the data on the tape was undertaken. The tape shows that the experiment started as planned, found the temperature of the system within acceptable range, started the heart pumping, and began recording pressure and flow data to the tape. After a short period of time, the tape becomes blank (was never recorded on) indicating the time the capacitor must have blown and shutdown the experiment, except for the independent temperature recorder. Data analysis of the recorded part of the tape produced several distinct clusters of physiologic waveforms recorded in microgravity that yielded 6 discrete data points on a cardiac function curve (Figure 8). The zero-gravity data is at the full-fill, full-eject physiologic region at the upper end of the function curve. These 6 data points are right-shifted from the 1-G data line and fall within the region predicted by the hypothesis. Although incomplete, this limited data set is strongly supportive of the experimental hypothesis, at least at the upper end of the graph.

Conclusion

The investigators are convinced they are close to proving their hypothesis but recognize that they must have a much larger data set with 2-3 replicates of each point along the curve for proper statistical analysis. This is what the experiment should produce when it runs to completion. Therefore, we have submitted a request to be manifested for a third shuttle flight in order to complete the data collection and to rigorously test the experimental hypothesis.

Lessons Learned. The Hearts in Space Project, 1985 to 1999

1. The folks at NASA are your friends especially the staff of the Get Away Special Division of the Goddard Space Flight Center Shuttle Small Payloads Projects Office. Your payload manager is on your side and wants your project to succeed. He/she will work with you during each step of the process.

2. Plan on spending more time on paper work than you originally budget. The PAR and SDP will be meticulously gone over, word-by-word (and I thought the IRS was tough…). Do not be afraid to ask someone who has gone through the process for advice to avoid potholes, pitfalls, and reinventing the wheel. Who knows you might even get a collaborator and make a new friend.

3. Solve your problems on paper before your begin construction. It saves both time and money. This is where the PAR and SDP can really help you focus your ideas. Bounce your ideas off others.

4. It helps to have a generous sponsor but you can do a whole lot by asking companies for parts, secondhand equipment, free services, or loaner items. Always acknowledge your donors prominently.

5. Encourage media coverage of your project. Have your school or organization write press releases and contact local media outlets. Positive press will get students and your campus interested. It can help you when you seek funding if a sponsor has heard about your project.

6. For payload integration, have duplicates of all mission critical components with you in case a primary system fails and needs replacement. Murphy's Law is true and universal.

7. Locate all fuses, diodes, etc. in an easily accessible location for quick replacement and ease of inspection for the safety engineer.

8. If space, weight, and power limits allow, build in redundant data recording systems.

9. Do not arrive at integration with an overweight payload!

10. Finally, be patient and have a sense of humor. It never works perfectly the first time. Relax and enjoy life.
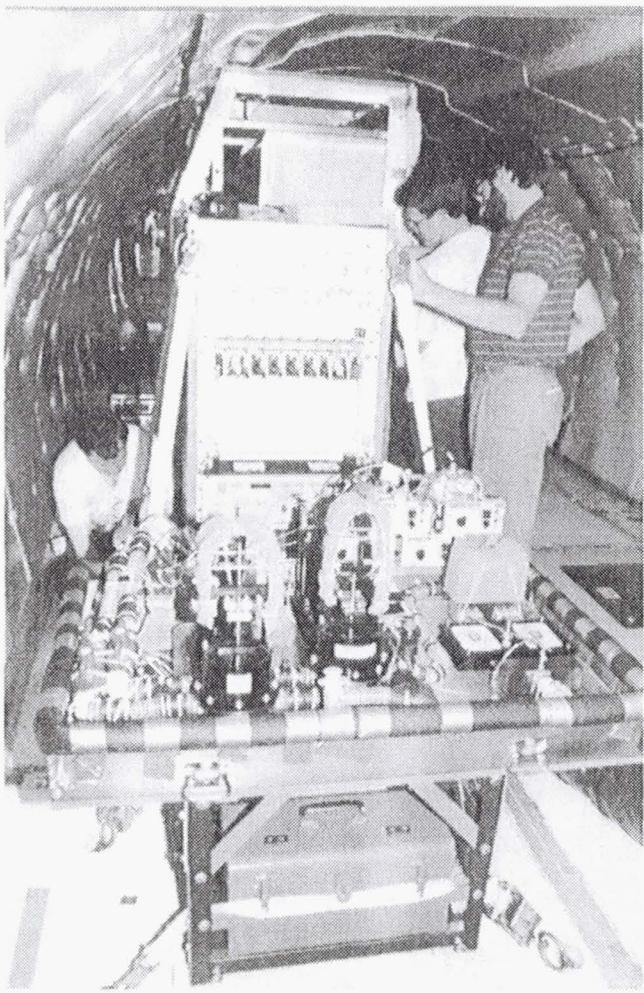
Figure 1. Photograph of the first design of an artificial heart driven, mock human circulation and support equipment chassis mounted aboard NASA's KC-135 airplane (August 1992). The total size and weight (over 600 lb) of the two components far exceeds the limitations for space and weight required for a Get Away Special canister.
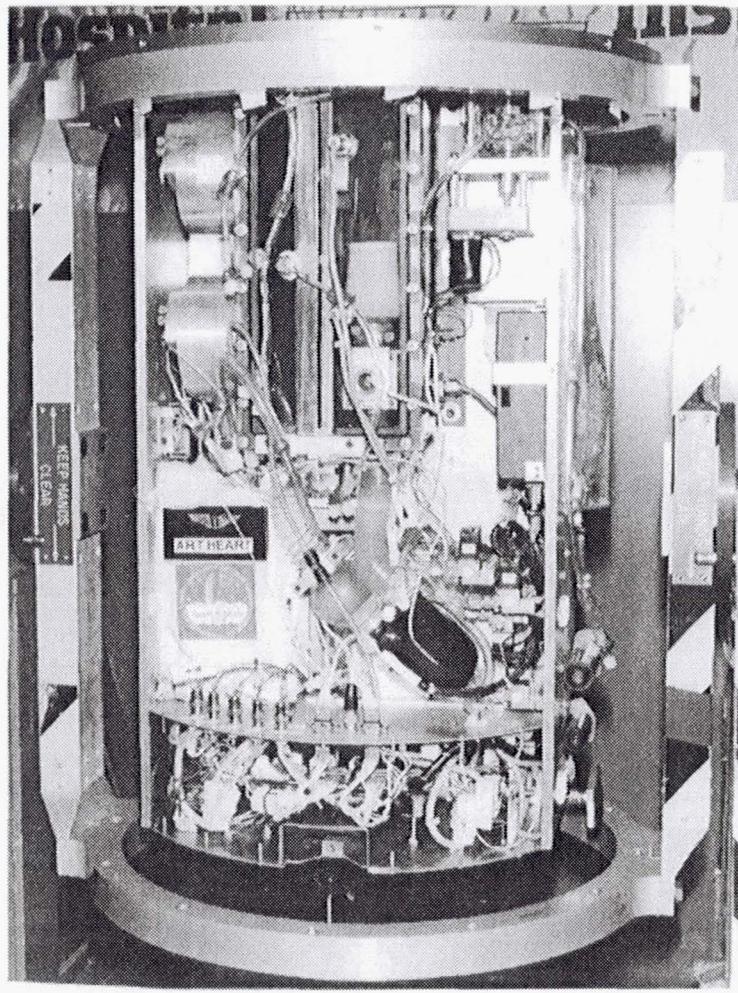
Figure 2. Photograph of the final flight-ready payload affectionately called 'Art Heart' prior to insertion into a Get Away Special canister on STS-95 (October 1998). The experiment weighs 200 lb and occupies 5 cu ft.
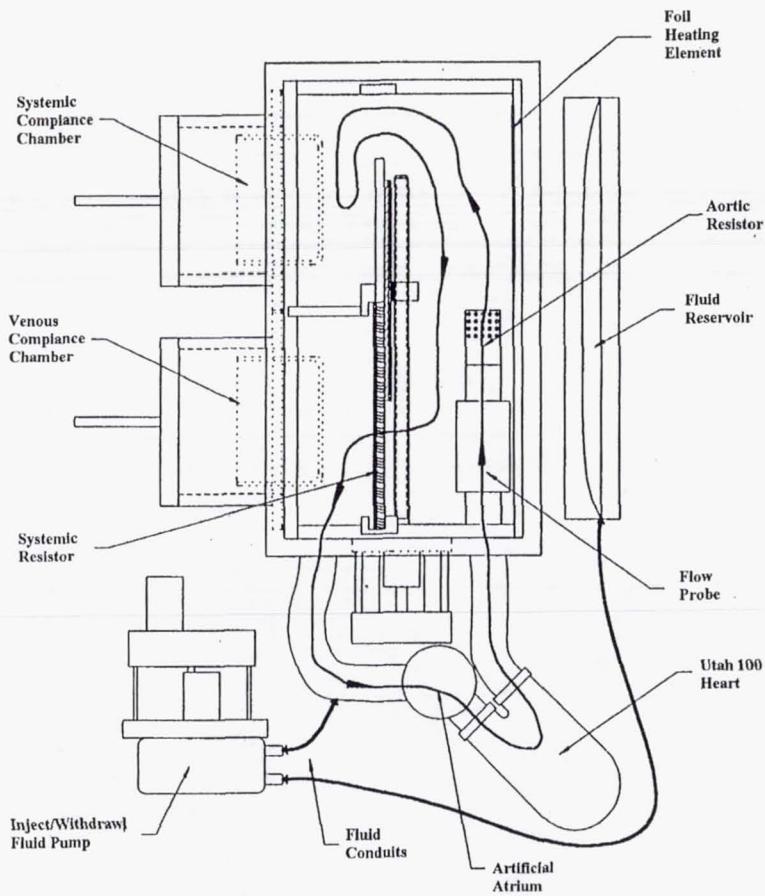
Figure 3. Schematic diagram of the circulatory simulator found in the GAS canister configuration of the Hearts in Space experiment. Key components are identified. (Note: the inject/withdrawl pump is shown out of place for clarity.)

Physical Diagram of Battery Box Contents
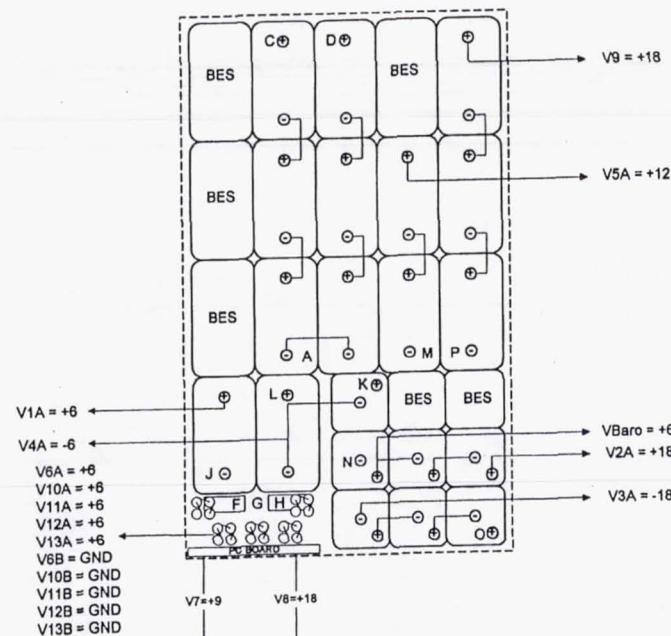
Figure 4. Internal battery configuration as flown on STS-95. Alkaline batteries (Duracell) are arranged in various parallel and series configurations to match the power and voltage requirements of payload components. There are 13 large 6V batteries (MN918), 7 small 6V batteries (MN915), 20 AA 1.5V batteries (MN1500), two 9V batteries (MN1604), and 6 foam battery equivalent spacers (BES) that fill the aluminum battery box.
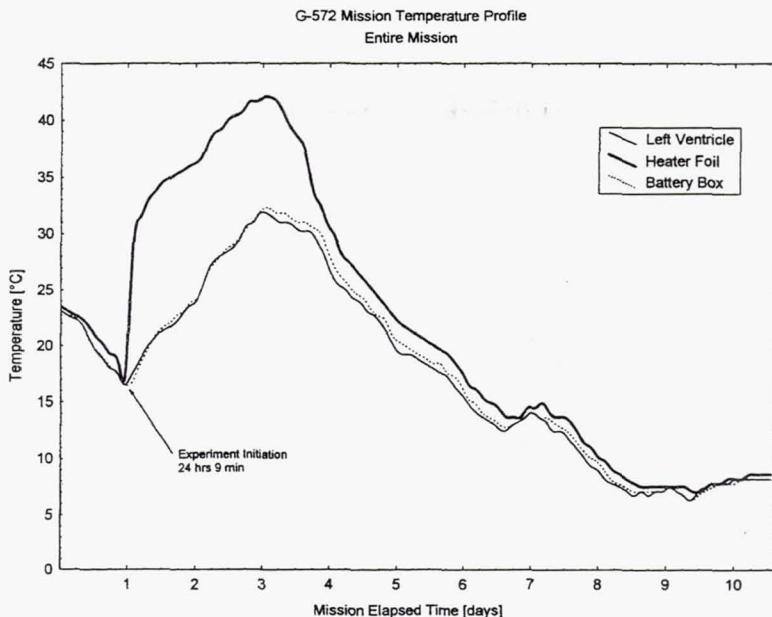
Figure 5. Temperature profiles for the ventricle, heater, and battery box during the first mission of the Hearts In Space experiment, STS-85 in August 1997. When the experiment was turned on at 24 hours MET, the temperature was below the minimum required temperature of 20° C. so heating of the experiment was initiated. After 3 hours of heating, the experimental protocol was initiated, that resulted in a continued temperature increase until termination 48 hours later.
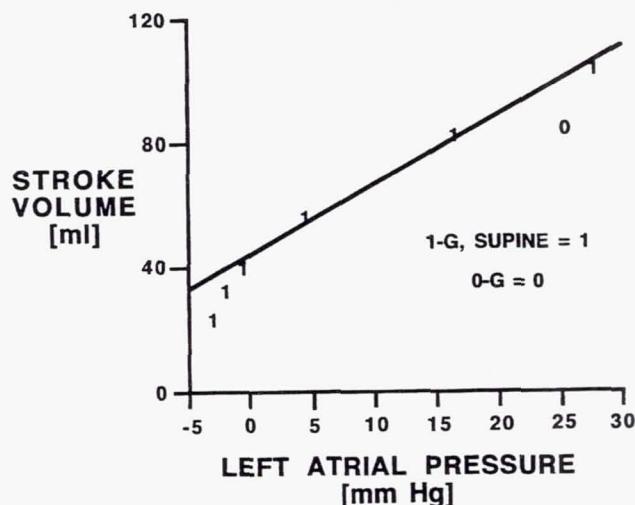
Figure 6. Ventricular function data for the 1-G supine condition (1) and the microgravity condition in orbit (0) during the first mission of the Hearts In Space experiment, STS-85 in August 1997. Consistent with the hypothesis, the microgravity data point lies a few mm Hg to the right of the ventricular function curve for the 1-G condition. This means that the heart requires a greater inlet pressure to achieve the same amount of filling in microgravity than it does in 1-G.

105
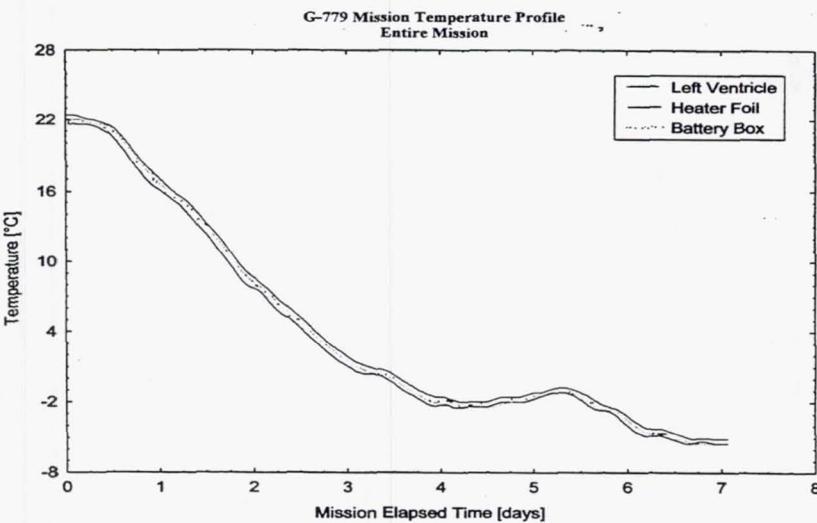
Figure 7. Temperature profiles for the ventricle, heater, and battery box during the second mission of the Hearts In Space experiment, STS-95 in October/November 1998. When the experiment was turned on at 6 hours MET, the temperature was above the minimum required temperature of 20° C. so heating of the experiment was not needed. Since the experiment failed to continue function shortly after the activation of Relay B, heating could not be initiated when the temperature fell below 20° C approximately 12 hours into the mission. Consequently, temperatures slowly continued to fall to nearly -5 °C when Relay A was deactivated after 7 days into the mission.

G-779 VENTRICULAR FUNCTION CURVE
[STS-95]
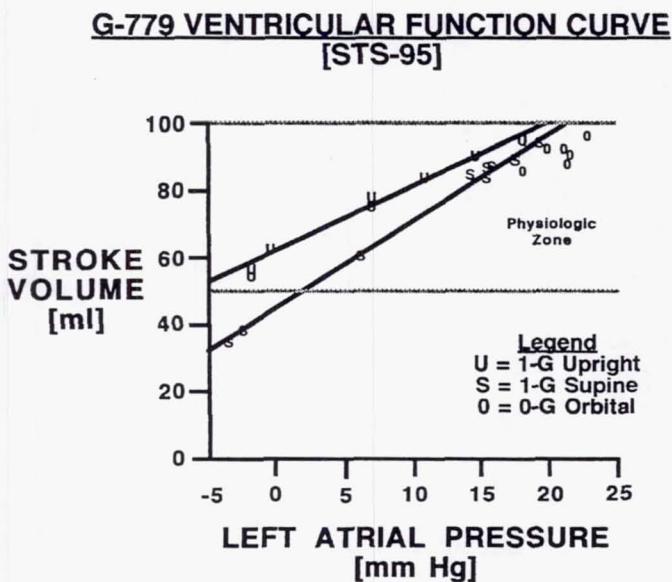
Figure 8. Ventricular function data for the 1-G upright (U), 1-G supine condition (S) and the microgravity condition in orbit (0) during the second mission of the Hearts In Space experiment, STS-95 in October/November 1998. Six complete data sets of blood pressure and blood flow data were successfully recorded before a power distribution failure shut down the experiment. Consistent with the hypothesis, the microgravity data points lie a few mm Hg to the right of the 1-G upright ventricular function curve for the 1-G condition. This means that the heart requires a greater inlet pressure to achieve the same amount of filling in microgravity than it does in 1-G. Also consistent with our hypothesis, the 1-G supine data (which has a smaller hydrostatic pressure to promote ventricular filling) lies in between the 1-G upright and the orbital microgravity data.

106

G-238: DUVAL HIGH SCHOOL'S ROACH *MOTEL*
(A *MICROGRAVITY OPPORTUNITY TO ENHANCE LEARNING* IN PARTNERSHIP WITH LOCAL AEROSPACE PROFESSIONALS)

Carolyn Harden, Aerospace Instructional Coordinator
Romain Deonarine and Kelli Staples, students
DuVal High School

ABSTRACT

In 1991, the National Capital Section of the American Institute of Aeronautics and Astronautics (NCS-AIAA) purchased a 2.5 cubic foot (cu. ft.) Get Away Special (GAS) canister reservation for the students and staff in the Aerospace Technology program at DuVal High School in Lanham, Maryland (MD). Thus began a unique partnership between a public high school and many active and retired aerospace and science professionals in the Washington, DC suburbs of Prince George's County, MD. Over the course of the next seven years, three different sets of teachers, over 75 different students, and more than 60 business professionals worked to develop and refine ideas for an experiment for the canister, design and fabricate the parts, and complete (while constantly revising) the required NASA documentation. In July of 1998, G-238 (DuVal's Roach MOTEL) was offered the opportunity to fly on STS-95, and a group of students, staff, and business partners was present at Kennedy Space Center for the October 29 launch of Space Shuttle Discovery. This long-term and, ultimately, successful partnership can provide a useful model for other schools and businesses who are looking to offer a unique educational opportunity for the students in their community. Our paper details the process as well as the specific information regarding the scientific experiment that flew in the GAS can and the results of that experiment. The paper also attempts to objectively analyze the positive and negative aspects of the experience so that the DuVal school community (or other communities who plan to replicate the model) will be able to learn from and correct mistakes while preserving the successful aspects of the model.

INTRODUCTION

Business partnerships with educational institutions are not new, but are becoming increasingly important (especially at the pre-college level) as education dollars are stretched more tightly. In 1991, the NCS-AIAA purchased from NASA a 2.5 cu. ft. GAS canister reservation for the students and staff of DuVal High School in Lanham, MD. During the next seven years, three different sets of instructors, over 75 different students, and more than 60 volunteer engineers and scientists worked to devise a scientific experiment, design and construct the GAS can components, and complete the required NASA paperwork to bring G-238 to the point that it was ready for launch on STS-95 on October 29, 1998. The effort was truly a learning experience for both the DuVal staff/students and the business professionals who acted as mentors throughout the design, fabrication, and integration of G-238.

BACKGROUND INFORMATION

DuVal High School is a comprehensive public high school of about 1400 students in Prince George's County, MD. The student population consists of approximately 91% African American, 6% White, 2% Asian, and 1% Hispanic. The school is located diagonally across Greenbelt Road (MD Route 193) from NASA's Goddard Space Flight Center (GSFC) and just to the west of a number of aerospace contractors' offices. During the late 1980's, in response to losing many of its talented students to nearby magnet programs and because of its proximity to GSFC and the contractors' offices, the school adopted an Aerospace Technology theme for its curriculum. With the purchase of the GAS can reservation in the

107

1991-92 school year by NCS-AIAA, students began meeting as an extra-curricular club activity two or three times a month to brain-storm ideas for one or more experiments to fly in the canister. During the second school year (1992-93), a dedicated class was formed as a technology education credit (*Independent Studies: Aviation*) and the class became affectionately known as the "GAS class!" The class was taught initially by Mr. William Davis, chairman of the technology education department, and was open to all grade levels and ability groupings of students who wanted to participate. The course's curriculum included elements of science, mathematics, English and technology education. Students worked in teams and had frequent interactions with volunteer consultants from the immediate community of scientific and aerospace professionals. Expenses for the GAS can components and experimental designs were paid in large part by NCS-AIAA, with a small amount coming from the DuVal Aerospace Technology budget (supplied by the county school system) and some in-kind donations of time and materials from the business community. With this continuous support, the groups of students during the seven school years from 1991 to 1998 were finally able to choose an experiment, go through several design phases and scientific investigations, and fabricate many of the components for G-238, which flew on Space Shuttle Discovery on October 29, 1998. The final three years of work (Fall, 1995-Fall, 1998) were directed by Dan Caron, technology education department chairperson, Carolyn Harden, Aerospace Instructional Coordinator, and John Henrici, a technical aide from the county school system's Howard B. Owens Science Center.

PURPOSE

The purpose of sending *Periplaneta americana*, the American cockroach, into space was to determine the effect of the microgravity space environment on the survival of the various developmental stages of the cockroaches and to determine the effects of launch vibrations on the cockroaches. A secondary purpose was to see if exposure to a microgravity environment would significantly alter the subsequent development of the various stages of the cockroach life cycle. Assuming that the cockroaches survive the launch vibrations and microgravity environment of the GAS can, they might pose a threat to future space travelers should they be able to stow away in a cargo container destined for the International Space Station (ISS) or other inter-planetary missions!

HYPOTHESIS

If we seal three adults, three nymphs, and three egg cases in separate compartments of a habitat inside of a GAS canister and provide each compartment with sufficient air, food, water, and life support systems for a journey into space, we expect the cockroaches to return alive. We also expect that our roaches will reproduce on the ground (before lift-off) and, possibly, in space. If the roaches return alive, we will compare and contrast the effect of microgravity on the subsequent developmental stages of the experimental roaches with those in the ground truth model.

PROCEDURE

A large number of steps and a much longer-than-anticipated time frame preceded the STS-95 launch opportunity. Students in the early 1990's had initially chosen three experiments to fill the GAS can: an experiment to test the tensile strength of metals; a seed germination experiment; and the cockroach experiment. As the students started designing the necessary components for all of the experiments, they soon realized that there wasn't enough space in the 2.5 cu. ft. canister for three experiments. Also, weight became a determining factor since we were limited to a total weight of 100 lb. (excluding the NASA experiment mounting plate). The first experiment that was eliminated was tensile strength of metals. The second experiment that was eliminated was seed germination, since the students had a difficult time trying to engineer a way to "plant" the seeds just before lift-off. The last experiment dealt with roaches and, because of the human interest factor, it was the one experiment that the students chose to keep.

After the roach experiment was chosen, students had to determine the amount of food, water, and air necessary for the survival of the roaches for the three months on the ground prior to launch, the length of time of the shuttle mission, and a period of about one month after the shuttle landed and before the

canister was returned to us. A retired entomological technician from Beltsville Agricultural Research Center helped students in the earlier years develop and perform the scientific experiments to determine these requirements. Students also had to determine how much g-force the roaches could withstand to be sure that they had a good chance of surviving launch acceleration forces. Additionally, students devised experiments to determine the optimum temperature range and critical extremes of temperature for survival of the roaches.

Progress was slow because, during the first three years of the dedicated GAS class, the class was taught individually by two different technology education teachers who had little knowledge of the life science parameters of the experiment. In the fall of 1995, under a team-teaching classroom partnership with a person well-versed in engineering design (Mr. Caron) and a former biology teacher (Mrs. Harden), the students were divided into teams to maintain the roach colony and verify the previous years' experimental results on the roaches (Life Science Team); configure the habitat, battery box, etc. (Structural Engineering Team); and determine the amount of power needed to run the equipment and keep the roaches at a constant temperature (Electrical Engineering and Thermal Teams). A Public Relations Team was charged with publishing regular newsletters, handling all communications to companies and consultants, and maintaining accurate records.

As the individual components were designed, they were put through rigorous tests. First, the habitat went through several different designs and tests, using different materials and compartment configurations. Second, a thermal analysis was performed to determine how much battery power would be needed to power the thermofoil strip heaters which would keep the habitat compartments at a constant temperature during the mission. These calculations were constantly modified as possible flight opportunities were offered and then withdrawn by NASA, since each different shuttle mission had a different thermal profile (depending upon the primary payloads manifested on the mission). Additional computations were performed to determine the amount of battery power needed to run a video camera which recorded events in the canister for two minutes every four hours during the mission. Third, we performed a "dry run" which consisted of an enclosed habitat with six roaches (three adults, three nymphs) and three egg cases, food, and water sealed in a plastic dissection animals' tub from June-September, 1997. At the end of the summer, a total of 75 roaches were counted in the habitat compartments!

After several design modifications, we agreed on the final flight hardware design. Many of the flight hardware components had to be fabricated at NASA/GSFC or at a private machine shop due to a lack of precision instruments at the school. Mr. Henrici's flexible work schedule (as a non-classroom-based employee) was essential to the timely accomplishment of the off-site work.

Our next challenge was to get assigned to a shuttle mission. This involved completing several required documents for NASA--the Payload Accommodations Requirements (PAR), the Preliminary Safety Data Package (PSDP), and the Phase 3 Safety Data Package (SDP). We were initially manifested on STS-91 (May, 1998, launch) and then moved to STS-88 (December, 1998, launch) when Johnson Space Center was dissatisfied with some parts of our SDP. We continued to work out the problems with our SDP and finally, in early July of 1998, we were offered an opportunity to fly on STS-95 which was scheduled to launch on October 29, 1998. We gladly accepted this launch invitation since it was considered to be a high-profile mission (Senator John Glenn's return to space). Several students from the Spring Term, 1998, GAS class participated in the integration of the canister at DuVal and GSFC for a portion of their summer vacation during the last week of July. These same students were also invited to the launch at Kennedy Space Center and had all but personal expenses paid by NCS-AIAA and the school system.

RESULTS

We feel that the Roach MOTEL Project was a success, even though the numbers of returning roaches (alive and dead) did not approach the numbers counted in our dry run habitat during Summer, 1997. There were two space roaches left alive in the nymph compartment when the GAS can was opened on December 8, 1998 during de-integration. This marked the first GAS can experiment involving insects which had returned live specimens from a space shuttle mission! One of the roaches had molted into adulthood and was identified as a male. The other roach was still in the nymph stage, and its sex could not be determined by examining external anatomy. In mid-January, 1999, the nymph survivor died before molting into an adult. The adult male is still alive and strong. In addition to the two original survivors,

there were 28 bodies and one partial carcass left in the flight habitat. Very little food (dog bone biscuits) mass had been consumed in the food cases by the roaches (Table 1) and a much smaller-than-expected quantity of water had been consumed or had evaporated from the water vials (Table 2). Examination of the water vial wicks indicated that at least one vial's wick in the nymph and adult compartments was not functioning as designed; therefore, it is assumed that the roaches were unable to get sufficient water and thus died of dehydration before launch. Videotape retrieved from the camera at deintegration also seemed to confirm that there were dead roaches in each compartment when the camera started recording activity in the habitat compartments during the mission. Another possible reason for the less-than-anticipated number of roach survivors may have been due to an insufficient amount of humidity in the can. As a result of the need to balance weight in the shuttle cargo bay, our experiment was placed in a 5.0 cu. ft. canister rather than in a 2.5 cu. ft. canister. This gave us a greater supply of air than needed for the roaches but also diminished the humidity in the canister.

The roaches in our original ground control habitat (set up in August, 1998, following integration of the flight unit) all died in a matter of days because the water vial wicks apparently soaked up the glue which held the wicks in place; the roaches, therefore, were unable to get any water. Our second ground control habitat (set up in mid-October) consisted of three adults, two nymphs, and one egg case. (We did not have enough nymphs and egg cases left in the population, so we were unable to make an exact ground truth replica of the flight unit.) The five roaches all survived but the egg case didn't hatch. The ground control unit was sealed up just before lift-off and, since the number of roaches in the habitat was less than the number loaded into the flight unit and the time of containment was different, we cannot scientifically compare the space roaches with the ground control roaches. Following the death of our surviving nymph, we added one of the ground control nymphs to the cage with the space-surviving adult male roach. In early April, 1999, the nymph molted into an adult and it's external characteristics appeared to indicate that it was a female. However, since no egg cases were produced by July (3 months), it would appear that both roaches are males! This means that we are unable to breed any hybrid space roaches without bringing in a new population of female roaches.

LESSONS LEARNED

As a result of this long-running partnership between our high school and the aerospace and science businesses, we have identified several problems that future experimenters may want to consider before embarking on a similar project. First, over the course of the seven-year period, we experienced three turnovers in the GAS class staff in the high school (due to retirements). This created a problem with continuity since there was a less-than-ideal paper-trail left by the two staff members who initially directed the effort from 1992-1995. Also, since the staff had retired, they were not always immediately accessible when we had questions about previous work done, calculations, etc. (A similar problem was experienced with some turnover in our volunteer consultant ranks as they changed job assignments and, in some cases, moved out of the area.) Second, we had an in-house problem in defining clear job descriptions or specific responsibilities for the three DuVal staff members involved in the final stages of the project. Third, none of the current nor former staff members had ever worked on a Get Away Special payload for NASA and we had no concept of the degree of effort involved in designing an experiment to fly on a manned mission under NASA's understandably strict safety constraints. We were assisted in large part by former GAS experimenters Michael Dobek and Stan Spencer from Sierra College in California and Dr. Stuart Ahrens (now retired) from North Carolina State A + T University who provided us with examples of their schematic drawings, pictures of their flight hardware, and/or copies of their PAR and SDP documents to act as models for us.

Student turnover in the class was another problem that was experienced until the school adopted a "4x4 Block Schedule" in the 1995-96 school year. In addition to providing 87-minute periods for each class, it also expanded the student elective opportunities (outside of the 21 credits required for graduation) from three elective courses to 11 elective courses over the student's four-year program. This allowed students to elect GAS class a number of times and remain with the program from year to year. Although time constraints within the day were eased greatly with the expanded 87-minute period, we still experienced problems with having to terminate work at the end of the class period rather than continuing to work on the

project throughout the day (as an aerospace engineer would be able to do at NASA or a private company). Also, the interruptions of weekends, school vacations, "snow days," etc. broke the work flow and frustrated our volunteer consultants who were used to working a project through to completion without regular work stoppages! And, lastly, there are many difficulties with trying to fly a life science experiment in a GAS canister due to the amount of time that must be planned for the experiment to be self-sufficient following integration and prior to lift-off (approximately three months) and during the one-month lag after the shuttle returns before the experimenters receive the sealed GAS can for de-integration. If we were to attempt a second GAS payload, we would probably try to avoid another life science experiment --unless we attempt to correct the faults of G-238 and fly the improved payload for better results!

CONCLUSION

Based on the experimental results, we conclude that *Periplaneta americana* is able to survive the launch accelerations and the exposure to microgravity for a period of nine days (the length of the STS-95 mission). We are unable to conclude whether the exposure to microgravity has any effect on the subsequent developmental stages of the cockroaches because we were unable to breed the two survivors before one of them died. Further studies would be necessary with a new experimental population of roaches and redesigned water-delivery tubes on another shuttle mission.

From the perspective of the staff and students of DuVal High School, we feel that the partnership with NCS-AIAA and the many volunteer engineers and scientists from the near-by aerospace and agricultural research communities has had a very positive effect on our school. The students gained a better understanding of how projects are completed in the government or private sector, and our volunteer business professionals gained a greater appreciation for the constraints of time and manpower under which educators have to work! We are also particularly grateful for the leadership role provided by C. David Eakman of The Boeing Company and NCS-AIAA who was with G-238 from start to finish, acting as our overall Project Manager and intermediary in locating consultants in the business community to assist us. We look forward to working cooperatively with the NASA/GSFC community and aerospace company professionals on many other NASA-related initiatives in the future.

TABLE 1: Food Case Results--all measurements in grams (g); dog bone biscuits--2 medium-size bones per food case in the adult and nymph compartments; 1 bone in the egg case compartment's food case; desiccant to retard mold formation in all food cases.

Habitat compartment	Initial mass-dog bone (food)	Final mass-dog bone (food)	Initial mass-desiccant	Final mass-desiccant
Adults	18.54 g	20.67 g	61.31 g	67.71 g
Nymphs	18.95 g	19.61 g	61.31 g	64.00 g
Egg Cases	10.42 g	46.46 g	46.46 g	46.46 g

(Note: Although there was visual evidence that some bone mass had been eaten in both the adult and nymph food cases, the bones apparently absorbed enough moisture to more than compensate for any bone mass consumed. More bone mass appeared to be missing from the adult bones than from the nymph bones--possibly due to the fact that the two surviving roaches in the nymph compartment appeared to have partially cannibalized the nymph that died!)

111

TABLE 2: Water Vial Results--all measurements in milliliters (ml); difference in initial and final amounts equals water consumption or evaporation from the water vials (2-50 ml vials in adult and nymph compartments; 1-50 ml vial in egg case compartment).

Habitat compartment	Initial amount	Final amount
Adult	100 ml	84 ml
Nymph	100 ml	83 ml
Egg cases	50 ml	38 ml

(Note: The wicks of only one vial in each of the adult and nymph compartments appeared to be wicking water.)

G-238: ROACH MOTEL (MICROGRAVITY OPPORTUNITY TO ENHANCE LEARNING) LESSONS LEARNED

C. David Eakman
G-238 Project Manager for the National Capital Section of AIAA
QSS Group, Inc.

ABSTRACT

The National Capital Section (NCS) of the American Institute of Aeronautics and Astronautics (AIAA) sponsored a Get Away Special (GAS) project for DuVal High School that flew on STS-95. As part of the NCS Educational Outreach Program, this project was sponsored to encourage high school knowledge of and interest in aerospace engineering as a career. Although a science return was a secondary objective, a program first by returning a live insect payload for future study thanks to the participating students, facility, and supporting local aerospace engineers.

This paper presents an overview of the program from the perspective of the project manager of the sponsoring organization. It provides lessons learned and practical advice on how to develop similar programs at the high school level. Topics covered include obtaining funding and service contributions, acquiring engineering consulting help, developing the required skill base and facilities at the educational institution, working within the NASA safety requirements, maintaining a reasonable schedule without compromising the educational benefits, and selecting an appropriate educational institution. This paper also describes several potential benefits that can be achieved from this type of program.

BACKGROUND

The NCS of the AIAA sponsored a GAS project for DuVal High School that flew on STS-95 in October of 1998. The experiment studied the effects of space travel on the behavior and developmental stages of Periplaneta Americana or the American cockroach. This specimen was chosen for its adaptability to environmental changes and ability to survive. NASA and aerospace contractor volunteers worked closely with the DuVal faculty to provide basic engineering information, develop a conceptual design, and further assist the students in understanding the experiment.

A video camera periodically recorded the behavior and the development of the adults, nymphs (teenagers), and egg cases of the roach colony. This data was evaluated against a ground control experiment to determine developmental differences affected by launch and zero-g. The total experiment consisted of a thermal control system, a battery power system, a video recording system, and controlling electronics. The design was validated with a prototype habitat experiment that was sealed in a dark space for 5 months. At the end of this time the colony of nine had grown to 75. The GAS can was designed to be modular so future experiments could be inserted with reuse of the support systems.

DuVal High School is located approximately one mile from the Goddard Space Flight Center (GSFC) in Maryland. The school enrollment is predominately minority and suffers a negative reputation, with many good students opting for a competing high school. But with dedicated support from the principal, a group within the facility has worked to turn this situation around, first by striving to get the school reclassified as an aerospace magnet school and second by developing an outstanding program to attract the superior students and encourage their science, math, and engineering skills.

113

RESULTS

Upon opening the canister and removing the Roach MOTEL experiment, it was determined that two of the original three nymphs had survived. The video camera and light system worked as programmed and two hours of videotape was obtained. Analysis of this tape provides insights into the behavior of the roaches while they were in space. One interesting result was that they adapted very rapidly to zero-g and were able to navigate their environment effectively after only a few hours exposure. Although disappointed that more roaches did not survive, the staff and students should be extremely proud that they were the first experimenters to bring back live insects in a GAS payload. A companion paper provides more details about the specific scientific results. I want to focus here on the institutional and human benefits.

First of all, in institution terms, the DuVal aerospace program received a tremendous boost as the class appeared on both the Good Morning America and Today shows, not to mention all local Washington, D.C. affiliates of the major networks. The BBC and Canadian Broadcast System also carried the story. The Washington Post and all of the local newspapers carried multiple articles about the project. A number of television stations and newspapers recorded the event as the canister was opened and de-integrated on Dec. 9 in Maryland.

The GAS project has become the center piece of the DuVal aerospace program. It has allowed the school to obtain additional resources for this program and to become involved with many other NASA and contractor organizations for the future expansion of the program. The number of students enrolled in the DuVal GAS program has tripled since the successful flight of the Roach MOTEL. This bodes well for the future of the entire aerospace program at DuVal.

In human terms, the successes were incalculable. Seven classes (over a hundred students) participated and received valuable problem solving skills and exposure to the fields of science and engineering in an exciting, hands-on process. Several students were persuaded to continue their education to the college level as a result of this class. Numerous personal successes were achieved, for example:
- One junior decided to enter aerospace engineering and the program provided him suffcent exposure to obtain three offers of summer employment from the local aerospace community.
- One parent revealed that her daughter suddenly had a renewed interest in school after having joined the GAS class and she felt sure that the girl would now attend college.

Finally, three of the DuVal High School facility received the 1999 AIAA Educator Achievement Award and were recognized at the annual honors banquet at Crystal City.

LESSONS LEARNED

1. Decide Early How it Will be Integrated into the School Program

Two options exist, a club approach and a class approach. In the former, a club organization meets after regular school. In a class approach, a regular class provides students with credits towards graduation.

The club approach was tried for the first year for the G-238 project with limited success. Most students must leave school on time in order to catch their school buses and obtaining school resources is more difficult. The regular class approach was more successful, but it also had disadvantages. Since at least two years is required to complete such a project, provisions must be made for multiple classes and continuity. The Roach MOTEL solution was to require each class to document the work accomplished each year so as to provide a starting point for the next class. This documentation process was turned into a positive by also requiring some students to present their results to an audience of NCS and NASA people and their parents. We were able to get some high visibility people, such as Joe Rothenberg, the then Director of the GSFC, to participate.

Detailed planning is usually required to incorporate any program into the curriculum with class plans, grading criteria, etc. This usually requires a collaborative approach between both engineering volunteers that understand the process and school facility that comprehend the school system requirements and how to construct such materials for an educational setting. The required lead time must also be considered in developing the project schedule, as numerous levels are usually required to approve new courses.

2. Required School Resources Need Definition and Commitment

Most schools do not realize the extent of their commitment for such a project and the number of unique resources required. It is essential that these issues be identified at the outset and committed to by the school principal and at the school district level.

At a minimum, the teacher must be allowed an additional free period to accommodate the extra coordination load. Technician skills are required to assist the students in performing the "hands-on" work on the project. This person should also have the free time to perform some of the more difficult tasks, to receive training in soldering and other skills to space-qualifications, and to coordinate with outside vendors such as fabrication shops. Depending on the project, additional facility members may be required who have backgrounds in subjects like biology, chemistry, or physics. For the Roach MOTEL, it was found that after the project really got started, we needed at least three facility members to dedicate a significant portion of the school day to keep the project on schedule.

In addition to the numbers of facility and the time allocated for GAS project work, the background and expertise of the selected facility must be adequate. We were fortunate to assemble a great team at DuVal to work the Roach MOTEL. However, this was accomplished only after several false starts and after recruiting one team member to work the program.

Since considerable coordination is required to work with volunteers, vendors, and other contributors, such as prior GAS experimenters, it is essential that direct phone lines, a fax machine, answering machines, and e-mail capability be available to the class. This also allows the students to be more involved in these processes.

A secure and relatively clean space must be provided for the experiment to be constructed. Depending on the school fabrication capabilities, access to some of these facilities may also be required. Although not essential, we found that access to video taping and photography capabilities was helpful in documenting progress and to providing public relations material.

A suggestion for future GAS projects might be to have the sponsoring organization, or even the school district, organize a process whereby a proposal is submitted by each interested school. The winner would be selected based on the proposed experiment, the resources available, and the educational benefits to be derived.

3. Public School Teachers and Engineers Do Not Speak the Same Language

Engineers speak in terms such as Work Breakdown Structures (WBS), waterfall schedules, thermal cycles, and space qualified parts while teachers speak in terms such as cognitive learning, daily lesson plans, and interdisciplinary learning. Engineers are taught to solve physical world problems while teachers are taught to impart knowledge while maintaining discipline in a class of thirty or more students.

Neither is right or wrong, they are just different approaches to the situation. The engineers involved in such a project should be aware of these differences and strive to bridge the gap as much as possible. The tools that we use such as WBS, waterfall charts, and action items need to be introduced carefully. Similarly, the schedule expectations must be kept reasonable as one is working with teachers and students who may have significant other commitments and may not possess the required background to perform these tasks as efficiently as an experienced aerospace engineer. Also, do not forget that education, not schedule achievement is the primary objective. In other words, slow it down!

Aerospace has evolved an extensive set of unique jargon, so care must also be taken to ensure communication is not impeded by using too much undefined jargon. Education also has jargon so the same message could be applied in reverse.

4. Expert Help is Required

Building a GAS project is really like building a small spacecraft. All of the spacecraft functions, with the exception of attitude control and communications, must be incorporated. This means that a structure, power system, thermal control system, and data system must be designed, fabricated, and tested. This only addresses the "spacecraft bus." In addition, the experiment must be designed, fabricated, and tested. The final product must be able to survive, in a functioning state, within the launch and on-orbit environment.

To accomplish the above functions, expert help is required. It is unrealistic to start such a project unless a pool of readily available engineers with experience in space projects is available. Such pools of experts can be found at the NASA centers, in universities with active space programs, and at aerospace contractor facilities. A possible exception might be to use the capabilities of modern communications to provide a "virtual pool" of experts. This approach, however, would require dedication and commitment on both ends to make it work.

Some projects also require specialized expertise and this should be considered when deciding on a project. As an example, for the Roach MOTEL, we required a roach expert (yes, they do exist). We were fortunate to get the assistance of a person recently retired from the Smithsonian and U.S. Department of Agriculture, who had spent many years researching Periplaneta Americana.

An ideal situation for providing expert help is using an organization such as the NCS of AIAA to provide a project manager and to aid in finding additional resources as required. Interestingly, getting volunteers to help with such a project is very easy. Most people are delighted to help with such a worthwhile project.

5. Learn From Past GAS Programs

The GAS project office at the GSFC has documents that describe previous GAS experiments along with points-of-contact. This resource proved very valuable in locating similar projects so that their experiences, and even the designs for various components, could be incorporated into our experiment development.

A unique use of this resource was to provide an unofficial preferred parts list. For example, the video camera that we flew was expensive, about $800, and we needed two to provide a spare. We could not afford to risk testing one of these cameras, so we found a previous GAS experimenter that had successfully flown a similar model and, based on this data, we decided to buy and fly this camera.

6. Keep Students Involved

As mentioned in Lesson 3 above, engineers tend to develop and work to schedules and to put in the required effort to achieve these schedules. A casualty of this process can be student involvement. As schedules are not met, the facility, or more usually the engineering volunteers, start performing the work to maintain the schedule. At times this may be justified to meet a NASA GAS project schedule or to make shipment to KSC for launch.

However, ideally sufficient slack should be incorporated into the schedule to remove the requirement for intervention by the experts. Adequate monitoring of progress towards schedule milestones also tends to prevent this situation.

7. All Schedules Are Closer Than They Appear

NASA schedules for the GAS program are very specific and unforgiving for certain deliveries such as the safety documents and the delivery of the integrated GAS can to KSC prior to launch. Sufficient slack

must be incorporated into the schedule to be certain that these can be met. Again, the capabilities and available time for the participating parties must be considered. The Roach MOTEL project actually missed it's first flight opportunity due to a late delivery of a corrected safety plan. This was partially due to late and incomplete feedback from NASA reviewing personnel. The experimenter must take responsibility for continually monitoring status with NASA to prevent the such occurrences.

Sufficient time must also be incorporated to accommodate failures and rework. On the roach MOTEL, our initial design for the battery box failed the overpressure test and required additional structure stiffening. Luckily we were able to accommodate the rework, but it would have been more comfortable to have a few additional weeks built into the schedule for these types of situations.

8. Budgets Estimation is Difficult

Developing a realistic budget for a GAS project is very difficult as the design must first evolve to a certain point prior developing this budget. In many cases, the involved organizations want a budget number prior to the design work. Also, the amount of donated money and services is hard to determine prior to a formal request.

On the other hand, if the budget estimate is too high, it may kill the project. We found no good solution on the Roach MOTEL project. Luckily, the sponsoring organization, NCS of the AIAA, was understanding and provided some of the required additional funds. We were also fortunate in getting either free or reduced prices on several hardware items and fabrication services. The DuVal High School personnel were very good at obtaining these free or reduced price deals (I was told that this was due to years of practice).

For the Roach MOTEL, we exceeded the original budget estimate by about 50% and this would have been closer to 100% except for the donated items. The budget lessons are that it always costs more than you expect, and one must always ask for vendors to support the project, as people are usually generous for a worthwhile program.

9. Develop a Mass and Power Budget Early

The GAS cans are limited as to allowable mass, and an inexperienced group can easily go over this limit. As soon as a list of components can be developed, the mass budget process should be started. Also a certain amount of reserve should be retained (the Roach MOTEL used 10%).

A related problem is the power budget. Since these payloads rely on batteries for power and batteries are very heavy, developing a power budget is a significant input to the mass budget. The power budget is dependent on two major power requirements: the thermal control required to conduct the experiment and keep the "spacecraft" functioning, and the power required by the experiment itself. Unfortunately, the thermal control power is also determined by the Shuttle attitude profile, which is mission dependent. NASA provides this Shuttle attitude profile, but sometimes very late in the design process. It may be subject to change as the mission itself changes. Protection can be provided by maintaining close coordination with the GAS project office and by incorporating as much additional battery-carrying capability as possible. If a mass problem does emerge late in the design, batteries or sets of batteries can be eliminated. Similarly, if the thermal requirement changes for the worse, the design can accommodate the additional batteries.

Putting this discipline in place early prevents expensive and schedule-consuming rework late in the project development cycle. This is one of those "engineering things" that would be new to the typical high school group, and the rationale must be thoroughly explained.

10. Plan the Public Relations Aspect to Maximinize the Returns

A project such as a GAS can requires a substantial commitment of time and resources. To maximize the total returns for the school system, an effective public relations campaign should be organized. School district personnel that specialize in media should be included in the team. The photography history of the

project development along with press packets explaining the project should be prepared prior to launch. Local newspapers and TV stations should be brought into the process a few months prior to launch so they are prepared to cover the story. A good logo also helps, and we had a great one for the Roach MOTEL, which, incidentally, was designed by the students.

SUMMARY

Developing a GAS project at the high school level is very challenging and requires a lot of dedication from the outside community, including the assistance of experienced aerospace engineers. It also requires a dedicated and committed staff at the high school and support form its management. Finally, it requires sufficient funding to develop the project.

When these conditions are satisfied, the payback can be tremendous. I cannot think of a single other type of program that could have impacted DuVal High School as positively as the roach MOTEL. For the dollars spent, the return was truly amazing. The program worked at DuVal, a largely minority high school, with mostly average students involved. I believe that it could also work well in more specialized high schools one which had a built-in mechanism to locate and encourage the most talented to consider a career in aerospace engineering. I hope that the success of the roach MOTEL will stimulate similar projects at other high schools and increase student interest in aerospace.

Personally, it has been a very satisfying experience and I recommend it to anyone. After a couple of years of rest, I may try it again myself.

For additional information on this project, I direct your attention to a web site where students and their teachers have chronicled their experiences over several years. The internet address is http://analyst.gsfc.nasa.gov/duval/GAS6.html.

118

COLLISIONS INTO DUST EXPERIMENT GAS PAYLOAD: SCIENTIFIC AND TECHNICAL LESSONS LEARNED

Joshua E. Colwell
Laboratory for Atmospheric and Space Physics, University of Colorado at Boulder

Martin H. Taylor
AlliedSignal Technical Services Corporation, Greenbelt MD

Barry Arbetter
Lucent Technologies

Lance Lininger
Lockheed Martin Missiles and Space, Sunnyvale CA

Adrian Sikorski
Colorado School of Mines, Golden CO

ABSTRACT

The Collisions Into Dust Experiment (COLLIDE) is a GAS experiment (G-772) which flew on STS-90 in April and May of 1998. The experiment was designed and built by a student-led team at the University of Colorado's Laboratory for Atmospheric and Space Physics. COLLIDE was designed to study the types of gentle collisions which occur between planetary ring particles and in the early stages of planet formation. The experiment provided the first data on low energy impacts into unconsolidated powders in a microgravity environment. Here we discuss the scientific motivation and results of COLLIDE, and we examine the technical and managerial process of developing a GAS payload with students on a short timescale and with a modest budget.

INTRODUCTION

Surfaces of asteroids, planetary satellites and planetary ring particles are continuously bombarded by interplanetary micrometeoroids at speeds in excess of 1 km/s. At these high impact speeds the mass of the ejecta produced in the impact is 10^3 to 10^6 times the mass of the impactor [1], and the bulk of the interplanetary micrometeoroid mass flux is in particles of a few 10^{-4} m in diameter [2]. Although no direct observations of an individual ring particle exist, the abundance of dust in planetary rings and protoplanetary disks suggests that this hail of impactors creates a coating of dust (the regolith) on the larger ring and disk particles. Because the ring particles and proto-planetesimals are small (cm to m-sized), the regolith is only weakly bound to the surface by gravity. This dust is knocked off the larger "parent bodies" by micrometeoroid impacts and presumably also by the lower velocity collisions between the parent bodies themselves [3,4].

In planetary rings and in the early stages of planetesimal accretion in the protoplanetary nebula, interparticle collisions occur at velocities on the order of 1 to 100 cm/s. In some regions of Saturn's rings the typical collision velocity inferred from observations by the Voyager spacecraft and dynamical modeling is even less: a fraction of a centimeter per second [5]. The particles in planetary rings undergo collisions on the short orbital time scale (~10 hours). The amount of dust released in these collisions is unknown, however. Because dust particles have short dynamical lifetimes (days to centuries), the abundance and distribution of dust is a sensitive tracer of the distribution and dynamics of the more massive parent bodies.

In planetary accretion, the details of the growth process in the critical centimeter-to-meter size range are not known, and depend greatly on the efficiency of mass loss during collisions. Collision velocities of 1 to 100 cm/s are significantly higher than escape velocities for centimeter-to-meter size particles, and so collisions must have been highly inelastic in order for growth to proceed. Dusty regoliths

covering particles may have helped to dissipate collisional energy, reducing the rate of mass loss during collisions and promoting accretional growth of larger bodies [6]. COLLIDE provides microgravity impact experiments to complement the extensive set of ground-based experimental data. Low velocity impact experiments simulating planetary ring particle collisions have been performed using hard ice particles and pendulums to achieve impact velocities less than 1 cm/s, typical of planetary ring particle impact velocities [7,8,9,10]. Our experiments provide data on the release of dust from ring particle regoliths in low velocity collisions. Regolith ejecta was produced in 5 m/s (and higher) ground-based impact experiments [11]; COLLIDE is an extension of those to a microgravity environment and impact speeds of less than 1 m/s.

COLLIDE is a GAS payload built at the University of Colorado's Laboratory for Atmospheric and Space Physics (LASP). The project was primarily implemented by students at the University of Colorado with the benefit of guidance and assistance from professional scientists, engineers, and machinists at LASP. Below we discuss the scientific results of COLLIDE as well as some of the technical and managerial aspects of implementing a GAS payload on a short time scale (< 2 years) with undergraduate students.

SYMBOLS AND ACRONYMS

COLLIDE	Collisions Into Dust Experiment
JSC-1	Johnson Space Center lunar soil simulant [12]
IBS	Impactor Box Subsystem
SMA	Nickel-titanium shape memory alloy
LED	Light emitting diode
LASP	Laboratory for Atmospheric and Space Physics, University of Colorado
v_i	impact velocity
v_n	normal component of the rebound velocity
ε_n	normal coefficient of restitution

EXPERIMENT

The number of parameters for an impact experiment is large, and includes impactor mass, radius, and velocity, impact angle, target material, target size distribution, and target depth. Because the impacts are into powder, it is not possible to re-use a target sample. The conceptual design of the experiment involved balancing the need for a large number of impacts (to explore as many different parameter values as possible) with the limited space of a GAS canister. A design which accomodates six independent impact experiments was selected, and impact velocity was chosen as the primary impact parameter for study. A schematic of the experiment is shown in Figure 1.

The experiment consists of six impact chambers or IBS's, each of which conducts a single impact experiment (Figure 2). Impact experiment data are typically recorded by high speed film movie cameras, however, the low velocities studied by COLLIDE enabled us to use standard 30 frame per second video. Camcorders provided a compact, simple, and economical means of recording science data. A compact consumer-grade digital video camcorder was selected for its small size and high quality digital video recording. We used two cameras, each of which observed three IBS's. For simplicity, the cameras are fixed and view three IBS's simultaneously. This results in a loss of resolution at each IBS in return for simplicity of design and increased reliability through reduction of motorized components.

Each IBS consists of a target tray at one end filled with JSC-1 ground basaltic powder [12]. The mean and median particle sizes of JSC-1 are near 10^{-4} m. The dimensions of the target sample are approximately 0.1 m by 0.1 m by 0.019 m deep. At the opposite end of the IBS is a launcher mechanism. The projectile was launched by a compression spring, and was held in place prior to firing by a spring loaded door which was in turn held in place by a spring-loaded plunger. Illumination for the camcorders was provided within each IBS by an array of 20 high-intensity light emitting diodes. A sliding door held the JSC-1 in place prior to the impact experiment, and was operated by a digital linear actuator. The IBS's were mounted so that the cameras view the target surface edge-on. A mirror in each IBS provided an orthogonal view of the impact.

Power was supplied by 18 alkaline D-cell batteries, and the experiment was controlled by a microcontroller.

TECHNICAL APPROACH AND LESSONS LEARNED

The primary guiding factor in the technical design and implementation of COLLIDE was to maintain simplicity. This resulted in lower costs, allowed students to do much of the actual design and fabrication`, reduced the number of failure points, and facilitated NASA safety certification. The cost of a simple design, however, is that the simplest design is often not the optimal design from a scientific standpoint. The development of COLLIDE involved a continuous balancing act between these two competing design considerations.

Mechanical

The experiment was designed to be safe by analysis, avoiding the cost and time necessary to certify safety by vibration testing. While having a structure that meets safety requirements by analysis makes the schedule much more flexible, it does not eliminate the need for vibration testing which would likely have identified fixable problems in the experiment (see below).

The choice of a consumer-grade camcorder for data recording had the benefits of low cost, low risk, and low development time. However, because the camcorder is not designed for extreme temperature environments or low ambient pressures, this decision imposed other constraints on the experiment design. Thermal control of the camcorders was necessary to insure that it remained within its operating temperature range, and it was necessary to house the camcorders in a sealed container at one atmosphere. This in turn raised the possibility of condensation obstructing the view of the camcorder.

The impacts studied in COLLIDE are sensitive to the presence of an atmosphere, and so an evacuated environment was required for the experiment. A sealed and evacuated container was chosen rather than having the experiment vent to space in order to simplify the safety certification process and avoid the need for electromagnetic interference testing. This decision made the schedule more flexible, but required sealed containers for the cameras which would hold pressure for the three to four month waiting period from integration into the GAS canister to launch, rather than just the few hours from launch to initiation of the experiment. This in turn required optical glass covers for the camera containers because they offer a better seal than the more sturdy polycarbonate windows used in the IBS's. Ultimately, this led to an in-flight failure, though with full vibration testing the failure could have been identified and remedied prior to launch.

A space project team comprised entirely of college level students does have a major disadvantage from a professional team, namely, lack of experience. However, there were some definite advantages to a student team. It was apparent throughout the COLLIDE design process that some options which would have been passed over by a professional team, were seriously entertained, and even implemented by the students. We used a more aggressive approach towards hardware and design concepts which did not have space flight heritage. Because COLLIDE would reside in a sealed environment (the GAS canister), use of non-space-rated hardware and electronics was deemed a low level of risk, and in fact, no anomalies on the experiment can be attributed to this approach of using non-space-rated hardware.

Professional engineers typically prefer to utilize proven design options. Our relatively inexperienced student team was open to novel approaches to problems. An example of this can be seen in the COLLIDE launcher system. The Nickel-Titanium shape memory alloy (SMA, or "muscle wire") actuation system was recognized by the students as a promising design option. The SMA is used to pull the spring-loaded plunger which holds the launcher door in place prior to launch of the projectile (Figure 2). In the initial trade studies, LASP professional engineers expressed concern with the SMA, as it had no design heritage within LASP. Suggestions leaned towards other actuation methods such as solenoids or paraffin actuators, which were used in past LASP experiments with flight-proven results. The SMA system was chosen, and it was built at a fraction of the time and cost that the other systems would have required. It is worth noting that dozens of tests were performed on the SMA launcher actuation system, and that the ease of assembly, testing, and refitting of the SMA were also factors in its selection. During flight, the SMA launcher actuation system performed flawlessly.

121

Electrical

Preliminary experiment designs called for digital temperature, pressure, and acceleration readings to be made and recorded during the experiment, and for active thermal control of the camcorders to prevent damage to them, even after completion of the experiment. Eventually, these non-critical options were omitted as budget and schedule constraints prevented their implementation. Nevertheless, a significant amount of planning and early design work was expended on these options. These options required increased power efficiency which suggested the use of a DC-DC converter, which ran up against space constraints within the experiment. . Within the short time-scale for a student project such as COLLIDE, this represents a costly inefficiency in the process.

Student turnover also put the electronics development behind the schedule of the mechanical development, with the effect that the electronics box dimensions were constrained without the necessary design work on the electronics. This resulted in an overcrowded electronics box which is difficult to assemble and disassemble. The mismatch in electrical and mechanical schedules also eliminated most of the time allotted for testing of the fully assembled and flight-configured experiment.

Flight electronics were soldered vector boards rather than printed circuit boards. Also, test connectors rather than the more expensive flight-rated gold-plated connectors were used for the wire harness of the experiment. An Intel Corporation 80C51GB microcontroller with a UV EPROM was used to controll the experiment. The microcontroller was programmed in the C language, providing readable and easily modifiable flight software. High intensity LEDs were used for illumination. These are lightweight, compact, have low power requirements, and are rugged. Aside from a transient problem with camera operation (see below), the flight electronics operated nominally.

Experiment Anomalies

Of the six IBS's in COLLIDE, three returned useful science data. The doors failed to open fully on two of the IBS's, and the projectile remained stuck in the launcher of another IBS. The doors were controlled by digital linear actuators, or stepper motors. A non-flight stepper motor controller was used to test door operation prior to flight, however most tests were conducted with empty target trays. Those tests that included JSC-1 powder in the target tray did not have the JSC-1 loaded in the same manner it was loaded for flight. The doors were not tested in their flight configuration following simulated launch vibration and in a vacuum. JSC-1 dust contamination of the stepper motor lead screws and the sliding door tracks may also have contributed to jamming of the doors in flight.

The experiment returned with fractured glass plates on the camera sealed containers, presumably due to launch vibrations. This resulted in elevated ambient pressure in the rest of the experiment in violation of science requirements and may have contributed to poor performance of the camcorders. The first time each camcorder was used the video quality was significantly degraded. In pre-flight and post-flight tests of the cameras using the fligh electronics (but in ambient laboratory conditions) the cameras operated nominally. Poor performance of the cameras was therefore due to the particular environmental conditions during flight. Voltage regulators for the cameras may have operated at high temperatures in the absence of air to carry heat away, resulting in noisy output and degraded camera performance. Although the regulators were thermally connected to the experiment hardware, all ground-based tests had the electronics in air.

Launchers did not in general meet their design specifications, with projectile speeds differing significantly from the design speeds. At 1 Earth gravity, a projectile launched upwards at 21 cm/s (one of our designed projectile speeds) will only travel 2.2×10^{-3} m. This rendered laboratory testing of the projectile speeds impractical.

Plans For Reflight

A reflight of the experiment, G-788, is planned. COLLIDE-2 will address the anomalies encountered on COLLIDE. Minor hardware modifications include a wider launcher barrel to reduce the amount of internal friction in the launcher, a larger lubricated barrier to prevent dust grains from jamming the door mechanism, a spring-driven lever for the lowest speed projectiles, and an improved camera

viewport design. These and other modifications will be tested through ground-based performance and vibration tests and NASA reduced-gravity aircraft tests for the launchers. As for the original experiment, however, the bulk of the work will be done by undergraduate students with oversight and guidance from professional engineers.

RESULTS

The scientific results are presented in detail in Colwell and Taylor (1999) [13] and are summarized here. A sample frame from one of the flight videotapes is presented in Figure 3. Contrary to expectations, virtually no ejecta was produced in the impacts observed on COLLIDE. Ground-based tests had demonstrated production of dust ejecta at speeds down to 1 m/s in vacuum, but at the lower velocities studied in COLLIDE, ejecta was absent. This could be indicative of a threshold for the production of ejecta, or it could be a result of the particular packing and vibration history of the target powder on COLLIDE.

Measurements were made of the normal and tangential coefficients of restitution of the impactors which are measures of the dissipation of energy in the collision and are important parameters in the collisional evolution of particulate disks such as planetary rings. The normal coefficient, $\varepsilon_n = v_n/v_i$, where v_n is the normal component of the rebound velocity, v_i is the impact velocity, and $1-\varepsilon_n^2$ is the energy dissipated in a head-on collision between particles with no spin. The results (Table 1) are consistent with ground-based experiments at higher velocities which show that the presence of a regolith drastically increases the dissipation of energy in low velocity impacts.

Table 1: Normal Coefficient of Restitution

IBS	Projectile Speed (cm/s)	Door Functioned	Normal Rebound Velocity (cm/s)	Coefficient of Restitution (ε_n)
1	14.80±0.09	Yes	0.41±0.02	0.028±0.002
4	17.10±0.21	Yes	0.37±0.02	0.022±0.002
6	90±15	Yes	2.8±0.5	0.03±0.01

Notes: Uncertainties are standard deviations from linear regression fits to displacement measurements. ε_n is the ratio of the normal component of the rebound velocity to the impact velocity.

CONCLUSIONS

The G-772 experiment COLLIDE returned novel and surprising scientific results. The experiment was primarily designed and built by undergraduate students at the University of Colorado, Boulder. The student team was innovative, hard-working, and built a successful flight experiment. Building the experiment with a large contingent of student labor allows cheaper experiments to built for flight, but more importantly it provides an incomparable educational experience for those involved, including students and professionals alike.

Key factors that contributed to the success of COLLIDE include the following. (1) Students were given a fair amount of decision-making power and autonomy in their work routines. This contributed to their sense of ownership and pride in the project. (2) The entire experiment schedule was kept short (19 months from initial design to delivery for integration). This kept the project within the scope of an undergraduate student career and helped minimize student turnover which introduces costly delays. Non-essential functionality was sacrificed in order to stick to this schedule. (3) The experiment design was kept simple. Complicating factors were eliminated unless they were critical for the fundamental success of the experiment. (4) Expertise of professional engineers was used as a frequent guide and resource. (5) Inexpensive off-the-shelf components were used whenever possible, including non-flight hardware. Items such as the SMA for the launcher, a consumer grade camcorder for data-taking, non-flight-rated electrical connectors, and alkaline batteries from the local hardware store all performed nominally. (6) Redundancy was included whenever possible. Multiple IBS's and two camcorders insured useful science data even though there were several anomalies with some components. The SMA circuits and most power lines were redundant.

The key factor that contributed to the in-flight failures of the experiment was inadequate pre-flight testing. This was due to a compressed schedule which could have been alleviated by earlier decisions to drop non-essential components from the design, freeing up valuable time and resources. Of course, in a small project with significant student involvement, the schedule is always at risk due to the very real demands of coursework and exams. This requires that more contingency be included in the schedule.

REFERENCES

1. Cuzzi, J. N., and R. H. Durisen, "Bombardment of planetary rings by meteoroids: General formulation and effects of Oort cloud projectiles," *Icarus*, Vol. 84, 1990, pp. 467-501.

2. Grün, E., H. A. Zook, H. Fechtig, and R. H. Giese, "Collisional balance of the meteoritic complex," *Icarus*, Vol. 62, 1985, pp. 244-272.

3. Colwell, J. E., and L. W. Esposito, "A numerical model of the Uranian dust rings," *Icarus*, Vol. 86, 1990, pp. 530-560.

4. Colwell, J. E., and L. W. Esposito, "A model of dust production in the Neptune ring system," *Geophys. Res. Lett.*, Vol. 17, 1990, pp. 1741-1744.

5. Esposito, L. W., "Understanding planetary rings," *Annu. Rev. Earth Planet. Sci.*, Vol. 21, 1993, pp. 487-523.

6. Hartmann, W. K., "Planet formation: Mechanism of early growth," *Icarus*, Vol. 33, 1978, pp. 50-62.

7. Bridges, F. G., A. P. Hatzes, and D. N. C. Lin, "Structure, stability, and evolution of Saturn's rings," *Nature*, Vol. 309, 1984, pp. 333-335.

8. Hatzes, A. P., F. G. Bridges, and D. N. C. Lin, "Collisional properties of ice spheres at low impact velocities," *Mon. Not. R. Astr. Soc.*, Vol. 231, 1988, pp. 1091-1115.

9. Supulver, K. D., F. G. Bridges, and D. N. C. Lin, "The coefficient of restitution of ice particles in glancing collisions: Experimental results for unfrosted surfaces," *Icarus*, Vol. 113, 1995, pp. 188-199.

10. Dilley, J. P., and D. Crawford, "Mass dependence of energy loss in collisions of icy spheres: an experimental study," *J. Geophys. Res.*, Vol. 101, 1996, pp. 9267-9270.

11. Hartmann, W. K., "Impact experiments. 1. Ejecta velocity distributions and related results from regolith targets," *Icarus*, Vol. 63, 1985, pp. 69-98.

12. McKay, D. S., J. L. Carter, W. W. Boles, C. C. Allen, and J. H. Allton, "JSC-1: A new lunar soil simulating," *Engineering, Construction, and Operations in Space IV*, American Society of Civil Engineers, 1994, pp. 857-866..

13. Colwell, J. E., and M. Taylor, "Low-velocity microgravity impact experiments into simulated regolith," *Icarus*, Vol. 138, 1999, pp. 241-248.
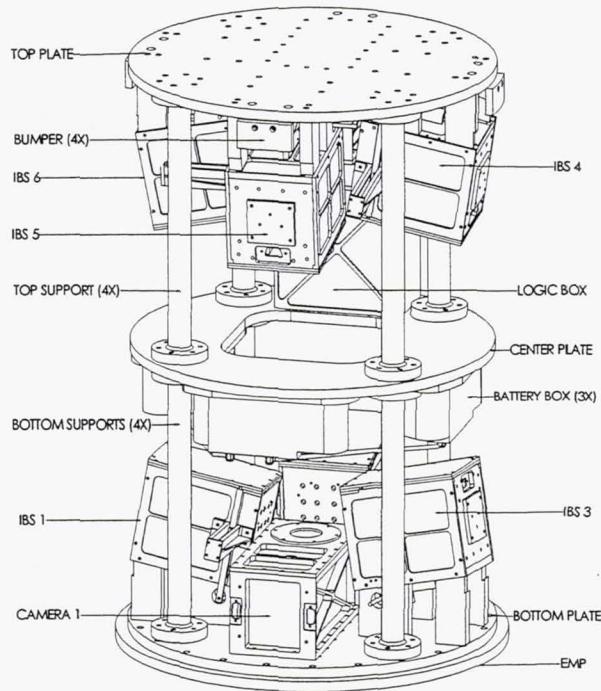
Figure 1: A schematic of the main COLLIDE assembly showing principle experiment components. Detailed information on the experiment is available from the web site: http://lasp.colorado.edu/collide/.
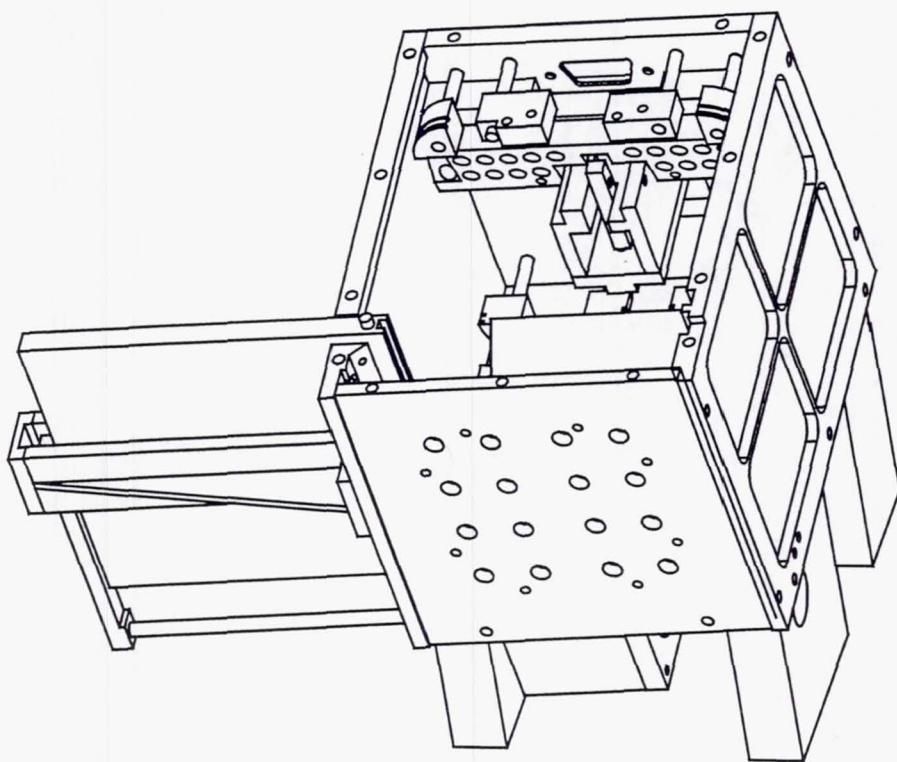
Figure 2: A view of an Impactor Box System (IBS). The door which holds the target powder in place until the experiment is run is open to the left of the IBS. Sixteen vent holes are visible in the back plate of the IBS which allow air to evacuate the pore spaces in the target JSC-1 powder through a filter inside the target tray. The launcher mechanism is visible at the opposite end of the box with the array of LEDs above the launcher. A canted mirror is mounted on the bottom of the IBS to allow the cameras a second view of the impact through the clear polycarbonate top of the IBS. The legs of the IBS orient it so that the camera has a direct edge-on view of the target surface.
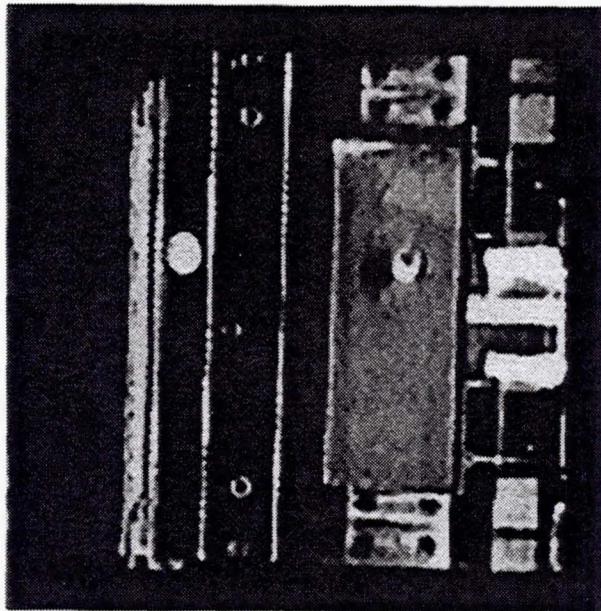
Figure 3: A frame from the flight video of COLLIDE. The target material is dark, to the left of the bright vertical band, and viewed edge-on. The projectile has just bounced off the target surface, and its reflection is visible in the mirror on the right half of the figure. The projectile's reflection shows a smudge of dust which stuck to the projectile. Almost no dust was released in the impact which dissipated 97% of the projectile's kinetic energy. Fiduciary grid marks are 2 cm apart for reference.

Page intentionally left blank

GET AWAY SPECIAL PAYLOAD G-093: THE VORTEX RING TRANSIT EXPERIMENT (VORTEX) FLIGHTS

Sven G. Bilén and Luis P. Bernal
(for the VORTEX Project team)

University of Michigan Students for the Exploration and Development of Space
François–Xavier Bagnoud Building
1320 Beal Avenue
Ann Arbor, MI 48109–2140

ABSTRACT

Get Away Special payload G–093 was designed and built by the University of Michigan Students for the Exploration and Development of Space. Also known as the VOrtex Ring Transit EXperiment (VORTEX), G–093 was flown on Shuttle mission STS–89 in January 1998 and again on STS–88 in December 1998. VORTEX was flown to answer some basic questions about fluid atomization—the process whereby a liquid is converted into small droplets. More specifically, VORTEX investigated the propagation of a vortex ring through a liquid–gas interface in microgravity. The scientific objective of the experiment was to conduct observations of the liquid drop-formation process in the case of surface-tension-dominated interface dynamics. The data returned should lead to better methods for atomizing fuel, producing metal powders of desired characteristics, aerosol generators for drug delivery, and inkjet printer technology. In addition to the important physics questions to be answered, the students learned how to work with industry, academia, and government. The students handled all project management, fund-raising, and technical aspects under the guidance of a Faculty Advisor who acted as the payload customer and NASA contact person. This paper discusses several aspects of the VORTEX project, including project timeline, how the payload was designed and constructed, and the project's educational impact.

INTRODUCTION

Payload G–093 was flown on Shuttle mission STS–89 in January 1998 and again on STS–88 in December 1998. Also known as the VOrtex Ring Transit EXperiment (VORTEX), G–093 was designed to answer some basic questions about fluid atomization—the process whereby a liquid is converted into small droplets. Without the effects of gravity, the physics of this process can be readily examined. More specifically, VORTEX investigated the propagation of a vortex ring through a liquid–gas interface in microgravity. As the vortex rings propagated through the interface, they formed one or more liquid drops. The scientific objective of the experiment was to conduct observations of the liquid drop-formation process in the case of surface-tension-dominated interface dynamics. In microgravity, the same interface dynamics can be examined in large drops thus facilitating detailed experimental observation. The data returned should lead to better methods for atomizing fuel (important in the operation of internal combustion engines), producing metal powders of desired characteristics (powder metallurgy), aerosol generators for drug delivery, and inkjet printer technology.

In addition to the important physics questions to be answered, the students learned how to work with industry, academia, and government. These students, who have ranged from first year to graduate students in fields ranging from engineering to liberal arts, gained valuable hands-on experience with a real-world engineering project. The students handled all project management, fund-raising, and technical aspects under the guidance of a Faculty Advisor who acted as the payload customer and NASA contact person.

The G–093 payload was designed and built by the University of Michigan Students for the Exploration and Development of Space (UMSEDS). UMSEDS is a student engineering organization that brings together UM students who have an interest in space and space exploration and helps them in exploring those interests by 1) providing its members with information and opportunities helpful to careers in space-related fields; 2) being a forum for the discussion and exchange of ideas in space-related areas of interest; and 3) educating students and the general public about the benefits of space exploration and development. By designing, building, and flying a GAS payload experiment, UMSEDS members were able to apply their interest in space exploration to a real-world engineering problem that will advance scientific knowledge.

Initial analysis of the returned data indicates that the STS–88 flight of VORTEX was successful in that several useful data sets were collected. These data sets are currently undergoing analysis. This paper will discuss technical and programmatic aspects of the VORTEX payload such as project timeline and how the payload was designed and constructed. This paper also discusses some of the lessons learned from the flight experience and the educational impact of VORTEX.

VORTEX PROJECT TIMELINE

In 1977, the University of Michigan reserved two GAS payloads for future flights. In 1993, a chapter of SEDS was started at Michigan, with one of its first goals to be the design and flight of a GAS payload. In Summer 1994, the first ideas for the payload were discussed and by Fall 1994 a core team of students had been assembled to work on the design. Over 70 students were involved with the project during its four-year lifetime. Figure 1 shows a timeline of the project from its inception to its launch on STS–89 and STS–88. The payload was also flown in the KC–135 reduced gravity airplane under the NASA Reduced Gravity Student Flight Opportunities Program in April 1997. The VORTEX team is currently analyzing data collected on the STS–88 mission.

July 1994	VORTEX Project Begun
	Payload Definition Stage
August 1995	PAR Submitted
	Payload Design
April 1997	VORTEX KC–135 Flights
August 1997	Phase III SDP Submitted
August 1997	SVD Submitted
	VORTEX Final Construction
October 1997	G–093 Integration
22–31 January 1998	STS–89 Mission
February 1998	G–093 De-integration
March 1998	Post–Mission Failure Analysis
	VORTEX Refurbishment
August 1998	G–093R Integration
4–15 December 1998	STS–88 Mission
January 1999	G–093R De-integration
February– 1999	VORTEX Data Analysis Begun

Figure 1 Timeline of significant events for payload G–093.

PAYLOAD DESCRIPTION AND OPERATION

Scientific Objectives

The microgravity environment provides an excellent opportunity to study surface-tension-dominated phenomena relevant to many earth-based engineering systems. This is particularly true for fluid interfaces with a large density change across the interface. On earth, the shape and dynamic evolution of the interface is dominated by the gravitational force. In the microgravity conditions of space, the shape and evolution of fluid interfaces is dominated by surface-tension effects, not gravitational effects.

The flow configuration for our experiments consists of a vortex ring that formed in the liquid below the liquid–gas interface and propagated towards the interface. If the vortex ring has sufficient impulse, then the collision of the vortex ring with the interface results in the formation of a droplet. The volume of liquid moving with the vortex ring determines the size of the droplet. The vorticity distribution in the vortex ring determines the motion of the liquid inside the droplet. This relatively simple flow captures many important dynamical processes relevant to the evolution of fluid interfaces in microgravity and in other flow systems. More information on the theory of this process, as well as images collected by G–093 on STS–88 showing the vortex ring propagation through an interface in microgravity, may be found elsewhere in these proceedings [1].

Experimental Component Overview

The main components of the G–093 experiment are a fluid test cell system, a laser-based illumination system, a digital imaging system, and a computer-based data acquisition and control system. All equipment was mounted on an equipment support structure as illustrated in Figure 2. For the experiments, the fluid test cell was partially filled with silicone oil to establish the liquid–gas interface. The vortex ring generator, which is located at the bottom of the test cell, consists of a piston moving inside a cylindrical cavity. For each test, the piston moved to the bottom of the cavity at which point the cavity was filled with silicone oil seeded with silver-coated hollow glass micro-spheres. The rapid upward motion of the piston generated the vortex ring that propagated to the liquid–gas interface. The laser system was used to illuminate a cross section of the fluid test cell. The digital imaging system captured images of the fluid motion and the drop-formation process, which were then transferred to computer memory. A data acquisition system simultaneously recorded the liquid temperature and the acceleration in the fluid test cell. All the data was stored on hard disk for analysis after the experiment was returned to earth. VORTEX was a self-contained experiment and was flown onboard the Space Shuttle in a 5-cubic-feet GAS canister.
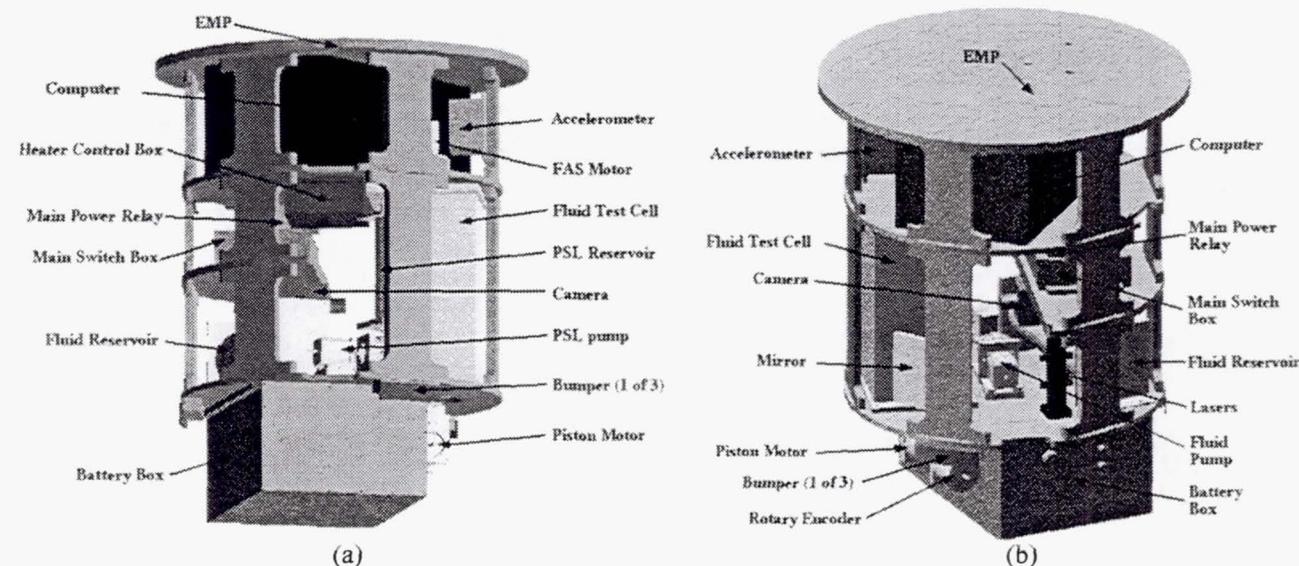
Figure 2 Illustration of G–093 components as they appear on the support structure: (a) view from one side, (b) opposite angle view.

The following sections contain brief descriptions of the experimental instrumentation.[1] A functional schematic of the payload's instrumentation and the flow of information between subsystems is shown in Figure 3.
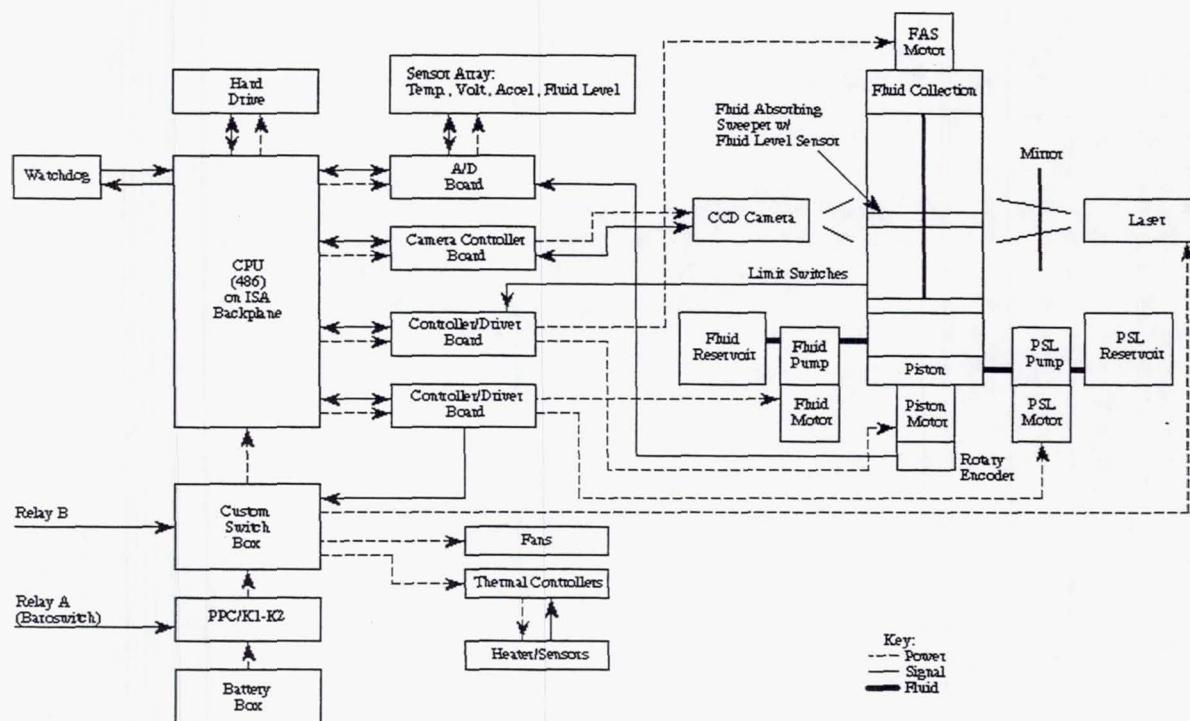
Figure 3 Diagram showing the interaction of the various G–093 system components.

Equipment Support Structure

The components of the VORTEX payload are supported by an equipment support structure (ESS) consisting of two complete shelves and one half shelf. The complete shelves are circular plates with a radius of 247.7 mm and a thickness of 9.5 mm. The half shelf has the same dimensions, but is a semicircle. The plates are separated by six "I"-shaped support beams, which are 124.9 mm wide at the ends, 74.1 mm wide in the center, and 12.7 mm thick. These beams are spaced equally around the perimeter of each plate as illustrated in Figure 4. The beams are bolted to the plates for easy removal and access to the components. The plates and beams are made of 6061–T6 aluminum and the entire shelving unit weighs approximately 23 kg. Two channels were machined into the full plates to provide room for cabling. Signal and power cables were routed in separate channels to avoid interference with the data signals.

---

[1] More detailed technical information on the G–093 payload may be found in the G–093 Phase III Safety Data Package, which may be downloaded from the VORTEX website: http://aoss.engin.umich.edu/vortex.
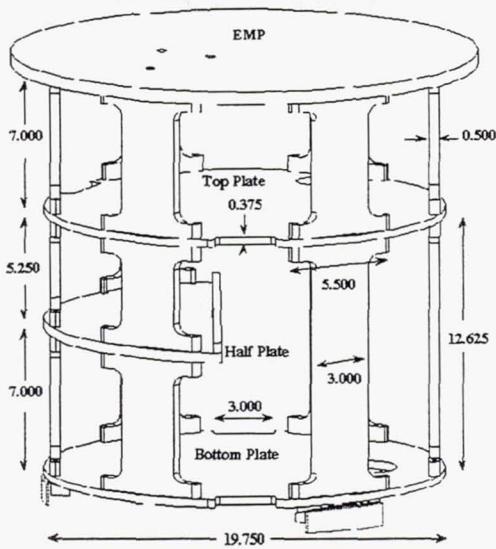
Figure 4 Schematic of the VORTEX equipment support structure (note: dimensions are in inches).

Three bumper assemblies were affixed to the edge of the ESS's bottom plate and contacted the inside surface of the GAS canister. Each bumper assembly provided about 25 cm^2 (4 sqaure inches) of surface contact area with the canister's inner surface. Each bumper has a pad made of 0.32-cm (0.125-in.) thick Viton. Easy access to the bumpers for adjustment and installation was ensured by their location on the bottom side of the bottom plate of the ESS.

Battery System

Power to the payload was provided by 120 Alkaline-Manganese Dioxide (Zn/MnO$_2$), 1.5 V, D-cell batteries arranged in six parallel strings containing 20 D-cells each, for a total of 30 V (nominal) per string. Total installed energy was 2565 Wh. Each string was individually diode isolated (each rated at 6 A, 100-V reverse voltage) so that no back charging could occur if one or more strings were to have failed. Each string was separately wrapped with shrink tubing, and the six strings were separated by Poron foam spacers, which prevented motion of the batteries within the box. In addition to the spacers, Pellon material was placed between the strings to act as an absorber should any electrolyte have leaked. Fusing of the batteries consisted of one in-line 10-A slow-blow fuse that was connected directly to the ground terminal of the batteries and housed inside the battery box.

All batteries were contained in a sealed 6061–T6 aluminum battery box internally coated with Conathane EN–11 and secured to the bottom side of the bottom plate. All joints were sealed with Conathane EN–11 and silcone RTV, except the front plate, which had a rubber gasket. The electrical contact with the battery box was made through a glass-sealed circular connector and purge-vent ports were connected to the experiment mounting plate's (EMP) battery pressure relief valve (PRV) via stainless steel (SS) tubing. The battery box was proof tested to 22.5 psid and was vented overboard using redundant SS tubes to the NASA-provided 15-psid PRV.

Electrical System

The design and operation of the power distribution is described in this section. Power was provided to the payload by a battery system, which is described in the following section. Power distribution is shown as a dotted line in Figure 3.

Payload G–093 was activated by a baroswitch, which activated the payload power contactor (PPC) and switched GAS control decoder (GCD) Relay A hot. Upon activation, power was provided from the battery box to the heater controllers and heaters that maintained the temperature of critical components until activation of the experimental sequence by GCD Relay B. All power could be removed from the payload by switching GCD Relay A to latent at any time. Switching GCD Relay B to latent would stop the experiment sequence.

Whenever power is provided to the payload, the heater controllers and heater elements are powered to maintain the payload components above 0 °C for mission success only. Each of the five heater modules controls a Kapton resistive

heating element and are rated at 10 W each. The heaters are located on the fluid reservoir, particulate-seeded liquid (PSL) reservoir, battery box, computer, and fluid test cell.

The payload sequence began when GCD Relay B was switched hot, which closed the VORTEX main power relay providing power to the four DC/DC converters that generate the ±12 V and ±5 V for distribution to the payload components. All four converters are properly sized with at least a 50% margin to provide the necessary power to the payload components.

Power was provided to the power bus and the data system's passive backplane. Attached to and powered from the backplane are the motherboard, A/D board, two stepper controller/drivers boards, and the camera board. The three A/D module boards and sensors are connected to and derive their power from the A/D board. The four stepper motors are attached to and derive their power from the two stepper controller/driver boards. The camera is attached to and derives its power from the camera board.

In addition to power being provided to payload components via the passive backplane, power is also distributed directly from the DC/DC converters to each of the two hard drives, two lasers, fan, and the accelerometer. Power to the two hard drives and accelerometer will flow through normally closed (NC) relays that are controlled by the stepper controller/driver board. The fan is attached via a normally open (NO) relay. Power to the two lasers is controlled via a NO relay as well. All relay signals are controlled by one of the stepper controller/driver boards.

Experiment Controller and Data Acquisition System

The computer system controlled the experimental sequence of events. The hardware consists of an industrial-grade motherboard with a 486 microprocessor, a passive back plane with five industry-standard architecture (ISA) expansion slots, a camera controller to capture digital image data that were stored on two 2-GB EIDE hard drives, A/D board, and two stepper motor controller/driver boards. To monitor experimental conditions for all sub-systems, the computer collected sensor data such as acceleration, piston speed, temperature, and voltages. A watchdog circuit was implemented to ensure that the computer was reset if it hanged. The watchdog was serviced every minute by the computer and if it did not receive a signal within five minutes, it would have reset the computer. More information on the experiment controller and data acquisition system can be found elsewhere in these proceedings [1].

An array of sensors, used to measure the G–093 payload environment, was implemented and their signals were conditioned as necessary and then sampled via an A/D board attached to the computer. Temperature sensors were located on the battery box, computer central processing unit (CPU), fluid reservoir, PSL reservoir, fluid test cell, both hard drives, and accelerometer and measured temperature for mission success only. The accelerometer measured the level of microgravity in the payload. The fluid level was measured with an infrared (IR) reflective sensor mounted on the fluid absorbing sweeper. The piston position was measured with an optical rotary encoder attached to the piston stepper-motor shaft. The FAS travel was limited with 2 hermetically sealed mechanical micro-switches located inside the fluid test cell. The charge-coupled device (CCD) camera captured image data, which were stored directly into computer memory and transferred to the hard disk between experiments.

Fluid Test Cell

The experiments were conducted in the fluid test cell (FTC), a diagram of which is shown in Figure 5. The liquid used in the FTC was silicone oil (2-cSt viscosity), which is a non-corrosive and non-flammable liquid that is compatible with all materials used in G–093. Silicone oil is also non-conductive with a high dielectric strength (350 V/mm) and a very low freezing temperature (much lower than –100 °C).
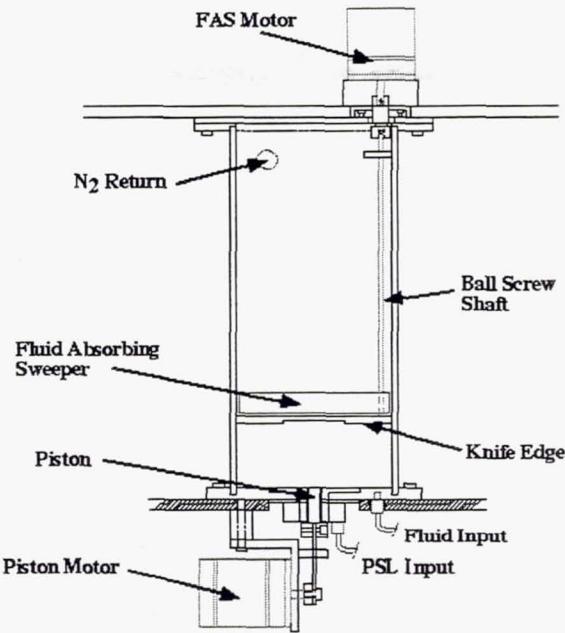
Figure 5 Fluid test cell diagram showing main components.

During launch, the fluid test cell was empty and the silicone oil resided in a separate fluid reservoir. Industrial bladders made of natural rubber were used for holding the silicone oil during launch and on orbit until needed. A constant displacement pump connected to a stepper motor pumped the silicone oil into the FTC from the bladder at the initiation of the experiment. This system was designed to add fluid to the FTC during the experiment to insure that each test was conducted with the proper liquid level. An infrared position sensor was used as a fluid level sensor to ensure that the fluid was filled to the proper height. Additional fluid was added, if needed, to replace the fluid that had been captured by the fluid absorbing sweeper (FAS) after each firing of the vortex ring generator, thereby re-establishing the liquid–gas interface at the proper height. A smaller bladder and a stepper-motor-driven constant-displacement pump were used to supply the PSL for each test.

The vortex ring generator is located at the bottom of the FTC and consists of a rapidly moving piston driven by a stepper motor. A piston stop was implemented so that it was not possible for the piston to withdraw completely from the test cell, thus ensuring all fluid remained in the test cell system. The PSL was added above the piston to enhance the visualization of the fluid droplet. After the PSL was injected into the system, the vortex ring generator created the vortex ring that propagated through the liquid–gas interface. The vortex ring generator and the injection system were operated under computer control. 100 experiments were conducted at piston speeds ranging from 5 cm/s to 25 cm/s (2 in/s to 10 in/s).

The FAS mechanism periodically "swept" the gaseous portion of the FTC free of any floating fluid droplets that could have potentially interfered with the imaging of subsequent trials. The FAS mechanism is an aluminum frame structure that supports a polyvinyl alcohol (PVA) absorbent material. The FAS is mounted on two SS linear ball bearings and moved up and down via a SS ball screw turned by a stepper motor. During each test, the FAS was positioned at the top of the FTC, which allowed the vortex ring to propagate freely in the FTC and be absorbed at the top by the FAS.

An important scientific requirement for these tests was a flat liquid–gas interface oriented normal to the direction of propagation of the vortex. A knife-edge was used to stabilize a flat interface (in microgravity, liquid–gas interfaces have a natural tendency to form spherical shapes). The knife-edge consists of a thin protrusion around the perimeter of the FTC to anchor the liquid–gas interface at a fixed point.

Laser Illumination System

The laser illumination system consists of two continuous-wave diode lasers (output power of 50 mW at 660 nm, rated Class IIIb) with a combined power output of 100 mW. Each unit includes a 30° laser line generator used to produce a plane of laser light from the lasers' pencil beam outputs. This light plane illuminates a single plane in the fluid test cell perpendicular to the camera plane. The laser was only operated during camera data acquisition. A front-surface mirror

mounted into an aluminum support extends the optical length of the laser system and also allows the laser plane beam to be perpendicular to the camera.

VORTEX FLIGHTS

KC–135 Flights

In April 1997, the VORTEX payload was flown in the KC–135 reduced-gravity airplane to verify the operation of several critical components in microgravity. These tests were conducted through the NASA Reduced Gravity Student Flight Opportunities Program. For the KC–135 verification flights, the payload ESS with all components except the computer was bolted to an angle iron mount, which was in turn attached to the cabin floor of the KC–135. The angle iron mount also supported an equipment rack with a computer, monitor, keyboard, and power supply. A picture of the payload during one of the KC–135 flights is shown in Figure 6. The results of the KC–135 tests were used to set up flow parameters for the STS–89 and STS–88 Space Shuttle flights.

Figure 6 VORTEX team member John Korsakas with VORTEX payload during the KC–135 flights.

Space Shuttle Flights

Payload G–093 was flown on Shuttle missions STS–89 in January 1998 and again on STS–88 in December 1998. Relevant data for both missions are listed in Table 1.

Mission and Emblem	STS–89	STS–88
	VOrtex Ring Transit EXperiment G-093 VORTEX (University of Michigan Students for the Exploration and Development of Space)	MichiganEngineering VOrtex Ring Transit EXperiment G-093R
Location	Aft, Starboard	Aft, Port (Bay 13)
Shuttle Launch	22 January 1998, 21:48:15 EST	4 December 1998, 03:35:34 EST
Experiment Sequence Started	Attempted at STS MET 003/12:26	STS MET 00/04:29
Experiment Sequence Ended	Never Began	STS MET 00/09:39
Payload Shut Off	STS MET 004/10:51	STS MET 00/14:01
Shuttle Landing	31 January 1998 at 17:35:09 EST	15 December 1998, 22:53:29 EST

Table 1 Mission data for payload G–093(R) on STS–89 and STS–88.

The first flight of VORTEX on STS–89 was not successful due to a switching sequence error. Tests conducted during G–093 de-integration at NASA Goddard Space Flight Center showed that the payload computer failed to turn on during the mission. Low temperature tests of the payload and battery pack were subsequently conducted at the University of Michigan to determine why the experiment did not turn on.

The results of the low temperature tests conducted at Michigan showed that there were most likely two causes for the failure of G–093 to turn on when commanded to at MET 003/12:26. The first is depletion of the battery pack due to payload heating during the time period from approximately MET 000/06:30 to MET 001/02:20, during which time the aft bay, starboard side temperature was below 0 °C, requiring G–093 heaters to be on. However, the total installed energy in the G–093 battery system was 2565 Wh and the maximum power dissipation by the onboard heaters was 50 W; it follows that there should have been enough energy remaining in the battery pack to activate the G-093 experiment at MET 003/12:26. The second likely reason is the cold temperature that existed in the payload when it was commanded on again at MET 003/12:26. The NASA-provided temperature data show that at the time when GCD Relay B was commanded hot the G–093 payload temperature was –10 °F (–23 °C). In the cold environment, not enough energy density was available from the batteries in order to turn on the computer. In addition, the payload temperature at that time was well below the minimum operational temperature for the G-093 onboard computer.

VORTEX was refurbished and flown again as G–093R on Shuttle mission STS–88. In this case, most payload systems performed as expected and scientific data were collected in 100 experimental sequences. The results are described in a companion paper [1].

EDUCATIONAL ASPECTS OF THE VORTEX PROJECT

As a project run by university students, the educational aspects of the VORTEX Project were of utmost importance. There is considerable interest among engineering students in obtaining hands-on experience with "real-world" projects. Building and flying an experiment on the Space Shuttle is just such a real-world engineering project, and as such can motivate learning in engineering and science fields, as well as in other fields such as business. Space experimentation provides a medium where faculty and students can work together with industry and government toward a common goal.[2,3] The VORTEX Project provided students with the opportunity to be involved in the design, fabrication, integration, and testing of a GAS payload project. Many students were able to experience the design and development of an engineering project from its beginning through its completion. For the VORTEX Project, this involved such activities as writing progress reports emphasizing technical writing, preliminary design via computer aided design (CAD), structural analysis, systems integration, and the establishment of industry investors.

During the course of the VORTEX project, we developed a strategy to engage students at three distinct levels: volunteers, directed-study students, and capstone design class students [4]. We found this strategy to be very effective and the feedback we received from students was very positive. It is interesting to note that many students who joined the project

at one level continued in another, *e.g.*, several students from the capstone design classes continued their involvement via directed studies and many students who began as volunteers switched to more structured directed studies. The VORTEX group held weekly meetings throughout the duration of the project. During these meetings, students were asked to present design results, ask questions of other members, and discuss problems and solutions. Students in all levels participated in the weekly meetings and were considered an integral part of the VORTEX group during their tenure.

As a final educational note, VORTEX is one of the reasons behind the establishment of the University of Michigan (UM) Student Space-Systems Fabrication Laboratory (S³FL) [5]. This facility will provide innovative educational opportunities for engineering, science, and other students to manage, design, fabricate, test, and ultimately fly small space systems and spacecraft.[2] It is fitting that this facility was started due to the success of *student-initiated* efforts in the realm of "space experimentation."

SUMMARY

The technical, programmatic, and educational aspects of the VORTEX project have been summarized in this paper. VORTEX was an investigation of the propagation of a vortex ring through a liquid–gas interface in microgravity. The VORTEX payload consists of a fluid test cell with a vortex ring generator, a digital imaging system, a laser illumination system, a computer-based controller, batteries for payload power, and an array of housekeeping and payload monitoring sensors. The VORTEX payload was flown on board the Space Shuttle STS–89 and STS–88 in a 5-cubic-feet GAS canister. While the STS–89 flight was unsuccessful, the STS–88 flight was successful and scientific data were obtained.

The VORTEX Project was entirely run by students at the University of Michigan but was overseen by a faculty advisor who acted as the payload customer and the NASA contact person. Our experience with the VORTEX Project, as outlined here, should prove beneficial to other GAS projects, especially student-run projects at universities. VORTEX maintains a webpage (http://aoss.engin.umich.edu/vortex) where information of a public and general nature about the project can be obtained.

REFERENCES

1. Korsakas, John V., Lindsay D. Millard, Avik S. Basu, Sven G. Bilén, and Luis P. Bernal, "The Vortex Ring Transit Experiment (VORTEX) Data System and Flight Results," 1999 Shuttle Small Payloads Project Office Symposium, Annapolis, MD, 13–15 Sept. 1999, NASA CP–1999–209476. (Paper 20 of this compilation.)

2. Gerondakis, G. G., "Get Away Special (GAS) Educational Applications of Space Flight," *IEEE Transactions on Education*, vol. 34, no. 1, 5–10, 1991.

3. Sacco, A., Jr., "The NASA GAS Program: A Stepping Stone to Education," *IEEE Transactions on Education*, vol. 34, no. 1, 27–30, 1991.

4. Bilén, Sven G. and Luis P. Bernal, "The Vortex Ring Transit Experiment Get Away Special Project: Using Projects Sponsored by Student Organizations to Enhance Engineering Education," ASEE 1998 Spring Conference, North Central Section, University of Detroit Mercy, Detroit, MI, 2–4 April 1998, pp. 211–215.

5. Bilén, Sven G., Luis P. Bernal, Brian E. Gilchrist, and Alec D. Gallimore "The Student Space-Systems Fabrication Laboratory: Enhancing Engineering Education Through Student-Run, Real-World Projects," ASEE 1999 Spring Conference, North Central Section, Pennsylvania State University Erie–Behrend, Erie, PA, 8–10 April 1999, pp. 68–72.

Kapton and Viton are trademarks of E. I. Du Pont de Nemours & Co., Inc. Poron is a trademark of Rogers Corp. Pellon is a trademark of Freudenberg Group. Conathane is a trademark of Conap, Inc.

---

[2] More detailed information on the S³FL may be found on its website: http://aoss.engin.umich.edu/s3fl.

THE VORTEX RING TRANSIT EXPERIMENT (VORTEX) DATA SYSTEM AND FLIGHT RESULTS

John V. Korsakas, Lindsay D. Millard, Avik S. Basu, Sven G. Bilén, and Luis P. Bernal
(for the VORTEX Project team)

University of Michigan Students for the Exploration and Development of Space
François–Xavier Bagnoud Building
1320 Beal Avenue
Ann Arbor, MI 48109–2140

ABSTRACT

Payload G–093, also known as the VOrtex Ring Transit EXperiment (VORTEX), was flown on Shuttle missions STS–89 in January 1998 and again on STS–88 in December 1998. VORTEX was flown to answer some basic questions about fluid atomization—the process whereby a liquid is converted into small droplets. VORTEX investigated the propagation of a vortex ring through a liquid–gas interface in microgravity. The primary data returned from the VORTEX payload are images of this process. The VORTEX experimental sequences were commanded by an experiment controller and data acquisition system. During the entire experimental sequence, the computer collected, interpreted, and stored sensor data. The VORTEX camera captured images of the fluid motion and the droplet formation process. A total of 100 experiments were performed, each collecting a sequence of 40 images. These images have been successfully retrieved from the on-board computer and are currently undergoing analysis. This paper discusses aspects of the VORTEX experiment sequence, the experiment controller and data acquisition system, and the imaging system. We also discuss our successes and concerns with utilizing commercial off-the-shelf components.

INTRODUCTION

The G–093 payload was designed and built by the University of Michigan Students for the Exploration and Development of Space (UMSEDS). Also known as the VOrtex Ring Transit EXperiment (VORTEX), G–093 was flown on Shuttle missions STS–89 in January 1998 and again on STS–88 in December 1998. VORTEX was flown to answer some basic questions about fluid atomization—the process whereby a liquid is converted into small droplets. Without the effects of gravity, the physics of this process was examined as never before. More specifically, VORTEX investigated the propagation of a vortex ring through a liquid–gas interface in microgravity. The primary data returned from the STS–88 flight of the VORTEX payload are images of this process.

Scientific Objectives

The microgravity environment provides an excellent opportunity to study surface-tension-dominated phenomena relevant to many earth-based engineering systems. This is particularly true for fluid interfaces with a large density change across the interface. On earth, the shape and dynamic evolution of the interface is dominated by the gravitational force. In the microgravity conditions of space, the shape and evolution of fluid interfaces is dominated by surface-tension effects, not gravitational effects.

The flow configuration is shown schematically in Figure 1. It consists of a vortex ring formed in the liquid below the interface propagating towards the interface (Figure 1a). If the vortex ring has sufficient impulse, then the collision of the vortex ring with the interface results in the formation of a droplet (Figure 1b). The volume of liquid moving with the vortex ring determines the size of the droplet. The vorticity distribution in the vortex ring determines the motion of the liquid inside the droplet. This relatively simple flow captures many important dynamical processes relevant to the evolution of fluid interfaces in microgravity and in other flow systems. Images of this process, which were collected by G–093 on STS–88 and show a vortex ring propagating through the interface in microgravity are shown in the data analysis section.
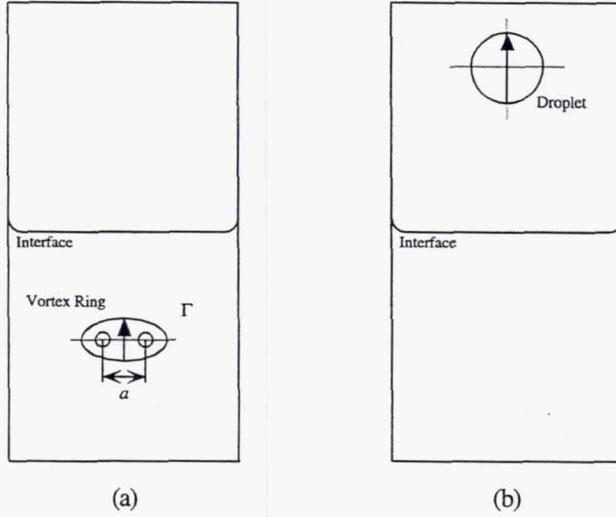
Figure 1 Schematic diagram of the interaction of a vortex ring with a liquid-gas interface: (a) idealized diagram before the interaction; (b) idealized diagram after the interaction.

Theoretical Considerations

To determine the relevant flow parameters for the experiment we follow the analysis of *Bernal et al.* [1]. The initial state before the interaction is characterized by the vortex ring diameter, a, and the circulation, Γ. The interface is characterized by the densities ρ_1 and ρ_2, the viscosities μ_1 and μ_2, and the surface tension σ. The ring moves toward the interface with speed V and collides with it. Generally, the collision and the subsequent evolution of the droplet depend on fluid inertia, viscosity and surface tension. Therefore, three nondimensional numbers define the problem: the Weber number, the Bond number, and the Reynolds number which are defined as

$$\text{We} = \frac{V}{\sqrt{\dfrac{\sigma}{\rho_1 a}}}, \quad \text{Bo} = a \sqrt{g \frac{\rho_1 - \rho_2}{\sigma}}, \text{ and } \text{Re} = \frac{\rho V a}{\mu_1} \tag{1}$$

respectively. In addition, the density ratio $r = \rho_2/\rho_1$ and the viscosity ratio $\lambda = \mu_2/\mu_1$ must be specified. Here, subscript 1 denotes the liquid below the interface and inside the droplet and subscript 2 denotes the gas or liquid above the interface. The Bond number characterizes the relative magnitude of surface tension and gravitational acceleration in the dynamics of the interface. It is important to recognize that for a fixed liquid-gas interface the Bond number depends only on $a\sqrt{g}$, thus atomization phenomena in 1 g with droplet size of the order of a few microns can be examined in microgravity (10^{-4} g) at a much larger scale.

To illustrate the implications of this Bond number scaling, consider the case of a vortex ring in water with a diameter of 1 cm propagating through the water-air interface, which are typical of VORTEX. The density ratio is $r = 10^{-3}$ and the Bond number is 0.07 at a microgravity level of 10^{-4} g. This value of the Bond number corresponds to a droplet size of 100 μm in a 1-g experiment. Clearly, this droplet diameter is in the range found in typical fluid atomization systems [see for example ref. 2]. VORTEX examined the details of interface breakup and droplet formation by a vortex ring at a range of parameters relevant to fluid atomization processes with a resolution that cannot be obtained in 1g experiments.

This paper discusses aspects of the VORTEX experiment sequence, the experiment controller and data acquisition system, and the imaging system. We also discuss our successes and concerns with utilizing commercial off-the-shelf (COTS) components. Analysis of payload environmental data and scientific return are also presented.

EXPERIMENT CONTROL AND DATA ACQUISITION SYSTEMS

The main components of the G–093 payload are a fluid test cell system, a laser-based illumination system, a digital imaging system, and a computer-based data acquisition and control system.[1] A digital imaging system captured images of the fluid motion and the drop-formation process, which were then transferred to computer memory. A data acquisition system simultaneously recorded the liquid temperature and the acceleration in the fluid test cell (FTC). All the data was stored on hard disk for analysis after the experiment was returned to earth. VORTEX was a self-contained experiment and was flown onboard the Space Shuttle in a 5 cu-ft GAS canister. A functional schematic of the payload's instrumentation and the flow of information between subsystems are shown in Figure 2. A more detailed description of the entire VORTEX payload may be found elsewhere in these proceedings [3].
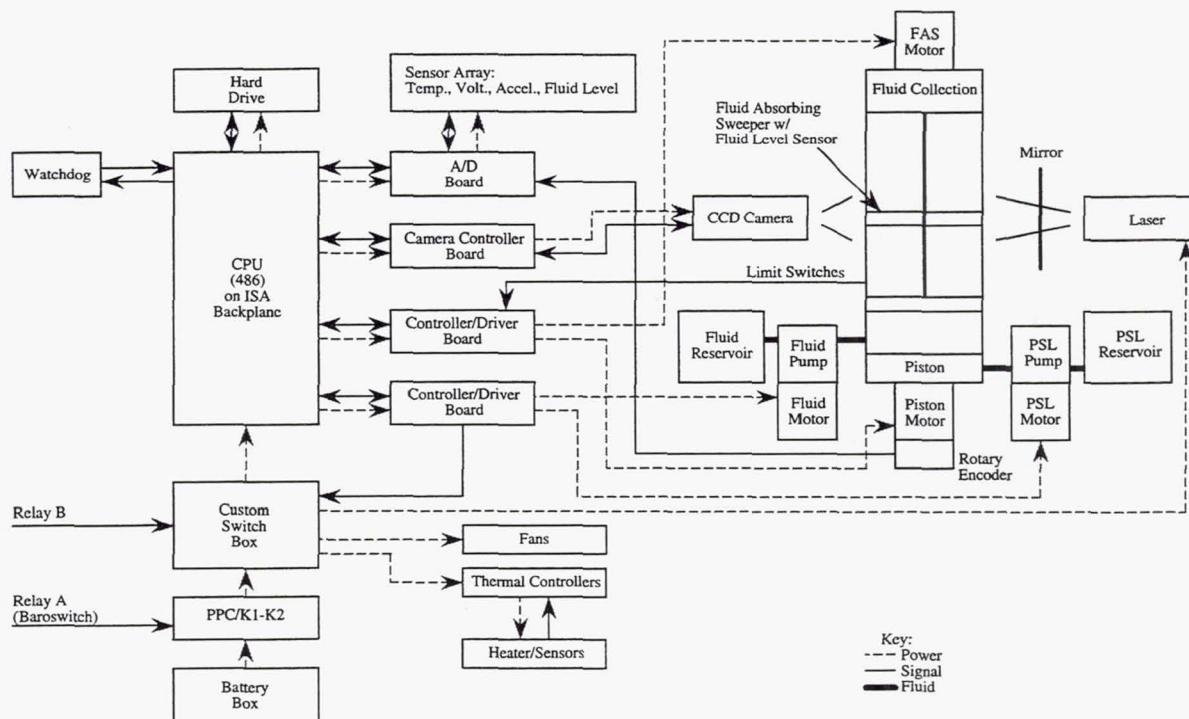
Figure 2 Diagram showing the interaction of the various G–093 system components.

Experiment Controller

The computer system served to control the experimental sequence of events and store the images and sensor data. The hardware consisted of an industrial-grade motherboard with a 486 microprocessor, a passive back plane with five expansion slots, a camera controller board to capture photographic data, two 2-GB EIDE hard drives, an A/D board, and two stepper motor controller/driver boards. The computer ran the MS-DOS ver. 6.22 operating system, while the experiment sequence and data collection were controlled by a dedicated program written in C/C++. The manufacturers of the motor boards, A/D board, and camera board provided linkable C/C++ subroutines that served as the software interface to the components.

The industrial computer assembly required several modifications so that it could be used as the payload's flight computer. One modification involved developing a mechanism to ensure that the five boards mounted in the passive backplane did not vibrate under launch loads, potentially causing an equipment failure. The solution was to machine a restraint from Delrin material such that it fit in the spaces between the computer cards and the computer box. This restraint included several grooves where the cards would securely be held in place and also included holes for screws to mount it against the steel walls

---

[1] More detailed technical information on the G–093 payload may be found in the G–093 Phase III Safety Data Package, which may be downloaded from the VORTEX website: http://aoss.engin.umich.edu/vortex.

of the computer casing. A second set of modifications included removal of all non-essential components (or incompatible pieces, *e.g.*, its 110 VAC power supply) and machining a notch for the NASA-provided pressure relief valve (PRV).

A watchdog circuit was implemented to ensure that the computer would reset if it hung. The watchdog was serviced occasionally throughout the experiment sequence, but if it did not receive a signal within five minutes, the computer would reset. The watchdog was implemented on a small board attached to the inside of the computer case. In order to properly handle a reset, the program had to be able to recover where it left off. Therefore, the program maintained a status file by occasionally saving information such as the experiment sequence number. On a reset, the program would read this file and be able to continue the experiment.

We used mostly "commercial off-the-shelf" (COTS) hardware rather than components that were space qualified due to cost considerations. We purchased industrial-grade hardware whenever possible. This kept the payload fabrication costs low, but there were several drawbacks. For example, although the computer was industrial grade and was housed inside the aluminum-walled GAS canister, it experienced some permanent damage during the flight. After de-integration, all attempts to boot the computer failed; the computer would freeze during the memory tests. We found evidence in the program's log file that the upset occurred approximately eight hours into the experiment, where it shows that the computer attempted to reboot several times. The last reboot listed in the log file has a date stamp of 01/03/80, which shows that some error caused the date to reset. Fortunately, this occurred after all 100 experiments were completed and the program was just waiting for the experiment to be shut down. The hard drives were not affected so we were able to connect them to another computer and retrieve the data.

Although we initially considered using the PC/104 format for our experiment controller, at the time of experiment design not enough components were available in this format. The situation has changed considerably such that future payloads should definitely consider this as an option.

Motors

Four stepper motors were used to actuate the payload components, with two motors connected to each of the two motor controller boards. Two motors were used for the two fluid pumps, one of which pumped the silicone oil into the FTC and the other pumped particulate seeded liquid (PSL) into the cylindrical cavity above the piston (see Figure 2). The remaining two motors drove the piston and the fluid absorbing sweeper (FAS). The computer controlled the speed and acceleration of the motors and the number of steps they rotated. For the case of the FAS, two limit switches were used to automatically stop the motor when the FAS reached the top or the bottom of the FTC.

Sensors and Data Acquisition System

An array of sensors, used to measure the G–093 payload environment, was implemented and their signals were conditioned as necessary and then sampled via an A/D board attached to the computer. Temperature sensors were located on the battery box, computer's central processing unit (CPU), fluid reservoir, PSL reservoir, FTC, both hard drives, and accelerometer. The accelerometer measured the level of microgravity in the payload. Acceleration data was collected from its three channels (x, y, and z) each at three different gains of ×1, ×10, and ×100. The fluid level was measured with an infrared (IR) reflective sensor mounted on the FAS. The piston position was measured with an optical rotary encoder attached to the piston stepper-motor shaft. The FAS travel was limited with two hermetically sealed mechanical micro-switches. The charge-coupled device (CCD) camera captured image data, which were stored directly into computer memory and transferred to the hard disk between experiments.

Digital Imaging System

The payload's camera was a 256-level grayscale, digitally controlled, CCD camera designed specifically for the computer technology market. The camera was capable of a resolution of 242×753, but the control program subsampled the number of horizontal pixels for an image size of 242×128. The FTC and image area are shown in Figure 3. The minimum exposure time for the camera was 1 ms and we used this minimum value since we wanted to maximize the image capture rate. It is important to note that exposure time is inversely related to bias and gain. For our experiments, we did not vary the exposure time but we did vary the gain (not the bias) to achieve a variety of images with different brightness and contrast levels.
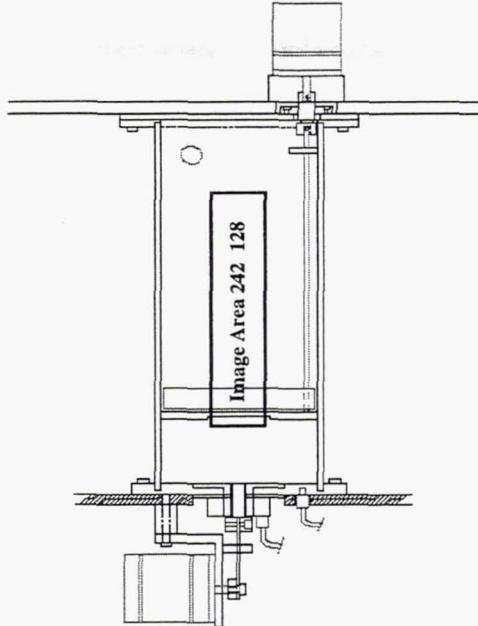
Figure 3 Diagram of fluid test cell showing image area.

The basic operation of the image acquisition system involved three major steps: memory allocation, image capture, and image storage. The program was able to store only one image at a time in random access memory (RAM); hence, only enough memory for one picture was allocated. The program then used the manufacturer-provided subsampling routine to capture a single picture and transfer the data to the allocated memory. To slightly increase the overall capture rate, instead of transferring the image from RAM to the hard drive, we chose to transfer it from RAM to a RAM disk. The image capture and transfer was repeated until there were 40 images in the RAM disk. Finally, the program transferred the image data from the RAM disk to the VORTEX hard drives via a special transfer buffer. The result was 40 separate image files stored in standard BMP format on both hard drives for each experiment.

EXPERIMENT SEQUENCE

The G–093 control program was written in C/C++, and compiled for MS-DOS ver. 6.22. Due to the limitations of MS-DOS, the program's commands had to run sequentially rather than in a concurrent or multitasked manner. The manufacturers of the motor board, A/D board, and camera board provided linkable C/C++ subroutines for DOS, which served as the software interface to the components. This made the programming task much simpler than having to write low-level code to communicate with each of the devices. In addition, the subroutines provided the capability of running board-level tasks in the background or concurrent with the main program. For example, the subroutine that controlled the A/D board sent a command to the board, which would then execute the command while the main program continued executing. This way the main program was capable of continuously collecting sensor data while performing other functions.

When the payload was turned on (via GCD Relay B), the main program executed by initially reading a status file that told it how to begin. This status file was updated frequently so if the computer should reboot for any reason, the program could continue where it left off. Throughout the experiments, the program also had to service a watchdog timer through a digital output on one of the motor controller boards. The watchdog would reset the computer if it was not serviced regularly (*e.g.*, the program stopped running or hung), but the program could start over again in the same place by reading the status file. Data for each of the 100 experiments were saved in directories—one for each experiment. After completion of an experiment, its directory contained a binary file of time-stamped sensor data, 40 bitmap images, and a log file of time-stamped text sentences of each step the program took.

For the duration of the mission, sensor data needed to be collected and saved. All of the sensors were connected to the computer through the A/D board. Using a manufacturer-provided subroutine, the A/D board could be commanded to collect data from any of the channels for a given sampling rate and amount of time. All the channels were sampled continuously at 10 Hz, and the encoder was sampled at 2.5 kHz only while the piston was firing. Depending on the part of the experiment,

data were collected in 5-, 10-, 20-, or 30-s blocks. The board could collect these data in the background and stream it directly into a memory data buffer while the main program would perform other tasks. Due to the sequential nature of DOS, after a background scan ended, there was a small delay before the next scan could begin. We minimized this delay by keeping two data buffers—when the board finished streaming data to one buffer, the program immediately commanded the board to begin the next scan into the other buffer. At this point the data from the first buffer was examined and saved to disk. These data were saved in binary format rather than ASCII. We found that a 30-s scan of data took close to 20 s to write to an ASCII file, while a binary file took approximately 1 s to write. A separate program was used after the mission to read the binary files and convert them to ASCII files for analysis.

Every five experiments, the program checked that the fluid level in the FTC was at the knife-edge. This was accomplished by lowering the FAS, which was actuated by a stepper-motor-driven ball screw. The FAS had two limit switches, also connected to the motor board, that would cause the motor to stop when the FAS reached the top or bottom of the FTC. Once the FAS was down, the program examined a 5-s average of data from the fluid level sensor. If more fluid needed to be added, the program commanded another stepper motor to pump more fluid into the FTC. Once the fluid level sensor read a value over a predetermined limit, the fluid fill stopped and the FAS returned to the top. Just in case all the fluid was used and the reservoir was empty, the program would keep track of the total amount of fluid (in motor steps) used so far and save that value in the status file. A parameter file, read at the startup of the program, had the number of motor steps of fluid originally placed in the reservoir, and if the program used more than this amount it would never try to fill again.

In addition to the above, the primary function of the program was to execute the actual experiment sequence. The program ran 100 separate experiments, varying parameters such as piston speed and camera gain. These parameters were specified in a file that was read upon program initialization. The experiment sequence began by lowering the piston and filling the cylindrical cavity with the PSL. The piston and PSL pump were each actuated by a motor connected to a motor controller board. Each motor was commanded to move a predetermined number of steps: 30 steps to lower the piston and 2000 steps to inject the PSL. At this point, the laser was turned on and the fan was turned off, each being controlled by a discrete output on a motor controller board. Five initial images were taken (to record the condition of the liquid–gas interface), the piston fired, then 35 images of the droplet formation were captured. The lasers were turned off and the fan was turned back on, the images were saved to the disk, and the program would move on to the next experiment.

Images were captured one at a time. The original plan was to capture as many images as possible directly into RAM and then transfer them to disk. The computer had 32 MB of extra RAM available, and due to the 640-kB limit imposed by DOS, the program would have been required to run in an "extended" or "protected" mode to access the extra memory. This was possible through some manufacturer-provided subroutines, and we were able to write a module that accomplished this. But once this module was integrated with the rest of the program, we found an incompatibility—some of the other manufacturer's subroutines were unable to operate in extended mode. We were unable to find a solution for this problem and therefore the program was limited to using only 640 kB of memory, which meant capturing only one image at a time. This significantly decreased the image capture rate, since capturing all images directly to RAM before transferring to disk is much faster than capturing one image and immediately saving it to disk to free the RAM for the next image. We attempted to speed the image capture as much as possible by creating a RAM disk, which is a portion of extended RAM that is assigned a physical drive letter. After capturing an image, the program saved it to the RAM disk. The program saw the RAM disk as a physical drive, and not extended memory, therefore it was able to use the extra RAM without operating in the extended mode. This was slightly faster than saving the image to a physical hard disk, but still not as fast as storing directly to RAM. Then after all 40 images were captured, they were transferred from the RAM disk to the hard disks.

Once all 100 experiments were completed, the program entered its shut down procedure. The program lowered the FAS and ran the fluid pump a predetermined amount of steps in reverse to evacuate the FTC of all the fluid. Once the FTC was empty, the FAS would move up half-way and wait for the shut down of the GAS canister.

The operational procedure described in detail above is outlined below:

- Baroswitch turns on Relay A, experiment thermal control begins, payload power is on
- GCD Relay B enables experiment
- Computer initializes
- FAS moved to bottom of FTC
- FTC is filled with silicone oil while monitoring fluid level sensor, stop when filled to knife edge
- Move FAS to the top of the test cell
- Experiment sequence begins
  - Lower piston
  - Fill cylindrical cavity with PSL

- Turn off fan
- Turn on laser
- Capture five initial images
- Initiate piston motion, record piston position
- Start image capture
- Turn off laser
- Turn on fan
- Transfer images to disk
- Run experiment sequence 100 times (approximately 5 hours)
- After 100 experiments completed, lower FAS to bottom of test cell
- Empty all silicone oil from FTC back into reservoir
- Raise FAS half way and wait for experiment to be turned off

DATA ANALYSIS

This section highlights data collected by G–093 on STS–88. Some of the data is specific to the VORTEX scientific mission, others are more general and should be useful to other payload designers. The VORTEX mission lasted a total of 5 hours, 10 min. VORTEX MET 00:00 occurred at STS–88 MET 000/04:29.

Internal and External Temperatures

When powered on, the electrical components of the VORTEX payload produced about 60 W on average. Almost all of this heat was contained within the canister. Figure 4 shows internal and external payload temperatures as a function of time during the VORTEX mission. The lines denoted by "Upper Thermister (V34T1118A)" and "Lower Thermister (V34T1118A)" are NASA-provided temperature measurements of the Shuttle's payload bay near bay 13 during the STS–88 mission.
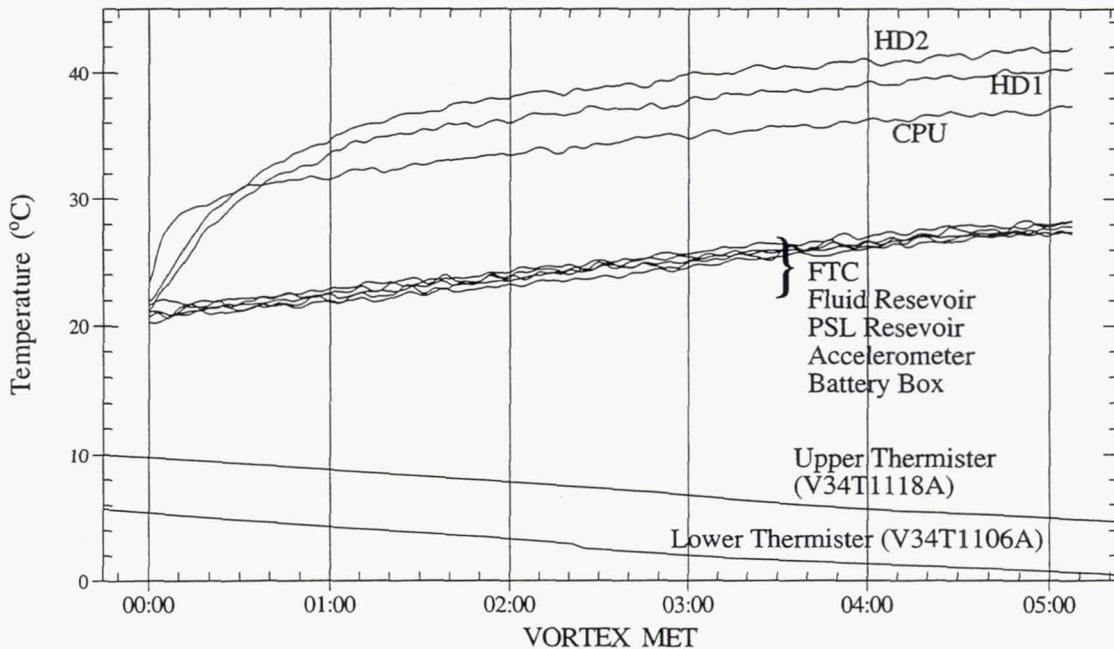
Figure 4 Internal and external temperatures of the G–093 payload.

There are several items to note about the temperature data. First, at no point during the VORTEX mission was the external temperature below 0 °C, and the internal temperature was always above 0 °C; hence, the payload's heaters were not used. Second, at the start of the VORTEX mission, the payload was about 20–23 °C. Third, the two hard drives and the

CPU had the highest localized temperatures, although this was expected. Finally, as seen by the fact that the other temperatures track very closely with each other, we see that the fan was able to adequately mix the payload's atmosphere to equalize the temperature between components.

Fluid Level

Figure 5 shows data collected by the fluid level sensor during the initial filling phase of the VORTEX mission. Filling cutoff occurred at 2365 counts and is indicated in Figure 5 by the rapid increase of signal at MET 00:20 (the sensor's response is nonlinear). As explained above, a 5-s running average was used to guard against the noise in the signal. The filling sequence was successfully stopped when the fluid reached the knife-edge. This shows that the knife-edge concept should prove useful for future missions wishing to establish a liquid–gas interface by this method.
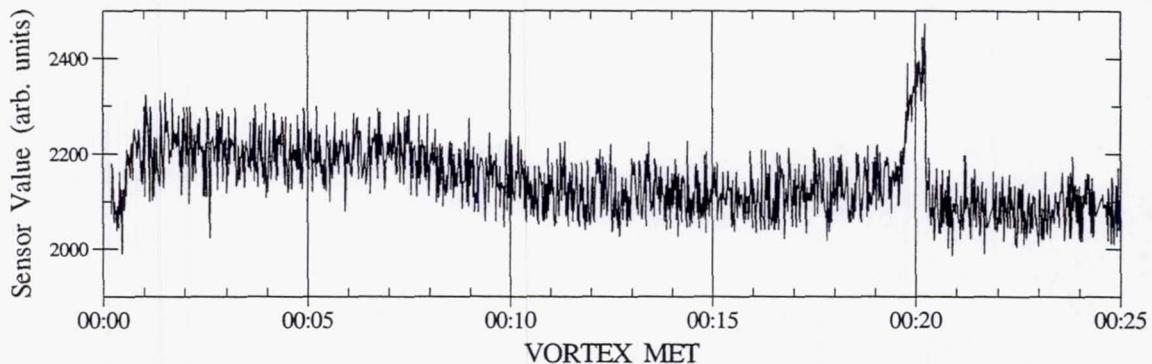
Figure 5 Fluid level sensor signal level during initial fill sequence.

Battery Box and Bus Voltages

Figure 6 plots the voltage of the main batteries during the VORTEX mission. Although data were collected on the other bus voltages, they are not shown because they held steady throughout the mission. These voltage data are important because they would indicate if a problem occurred due to an out-of-specification voltage level. This data also shows that the battery box design we developed, while inexpensive, provides a large energy source easily capable of running longer duration missions. One consideration for future payloads is the addition of a current sensor to determine total power usage directly.
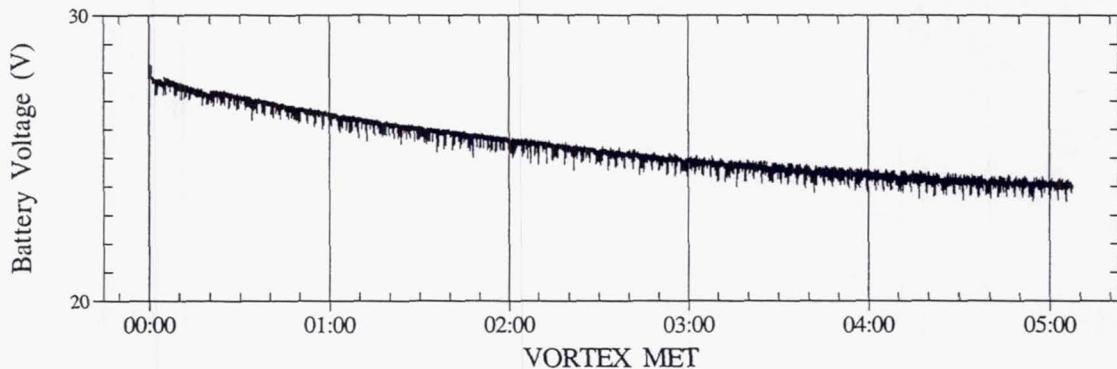
Figure 6 Battery voltage during VORTEX mission.

Encoder Data

Figure 7 shows the data collected form the rotary encoder and how it is interpreted to determine piston speed. The bottom panel shows the output of the rotary encoder, which is a TTL-level signal that toggles between high (1) and low (0) every 1.8° (200 toggles per full rotation). This data can be analyzed to show the piston distance as a function of time. For example, in Figure 7 the derivative of the smoothed piston position gives a piston velocity of 14.75 cm/s. Although the

146

computer controlled the piston speed, the rotary-encoder data provide independent confirmation that the piston did indeed move at a certain speed and that it moved the entire distance from 1.1 cm below the FTC bottom to the bottom (at 0 cm position).
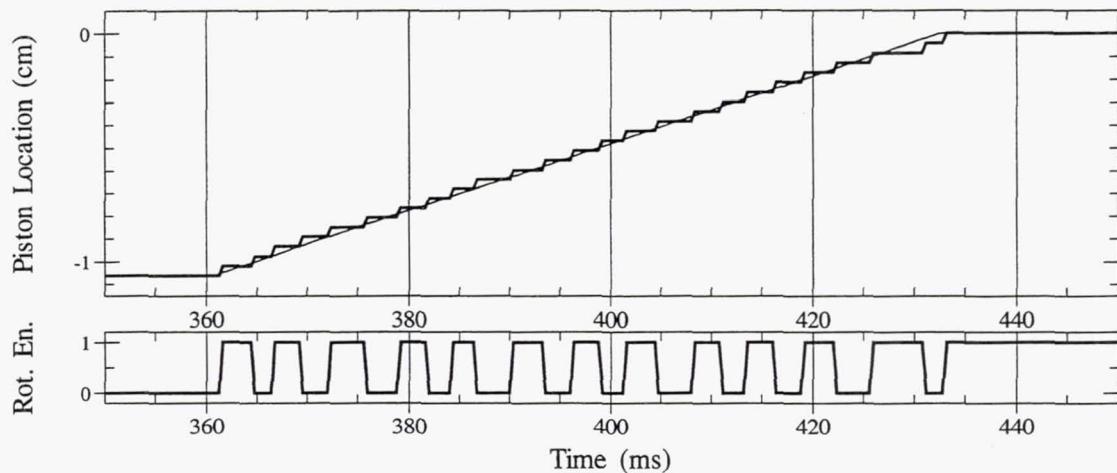
Figure 7 Piston position derived from rotary-encoder data during experiment 89.

Image Data

The VORTEX CCD camera captured images of the fluid motion and the droplet formation process. The images have been retrieved successfully from the on-board computer and are currently undergoing analysis. Figure 8 shows a sample sequence of images taken during experiment 89. We are currently examining these images to extract information on the droplet formation and sequencing the images to show clearly the propagation of the droplet. This information will then be combined with piston speed, temperature, and other experimental conditions collected during the experiments.
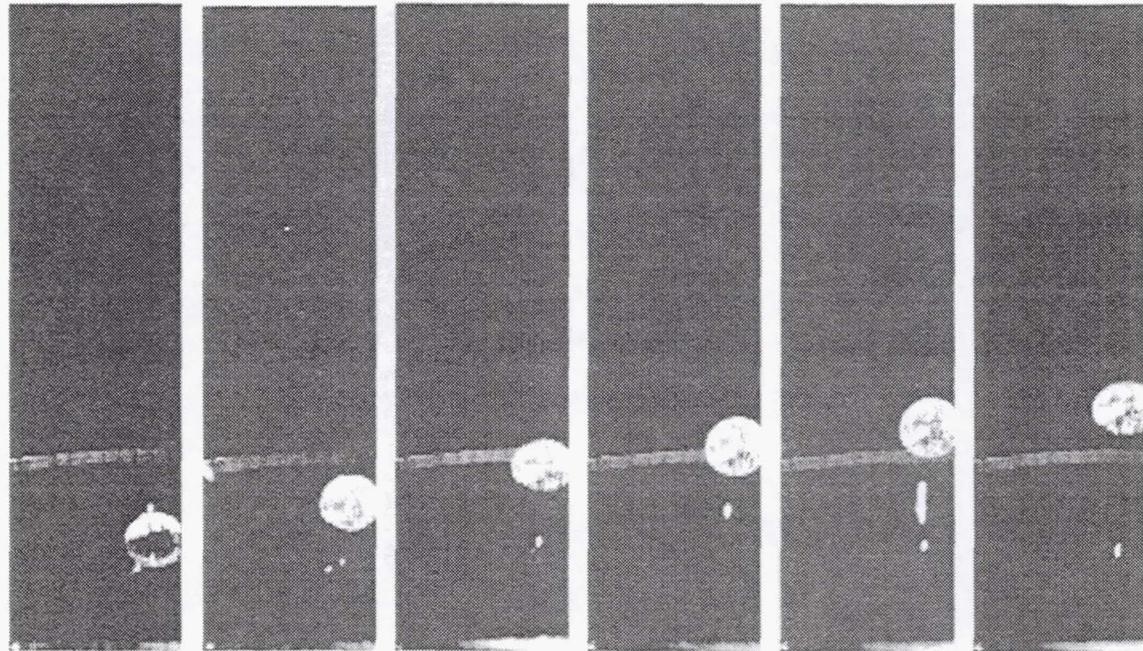
Figure 8 Sequence of images taken during experiment 89 showing propagation of a vortex ring through a liquid–gas interface.

The image data have been modified using a commercial graphics software package. Since the photos were stored in BMP format during the VORTEX mission, they remained in BMP format after adjustments were made so that no information would be lost. The images have been brightened and the color levels adjusted to include a smaller section of gray levels. The image data show that the camera was slightly off-center, possibly due to a shift during launch.

SUMMARY

VORTEX was flown on Shuttle missions STS–89 in January 1998 and again on STS–88 in December 1998. VORTEX was flown to answer some basic questions about fluid atomization—the process whereby a liquid is converted into small droplets. VORTEX investigated the propagation of a vortex ring through a liquid–gas interface in microgravity. The primary data returned from the VORTEX payload are images of this process. Although the STS–89 flight was unsuccessful, the second flight of VORTEX on STS–88 performed as expected and scientific data were collected in 100 experimental sequences. The image data have been successfully retrieved from the payload's on-board computer and are currently undergoing analysis. This paper discussed aspects of the VORTEX experiment sequence, the experiment controller and data acquisition system, and the imaging system.

REFERENCES

1. Bernal, L. P., P. Maksimovic, F. Tounsi, and G. Tryggvason, "An Experimental and Numerical Investigation of Drop Formation by Vortical Flows in Microgravity," AIAA paper 94–0244, AIAA 32nd Aerospace Sciences Meeting, Reno, Nev., Jan. 10–13, 1994.

2. Wu, P.-K., and Faeth, G. M, "Aerodynamic Effects on Primary Breakup of Turbulent Fluids," *Atomization and Sprays*, vol. 3, 265–289, 1993.

3. Bilén, Sven G., and Luis P. Bernal, "Get Away Special Payload G-093: The VOrtex Ring Transit EXperiment (VORTEX) Flights," 1999 Shuttle Small Payloads Project Office Symposium, Annapolis, MD, 13–15 Sept. 1999, NASA CP–1999–209476. (Paper 21 of this compilation.)

Delrin is a trademark of E. I. Du Pont de Nemours & Co., Inc. MS-DOS is a trademark of Microsoft Corp.

THE DEVELOPMENT OF THE USU GAS SYSTEM, G-001 TO G-090

Jason Sanders (USU GAS Coordinator)
Casey Hatch, Kait Williams, Steven Neville, Uyen Chau, Arlynda Wright, Leann Moody,
Mike Anderson, Jamie Jorgensen, Adam Margetts, Mel Torrie, Travis Whipple, Glen
Roth, David Hansen, Rayn Sharp, Stephen Fonnesbeck, and Rick Rambo

Student Experimenters, USU GAS Program
4415 Old Main Hill
Logan UT, 84322-4415, USA
435-797-2629 (voice)
435-797-2492 (fax)
jason.sanders@usu.edu (email)

Jan J. Sojka, David Peak

Faculty Advisors, USU GAS Program
Dept. of Physics, Utah State Universtiy
Logan UT, 84322-4415, USA
435-797-2857

ABSTRACT

The Utah State University Get Away Special (USU GAS) Program has flown a
total of 11 GAS payloads since G-001 back in 1982. From that first payload, USU
undergraduate students have learned many valuable lessons. These lessons have been use
to implement our new GAS payloads. We have developed a system for integrating
multiple experiments into a single GAS payload. Along with this integration scheme, we
have developed reusable GAS hardware designed for flexibility and modularity.

This paper will consider the hardware developed by USU GAS from a historical,
motivational and educational viewpoint. The major hardware discussed will be the
program's Iso-Spacepak structure, battery box, micro-controller system, and GAS
Environment Monitoring System (GEMS). The thrust of the paper's exploration will be
to describe the modularity, flexibility and simplicity of these USU GAS systems. We
believe the lessons we have learned over the years will be beneficial to future GAS
student experimenters.

We will be describing the history of the program's structure. Included in this
history will be the development of a aluminum supported, foam and epoxy resin
Spacepak. In addition we detail the current reusable, modular, lightweight, aluminum
Iso-Spacepak.

The current sealed battery box design will be reviewed. It will be compared with previous attempts and failures. Also, we will take a look into the past when battery boxes were not a requirement.

Micro-Controller development will be analyzed. We will describe the current control board designed and built by USU GAS students. It incorporates the commercial micro-controller (the Stamp II). The history of USU GAS micro-controllers begins with the early payloads' student-made, bulky, yet modernly powerful Sawat Controller.

The final content of the paper will involve the GAS Environment Monitoring System (GEMS). It is being developed for G-221. GEMS is a system, independent of all experiment control systems. It monitors the electrical activities of multiple GAS experiments along with the GAS canister environment.

STRUCTURE

Over the years the USU GAS program's standardized payload structure has gone through four major revisions. These revisions reflect the program's desire to build strong, lightweight, reusable and modular GAS components.

The first structure was used once for G-001, in 1982. This structure is shown in a Figure 1. The structure was a great starting point for GAS experiments. The structure consisted of three vertical walls joined in the center of the GAS Canister and each extending outward to the edge of the plate. The individual experiments, power supplies and electronics were mounted to these three walls.

Figure 1 - The first USU GAS structure.

During construction and integration of this payload it was discovered that this design was not very modular for the implementation of many experiments. This lack of modularity made it difficult for separate experimenters to simultaneously work on their respective experiments in the structure. It also caused difficulty in mounting all the separate experiments into the single GAS Canister. These structural problems inspired the spacepack concept.

Figure 2 - Spacepak concept.

The second structural revision was the first to implement the spacepack concept. Used in G-004, G-008, G-518, and partially in G-254. The spacepak concept is founded on keeping the structure modular and convenient for multiple GAS experimenters. A full structure outline is shown in Figure 2. Figure 3 shows three students with their individual spacepaks filled with their experiments. The bottom half of Figure 2 shows three of the six spacpaks stacked on top of each other. Each hexagonal spacepak is designed to house a single experiment. Each experiment is designed, fabricated, built and fitted into its individual spacepak. At integration all six spacepaks are stacked on top of each other and attached to vertical aluminum struts. These struts

Figure 3 - David Prince, Sawat Tantiphanwadi and Scott Thomas proudly display their spacepaks for G-004

are securely attached to the mounting plate and provide lateral support. This spacepak structure simplifies integration of all the payload experiments and simplifies the construction of individual experiments.

Each Spacepak was easily constructed out of lightweight aircraft foam and coated with fiberglass. The foam hexagonal spacepak walls and base were cut from a foam sheet. These wall and base pieces were then assembled and glued together with epoxy. Following, the foam assembly was coated with epoxy and covered with fiberglass to harden and strengthen the structure. Each fiberglass spacepak was remarkable strong; to test the strength of each student's structure, it is reported that Dr. Rex Megill, would stand on the completed spacepak before it was deemed "flight worthy".

The third major structural change occurred as part of the G-254 payload. A stronger, completely reusable structure was desired. The first of the iso-spacepaks was developed. Iso-spacepak is an
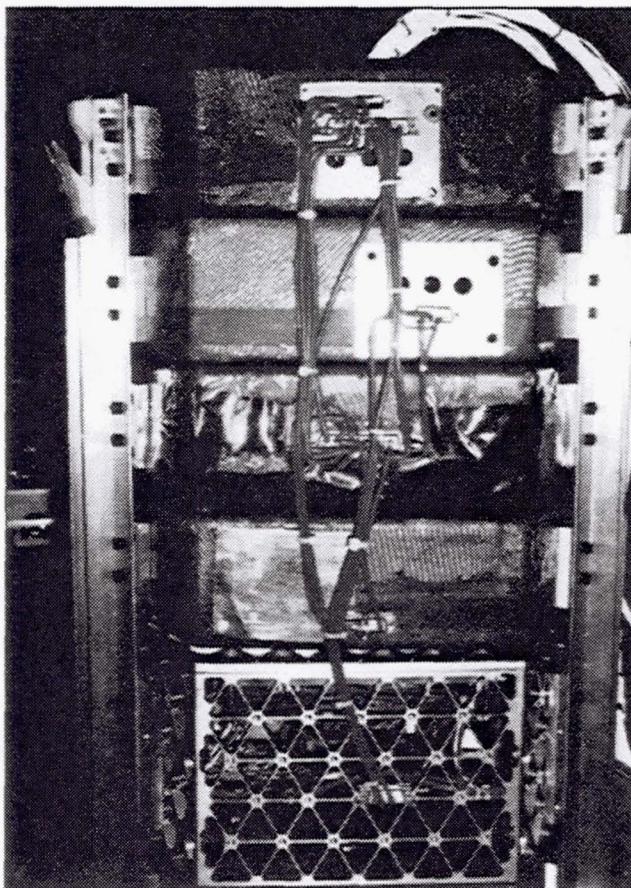
Figure 4 - G-254 structure showing both the old fiberglass spacepak and the new iso-spacepak structure.

Figure 2.1.1 G-090 Structure

Iso-spacepak Level 1

Bumper

Struts

MID PLATE

spacepak Level 2

Mounting ring
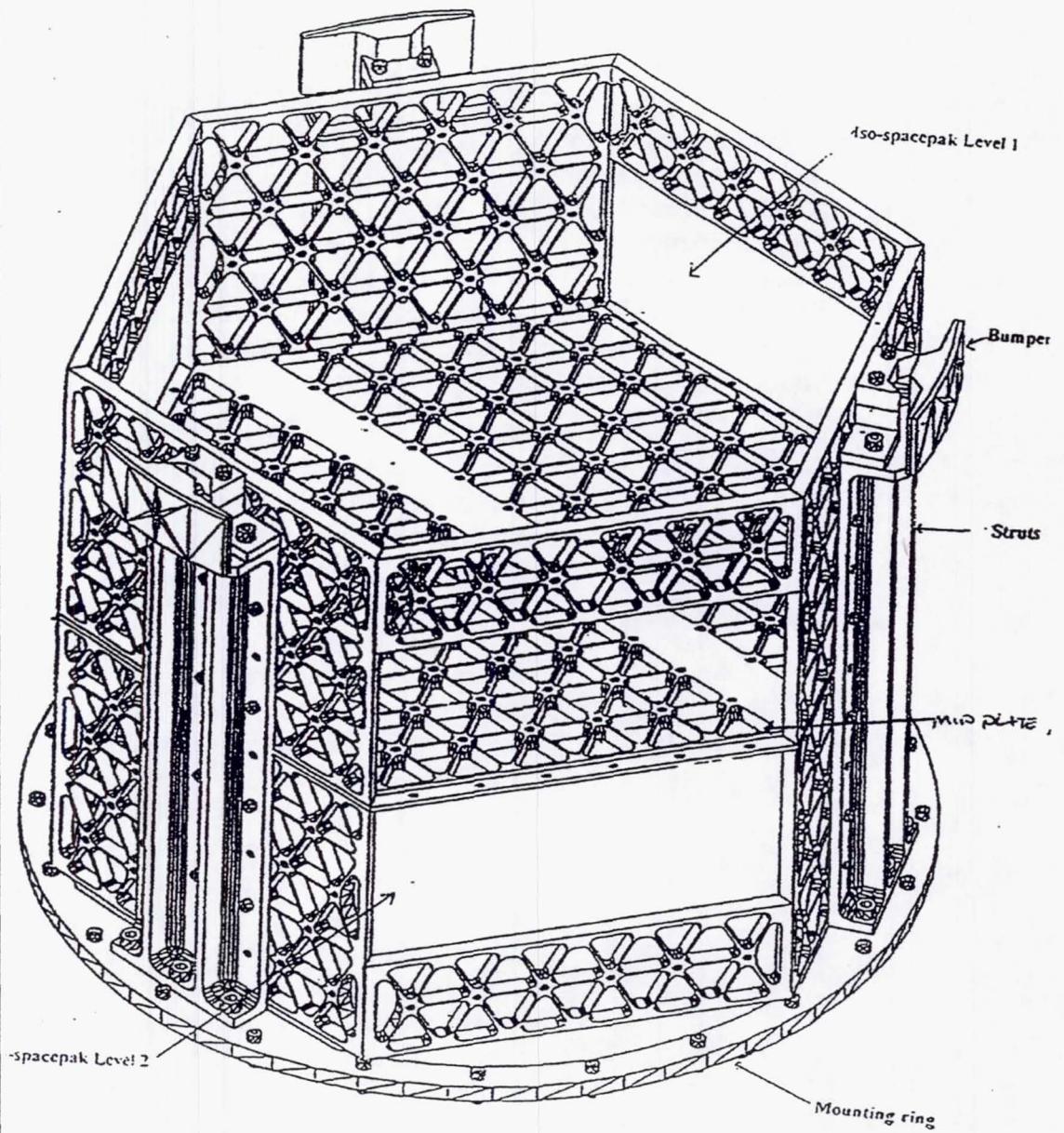
Figure 5 - Iso-spacepak structure used in G-200 and G-090

aluminum structure with a milled iso-grid pattern. Only one was made and implemented into the full spacepak structure as seen in figure 4.

This first iso-spacepak was a new step in the evolution of the USU GAS structure. The structure kept its convenient modularity of the spacepaks and added reusability and

increased strength. The iso-spacepak also added a touch of elegance and sophistication to the structure.

The final step in the evolution of the USU GAS structure was the implementation of a structure made completely out of iso-grid. Building on the success of the iso-spacepak of G-254, USU students built a fully reusable half can iso-grid structure (see Figure 6 & 7). This structure was used in G-200, G-090 and will be used for G-221. This iso-spacepak structure is modular, strong and remarkably lightweight.

BATTERY BOX
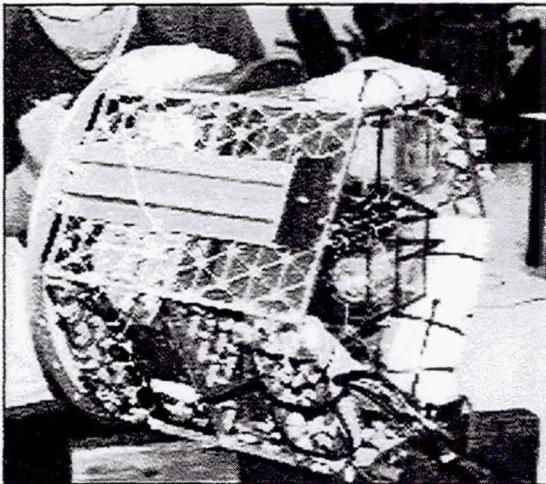
Figure 6 - Iso-spacepak structure. Photo taken during G-090 safety inspection at KSC.
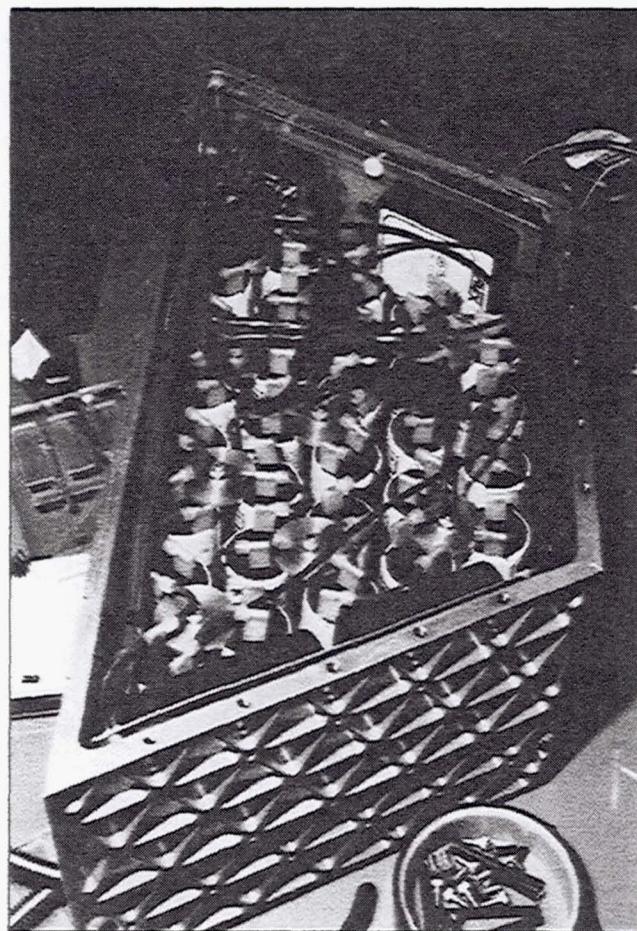
Figure 7 - G-200 battery box.

Battery boxes have gone through a number of transitions through the years. The first payloads were not required to have any formal battery boxes. In G-001, for instance, (see figure 1) the batteries are not contained in a battery box. For these first payloads the batteries for each experiment were contained separately and not enclosed in a sealed battery box.

USU's first attempt at the sealed battery box was initiated with G-200. This battery box was designed and built into the new iso-spacepak structure. The battery box was contained in half of one of the hexagonal spacepaks (see figure 7). Unfortunately, the battery box was a failure. The box could not hold a pressure and thus failed pressure tests at KSC during integration. The half-hexagonal shape made it difficult to create a pressure seal and the power connector to the battery box was not hermetically sealed. This failure, however disheartening, inspired the current battery box.

153

The current USU GAS battery box is shown in Figures 8 & 9. The conical shape was chosen for its ease in being sealed with an O-ring. The design was inspired by the NASA GAS Canister. A full description of the battery box follows.
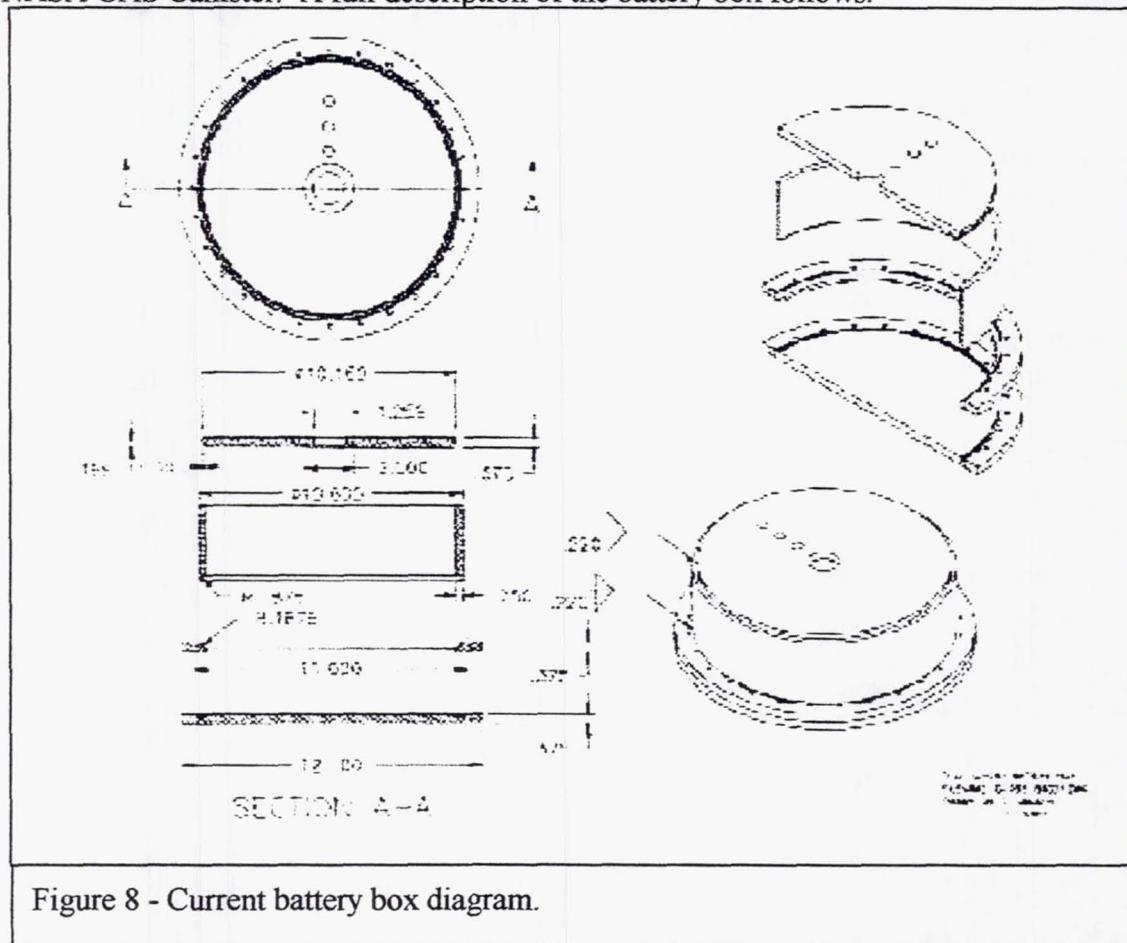
Figure 8 - Current battery box diagram.

40 cells are enclosed in a sealed circular battery box made of 6061-T6 Aluminum (see figures 8 & 9). The batteries sit in 1/8 inch seats milled out of ¼ inch plexiglas plate. This plexiglas plate is attached to the bottom of the battery box, and secures the batteries into position. The batteries are tightly secured from the top by another Plexiglas plate, which then sandwiches the batteries securely in place. The top Plexiglas plate is secured to the bottom Plexiglas and aluminum plate by 8 -3" bolts. The circular top plate is welded to the cylindrical sides and is secured to the bottom aluminum plate and over the batteries and Plexiglas by 28 -.75" bolts
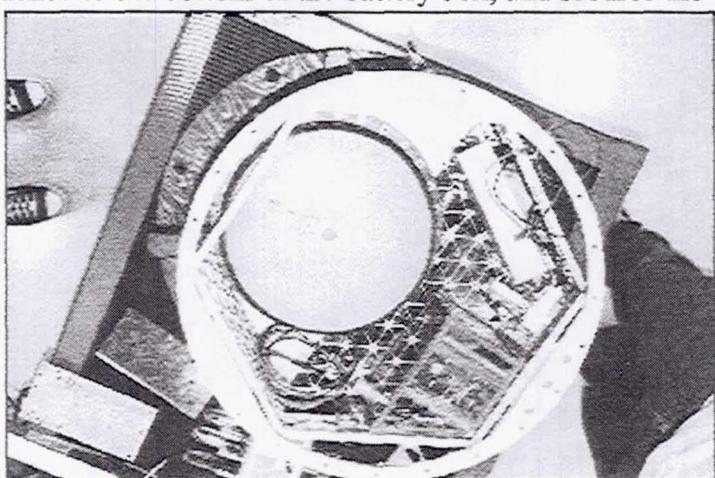
Figure 9 - Iso-spacepak structure with battery box.

154

which are coated with Epon 828 cured with Versamid 140. To ensure a seal, an ethylene propylene o-ring is placed in a groove between the lid and the box. Prior to sealing a layer of Parker O-lube vacuum grease is applied around the o-ring. The box is vented through the upper aluminum plate through two NASA standard 15-psi differential pressure relief valves. Power connection to the box is provided by a 9 pin hermetically sealed connector. The inside of the box is coated with a non-conductive coating, Epon 828 cured with Versamid 140, which is chemically inert to the battery electrolyte. The terminals are also coated with the same non-conductive material. The free volume of the box has been minimized by design. The battery box is proof pressure tested to 22.5 psig.

MICRO-CONTROLLER

The first reusable, student designed control board was built by Sawat Tantiphanwadi, in 1983. The Sawat controller was used on the student payloads G-004, G-008, and G-518. The board was designed around the 65C02 processor. It had 16 analog input channels, 8 digital input control channels, and 8 output control signals. The controller had 128k of program storage, 64k temporary data storage, and 32k of permanent data storage. The board was programmed in machine language.

The current control board is designed around the Basic Stamp II micro-controller (see figure 10). This controller has been used on G-200, G-090 and will be used again on G-221. This control board is highly flexible it has 16 digital or analog input/output-control channels. The Stamp II itself has 2k for program and data storage, and can easily be expended to 96k of data storage. The Stamp II is programmed in PBasic.

Although the Sawat controller has more input/control channels and more storage space the transition to the Stamp controller was made because of the Sawat controller's inflexibility and because of the difficulty involved with programming machine language. Over the years only a couple students were able to program the Sawat Controller. The Stamp II is very flexible. It can easily expand its input/output-control channels and its data storage. The PBasic programming language is very simple and is easy to use, even by non-technical students. With the Stamp control board individual GAS experimenters are able to easily program their own control and data recording sequences.

Figure 10 - The Stamp II control board, used in G-090.

GAS ENVIRONMENT MONITORING SYSTEM (GEMS)

The GEMS concept was brainstormed during G-090's deintegration and evaluation period. G-090's payload consisted of four high school student experiments. These experiments were designed, built and tested by separate high schools under the supervision of USU (ref 1). The experiments ran independently in the GAS Canister, while in orbit. During deintegration a number of questions arose about what actually occurred in orbit. For instance it was unknown if power made it to a certain component. It was unknown exactly how long one experiment was powered on. The temperature of the GAS Canister is in question. These questions and others inspired GEMS.

GEMS is being designed to monitor the occurrences of multiple GAS experiments as well as the GAS Canister environment independently. Currently the design calls for GEMS to monitor: GAS Canister temperature, humidity and radiation as well as individual experiments power switching, voltage and current draws. Also included in GEMS will be visual indicators. These indicators will give us visual confirmation about electrical power being switched by certain components, rather than relying on electrical indications.

GEMS is being designed for simple integration into the current USU GAS hardware. The system's probes and controller is being designed to be easily implemented into the structure. The individual experiment power, voltage and current indicators are being designed around the Stamp II control board.

It is hoped that GEMS will provide a reusable independent monitoring system to aid in the deintigration and evaluation of GAS experiments.

The GAS Program at USU has had many years of GAS experience. Throughout these years we have accumulated a lot of experience, much of it the hard way, by trial and error. It is our hope that our experiences will be shared with future GAS experimenters.

REFERENCES

1. Leann Moody: USU's High School Companion, G-090. The Shuttle Small Payloads Project Office Symposium, NASA CP–1999– 209476. (Paper 22 of this compilation.)

Page intentionally left blank

USU'S HIGH SCHOOL COMPANION, G-090

Leann Moody

Casey Hatch, Kait Williams, Steven Neville, Uyen Chau, Arlynda Wright, Jason Sanders, Mike Anderson, Jamie Jorgensen, Adam Margetts, Mel Torrie, Travis Whipple, Glen Roth, David Hansen, Rayn Sharp, Stephen Fonnesbeck, and Rick Rambo

Student Experimenters, USU GAS Program
4415 Old Main Hill
Logan UT, 84322-4415, USA
435-797-2629 (voice)
435-797-2492 (fax)
slf53@cc.usu.edu (email)

Jan J. Sojka, David Peak

Faculty Advisors, USU GAS Program
Dept. of Physics, Utah State Universtiy
Logan UT, 84322-4415, USA
435-797-2857

ABSTRACT

In conjunction with NASA, the Get Away Special (GAS) Program is an academic program at Utah State University (USU). It's designed to give undergraduate students an opportunity to participate in Space Shuttle flights by developing their own science experiments. G-090 was flown aboard Shuttle Discovery (STS-91) in June, 1998. It consisted of three experiments designed and crafted by high school students from Utah and Idaho, as well as a small experiment for elementary school.

USU worked along with high schools to give them the opportunity to gain experience in space research. USU seeks to help students develop knowledge and gain a better understanding of space flight experimentation. High school students are recruited in hopes of sparking interest in space and furthering their education.

The following four experiments have been flown and will be flown again.

Experiment 1: *Chemical Unit Process (CUP)* was built by students from Shoshone-Bannock High School in Fort Hall, Idaho. This experiment was designed to test the effects of micro-gravity on the extraction of phosphate ions from phosphate ore using conventional industrial methods. Throughout the experiment, we experienced many difficulties. We learned that testing and running a program is vital to its success. We also learned we must account for the three month dormancy period (between integration and launch).

Experiment 2: *Crystal Growth* was built by students who originally attended Moscow High School, in Moscow, Idaho. This experiment was designed to study the formation and growth of chemical crystals in a micro-gravity environment. Our expectations for this experiment were highly met. Unfortunately, it was learned that what had taken place may have happened on Earth and not in space.

Experiment 3: *Nucleic Boiling* was built by students at Box Elder High School in Brigham City, Utah. The purpose was to study the effects of micro-gravity on temperature gradients and bubble formations in nucleic boiling water. Upon conclusion of the flight, we found a few things had gone wrong and a few others had worked in ways different from expectation. The paper will reveal these differences.

Experiment 4: *Space-Popcorn* was a latent experiment for St. Vincent Elementary School in Salt Lake City, Utah. They popped the popcorn and grew radish seeds to compare with similar samples maintained on earth. The purpose of this experiment was to promote interest in space among young

children. The process did have a few scientific mistakes, but it exposed the students to a unique space experience.

We can safely say that the total lessons learned have more than out weighed the downfalls made along the way. The lessons we learned will be incorporated throughout the experiments as we prepare to fly again on G-221 in March of 2000.

INTRODUCTION

The GAS program at Utah State University (USU) encourages students to participate in microgravity science by giving the students an environment to design and fabricate GAS experiments. The goal of the GAS program at USU is to develop undergraduate student skills associated with building and conducting individual experiments and to provide an extraordinary space related experience. Proudly, USU has flown a number of GAS payloads include the first payload, G-001, back in 1982. The most recent payload, G-090, flew on STS-91 aboard the Space Shuttle Discovery in June 1998. As an outreach program, G-090 incorporated four experiments designed and built by three high schools and one elementary school in Utah and Idaho. USU provided supervision, support, and acted as a liaison with NASA. We will detail the four experiments, describe the experimental results, discuss the lessons learned, and outline a path to a future reflight.

G-090

Using the spacepak concept similar to G-008, G-004, G-518, and G-006; and the iso-spacepak concept of G-254, and G-200 (ref 1), the external shape and dimensions of each experiment was standardized, and each experiment was independently controlled to allow easy interchange within the canister. The experiments were housed in a sealed 2.5 cubic foot canister with a nitrogen purge. The GAS Canister was comprised of four experiments, the battery box, and control and measurement electronics. The experiments and the developing schools were: Experiment 1, Chemical Unit Process in Space, Shoshonne-Bannock (ShoBan) Sr/Jr High School, Fort Hall, Idaho; Experiment 2, Crystal Growth Experiment, Moscow High School/University of Idaho, Moscow, Idaho; Experiment 3, Nucleic Boiling in
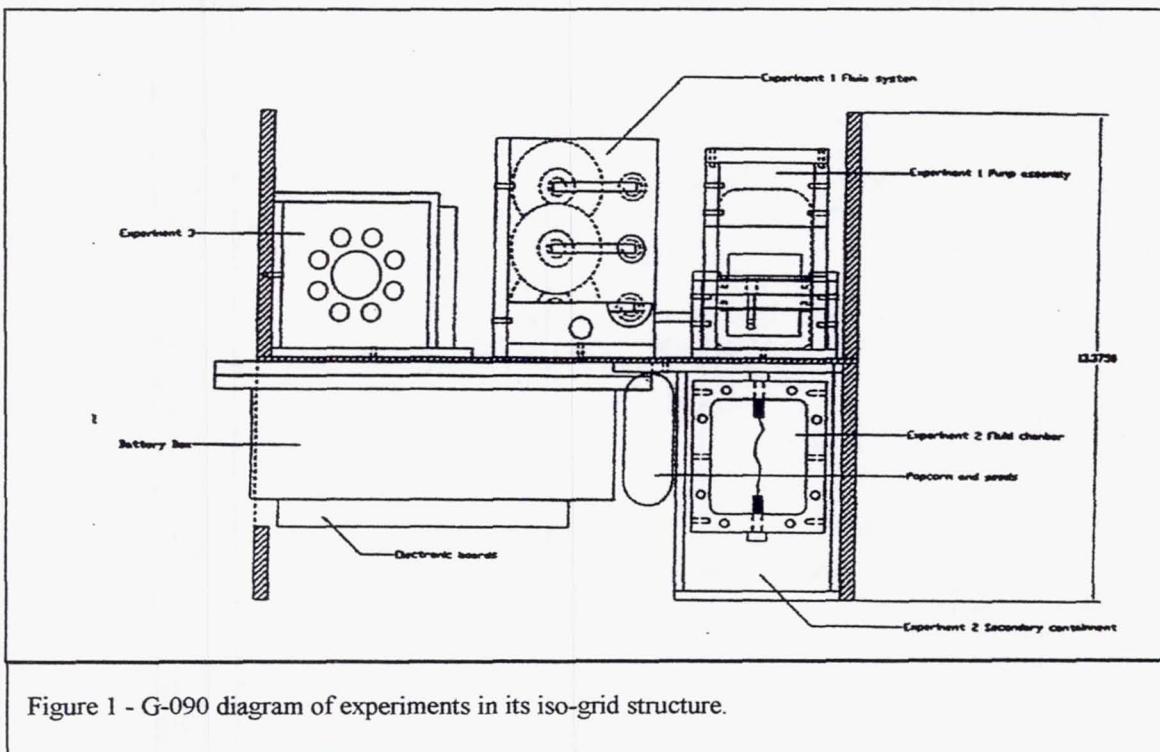
Figure 1 - G-090 diagram of experiments in its iso-grid structure.

160

Space, Box Elder High School, Brigham City, Utah; and Experiment 4, Space Popcorn, St Vincents Elementary School, Salt, Lake City, Utah.

Experiment 1 – Chemical Unit process

Experiment 1 was designed, tested, and fabricated by Native American students from Shoshonne-Bannock (ShoBan) Sr/Jr High School, Fort Hall, Idaho. The experiment was the first completely Native American designed experiment to fly in the Space Shuttle. In the local area the mining and extraction of phosphate ore is a major industry. The students, wishing to design an experiment reflecting their land and culture, choose to design an experiment involving the extraction of phosphate ions from phosphate ore. Figure 2 shows the students from ShoBan High School.

On Earth, phosphate ions are used as a fertilizer and would be dire to sustain life in an independent space colony. This experiment was designed to test the effects of micro-gravity on the extraction of phosphate ions from phosphate ore using conventional industrial methods. Also, this experiment was designed to test the chemical unit process is space. On earth gravity is a factor, therefore the extraction of the ion is easily performed and understood. It was the desire of ShoBan High School to perform the same process in a micro-gravity GAS canister.

The experiment percolates water through three samples of phosphate

Figure 2 - Students from ShoBan High School in the USU GAS Maragoni Lab

ore, creating a phosphate-water solution. The main experiment action consists of pumping water through a system of chambers with phosphate ore, filters, tubing, and plastic bladders (see figure 3). A solenoid valve opens as the first of the two linear actuators pushes a push plate against a water bladder. The solenoid valve then closes. The water bladder is a 450-ml medical IV bladder containing 300 ml of deionized water, encased with the push plate in a lexan chamber. The bladder is filled to 67% of its capacity to account for any expansion of the water if it should freeze during flight. The first linear actuator sits on a sliding Plexiglas plate above the second linear actuator, which is mounted to two Plexiglas mounts. Both actuators push the water throughout the entire system. The first acutator continues to push for nine seconds and then stops for nine seconds along with the opening and closing of the solenoid valve. The second actuator is then activated and continues the same process. The second actuator pushes the sliding plate, which the first actuator sits upon, then in turn, pushed the push plate into the water bladder. The water is pushed out of the bladder through nylon tubing then split into three identical systems. The water then percolates throughout three separate mixing chambers; each containing phosphate ore and two coned pre-filters, one prior to the phosphate ore and one after. In the mixing chambers the water and phosphate produce a water phosphate solution. The phosphate solution passes through the pre-filters in the mixing chambers and then through primary filter (coffee filter) before being stored into three collection bladders. In the tubing between the filters lies a check valve, which keeps the fluids from flowing back throughout the system. The experiment lasts for a total of thirty minutes, in which time the solenoid is closed permanently and the entire system becomes dormant.

During deintegration at KSC, it was quickly noted that no water had been pumped from the main bladder, and no solution was found in the collection bladders. This was a heart-breaking discovery. It appeared, at first, that the push plate had jammed during launch vibrations and thus not pushing the water through the system. However, upon complete dismantling of the experiment, it was found that the
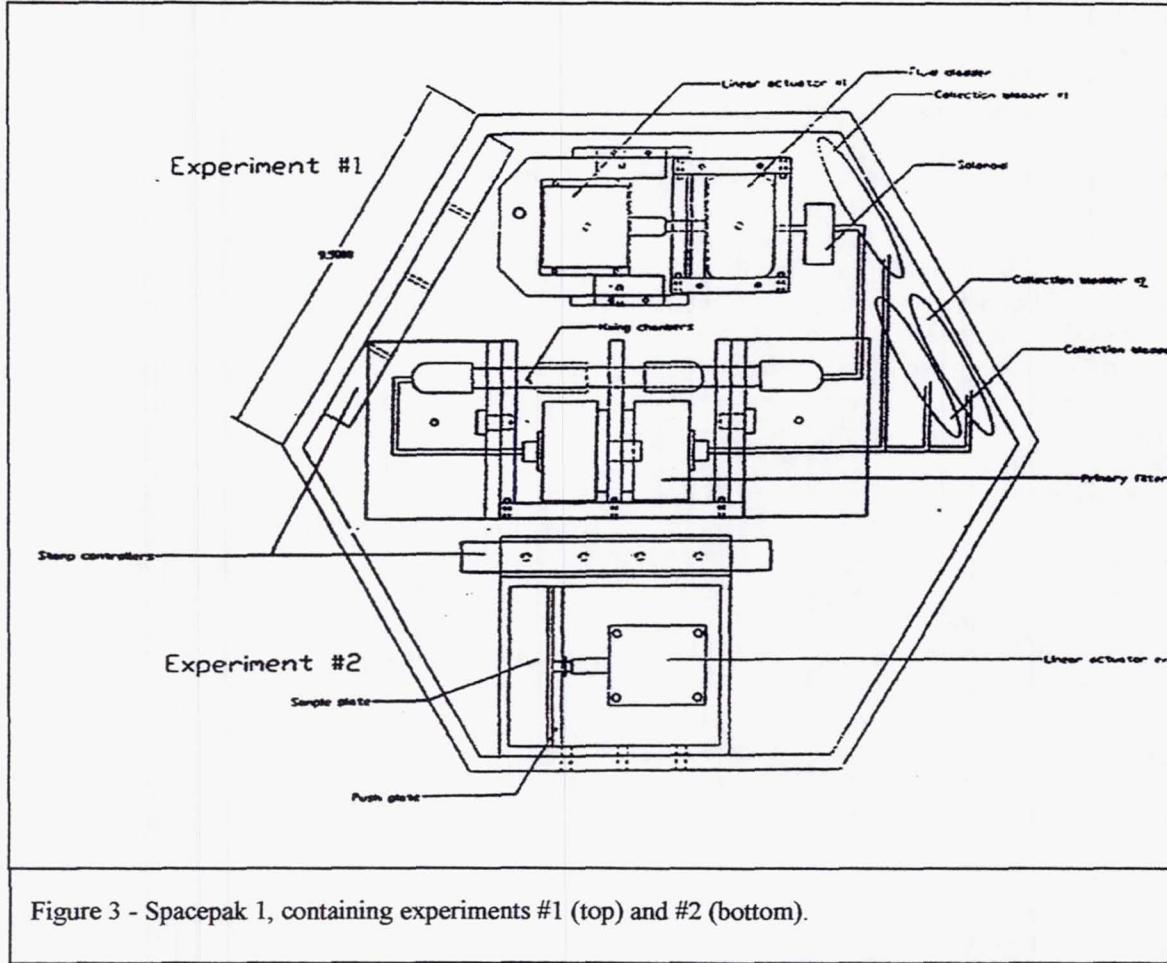
Figure 3 - Spacepak 1, containing experiments #1 (top) and #2 (bottom).

phosphate powder in the mixing chambers was hard as cement, thus blocking the chambers and not allowing the water to percolate through the ore. The moisture within the pumps and tubes allowed the phosphate to accumulate into cement and the experiment was unable to perform at all. This oversight allowed the moisture in the tubes to mix with the ore and harden like cement.

Perhaps 'learning patience' can sum up the major lessons learned from this experiment. Many tests and demonstrations were simulated. Yet the experiment was not allowed time to sit dormant, as it normally would have done on the pad before a flight. Tests are currently underway to test the experiment's performance after a three month dormancy period.

Experiment 2 – Crystal Growth

This experiment was conducted by students from Moscow High School, Moscow, Idaho. At the time of flight these students had graduated and carried their experiment production to the University of Idaho, also located in Moscow, Idaho (see figure 4).

On earth the formation and growth of the crystal structure is well known and documented and therefore the desire to study the formation and growth of chemical crystals in a micro-gravity environment sparked the interests of these students. The experiment was designed to test crystal growth of four compounds under micro-gravity conditions. The four compounds were Copper sulfate, urea, sucrose, and cobalt chloride. The compounds (in aqueous form) were sealed in a reservoir containing a filter paper surface. A sealing plate pressed against the sample plate formed the seal (figure 3). Vaseline was used to ensure it was a good seal. Once the experiment was activated, a control board activated a linear actuator, which pulled a sealing plate away from the sample plate. The aqueous solutions evaporated the water in to the air and formed crystals. A drying agent (calcium sulfate) was used to absorb water if the air became

162

saturated. Thermistores were used to gather temperature data. After two days, the control board closed the sealing plate and resealed the reservoirs. Two samples of each compound were used.

At deintegration at KSC small crystals could barely be seen on the filter paper, a positive indication. Upon dissecting the experiment we found a number of fully grown crystal formations that appear to have formed in microgravity (see figure 5). Copper Sulfate:

Figure 4 - Eric Chin, Bryan Fullerton, Sam Kirchmeier from the University of Idaho during the deintegration and evaluation of their experiment.

Crystals appeared completely formed. No evidence of liquid could be found. Four to five large crystals had grown vertically (in both directions), as opposed to the somewhat flat, uniformly distributed crystals that had grown in the lab. Small "spikes" were present around each crystal. Urea: Appeared completely
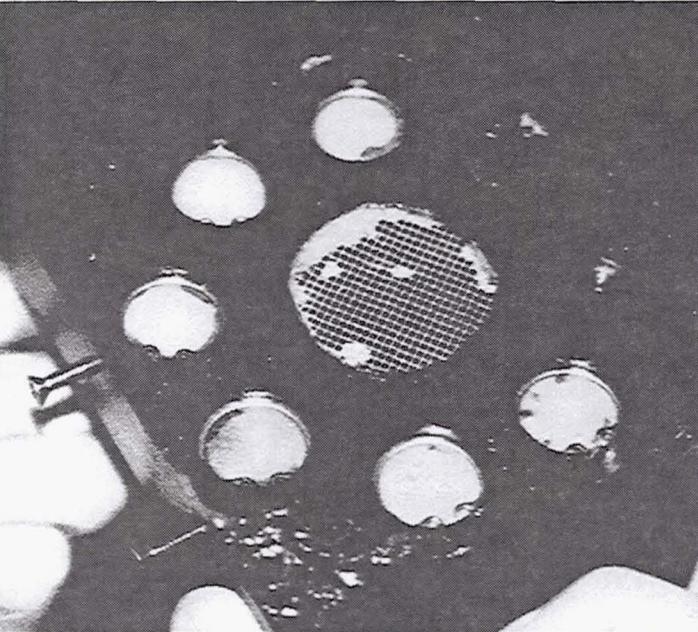
Figure 5 - Crystal Growth sample plate. Crystals counter-clock wise from Bottom Center – Copper Sulfate, Copper Sulfate, empty, Cobalt Chloride, Urea, Urea, Sucrose, Sucrose.

formed with no evidence of liquid. The crystals shown appeared long and flat which is no different that those grown in the lab. Sucrose: At first glance appear wet, yet when touched lightly with a piece of frayed filter paper they were in fact solid, leaving no water absorbed onto the filter paper. Crystals were small and uniform across the paper. One of the samples appeared to have a slight blue color, something of an unknown origin. Cobalt Chloride: The cobalt chloride crystals appeared slightly wet. When touched with filter paper, the paper turned slightly red. Indicating that these crystals didn't completely form within the time that the experiment was run. These crystals took longer in the lab setting to form as well. Perhaps the wet look of the crystals may be attributed to small crystals on the surface of the filter paper, or to some Vaseline contamination. Each crystal was allowed to sit for several minutes and was monitored to see if there were

any changes due to incomplete crystal formation. The cobalt chloride samples appeared to turn a darker color. One sample from each crystal was removed and examined. There were no crystals on the reservoir walls (all crystals were on the filter paper). When the filter paper (with the crystals was removed, it was noticed that the crystals grew equally on the bottom of the filter paper as the top. This suggests a lack of orientation constant with a microgravity environment.

We also found streaks of smeared Vaseline and a flattened blob of Vaseline on the ceiling of the main container. This suggests that the sealing plate did in fact retract during flight, thus smearing and flattening as it pulled back.

When the temperature data was downloaded, unfortunately only half of the data was retrieved. The problem was traced to a small program error. Only the temperature data from the first half of the experiment was recorded, and causing the experiment to shut down prematurely after 1.42 days, rather than the full two days. Yet the temperature appears to remain relatively constant, a control experiment can still be devised. Temperature readings appear to be on the hotter side rather than the cooler.

Many more experiments are being done in hopes to reveal more information about the crystals and their structure.

In preparation for reflight the implementation of a physical switch on the ceiling of the main container will be added to give a visual verification on the opening of the sealing plate. When the plate is pulled open the switch will flip on. Also, more reservoirs are being added to incorporate the growth of more crystals.

Experiment 3 – Nucleic Boiling in Space

Nucleic Boiling in Space was designed and built by students at Box Elder High School in Brigham City, Utah. Three of the students participated in a summer long mini-internship at USU during the development of their experiment. These students are shown in Figure 6.

On earth gravity is a factor in the mixing of liquids due to density gradients, convection currents created by the rising of more dense warm currents, the sinking of less dense cooler currents, and the rising action of bubbles. The experiment was developed to study the effects of micro-gravity on this reaction. The students were curious to see what happens when you boil water in space; where the bubbles go, what they do, and how they react, as well as what temperature gradients may appear.

The experiment apparatus consists of a sealed Lexan chamber filled

Figure 6 – Amy Whitworth, Leann Moody, Zeb Fiefield, Ron Cefelo (Teacher) from Box Elder High School, with G-090.

with deionized water. The chamber is filled with deionized water through a hole in the lexan block which is then plugged (with a metal bolt and sealed with Armstrong epoxy) after filling (see figure 7). All of the experiment were held together with Armstrong's epoxy as well as a few bolts. Distilled water is necessary in order to stop corrosion and make the components easier to see. Within the lexan block were two stainless steel bolts, located at opposite ends, used to hold our nichrome wire, to eliminate melting of our block. The wire was looped twice to abolish the need of resistors. The wire was then put through a hole, one end through each bolt, and then tied. Located at the back of the experiment was a sheet of rubber instead of a lexan plastic back. This was used to relieve pressure from the thermal expansion of the water. A lexan secondary chamber surrounds the entire experiment in case of any leakage that may occur. Within the block

164

Figure 7 - Isospacepak 2 with Experiment #3 and the battery box.

were located five thermisters. The thermisters were used to record temperature data. The controls of the experiment and data collection from the thermisters was programmed into the USU Stamp control board. Four lights were placed within the walls of the lexan block, one in each corner, to aid video recording.

The experiment started by recording temperature data from the thermisters, which is repeated periodically throughout the experiment. The video camera and recorder is turned on minute prior to the heating wire. Once the wire is turned on the experiment runs for 20 minutes. During this time temperature and video data is being recorded. Many ground-based tests were conducted. Figure 8 shows a ground based test video image of the heating wire and many bubbles seen through the view window.

At deintegration it was noted that the ground wire to the video recorder was loose. We suppose that this wire was not secured tightly enough and was freed during lift off vibrations. Without power to the recorder no video data was recorded. We also

Figure 8 - Nucliec Boiling in Space ground based video image.

found a huge air bubble in the chamber. We are unable to determine if the bubble is water vapor, or the dissociation of Hydrogen and Oxygen from water, or if it is from corrosion of the bolts, or even due to some battery action in the water from some of the free ions. We did note that the heating wire was broken.

165

Our hypothesis was that the bubbles caused from boiling would stick to the wire and create a huge air pocket, which would allow the wire to burn up. Because of the broken wire we strongly believe the water was heated and boiling occurred.

As we prepare for reflight we are making a number of additions and changes to better our experiment. Instead of using bolts to secure the heating wire, we are testing graphite rods to increase the amount of power that can be applied to the wire. Two rods will be placed at opposite ends, used to hold one wire each. We are also implementing a back-up heating wire. The first strand of wire will consist of three wires braided together tightly. We found that this produced the greatest results and worked more efficiently. The next wire will be our back up wire (one straight wire), it will be turned on after the first has run and had time to respite. Many tests have been done on the wire; it being very difficult to break will burn and snap when surrounded by air. Further testing needs to be done to be sure of the wire's outcome. We also plan more extensive tests with the thermisters and the data collection involved. The biggest thing that was learned from this experiment at this time was not to put off final details until the night before. If you're not the one doing it then by all means supervise it.

Experiment 4 – Space Popcorn

Does popcorn exposed to micro-gravity change? This was the most successful of all the experiments in terms of post-flight analysis. The elementary students from St. Vincents Elementary School (figure 9), Salt Lake City, Utah, executed examination of popcorn, which was flown in the G-090 container compared with popcorn, which was maintained on earth. The popcorn and seeds used were placed inside plastic ziploc bags then mounted on the sides of the Isospacepak walls using nylon cable ties (see figure 10).

The students collected data and worked in an efficient effective manner taking weights of the popcorn bags before and after popping, odor of the popcorn, number of popped and unpopped kernels, the size, color, as well as many other experiments.

The whole process was carried out for many hours. The students collected the

Figure 9 - Students from St. Vincents Elementary School.

data and worked in an efficient manner. The following data were compiled:
1. The students found an average of ten-gram difference in the weight of the space popcorn compared to the weight of the earth popcorn. The space popcorn is lighter.
2. Students found that the space popcorn had a difference of about 200 more kernels pop per bag than the earth popcorn.
3. Students rated the popcorn according to its crunchiness on a scale from 1-5 with 5 being the crunchiest. Space popcorn rated around 4.0 while earth popcorn rated a 3.0
4. Students then rated the popcorn according to the amount of after-taste. The earth popcorn rated a 5.0 as the space popcorn had a 2.0 – on a scale of 1-5, with 5 having the most after-taste.

166

The examination of the popcorn did have a few scientific deficiencies yet it did have a remarkable impression on all that were involved. The impact that was brought about was extraordinary and hopefully will be carried with the students throughout the years to come. Within the school the students had the opportunity to become the investigators of a real life experiment that had taken place where they themselves will probably never get to go.

Figure 10 - Space Popcorn mounted to the structure of G-090.

Perhaps the field of space exploration is so captivating because it is the unknown. Those who remain on earth look to space with feelings of admiration and respect. Our research and exploration has brought us to places and experiences that were needed to complete our learning.

REFERENCES
1. Jason Sanders: The Development of the USU GAS System, G-001 to G-090USU's High School Companion, G-090. The Shuttle Small Payloads Project Office Symposium, NASA CP–1999–209476. (Paper 23 of this compilation.)

Page intentionally left blank

PAYLOAD G-768
A SPACE PROBE INTO THE CHEMISTRY OF LIFE

MIKE MUCKERHEIDE-PAYLOAD MANAGER
JOSEPH HORN-ALIEN TECHNOLOGY
DANIEL P. GLAVIN, JEFFREY L. BADA, MATT LEVY, KEVIN NELSON,
JIM CLEAVES AND STANLEY L. MILLER
UNIVERSITY OF CALIFORNIA, SAN DIEGO

ABSTRACT

The early work of Miller and Urey in 1953[1] proved that discharging an electric spark into a mixture of water, hydrogen, methane and ammonia could generate amino acids, the building blocks of life.

The laser system which is configured to meet the criteria of the G-768 NASA PAR (Payload Accommodation Requirement) has also produced amino acids. The laser system is designed to utilize electronics and optical parameters which make it possible to produce a laser spark (plasma). The production of an electrode free spark within a series of closed spheres, can provide the energy necessary to synthesize amino acids from a mixture of water, methane, ammonia and nitrogen.

The system design and orientation is dependant upon phase I, phase II and phase III of the Payload Safety Package required by NASA in the GAS Payload Program. Rugged system design is essential to successful operation in the harsh environment of space.

Special attention is given to compartment integrity. Paramount to the investigation is a determination of differences that may be present between Earth based experiments and experiments done in the reduced gravity, severe temperature swings, and cosmic radiation conditions of space. Advance state of the art analysis will be performed post flight.

INTRODUCTION

The payload G-768 complies with the Payload Accommodations Requirements which defines the technical agreement between NASA/Goddard Space Flight Center (GSFC) and Alien Technology. The Payload Accommodation Requirement contains the information needed for the preparation, flight and disposition of the payload. The general plans are compliant with the GAS Experimenter Handbook and the

Payload Integration Plan (PIP), Space Transportation System and Get Away Special Carrier (NSTS-44000) criteria.

DESCRIPTION OF PAYLOAD G-768

The payload will be flown in a standard 5 cubic ft GAS container and will weigh 200 lbs. This paper will not address the non-related passive experiments of the payload. It will however address the active experiment in which a Neodymium YAG Q-switched laser will be focused into a series of vials containing methane, nitrogen, and aqueous ammonium chloride (0.05M) Amino acid potential synthesis in the experiment include: aspartic acid, alanine and glycine and possibly α-aminoisobutyric acid (AIB). This experiment is a continuation of previous Earth based experiments involving prebiotic organic compound systhesis which originated with Dr. Stanley Miller's "electric spark" experiment in 1953[1] (commonly known as the Miller-Urey experiment). It is theorized that the space environment (microgravity and high cosmic radiation condition) may affect the formation of organic compounds i.e. yields, molecular structural formation and distribution. Microdroplets formed during the experiment as a result of weak gravitational interactions, could effect amino acid synthesis. We can not duplicate this effect on Earth. Cosmic radiation hits and X-ray exposure will be monitored using passive detectors, CR-39 and X-ray step wedge dental film respectively. The results of the experiment will be evaluated and compared against the compounds produced under an identical Earth based experiment. The successful production of organic compounds from this space based experiment will begin to provide an understanding as to how organic compounds are presently being created in the interstellar regions.

PAYLOAD AND DEVICE STRUCTURE

The payload support structure consists of 4 6061T6 0.25" thick aluminum decks mounted to four vertical support columns. The payload has a diameter of 19.75 inches and an overall height of 28.25 inches. The first deck will contain the payload batteries and 3 passive experiments (not addressed in this paper). The batteries and experiment will be contained in separate compartments (303 stainless construction). The second deck compartment (303 stainless) will contain the laser system and controls for the two active experiments. The third deck will contain the flasks (20) and optical actuator for the amino

170

acid experiment. The fourth deck will be bolted to the experiment mounting plate (EMP) supplied by NASA.

The amino acid experiment which is the primary concern of this paper will utilize a Q-switched Nd:YAG laser which will be activated by a timer to fire pulses of 200 millijoules at 10Hz to 20Hz repetition rates into the 20 flasks of the gas mixture. The laser beam at 1064 nanometers (nm) wavelength will be rotated through 360 degrees into each of the 20 flasks. The laser beam will be tightly focused by a special glass lens to the center of each flask. Each flask will have it's own focusing lens. Laser power will be provided by Gates batteries.

The laser system will be mounted on a deck below the flask deck and the beam will be configured through a glass flat, mounted at the Brewster angle. The glass flat will provide an additional integrity between the two compartments. The beam will be directed by a front surfaced mirror mounted on a stepped galvanometer. The laser beam will produce a plasma (4th state of matter) in each flask as it rotates through its menu. The laser will be activated after a two-hour delay by the timer which will be triggered by the Baroswitch. Exposure times of the beams on the flask optics will range from 5 to 20 minutes. Upon completion of the cycle translation through 360 degrees the system will shut down.

Three stages of flask integrity are needed for compliance with safety parameters. The flask compartment will be made of 303 stainless steel to prevent corrosion in the event of flask failure. There are methods and parameters of function, which this paper will not address do to the proprietary nature of the experiment. Suffice it to say that the micro gravity and cosmic radiation of space will be exploited to produce a maximized condition for the highest potential of generating amino acids in space.

CONTROL

A standard mixture of amino acids contained in two passive flasks will not be exposed to laser radiation in space. This control is to determine effect of cosmic radiation on amino acids. Although high doses of gamma-radiation less than 1 Mrad have been shown to contribute to some racemization of amino acids on Earth, the extent of racemization due to cosmic radiation in space is unknown.

EXPERIMENTAL

The glass test vials used in the laser induced plasma (LIP) experiments were filled under the supervision of Stanley Miller. Each 100ml flask contained a liquid/gas mixture similar to that used in previous spark discharge (SD) experiments (10 ml; 0.05 M NH_4Cl, ~100 torr CH_4 and N_2). The flasks were flame sealed and then shipped to Alien Technology where the LIP experiments were conducted. A hot plasma was generated by focusing the beam of the Nd:YAG laser (1064 nm) into the center of the round glass flask containing the gas mixture. Each laser pulse contained an average energy of 0.20 J and were produced at a rate of ten every second (10 Hz). The total energy consumed by the gas mixture during the laser experiment (600-1200 J) was a few thousand times less than used by spark discharge[1,2]. After exposing the gas mixture to the laser beam for a few minutes, the synthesis of organic compounds was observed as the previously clear ammonium chloride (NH_4Cl) solution at the bottom of the flask began to turn yellow.

The solution was then analyzed for the presence of amino acids at the Scripps Institution of Oceanography. The flasks were opened under a fume hood and approximately 1 ml of the NH_4Cl solution was removed from each flask and vacuum dried in a separate glass test tube. The dried samples were then hydrolyzed in 1 ml of double distilled 6 N HCl at 100°C for 24 hours and then desalted using cation-exchange chromatography (Bio-Rad AG50W-X8 resin was used). Final desalted aliquots were then analyzed for amino acids by O-phthaldialdehyde/N-acetyl-L-cysteine (OPA/NAC) derivatization and high-performance liquid chromatography[5].

RESULTS AND DISCUSSION

The results of the LIP experiments are summarized in Table 1. The most abundant amino acids produced in the experiments included glycine and racemic mixtures of alanine and aspartic acid, with much lower concentrations of α-aminoisobutyric acid. The distribution of amino acids produced by LIP is consistent with that found in spark discharge[3]. The percent yield of amino acids in the LIP experiments (based on the amount of carbon present in the system as methane) ranged from 0.02 to 0.1 % and is lower

172

than the amino acid yield reported from spark discharge (see Table 1). This is not surprising, given more energy was applied in the spark discharge experiment to optimize amino acid yields. Future work is still necessary to optimize carbon yields using LIP.

TABLE 1:

Yields of amino acids after exposing a mixture of CH_4, NH_3, N_2 and H_2O to a Nd: YAG laser source.

| Amino acid | Yield | | | Energy Yield | |
| | nmoles | % | | nmoles HCN/J | |
	LIP	LIP	SD[†]	LIP	SD[*]
Glycine	380	0.10	(0.5-2.1)		
D/L Aspartic acid	95	0.06	(0.02)		
D/L Alanine	105	0.05	(0.08-1.8)		
α-Aminoisobutyric acid	5	0.02	(0.10-0.6)		
Total	585			9.6	(4-10)

Although the carbon yields from LIP were lower than spark discharge, the energy yield (based on moles of HCN produced per joule of laser energy input) was found to be 9.6 and is consistent with spark discharge. The energy expended in to the gas mixture can be more accurately determined with the LIP technique, due to the uncertainty in the magnitude of the resistance across the electrode in spark discharge, hence the greater precision in the LIP energy yield.

CONCLUSTION

We have demonstrated that the laboratory based synthesis of amino acids using a laser induced plasma can be used as an alternative to electric spark discharge. With the LIP technique, amino acids can be synthesized in just a few minutes (exposure times of a day to a week are required by spark discharge), which makes this technique favorable for testing in space.

We have no idea how the synthesis of organic compounds in space will compare to laboratory based experiments. This space based experiment offers for the first time a unique opportunity to understand how amino acids, the building blocks of life, can be produced in the micro gravity environment of the interstellar regions of space.

Portions of the proceeding payload text contains excepts from the G-768 Payload Accommodations Requirement.

REFERENCES

[1] Miller, S.L. (1953) *Science* 117, 528

[2] Miller, S. L. (1955) *J. Am. Chem. Soc. 77, 2351*

[3] Miller, S. L. (1987) In: Cold Spring Harbor Symposia on Quantitative Biology, vol. LII, pp. 17-27.

[4] Stribling, R. and Miller, S. L. (1987) *Origins of Life Evol. Biosph.* 17,261

[5] Zhao, M and Bada, J.L. (1995) *J. Chromatography a* 690, 55.

[†] Yield based on total carbon present in the mixture as methane (Miller 1953, 1955).

[*] Energy yield based on moles of hydrogen cyanide generated per joule of laser energy input (Stribling and Miller 1987).

A Novel Technique for Performing Space Based Radiation Dosimetry Using DNA : Results from GRaDEx -I and the Design of GRaDEx -II

Joe Ritter[1,2], R. Branly[2,3], C. Theodorakis[4], J. Bickham[4], C. Swartz[4], R. Friedfeld[5],
E. Ackerman[3], C. Carruthers[3], A. DiGirolamo[3], J. Faranda[6], E. Howard[7], C. Bruno[3]

1) Space Optics Manufacturing Technology Center SD 71,
   NASA George C. Marshall Space Flight Center AL. 35812 Email: Joe.Ritter@msfc.NASA.gov
2) Florida Space Institute, University of Central Florida, Orlando FL
3) Broward Community College, Department of Natural Science, Davie FL
4) Texas A&M University, Department of Fisheries and Wildlife, College Station TX
5) Steven F. Austin State University, Nacogdoches TX
6) Georgia State Department of Physics, Atlanta GA
7) Florida International University, Miami FL

Abstract

Because of the large amounts of cosmic radiation in the space environment relative to that on earth, the effects of radiation on the physiology of astronauts is of major concern. Doses of radiation which can cause acute or chronic biological effects are to be avoided, therefore determination of the amount of radiation exposure encountered during space flight and assessment of its impact on biological systems is critical.

Quantifying the radiation dosage and damage to biological systems, especially to humans during repetitive high altitude flight and during long duration space flight is important for several reasons. Radiation can cause altered biosynthesis and long term genotoxicity resulting in cancer and birth defects etc. Radiation damage to biological systems depends in a complex way on incident radiation species and their energy spectra. Typically non-biological, i.e. film or electronic monitoring systems with narrow energy band sensitivity are used to perform dosimetry and then results are extrapolated to biological models. For this reason it may be desirable to perform radiation dosimetry by using biological molecules e.g. DNA or RNA strands as passive sensors.

A lightweight genotoxicology experiment was constructed to determine the degree to which in-vitro naked DNA extracted from tissues of a variety of vertebrate organisms is damaged by exposure to radiation in a space environment. The DNA is assayed by means of agarose gel electrophoresis to determine damage such as strand breakage caused by high momentum particles and photons, and base oxidation caused by free radicals. The length distribution of DNA fragments is directly correlated with the radiation dose. It is hoped that a low mass, low cost, passive biological system to determine dose-response relationship (increase in strand breaks with increase in exposure) can be developed to perform radiation dosimetry in support of long duration space flight, and to predict negative effects on biological systems (e.g. astronauts and greenhouses) in space. The payload was flown in a 2.5 cubic foot Get Away Special (GAS) container through NASA's GAS program. It was subjected to the environment of the space shuttle cargo bay for the duration of the STS-91 mission (9 days). Results of the genotoxicology and radiation dosimetry experiment (GRaDEx-I) as well as the design of an improved follow on payload are presented.

Introduction

Traditionally, radiation dosimetry has been accomplished using narrow energy bandwidth devices such as electronic detectors or radiation-sensitive film badges. Extrapolation of the measured doses to biological effects can be problematic, especially when people are exposed to radiation with a complex energy spectra (Pissarenko 1993). It would be advantageous to develop dosimeters, which could provide more biologically relevant data.

Because many of the more serious effects of radiation toxicity are due to damage of DNA molecules, any dosimeter which could incorporate DNA in its design would be a likely candidate for such a biological dosimeter. These types of dosimeters are currently being developed for measuring terrestrial exposure to solar ultra-violet radiation (unpublished data), but their use for monitoring cosmic ionizing radiation has yet to be realized.

The purpose of this study is to develop a low cost, high sensitivity, DNA dosimeter with a wide dynamic range, which can be used in space e.g., aboard space shuttle flights, on the International Space Station, and eventually on long duration flights e.g., to Mars, for monitoring cosmic radiation exposure. These simple dosimeters consist of a naked DNA solution sealed into quartz cuvettes. After exposure, the DNA is analyzed for radiation-induced damage via agarose gel electrophoresis.

Biosynthesis is essential to life. Altered biosynthesis can occur in several ways. Radiation can damage DNA, RNA, and proteins. Proteins can be replaced, new RNA can be pattered from DNA, but radiation damage to a cells DNA can be catastrophic. If a cell undergoes extreme radiation damage it usually is no longer viable, can not reproduce, and simply dies. Replicating cells are particularly sensitive to such damage. Of concern e.g. to astronauts are smaller radiation doses, which may not cause immediate cell death but can show up later when a cell tries to duplicate. For example of serious concern are genetic mutations which do not impair cell reproduction, but impair the function of future generations of cells. Such cells may become cancerous, or in the case of mutation to e.g. a sperm cell, offspring of radiated subjects can be affected.

Radiation can cause nucleotide substitutions. The process involves the initial production of single or double strand breaks, either as a result of the direct interaction of the DNA with the particle or photon, or by interaction with radicals. Radiation-induced DNA damage occurs primarily by the production of unstable free radicals by the ionizing radiation. If a radioactive particle interacts with a DNA molecule, it can produce a DNA radical (Drouin et al. 1996). Such a DNA radical is unstable, and quickly leads to a break in the DNA strand (Kraft et al.1989). DNA is a long, double-stranded molecule, so strand breaks can occur in adjacent sites in both of the adjacent strands or in only one of the strands. Alternatively, the high momentum particle or photon may interact with a molecule in solution, most commonly an oxygen or water molecule, leading to the production of oxy- or hydroxy- free radicals. If these free radicals encounter a DNA molecule, they may strip away an electron, which can form a strand break. Free Radicals may also form covalent bonds with the DNA itself, thus leading to oxidation of a portion of the DNA molecule (Shulte-Frohlinde and Von Sonntag 1985). After the dosimeters returned from the shuttle flight, the DNA within them was analyzed for DNA strand breakage and oxidation.

Only strand breaks and base oxidation are measured with this experimental design; however, there is a direct correlation between the number of strand breaks and the mutation rate. In order to detect another type of mutation in in-vivo DNA, seeds of the mustard plant Arabodopsis were flown, and will be grown on earth to look for the effects of chromosome damage in somatic cells by means of flow cytometry. This plant s frequently used by plant geneticists as its genetic sequence is known. Results of the Arabodopsis assay are not presented here.
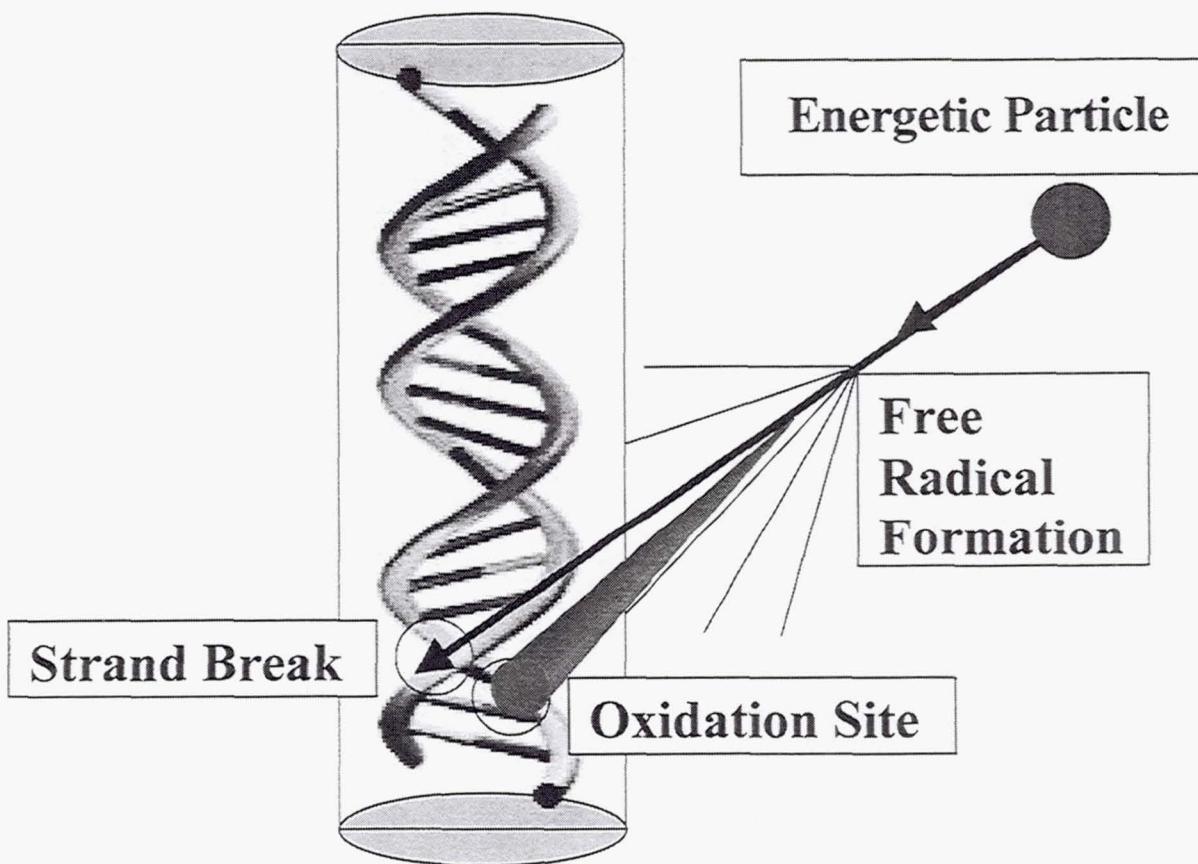
Figure 1 DNA damage mechanisms.

The Payload

ASPR-GRaDEx-I (Genotoxicology and Radiation Dosimetry Experiment I) was a variant of another experiment ASPR and Texas A&M are constructing (MET4-GPSE) which will fly as part of the TAMSE GAS payload (Ritter et al., 1998). Because of TAMSE's complexity (9 instruments) an opportunity for an early flight of the simpler GRaDEx payload arose.

Naked DNA was sealed in quartz cuvettes, and then placed in an airtight monolithic 6061-T-6 aluminum container having 1/4 inch thick walls. This was then installed in and flown in a standard, 2.5 cubic foot Get Away Special (GAS) container through NASA's GAS payload program. The payload was subjected to the environment of the space shuttle Discovery's cargo bay for the duration of the STS-91 mission (9 days).
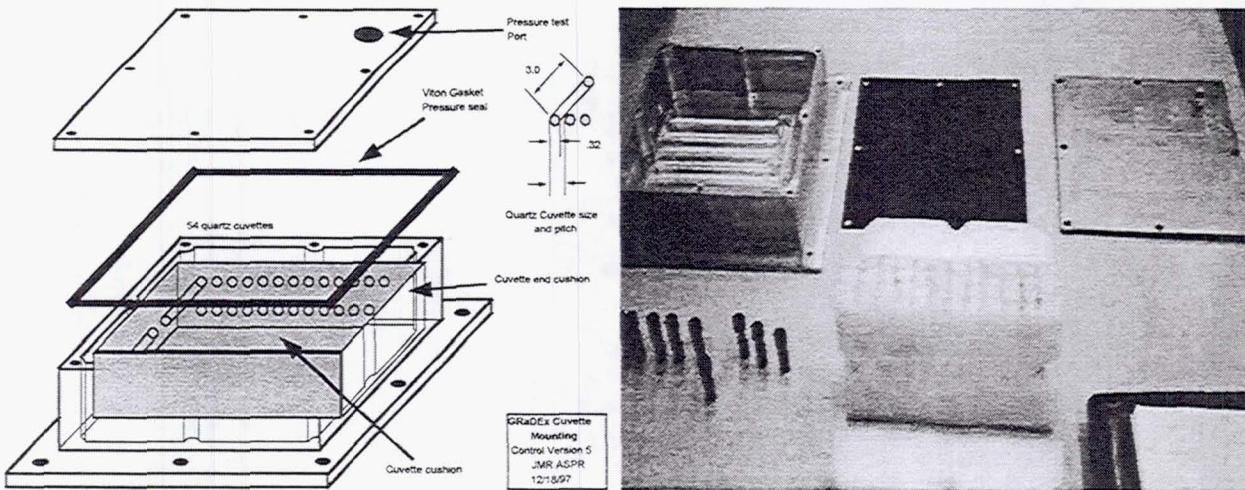
Figure 2   Genotoxicology and Radiation Dosimetry Experiment (ASPR-GRaDEx-I)

Methods

DNA single-stand breaks were determined by alkaline gel electrophoresis. The alkaline treatment separates the double-stranded DNA into single-stands, allowing determination of single-strand breaks. Double-strand breaks can be caused not only by radiation but also by shearing of the molecule due to physical disruption by shake, thermal cycling, and even the formation and shearing of ice crystals in the buffer solution. Thus, the number of double-strand breaks is not determined because it is difficult to distinguish between double-strand breaks caused by shearing and those caused by radiation using our current techniques.

The number of oxidized bases was determined by digesting the DNA with enzymes which produce single-stranded DNA breaks at each site of oxidation damage (Boiteux et al. 1992, Dizdaroglu et al. 1993). The number of single-strand breaks produced by this treatment, and thus the number of oxidized bases, can be determined by comparing the number of single-strand breaks with and without such treatment (Freeman and Thompson 1990).

DNA was extracted from mosquitofish (Gambusia affinis), chicken (Gallus gallus), and tiger salamander (Ambystoma tigrinum) by homogenizing approximately 200 mg tissue in 500:1 TEN buffer (10 mM trizma base, 1mM EDTA, 100 mM NaCl) plus 1% sarcosyl. The homogenate was then extracted with 500:1 phenol/chloroform/isoamyl alcohol (25:24:1, v:v:v) and then 500:1 chloroform. The DNA was precipitated with 2 volumes of ice-cold ethanol.   The precipitate was then resuspended in 50 mM phosphate buffer (sterile) at a concentration of 20 mg/ml. Human placental DNA was purchased from Sigma Chemical Co. (St. Louis, MO) and resuspended in phosphate as above. Five hundred μl of DNA solution was then loaded into quartz cuvettes and heat-sealed. Some of the cuvettes were flown on the space shuttle Discovery on STS-91 (flight samples), while some were kept in the laboratory (control samples).

After exposure to cosmic radiation, the flight DNA was precipitated by adding 50:1 3 M sodium acetate, 100 g mussel glycogen and 1 ml ice-cold ethanol, and cooling this mixture for 15 min at -80° C. The DNA was then pelleted by centrifugation at 13,000 rpm for 10 minutes in a microcentrifuge. The pellet dried for 10 min under vacuum and was then resuspended in 50:1 TE (10 mM trizma base, 1 mM

EDTA, pH 7.0). The DNA concentration was then quantified spectrophotometrically at 260 nm (1 AU = 50 µg DNA).

For enzymatic digestion, 1.1µg DNA was diluted in digestion buffer (5 mM HEPES buffer, 100 mM KCl final concentration), and 2µg each of endonuclease III and formamidopyrimidine (FaPy) glycosylase (Fpg protein), in a final volume of 30:1. This mixture was incubated at 37° C for 1 hour. Then proteinase K and NaCl were added to a final concentration of 20 mg/ml and 50 mM, respectively, and the mixture was incubated for an additional 1 hour. Samples were incubated both with and without endonuclease. The digested DNA was then analyzed via alkaline or neutral gel electrophoresis.

For alkaline gel electrophoresis, 10.5 ml digestion solution, 3 ml tracking dye (15% Ficoll, 0.025% bromophenol blue), and 1.5 ml of 1 N NaOH and incubated for 15 min. at room temp. All of this mixture was then loaded into a 1% agarose gel and subjected to electrophoresis in alkaline solution (30 mM NaOH, 2 mM EDTA, pH 12.5) at 7 V/cm for 5 hours. The gels were then stained with ethidium bromide (a fluorescent DNA-binding stain) and photographed under ultra-violet light.

For neutral gel electrophoresis, 4 ml digestion reaction was loaded into a 0.3% agarose gel and subjected to electrophoresis in TBE (90 mM trizma base, 90 mM boric acid, 1 mM EDTA, pH 8.0) at 1.5 V/cm for 15 hrs. The gel was then stained and photographed as above.

The average molecular length (Ln) of each sample was calculated with molecular length standards (coliphage T4 DNA, lambda phage DNA Hind III digestion, and 100 base pair ladder) using the methods of Freeman and Thompson (1990) . The amount of DNA damage was calculated according to the formula: $D = (1/Ln1 - 1/Ln2) \times 100$.

The number of oxidized bases, Ln1, is the molecular length of the sample with enzyme and Ln2 is the molecular length of the sample without enzyme (both determined using alkaline gel electrophoresis). For number of single-strand breaks, Ln1 is determined using alkaline gel electrophoresis, and Ln2 is determined using neutral gel electrophoresis (both are without enzyme). The amount of damage is reported as number of oxidized bases or number of single strand breaks per 10^5 base pairs.

Results
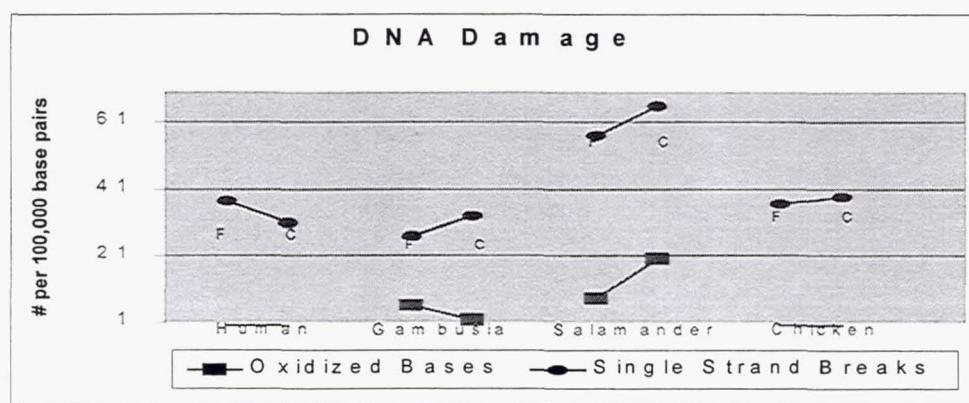
Figure 4 Electrophoresis strand break analysis results.

The number of oxidized bases in the Gambusia flight (F) DNA was greater than that in the control (C) DNA. The opposite was true for the salamander DNA. No other samples showed evidence of

oxidized base damage. Unlike the positive (irradiated) controls in prior ground experiments, there were no obvious trends in the number of single-strand break data. For the human DNA, the flight samples had roughly 7 more strand breaks/10^5 base pairs, but for the other species this trend seemed to be reversed.

Species	# Oxidized Bases	# Single Strand Breaks
Human Flight	0.00	37.56
Human Control	0.00	30.78
Gambusia Flight	5.98	26.92
Gambusia Control	1.49	32.82
Salamander Flight	8.19	56.76
Salamander Control	19.97	65.76
Chicken Flight	0.00	36.57
Chicken Control	0.00	38.71

Table 1 - Number of DNA single-strand breaks and oxidized nucleotide bases (per 105 bases) in DNA samples from different species exposed to cosmic and solar radiation. "Flight" samples were exposed to cosmic and solar radiation aboard the space shuttle. "Control" samples remained in the laboratory during the same period of time.
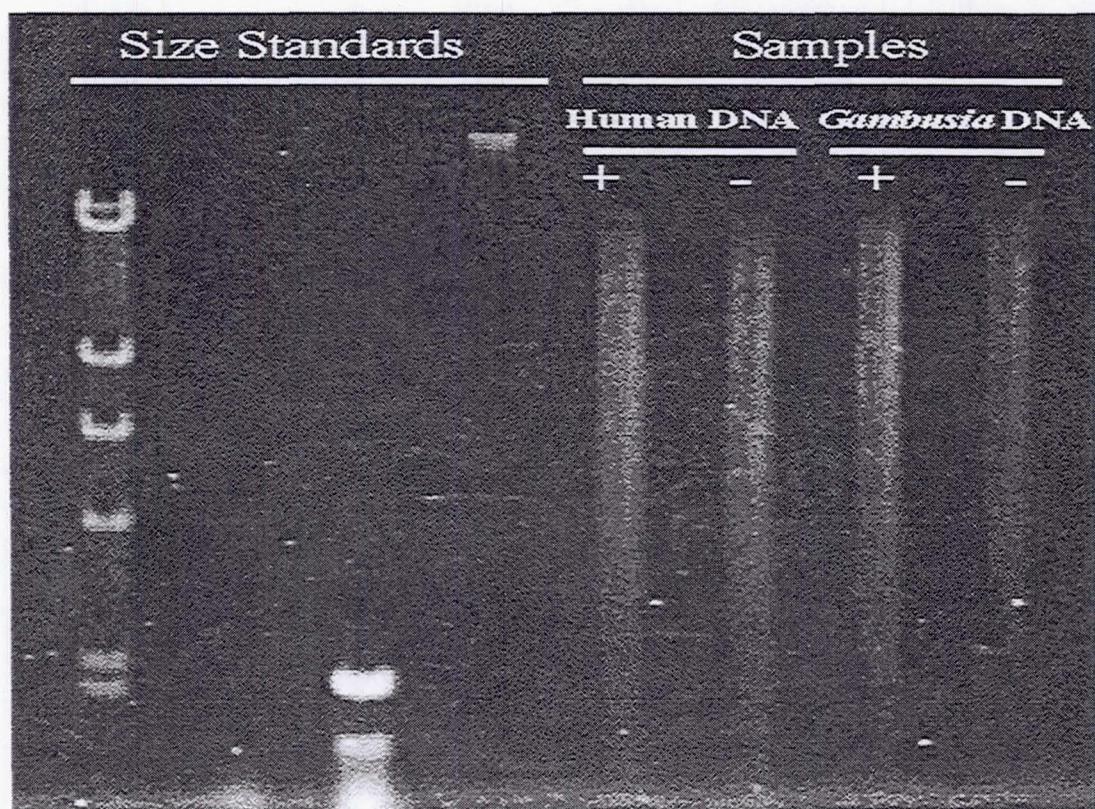
Figure 5 An agarose gel stained with ethidium bromide and photographed under UV light. "Size standards" are DNA fragments of known molecular length. The 1st 3 lanes on the left of the gel are standards: Lambda phage DNA cut with Hind III (high ladder) ; 100 base pair ladder (low ladder); and coliphage T4 DNA (single band). The next 4 lanes are samples from cuvettes. The samples are human flight (with then without enzyme digestion) and gambusia flight DNA (with then without enzyme digestion).

Conclusions

There was no clear evidence of cosmic radiation-induced DNA damage. It could be that the amount of damage from the cosmic radiation was so small that it is beyond the *current* detection limit of this assay. However, the DNA samples also had small amounts of trizma and EDTA mixed in with them. It is known that trizma (tris(hydroxymethyl) amino-methane) is a radioprotectant free-radical scavenger (Stanton et al. 1993), and EDTA may also be a free-radical scavenger, as are many other organic acids. Thus these compounds may have had a protective effect on the DNA in the samples. Also, the amount of DNA used in this experiment was low, so that the fluorescence of the DNA was small compared to the background fluorescence of the ethidium bromide stain in the gel. Thus the background fluorescence may have contributed extraneous variation when reading data from the gels.

In GraDEx-II, an effort will be made to ensure that no radioprotective compounds are included in with the DNA samples. Also, more DNA will be used in the cuvettes, so that a higher concentration of DNA can be loaded into a well, thus minimizing the effect of background fluorescence in the determination of Ln. Additionally strands of known length e.g., a Coliphage enzymatically cut to a known length may be used as a substrate. Future work will also include a new series of ground experiments to determine the dose response relationship for various energy spectra as well as to determine the effects of mechanical stress on the DNA.

The authors' goals are not only to support future technical needs of the manned space program, but also to support education. Scientists as well as students from fields as diverse as Chemistry, Biochemistry, Physics, Engineering, Astronomy, and Environmental Science benefited from involvement in every level of design, fabrication, testing, and data analysis. The design and fabrication of the TAMSE and ASPR-GRaDEx-I payloads represent several years of time and learning invested by students and their mentors. The investigators and authors of this paper believe that interdisciplinary technical training of American youth is critical to the long-term interests of the United States. Only by maintaining a competitive technical edge will the United States continue to be a world economic and space leader. We are both grateful and proud to live in a country where opportunities like NASA's GAS program are made available to educators, students, and other researchers. In the same spirit, data from the TAMSE and ASPR-GRaDEx-I payloads will be made available to educators who contact the authors (Joe.Ritter@msfc.nasa.gov and rolando@nsu.acast.nova.edu.). Those interested may visit the ASPR website at http://fs.broward.cc.fl.us/north/ecs/nasa/ .

The authors believe that this technique can eventually be improved to a point where radiation dosimetry from very negligible to lethal doses can be accomplished in a single small lightweight inexpensive package suitable for use on both robotic flights, and in support of manned space flight.

Acknowledgments

References

Boiteux, S., E. Gajewski, J. Laval and M. Dizdaroglu (1992) Substrate specificity of the Escherichia coli Fpg protein: recognition and cleavage of oxidatively damaged DNA. J. Biol. Chem. 269: 15318-15324.

Dizdaroglu, M., J. Laval and S. Boiteux (1993) Substrate specificity of the Escherichia coli endonuclease III: excision of thymine- and cytosine-derived lesions in DNA produced by radiation-generated free radicals. Biochemistry 26: 8200-8206.

Drouin, R., H. Rodriguez, G.P. Homquist and S.A. Akman (1996) Ligation-mediated PCR for analysis of oxidative DNA damage. In Technologies for Detection of DNA Damage and Mutations. G.P. Pfeifer (ed.). New York: Plenum Press. pp. 211-290.

Drouin, R., S. Gao and G.P. Holmquist (1996) Agarose gel electrophoresis for DNA damage analysis. In Technologies for Detection of DNA Damage and Mutations. G.P. Pfeifer (ed.). New York: Plenum Press. pp. 37-44.

Freeman, S.E., and B.D. Thompson. (1990) Quantitation of ultraviolet radiation-induced cyclobutyl pyrimidine dimers in DNA by video and photographic densitometry. Anal. Bioch. 186: 222-228.

Kraft, G., W. Kraft-Weyrather, S.Ritter, M. Scholz, and T. Stanton (1989) Cellular and subcellular effects of heavy ions: A comparison of induction of strand breaks and chromosomal aberrations with the incidence of inactivation and mutation. Ad. Space Res. 9: 59-74.

O'Connor, T.R. (1996) The use of DNA glycosylases to detect DNA damage. In Technologies for Detection of DNA Damage and Mutations. G.P. Pfeifer (ed.). New York: Plenum Press. pp. 155-167.

Pissarenko, N.F. (1993) Radiation environment during the long space mission (Mars) due to galactic cosmic rays. In Biological Effects and Physics of Solar and Galactic Cosmic Radiation. Part B. C.E. Swenberg, G. Hornbeck and E.G. Stassinopoulos (eds.). New York: Plenum Press. pp. 1-14.

Ritter, J.M., R. Branly, E. Ackerman, R. Friedfeld, J. Bickham, A. Blitz, J. Faranda, C. Dahl, C. Theodorakis (1998) An interdisciplinary payload to perform space based remote sensing and to measure microgravity and radiation effects. Proceedings of the 35th annual Space Congress.

Ritter, J.M., R. Branly, C. Theodorakis, J. Bickham, C. Swartz, R. Friedfeld, E. Ackerman (1999) Passive orbital radiation dosimetry on STS-91 using DNA : initial results from ASPR-GRaDEx-I. Proceedings of the 36th annual Space Congress.

Shulte-Frohlinde, D. and C. Von Sonntag (1985) Radiolysis of DNA and model systems in the presence of oxygen. In Oxidative Stress. H. Seiss (ed). London: Academic Press.

Stanton, J., G.Taucher-Scholz, M. Schneider, J. Heilman and G. Kraft (1993) Protection of DNA from high LET radiation by two OH radical scavengers, tris(hydroxymethyl)amino-methane and 2-mercaptoethanol. Radiat. Environ. Biophys. 32: 21-32.

Results From the First Two Flights of the
Static Computer Memory Integrity Testing (SCIMT)
Experiment

Thomas M. Hancock III
AverStar
Marshall Space Flight Center
M/C JT-04 Huntsville Alabama 35812
thomas.hancock@hsv.boeing.com

ABSTRACT

This paper details the scientific objectives, experiment design, data collection method, and post flight analysis following the first two flights of the Static Computer Memory Integrity Testing (SCMIT) experiment. SCMIT is designed to detect soft-event upsets in passive magnetic memory. A soft-event upset is a change in the logic state of active or passive forms of magnetic memory, commonly referred to as a "Bitflip" (see Fig. 1). In its mildest form a soft-event upset can cause software exceptions, unexpected events, start spacecraft safeing (ending data collection) or corrupted fault protection and error recovery capabilities (see Fig 1.1). In it's most sever form loss of mission or spacecraft can occur. Analysis after the first flight (in 1991 during STS-40) identified possible soft-event upsets to 25% of the experiment detectors. Post flight analysis after the second flight (in 1997 on STS-87) failed to find any evidence of soft-event upsets. The SCMIT experiment is currently scheduled for a third flight in December 1999 on STS-101.

INTRODUCTION

Over the years several different spacecraft have suffered soft-event upsets (bit-flips) of their onboard memory. The most famous instance occurred in 1986 when the Voyager 2 spacecraft was encountering the planet Uranus. The spacecraft suffered soft-event upsets to its Flight Data Subsystem (FDS) during far-encounter. This caused a loss of guidance and control for several hours that resulted in the spacecraft pointing its instruments out into deep space away from the planet. Similar events have impacted the Galileo Jupiter Orbiter Command and Data Subsystem (CDS) during encounters with the moons Io and Europe.

Today as larger, more complicated systems are developed and planned (International Space Station, human missions back to the Moon and on to Mars) the possibility of soft-event upsets affecting static memory is becoming a concern. Large systems should not relay on mass uplinks for reloading embedded command and data handling, attitude control and related subsystems. A safer approach is to carry back-ups of the embedded flight software on static memory (* note though not related to a soft-event upset, but significant coding errors the Magellan spacecraft required each block of its flight software be uplinked from Earth overwriting privileged memory shortly after Venus orbit insertion. This significantly raised the risk of permanently losing the spacecraft after the initial recovery).

SCIENTIFIC OBJECTIVES

The objectives of this experiment are:
- Observe Soft-event upsets
- Determine the frequency of soft-event upsets
- Determine the characteristics of soft-event upsets
- Determine the possible effectiveness of different types of shielding material
- Evaluate the possibility of using static memory as a type of passive detectors

EXPERIMENT

General
The experiment uses a number of commercial floppy disks. Each disk was loaded with a text file/bit-map identical in size and format (see Fig.2). This method made it simple to determine when a soft event upset had occurred by observing a change in the logic state (character representation) of any area on the bit maps during post flight analysis (see Fig.3). Each disk contained one large text file/bitmap

STS-40
For the first flight as part of GAS payload G-616, ten disks were inserted into each of four storage containers (see Fig. 4). Several of the disks were covered in one of three types of shielding material:
- Normal anti-static nylon
- Aluminized Mylar mesh
- Field dispersing (electrically neutral) nylon

STS-87
For the second flight as part of GAS payload G-036 five disks were inserted into a one storage container and three disks were each covered with one of the three types of shielding material (see Fig. 5).

Procedure

General
The experiment was constructed by:

- Developing a standard text file/bitmap
- Copying an identical standard text file/bitmap on each disk
- Testing to assure the integrity of each text file/bitmap
- Covering a number of the disk with one of the three types of shielding material
- Inserting disks into storage containers
- Integrating the disks and storage containers into the GAS canister

STS-40
For the first flight the experiment was integrated into the GAS canister in June of 1990. The experiment remained on the GAS Bridge assembly until after landing in June 1991. The experiment remained in orbit for 9 days. Post flight recovery and analysis took place within 30 days of landing.

STS-87
During the second flight SCMIT was integrated in the GAS canister and flown as part of STS-87. The experiment remained in orbit for 16 days. Floppy disks that had not shown any affects (no evidence of soft-event upsets, text file/bitmap intact) from the STS-40 flight were re-flown during STS-87. Post flight recovery and analysis took place within 30 days of landing.

POST FLIGHT ANALYSIS

General
After each flight every disk was analyzed for evidence of soft-event upsets. Each text file bit was viewed/compared and verified.

STS-40
During the first flight, single event, soft event upsets were not observed. However ten disks in one of the four storage containers did exhibit characteristics that could be attributed to a massive number of soft-event upsets. Preflight testing was conducted that verified the integrity of each text file/bitmap before integration and launch. Preflight tests should have captured the types of errors discovered during post flight analysis if these errors had occurred during experiment development and construction. The disks that exhibited these characteristics where not shield during the flight. It is important to note the experiment was stored for one year on the GAS Bridge assembly prior to launch in June of 1991.

STS-87
During the second flight, single event, soft event upsets were not observed. In addition the massive errors observed in 10 disks from the first flight were not present in any shielded or unshielded disk re-flown during STS-87.

CONCLUSIONS

General
The data supports an anomalous event occurring to 10 disks flown on STS-40. Additional exposure (16 days on orbit) on STS-87 of five disks did not reproduce the types of errors observed during STS-40. Storage of the experiment on the GAS Bridge for one year prior to the launch of STS-40 may have contributed to the observed errors. However, 30 additional disks in 3 other containers did not suffer any affect. The third flight on STS-101 will repeat the experiment has flown during STS-87.

STS-40
The types of soft-event upsets anticipated prior to flight were not observed. However a massive number of changes were observed in the logic state of 10 disks from a single container (25% of the total number). This indicates the possibility that soft-event upsets or a similar type of event occurred. It is also possible that while the experiment was stored on the GAS Bridge (1 year prior to flight) it was exposed to a magnet field or high-energy event could have created the type of changes observed. However it is worth noting 30 other disks divided among 3 different containers did not show any affect from the flight (including pre and post). It is also possible the errors occurred during construction of the experiment. However this is considered unlikely.

STS-87
During the second flight exposure to the environment of low earth orbit increased to 16 days.
A smaller number of disks served as detectors and all five were contained in a single box.
Three of the five disks were covered by one of the three types of shielding material.
Soft-event upsets were not observed in any disk. In addition the type of massive errors for the first flight were not observed. This is contra to the result of the first experiment. The third flight on STS-101 will repeat the experiment has flown during STS-87.
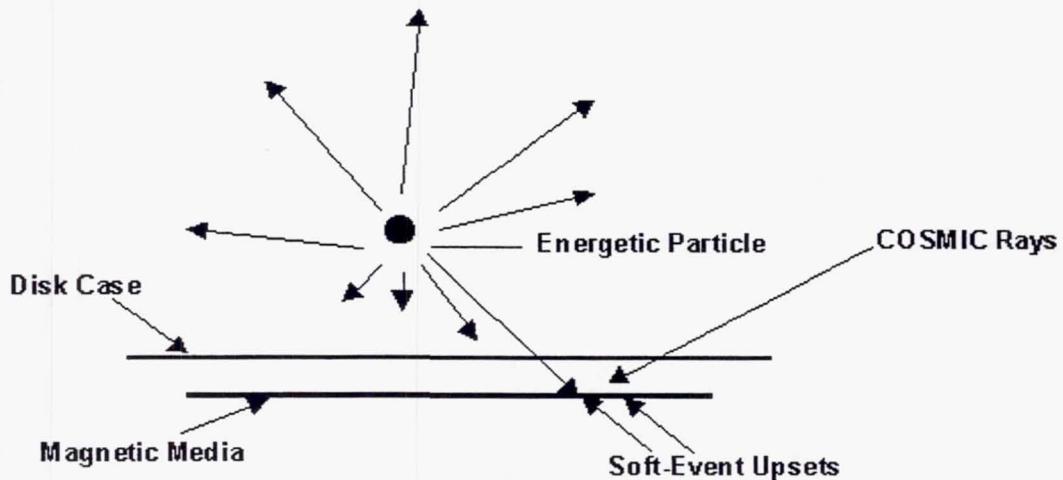
Figure 1. Soft-Event Upsets

```
type Acquisition_Data_type is record
   Total_Exception_Counter   : UAS_MDM_types.Byte_t;
   Spare                : boolean;
   Ada_Exception_Counter    : Ada_Exception_Counter_type;
   Spare2               : boolean;
   Ada_Exception_per_CSC    : Ada_Exception_per_CSC_type;
end record;

for Acquisition_Data_type use record at mod 2;
   Total_Exception_Counter    at 0 range 0..7;
   Spare                at 0 range 8..15;
   Ada_Exception_Counter     at 2 range 0..55;
   Spare2               at 9 range 0..7;
   Ada_Exception_per_CSC     at 10 range 0..
     (Scheduler_Objects.CSC_Type'POS(Scheduler_Objects.CSC_Type'LAST) +1)
     * Scheduler_Objects.CSC_Type'SIZE - 1;
end record;
```

Example of uncorrupted Code

```
type Acquisition_Data_type is record
   Total_Exception_Counter   : UAS_MDM_types.Byte_t;
   Spare                : )(*%^ean;
   Ada_Exception_Counter    : Ada_Exception_Counter_type;
   Spare2               : boolean;
   Ada_Exception_per_CSC    : Ada_Exception_per_CSC_type;
end record;

for Acquisitionsereaqsz_Data_type use record at mod 2;
   Total_5642356bxception_Counter    at 0 range 0..7;
   Spare                at 0 range 8..15;
   Ada_Exception_Counter     at y7nthdftrs 0..7;
   Ada_Exc*&Rion_per_CSC     at 10 range 0..
     (Scheduler_54wdfcy.CSC_)_(*%*^%6555555fdgsc mh7778@%$%^%%$%@#
_Objects.CSC_Type'LAST) +1)
     * Scheduler_Objects.CSC_Type'SIZE - 1;
end record;
```
Example of Code Impacted by Soft-Event Upsets

Fig 1.1 Flight Software Impacted by Soft-Event Upsets

```
1111111111111111111111111111111111111111111111111111111111111111111
1111111111111111111111111111111111111111111111111111111111111111111
1111111111111111111111111111111111111111111111111111111111111111111
1111111111111111111111111111111111111111111111111111111111111111111
1111111111111111111111111111111111111111111111111111111111111111111
1111111111111111111111111111111111111111111111111111111111111111111
1111111111111111111111111111111111111111111111111111111111111111111
1111111111111111111111111111111111111111111111111111111111111111111
1111111111111111111111111111111111111111111111111111111111111111111
1111111111111111111111111111111111111111111111111111111111111111111
1111111111111111111111111111111111111111111111111111111111111111111
1111111111111111111111111111111111111111111111111111111111111111111
1111111111111111111111111111111111111111111111111111111111111111111
1111111111111111111111111111111111111111111111111111111111111111111
1111111111111111111111111111111111111111111111111111111111111111111
1111111111111111111111111111111111111111111111111111111111111111111
1111111111111111111111111111111111111111111111111111111111111111111
1111111111111111111111111111111111111111111111111111111111111111111
1111111111111111111111111111111111111111111111111111111111111111111
1111111111111111111111111111111111111111111111111111111111111111111
1111111111111111111111111111111111111111111111111111111111111111111
1111111111111111111111111111111111111111111111111111111111111111111
1111111111111111111111111111111111111111111111111111111111111111111
1111111111111111111111111111111111111111111111111111111111111111111
1111111111111111111111111111111111111111111111111111111111111111111
1111111111111111111111111111111111111111111111111111111111111111111
1111111111111111111111111111111111111111111111111111111111111111111
1111111111111111111111111111111111111111111111111111111111111111111
1111111111111111111111111111111111111111111111111111111111111111111
1111111111111111111111111111111111111111111111111111111111111111111
1111111111111111111111111111111111111111111111111111111111111111111
1111111111111111111111111111111111111111111111111111111111111111111
1111111111111111111111111111111111111111111111111111111111111111111
1111111111111111111111111111111111111111111111111111111111111111111
1111111111111111111111111111111111111111111111111111111111111111111
1111111111111111111111111111111111111111111111111111111111111111111
1111111111111111111111111111111111111111111111111111111111111111111
1111111111111111111111111111111111111111111111111111111111111111111
1111111111111111111111111111111111111111111111111111111111111111111
```

Figure 2. Sample of a Text File/Bitmap

```
11111111111111111111111111111111111111111111111111111111111111111111111111111
11111111111111111111111111111111111111111111111111111111111111111111111111111
11111111111111111111111111111111111111111111111111111111111111111111111111111
11111111111111111111111111111111111111111111111111111111111111111111111111111
11111111111111111111111111111111111111111111111111111111111111111111111111111
11111111111111111111111111111111111111111111111111111111111111111111111111111
11111111111111111111111111111111111111111111111111111111111111111111111111111
11111115t4890751111111111111111111111111111111111111111111111111111111111111
111111111eewreds1111111111111111111111111111111111111111111111111111111111111
11111111000011we5431sds111111111111111111111111111111111111111111111111111111
111111111111111lsd1111111111111111111111111111111111111111111111111111111111
11111111111111111111111111111111111111111111111111111111111556432sd10011111
111111111111111111111111111111111111111111111111111111111111111101001111
11111111111111111111111111111111111111111111111111111111111110011000111
11111111111111111111111111111111111111111111111111111111111111111111111111
11111111111111111111111111111111111111111111111111111111111111111111111111
11111111111111111111111111111111111111111111111111111111111111111111111111
11111111111111111111111111111111111111111111111111111111111111111111111111
11111111111111111111111111111111111111111111111111111111111111111111111111
11111111111111111111111111111111111111111111111111111111111111111111111111
11111111111111111111111111111111111111111111111111111111111111111111111111
11111111111111111111111111111111111111111111111111111111111111111111111111
11111111111111111111111111111111111111111111111111111111111111111111111111
11111111111111111111111111111111111111111111111111111111111111111111111111
11111111111111111111111111111111111111111111111111111111111111111111111111
11111111111111111111111111111111111111111111111111111111111111111111111111
11111111111111111111111111111111111111111111111111111111111111111111111111
11111111111111111111111111111111111111111111111111111111111111111111111111
11111111111111111111111111111111111111111111111111111111111111111111111111
11111111111111111111111111111111111111111111111111111111111111111111111111
11111111111111111111111111111111111111111111111111111111111111111111111111
3fdsd3#^&$%&^%1111111111111111111111111111111111111111111111111111111111111
111111111111111111111111111111111111111111111111111111111118870p908udfhg
```

**Figure. 3 Example of Soft-Event Upsets anticipated before flight**

Figure 4. Position of SCMIT Experiment in GAS Canister - STS-40
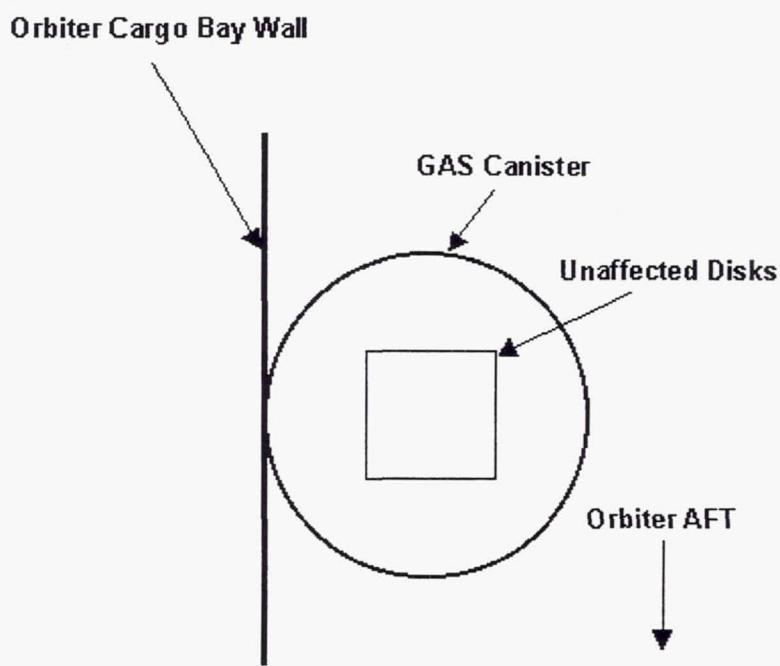
Figure 5. Position of SCMIT Experiment in GAS Canister - STS-87
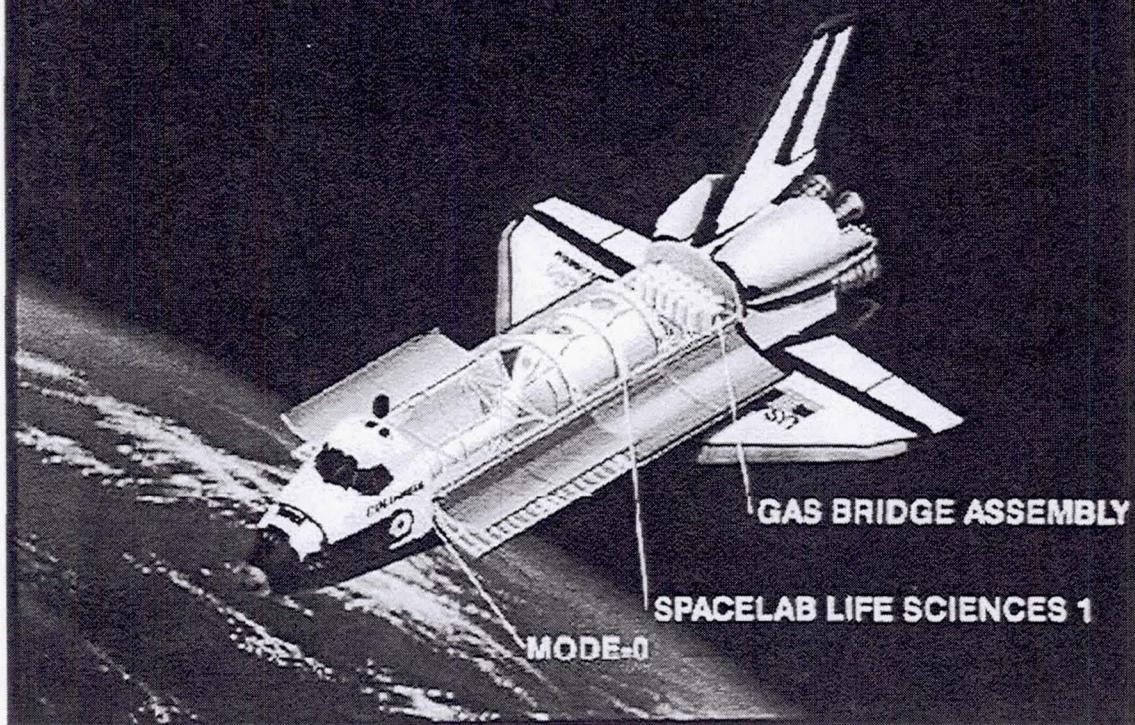
GAS Bridge Assembly STS-40

SCMIT in G-037 on STS-87

ESAJECT: ESA EJECTION SYSTEM

Jo Bermyn – Verhaert Design and Development
Hogenakkerhoekstraat 9, B-9150 Kruibeke, Belgium

Ralph Engelhardt - ESA/ESTEC
Keplerlaan 1, 2201 AZ Noordwijk, the Netherlands

ABSTRACT

Esaject (ESA Ejection System) is an ejection system developed for the ejection or jettison of small payloads from the Hitchhiker Bridge located in the Shuttle Cargo Bay. The system is developed under ESA's Technology Demonstration Program and will make its first flight for the ejection of the satellite Sloshsat, built by NLR, the Dutch National Aerospace Laboratory (as part of the Hitchhiker TAS-03 mission). The system is compliant with the stringent Shuttle safety requirements and is equipped with a "jamming free" power and data transfer system.

INTRODUCTION

Esaject is developed respecting the stringent safety requirement for Shuttle missions. As such, no guiding system is used and a single-failure tolerant system is built. This means the system can be used as well as a "safety backup" device to jettison failed payloads (e.g. blocked robotic arm). The Firing circuit is protected with three independent inhibits to prevent unintentional firing of the system; as such it will be remotely activated by the flight crew from the Standard Switch Panel (SSP) on the orbiter Aft Flight Deck (AFD).

Furthermore, the system has some specific features such as a contactlesss (inductive pot cores) power and data transfer system to allow powering and checkout the payload before ejection. As an option, the system can be equipped with a battery to be independent of the orbiter power supplies to provide power to the 'firing circuit' for ejection/jettison.

Main design drivers are :
- Ejection and Jettison function (use as safety backup device)
- Single-failure tolerant against refusing to fire (eject)
- Two-failure tolerant in combination with payload in jettison case (first failure on payload)
- Two-failure tolerant against unintentional firing
- Prevent inadvertent ejection with a minimum of three independent inhibits
- May not be initiated from ground
- Design-Lifetime three missions
- Ejection of payloads from 50 - 150 kg with a nominal ejection velocity of 0,8 m/s (min 0,3 m/s)
- Battery pack (development not part of actual contract) can be provided to be independent from Orbiter power for ejection/jettison

ESAJECT CONCEPT DESCRIPTION

Esaject consist of a main structure, bolted on the Hitchhiker Pallet, and a payload interface ring bolted to the payload. Both are interconnected by means of a marman clampband. The two identical clampband halves are interconnected with two pyrotechnic separation bolts. The clampband halves are connected to a retraction and retain system to properly retract and hold the clampband halves after separation

Firing of the two separation bolts will allow the ejection of the payload, however proper release is already guaranteed when only one bolt functions (single-failure tolerant system). After firing, the ejection is initiated by means of eight ejection spring assemblies, equally distributed around the main structure's perimeter. Adjusting the pushrod length allow for mission specific adjustments coping with COG offset and mass differences of different payloads
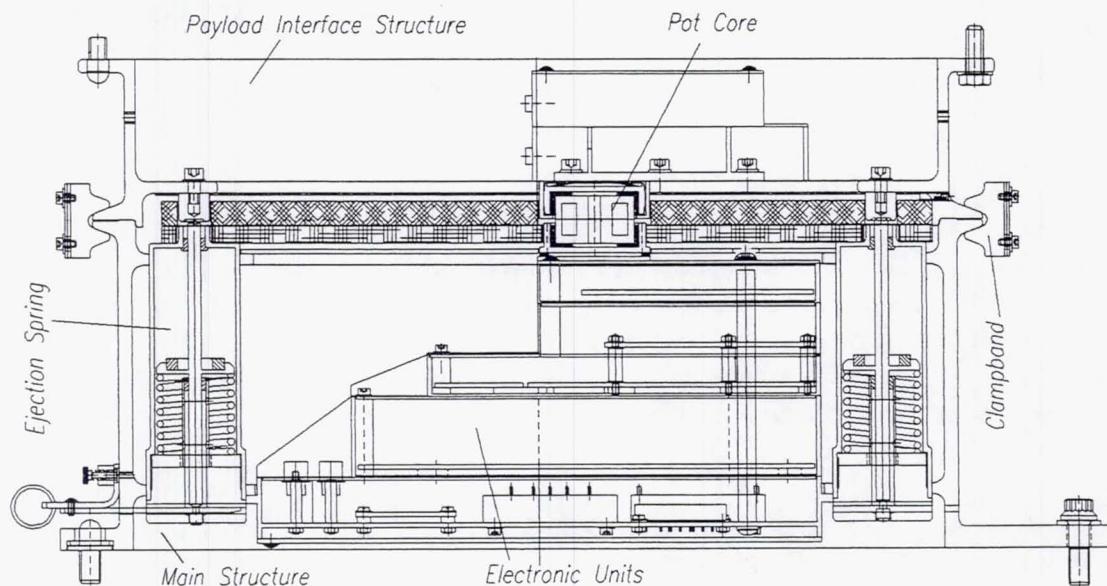
FIG 1 ESAJECT CROSS-SECTION

Mechanical Subsystem

The ESAJECT mechanical subsystem is comprised of the main structure, the ejection spring assemblies, the marman clamp band, debris capture devices and the external housing. The total mass of the ejection system is approximately 38.5 kg.

ESAJECT Structures

There are three structural subsystems associated with the ESAJECT: the main structure, the payload interface structure and the outer structure.

Main Structure

The main (inner) structure, fabricated from AA 7075-T7352, transfers the loads to the HH Double Bay Pallet. The main structure is 155 mm high and is made from a single part to reduce the number of bolts and joints. The electronics box is mounted inside, with remaining subsystems mounted on the structure itself. Connectors and harness to the outside are routed via feed through in the structure. The top portion is one half of the separation interface, and the bottom side is bolted to the HH Pallet.

Payload Interface Structure

The Payload Interface Structure, fabricated from AA 7075-T7351, provides the interface between the lower part of the ESAJECT system (main structure) and the payload. It is mechanically bolted to the underside of the payload. The other side interfaces with the marman clamp band. The structure also houses the payload-side part of the pot core based power and data transfer system. It is keyed to provide for correct installation on the main structure. The contact surfaces of the separation interface plates with the marman band will be coated with NiFlor (Ni coating with PTFE) to reduce friction effects. The shear forces between the main structure and the payload interface ring are limited by a border with a slope of 15 degrees.

Outer Structure

The outer structure is actually a non-load bearing cover which is mounted to the retraction spring brackets. It provides for installation of the Multi-layer Insulation (MLI) thermal blanket. It is currently designed in two sections, any of which may be removed without disturbing the payload. The outer structure and MLI will be vented to prevent pressure differentials within the system.

Spring Assemblies

There are 8 spring assemblies equally spaced around the perimeter of the main structure (approximately 150 mm around the ESAJECT vertical center line). Each spring assembly is identical and is comprised of the following components:

separation spring - cold coiled stainless steel (AISI 301)
push rod - stainless steel (AISI 431)
bushing - vespel
guide and housing
nuts and washers

The nominal ejection velocity is 0.8 m/s and the minimum is 0.3 m/s in case of spring failure. This nominal velocity for future payloads of varying weight will be maintained through pre-flight calculations which will lengthen or shorten the stroke, as is dictated by the payload mass. The stroke will be pre-determined prior to integration, and is not adjustable once the payload has been attached to the ESAJECT system. Shims can be used to adjust the spring assemblies to the same initial force within +/- 7.5%. Future payloads with offset centers of gravity may be compensated for through asymmetric compression by using different pushrod lengths. The spring is designed to be loaded not higher than 80% of its rated force. The assemblies may be locked/unlocked in a compressed position in order to allow proper installation of the payload interface ring and the marman clamp band without forcing.
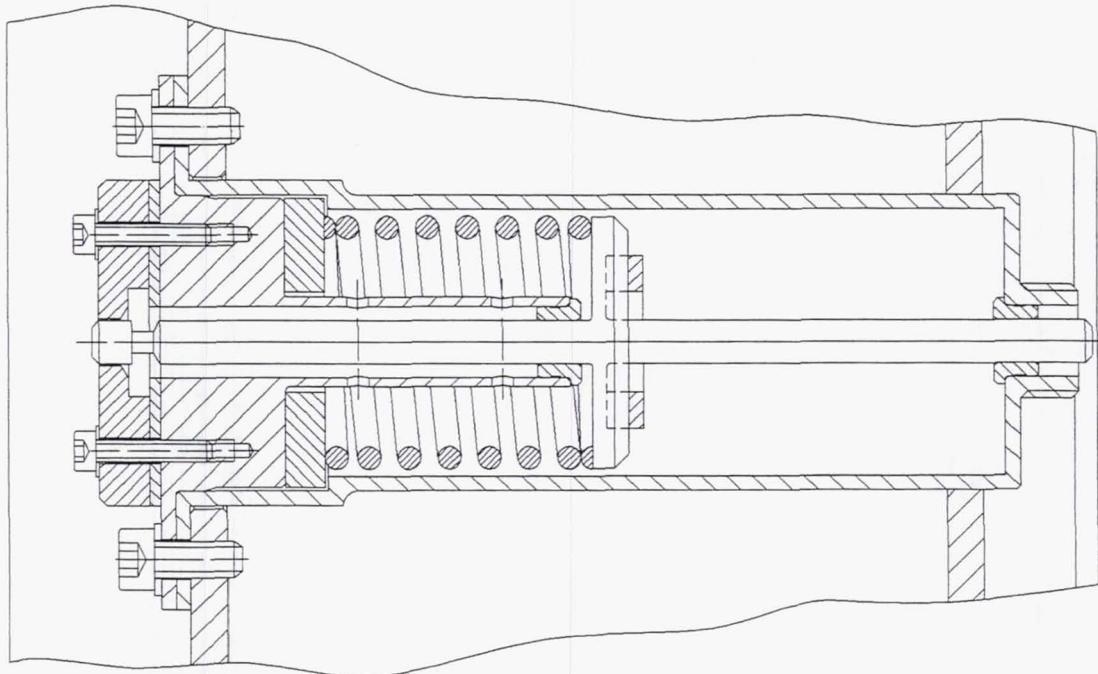

FIG 2 SPRING UNIT CROSS-SECTION

Marman Clamp and Separation Bolt

The marman clamp consist of two nickel-alloy bands (Ni 718) with three floating Aluminium-alloy clamps on each side of the two bands. The clamp band halves are held in place by two pyrotechnically operated Separation Bolts which are set 180 degrees apart. The pre-tension of the clamp band can be monitored at any time through redundant sets of strain gauges. The inner and outer surfaces of the clamps, clamp band and trunnions are coated with XYLAN 1010 dry lubricant (0.11 static coefficient of friction) which improve disengagement of the clamp during retraction and ease installation.

The release of the marman clamp is achieved through pyrotechnically initiated separation bolts. The energy for actuation is provided by a NASA Standard Initiator (NSI)-actuated booster cartridge. This bolt is known as a "velocity piston" design because it efficiently uses the kinetic energy of the piston to effect separation. Only a small amount of propellant is required and the separation event is quite gentle. The separation bolts are purchased from PyroAlliance, Les Mureaux, France (affiliated with OEA Corp., USA).

Separation of either bolt will release the clamp and allow the payload to be ejected. After pyrotechnic firing, the clamp band will be retained by means of a retraction and retention mechanism (see next paragraph). Breadboard testing of the ejection system has shown high induced forces from the separation of these bolts, therefore an additional locking device, based on a ty-rap concept, is incorporated to prevent rebound of the clamp band. Redundant sets of strain gauges on each clamp band half will allow monitoring of the stresses during integration and in orbit.
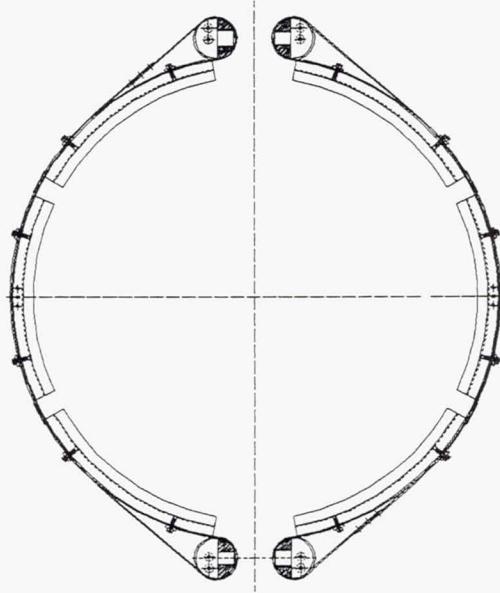

FIG 3 MARMAN CLAMPBAND

Retraction and Retention Mechanism

The retraction and retention mechanism consists of a set of spring loaded devices which pull the halves of the marman clamp band away after pyrotechnic operation . These devices respond quickly enough to prevent an asymmetric ejection of the satellite due to interference with the clamp band. They are also designed to prevent rebound and possible recontact with the ejecting payload. Each mechanism consists of 3 sets of springs attached on one side to the clamp band halves and to bridges. These bridges act as "guides" and are part of the restraint scheme for the retracted clamp band halves. Each set of springs consists of a right-hand and left-hand wound spring to avoid blocking or interference with adjacent springs. In the event that only a single bolt is separated, the mechanism allows for a tangential retraction with a minimum of friction, still providing for full clearance of the separation interface.
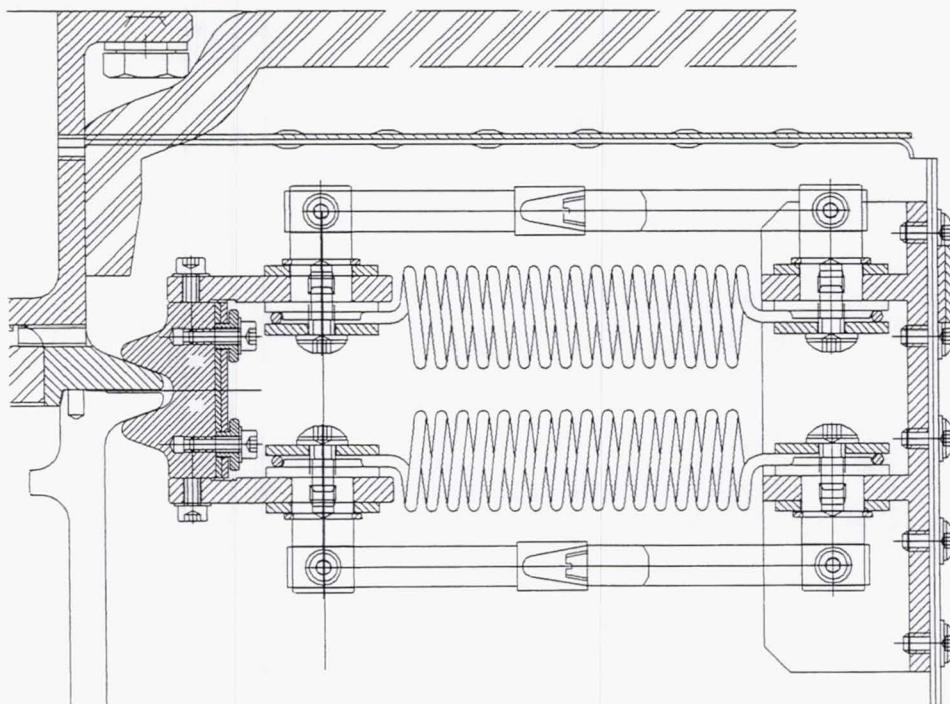
FIG 4   RETRACTION SYSTEM

Debris Capture Device

The debris capture device implemented in the ESAJECT design is derived from a concept, first used on ESA's ERS-1 satellite. It consists of four silicon rubber membranes separated with spacers. Each membrane has a 90 degree slit and they are set 90 degrees shifted in the assembled configuration. The proposed silicon rubber is "SILICONE ERICA" from Eriks. This silicon has been shown to provide the best performance with respect to temperature range, permanent deformation, tear strength, surface friction and out gassing.
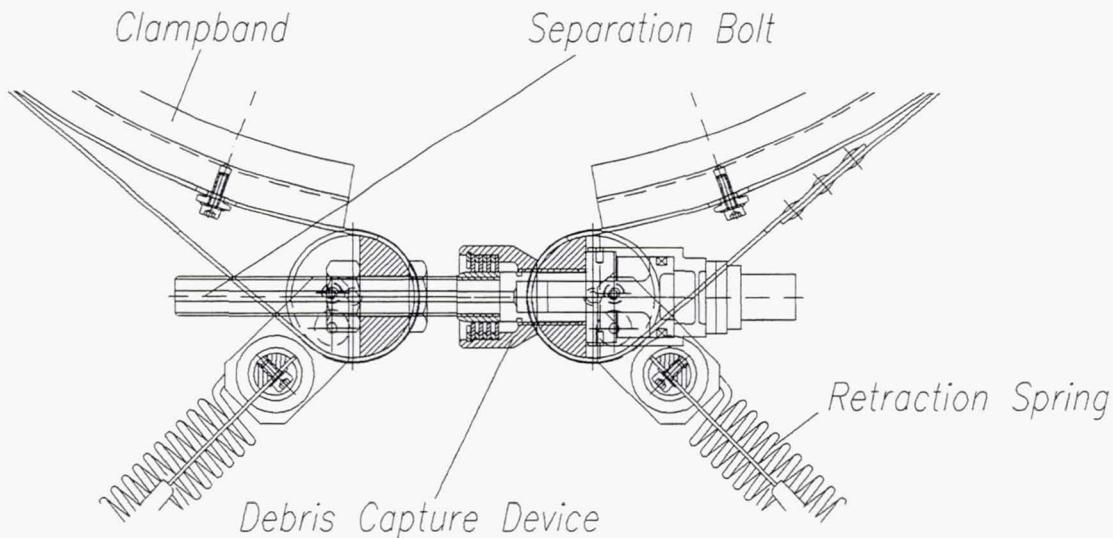
FIG 5   SEPARATION BOLT - DEBRIS CAPTURE DEVICE

ELECTRICAL SUBSYSTEM

The electrical subsystem consists of the following: the electronics box, the Data Transfer System (DTS), the Power Transfer System (PTS), the Pyrotechnic Firing System (PFS), and test hardware (including ground shorting plugs). The ESAJECT in its current configuration, used to eject Sloshsat does not contain a battery subsystem.

Electronics Box

The electronics box will house the ESAJECT command and monitoring circuitry, including associated pyrotechnic circuitry. The box will interface through the standard Hitchhiker electrical interfaces. No payload functions are associated with this unit.

Data Transfer System

The DTS provides for data transmission to the payload prior to ejection. The connectors will actually be two ferrite pot cores, which use electromagnetic induction to transmit the desired data. The pot cores make contact at the separation plane, thus half of the connector is on the payload side of the interface, and will be ejected as part of the satellite. The magnetic coupling of the data across the separation plane is done using a Ferroxcube pot-core. This method will avoid the problems associated with separating the typical pin connector (contact forces may cause jamming). There will be two redundant sets of pot cores, one set for transmitting and another set for receiving.

The pot core transformer consists of a primary (transmitter) side of the transformer made by 2 windings of 15 turns each of copper wire. The secondary (receiver) side is 1 winding of 15 turns of copper wire. The winding is fixed inside the pot core half. A spring-loaded mechanism located in the upper part will provide the necessary mechanical pressure between the two halves.

Data Transfer

ESAJECT will provide for 16 bit bi-directional parallel data transfer at the separation plane. This will be achieved through redundant Manchester-coded serial data links using shift-registers for parallel/serial data conversion. The actual data transfer is made via the pot core magnetic coupling. The electronics are based on a commercially available CMOS Manchester Encoder-Decoder Chip per MIL-STD-1553. Independent encoder-decoder sections on the chip allow full duplex data communication. A second of these chips will provide the desired redundancy. The data rate is 1 Mbit/sec, which corresponds to a transfer rate of 50 Kwords per second. Included in this data transfer is the asynchronous uplink and downlink for communication with the payload while attached to the ESAJECT system.

Power Transfer System

As with the data transfer, power is routed to the payload via pot cores across the interface plane. There are two identical systems in parallel for redundancy. A shutdown circuit stops the switching of the primary part of the power system after ejection of the secondary part with the satellite. The pot core halves are pressed together with using a spring located in the upper part.

Power Transfer

To meet galvanic isolation requirements, the power transfer system utilizes a DC/DC converter, powered via an Electromagnetic Interference (EMI) filter from the HH avionics port. After the DC/DC converter, the PTS converts the output (28V) to the output on the satellite (28V @ 3A).

Pyrotechnic Firing System

The PFS fires the NASA Standard Initiators by sending a current of 5A through the bridge wires. The power is provided by the avionics power port via a DC/DC converter which produces the required 28V. The current through the initiators is limited to 6.5 A via a protection fuse resistor. The electrical connections to the firing electronics are through separate connectors to provide redundancy downstream of the avionics box. Bleed resistors provide protection against EMI or other extraneous currents. The system is operated via three SSP switches on the orbiter Aft Flight Deck.

Test Hardware

Safe and Arm Plugs

A Safe Plug is installed at all times during ground processing to allow for handling, testing and integration of the ESAJECT hardware without the potential for firing of the NSI pyrotechnics. The Safe Plug will be equipped with a "Remove Before Flight" label. During ground processing, the Safe Plug is installed to allow for health checks of the system.

The Arm Plug will be installed as late as possible and will connect the NSI to the firing circuit. A continuity check with a commercial bridge wire resistance meter (Alegany technology, model 101-5AI) can be performed at any time.

Test Connectors

Two test connectors are available for use on ground and allow for testing of the data and power transfer systems, and for measuring current, voltage and continuity. During testing, power will be provided via the avionics power interface connector.

OPERATIONAL SCENARIO

The main power control to provide power to the pyrotechnic circuitry is provided through a combination of the HH Avionics and the Standard Switch Panel (SSP) controls. The HH Avionics will be enabled by the crew through the SSP S1 switch which enables ground commanding and telemetry feedback. In addition, the HH Experiment power bus will be enabled by the crew through the SSP S2 switch. Ground commanding via the HH Avionics will be used to enable pyrotechnic fire-control circuitry, however, complete commanding for pyrotechnic fire will be given to the crew via the SSP interface.

Four switches located on the Aft Deck Switch Panel are used for the ejection (Pré-Arm, Arm, Fire 1 and Fire 2). Any combination of three switches out of four will initiate the ejection, the fourth switch is used for redundancy. The status of the 3 independent inhibits is indicated by the PRE-ARM and ARM indicators.

A redundant set of inductive separation switches is located in the main structure and give a feedback on the separation status (separated or not) through the housekeeping data to the customer ground support equipment.

PROJECT STATUS / PLANNING

Esaject is built according the protoflight philosophy, this means we immediately build the flight hardware and breadboarding was performed on new and critical elements only. During phase B, one of the major activities was the evaluation of the ejection trajectory, were we had to prove to stay within an full cone ejection angle of 20°. A dynamic analysis was performed with DCAP and verified afterwards by ejection tests performed on a mechanical breadboard. The ejection tests were recorded with a high speed camera, giving sufficient information to validate the retraction and ejection phenomena of the system. On electronics level, the inductive pot core system was breadboarded and functionally tested.

The flight model is currently under integration and qualification testing will take place in August-September 99. After testing, Esaject will go to NLR for system integration and testing with Sloshsat, after which it will be ready for shipment to GSFC for integration on the Hitchhiker.

Esaject with Sloshsat (STOF) is planned to fly on the Hithchiker TAS-03 mission, of which the real launch is not yet manifested (in 2000 - 2002 time frame).
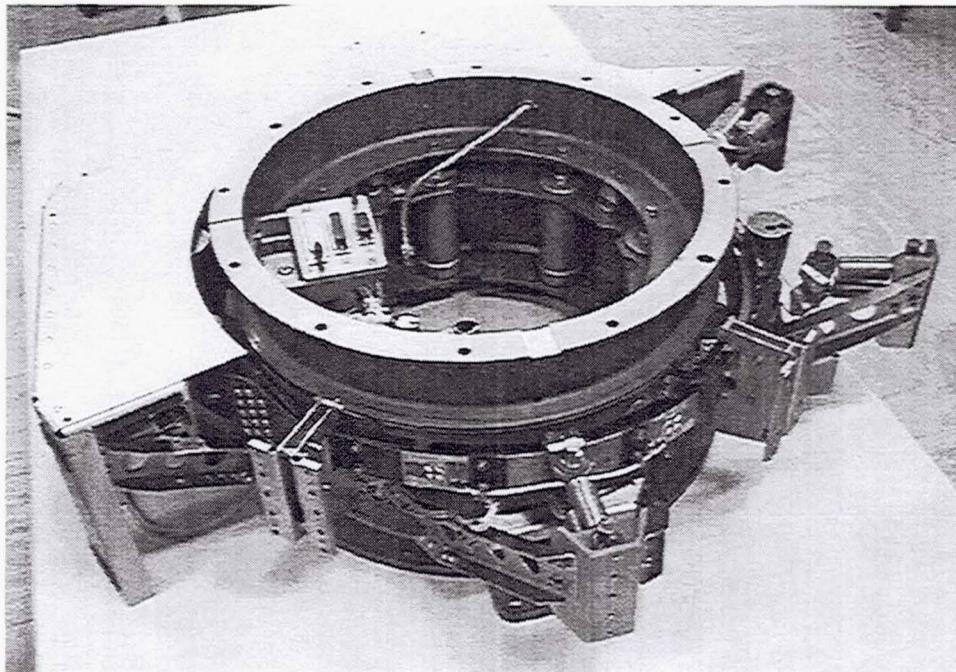

FIG 6 ESAJECT

Page intentionally left blank

ESA ATACHED PAYLOADS DURING THE SPACE STATION EARLY UTLISATION PHASE.

Henk Olthof
ESA/ESTEC, Noordwijk, The Netherlands

ABSTRACT

Following the agreement between ESA and NASA on the development of the external accommodation capabilities, ESA has selected a number of small experiments in the various domains of space science (e.g. space physics, solar physics, astronomy, etc) to be flown in the early utilisation phase of the space station. Experiments of similar nature and requirements are examples for European interest in future Hitchhiker and/or Get-Away-Special flight opportunities.

INTRODUCTION

When preparing the long term space science programme for Europe the Survey Committee in charge of this task has addressed the potential of the Space Station as a complement to the free flying missions in order to take advantage of the unique capabilities of this new system.

These include:

-Long term monitoring of known astronomical sources over a wide range (uv/x-rays, gamma-ray burst sources). Such observations could be carried out with small multipurpose telescopes which would be used also to observe targets of opportunity.

-Continuous space based measurements of the solar total and spectral irradiance from the ultraviolet to the infrared. The International Astronomical Union (IAU) is strongly encouraging such an activity which could be carried out by an international set of instruments dedicated to these measurements in various wavelength bands.

-Continuous monitoring of the Space Station environment with the aim of studying the distribution of natural particles and artificial debris.

-Validation and qualification of enabling technologies for the next generation high energy astrophysics instrumentation.

A NEW EXPERIMENT PHILOSOPHY

The International Space Station (ISSA) is very different from a free-flyer. It is rather a facility which can accommodate a variety of experiments in different scientific disciplines. A possibility for European scientists to access ISSA was offered in the ESA Announcement of Opportunity for externally mounted payloads that was issued in 1997. To allow many participants and rapid turn-around a new approach has been taken:
--small payloads
--short development time
--limited financial resources.

which in turn means that;
--science objectives are focused
--state of the art technologies are being used
--resources from science institutes and industry are optimised
--science objectives complementary to other space missions.

THE EARLY UTILISATION PHASE

The first steps to implement the above mentioned strategy have been
taken. After the scientific evaluation of the proposals received in
response to the Announcement of Opportunity for the early utilisation
phase of the Space Station (timeframe 2001-2005) the following
experiments have been selected:

--The sky polarisation observatory, SPORT (PI: Cortiglioni,I,ref. 1),to
measure the polarisation of the cosmic background radiation in the
microwave region, 20-90 GHz

--A solar package (ref. 2), including
 -Solar Variability and Irradiance Monitor, SOVIM (PI: Froehlich, CH)
for total spectral irradiance measurements at three wavelength.
--Auto-calibrating EUV/UV Spectrometers, SOL-ACES (PI Schmidtke, D) for
spectral irradiance measurements below 220 nm
--Solar Spectral Irradiance Measurements, SOLSPEC (PI: Thuillier, F) for
spectral irradiance measurements from 180 to 3000 nm

SCIENTIFIC BACKGROUND

THE SKY POLARIZATION OBSERVATORY - SPORT

Multifrequency full sky polarisation measurements very high frequency
(where Faraday rotation and depolarisation is negligible) to be made by
SPORT allow to study the radio spectrum of the total Galactic
synchrotron emission. The knowledge of this spectrum helps to separate
different components of the Galactic radio emission and the cosmic
background. In addition it will obtain valuable information on the
energy spectrum of the relativistic electrons and on the structure of
the interstellar magnetic field. Space observations greatly improve the
quality of the polarisation measurements because ground based
measurements are affected by tropospheric, ionospheric and by partly
polarised (not constant) ground radiation.

SPORT represents the first scientific payload operating at microwave
wavelengths so far realised in Europe and the first microwave scientific
polarimeter for space. Main aims of SPORT are:
-- to carry on accurate mapping of galactic linearly polarised emission
over >80% of sky
-- to attempt a detection (or to at least to improve current upper
limits) of the linear polarisation of the Cosmic Microwave Background
(CMB)

SPORT is a set of four identical correlation receivers respectively
tuned at 22, 32, 60 and 90 GHz with 10% of bandwidth, fed by quasi-
geometrically scaled corrugated horns with a FWHM=7 deg scanning
directly the sky at the ISSA zenith.

SPORT will provide scientific data complementary to other important
future space missions, like NASA-MAP (from 2001) and ESA-PLANCK (from
2008), devoted to investigate CMB anisotropies. SPORT will represent a

natural step between the COBE era and the MAP-PLANCK era. COBE, in fact, has done the first detection of CMB anisotropy by observing the full sky with spatial resolution of 7 degrees at three frequencies (31, 53 and 90 GHz). This important result has been obtained through the accurate subtraction of galactic foreground, but without taking into account its linear polarisation.

THE SOLAR PACKAGE

The three solar instruments placed on the space Station will explore for the first time a wide spectral range from EUV to infrared representing more than 99% of the total solar irradiance; the data from the three instruments will be taken simultaneously. The measurements are relevant to atmospheric physics, climatology and solar physics. Accurate solar spectral irradiance measurements are needed because this energy in particular UV radiations, is the primary source of chemical, radiative and dynamical processes that impact the ozone content, the production and destruction of the latter and other minor atmospheric constituents through many catalytic reactions. Absolute measurements of the solar spectral irradiance as a function of time are essential to understand natural variations of the composition of the Earth' atmosphere.
EUV measurements are important for the physics of the upper atmosphere, satellite orbit predictions and total electron content needed for modelling the behaviour of navigation and communication satellites. There is no other way to assess the primary energy input to the Earth's upper atmosphere than by continuously measure the solar EUV/UV radiation directly. Moreover, an accurate knowledge of the status of the upper atmosphere is needed for navigation, for communication, for space-weather phenomena.
For the understanding of the solar internal mechanisms, it is important to know the absolute value of the total and spectral irradiance is varying as a function of the solar cycle characteristics.

SOL-ACES (Solar Auto-calibrating EUV/UV Spectrometers with absolute, in flight calibration) will measure the solar spectral irradiance of the full disk from 17 to 220 nm at 0.5 to 2 nm spectral resolution. This instrument will provide the most accurate EUV/UV observations so far achieved and, among others, will provide the foundation for more accurate thermospheric-ionospheric models.

An investigation of the ISSA environment will be another result. The instrument consist of four spectrometers and four ionisation chambers each equipped with a pre-calibrated photodiode. The filter wheel allows to place the filters (with bandwidth of 10-20 nm) in front of each spectrometer and each ionisation chamber. The filter wavelength domain allows to cover the EUV and UV domain with overlap. The spectrometers are working at grazing incidence.

SOLSPEC will determine the solar spectral irradiance from 180 to 3000 nm with an accuracy of 2% in UV and 1% above at 1 nm resolution below 900 nm and 4 nm above, and the variability in that wavelength domain. The instrument is made of three spectrometers to cover the 180 to 3000 nm region. Each spectrometer consist of a double monochrometer using holographic gratings which reduce the scattered light. The wavelength positioning is of the order of 0.01 nm. The detectors in the UV and visible domains are photomultiplier tubes and a PbS cell in the infrared.

SOVIM will observe the total solar irradiance at three wavelength to obtain quasi-continuous high quality measurements of the solar irradiance variations.
The instrument consists of electrical substitution radiometers operating at ambient temperature.

REFERENCES

1.S.Cortiglioni et al, proceedings of the 2nd European symposium on the utilisation of the international space station, 1998, ESA SP-433 pg 613

2.G.Thuillier et al, proceedings of the 2nd European symposium on the utilisation of the international space station, 1998, ESA-SP433 pg 605

FAR-ULTRAVIOLET STELLAR EMISSION MEASUREMENTS FROM UVSTAR[1]

Roberto Stalio[1,2], Anna Gregorio[1,2], Paolo Trampus[2]
[1]Astronomy Department, University of Trieste
[2]CARSO, Center for Advanced Research in Space Optics, Trieste

ABSTRACT

We present UVSTAR and some of the relevant science results from the three UVSTAR missions performed so far: on STS69, STS85 and STS95. In particular we discuss hot sub-dwarf stars, β Lyr and ε CMa (500 - 1250 Å) observations.

INTRODUCTION

UVSTAR, UltraViolet Spectrograph Telescope for Astronomical Research operates in the 500 - 1250 Å waveband at spectral resolutions of 1, 4.5 and 12 Å which can be selected according to the observation requirements; it has capability for long slit spectral imaging of extended cosmic sources such as planets, planetary nebulae, supernova remnants, H II regions, and external galaxies. UVSTAR has flown as a Hitchhiker-M payload on the STS 69 mission (September 7-18, 1995) of the Shuttle Endeavour, and on the STS 85 (August 7 -19, 1997) and STS 95 (October 29 - November 7, 1998) flights of the Shuttle Discovery. These are the first three of a series of flights that NASA has allocated to the IEH (International Extreme-ultraviolet Hitchhiker) program, an international scientific collaboration which includes UVSTAR and the Solar Extreme-ultraviolet Hitchhiker (SEH) as well as other instruments. UVSTAR, a joint collaboration between the Universities of Arizona and Trieste, consists of a movable platform and an optical system. The platform provides fine pointing (±5 arcsec) within ±3 degrees from the nominal view direction, which is near the Shuttle +Y axis, i.e. perpendicular to the long axis of the Shuttle and in the plane of the wings. The optical system has two channels, each consisting of a telescope and Rowland concave-grating spectrograph with intensified CCD detector. One channel, EUV, operates at wavelengths shorter than 912 Å, while the second, FUV, operates above the Lyman discontinuity.

Pointed observations are obtained at any time the Shuttle is on celestial lock and the +Y axis is near a program target and at any time the Shuttle is in a LVLH attitude with the +Y axis directed towards one of the orbit poles. Priority UVSTAR pointed targets are Jupiter and the Io Torus, calibration stars, ultraviolet (including EUV) stellar and extended sources such as comets, planetary nebulae, globular clusters, HII regions, supernova remnants, nearby galaxies.

UVSTAR

The instrument, described in detail in Broadfoot, Sandel and Stalio (1993), consists of two spectrographic channels, EUV and FUV, which are nearly identical and observe the same target simultaneously (figure 1). Each channel consists of a telescope mirror, and a concave grating spectrograph with its own intensified CCD detector. The telescopes form images of the target at the entrance slit of the spectrographs. The concave gratings of the spectrographs both disperse and re-image the light from the target onto the 2-D detectors. Spatial resolution along the slit is preserved, so that in the cross-dispersion direction the detectors records many spectra corresponding to different part of an extended source simultaneously. The optical design is driven by the facts that at the EUV wavelengths of interest only reflective optics can be used and that reflectivity is poor, which requires minimizing the number of reflections if weak sources are to be detected in a short period of time.

Optical configuration

The telescope mirrors are off-axis parabolic mirrors of 30 cm diameter and 1.5 m focal length. They are SiC coated for maximum reflectivity, are made by Zerodur to prevent defocusing due to thermal changes, are joined to the spectrographs by rods of a carbon composite material of about zero thermal expansion coefficient along its length. The spectrographs employ concave, holographic gratings to disperse the radiation and focus it on the detector. Gratings dimensions are 70×100 mm with a radius of curvature of 275 mm. They achieve aberration correction and a flat focal plane over a length of 8 mm in the cross-dispersion, and 15.4 mm in the dispersion directions. To maintain good focus over a range of temperatures, the gratings are fabricated on Zerodur blanks; coating is BC. The grating cell is mounted to permit small motions relative to the spectrograph housing. The position of the grating relative to the entrance slit and detector is established by invar rods that extend from the grating cell to fixed positions near the entrance slit and detector.

The spectrographs cover the overlapping spectral ranges for a total band of about 485 Å each. The spectrum is dispersed along 1024 pixels, giving a dispersion of ≈ 0.47 Å per pixel. The array is 256 pixels wide. In the image mode the spectral/spatial images consist of $2 \times 1024 \times 256$ pixels, that is, nearly 5.3×10^5 pixels or 1.06×10^6 bytes if each pixel is digitized to 16-bit accuracy. Each of the spectrographs is equipped with a mechanism for selecting among three entrance slits. All slits have the same length of $0.25°$ but differ in width. The slit widths and their uses are: a) Narrow slit (3 pixels, 9 arcsec). This slit provides about 1 Å resolution and spatial resolution along its length. b) Medium slit (13 pixels, 39 arcsec). This slit gives global images of extended sources (planetary nebulae, SN remnants, Jupiter's disk) at the wavelengths of most intense emissions. Resolution is 4.5 Å. c) Wide slit (33 pixels, 100 arcsec). This aperture allows the whole image of the Io plasma torus to be dispersed into its major emissions and re-imaged with 12 Å resolution.

Detectors

The intensified CCD (ICCD) detectors (Bucconi et al. 1999) consist of standard proximity-focused image intensifier tubes (MCP) that are fiber-optically coupled to CCDs. The image intensifiers are windowless and have KBr photocathode. Charge from photoevents is amplified by the microchannel plate and electrostatically accelerated to a phosphor screen on a fiberoptic window. The visible-wavelength image from the phosphor is transferred to the CCD by fiber optics for readout. A special position of the slit changing mechanisms seals the spectrograph enclosures to protect the detectors and gratings from contamination. Each spectrograph is equipped with an ion pump to assure a satisfactory vacuum environment for operating the windowless intensifiers on orbit.

Pointing and tracking system

UVSTAR includes capabilities for independent target acquisition and tracking. The spectrograph package has internal gimbals that allow angular movement of $\pm 3°$ from the central position. Rotations about the azimuth axis (parallel to the Shuttle Z axis) and elevation axis (parallel to the Shuttle X axis) will actively position the field of view to center the target of interest in the fields of the spectrographs. Two dedicated visible imagers (Finder and Tracker) having different fields of view provide pointing and guiding information. Finder and Tracker have their own ICCD detector, 384×288 pixel arrays. Tracker ICCD has the same plate scale as the spectrograph.

The Finder has 60 mm focal length and f/1.4 optics giving a field of view of $4.8° \times 6°$. It operates in two modes (De Carlo et al. 1994; Trampus *et al.*, this symposium): in the finder mode, from a coarse knowledge of the pointing direction ($\pm 3°$), it recognizes autonomously the acquired stellar field and point to the chosen direction within $\pm 3"$. In the tracker mode, after having reached the wanted direction, it tracks a target with two different techniques: 1) triangulation, the system chooses three stars out of the stars selected in the finder mode and by means of a triangulation procedure, computes the position of the center of the sensor which coincides with the chosen pointing direction; 2) star pointing, the target star is at the center of the sensor; its position is corrected at every acquisition to keep it at the center. In both cases the algorithm takes a few milliseconds of processing time. As an alternative to the above

mentioned routines the system can run a procedure (called planet mode) which doesn't use any identification procedure, but simply searches for the brightest object in the FoV, brings it at the sensor center and tracks it with the algorithm 2). During the observations the target is captured and tracked by time tagging the "start track" command.

The Tracker is a 100 mm diameter cassegrain telescope with a 1.5 m focal length and a 0.24°×0.32° field of view. The tracker telescope is also equipped with an intensified quadrature diode which tracks a 8-9 magnitude star with negligible processing time. The tracking accuracy is better than ±3". The tracker telescope is both used for in-flight alignement of the spectrographs and as a back-up system for the Finder.

UVSTAR as an attached payload

An attached payload, like UVSTAR, has the advantage that 1) it uses resources from the Shuttle: power, telemetry, attitude, 2) it does not have strong weight and mass reduction requirements or need of long life - high quality parts and components, and 3) in the framework of a multiple flight program, it can be fixed, upgraded and adjourned each time it comes back to ground and is prepared for another flight. Compared to an independent payload operating from a satellite, this results in a strong cost reduction which is only partly counterbalanced by the cost increase due to safety requirements for a manned flight, and in a continuous search of new technological solutions indicated by the lessons learning experience from previous flights. For an astronomy payload, the main disadvantages of being attached are that the Shuttle is not a stable base and that most of the time it operates on a LVLH attitude. Most of these advantages/disadvantages will be found for pointing astronomy payloads which will operate from the International Space Station.

UVSTAR capabilities for independent target acquisition and tracking by means of dedicated visible imagers, described in the previous section, make the instrument unaffected, to a large extent, by the Shuttle motion. Viceversa, an important limitation of the instrument autonomy is the small, ± 3°, tracking box for both elevation and azimuth motions. This means that UVSTAR needs that the Shuttle points a target and stays on an inertial attitude for the duration of the observations. The plan for the series of missions we are carrying on is to have the Shuttle pointing celestial objects for 12 hours during the flight. However, this limitation is relaxed by the possibility of serendipitous observations which can be made every time that the Shuttle is on a inertial attitude or when it operates on a fixed, low energy requirement, LVLH attitude with the tail in nadir or zenith direction and the telescope line of sight pointing near one of the orbit poles. In this last case the instrument can track stars near the pole (up to about 10 degrees away) since it sees the targets making a complete circle around it in about 90 minutes, which is the typical duration of a Shuttle orbit. The equatorial coordinates of the orbit poles are determined by the initial orbit parameters; due to precession their right ascension changes with time at a rate which depends on the orbit inclination.

The STS 69 flight

UVSTAR has flown for the first time from September 7 to 18, 1995 on the Shuttle Endeavor (STS 69 mission). Unfortunately, two major failures hindered the mission: a mechanical/elevation drive failure which resulted in the inability of tracking a star and an electrical failure in the Finder which made it more difficult to identify the pointed direction and align the Finder and Tracker with the spectrograph slits. These failures have limited the instrument performances and influenced the science product. In fact, UVSTAR only acquired spectra when the Shuttle was on an inertial hold with pointing direction controlled up to 0.05 degrees. Without a tracking system, we made the choice of using the widest slit on these stellar spectroscopy observations in order to maintain the star within the slit as long as possible. This resulted in a degradation of the nominal (1 Å) spectral resolution due to Shuttle motion along the dispersion direction. FUV data from two bright stars: ε CMa, B2 II, and α Eri, B3Vp were obtained. In Table 1 we report the mission orbital parameters.

Table 1: **Shuttle orbital parameters for STS 69**

orbital parameters - STS 69				
a (km)	e	i (°)	Ω (°)	ω (°)
6728	0.0003	28.4	191.92	69.06

The STS 85 flight

The second flight of UVSTAR occurred from August 1 to18, 1997 on the Shuttle Discovery (STS 85 mission). The main science objectives were to observe Jupiter and the Io plasma torus, hot stellar sources at wavelengths down to the interstellar hydrogen absorption cut-off at 912 Å, and the comet Hale-Bopp as a target of opportunity. During this flight the internal pressure of the spectrographs was too high and prevented us from getting the low noise required to record the Jupiter and Torus emissions as well as the faint line emissions from the comet. Viceversa, the stellar observations were very good.

We pointed and tracked stellar targets, Jupiter and Hale-Bopp. In addition we monitored continuously the day and night Earth glows at both high and low spectral resolution. A target spectrum consisted of several observation frames; each frame was acquired by co-adding in flight a sequence of six 5-second images. In this way we were able to maintain the spatial information in the Ly-α geo-coronal flux without saturating. The 30 second integrated spectral image was then transmitted to ground for quick look analysis and storage. A target spectrum was formed by co-adding the number of observation frames necessary to get the required S/N ratio. The sky background was recorded both before and after an observation run. The pointing system images were also transmitted to ground at a faster rate. The STS 85 orbital parameters and the 1950 (M50) celestial coordinates of the poles at the beginning and end of the mission are reported in Table 2. Table 3 provides the UVSTAR observation journal.

Table 2: **STS 85 orbital parameters and 1950 (M50) celestial coordinates of the poles**

orbital parameters - STS 85				
a (km)	e	i (°)	Ω (°)	ω (°)
6673	0.0003	57.027	75.5896	69.06

coordinates of south pole		coordinates of north pole	
beginning	end	beginning	end
α=165°.6	α=110°.4	α=345°.6	α=290°.4
δ= -32°.97	δ= -32°.97	δ= 32°.97	δ= 32°.97

*Table3:*Journal of observations (UVSTAR - STS 85)

ET[1]	Target	Name	m_V	Spectrum	Data[2]	MET[1]	Target	Name	m_V	Spectrum	Data[2]
04/15:10	124	γ Peg	2.9	B2 IV	Y	08/01:48	Jupiter	Jupiter			Ly_α
04/20:48	904	HD176301	6.5	B7III-IV	Y	08/06:30	Serend.	HD74824	5.7	B2III	Y
05/01:25	420	10 Lac	4.9	O9V	Y	08/07:30	Serend.	HD75547	1.4	B9.5IV	Y
05/01:45	Serend.	12 Lac	5.3	B2III	Y	08/07:40	Serend.	LS1153	12	B	Tba
05/15:40	204	ζ Per	2.9	B1Iab	Y	08/15:01	Jupiter	Jupiter			Ly_α
05/16:31	407	HBV 475	12	M4	Tba	09/02:01	Serend.	PT Pup	5.7	B2III	Y
06/13:17	Jupiter	Jupiter			Ly_α	09/02:06	TOO	Hale-Bopp	5		Y
06/14:55	Jupiter	Jupiter			Ly_α	09/03:30	Serend.	PT Pup	5.7	B2III	Y
06/18:05	904	HD176301	6.5	B7III-IV	Y	09/03:32	TOO	Hale-Bopp	5		Y
06/19:38	904	HD176301	6.5	B7III-IV	Y	09/04:10	126	α Lyr	0.03	A0V	Y
07/04:53	TOO	Hale-Bopp	5		Y	09/04:45	111	NGC 104	4.9	Glob. C.	Tba
06/13:17	Jupiter	Jupiter			Ly_α	09/06:25	115	3 in η Car		WR & O	Y
07/15:10	112	NGC 246	11.8	Op	Y	09/06:25	Jupiter	Jupiter			Ly_α
07/15:27	Serend.	BD-11 162	11.2	SdO	Y	09/09:32	121	NGC 6818	9.9	PNN	N
07/15:37	Serend.	HD 4188	4.8	K0III	N	09/22:51	Jupiter	Jupiter			Ly_α
07/19:56	903	HD175803	8	B3V	Y	10/00:25	416	B+284211	10.5	SdO	Y
07/21:15	903	HD175803	8	B3V	Y	10/00:46	Serend.	B+284177	9.8	B1IV	Y
08/01:48	Jupiter	Jupiter			Ly_α	10/01:05		Calibration			

[1] Mission elapsed time (day/hour:min: launch = 00/00:00); [2] TBA = to be analyzed; N = no data

The STS 95 flight

The third flight of UVSTAR occurred from October 29 to November 7, 1998 on the Shuttle Discovery (STS 95 mission). The main science objectives were again to observe Jupiter and the Io plasma torus and hot stellar sources at wavelengths down to the interstellar hydrogen absorption cut-off at 912 Å.

The changes made to the spectrographs for decreasing the internal pressure included enlarging the pumping port by a factor of twenty and placing 50 watt heaters in the spectrograph bodies. The heaters were used during the first day, holding the temperature in the 20° C to 40° C range. When the heaters were turned off, the internal pressure dropped to $< 5 \times 10^{-7}$ torr and remained there throughout the mission. Jupiter was acquired on the first opportunity and held in the center of the slit by the star tracker with an accuracy of less than four seconds of arc. The shuttle limit cycle effect was minimized by working with a dead-band of plus or minus one degree. Very little data was lost due to identifying and pointing the program targets.

The observational strategy was basically the same as for STS 85. The calibration source, ε CMa; has been observed twice: with the first series of images we have been able to align the telescope and the FUV spectrograph; with the second series we succeeded in aligning the EUV channel with the telescope. This lead us to acquire both Jupiter system and ε Cma EUV spectrum. Other important celestial targets obtained are the weak Seyfert galaxy F9 and the Large Magellanic Cloud sources 30 Dor and S Dor. The STS 95 orbital parameters and the 1950 (M50) celestial coordinates of the poles at the beginning and end of the mission are reported in Table 4, the journal of observations is given in the paper by Trampus *et al.* (this symposium).

Table 4: **STS 95 orbital parameters and 1950 (M50) celestial coordinates of the poles**

orbital parameters - STS 95				
a (km)	e	i (°)	Ω (°)	ω (°)
6950	0.0003	28.45	151.8	200

coordinates of south pole		coordinates of north pole	
beginning	end	beginning	end
α=61°.8	α=119°.4	α=241°.8	α=184°.2
δ= -61°.55	δ= -61°.55	δ= 61°.55	δ= 61°.55

SELECTED SCIENCE RESULTS

FUV Spectra of BD +28° 4211, NGC 246 and BD-11°162

The sdO star BD +28° 4211 is of particular interest as it is used as a secondary flux standard. It has been observed at wavelengths below 1150 Å by the Voyager UVS on January 13, 1981, by an absolutely calibrated sounding rocket (Cook, Cash and Green, 1991) and by HUT (Kruk et al. 1997). A detailed discussion of the calibration results for this star, and in general for the spectral band below 1150 Å, is given in Holberg et al. (1991) and in the above mentioned papers by Cook, Cash and Green and by Kruk et al. We have used the Voyager data of BD +28° 4211 with the revised absolute calibration by Holberg (1997) for this analysis. A correction curve has been obtained by calculating the ratio Voyager UVS to UVSTAR and fitting the resulting curve with a second order polynomial. The same correction curve has been then adopted for the central star of NGC 246 and for BD-11°162.

The central star of the planetary nebula NGC 246 is one of the hottest planetary nebula nuclei known; it is considered a hydrogen deficient PG 1159-type star with a optical spectrum characterized by strong OVI emission lines (Smith and Aller 1969). It is a X-ray source (Apparao and Taradfar 1989) and an EUV source (Bowyer et al. 1996). Feibelman (1995) studied the high resolution IUE absorption spectrum of the nucleus (hereafter referred to simply as NGC 246) stating that it is mostly strong and broadened high excitation CIV and OVI lines; NeVII lines are also very strong. He also detected OVII λ-1522 (Feibelman, 1999). The CIV resonance doublet is the only feature to exhibit a P Cygni profile, although weak, with a maximum absorption velocity at 2700 ± 250 km/s and a terminal velocity, v_∞, at 4100 ± 200 km/s (our measurements from 9 IUE SWP high resolution spectra co-added); Koesterke, Dreizler and Rauch (1998) report a v_∞ value of 3500 km/s and estimate a mass loss rate of 1.2×10^{-7} M_{sun}/year. The CIV P Cygni profile also displays two absorption component at -10 and -66 km/s which are probably of circumstellar origin. Other information on NCG 246 are given in Acker et al. (1992): the spectral type is WC-OVI, the systemic radial velocity is -46 ± 7 km/s, the diameter of the nebula is 245", the distance is 0.47 kpc. Koesterke and Werner (1998) report an effective temperature of 150000 K and log g = 5.7.

Very little is known on BD $-11°162$: it is 11.2 visual magnitude hot SdO star with UV enhanced flux.
In figure 2 we compare the UV spectral energy distributions of BD $+28°$ 4211, NGC 246 and BD-11°162 using UVSTAR fluxes derived from the calibration curve described above and IUE ($\lambda > 1250$ A) fluxes. NGC 246 is slightly fainter, but its spectral distribution is very similar to that of BD $+28°$ 4211. BD-11°162 is slightly fainter than NGC 246 but not as much as it appears in figure 2 where its flux profile has been decreased by 0.5 (in the log) for clarity reasons. Striking spectral differences lie in the profiles of the OVI resonance doublet, $\lambda\lambda$ 1032-1038 and the CIII λ977 resonance line. In figure 3 we report these profiles on a relative normalized intensity vs Doppler-velocity scale. The far left edge of the profile gives the terminal velocity of the stellar wind. While in BD $+28°$ 4211 the wind in these ions is not noticeable, it is strong in NGC 246 and moderate in BD-11°162 (note that the strength of a wind profile is related to the spectrum-absorption area on the part of negative velocities). In particular one notices that the wind in OVI reaches velocities as fast as -6000 km/s in both stars while the wind in CIII has terminal velocity of -6000 km/s (in NGC 246), consistently with OVI, and of "only" 4700 km/s in CIII. An explanation for this difference lies probably in the different ionization structure of the wind in the two stars: if, as predicted by radiation pressure wind models, the velocity law is increasing with distance to the asymptotic value of v_{term}, then the CIII density decreases with distance faster than the density of the OVI ions.

In figure 4 we compare on a relative normalized intensity vs. velocity scale the P Cygni profiles of CIII-977, CIII-1175 and CIV-1550 in NGC 246. The CIV profile lies in a UV spectral band where UVSTAR does not operate; to derive it we have co-added 9 high resolution IUE archival spectra of NGC 246. Our data agree with literature data by Feibelman (1995) and Koesterke, Dreizler and Rauch (1998): the terminal wind velocity of CIV is of the order of 3500 km/s, i.e. much less than the values measured from OVI and CIII with our UVSTAR spectra; in addition the wind in CIV is definitely "weaker" than the CIII and OVI. This is inconsistent with any single flow modeling of stellar winds and deserves a thorough analysis, which is in course, to explain the concomitant presence in the wind of comparably strong CIII and OVI and relatively weak CIV. Since the rates of mass loss from NGC 246 have been calculated from the CIV profiles to be of the order of 1.3×10^{-7} solar masses per year, this has to be revised too.

β Lyr

According to Hack and collaborators (1975, 1976, 1977) the β Lyr system is a very complex one consisting of a B8 primary star, an unknown companion, an envelope and a disk. Visual data (Wilson, 1974) indicate that, if, as it is likely, the primary star fills it Roche lobe, then the radius is between 11.7 – 15.7 solar radii. This would correspond to a luminosity class about II. The eclipsing body seems to be formed by a star and a disk; the secondary star has a radius R_2 < polar radius of the disk < 9.4 R_{sun}. The envelope is extended and multi-structured being the origin of emission and absorption components from a range of molecules, atoms, ions: H_2, H, neutral and ionized abundant elements. Similarly, the FUV spectrum is very difficult to understand being dominated by high ionization emission lines (OVI, SVI, NV, SIV, CIII, NIII, etc.) and by many absorption lines of molecular and atomic hydrogen. No signatures of the stellar spectra are evident. The spectrum seems rather insensitive to phase, as can be seen in figure 5. Here we compare two observations obtained during the STS 95 mission taken 3.75 days a part, i.e. at Δphase = 0.29. Similar

results were obtained by Hack and collaborators when studying Copernicus data taken over the whole system period. The variations with phase which they measured are not detectable at UVSTAR resolution.

The lower spectrum of figure 5 has been taken on November 4, 1998 at TU = 0h 38m; the upper spectrum has been observed on November 7, 1998 at TU = 18h 40m. The two tracings are shifted for reasons of clarity. The S/N ratio is quite good, probably of the order of 30 or higher. The reason why we don't have a firm evaluation of it is that there is still work to be done for characterizing science and calibration data of this last mission.

In figure 6 we present enlarged sections of the spectra and the identification of the major spectral features. In the upper left panel Ly_α and N V are displayed. Ly_α has not been properly corrected for geocoronal light. This fact makes the short wavelength wing of the NV profile somehow undefined. Other major emission lines, all resonance, are present in the nearby region: the Si II lines of multiplet 5, which is among the strongest multiplets of the ion, Si III - λ1206 and the S III lines of multiplet 1, which are dominating the blend with multiplet 5 of Si II. The top right panel covers the 1090 - 1190 Å region which is characterized by the following emission lines of high excitation: C III - λ1175, Si III - multiplets 32 (around 1140 Å) and 5 (around 1110 Å), Si IV - multiplet 3. In the two lower panels, below the system spectra, we have marked the position of the absorption features resulting from atomic and molecular hydrogen and from He II. The upward dips in the lowest part of the panels are H_2; those above indicate atomic hydrogen and the He II Balmer series (taller marks). The effect of H_2 is quite substantial. It affects, among other features, the strength of the 1073 Å line of the SIV resonance lines (multiplet 1) and, together with the C II - multiplets 1, 2, the strength of the λ1037 component of the O VI resonance doublet. It has to be noted that Hack and collaborators do not consider the presence of O VI likely due to the absence of the longward component of the doublet. The strongest multiplet of S III resonance is also present in this band. Note that the S III - λ1015 is made weaker by the H_2 Lyman absorption. Turning to the last panel which covers the region 910 – 1010 Å, we clearly identify the resonance lines of C III - λ977, P IV - λ951 and S VI - $\lambda\lambda$933-944. They are all somewhat unaffected by atomic or molecular hydrogen absorption; viceversa, the NIII resonance lines (multiplet 1) are. There is evidence of a possible presence of He II - λ942, - λ959; if this is true, then the line that we have ascribed to NII at λ1085 may be He II, at least partially. The possible presence of emission from the He II Balmer series was also discussed by Hack and co-workers. They excluded He II on the basis of its absence in the visual range. However, they didn't have the UV spectrum at wavelengths shorter than 1000 Å. Another important ion showing up in this band is P III in the multiplets 2 and 3. This last multiplet, in particular, might explain the emission flux at wavelength immediately above the Lyman limit.

Adhara (ε CMa)

Adhara is the brightest EUV source in the sky; its spectral type is B2 II (MK standard). The visual magnitude is m_V=1.5 and the distance is 132.1 pc (from Hypparcos data). Its stellar radius has been measured with an intensity interferometer as $3.878509 \, 10^{-9}$ rad. This corresponds to a radius of $(11.4 \pm 0.7) \, R_{sun}$. The star has moderate periodic spectrum and light variability due probably to radial and non radial pulsation. Other information is given in Table 5.

Table 5: **Basic parameters for Adhara**

T_{eff}	(20990 ± 750) °K
log g	3.20 ± 0.15 (cgs units)
N_H	$(0.7 - 1.2) \, 10^{18}$ cm^{-2}
V sin i	35 km/sec
dM/dt	$10^{-7} \, M_{sun}$/year

UVSTAR has observed Adhara both during the STS69 and STS95 missions. In this last mission, Adhara has been observed both in the EUV and in the FUV bands. The observations in the EUV bands are particularly difficult in reason of the strong extinction due to interstellar hydrogen absorption. Only EUVE has taken EUV spectra of Adhara in a band which is comparable with ours and at a similar spectral resolution. The EUV band is particularly interesting for several reasons: 1) it could help us in understanding the density and ionization structure of the local interstellar medium (i.e.

that region around the solar system which extends up to about 5 pc from the Sun) and of the solar plasmasphere, 2) it provides key information for testing advanced model atmosphere codes in reason of the different depth in the atmosphere from where the EUV radiation comes; 3) it provides new information on the stellar wind properties in reason of the larger variety of ionization degrees of abundant species. We here report only on preliminary analysis results.

Figure 7 displays an example of the observations. The top panel gives a 15 sec integration FUV spectrum (S/N approx 100). The lower three panels show 15 sec integration EUV spectra taken at different intensifier gains. This shows the difficulty in deriving high quality EUV data. Figure 8 shows a merged EUV and FUV spectrum and a comparison with classical model atmosphere. One notices the inadequacy in fitting the EUV spectrum, whilst the FUV spectrum fits quite well with a model built with the stellar parameters of Table 5. Finally, figure 9 shows the quite unexpected discovery of rapid flux variations in two FUV bands and their counter-phase characteristics. At this stage we do not have an explanation for it.

Conclusions

UVSTAR low cost and fast reaction time approach has been successful both from the point of view of science and of technology. In this second and third flights, UVSTAR has collected a large amount of interesting data: in this paper we have presented just a few. The spectral imaging characteristics allow for the first time to obtain UV spectra at moderate resolution of extended sources. Data of the Jupiter system (this symposium) and the Hale-Bopp comet (in press) are good examples.

The experiment also demonstrated the utility of the Shuttle as a remote sensing observational platform. Stars were tracked with a "up to" 2 arcsec accuracy, depending on the magnitude, off-set guiding was demonstrated as well as the autonomous pointing system.

REFERENCES

Acker, A. et al.: 1992, Strasbourg-ESO Catalogue of Galactic Planetary Nebulae (ESO)
Apparao, K.M.V. & Tarafdar, S.P.: 1989, Ap. J. 344, 826
Bowyer, S., et al.: 1996, Ap. J. Suppl., 102, 129
Broadfoot, A.L., Sandel, & Stalio, R.: 1993, Optical Eng. 32, 3009
Bucconi, A., Gregorio, A., Stalio, R., Zennaro, G.: 1999, The Ultraviolet Italian Sky Surveyor (UVISS) for the International Space Station (ISS), ASI/ARS SP-98-40
Cook, T.A., Cash, W, & Green, J.C.: Adv. Space Res. 11, 29
De Carlo, F., Stalio, R., Trampus, P., Broadfoot, A.L., Sandel, B.R., Sicuranza G.: 1994, Optical Eng. 33, 2781
Feibelman, W.A.: 1995, PASP, 107, 531
Feibelman, W.A.: 1999, PASP, 111, 221
Hack, M., et al.: 1975, Ap. J., 198, 453
Hack, M., et al.: 1976, Ap. J., 206, 777
Hack, M., et al.: 1977, Ap. J. Suppl. Series, 34, 565
Holberg, J.B. et al.: 1991, Ap. J. 375, 716
Holberg, J.B. 1997, private communication
Kosterke, L., Dreizler, S., Rauch, T.: 1998, A,A., 330, 1041
Kosterke, L., Werner, K.: 1998, Ap.J.., 500, L55
Kruk J.W. et al.: 1997, Ap. J. 482, 546
Smith, L.F. & Aller, 1969, Ap. J. 157, 1245
Trampus, P., Bucconi, A., Zennaro, G.: 1999, this symposium
Wilson, R. E.: 1974, Ap. J. 141, 155
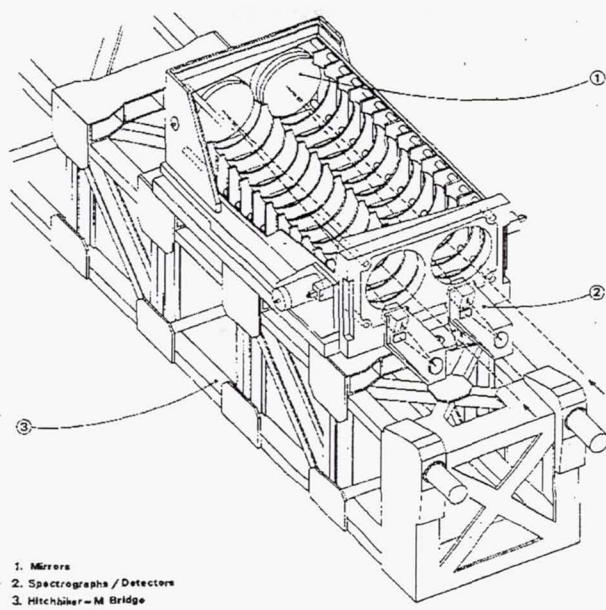
**Figure 1: Schematic drawing of USTAR on the Hitchhiker bridge**
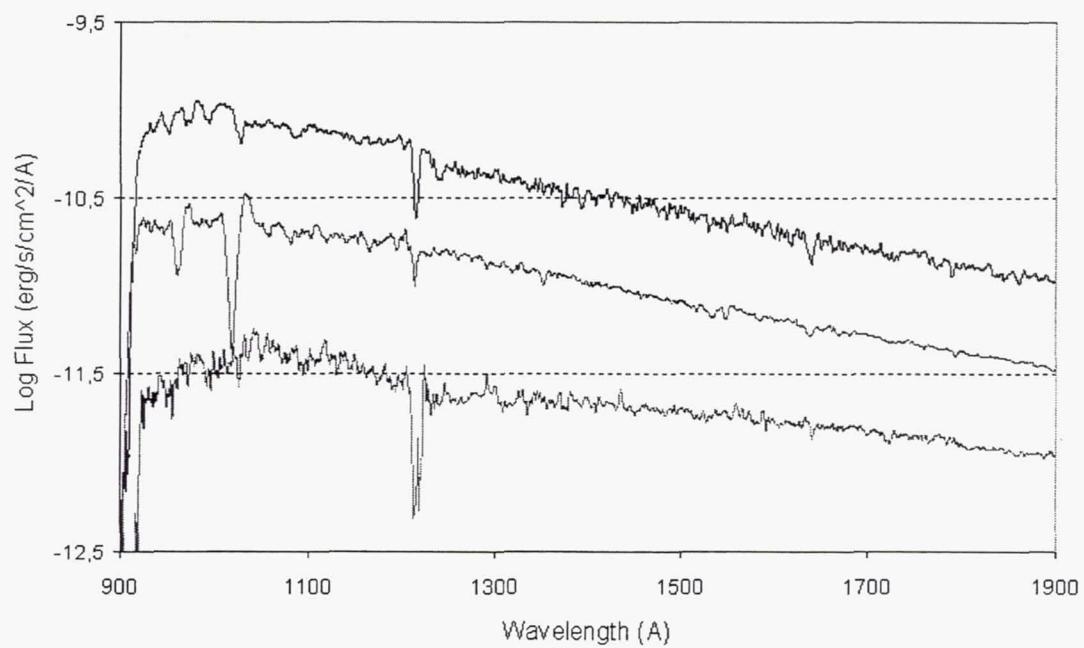
Figure 2 : BD +28° 4211 (top), NGC 246 (middle) and BD-11°162 (bottom) calibrated spectra (UVSTAR + IUE, see text)
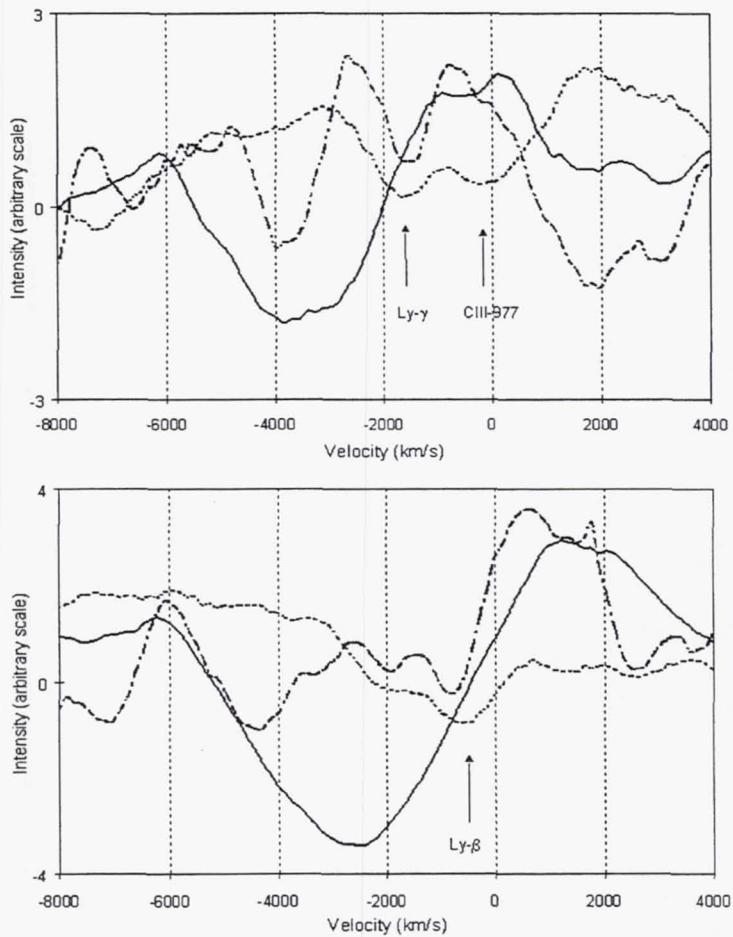
Figure 3 : Stellar wind profiles: BD +28° 4211 (dashed line), NGC 246 (full line) and BD-11°162 (long/small dashes). The top panel shows the CIII profiles. The arrows indicate the positions of the photospheric CIII and Ly-γ. The bottom panel shows OVI ; the arrows indicates Ly-β.
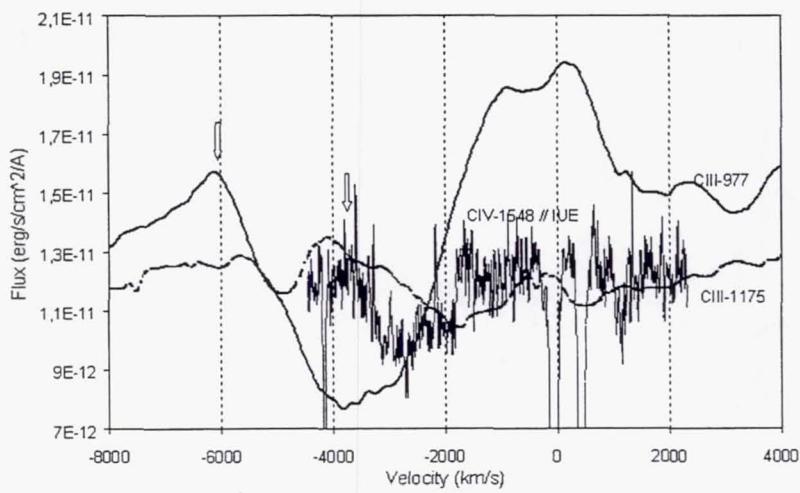

Figure 4 : NGC 246: CIII (UVSTAR) and CIV (IUE) wind profiles
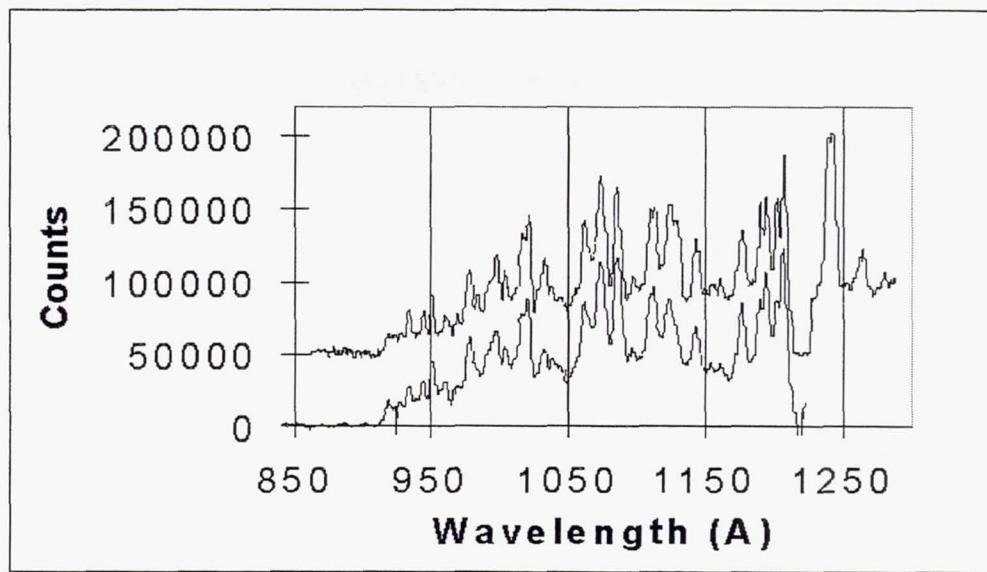
Figure 5 : Spectra of β Lyr taken on Nov. 4, 1978 at TU= 0h 38m (bottom) and on Nov. 7, 1998 at TU = 18h 40m (top).
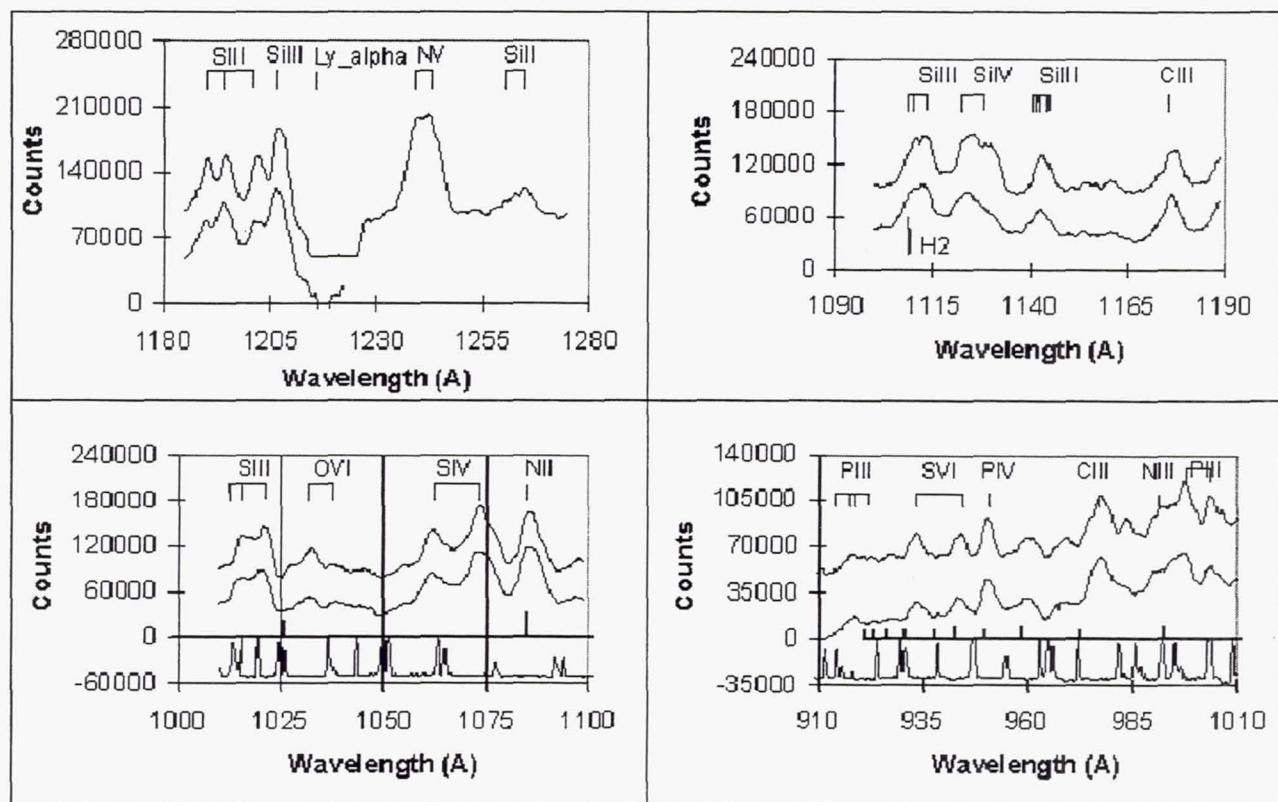
Figure 6 : Identification of the major spectral features. The very bottom spectrum, at negative counts, is the laboratory molecular hydrogen spectrum. Position of the H-Lyman lines are also indicated.
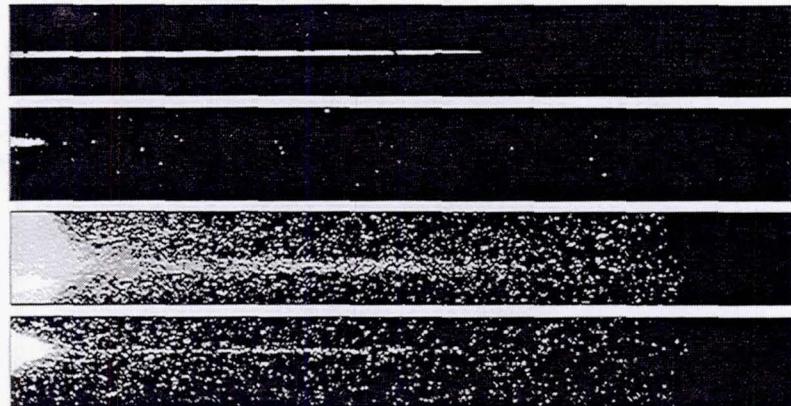
Figure 7 : Four observations of Adhara: FUV spectrum (top) and three different EUV spectra (see text).
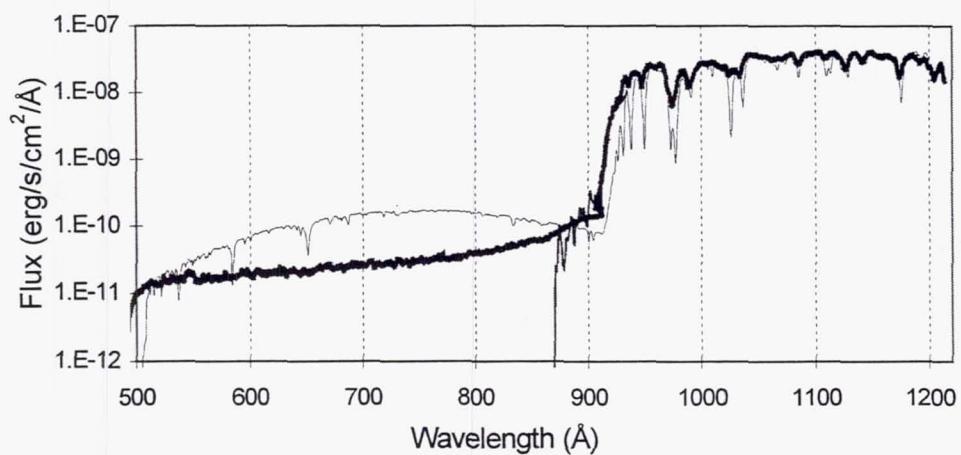

Figure 8 : Merged EUV and FUV spectra compared with classical model atmosphere.
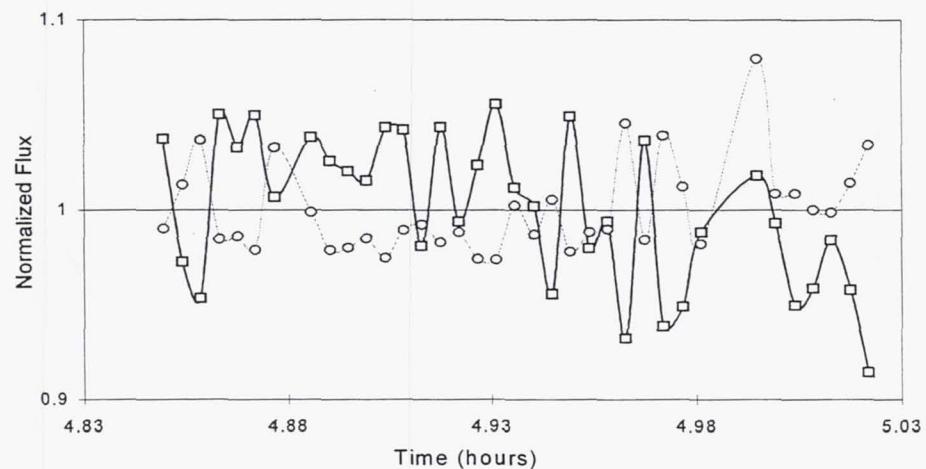

Figure 9 : Flux variations in two FUV bands (1048-1066 A, thick marks; 960-978A, thin marks).

213

THE STARSHINE HITCHHIKER MISSION ON STS-96

Gil Moore
Project Starshine

Ben Y. Lui
NASA Goddard Space Flight Center

ABSTRACT

A mirrored, spherical "Starshine" satellite was ejected by NASA into a circular low Earth orbit from a Hitchhiker canister in the cargo bay of Space Shuttle OV-103 Discovery at 07:21 Universal Time on June 5, 1999, near the end of Discovery's STS-96 mission to the International Space Station. Starshine's initial orbital altitude was 218 Nautical Miles (387 km), and its orbital inclination was 51.6 deg. The satellite is expected to orbit Earth until sometime in January 2000, when it will reenter the atmosphere and vaporize. Some 25,030 students in 700 schools around the world participated in the construction of this satellite by polishing 878 small, front-surface aluminum mirrors that stud its outer surface. A small fraction of those students is presently tracking the satellite and measuring its angular position at specific times.

The Naval Research Laboratory is combining the students' measurements with Naval Space Command radar tracking data to compute the satellite's orbit on a daily basis. From the rate of decay of the orbit, the students are able to calculate the density of the atmosphere at the satellite's present altitude. The students are also accessing the project's web site to observe ground-based and space-based images of the sun and other indices of solar activity. They are then using these data to make correlations between the intensity of solar storms and fluctuations in the density of the earth's upper atmosphere. The number of students participating in the tracking phase of the project is expected to increase dramatically at the start of the fall school term in the northern hemisphere. At the conclusion of the Starshine mission, the student team will attempt to predict when and where the satellite will re-enter the atmosphere, so they can compete for a cash prize for the best photograph of the satellite's fiery demise.

INTRODUCTION

Our sun experiences substantial changes in activity during an approximately eleven-year interval known as the sunspot cycle. It is now approaching the peak of activity in its present cycle. As the peak approaches, the sun exhibits several interesting phenomena, such as an increase in the numbers of sunspots in its photosphere (Figure 1) and in the occurrence of plages, flares, prominences, and coronal mass ejections in which enormous quantities of ionized particles randomly erupt from its surface. Earth's upper atmosphere, ionosphere and magnetosphere respond to these outbursts of solar activity in various ways, including magnetic substorms, auroral displays (Figure 2) and fluctuations in atmospheric density. During the next year or so, aurora will be observed at latitudes unusually far south in the northern hemisphere and unusually far north in the southern hemisphere. In addition, it is possible that power blackouts will occasionally occur in northern locations, such as Canada, as they did in 1988 during the previous sunspot peak. Furthermore, unprotected commercial communication satellites may experience temporary or even permanent damage to their electrical circuits and processors following very large coronal mass ejections.

Project Starshine was initiated in 1997 by a volunteer consortium of individuals and institutions involved in educational outreach (Table 1), for the purpose of bringing this cyclical behavior of the sun and its effect on the earth's atmosphere to the attention of pre-college students and their parents around the world. In order to give them a sense of participation in an experiment designed to measure some of these solar-terrestrial effects, large numbers of students were recruited in 1998 to polish small aluminum mirrors (Figure 3), that were then mounted on the surface of a spherical satellite (Figure 4). This satellite was installed in a Hitchhiker canister in the cargo bay of Space Shuttle OV-103 Discovery (Figure 5). Discovery was launched on the STS-96 mission to the International Space Station on May 27, 1999, and its crew deployed Starshine into its own orbit on June 5, 1999 (Figures 6 and 7). This particular mission was chosen for the satellite deployment, because its orbital inclination to the equator was 51.6 degrees, and its orbital altitude at deployment was 218 nautical miles (387 kilometers). In this orbit, the satellite passes over almost all the

populated regions of the globe (Figure 8) and is visible at civil twilight to all the students who polished its mirrors. The deploy altitude and the area-to-mass ratio of the satellite were chosen to insure that the satellite's orbit will be steadily reduced by atmospheric drag and will result in the satellite's fiery destruction by aerodynamic heating in approximately eight months. By observing the change in the satellite's orbital altitude (Figure 9), the students are able to measure the drag on the satellite and thus the atmosphere's density at the present altitude of the satellite.

EARLY RESULTS

Many sunlight flashes from Starshine's mirrors have been observed and reported by a mixture of students, teachers and skilled amateur satellite observers all over the world. The brightness of these flashes is slightly greater than predicted, ranging from +5 to –2 in equivalent stellar magnitude, depending on the distance of the satellite from the observer and the phase of the mirror at the time of the flash. However, the frequency of the flashes is much lower than expected. The mirror pattern on Starshine was laid out with the expectation that its Hitchhiker deployment system would impart to it sufficient tip-off and spin torques to make it rotate about its principal axes at a combined rate of approximately five degrees per second, or one revolution per minute. The designers chose this approach, since similar motions had been experienced by the three previous satellites deployed by the Hitchhiker ejection system.

This rotation rate, combined with the pattern in which its 878 mirrors were installed on its surface, was expected to produce a reflected sunlight flash to an observer on the ground every two to five seconds. However, the Hitchhiker project office made several improvements to the Hitchhiker system following the deployment of MightySat I during the STS-88 mission in December of 1998. Those improvements apparently eliminated essentially all tip-off torques, with the result that Starshine experienced no observable motion about any of its principal axes following deploy, as can be seen in the deployment videos taken by the STS-96 crew. Consequently, the only motion now producing mirror flashes is the satellite's orbital translation across the sky. During the first few months of the mission, flashes are being seen by observers around the world at rates varying from once per five seconds to once or twice per pass, to no flashes at all, depending on how the rows of mirrors line up with the sun-satellite-observer plane during a given pass. Therefore, it is very difficult for observers to make precise measurements of the satellite's position.

It is anticipated that the flash rate will increase when the satellite descends into denser air later in the mission and begins to experience continuum-flow aerodynamic torques. The satellite is slightly asymmetric, due to the presence of the deployment foot at its base. It is therefore statically stable, but dynamically unstable, and should wobble in the manner of a badminton shuttlecock late in the mission and thereby produce the desired increase in flash rate. In the meantime, project officials have suggested to the observer team that they should concentrate on making and reporting observations of flash rates and help determine when it will be possible to return to the standard tracking procedures. In addition, they have suggested that the students practice tracking Mir and ISS, which are in orbits very similar to Starshine, so as to become adept at tracking by the time Starshine's flash rate improves. Near the end of the mission, an attempt will be made to increase the numbers of student observations greatly, since drag effects will ramp up sharply, and atmospheric density measurements will be at their most meaningful. A cash prize is being offered for the best photo of the flaming fireball that will occur at re-entry, as a means of focusing interest on this portion of the mission. Although the students have been advised that is extremely unlikely the satellite will come down over land on a non-cloudy day or night, many of them have exhibited great interest in making the attempt to obtain the prize-winning photograph.

FUTURE PLANS

The interest expressed by students and teachers around the world in participating in this first mission would seem to justify a continuation of the Starshine project. The mirror-polishing phase has been very popular, since it is relatively easy to accomplish, and it produces a tangible piece of shiny space hardware. The tracking and reporting phase of the project has been more difficult to get underway, since it is intellectually more challenging and more esoteric in nature for the target audience. Additionally, the fact that the Shuttle launch and satellite deploy took place after many schools in the northern hemisphere had closed for the

summer has delayed the start of most of the tracking effort till the beginning of the 1999 fall term. The degree of success of the tracking and atmospheric density determination phase will become apparent only near the end of the project, after the mirror flash rate has increased, and after a larger number of students has been recruited and trained to track the satellite at the start of the fall school term.

In anticipation of the successful conclusion of this first experiment, a request for flight assignment to a Space Shuttle mission in 2000 has been submitted to NASA. The external structure for a second satellite has been fabricated, and a self-contained, spin-inducing mechanism is being designed to insure proper spin at the start of the next mission. A full complement of mirror blanks has been machined for a second satellite, and mirror-grinding and polishing kits are being assembled. A deluge of applications to polish mirrors for this next satellite is expected to arrive at the start of the fall school term in the northern hemisphere, well in excess of the number of mirrors that can be flown. Selection criteria are being developed to insure fairness in assigning mirrors to the most deserving schools for Starshine #2.

Further details about the fabrication, launch, and tracking phases of the project may be found at http://www.azinet.com/starshine.
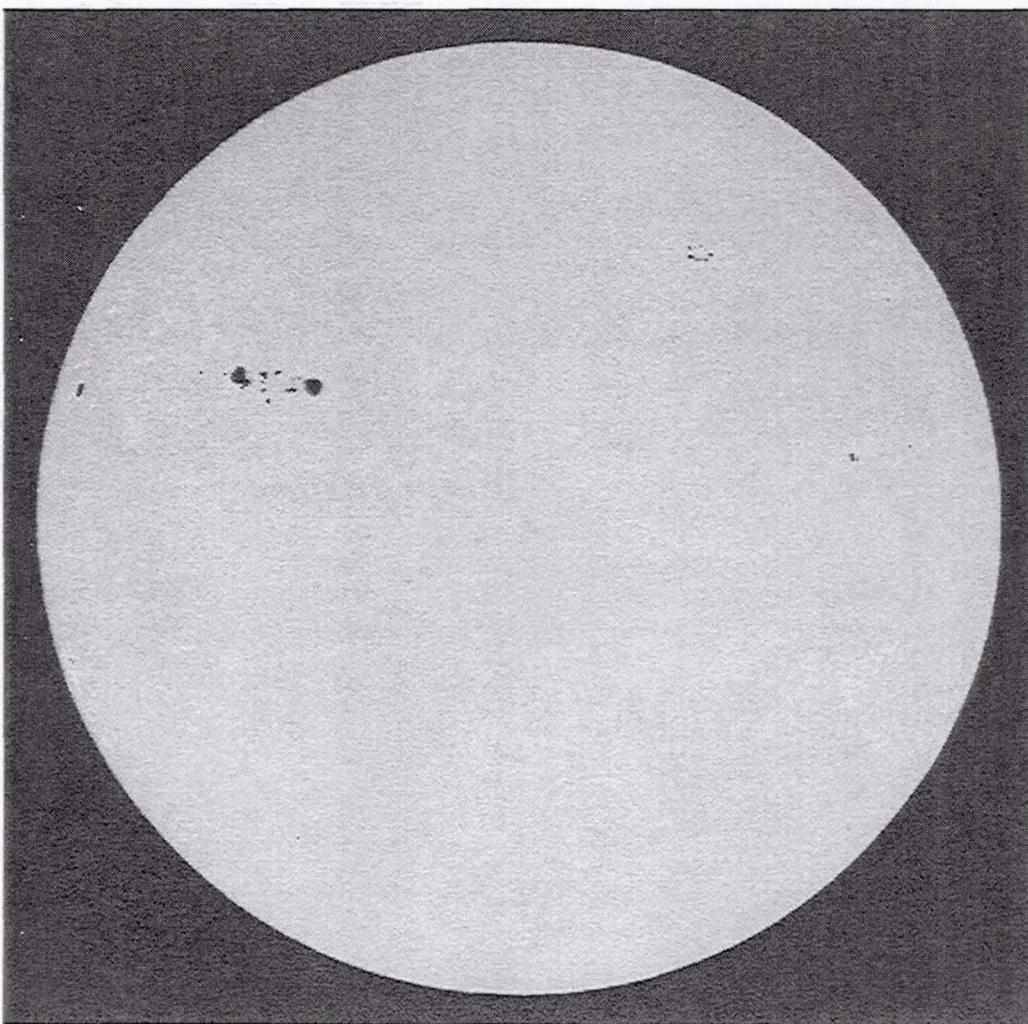

Figure 1
Sunspots
SOHO Image

221

Figure 2
Aurora Borealis
Jan Curtis Image
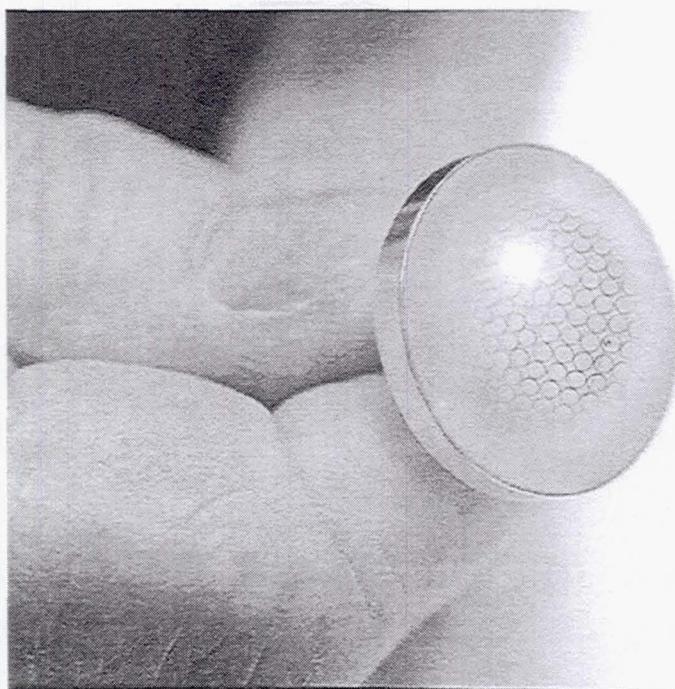

Figure 3
Student Mirror
USAFA Image
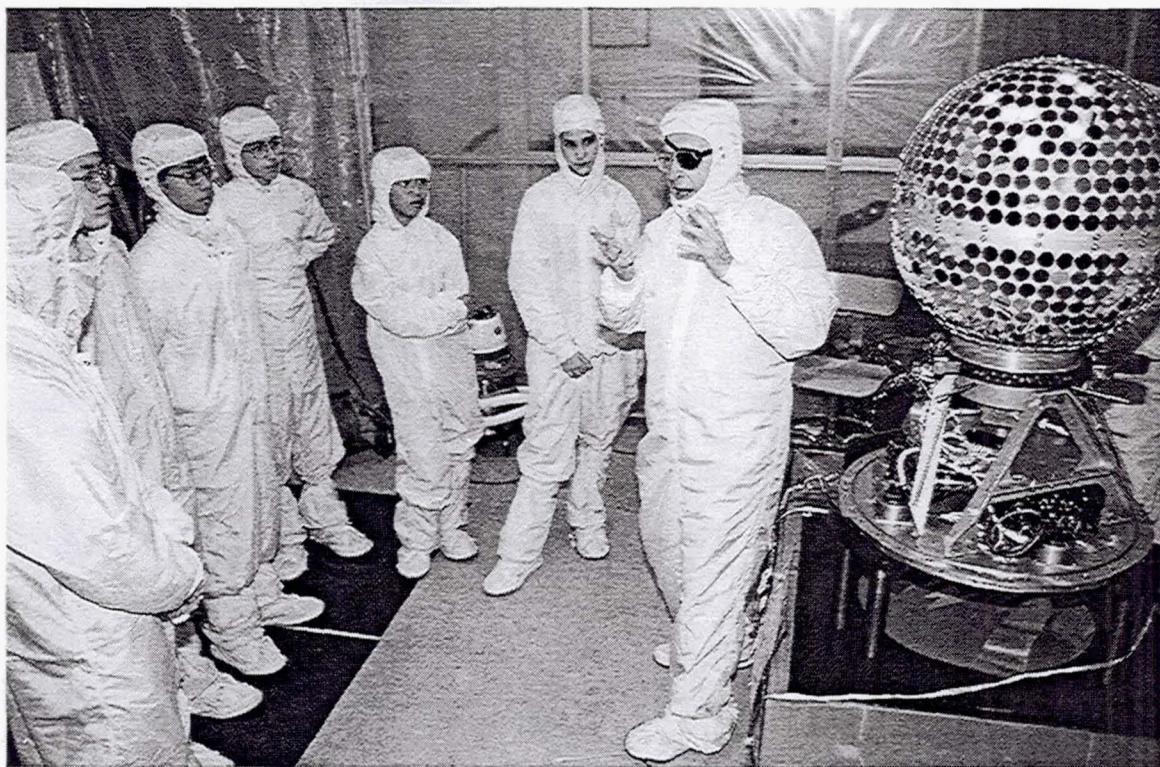
Figure 4
Starshine Satellite
NASA Image
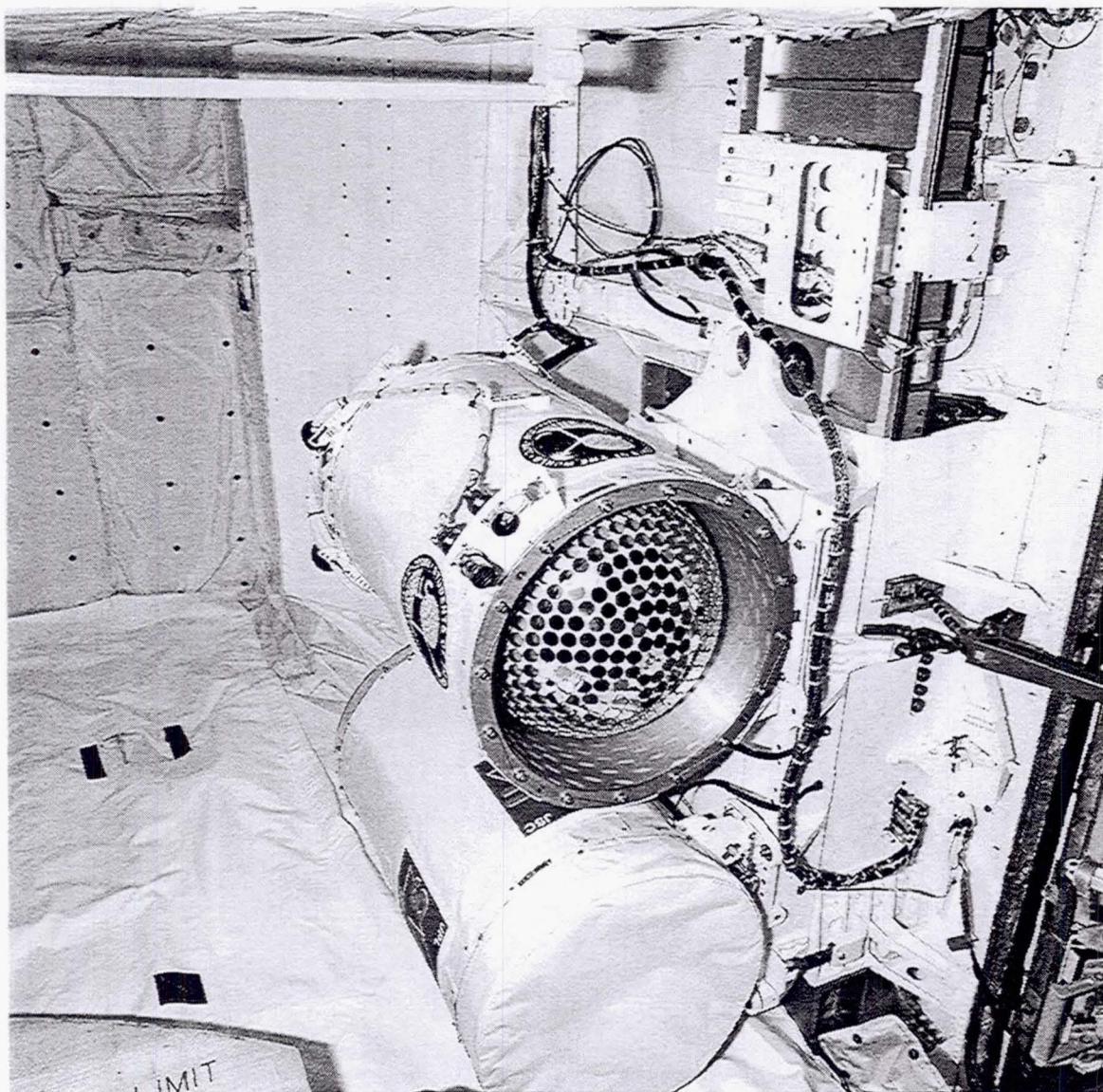
Figure 5
Hitchhiker Canister
NASA Image
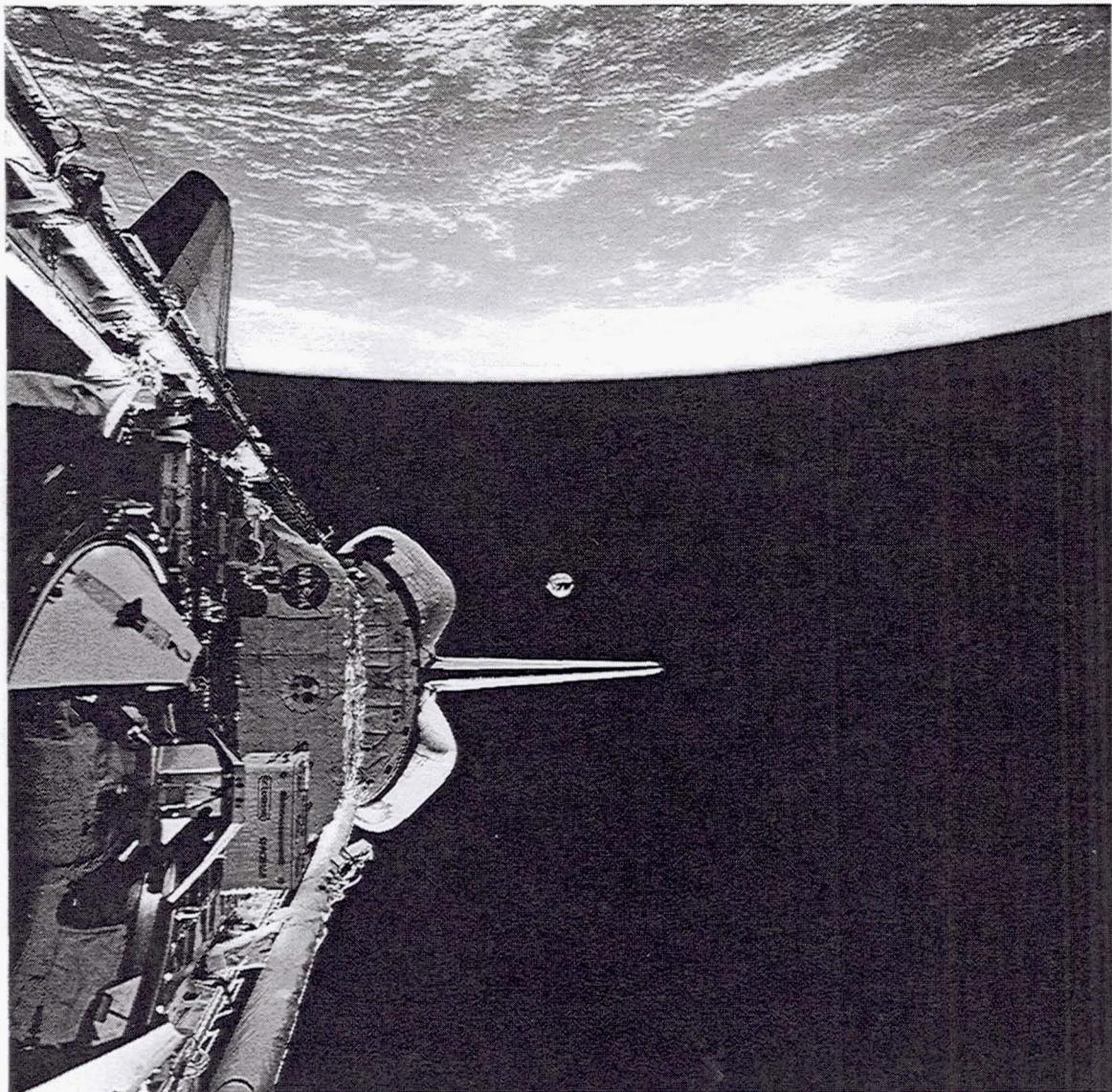
**Figure 6**
Starshine Deploy / NASA Image

Figure 7
Mirror Flash / NASA Image
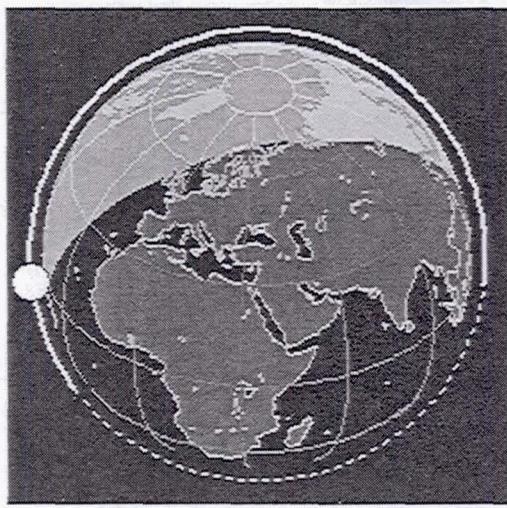
View from above orbital plane
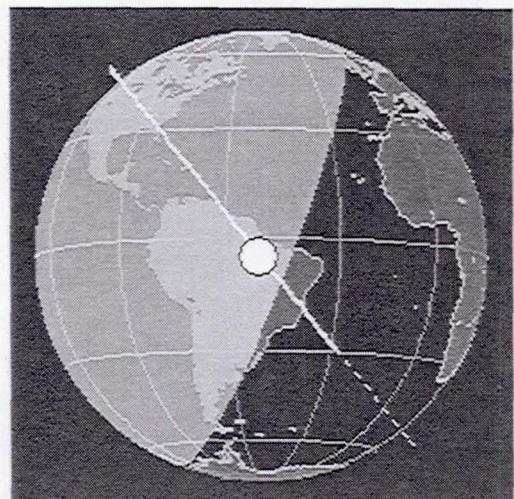
View from above satellite
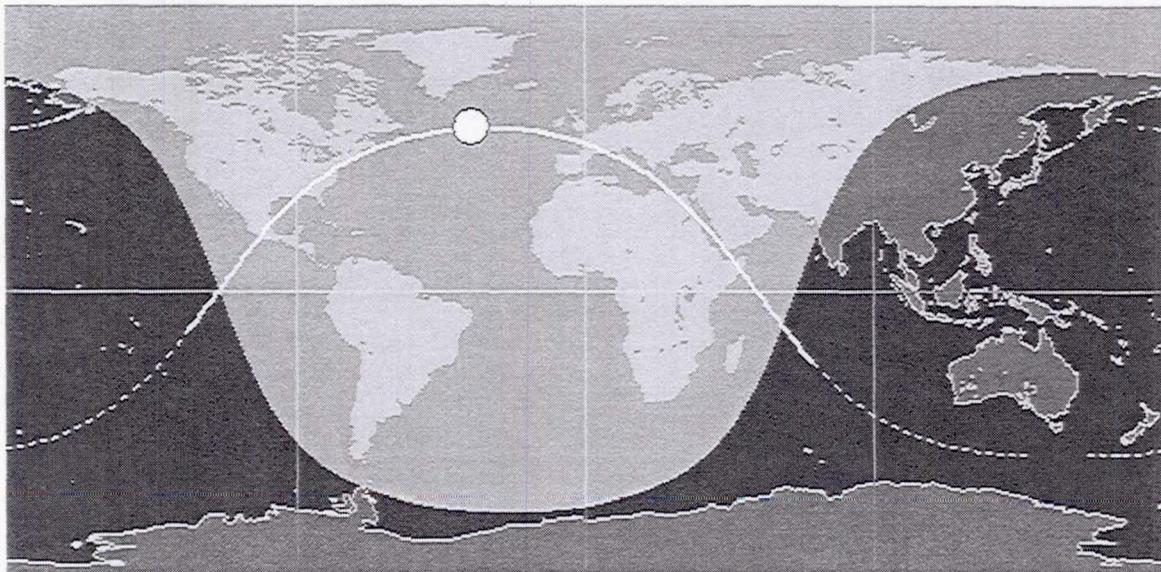

Ground Track

Figure 8
Starshine Orbit
GSOC Web Site
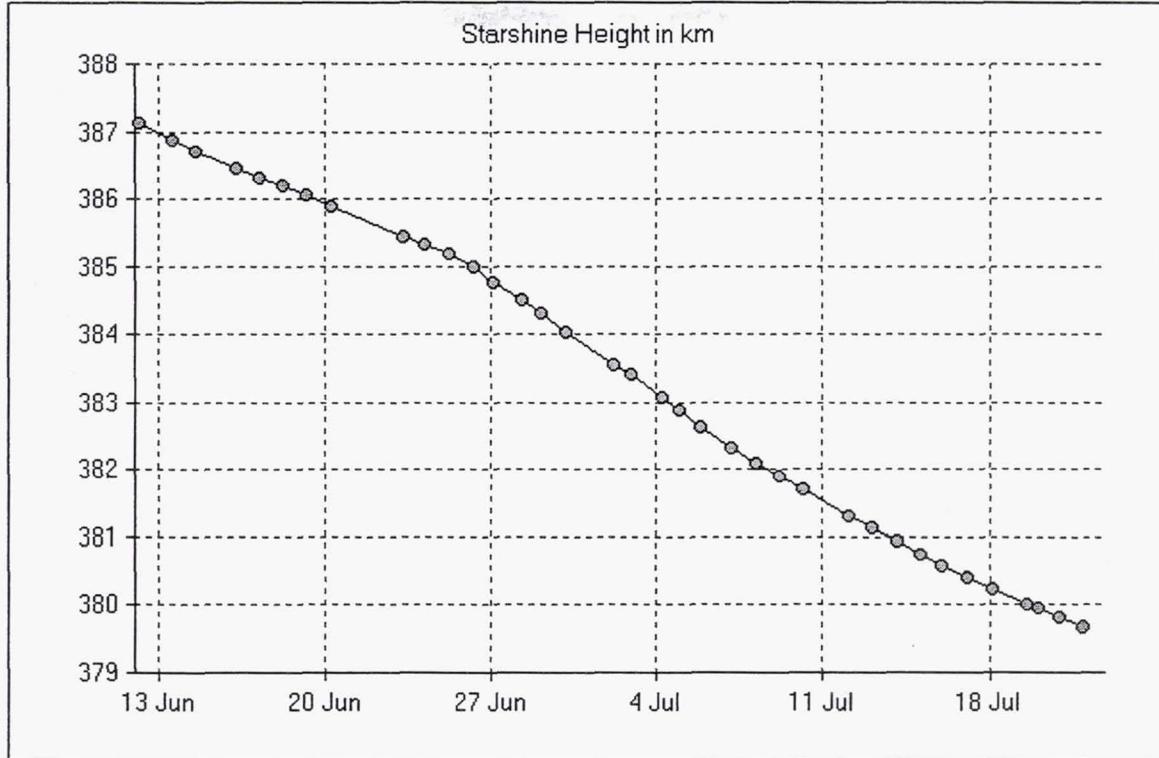
Figure 9
Starshine Orbit Decay
GSOC Web Site

Table 1
Participating Institutions

Institution	Responsibility
NASA Headquarters	Provision of Shuttle launch at no charge to project, coordination of launch attendance by students, parents, teachers, addition of Starshine web page to Spacekids web site
NASA Goddard Space Flight Center	Mission management, Hitchhiker system modification and testing, satellite integration, cargo bay installation, L minus 2 week press briefing, coordination of launch attendance by students, parents and teachers
NASA Kennedy Space Center	Satellite installation and checkout, Shuttle launch, provision of facilities and tours for students, parents and teachers, pre-launch press briefing
NASA Johnson Space Center	Cargo integration, astronaut deploy training, Shuttle launch and on-orbit operations, satellite deploy, post-deploy press briefing
Naval Research Laboratory/Naval Center for Space Technology	Satellite structural design, fabrication, testing, mirror mounting, orbit determination
Naval Space Command	Satellite tracking
Air Force Space Command	Software development for orbit determination
Starshine Headquarters	Project direction, mirror polishing kit assembly and shipping, data base management, signature sheet scanning
Rocky Mountain NASA Space Grant Consortium	Project coordination, web site development, data base management, mirror-coating liaison, monetary support
Utah State University	Mirror design
Bridgerland Applied Technology Center	Machining of mirror blanks
White Sands Missile Range	Development of mirror polishing methodology
Students & Teachers in 700 Schools in 18 Countries	Mirror polishing, satellite visual tracking
Packager, Inc.	Manufacture of shipping boxes for polishing kits
Lightpath Technologies	Manufacture of optical inspection flats
Hill Air Force Base	Inspection and coating of polished mirrors
U.S. Air Force Academy	Mirror flatness measurement, photographic support

German Space Operations Centre	Web site development, orbit determination, generation of sighting opportunities and orbit decay analysis
Azinet Internet Business Solutions	Web site development and operation
Gates Planetarium	Teacher education
Hansen Planetarium	Teacher education
U.S. Space Foundation	Teacher education
Starfire Optical Range	Teacher education, satellite optical tracking
U.S. Space and Rocket Center	Teacher education, monetary support
Albuquerque Chapter of Optical Society of America	Teacher education, monetary support
Aerospace States Association	Monetary support
Clark Foundation	Monetary support
Young Oak Foundation	Monetary support
Utah Section of American Institute of Aeronautics and Astronautics	Monetary support

Page intentionally left blank

THE PETITE AMATEUR NAVY SATELLITE (PANSAT) HITCHHIKER EJECTABLE

Daniel Sakoda
Aerospace Engineer, Naval Postgraduate School

ABSTRACT

The Petite Amateur Navy Satellite (PANSAT) was successfully launched aboard the STS-95 *Discovery* Shuttle as part of the third International Extreme Ultraviolet Hitchhiker (IEH-3), and placed into a circular, low-Earth orbit with 555 km (300 nmi.) altitude and 28.5° inclination. The culmination of approximately 50 graduate student theses, PANSAT provides the amateur radio community with digital, store-and-forward, direct sequence, spread spectrum communications, as well as providing officer students at NPS a space-based instructional laboratory. The spacecraft hardware was built and tested almost entirely at NPS to the component level. Rigorous analysis and testing was performed to ensure compatibility with Shuttle payload requirements. This paper describes the spacecraft design as relates to both compliance with Shuttle safety requirements and ensuring overall mission success. Specifically, PANSAT design requirements for structures, radio frequency emissions, and batteries will be discussed along with some lessons learned in the verification process.

INTRODUCTION

The Petite Amateur Navy Satellite (PANSAT) is the Naval Postgraduate School's (NPS) first satellite in space. The main objective is to provide a hands-on, educational tool for the officer students at NPS in the Space Systems Engineering and Space Systems Operations curricula. The satellite, itself, provides a global, digital messaging system in the amateur radio ultra-high frequency (UHF) band utilizing direct sequence spread spectrum techniques. More than 50 Master's theses have been published related to the PANSAT project. These theses were primarily focused on the spacecraft, largely to the benefit of the Space Systems Engineering officer students. Following the deployment of PANSAT from the STS-95 Discovery Orbiter, the project has shifted more in the direction of Space Systems Operations.

PANSAT was designed as a secondary payload, or payload of opportunity. Because an initial design could not start without system-level requirements, the Shuttle was chosen to derive the baseline launch carrier requirements. This allowed preliminary designs to proceed using the Hitchhiker requirements and capabilities for such things as payload envelope, structural load requirements, thermal environment, orbitology, and factors of safety, as well as requirements derived from safety issues. It was presumed that if PANSAT could be certified to fly aboard a man-rated system, the design would be sufficient for expendable launch vehicles as well. The decision to use the Shuttle requirements as a baseline turned out to be a self-fulfilling prophecy, albeit a beneficial one.

The decision to use the Shuttle as the launch carrier had an additional effect of focusing on system safety. Generally speaking, safety concerns are dealt with at the cost of system reliability or functionality. In the case of PANSAT, early decisions were made to remove any propulsion, and to use only passive attitude control, if any. As the configuration matured, PANSAT became a tumbling satellite with neither attitude control nor propulsion. Except for the mechanical inhibit microswitches, the spacecraft consists of no moving parts; only solid state electronics and the structure. The satellite configuration is depicted in Figure 1. Note that some solar panels are removed to show the spacecraft interior.
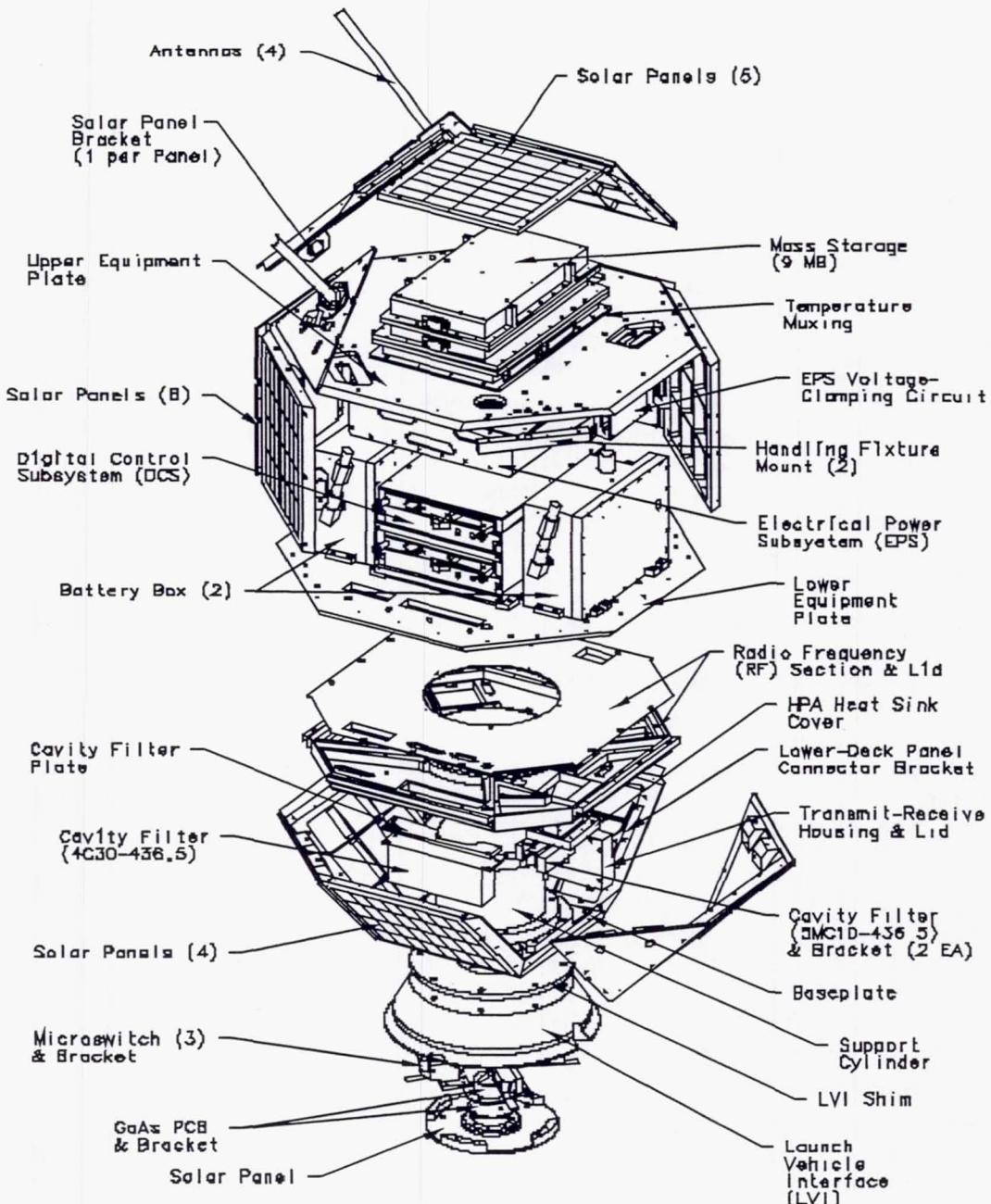
Figure 1. PANSAT Configuration.

DESIGN REQUIREMENTS

Overall mission requirements for PANSAT are to provide store-and-forward digital communications using direct sequence, spread spectrum techniques in the amateur radio, ultra-high frequency (UHF) band, centered at 436.5 MHz both for the up-link and down-link. FCC rules for amateur radio spread spectrum (Ref. 1, §97.311) resulted in a 9800 bps data rate, given a 7-bit shift register (with taps at 7 and 1) for generation of the pseudo-noise (PN) code for spreading, one PN code sequence per bit, and approximately three megahertz of allowable bandwidth. A two-year mission life was determined sufficient for system evaluation and to allow involvement with the amateur radio community as users develop spread spectrum capable ground stations.

Orbital requirements were constrained such that communications could be performed from a ground station located at the Naval Postgraduate School in Monterey, California and that the altitude would provide the minimum

orbital life while allowing sufficient margin in the communications link budget. A nominal Shuttle altitude was deemed sufficient provided that the launch would occur at or near the minimum of the 11-year solar cycle (Ref. 2, p. 47). As a secondary payload, however, orbital options are limited. Thankfully, though, the STS-95 mission altitude was extremely high which results in a much higher orbital life than originally expected from a Shuttle launch. Current estimates provide an orbital life greater than ten years which will far exceed the operational life of the satellite.

PANSAT requirements derived from the Shuttle Hitchhiker (HH) carrier are outlined in the *Hitchhiker Customer Accommodations and Requirements Specification* (CARS) document. Table 1 shows the design limit loads required of the primary structure for a Shuttle HH payload. Table 2 shows the design limit loads for tertiary equipment (Ref. 3, p. 3-6). The factors of safety are 2.0 times the limit load for yield and 2.6 times the limit load for ultimate. These factors of safety were selected for structural verification by analysis alone.

Table 1. Shuttle Design Limit Loads.

Payload/Instrument structure					
Load Factor, (g)			Angular Acceleration (rad/sec^2)		
NX	NY	NZ	R_X	R_Y	R_Z
± 11.0	± 11.0	± 11.0	± 85	± 85	± 85

Table 2. Shuttle HH Tertiary Assembly/Component Design Load Factors.

Tertiary Assembly/Component	
Weight, (lbs)	Load Factor, (g)
<20	40
20 – 50	31
50 – 100	22

Payload Envelope

The payload envelope for a Hitchhiker ejectable is shown in Figure 2, with PANSAT and the Pallet Ejection System (PES). The PES is similar in function and interface to its predecessor, the Hitchhiker Ejection System (HES) but requires less vertical space. PANSAT attaches to the PES via a Marmon clamp with pyrotechnic bolt cutters. When the bolt cutters release the Marmon clamp, a spring, compressed inside the PES, extends and pushes the satellite at a rate of 1.13 meters per second (3.7 feet per second). The maximum weight for the satellite is 68 kg (150 lbs). The weight of PANSAT was 57 kg (125.5 lbs).
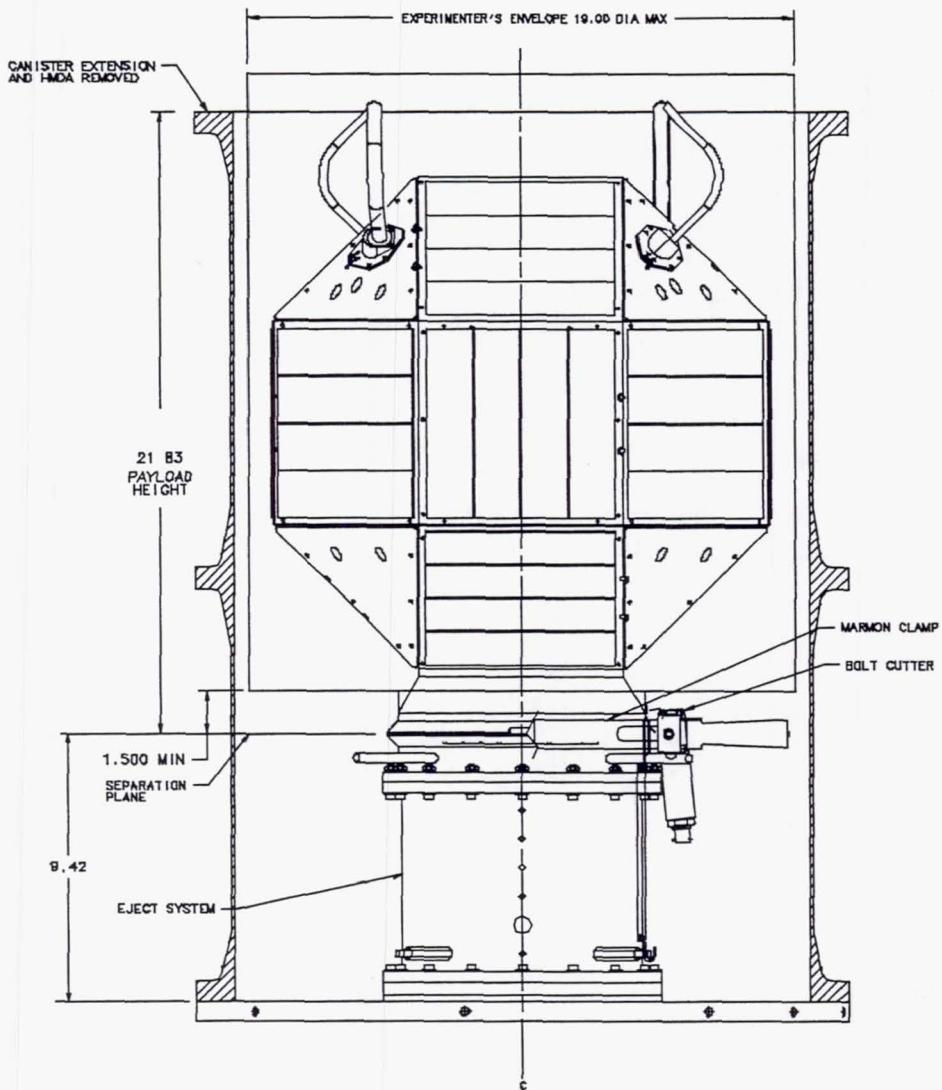
Figure 2. PANSAT in Hitchhiker Canister.

Testing Requirements

Testing can be divided into two categories. The first category deals with reliability and workmanship and the second with verification of compliance with Shuttle safety requirements. Some testing overlapped both types such as in the case of system-level random vibration testing, a structural verification requirement but also a survivability test for PANSAT electronics. Because the development environment for PANSAT was in the academic arena, emphasis was placed on thorough testing at the subsystem level. As was anticipated, the hardware delivery precluded the ability to perform some of the desired system-level testing, such as thermal cycling and thermal balance. It can generally be said that functional testing of the integrated payload will demand as much time as the schedule and cost will allow in order to test any and all identified operational states and scenarios.

PANSAT subsystem environmental testing included random vibration and thermal cycling. A detailed discussion of PANSAT subsystem environmental testing is given by Overstreet (Ref. 4). All the electronics, with the exception of the communications modem and radio frequency (RF) section were tested to at least the acceptance level. The modem and RF section were late in hardware development and was subsequently needed to support software development. Although certainly a gamble, like practices in the fabrication of these modules were duly followed to ensure good workmanship; and no anomalies were evident in functionality following system-level random vibration testing.

Shuttle safety verification testing for PANSAT included component testing to verify the cracking pressure of pressure relief valves and random vibration of individual battery cells. Testing for verification of a 15-second timer inhibit in the RF section and an open-circuit state for the microswitches was performed during integration at NASA/GSFC. Testing at the system level was performed at NASA/GSFC as well for random vibration, fundamental frequency measurement, and center-of-gravity (CG) location determination.

Launch Vehicle Interface

PANSAT mated to the PES via the launch vehicle interface (LVI). The LVI was milled from a single billet of 6061-T6 aluminum and was shown by analysis to be very robust (Ref. 5). Available user space below the actual PES-to-LVI interface plane was used to accommodate a small gallium-arsenide (GaAs) solar panel. No electrical interfaces are provided by the PES to the spacecraft. The pusher plate, however, was used as a mechanical interface to contact three active microswitches and one dummy switch which, along with the LVI, remained with the spacecraft. These microswitches were used as inhibit switches to cut off power to the spacecraft electronics, thus ensuring that PANSAT was non-operable while attached to the Shuttle. Special care was taken in the fabrication of the microswitch brackets and their installation with the LVI in order to avoid any over-travel damage. Figure 3 shows the bottom view of the LVI with its solar panel and microswitches attached. For each lever arm of the microswitches a shallow pocket was recessed in the LVI to accommodate them in the open-circuit position forced by the PES pusher plate.
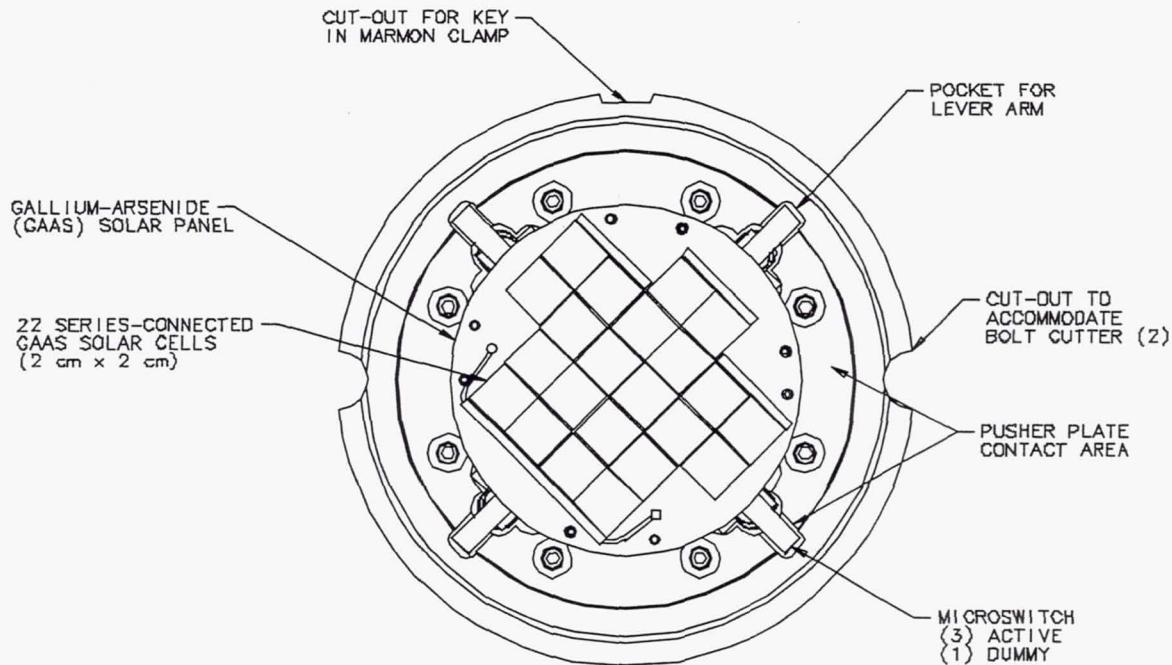

Figure 3. Bottom View of LVI with GaAs Panel.

Launch Environment

The launch environment for PANSAT included the vibroacoustic and acceleration loads acting on the structure as well as the thermal environment. Consideration was also given to the thermal environment prior to launch where the Shuttle was on the launch pad. Verification of the structure design to withstand the vibrations induced by launch was performed through random vibration testing. Analysis using the worst-case, combined limit loads of Table 1 and appropriate factors of safety showed positive margins of safety for the structural components as well as for all load-bearing fasteners. Thermal concerns were solved largely in the design phase through appropriate component selection to accommodate a large temperature range. Thorough testing on each subsystem provided assurances that PANSAT electronics would survive both the vibroacoustic loads as well as the extreme temperatures. As stated earlier, PANSAT was also designed not to operate while attached to the Orbiter.

Requirements on structural verification are discussed later. Another issue related to the launch environment which may be of concern to experimenters but, eventually had no effect on the PANSAT payload, is venting of the

payload as it reaches the vacuum of space. The Shuttle payload bay reaches a maximum decay rate of 5240 Pa/sec (0.76 psi/sec), (Ref. 6, p. 10B-1) during its ascent. This is of particular concern where thermal blankets are used which may be released, inadvertently, into the cargo bay.

On-Orbit Requirements and Issues

On-orbit concerns include issues related to the pre-deployment, deployment, and post-deployment phases of the mission. Prior to deployment, PANSAT is inhibited by the three microswitches. A concern of maintaining the nickel-cadmium batteries within manufacturer's suggested storage temperatures required the use of strip heaters located on the interior of the Hitchhiker canister which provided radiative heating to the PANSAT satellite. The use of heaters, in addition to Shuttle attitude maneuvers, allowed the batteries to be kept within appropriate temperature limits. This was determined analytically using the PANSAT thermal model, generated at NPS, integrated into the NASA/GSFC IEH–3 thermal model. The analysis also suggested that although the batteries would be within storage temperature limits, they would be too cold for operation. Therefore, a sun soak was requested prior to deployment to allow for the satellite and batteries to warm to approximately 23°C. Because of a concern of conserving Shuttle energy, the timeline set PANSAT ejection within 24 hours after launch to allow turning off the canister heaters for the remainder of the STS-95 mission.

The PES deployment of PANSAT introduced an initial rotation of approximately one revolution per minute about its axis of symmetry, probably due to uncoiling of the spring from the compressed state to a relaxed state, as evidenced from NASA video and downloaded telemetry data of the solar panel currents. Although PANSAT was designed as a tumbling satellite, future experimenters may find this fact noteworthy. PANSAT deployment released the microswitches and allowed the spacecraft to operate. Nominally, the spacecraft would receive power from the solar cells and the processor would boot from read-only memory (ROM) to perform hardware initialization, battery charging, and intermittent listening for NPS ground station commands. A 15-second timer in the radio frequency section inhibited PANSAT from transmitting until it reached a safe distance from the Shuttle. PANSAT software precluded any spacecraft transmissions unless commanded by the ground.

SAFETY REQUIREMENTS

Hitchhiker payload safety requirements are outlined in the *Hitchhiker Customer Accommodations & Requirements Specification* (Ref. 3). Experimenters should also have the following necessary documents, as a minimum.

- *Safety Policy and Requirements for Payloads Using the Space Transportation System* (Ref. 7)

- *Space Shuttle Program Payload Verification Requirements* (Ref. 8)

- *Implementation Procedure for NSTS Payloads System Safety Requirements for Payloads Using the Space Transportation System* (Ref. 9)

- *Interpretations of NSTS Payload Safety Requirements* (Ref. 10)

- *Design Criteria for Controlling Stress Corrosion Cracking* (Ref. 11)

- *Fracture Control Requirements for Payloads Using the Space Shuttle* (Ref. 12)

- *Manned Space Vehicle Battery Safety Handbook* (Ref. 13)

- *Shuttle Orbiter/Cargo Standard Interfaces* (Ref. 14)

- "Fastener Integrity Requirements," (Ref. 15)

Shuttle safety requirements compliance begins at the design phase. Experimenters should be aware of all safety issues apparent in the design at both the board level as well as the system level. Because the Shuttle was selected as the baseline launch vehicle for PANSAT, initial design decisions were predicated on safety concerns. As stated earlier, both the propulsion and attitude dynamics and control subsystems were purged. The incorporation of the three microswitches ensured that the spacecraft would not operate while attached to the Shuttle. On the operational side, the batteries were fully discharged prior to integration with the Shuttle. This removed a number of potential safety concerns, although, it is understood that few Hitchhiker experiments can afford this mode of operation. At the component level, the selection process needs to consider materials usage to remove the risk of contamination

due to outgassing. Additionally, failure scenarios should consider materials reactivity, such as electrolyte leakage from batteries on metal casings and electronics. Experiment design should reasonably address all likely failure scenarios which could impact safety. Following is a discussion of PANSAT-specific safety designs for the batteries, microswitch and timer inhibits, and the structure.

Nickel-Cadmium Batteries

The PANSAT batteries were designed with full adherence to (Ref. 13). Nickel-cadmium (NiCd) battery cells were used in the two PANSAT batteries. The battery cells are the Sanyo Cadnica, D-size cell, model no. KR-4400D. These cells were chosen for a number of safety-related reasons. Although, these cells are not hermetically-sealed, space-qualified battery cells, they are fabricated such that they are electrolyte-starved (with only two drops of electrolyte), and the Sanyo Cadnica cells do have a flight history. The Sanyo Cadnica N-4000DRL, which is the fast-charge version of the same NiCd cell, has flown on four Space Test Experiment Platform (STEP) spacecraft and both the REX-1 and REX-2 spacecraft. The N-4000DRL has the same mechanical construction as the KR-4400D cell. The KR-4400D cell is targeted for use in the Space Station Assembly sequence for the "pistol-grip tool."

A sealed aluminum container is used for the housing of the batteries in order to space-qualify the commercial, off-the-shelf (COTS) NiCd cells. The battery housing is made of aluminum 6061-T6 and is designed with the factor-of-safety of 2.5 times the maximum design pressure (MDP), per the letter JSC TA-94-057 (Ref. 10). The housing is fitted with a sub-micron filter in line with a pressure relief valve set at 32 psig cracking pressure, thus providing a MDP of 32 psi. Each pressure relief valve was tested to verify the advertised cracking pressure. Prior to installation of the battery with the PANSAT structure, the battery housing was purged with dry nitrogen at ambient pressure.

Although the nickel-cadmium battery cells are sealed containers, themselves, they are fully contained within the battery housing. The housing major dimensions yield a volume of 0.05 cubic feet, less the thickness of the housing material, and volume of the battery cells, wiring and other features within the housing. Interior voids of the housing were filled with glass wool in order to further reduce the volume for gas to accumulate, as well as to help contain any electrolyte leakage. The interior of the aluminum battery housings were insulated with a thin Teflon film, and thermal cut-outs were implemented to take the batteries off-line above 55°C. As stated earlier, the batteries were also fully discharged as a final step at NASA/GSFC integration to further ensure that the PANSAT payload was inert while in the Hitchhiker canister. Figure 4 shows the interior of an assembled battery.
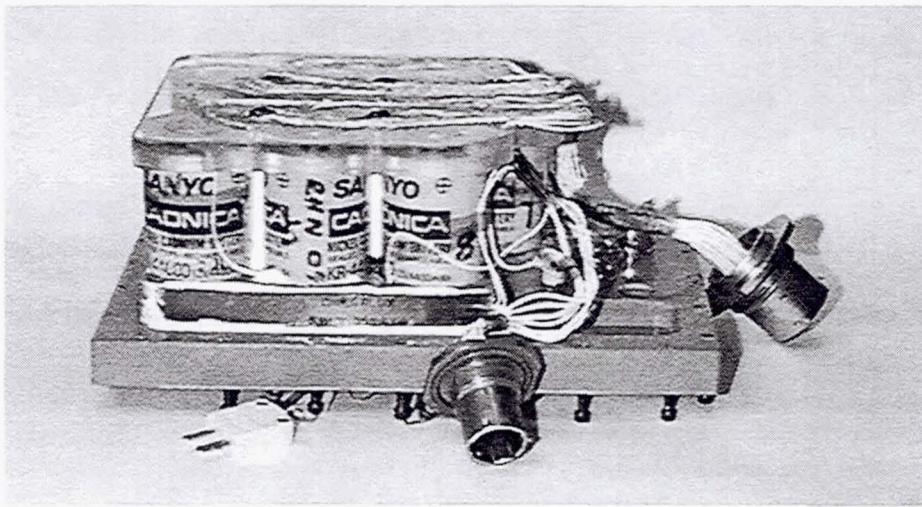

Figure 4. PANSAT Nickel-Cadmium Battery.

Microswitches and Timers

The PANSAT electrical power subsystem (EPS) provides electrical power distribution for all the spacecraft electronics. The EPS is not activated until after ejection from the PES. This is ensured through the use of three microswitches attached to the spacecraft's launch vehicle interface (LVI). Two microswitches are connected in series

237

on the power leg of the solar panel power bus, and one microswitch is connected in-line on the ground leg of the solar panel power bus. The Honeywell microswitches (model no. 1HS41) are normally-closed, hermetically sealed mechanical switch contacts which are held in the open state by the physical mating of the spacecraft LVI to the PES. While the microswitches provide three independent inhibits, they also constitute three single-points-of-failure should any one of them fail in the open position.

Microswitch status verification was performed following mating of the PANSAT with the PES. A simple resistance measurement was taken through lead wires which traveled from a spacecraft test port on the upper section of the satellite down to the LVI and microswitches at the spacecraft's base. The very high resistances provided in the test showed that the microswitches were indeed in the open position.

Release of the three microswitches also meant the loss of three independent safety inhibits. A 15-second timer circuit in the PANSAT design ensured that no radio frequency (RF) emissions occurred until PANSAT was a safe distance away from the Shuttle. Worst-case assessment of this phase included the following assumptions: a broken spring in the ejection mechanism resulting in a reduced separation velocity of 1.0 m/sec (3.3 ft/sec), a processor/software failure which would configure the RF electronics to transmit at maximum power, and the assumption that all electrical power available would be converted into RF energy, noting that the batteries are already fully discharged and could not provide any energy for RF emissions. The 15-second RF timer provided the required second, independent safety inhibit for the seven seconds between separation from the PES and the safe distance traveled by PANSAT of 3.44 m (11.3 ft).

Structural Verification

Structural verification for the PANSAT payload was outlined by the "Structural Integrity Verification Plan, (SIVP)" a document which describes the design philosophy for the payload structure and the means by which the structure is verified. The SIVP enumerates the other reports and documents which support the verification process through detailed analysis or testing. Specifically, the document describes verification of the structure by analysis alone, identification and classification of structural components for fracture control, fastener analysis, and descriptions of tests to be performed. Additionally, the SIVP describes structural verification of any ground handling equipment which is required for payload handling or testing.

Structural Strength

Payload structural strength was verified by analysis alone using factors-of-safety of 2.0 for yield and 2.6 for ultimate times the design limit loads of Table 1. The load-bearing structure was modeled and analyzed using the Structural Dynamics Research Corporation (SDRC) I-DEAS® finite element modeling and analysis (FEA) tools. The FEA model was validated through modal test on a prototype structure by comparing and matching the fundamental mode from the test data with that of the FEA results. Correlation of the fundamental frequency between analysis and test was within 6% (Ref. 16).

Figure 5 shows the load-bearing structure. Table 3 shows a summary of the element types used. Lumped mass elements were used to simulate the various electronics, housings, and other non-structural parts. The FEA model and results were also used in the fracture analysis for classification of parts for fracture control.

Table 3. Summary of Elements.

| Element Type	Quantity
thin shell parabolic quadrilateral	24
thin shell parabolic triangle	616
parabolic beam	312
lumped mass	112
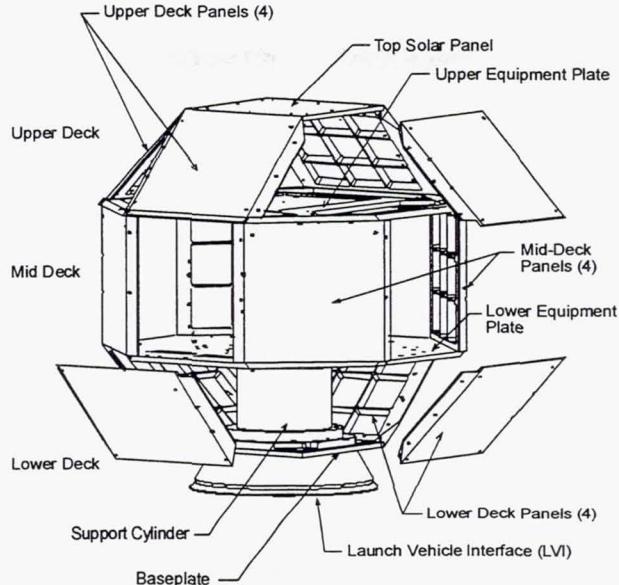
Figure 5. Load-Bearing Structure.

Fracture Control

The primary method in the fracture classification of parts was to perform stress analyses using finite element methods. Because of the robustness of the PANSAT structure, the stresses resulting from static loads analysis was sufficiently low to show low-risk fracture classification. Additionally, the finite element analysis (FEA) model was used to show that structural redundancy is present as relates to the lower deck panel where the highest stresses occur in worst-case, combined loading. Structural redundancy was shown by simply removing the elements of the model which comprised the part and running the analysis using the same loading and boundary conditions.

Low-risk classification of PANSAT structural components was done by showing the following three conditions applied: low stresses in the parts, (<30% of ultimate tensile strength, F_{tu}); all parts were manufactured from materials from Table 1 of (Ref. 11); and that maximum cyclical stresses were less than or equal to $F_{tu}/6$, with worst case selection for the ratio of minimum to maximum stress in a fatigue cycle, R = -1.

$$S_{max} \leq \frac{F_{tu}}{4(1-0.5R)} \qquad (1) \qquad (\text{Ref. 12, p. 12}).$$

It should be noted that for eq. (1) and other stress calculations for fracture analysis, a factor of safety (F.S.) of 1.0 was used. Because the FEA results were all in the linear regime, stresses could be scaled proportionally from the stress analysis F.S. Figure 6 shows the process flow for the PANSAT fracture analysis. Other considerations, as shown in the figure, are given to the battery housings which are sealed containers, as well as non-load-bearing components which are actually exempt from fracture control.

Fracture Control Analysis

Load-Bearing Structure

Static Loads FEA Model

Lower-Deck Panel Identified as High Stress Component

Show Lower-Deck Panel Structurally Redundant

Fail Safe Part

Show Rest of Load-Bearing Structure is Low-Risk

Satisfies Stress < 30% of Ultimate Tensile Strength

Parts Are MSFC-SPEC-522B, Table I, Compliant Material (6061-T6)

Parts Are Machined (not cast or welded)

Show Smax <= Ftu/6 (Using conservative loads & worst-case, R=-1)

Non-Load Bearing Parts

Sealed Containers Compliant w/ Sect. NASA-STD-5003, 3.39

Material is Aluminum 6061-T6

Pressure is 1 Atm.

Exempt from Fracture Control

Show Low-Risk Suitability

Figure 6. PANSAT Fracture Analysis Flow Diagram.

Fasteners

A detailed fastener analysis was performed using a F.S. of 2.0 for yield times the design limit loads of Table 1 for load-bearing fasteners. Angular acceleration loads were applied as a resultant force acting on the fastener derived from the 85 rad/sec^2 of Table 1, multiplied by the maximum moment arm (from the launch vehicle interface to the top of the spacecraft) multiplied by the weight of the component(s) being held by the fastener, and multiplied by the factor of safety of 2.0. It is clear that using the simplification of force derived from the angular acceleration, the results were very conservative.

Tertiary limit loads, from Table 2, were applied to fasteners used for mounting purposes, such as those used to mount a cover panel to the structure, or a housing to the equipment plate. Again, a factor of safety of 2.0 was applied to the limit loads and combined stresses were calculated for linear and angular accelerations in both axial and shear directions. For tertiary limit loads, the full load was applied in the worst case direction, namely shear, and 30% of the load was applied in the other two directions per (Ref. 3, p. 3-6). All fasteners used in PANSAT were in compliance with Table 1 of (Ref. 11) for materials selection. Some tensile testing was also required per (Ref. 15) for bolt sizes of #10 and larger which was performed at NPS. During integration safety wire was used on all fasteners with exposed heads which would contain the released mass in the event that any might break off.

Environmental Testing

Environmental testing for PANSAT as a Shuttle payload included only random vibration testing. Random vibration was performed on the spacecraft as part of the structural integrity verification process. Electromagnetic compatibility (EMC) testing is generally required for all Hitchhiker experiments, however, since PANSAT was non-operable while in the canister and integration of PANSAT with the PES followed EMC testing of the IEH-3 bridge, EMC testing was not performed on PANSAT. Other required testing for PANSAT was done to determine the location of the center-of-gravity (CG) and to determine the fundamental frequency. The CG requirement for a Hitchhiker ejectable is

an envelope of ±1.27 cm (±0.5 in) from the canister centerline and 26.03 cm (10.25 in) from the separation plane. The PANSAT computer-aided design (CAD) model yielded an error of only 0.18 cm (0.07 in) from the canister centerline for the 56.9 kg (125.5 lbs) satellite. The fundamental frequency of the structure was found through a sine sweep test performed in conjunction with the random vibration testing and shown to be higher than the minimum required 50 Hz.

Random vibration testing was done to protoflight levels. The acceleration spectral density (ASD) was determined from Table 3.6 of (Ref. 3, p. 3-13), which derated for PANSAT's weight, resulted in a 8.2 g_{rms} acceleration. Prior to, and following each random vibration test a sine sweep was performed. This was done to measure the fundamental frequency as well as a means of seeing whether a failure occurred which would change the dynamic response of the structure. Testing was performed in each axis followed by a functional test of the payload electronics.

The PANSAT payload underwent final functional testing and was partially disassembled in order to discharge the batteries. At this point, it was discovered that a screw had broken. Following many discussions, it was generally agreed that the failure was due to workmanship and that the payload would be fully disassembled and re-assembled utilizing a staking compound for each screw and verifying installation torque values. Random vibration testing was again performed. This second set of random vibration tests was performed at the workmanship level which after derating for the spacecraft weight resulted in 4.7 g_{rms} acceleration (Ref. 16, p. 2-18).

LESSONS LEARNED

The PANSAT project offered many lessons learned, especially for the many officer students who worked on the satellite development. Many early decisions proved to be wise for such a complex project in an academic environment. Specifically, removing safety hazardous from the design, such as the attitude dynamics and control subsystem and propulsion subsystem, simplified not only the safety process, but the development process as well with little sacrifice in capability. Placing an emphasis on rigorous testing, both in environmental effects as well as functionality, on subsystem development provided added confidence in the robustness of the design as a whole.

Another design philosophy which was embraced was to design for test. Ease of functional testing was a design objective from the subsystem level to the system level. This allowed reuse of software test modules and a highly effective ground support system used during integration. The ground support equipment (GSE) for functional testing used during integration of PANSAT at NASA/GSFC consisted of little more than a power supply, two laptops, and a brief-case-sized RF modem. A detailed description of the GSE and development tools is given by Horning (Ref. 18) in this same proceedings.

A few anomalies did occur, however, which were mainly due to the tight schedule just prior to hardware delivery and the minimal staff labor available for the tasks at hand. This was evident in the workmanship issue concerning the failed screw during vibration testing. A second issue was a dimensional error regarding the antenna placement in the Hitchhiker canister which resulted in PANSAT breaking the user envelope of the Hitchhiker and having the antennas touch the interior of the canister. As a result the antennas were bent to avoid their contact with the interior of the canister. Later analysis showed that the bending of the antennas probably exaggerated the original antenna pattern, forcing the lowest nulls in the radiation pattern to be deeper while making peaks in the pattern higher.

CONCLUSIONS

The successful launch, deployment, and operation of the PANSAT small satellite marked the climax of a decade of work by officer students, faculty, and staff at the Naval Postgraduate School. Although some obstacles were presented in the development, an autonomous, digital communications satellite in full compliance with NASA Shuttle safety requirements was completed and is operating in low-Earth orbit. The satellite in many ways validates the educational process in Space Systems Engineering and Space Systems Operations at NPS and further serves in educating officer students while in orbit.

REFERENCES

1. *Code of Federal Regulations, Part 80 to End,* U. S. Government Printing Office, October 1997.

2. *Lifetime and Reentry Prediction for the Petite Amateur Navy Satellite (PANSAT),* Daniel J. Cuff, Master's Thesis, Naval Postgraduate School, Monterey, CA, Sept. 1994.

3.   *Hitchhiker Customer Accommodations & Requirements Specification,* NASA/GSFC HHG-730-1503-07, 1994.

4.   *Environmental Testing of the Petite Amateur Navy Satellite (PANSAT),* Paul J. Overstreet, Master's Thesis, Naval Postgraduate School, Monterey, California, December 1997.

5.   *Design and Analysis of the Launch Vehicle Adapter Fitting for the Petite Amateur Navy Satellite (PANSAT),* Brian B. Gannon, Master's Thesis, Naval Postgraduate School, Monterey, California, September 1994.

6.   *Shuttle Orbiter/Cargo Standard Interfaces,* ICD-2-19001, Rev. K, Change Pkg. No. 62, NASA/JSC, June 30, 1993.

7.   *Safety Policy and Requirements for Payloads Using the Space Transportation System,* NSTS 1700.7B, NASA/JSC, January 1989.

8.   *Payload Verification Requirements, Space Shuttle Program,* NSTS 14046C, NASA/JSC, April 1994.

9.   *Implementation Procedure for NSTS Payloads System Safety Requirements for Payloads Using the Space Transportation System,* NSTS 13830B, NASA/JSC, November 1989.

10.   *Interpretations of NSTS Payload Safety Requirements,* NSTS 18798, Rev. A, NASA/JSC, April 1989.

11.   *Design Criteria for Controlling Stress Corrosion Cracking,* MSFC-SPEC-522B, NASA/MSFC, July 1, 1987.

12.   *Fracture Control Requirements for Payloads Using the Space Shuttle,* NASA-STD-5003, October 7, 1996.

13.   *Manned Space Vehicle Battery Safety Handbook,* JSC-20793, NASA/JSC, September 1985.

14.   *Shuttle Orbiter/Cargo Standard Interfaces,* ICD-2-19001, rev. K., June 30, 1993.

15.   "Fastener Integrity Requirements," Rev. A, S-313-100, NASA/GSFC, April 10, 1993.

16.   *Structural Design, Analysis, and Modal Testing of the Petite Amateur Navy Satellite (PANSAT),* Daniel J. Sakoda, Master's Thesis, Naval Postgraduate School, Monterey, California, September 1992.

17.   *General Environmental Verification Specification for STS & ELV Payloads, Subsystems, and Components,* GEVS-SE, NASA/GSFC, January 1990.

18.   Horning, James A., "PANSAT Functional Testing Software and Support Hardware," NASA Shuttle Small Payloads Project Office Symposium, Annapolis, MD., NASA CP–1999–209476.
        (Paper 31 of this compilation.)

MIGHTYSAT I: IN SPACE

Capt Barbara Braun, USAF Research Laboratory
Robert Davis, The Aerospace Corporation
Thomas Itchkawich, Orbital Sciences Corporation
Todd Goforth, Maxwell Laboratories

ABSTRACT

MightySat is a United States Air Force (USAF) Research Laboratory multi-mission, small satellite program dedicated to providing frequent, inexpensive, on-orbit demonstrations of high-payoff space system technologies. MightySat platforms provide the on-orbit "lab bench" for responsively testing emerging technologies to ensure their readiness for operational Air Force missions. MightySat I, the 140lb pathfinder satellite of the MightySat series, was ejected from the Space Shuttle Endeavor on the 15th of December, 1998. Contact with the satellite was established one hour after ejection, and MightySat I has been performing robustly on-orbit ever since. This paper provides an overview of the MightySat I satellite and its experiments: a lightweight composite structure, high-efficiency solar panels, low-power microelectronics, low-shock release devices, and micro-particle impact detectors. The design, integration, and test process is described, as is the process of Space Shuttle integration and final testing. The paper then discusses the on-orbit operations, coordinated from the Space and Missile Systems Center's Test and Evaluation directorate (SMC/TE) at Kirtland AFB, NM, and conducted using two UHF ground stations in Virginia and New Mexico. The launch, initial contact, and early-orbit checkout sequence of events is described. The paper describes payload initialization and on-orbit data collection, and highlights some of the payload data currently being collected. A brief discussion of the upcoming MightySat II satellites and missions is also included.

MIGHTYSAT PROGRAM

The introduction of advanced, often enabling, space system technologies into USAF operational satellites has traditionally been a challenging problem. The term "operational systems" refers to the critical surveillance, communications, navigation, and other missions performed by the fleet of satellites in the US Department of Defense space architecture. These systems are generally complex and expensive, often requiring a decade to develop and hundreds of millions of dollars to build and launch. Accepting the risk associated with introducing advanced technology components into programs of this magnitude is very difficult for USAF program directors. Even when such technologies are key to the success of the mission, the introduction of unproven technology into new operational space programs or block-changes to existing systems has traditionally been a source of significant program cost growth and development delays. More importantly, on-orbit failure or unexpected degradation of advanced technology components in critical defense systems is simply not acceptable for the successful execution of the Air Force's space mission.

The primary objective of the MightySat program is to reduce the risk of transitioning advanced space system technologies from the laboratory to operational USAF space applications by providing on-orbit demonstration of emerging technologies. The US Air Force Research Laboratory (AFRL) Space Vehicles Directorate, based in Albuquerque, New Mexico, is the USAF center for space systems research and development, with the charter to explore, develop and transition enabling technologies to the operational users. The Space Vehicles Directorate has advanced technology development programs underway in nearly all elements of space systems. These programs are in various stages of maturity, from fundamental scientific research to conceptual design to actual hardware fabrication and testing. Promising technologies that emerge from this process are candidates for demonstration on a MightySat mission. Data from the MightySat missions will then be used to support decisions on the readiness of the specific technology for application in USAF missions. The difficult technology insertion decision can then be made with increased confidence and with considerably reduced risk.

In order to effectively make emerging technologies available to operational systems, the technologies must be demonstrated in a timely manner. Thus MightySat seeks to shorten the timeline for technology demonstration to something on the order of 2-3 years from payload conception to launch. Demonstrating emerging technologies is also risky, and fiscal constraints dictate that MightySat technology demonstration missions be significantly less expensive than historical military experimental satellite programs. The total cost goal of each MightySat mission, including contracted spacecraft development, government program execution expenses, payload integration, system testing, launch, and mission operations is $10M. For MightySat I, a simple pathfinder mission for the long-term MightySat program, the total mission cost (including all of the above) will be near $7M.

Although technology demonstration and transition is the primary mission objective for the MightySat program, the Air Force also realizes several collateral benefits from this effort. An intangible but very important benefit of the MightySat effort is the invaluable experience gained by lab personnel who support the many aspects of the MightySat program. MightySat is a microcosm of the larger, more complex space programs in which many of the Research Laboratory's Air Force officers will eventually hold positions of significant responsibility. MightySat offers real-world lessons in systems engineering, payload integration, environmental test, launch operations, and on-orbit satellite command & control.

The MightySat I program is managed by AFRL's Space Vehicles Directorate in Albuquerque, NM. The contractor for the MightySat I spacecraft bus (a refurbishment of the existing "XSAT" bus, intitiated under a NASA contract in 1988-90) is Orbital Sciences Corporation (OSC) in McLean, VA (formerly CTA Space Systems). MightySat II is a series of up to five small satellite missions occurring over the next decade, with the spacecraft bus being developed by Spectrum Astro, Inc. of Gilbert, AZ. The USAF Space & Missile Systems Center's Test and Evaluation Directorate, also based in Albuquerque, leads mission operations and launch coordination. Since the Space Shuttle is the primary launch vehicle for the MightySat program, NASA is also a key member of the MightySat team.

The MightySat effort has two distinct groups of customers for whom the advanced demonstrations are conducted: technology users and technology developers. The ultimate customers for the MightySat program are the developers and users of USAF operational space systems at the USAF Space & Missile Systems Center (Los Angeles, CA), US Space Command and Air Force Space Command (Colorado Springs, CO). These organizations make the decisions about insertion of advanced space systems technologies into operational applications. The second, more immediate customers for the MightySat program are the technology developers within AFRL who propose experiments or technology demonstrations.

Table 1: MightySat I Key Parameters

| Total Space Vehicle Weight	140 lbs
Payload Weight	37 lbs
Power Generation	0 - 32W
Orbit Average Power	14-27W
Spacecraft Orbit Avg Power Usage	12W
Uplink Rate/Downlink Rate	2400/9600 bps
Attitude Knowledge	+/- 5 deg
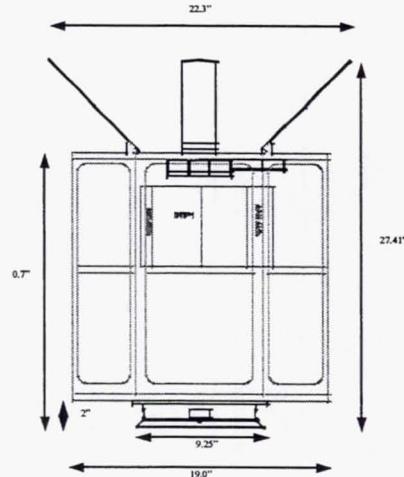
Figure 1: MightySat I Dimensions

MIGHTYSAT I SPACECRAFT

The drawing of Figure 1 shows the overall dimensions of the MightySat I vehicle. The vehicle size was dictated by the static and dynamic envelope constraints of the Shuttle Hitchhiker canister, and the vehicle weight was limited by the capability of the ejector. In order to avoid deployable antennae (which NASA discourages for safety reasons), four fixed UHF antenna blades are hard-mounted to the top of the vehicle. This configuration results in the MightySat I vehicle protruding above the Hitchhiker canister, which is flown without the traditional motorized lid for this flight.

The MightySat I structure is characterized by three decks supported by six structural frames, which make up a six-sided, quasi-cylindrical body. The bottom deck houses spacecraft components, such as the card cage and power, communications, and attitude control system hardware. The middle deck is used primarily for two of the payloads. The upper deck supports a solar panel, some experimental thermal control hardware (calorimeters & thermostats) sponsored by the spacecraft contractor, and four paddle antennae. The center of mass for the MightySat I vehicle meets the NASA requirements of no more than 10.25" from the separation plane in the Z direction, and no more than 0.25" from the geometric center in the X and Y directions.

Table 1 provides a top-level overview of key performance parameters for the MightySat I spacecraft. Although the MightySat I spacecraft does not have a large degree of flexibility or redundancy, the system is a very capable space platform for meeting the requirements of this specific mission, especially in light of the cost and development schedule.
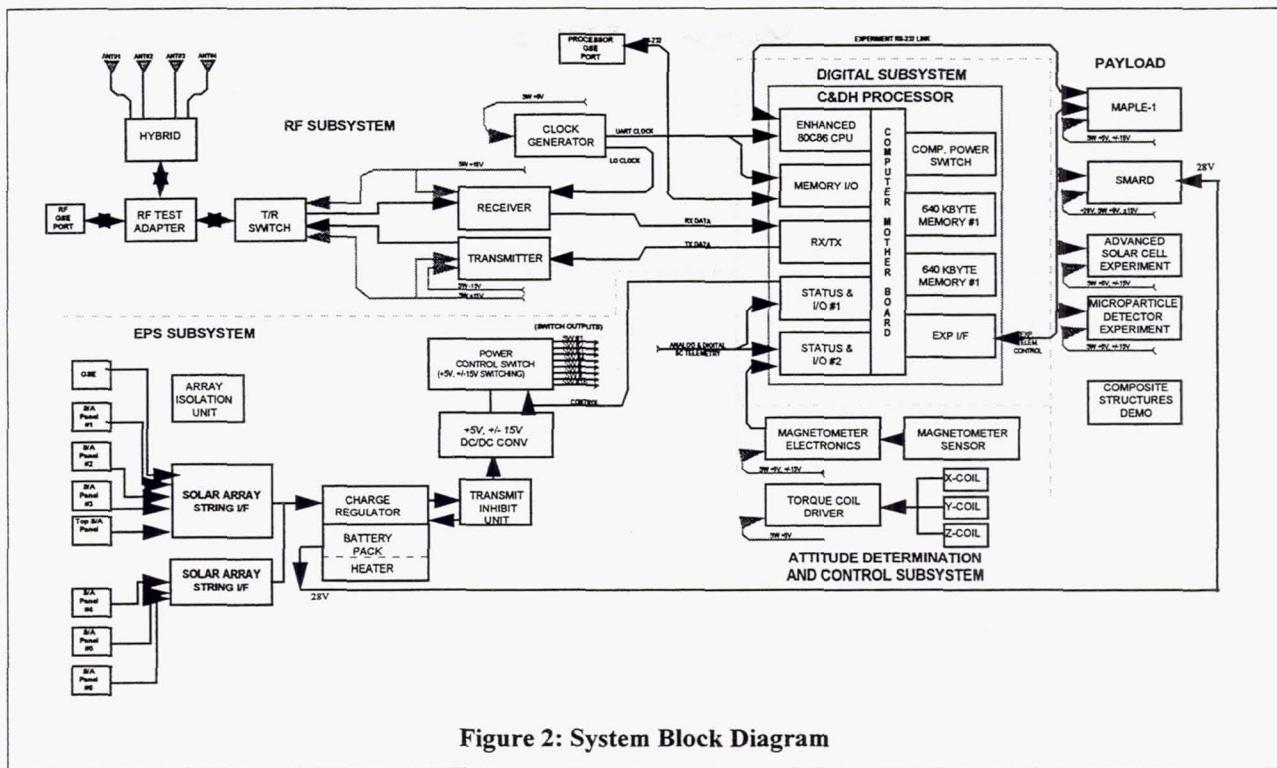
Figure 2: System Block Diagram

Figure 2 is the overall system block diagram for the MightySat I vehicle. Functionally, the spacecraft has four major elements: Command & Data Handling (C&DH) Subsystem, Electrical Power Subsystem (EPS), Communications Subsystem (RF), and the Attitude Determination and Control Subsystem (ADACS). In addition, there are mission unique components that were developed for collecting solar cell performance data, and for addressing NASA safety concerns.

Command & Data Handling Subsystem

At the heart of the MightySat I system is the C&DH, which controls all spacecraft functionality. Nine electronic boards make up the C&DH subsystem, which performs the following functions: 1) accepts and executes ground commands, 2) controls all power switching and commanding of the payload and spacecraft elements, 3) collects and stores spacecraft and payload telemetry, 4) schedules and controls communications with the ground, 5) performs all spacecraft housekeeping and spacecraft state-of-health functions.

Flight Software

The MightySat Flight Software has heritage from many other CTASS satellites, including the STEP and REX series. Processor software is written in Assembly language and "C", and operates under Ready Systems' Virtual Run Time Executive (VRTX) operating system.

Like the C&DH hardware, the MightySat I software architecture is relatively simple. Following a Start-up Routine, software control is passed to the VRTX operating system, which runs the MAIN task. MAIN, which is the highest priority task after satellite initialization, maintains the schedule, initiates execution of routines based upon ground commands, and passes control to the various sub-tasks as required.

Electrical Power Subsystem

The MightySat EPS consists of seven solar panels, a single 21-cell NiCd battery, a charge regulator, a DC/DC Converter, and a Power Control Switch. Although most of the EPS design has flight heritage, the Solar Array String Interface (SASI) was modified significantly to permit precise measurement of solar panel performance as part of the ASCE payload. Power from the solar panels is routed through the Solar Array String Interfaces (SASI's) to the battery charge regulator. The battery charge regulator is connected to the bus loads through an isolation diode, and permits the battery to supply power when the need exceeds the power generated by the solar panels. The MightySat I battery is a single 4 Amp-hr unit made of 21 Sanyo NiCd "D" cells wired in series. From the battery, power flows through a DC/DC converter to the Power Control Switch, a bank of 16 transistors that switch power to all bus and payload components based upon commanding from the C&DH.

Attitude Determination and Control Subsystem

The Attitude Determination and Control Subsystem (ADACS) configuration consists of a three-axis magnetometer and two coarse sun sensors for attitude determination, plus three torque coils and associated driver electronics for attitude control. In order to optimize power generation and maintain a simple, low-cost approach, the vehicle spins at 3 rpm about the vehicle "Y" axis, with the spin axis oriented normal to the orbit plane. This attitude is best illustrated in the orbit visualization depiction of Figure 5. Though the "Y" axis would appear to be an unconventional choice, it is the maximum moment of inertia axis and is acceptable from a power generation perspective.

RF Communications Subsystem

The MightySat I communications architecture consists of a simple, half-duplex (306.775 MHz) approach with a 2400 bps FSK uplink and 9600 bps BPSK downlink. The spacecraft RF Subsystem consists of a receiver, transmitter, transmit/receive switch, antenna hybrid, four blade antennae, RF test adapter and clock generator. The BPSK modulated transmitter has an output power of 14W with an efficiency of 60%. The receiver is a fixed frequency, single conversion unit with a 2.5 dB noise figure and a 10 dB S/N ratio at an input signal level of -120 dBm. Four quarter-wave monopole antennae are mounted 90 degrees apart on the top deck of the MightySat vehicle to produce a quasi-omnidirectional pattern. The MightySat RF communications link has about a 20 dB margin for both uplink and downlink at a 5 degree elevation angle.

Payloads

MightySat I has five advanced technology demonstration experiments. Two of the demonstrations are considered Experimental Bus Components, because they provide essential bus functionality to MightySat I, in addition to acting as advanced technology demonstrations. These are the Advanced Composite Structure and the Advanced Solar Cell Experiment (ASCE). The remaining three experiments are considered Stand Alone Experiments. These include the Microsystem And Packaging experiment for Low-Power Electronics (MAPLE-1), the Shape Memory Actuated Release Devices (SMARD) experiment, and the Microparticle Impact Detector (MPID) experiment. Details on each of these experiments can be found in the section on on-orbit results.

LAUNCH APPROACH

The primary launch approach for the MightySat program is ejection from the Space Shuttle. The MightySat I vehicle was designed and built for direct compatibility with the standard STS Hitchhiker Ejection System (HES). The chief reason for this approach is cost; as a USAF payload, the cost of launching from the Space Shuttle is consistent with the cost goals of the program. Launch system reliability, and a relatively high frequency of launch opportunities as a secondary payload are other attractive features of the Shuttle. However, Space Shuttle launch does have some rather significant drawbacks, such as the program impact and manpower costs of navigating through the extensive NASA Safety Review Process. Also, the Shuttle orbits are not always optimal for technology demonstrations that require special orbits, such as sun synchronous or high-radiation. For this reason, the MightySat II series is being designed with alternate launch systems in mind, to take advantage of any potential low-cost launch opportunity that may arise.

MightySat I has a standard Marman Ring interface with the HES. Figure 3 shows the MightySat I vehicle in the Hitchhiker canister with the standard motorized lid removed. The interface with the HES is strictly mechanical; no power, telemetry, or command interface exists between the Shuttle and the MightySat I vehicle. MightySat is essentially "inert" while in the canister; all spacecraft components are isolated from power sources. The canister is equipped with survival heaters that will keep the satellite temperature above 0°C in the cargo bay; aside from these survival heaters, no other active thermal control exists in the Hitchhiker canister. Safety issues associated with launching on a manned system have impacted the MightySat I program from many aspects. The design of two MightySat I components were particularly driven by safety-related concerns: the Transmit Inhibit Unit and the Nickel-Cadmium battery. The Transmit Inhibit Unit (TIU) is an electronic
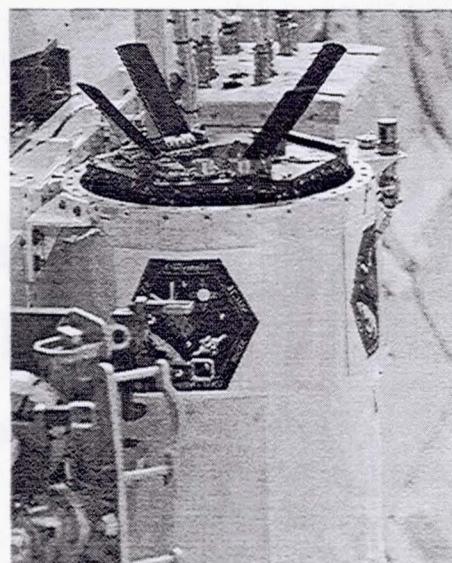

Figure 3: MightySat I in Hitchhiker Can

component that was added to the MightySat I design specifically to address the safety concerns of launching on the Shuttle. This unit essentially contains a series of electrical inhibits that block power from reaching "hazardous" components, such as the spacecraft transmitter. NASA requirements prohibit MightySat transmitter activity within 30 feet of the Shuttle. Other hazards associated with electronic board shorting were most easily addressed by simply ensuring that the MightySat system was powered OFF while in the canister.

Another serious concern of the NASA Safety Review Panel was the MightySat battery. MightySat uses commercial Sanyo Nickel Cadmium "D" cells, which do not have the typical design and test documentation associated with hardware developed for aerospace applications. Although these cells have flown for a decade on many OSC small satellites without a single cell failure on orbit, the MightySat team faced several design and testing challenges to meet NASA requirements. In order to better understand the nature of the NiCd cells, the MightySat program sponsored a series of tests at The Aerospace Corporation to experimentally determine the maximum operating pressure of the cells in off-nominal conditions, such as overcharge and reversal. The pressure at which the cells would vent was also determined experimentally.

In addition to testing the cells, the MightySat team was tasked with designing a battery "box" which would absorb and contain the potentially hazardous potassium hydroxide (KOH) electrolyte in the event of cell venting. The design solution was an aluminum box with special cut-out regions adjacent to cell vents that is filled with an absorbent material. These regions contain any leaked electrolyte in the absorbent material, while not permitting shorting across paths of leaked electrolyte. A microporous Teflon filter is also used over a vent hole in the battery box, so that hazardous gases will escape from the battery box. In this case, an originally low-cost battery approach became significantly more expensive due to the manpower and testing required to meet the requirements of the NASA safety process. The MightySat I battery experience is a valuable "lesson learned" for the long term MightySat program.

MISSION OPERATIONS CONCEPT

Three stand-alone, UHF Ground Control Stations (GCS) were developed for the MightySat program. Two were designed for satellite mission operations, and the third was dedicated to ground testing. The system shown, which connects to a steerable 10 ft diameter dish antenna, was installed at Kirtland Air Force Base (Albuquerque, NM) and at OSC (Dulles, VA) to provide two locations for satellite contact. The GCS was designed and built by Deskin Research Group (DRG), Inc of Santa Clara, CA using a large amount of existing hardware from previous government programs. This allowed the ground control stations to be acquired at low cost, but also produced some ground station problems. Because the components of the ground stations were acquired from several different programs, the antenna's positioner was undersized for the weight of the antenna and hood assembly. This led to problems with maneuvering the antenna through elevations near 90°. The wear and tear on the positioners was also extensive, requiring rework and the addition of counterweights to prevent positioner breakdowns.

MightySat I's ground control architecture is based upon the use of two PCs, as shown in Figure 4. The Mission Planning Computer (MPC) is the primary operator interface. Commands are selected from a database stored on the MPC for uplink to the satellite, and downlinked telemetry is displayed on the MPC for operator viewing and post-processing. Also, the MPC contains orbit visualization and propagation software for use in scheduling satellite contacts and other mission planning needs. The second PC, in the Signal Processing Unit, controls the GCS hardware and orchestrates the communications session between the ground and the satellite. This PC interfaces directly with the MPC to generate a track file for steering the dish antenna during contact with the satellite. In addition to the transmitter, dual receivers, and modems, the GCS contains a timing source (WWV or GPS) and Doppler correction hardware. Other PCs in the operations area are used to process telemetry, develop long-range planning boards, and place data on a public FTP site for retrieval by payloaders.

The Concept of Operations for the MightySat I vehicle is based largely upon experience from similar small satellite programs, most notably RADCAL. MightySat vehicles are operated by personnel from the Space & Missile Systems Center's Test and Evaluation
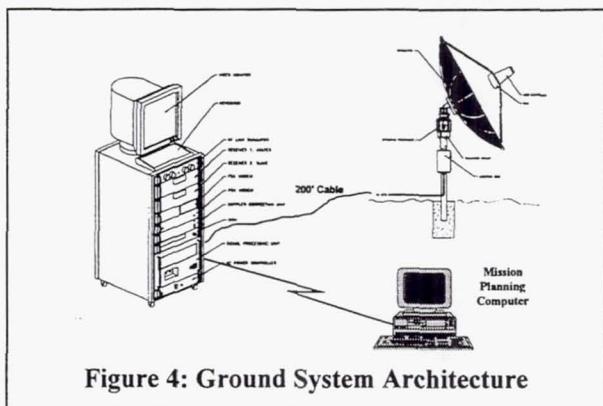

Figure 4: Ground System Architecture

Directorate (SMC/TE), an organization with a long history of performing mission operations for non-operational Air Force space systems. The main center for MightySat I operations is at KAFB. Contacts at the Dulles ground site are managed through remote link from KAFB, using modems, phone lines, and special remote software.

After preparation by the operations team, the actual MightySat I communications session occurs autonomously. Several minutes before a contact, the ground system prepositions the antenna at the start of the satellite's track. At the satellite's "rise time," the ground system begins executing its track file, positioning the antenna to follow the satellite's track through space. The satellite initiates all communications events, based upon a time-tagged communications event in its Scheduler. In a typical pass, the satellite begins by downloading payload data to the GCS, which stores the data for post-pass processing. Towards the middle of the pass, the satellite and ground station conduct bi-directional communications, in which commands are uplinked to the satellite Scheduler and MightySat I state-of-health data is downlinked. After this exchange, the satellite resumes downlink of payload data.

The Aerospace Corporation developed a MightySat I mission simulation model for visualization of the orbit and to gain a better understanding of power and communications issues. Figure 5 shows an image from this simulation tool, with the MightySat I vehicle in its expected orbit and attitude. The spin axis for the vehicle is oriented directly out of the orbital plane, which causes the antennae to alternately point towards then away from the earth. MightySat I has between six and nine passes each day, divided fairly evenly between the KAFB and the Dulles ground sites. Each pass can be
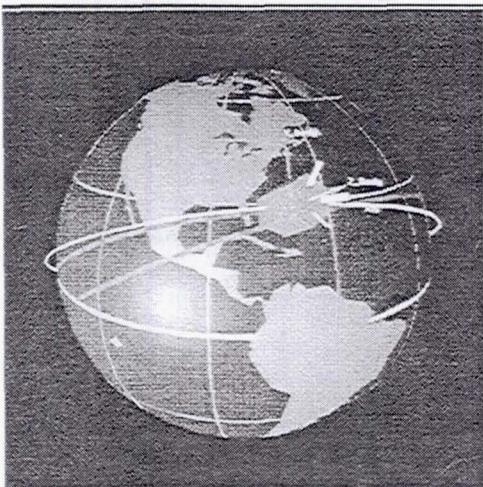

Figure 5: MightySat I Simulation
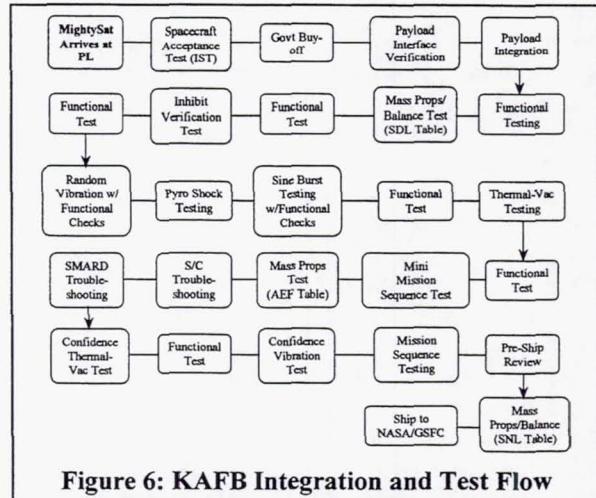
Figure 6: KAFB Integration and Test Flow

from one and five minutes long. The passes occur about 90 minutes apart, followed by a long period (up to 14 hrs) of no contact with the vehicle.

INTEGRATION AND TEST

During spacecraft development at OSC, each of the spacecraft components was subjected to thermal cycling and random vibration acceptance testing to ensure quality of the workmanship. In some cases, the component was of a new design (e.g. TIU), and the testing served as a qualification as well as acceptance test. Once assembled, the spacecraft (without payloads) underwent EMI/EMC testing and thermal cycle testing with electronic check-outs of the full functionality of the spacecraft at hot and cold dwells.

In parallel, each of the MightySat payloads underwent its own thermal cycle and vibration testing. A second composite structure, identical to the flight unit, was fabricated and tested in order to gain an early understanding of the structural dynamics of the vehicle. With mass mock-ups in place for the internal components, the "engineering structure" was put through random vibration testing, sine burst testing for structural qualification, and sine sweep testing to measure the spacecraft's natural frequency. As a result of this testing, modifications were made to the flight structure to make it more robust. The use of an engineering structure saved countless hours of rework to the flight structure, and reduced the risk of damaging critical flight components.

Payload Integration
Figure 6 outlines flight model integration and test effort at KAFB. Upon delivery of the spacecraft to the USAF in November of 1996, the government took the lead in integrating and checking the MAPLE-1, SMARD, ASCE, and MPID payloads. Payload integration took

248

nearly two months. During this time, several modifications to the electrical wiring harness were made, and mechanical modifications to some of the payloads were required to fit the payloads into the very tight confines of the MightySat I spacecraft. At the completion of payload integration, an integrated systems test and a functional test were performed to verify the space vehicle's performance.

Several tests required by the NASA safety process were accomplished following payload integration. These included tests to verify the TIU and the satellite's startup sequence. An initial spin balance verified that the satellite's center of gravity was within the 0.5" envelope specified by NASA. The spin balance also attempted to lower the satellite's products of inertia to near zero. Because MightySat I is spin-stabilized using magnetic torque coils, the stability of its spin is highly dependent on its moment of inertia matrix. Large products of inertia produce a spin that decays quickly. Subsequent evaluation revealed that this initial spin balance process was inadequate to reduce the satellite's products of inertia to a low enough level. Late in the test flow, therefore, the spin balance test was repeated at the more capable Sandia National Laboratories spin balance table.

Vibration Testing
Following the initial spin balance testing, the satellite was readied for vibration testing. Four vibration tests were performed to verify the satellite's readiness for launch: sine sweep testing, random vibration testing, pyroshock testing, and sine burst testing. The simplest of the four tests was the sine sweep test, which subjected the satellite to a 0.5g frequency sweep from 20Hz to 2000Hz. The sine sweep test was used throughout vibration testing to verify the satellite's integrity. The sine sweep tests conducted during the sine burst testing also demonstrated the satellite's lowest natural frequency to be 51Hz, above NASA's minimum of 50Hz.

Random vibration testing subjected the satellite to the NASA-specified protoflight vibration profile, which simulates the launch vibration environment of the shuttle. Figure 7 illustrates the test setup for random vibration testing. To emulate launch conditions, the MightySat I space vehicle was secured to a non-flight version of the Hitchhiker Ejection System (HES), called the Milkstool, for the random vibration test. The Milkstool was secured to a Ling 4022LX vibration table using an interface plate, and the table's control accelerometer was situated at the base of this interface plate. The rest of the data, or auxiliary, accelerometers were distributed throughout the test assembly to measure the satellite's response to the random vibration
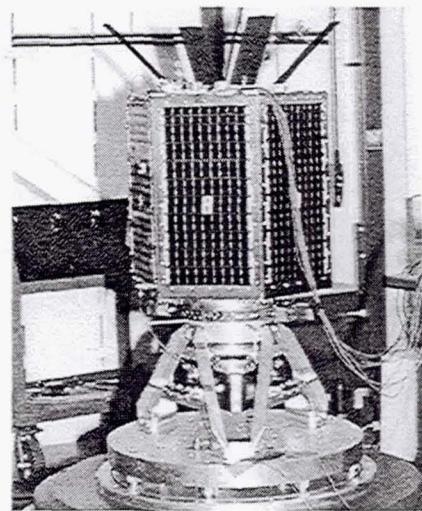

Figure 7: Random Vibration Test Setup

profile. Following setup, the vibration test profile was executed in each of the three spacecraft axes, with functional testing and sine sweep testing conducted between each axis to check for structural or component damage. The MightySat I space vehicle sustained no damage during the random vibration test, in part thanks to the modifications made as a result of engineering model testing.

After the successful completion of random vibration testing, the satellite underwent pyroshock testing. The pyroshock test was designed to verify that all satellite components could withstand the shock produced by the ejection system's pyrotechnic boltcutters. Figure 8 illustrates the test setup for pyroshock testing. The HES Milkstool, without its ejection spring, was secured to the MightySat I space vehicle as if for flight, with a marmon ring, bolts, and two pyrotechnic boltcutters.
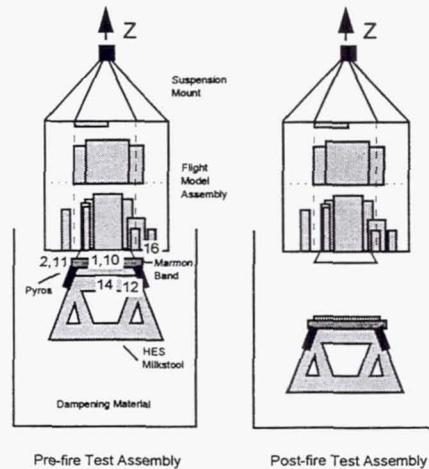


Figure 8: Pyroshock Test Setup
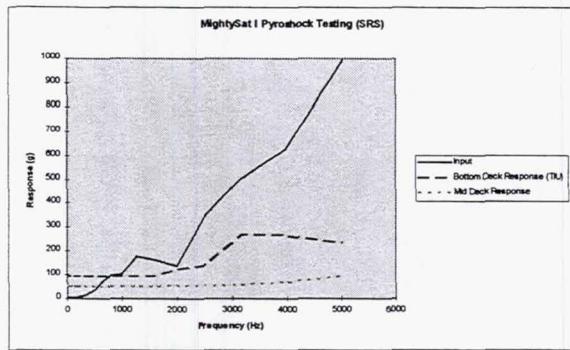
Figure 9: Shock Response Spectra

The entire test assembly was suspended over a catch box lined with dampening material. The internal accelerometers from the random vibration testing were left in place to measure the shock produced by the boltcutters as it propagated through the satellite. MightySat I underwent two ejection simulations. The NASA Standard Initiators (NSIs) for the first ejection simulation contained 125% of the standard charge; during the second ejection simulation, the NSIs contained 85% of the standard charge. Figure 9 shows the shock response spectra measured by several of the accelerometers. Following each of the simulations, a visual inspection documented proper HES release and no spacecraft damage. A lights-on test verified proper spacecraft operation.

The final structural test was a sine burst strength test. NASA Hitchhiker safety requirements dictate that composite structures cannot be strength qualified through analysis alone. Therefore, MightySat I was required to undergo a sine burst test to verify its ability to withstand worst-case shuttle launch and landing loads. To accomplish this, MightySat I was secured to the vibration table using a low mounting fixture. The vibration table imparted a low-frequency (17 – 25 Hz) sine wave to the base of the fixture. At low frequencies and large deflections, the force imparted to the base of the satellite reaches values greater than 25g's. Amplification in the satellite structure increases the force seen by different parts of the structure; as a result, portions of the satellite experienced forces in excess of 40g's during the sine burst strength test. The sine burst profile was executed in each of the three spacecraft axes, and followed by sine sweep testing and satellite functional testing. MightySat I survived sine burst testing in all three axes, proving it capable of handling worst-case shuttle launch and landing loads. Some restaking of internal components, however, was required to reduce destructive force amplification on these components. Again, the experience gained in the engineering model testing proved invaluable.

Thermal Vacuum Testing

Following structural verification, MightySat I underwent thermal vacuum testing. Thermal vacuum testing assessed the satellite's ability to operate in the launch environment, and addressed NASA safety concerns regarding the satellite's battery. The MightySat I space vehicle was subjected to temperature extremes ranging from -20° C to +40° C in order to thermally stress the spacecraft. A thermal vacuum functional test was conducted at each temperature dwell
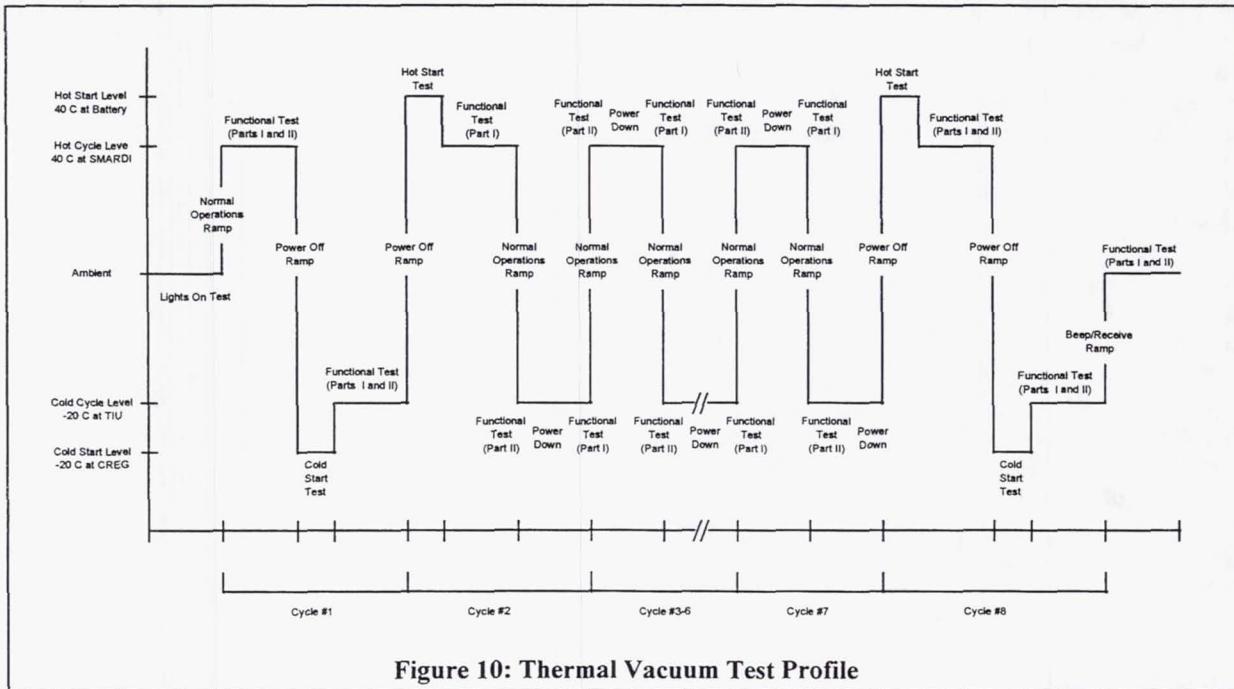

Figure 10: Thermal Vacuum Test Profile

250

and during the temperature ramps. This functional test validated the MightySat hardware and software by functionally exercising all of MightySat I's subsystems. All basic normal and abnormal modes of spacecraft operation were run during the thermal vacuum functional test.

Each thermal vacuum functional test consisted of two parts. The first part, based on the plan for early orbit checkout, initialized and exercised all normal operations of the spacecraft, much as they would be exercised in early orbit. Following this checkout, the satellite was allowed to run in its nominal on-orbit configuration for a period of time. This period of nominal operations was normally conducted during the ramp from one temperature extreme to another. The second part of the thermal vacuum functional test exercised several off-nominal operations. Figure 10 is a graphical representation of the thermal vacuum test approach.

Several software problems were uncovered during the extensive functional testing that accompanied thermal vacuum testing, but none of the problems arose out of the thermal vacuum conditions themselves. The satellite's start-up circuitry functioned properly during two cold boots and two hot boots. The cold boots also demonstrated the functioning of the satellite's battery heaters. During the thermal vacuum testing, two of the SMARD devices were also fired, but the fires were unsuccessful. This prompted a several-week reevaluation and redesign of the SMARD experiment, which occurred after the mission sequence test. The ground failure of the SMARD experiment also prompted a redesign of the shape-memory devices by the payloader.

Mission Sequence Testing

The mission sequence test exercised MightySat I's ability to function operationally. This test, virtually impossible for anything but a small satellite, consisted mainly of a five-day, completely plugs-out functioning of the satellite. Figure 11 is a photograph of the setup of the mission sequence test. The MightySat I satellite was mounted to a spin table, with the satellite's Y-axis (its nominal spin axis) pointing up. The spin table was set to rotate at three revolutions per minute, MightySat I's nominal rotation rate. A Xenon lamp was used to illuminate the satellite's solar panels, and the satellite's ground equipment was set up a short distance away. A small antenna was attached to the operational RF ground station rack to receive RF signals transmitted from the satellite, and to uplink commands to the satellite. The signal from both the uplink and the downlink paths was attenuated at the ground station to simulate nominal predicted link margins.
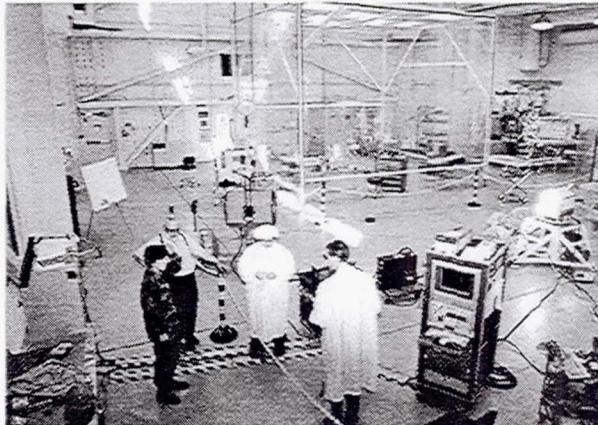

Figure 11: Mission Sequence Test

After setup and initial testing, the MightySat I satellite was taken through its startup sequence. A pusher plate was used to hold the TIU microswitches closed, much as the HES ejection system would hold them closed in the shuttle cargo bay. After a short countdown, the pusher plate was removed, releasing the microswitches. The Xenon lamp was turned on, causing the photodetectors built into the startup inhibit system to sense the "sun". Test conductors then waited for the first telemetry from the satellite. Following satellite acquisition, MightySat I's early orbit checkout procedure was executed. When the command to initiate the satellite's spin-up procedure was sent, the spin table was turned on to spin the satellite. Throughout the test, the Xenon lamp was turned on and off to simulate the satellite's normal sunlight-shadow orbital cycle. All satellite power was generated by the solar panels from the illumination of the Xenon lamp. All satellite commanding, and all telemetry downlink, was radiated through the air using the satellite's RF system.

Following the early orbit checkout procedure, MightySat I was placed in its nominal operating state, with the MAPLE, MPID, and solar cell experiments on and collecting data. Satellite contacts were scheduled periodically. The Xenon lamp was cycled on and off at the appropriate times to simulate sunlit and shadowed portions of the satellite's orbit. The satellite was allowed to run in this state, generating its own power, for five days. In this way, MightySat I was exercised in as close to on-orbit operational conditions as possible, greatly increasing the team's confidence in its ability to function on-orbit. The team that would operate the satellite in space practiced building commands, conducting satellite passes, and downloading telemetry as they would during on-orbit operations.

The Mission Sequence Test completed the KAFB portion of MightySat I integration and test. Following the SMARD repair, abbreviated vibration, thermal

251

vacuum, and mission sequence testing was conducted to verify that the satellite had suffered no damage and that the SMARD experiment was now functional. Then the satellite was readied for shipment to NASA's Goddard Space Flight Center (GSFC).

LAUNCH PREPARATION

At GSFC, MightySat I underwent testing at specialized facilities unavailable in Albuquerque. An anechoic chamber was used to measure the satellite's antenna pattern in the final spacecraft configuration. GSFC's magnetic test facility was used to check out the satellite's attitude determination and control system (ADACS), uncovering several ADACS software bugs. The satellite was secured to NASA's Hitchhiker Ejection System and placed in the lidless canister that would mount to the side of the shuttle's cargo bay. The satellite's battery was charged, and an inhibit verification test was performed prior to the satellite's shipment to Kennedy Space Center (KSC).

Upon arrival at KSC, final functional testing was conducted on MightySat I. The satellite was installed into the shuttle's cargo bay at the Orbiter Processing Facility. During a battery charge procedure following the satellite's installation into the shuttle cargo bay, and fastener from a piece of NASA-provided GSE was discovered to be missing. This necessitated a removal of MightySat I from the shuttle cargo bay, so that technicians could inspect the ejection system for the missing fastener. NASA was concerned that should the fastener lodge in the satellite's ejection system, it could interfere with ejection, leaving MightySat I in a partially ejected state. This would be a considerable safety risk. The fastener was never found; however, the visual inspection determined that the fastener had not compromised the ejection system. The MightySat I canister was reassembled and reinstalled in the shuttle cargo bay.

While STS-88 awaited launch, MightySat I technicians performed three battery top charge and inhibit verification procedures on the satellite in the shuttle cargo bay. The last two tests were performed on the launch pad itself, and the final procedure was executed less than a week before launch. These tests verified that MightySat I's startup inhibit circuitry, required by NASA Safety, had not been compromised in the days leading up to launch. The procedures also charged MightySat I's battery.

In parallel with these efforts, MightySat I's operational team was also preparing for launch. Three intensive mission operations rehearsals were conducted to exercise the team's operational procedures. Data from satellite testing was massaged using special software to simulate real on-orbit telemetry. Simulated passes were conducted, the results observed, and follow-up actions orchestrated. During some of the rehearsals, satellite anomalies such as spacecraft resets and thermal problems were simulated. As a result of these rehearsals, many of the operational procedures were refined or re-written.

LAUNCH AND EARLY ORBIT CHECKOUT

On December 4th, 1998, the Space Shuttle Endeavor lifted off from Kennedy Space Center to begin STS-88. During the deployment of the Unity module, and during its linkup to the Russian Zarya module to form the first elements of the International Space Station, MightySat I remained in the shuttle cargo bay. During one of the flight's many extravehicular activities, an astronaut accidentally grazed the side of one of MightySat I's four paddle antennas with his foot. After inspecting pictures and videotapes of MightySat I during and after the accidental contact, MightySat I engineers determined that the encounter had not damaged MightySat I in any way. Therefore, ten days into the mission, the way was clear for MightySat I to eject.

The shuttle crew ejected MightySat I about ten days into the shuttle's mission, at approximately 1900 hours Mountain Standard Time (MST) on the 14th of December, 1998. Based on the satellite's predicted orbit, the first satellite contact was expected to occur at the KAFB ground station approximately 2.5 hours following ejection. Closer examination of the satellite's visibilities, however, revealed a low-elevation (approximately three degrees) pass over the Dulles ground station about an hour after ejection. The decision was made to point the Dulles antenna toward the low elevation pass and listen for satellite telemetry. At approximately 2000 hours MST on December 14th, the first telemetry from MightySat I was received at the Dulles ground station.

The initial telemetry from MightySat I indicated a healthy satellite, with a good battery state of charge and a good thermal profile. The satellite was in its initial startup mode, called "beep/receive." In this operational mode, the satellite transmits its routine telemetry to the ground every minute, and then listens for a response. Because the satellite initiates all contacts, this increases the chances that successful contact will be made with the ground station.

Initial attempts to upload commands to MightySat I were unsuccessful, due to RF interference and doppler correction problems with the ground stations. By the end of the first sequence of passes, however, an uplink

to the satellite was achieved. MightySat I was left in beep/receive mode during the 12-hour outage when the satellite remained out of view of both ground stations. During this 12-hour outage, modifications to the ground stations were made to make it easier to contact the satellite.

During the second group of passes, more successful contacts were made with MightySat I. The picture of the satellite's state of health was refined with the first few dumps of the satellite's complete telemetry. A rudimentary communications schedule was uploaded to the satellite, taking it out of beep/receive mode. The solar cell experiment was activated at a low rate, to characterize the power generation of the satellite, and a magnetometer data collection was run to identify the satellite's spin profile. The solar cell and magnetometer data indicated healthy power generation, and a satellite wobbling predominantly around its "Z" axis approximately once per minute.

At the start of the third group of passes, ground controllers set the satellite's clock and briefly functioned the satellite's attitude control system for the first time. The Microparticle Impact Detector experiment (MPID) was also powered on during the third set of passes. The forth and fifth days of satellite contact were devoted to functioning the satellite's attitude control system. Several short, 20-minute functionings of the ACS were interspersed with solar cell and magnetometer data collections, as the mission control team evaluated the effect of each functioning on the attitude and spin of the satellite. Finally, on the fifth day after launch, the ACS was run for a full hour. Following this series of activations, the satellite was determined to be spinning in its nominal orientation around the Y axis, with a period of about 35 seconds.

Ground controllers sent a command to MightySat I to change its battery charging characteristics on the sixth day of operations. Temperatures measured at the satellite's battery were nearing 40°C, high enough to cause degradation to the battery over the long term. Changing the satellite's Taffle curve setting allowed more power to be left on the satellite's solar arrays, and caused a dramatic drop in the battery's temperature, with only minimal impact on the battery's voltage. With the battery's temperature stabilized, the way was clear to turn on the MAPLE-1 experiment on the seventh day of satellite operations. This completed MightySat I's early orbit checkout. SMARD, the one remaining experiment, would not be functioned until six months into the mission.

Despite ground station problems, the MightySat I early orbit checkout was completed in seven days, several days earlier than expected. Over the next several weeks, MightySat I engineers would track down the ground station problems, allowing operations to become fully autonomous by the end of January 1999. Since that time, all MightySat I's payloads have been functioned, and months of on-orbit data has been collected.

MIGHTYSAT I EXPERIMENT RESULTS

Advanced Composite Structure

The Advanced Composite Structure, which serves as the structure for the vehicle, has no real data or command interfaces with the spacecraft. The structure, developed by Composite Optics Inc. under an Air Force Research Lab contract, consists of a composite frame, three decks, and seven solar panel substrates, as shown in Figure 2. The composite material used throughout the structure is a prepreg of K1352U graphite fiber with a 954-3 cyanate resin. The spacecraft frames were fabricated by using a SnapSat™ approach [Reference 1], in which the elements are cut from cured flatstock layups and fitted together using a mortise & tenon technique. In addition to the well-documented weight savings of composite structures, the SnapSat™ approach reduces fabrication time by as much as 40%, and introduces greater flexibility in the process of design and fabrication of the spacecraft structure. The electrical resistivity of the structure is comparable to metallic designs, and only straps to ground the solar panels to the frame were necessary.

Pertinent data on the structure was acquired in ground testing, and particularly during the vibration testing designed to strength qualify the structure for flight on the shuttle. During early engineering model tests, a few of the metal spools used to secure the satellite's components to the composite structure broke loose under vibration and sine burst loads. The composite structure was reinforced and tested again, this time passing all structural verification testing. By surviving ground testing and satisfying all of NASA's safety requirements, the composite structure was verified as a viable structural platform for small satellites. MightySat I, however, had a robust weight margin in its final configuration, and therefore the weight savings introduced by the composite structure was not crucial. Future small satellites may wish to trade the weight savings against the difficulty of navigating the launch safety process, particularly for shuttle secondary payloads.

Advanced Solar Cell Experiment

The Advanced Solar Cell Experiment (ASCE), the second Experimental Bus Component, provides all the power generation for the MightySat I spacecraft.

MightySat I is one of the first space missions to use dual-junction solar cells, which offer a 15% performance gain over conventional GaAs cells. The dual-junction cells have a layer of Gallium Indium Phosphide (GaInP), which captures and converts shorter wavelength solar energy, relative to GaAs. The longer wavelength energy passes through the GaInP layer to be converted to electrical power in the underlying GaAs layer. Dual-junction cells can provide power at an average efficiency of over 21%, compared with 18-19% efficiency of GaAs cells and 14-16% from silicon cells. They are also an important step toward triple-junction technology with the potential for over 25% efficiency. This advance in space power generation technology is critical for many power-intensive sensors of the future, and could be particularly enabling for small satellite missions, which are often power-limited.

The ASCE payload consists of 13 strings of 40 GaAs cells (2x4 cm) and 6 strings of 18 GaInP cells (2x2 cm). A side panel, with one string of dual-junction cells and two strings of GaAs cells, is shown in Figure 12. The cells are bonded directly to a kapton-coated, monocoque, composite substrate (0.060" thick). The use of both solar cell technologies on the same mission provides a side-by-side comparison of cell performance on-orbit. The solar panels have been extensively tested to characterize cell performance, both at the vendor site and at AFRL's Space Power Laboratory. However, the ability of the ground-based solar simulators to match the precise spectrum of the sun is limited. Thus, one of the objectives of this experiment is to resolve uncertainties in the beginning-of-life modeling of the performance of the dual-junction cells. Another objective is to determine the effects of the space environment on the efficiency of the cells, although the MightySat I orbit and lifetime are not expected to produce large-scale changes in cell performance.

The Advanced Solar Cell Experiment (ASCE) has been collecting data since the second day of MightySat I operations. Each solar cell collection sample records the array voltage produced by the solar panels, the current
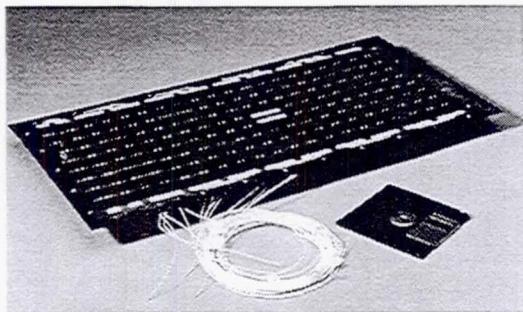

Figure 12: ASCE Side Panel

from each of the satellite's solar array strings, and the temperature of each panel. In addition, each data sample records the satellite time, the satellite magnetometer readings, and the readings from the satellite's coarse sun sensors. In order to compare ground test data to the string performance on-orbit, several corrections need to be made. Foremost among these corrections are the ones for solar incident angle and earthshine. In the laboratory, each panel is carefully mounted perpendicular to the carefully calibrated light source. On-orbit, the panels receive light from the sun at many different angles, and are also exposed to solar energy that is reflected off the Earth. Using data from the magnetometers on the MightySat-1 spacecraft, ground processing allows a reasonably accurate estimation of the solar incidence angle and earthshine angle at the time of solar panel data collection. After making the needed corrections, the on-orbit performance of the solar cells can be directly compared to the ground test results. Results for the MightySat-1 solar cell experiment are still being calculated, but initial side-by-side comparisons of the GaAs cells and the GaInP cells indicate that the GaInP cells are producing approximately 6-8% more current per unit area than the GaAs cells.

MAPLE-1

The Microsystem and Packaging for Low Power Electronics (MAPLE) experiment is a demonstration of advanced microelectronics and electronics packaging techniques. The objective of this experiment is to provide the first on-orbit demonstration of the latest advances in low power electronics, and characterize their performance in the collective space environment. This space experiment is seen by AFRL/VSSE as the first unit in what is hoped to be a series of experiments designed to evaluate emerging electronics and packaging technologies in space. As in the case of the solar cells, the expected MightySat I environment is not stressing to electronics from a radiation perspective. However, gaining space heritage for any of the emerging electronics technologies provides a larger performance database for assisting in the transition of the technology.

The MAPLE-1 space electronics experiment fielded involved five separate primary experiments and one very exciting "add-on" experiment. The payload, shown in Figure 13, consists of six electronic boards or "slices" containing several advanced technology items. The Advanced Electronics Board (AEB) was developed to determine the differences between the response of a radiation hardened and a military grade field programmable gate array. The purpose of the experiment was to examine how the gate logic unit degrades with time-in-orbit. This was done by testing
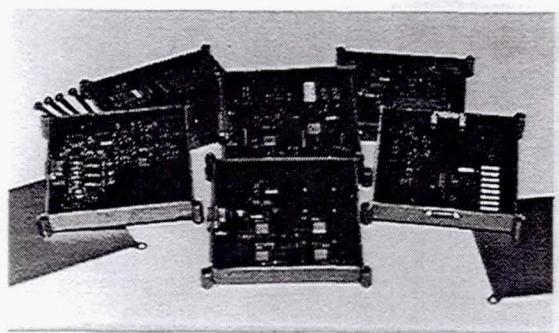
Figure 13: MAPLE-1 Experiment

approximately 80% of the 20,000 gates (PLD equivalent gates) available on each of the arrays by using identical programs to setup software instruction sets and then measuring the errors at the output of the arrays.

The Packaging Reliability Board (PRB) was developed to evaluate the reliability of packaging used on the ATC04 devices, which are Sandia National Labs (SNL) designed test chips. The reliability was examined by measuring the frequency of eight oscillators housed in four ATC04 chips and determining how the electronics degrades with time-in-orbit. During laboratory tests the oscillation frequency dependence on temperature and bus power was determined (-0.07 MHz/°C and +3.2 MHz/V respectively). The Solid State Recorder Board (SSRB) was designed to evaluate the performance of the High Capacity Spaceborne Memory (HCSM) SRAM module in a space environment. The HCSM is a 40 bit x 512K bit deep static RAM on a high-density 2D multi-chip package. The test involved writing various 40 bit word patterns to the memory (00H, FFH, 55H, AAH), waiting for approximately 30 seconds, and measuring the single bit upsets in memory locations.

The Environment Monitor Board (EMB) was designed to measure the temperature inside the Maple-1 enclosure and the cumulative total dose radiation seen by the experiment during time-in-orbit. The Micro Electro-Mechanical Systems (MEMS) Evaluation Board (MEB) was developed to evaluate the electronics functionality of the MEMS device technology used to process the signals from 3-axis accelerometers. Two accelerometers were fielded on MAPLE-1, a local 5-g full scale unit and a remote 2-g full scale unit mounted near the Shaped Memory Actuated Release Device

(SMARD) experiment. Electronic health tests were incorporated into the programs used to monitor the operation of the accelerometers as well as a "solenoid plunger" used to mechanically 'ping' the local accelerometer.

MAPLE-1 was powered on at 0800 Zulu time on December 21, 1998 and has been operating continuously since that time. All of the five experiments are in excellent health and are operating as expected.

Of the five experiments, the data from the EMB and the PRB experiments is the most interesting. This is because, for the AEB and the SSRB experiments, success means minimal errors - which is what has been observed to date. The single event upset (SEU) rate observed with the SSRB has been almost non-existent, but even with the limited data available a few observation can be made. A '00H' pattern written to memory is more likely to 'upset' than a 'FFH' pattern. Future efforts would want to determine if this pattern dependence is attributable to the layout of the memory gates on the chip -- or possibly is due to some other cause. The SEU rate is also expected to be independent of the physical location of the memory gate on the chip (the complete SRAM is composed of 4 separate chips mounted in adjacent locations on the support structure). Because of the low upset rate (low statistics), the dependence on physical location will be examined using the entire date set available at the end of MightySat's life-in-orbit.

The data from the "add-on" SMARD experiment is perhaps the most exciting. MAPLE-1 participation in the SMARD experiment involved measuring the response of the 3-axis MEMS accelerometer to the shock wave generated when a test "separation bolt" was fired. The SMARD firings consisted of four separate events. The MAPLE-1 remote accelerometer successfully captured the SMARD events and clearly showed the dramatic difference between the two types of devices. The shock from the two pyrotechnic devices propagated in three axis throughout the satellite mid-deck to all components located there. In contrast, the shock of the shaped memory devices was felt in only one axis, with the amplitude being several orders of magnitude less than for the pyrotechnic devices.

The next most interesting experimental result is the strange temperature dependence of the oscillator frequencies of the ATC04 chips. As the satellite permeates in its orbit, it moves from approximately 50% sun exposure to 100% sun exposure. As it does so, the satellite surface temperature increases. The temperature of the interior of the satellite, as measured by the EMB, follows the surface temperature. Figure 14a is the MAPLE-1 temperature over a two-week period in January. Figure 14b is the frequency of one of the oscillators (F8) over the same two-week period. Combining the two data sets, Figure 14c is a plot of the F8 oscillator as a function of the local temperature.

Some observations can be made from this data. First, the overall temperature dependence (-0.05 MHz/°C) is similar to the observed during ground testing (-0.06 MHz/°C). Second, the plateaus observed were totally unexpected. The flat regions are where the oscillator frequency is independent of temperature, while the sloped regions (-0.16 MHz/oC) correspond to a very strong temperature dependence (almost three times the overall dependence!). Finally, the plateaus are all separated by 250 kHz and have almost the same duration in temperature (approximately 4°C). This data has been made available to SNL, who are also puzzled by this rather bizarre temperature dependence.


Figure 14: MAPLE-1 Oscillator Temperature Dependence
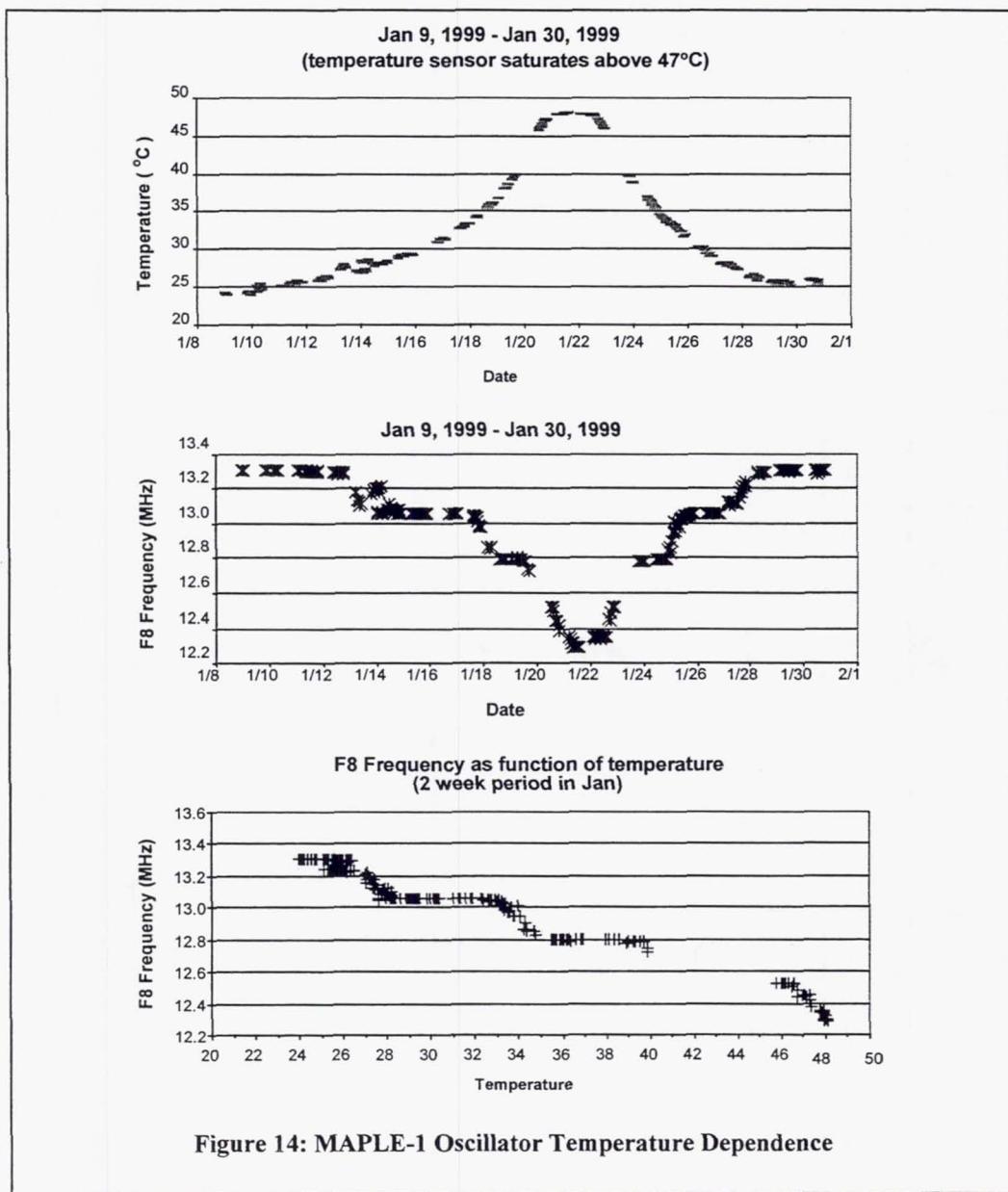
Shape Memory Actuated Release Devices

The Shape-Memory Actuated Release Device (SMARD) payload is an on-orbit demonstration a new class of low-shock release devices. Such devices have application in nearly all space systems, and are essentially replacements for conventional pyrotechnic units. The SMARD devices are based upon a shape-memory alloy (Nitinol) which is used as the driving force to actuate the release of a fastener. Release devices in general are used to separate satellites from launch vehicle adapters, or to deploy antennae, solar arrays, sensor covers, or other elements of space systems. Studies have shown that the shock imparted on space systems from the firing of conventional release devices, such as pyrotechnic bolt cutters, can potentially damage sensitive electronics. Table 3 shows some ground performance data from the SMARD release devices, relative to commonly-used pyrotechnic and linkwire technologies. Shape memory Actuated (SMA) devices offer greatly reduced shock levels at the expense of slightly longer separation times. They are also relatively low-cost, and have the added benefit of being completely resettable. Thus, the specific flight unit can be ground tested to ensure functionality. SMARDs also offer reduced contamination and safety concerns, since there are no pressurized gases or explosion hazards.

Table 2: Comparison of Release Devices

Device	Shock (G's)	Separation Time (msec)	Resettable
Pyro	7000	2	No
Link Wire	5000	20	No
SMA Low Force Nut	500	40	Yes
SMA Two Stage Nut	200	30	Yes

The MightySat I SMARD payload consists of four release devices mounted to a common, instrumented deck, as shown in Figure 16. A neighboring electronics box performs the arming and firing of the devices, and routes the data collection channels to the spacecraft. The four release devices use different technologies to perform the release of a 0.25" bolt, which is captured in the volume below the mounting deck. A conventional pyrotechnic device, a linkwire device, and two shape-memory actuated devices are used in this experiment. During the on-orbit actuation of the SMARD experiment in May 1999, the devices were "fired" one at a time, while actuation current & voltage, shock levels, release time, and temperature data were collected. The data was stored in spacecraft memory, and later downlinked to the ground for post-processing. Figures 15 shows the accelerometer data collected during the on-orbit actuation of each of the four devices in the SMARD experiment. Two accelerometers


Figure 15: SMARD On-Orbit Data

257
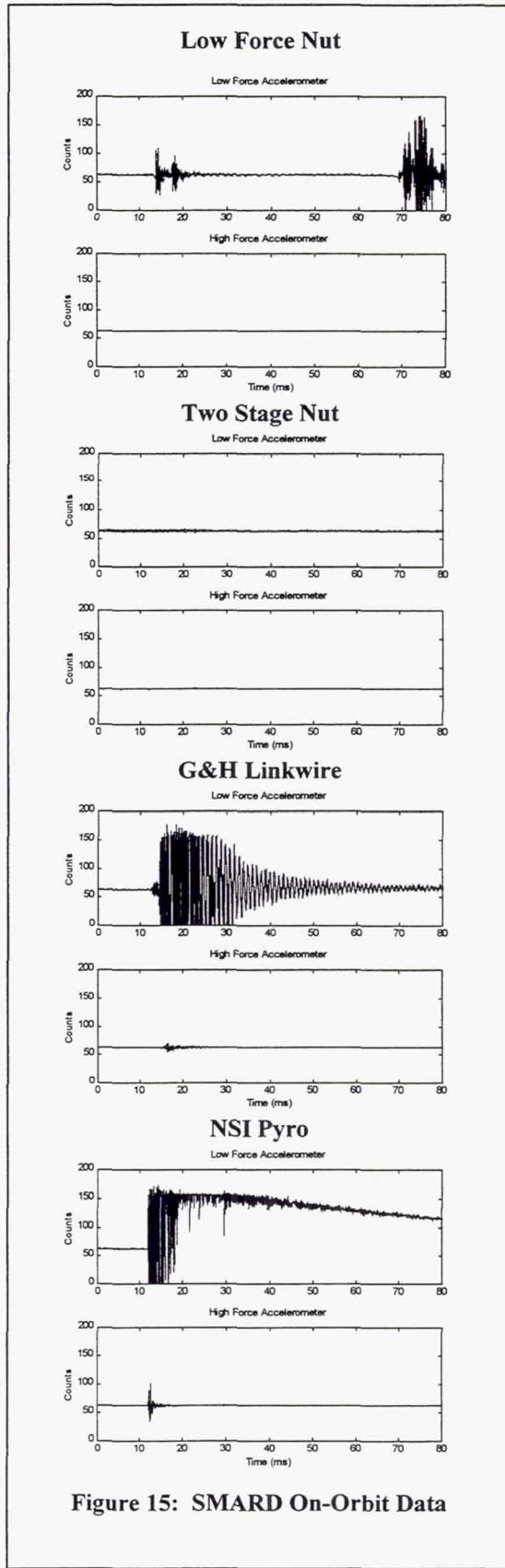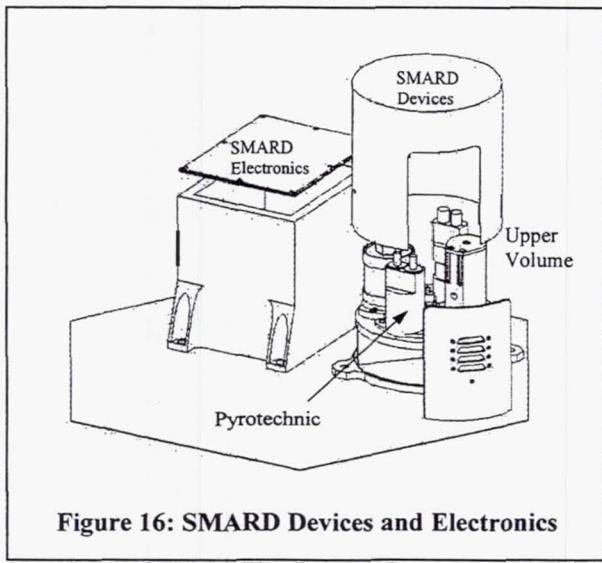
Figure 16: SMARD Devices and Electronics

recorded each event. The first accelerometer was a low-force accelerometer selected to pick up the low shock levels generated by the shape memory devices. The second accelerometer was a high-force accelerometer chosen to pick up the higher shock levels produced by the standard release devices. During the NSI device fire, the low-force accelerometer saturated, producing the unusal graph shown at the bottom of Figure 15. While the data is still being analyzed, the plots show that the shape memory devices do present a significant reduction in the shock loads seen by the surrounding accelerometers. The MAPLE MEMS accelerometer also recorded data from the device actuations of the SMARD experiment.

The execution of the SMARD experiment by the MightySat I spacecraft presented several challenges. The release devices needed a 1200W burst of energy for actuation; delivering this power without affecting the spacecraft functionality or data collection required a specially-designed power system with a very capable battery. Fortunately, no adverse affects to the MightySat I vehicle were noted during the actuation of the SMARD experiment.

Micro-Particle Impact Detector
The MPID payload was a late addition to MightySat I, proposed just two months before shipment of the spacecraft to AFRL. The objective of this experiment is to measure direction and time of impact of spaceborne micron size particles with time of impact resolution of 0.1 s. By recording the time of impact and referencing to the vehicle ephemeris, the orbit position at time of impact can be determined. The objective of the overall MPID effort is to place as many detectors as possible into the space environment. These detectors can then contribute to the information database for natural and man-made orbital "debris."

The primary elements in this experiment are two Metal-Oxide-Semiconductor (MOS) discharge capacitor detectors that discharge upon hypervelocity particle impact. The detectors were developed by Prof. J.J. Wortman from North Carolina State University, and are capable of detecting particle sizes of at least 0.4 μm. Each MOS particle detector is 3" x 1-1/2" in size and approximately 0.013" thick, providing a total impact detection area of 3.7 in^2. Each detector is bonded to a detector holder assembly that is in turn mechanically fastened to the external bottom plate of the MightySat I spacecraft. The detector assembly and associated electronics weigh less than 0.4 lb. A particle impact causes an impact event record to be stored in the spacecraft control unit for later downlink. Each impact event record will store time of impact and output from two coarse sun sensors. Data from the coarse sun sensors is used to help determine the attitude of the spacecraft.

The MPID experiment was turned on during the first week of MightySat I on-orbit operations. To date, the experiment has recorded no impacts. Model data suggests that the lack of impacts may be due to the low impact detection area of this experiment, and the relative scarcity of hypervelocity particle debris. MPID will continue to operate until the end of MightySat I's on-orbit life, however, and it is hoped that the detectors will measure an impact sometime in the future.

MIGHTYSAT I LIFETIME

At this time, MightySat I is operating nominally. The Advanced Composite Structure has been demonstrated. The SMARD experiment, once operated, lies dormant. The MAPLE-1 and MPID experiments operate continuously, and the ASCE experiment is functioned at least once a day. Telemetry data continues to indicate a robust satellite. Based on the satellite's orbital observations for the first several months of its operation, MightySat I is expected to reenter the earth's atmosphere in the early part of November 1999. This is just shy of its one-year on-orbit lifetime goal. The early reentry is predominantly due to the increase in atmospheric drag due to the solar sunspot maximum. Toward the end of MightySat I's lifetime, the rapidly-changing orbit may require more updates to the satellite's visibility schedule than can be reasonably accommodated. If this occurs, the satellite will be contacted less frequently, and will be placed in a quiescent mode between contacts to reduce spurious radiation by the satellite.

MIGHTYSAT II

As mentioned earlier, MightySat I is a single-mission pathfinder for the Space Vehicle Directorate's long term program for technology demonstration flights, MightySat II. As MightySat I was starting in June, 1995, a competition was being held to select a spacecraft contractor to develop 3-5 small satellite missions over the next decade. This contract was awarded to Spectrum Astro, Inc., a small satellite company in Gilbert, AZ with experience from the MSTI program. The program was initiated in March 1996, and the first satellite in the series, dubbed Sindri, was delivered to the Air Force for integration and test in April 1999. Launch of Sindri is scheduled for April of 2000, on board the second launch of OSC's Orbital/Sub-Orbital Program (OSP) launch vehicle.

A drawing of the MightySat II spacecraft is shown in Figure 17. MightySat II is a highly capable small satellite, which can perform a wide array of technology demonstration missions. Most notably, the spacecraft is twice as large as MightySat I, and is three-axis stabilized with deployable, articulated solar arrays. Some basic performance parameters for the MightySat II system are also shown in Figure 17. In some cases such as the downlink rate, reduced performance was accepted in order to maintain a low-cost approach. In other areas, however, such as attitude determination and control, the contractor was able to offer a relatively high level of capability at a reasonable cost. In this case, use of a flight proven OCA Star Camera, which has heritage from the Clementine small satellite mission, enabled a high performance yet low-cost attitude control system.

MightySat II is designed to host a large set of technology demonstration payloads, including earth-pointing or space-pointing sensors. Although volume, weight, and power limitations will still exclude large-scale payloads, MightySat II should be capable of supporting the needs of the large majority of AFRL technology developers. The MightySat II program will attempt to manifest as many payloads as possible on each MightySat II mission. The first mission features space demonstration of a Fourier Transform Hyperspectral Imaging system. Hyperspectral imagery is considered to have great potential for military applications, including characterization of soil conditions and detection of camouflaged targets. The MightySat II sensor, however, is strictly a technology concept demonstration, with no direct operational utility. This imaging system will stress the data collection and downlink capability of MightySat II, since it acquires 160 Mbytes of imagery data in only 8 seconds.
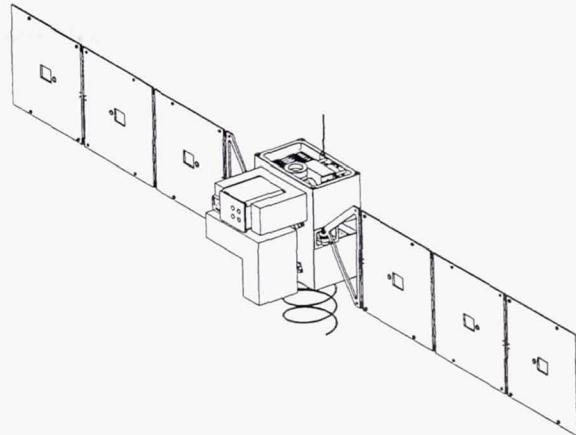
Vehicle Weight	275 lbs
Payload Weight	125 lbs
Maximum Power Generation	325 W
Payload Power Budget (sun/eclipse)	100/30 W
Attitude Knowldge/Control	0.15/0.25 deg
Uplink Rate/Downlink Rate	2/256 kbps

Figure 17: MightySat II Performance Parameters

Other follow-on technology demonstrations are in the area of composite structures. The MightySat II primary structure will use composite materials with built-in thermal management properties. Other structures demonstrations include a shape memory film that minimizes thermal distortion of solar arrays, a multi-functional film to transport power and data signals without cumbersome wire harnesses, and experimental solar array substrates using an isogrid design.

SUMMARY

This paper has provided an overview of AFRL's MightySat program, focusing primarily on the MightySat I mission. The primary objective of the MightySat effort is to provide a low-cost space-based platform for frequent demonstrations of advanced space system technology. Demonstration of emerging technology will expedite transition of advanced capabilities from the lab bench to operational Air Force space systems, which is a critical element of AFRL's charter. An overview of the MightySat I spacecraft was given. The satellite's integration and test process, launch and operations, and initial payload results were described in detail. A brief overview of the MightySat II effort was also included.

Perhaps the most notable features of the MightySat program are the focus directly on technology demonstration as a mission, and the attempt to execute a DoD small satellite mission in a new cost regime. Is MightySat "smaller, faster, cheaper, better?" MightySat

seeks to build on the success of highly effective small satellite programs accomplished by the USAF over the past decade, including the STEP, MSTI, and REX series, RADCAL and APEX. These pioneering programs have built an infrastructure for the rapid development of highly capable small satellite missions at a greatly reduced cost. In some respects, these programs have paid the non-recurring cost of developing a government/industry environment where programs such as MightySat can succeed. In addition, international small satellite efforts have provided the models for performing very effective space missions at a fraction of what is typically spent on US DoD programs. In essence, MightySat represents an attempt to perform a USAF mission (technology demonstration) at a cost comparable to the scientific missions of our colleagues overseas. So how do we answer the above question? Relative to past USAF missions, MightySat I has been somewhat smaller, perhaps faster, and certainly cheaper. Since the MightySat mission of focusing strictly on technology demonstration is significantly different from that of past programs, judgment on "better" is not really possible. But the success of MightySat I is due in large part to those small satellite missions that preceded it.

REFERENCES

1. "Affordable Polymer Composite Structures for various Spacecraft Structural Components", G.C. Krumweide, 9th Annual AIAA/USU Conference on Small Satellites, Logan, Utah, September, 1995.

THE TRACKING AND POINTING SYSTEM OF UVSTAR[1]

Paolo Trampus, Andrea Bucconi, Giovanna Zennaro
CARSO, Center for Advanced Research in Space Optics, Trieste (Italy)

ABSTRACT

Uvstar is an ultraviolet telescope that has flown three times as a SSP on STS 69, STS 85 and STS 95. The instrument has been improved every new mission. For the second flight an independent pointing and tracking system, the Finder and Tracker Control Unit (FTCU) based on the DSP 21020 was developed. The tracking algorithm was further improved for the third flight and two electronic boards, used as back-up units during the second flight, were removed from the FTCU. The FTCU architecture, the different target catching and tracking modes and the results of more than fifty tracking sessions are presented.

INTRODUCTION

Uvstar, UltraViolet Spectrograph Telescope for Astronomical Research, operates in the 500÷1250 Å waveband at a spectral resolution of 1, 4.5 and 12 Å (ref. 1, 2). Uvstar consists of a movable platform and an optical system. The platform provides fine pointing within ± 3 degrees from the nominal view direction. The Uvstar position and observing direction U_V are shown in Fig. 1. When Uvstar is in the default position the U_V vector corresponds to the Shuttle Y axis rotated by a roll angle of $-5°$. Both the Uvstar axes can rotate of $±3°$: this means that when the Shuttle is in LVLH (Local Vertical/Local Horizontal) attitude and its Y axis is pointing to the pole of the orbit, the Uvstar pointing direction performs a quasi-anular trajectory during a Shuttle orbit (≈96 minutes) with a radius in the range 3 to 8 degrees and velocities 12 to 33 arc-sec/s. The optical system has two channels, each formed by a telescope and a Rowland concave-grating spectrograph with an intensified CCD detector. One cannel, EUV, operates at wavelengths shorter than 912 Å, while the second, FUV, operates above the Lyman discontinuity. The telescope mirrors are off-axis parabolic mirrors of 30 cm diameter and 1.5 m focal length.

FTCU (FINDER TRACKING CONTROL UNIT)

During the first flight Uvstar was equipped with a tracking system based on a 68020 CPU inserted in the ICU (Instrument Control Unit) provided by the University of Arizona Lunar and Planetary Laboratory. The acquisition from the tracking detectors and from the spectrograph CCDs was performed by the same CCD controller, with functional limitations. The maximum acquisition frequency was about 1 Hz, the image data were available for elaboration with a transfer delay of 300 ms and during the scientific data acquisition, every 15÷30 s, the tracking image acquisition had to be skipped. For the second mission an independent tracking control unit based on a VME bus (FTCU) was developed. This electronics is mostly dedicated to the tracking functions of the Uvstar platform. The FTCU has a 1200 baud bidirectional channel in order to receive the commands from the CGSE (Customer Ground Support Equipment) and transmit the telemetry providing information on instrument and tracking status. A video board inside the FTCU sends real time images from the tracking telescopes when the video channel is available.


Fig. 1 Uvstar accommodation on the Shuttle bay

Processor Board

The FTCU processor board is based on the 21020 DSP. This board directly interfaces the Finder and Tracker cameras and has 1 Mbyte dedicated memory for the tracking images. In addition it has: two banks of 1 Mbyte Eeproms that allow to store two program versions and a stellar catalog, a 768 Kbyte program memory, a 640 Kbyte data memory with Edac, two RS422 serial interfaces, a real time clock and a watch-dog (Fig. 2).
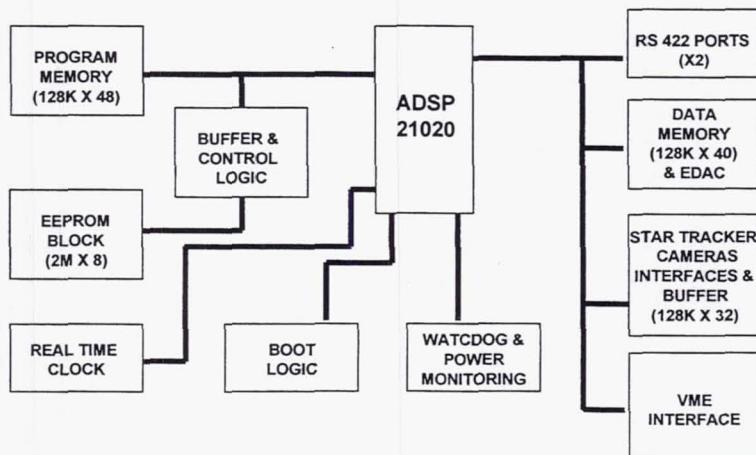

Fig. 2 FTCU Processor Board

262

Housekeeping Board

This board, dedicated to the housekeeping functions, has 16 differential analog inputs for voltage and current monitoring, 16 single ended analog inputs for temperature measurements, 16 digital inputs to read the status of the platform limit and zero switches, three analog outputs to control the intensifier gain, 16 digital outputs for actuation, one RS422 interface and two axes stepper motor controller with dedicated inputs for the two encoders (Fig. 3).

The power consumption of the DSP board is 8W and that of the housekeeping board is 4W.
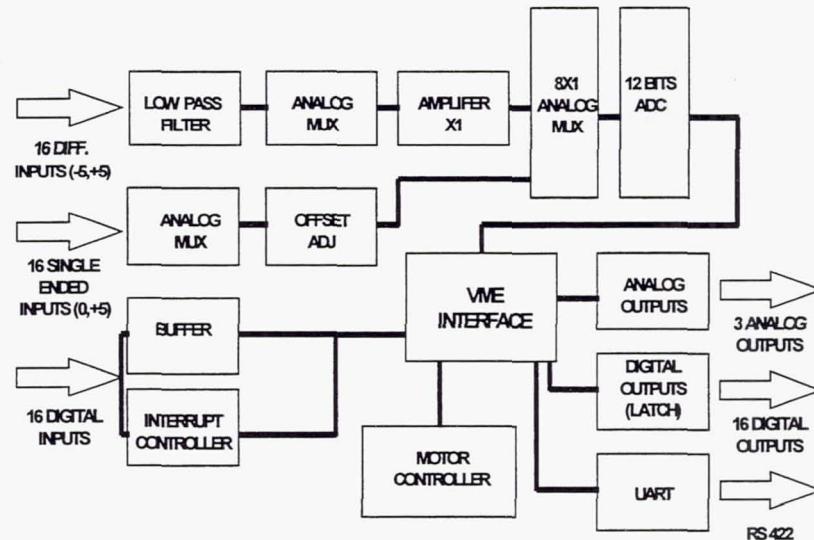

Fig. 3 FTCU Housekeeping Board

FINDER AND TRACKER TELESCOPES

The tracking telescopes are based on intensified CCDs. The frame transfer CCDs have 385×288 pixels and the intensifiers have wrap-around high voltage supply with gate control, S20 photocathode and P20 phosphor screen. The Finder telescope is a f/1.2 lens with 75 mm focal length and 6.5°×4.8° field of view. The Finder dimensions are 112×125×385 mm (with baffle). The Tracker is a f/15 Cassegrain telescope with 1500 mm focal length and 0.32°×0.24° FoV, dimensions of 179×210×403 mm. The frame frequency of the tracking cameras is 16 Hz with 2 MHz pixel clock.

This paper is concerned with the characteristics of the Finder telescope since the tracker has only been used during the missions for alignment of the science and pointing instruments.

In order to illustrate the pointing performances of the Finder telescope, we report in Fig. 4 the deviation from a (X,Y) position of a light spot acquired by the Finder without the intensifier. 500 data were acquired by the Finder with an acquisition frequency of 4 Hz; the position was determined by using a centroid algorithm. The standard deviation on the X coordinate of the point is 0.0027 pixels (0.16 arc-sec) and that of the Y coordinate is 0.0048 pixels (0.29 arc-sec), where a pixel corresponds to 60 arc-sec.
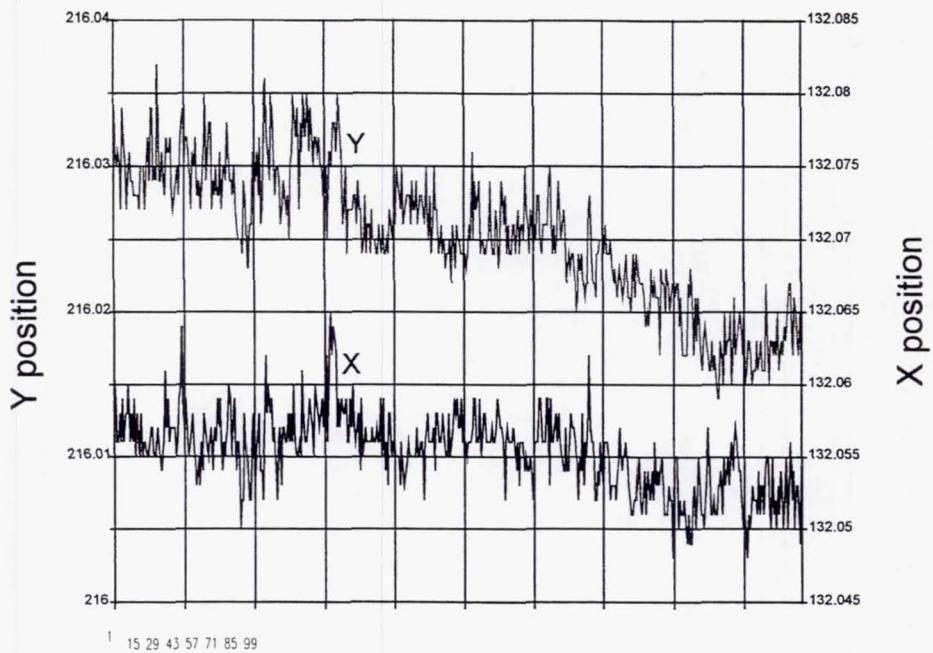
Fig. 4 FTCU Finder Resolution

An example of system response (point-spread function) when two stars in the same frame are acquired is illustrated in Fig. 5. The figures to the left correspond to a 1.6 visual magnitude star while the figures to the right to a 3.7 magnitude star. The analysis is performed using images obtained during the STS-95 mission. The two graphs at the top show the distribution of illuminated pixel intensities; the second row of graphs shows the same distribution projected on the detector plane and allow a better estimation of the defocusing. The defocusing of the Finder telescope was analyzed during the instrument integration phase and was adjusted so that the star dimension on the CCD at 20% of the maximum intensity (set to 100) is $\approx 4 \times 4$ pixel. The third row of graphs show the distribution of the signal along CCD columns and rows in correspondence of the maximum intensity.

These measurements were performed with the intensifier voltage gain at 65% of the maximum value corresponding to a gain of ≈ 50 in terms of number of electrons on the CCD output with respect to a unintensified detector. The images were compressed by sending one pixel every two and re-sampled during the transmission. For transmission we used two different video boards, FTCU and ICU frame grabbers. This procedure can affect the result of the reconstruction analysis. The ratio between the total sum of the pixel amplitudes of the two stars is 7.1, close to the ratio of their fluxes of 6.9.
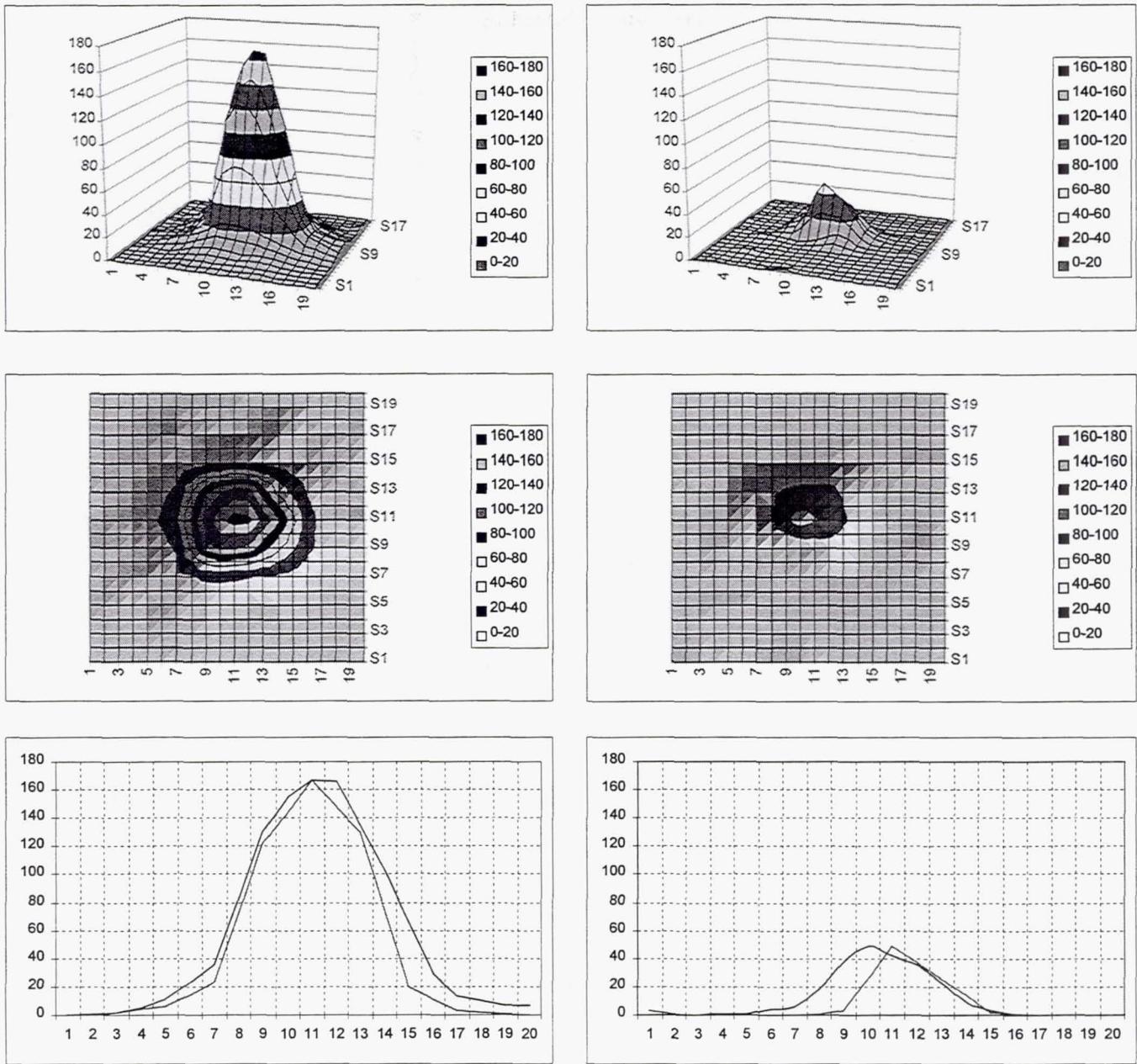
Fig. 5 Point spread functions

POINTING AND TRACKING

Autonomous Attitude Recognition

The star recognition algorithm needs as input the estimated coordinates of the observed target within ≈2° (ref. 3, 4). The system loads from the on-board catalog the stars around the observing direction and compares them with stars within the acquired FoV. Before comparison the catalog stars are projected on the CCD plane. The program looks for a one-to-

one correspondence between measured interangles and corresponding interangles calculated from the catalog stars. Two interangle tables are built for the acquired and catalog stars. An hypothesis of correspondence between stars listed in the two tables is performed. This hypothesis is accepted or rejected by the orientation algorithm. In the case of rejection another hypothesis of correspondence is made, and the procedure is repeated. The algorithm minimizes the distance between acquired stars and the corresponding ones determined from the catalog.

The on-board stellar catalog is derived from the SAO catalog and contains 15945 stars brighter than the 7th magnitude. (ref. 5). A failure in determining the orientation of the platform occurs when less than three stars are present in the detector FoV. The simulation performed using the Uvstar configuration parameters shows that this happens 0.6% of times.

Pointing and Tracking Modes

The system allows different pointing and tracking modes. Two operating modes using the Finder are available during the pointing phase: the attitude mode, where the right ascension and declination of the observing target have to be provided for operating the attitude recognition, and the star mode, where the brightest or the nearest target in the FoV is chosen. When the system moves the platform close to the selected direction the tracking phase begins. The tracking phase allows different options: attitude algorithm, triangulation algorithm with three or four stars, tracking with a bright target (this algorithm is also used with the Tracker telescope).

During the tracking it is possible to change the observing direction in terms of fraction of pixel in order to align the system or to observe different regions of extended sources. Other commands allow to change the intensifier gains and the tracking CCD acquisition period.

The system includes capabilities for independent target acquisition and tracking: it is possible to program a set of commands to be executed at a given MET (Mission Elapsed Time). During the STS-95 mission a few observations were performed successfully in this way. This occurred when the Low Rate channel was not available. When the Medium rate was also unavailable both tracking telescope images and science data are recorded in the DRU (Data Recorded Unit), that can store up to 500 Mbytes of data.

Tracking Control

The control system has to maintain the target on the spectrograph slit independently on the Shuttle oscillations. A basic scheme of the tracking control loop for one of the tracking telescopes is shown in Fig. 6. The offset angle α, corresponding to the observing direction of the main telescope with respect to the detector center, is defined through the instrument alignment.

At a time t the system recognizes the target position on the tracking telescope that corresponds to an angle α_M. The difference $(\alpha - \alpha_M)$ gives an estimation of the error on the distance. The control system sends this value to the motors and brings back the target to the spectrograph slit.

We recall that one pixel on the Finder CCD corresponds to 60 arc-sec FoV, one azimuth axis step corresponds to 0.108 arc-sec and an elevation axis step corresponds to 0.0556 arc-sec. The rows on the Finder CCD are aligned with the azimuth axis, the columns with the elevation axis. During the tracking control, the axes can be moved by using two different movement commands: the position or the velocity. The position movement command brings the platform to the given position with the selected motor velocity and acceleration while the velocity movement changes the motor speed with the given acceleration. During the catching phase the system brings the target in the observing direction by position movement. When the target is close to the observing direction (less that 10 pixels) the tracking phase starts and the system moves the axes by using velocity commands.
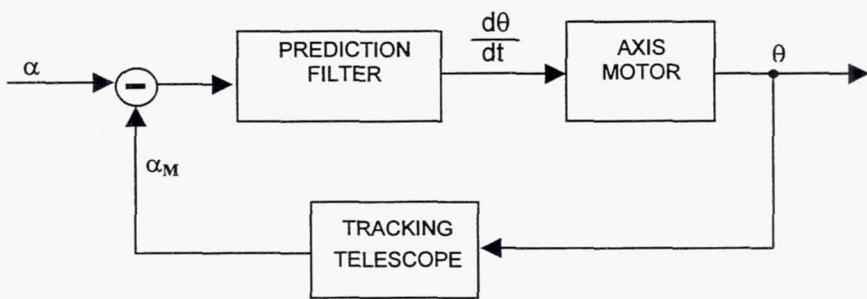
Fig. 6 Tracking control loop

Even supposing a perfect measurement, the target direction is available for moving the axes after a delay as shown in Fig. 7. This delay is the sum of different terms: (1) half the detector integration time (since the centroid algorithm "integrates" over that time and a uniform motion during this time can be assumed), (2) the image transfer time from the CCD to the memory and (3) the time required to compute the correction (mostly due to the process of star searching). A second source of error is related to the finite axis acceleration.

To compensate this error a control filter is adopted during the tracking phase. The Uvstar system allows a selection between two different filters: a PID regulator and a FLS (fast Kalman algorithm). The two filters show a comparable behavior in terms of tracking errors but usually the first filter is used because the second one could oscillate in presence of discontinuities.

The result of a tracking session with no PID regulator is shown in Fig. 8. This is a tracking session dedicated to instrument alignment. In fact, the alignment between the tracking telescopes and spectrographs is performed both on ground during the instrument integration phase, and in flight during the first observation session using bright star. The tracking error is much larger than in the case where PID regulator is adopted.
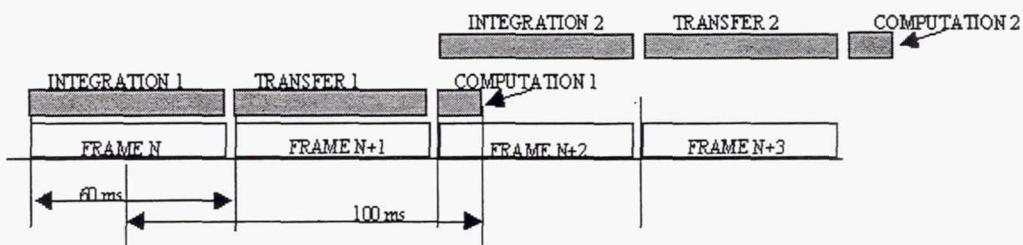

**Fig. 7** Time profile of the control loop
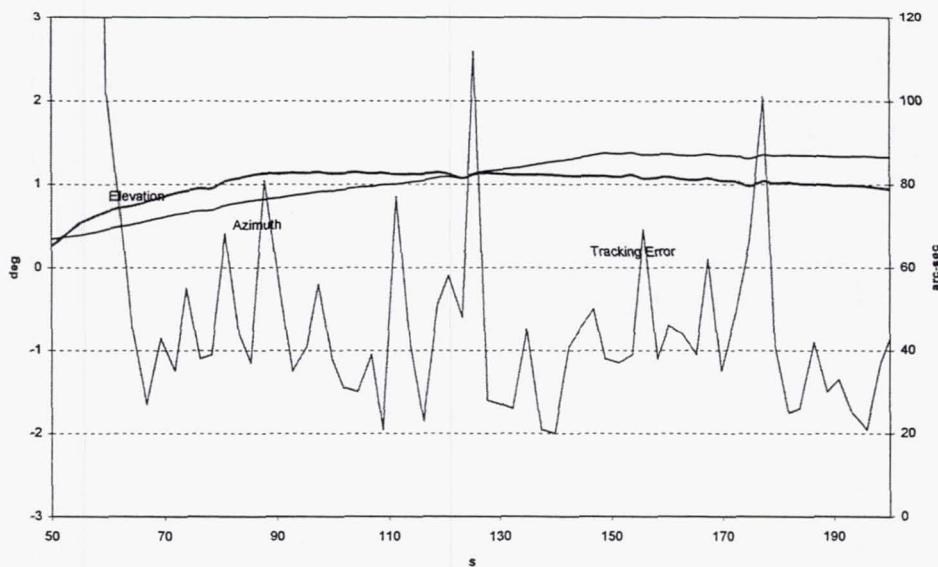
Fig. 8 Tracking session; no filter

TRACKING PERFORMANCE

Most of the tracking was performed during the night part of the orbit. Sun light reflections in the Finder telescope limit the tracking capabilities during day time. The baffle length of 280 mm is the maximum allowed due to the Uvstar position in the Shuttle bay. Day time tracking was possible only with bright objects, i.e. stars with visual magnitude brighter than 2nd.

The list of all the observations performed by the Uvstar telescope during the STS-95 mission are reported in Table 1. There are two sets of observations: celestial and planetary (Jupiter). The celestial observations could be further subdivided in two groups:
- pointed targets (scheduled observations) when the Shuttle assumes a specific attitude in order to allow the telescope pointing in the required direction ;
- "targets of opportunity", observations performed either when the Shuttle is in LVLH attitude and the Shuttle Y axis is oriented towards the pole of the orbit or the Shuttle is in inertial attitude for other reasons.

Table 1 also reports the observation starting MET in days, hours and minutes, the Shuttle attitude the tracking duration in seconds and the tracking mean error in arc-sec defined as the angle the telescope forms with the nominal observing direction. In the last three columns the target name, its visual magnitude and tracking mode (triangulation or star on center) are specified. The targets indicated with asterisk were used for instrument alignment.

268

Table 1 STS-95 Journal of observations

| Nr | MET | | | SHUTTLE ATTITUDE | Tracking | | Target | mgv | |
	DAY	HOUR	MIN		Time (s)	Error (arc-sec)			
1	1	19	43	M50	1325	8.6	εCMa(*)	1.5	soc
2	2	1	53	M50	1321	7.2	(*)		soc
3	2	13	27	M50	611	1.8	αAur	0.1	soc
4	2	14	25	M50	2777	5.2	Jupiter (*)		soc
5	2	16	8	M50	2356	1.1	Jupiter		soc
6	2	17	52	M50	1525	1.9	Jupiter		soc
7	3	2	2	LVLH	46	6.4	HD141318	5.7	triang
8	3	2	8	LVLH	690	5.6	βTrA	2.9	soc
9	3	3	35	LVLH	167	4.1	Tnor	4.6	triang
10	3	3	44	LVLH	162	2.5	βTrA	2.9	soc
11	3	5	19	LVLH	74	5.3			triang
12	3	6	56	LVLH	38	7.5	HD142138	7.9	triang
13	3	6	58	LVLH	61	4.6			triang
14	3	7	4	LVLH	216	7.1	HD142514	5.7	triang
15	3	16	1	M50	2461	2.7	Jupiter		soc
16	3	17	44	M50	1727	2.7	Jupiter		soc
17	3	21	9	M50	557	3.2	αEri	0.5	soc
18	3	21	21	M50	195	2.5			triang
19	3	21	29	M50	202	3			triang
20	3	22	38	M50 (SEH)	606	3.1			triang
21	3	23	51	M50	2869	2.3	Jupiter		soc
22	4	3	18	M50	828	6.9	F9	13.2	triang
23	4	3	35	M50	1075	2.3	αEri	0.5	soc
24	4	4	58	M50	236	8.5	HD200856	6.7	triang
25	4	6	20	M50	822	5.3	βLyr	3.2	soc
26	4	6	36	M50	402	4.9	RingNeb	15	triang
27	4	7	54	M50	380	3.2	8Lyr	5.9	triang
28	4	8	4	M50	250	6.19	HD174179	6.1	triang
29	4	8	11	M50	473	4.6	γLyr	3.2	soc
30	4	17	43	M50	1706	1.9	Jupiter		soc
31	4	19	38	LVLH	347	3.3	HD133792	6.3	triang
32	4	19	46	LVLH	171	6.2	HD131058	6.1	triang
33	4	20	55	LVLH	218	7.8	βCir	4.1	triang
34	4	21	6	LVLH	250	4.6	HD135160	5.7	triang
35	4	22	54	LVLH	113	2.2			triang
36	5	1	44	LVLH	70	4.1	αCir	3.2	soc
37	5	3	18	M50	268	6.6	HD226676	8.7	triang
38	6	1	50	M50	878	2.2	Jupiter		soc
39	6	3	32	M50	878	2.9	αAur	0.1	soc
40	6	3	48	M50	484	6.4			soc
41	6	4	50	M50	1601	2.4	εCma	1.5	soc
42	6	12	32	M50	2607	1.5	Jupiter		soc
43	6	14	5	M50	2580	1.5	Jupiter		soc
44	6	16	16	M50	416	5.6	MXPup	4.8	triang
45	6	17	28	M50	1676	2.1	Jupiter		soc
46	7	17	23	M50	1345	2.1	Jupiter		soc
47	7	19	7	M50	673	1.5	Jupiter		soc
48	7	23	20	M50	950	5.3	βLyr	3.2	soc
49	7	23	42	M50	747	2.7	8Lyr	5.9	triang
50	8	0	14	M50	1182	5.6	HD68450	6.5	triang
51	8	3	18	M50	1499	4.5			triang
52	8	4	38	M50	2363	5.7	SDor	10	triang

269

In Table 2 we summarize the tracking performances during the STS-95 mission. Tracking duration and the corresponding error are reported for Jupiter and celestial observations separately and jointly.

Table 2 Performances

	Jupiter	Celestial	All	
Tracking sessions	13	39	52	
Total observation time	420	327	747	min
Mean tracking error	2.31	4.89	3.73	arc-sec
Mean tracking error without alignment phases	**1.95**	**4.48**	**3.35**	**arc-sec**
Mean tracking session duration	32.3	8.4	14.4	min
Longest observation	47.8	39.4	47.8	min
Shortest observation	11.2	0.6	0.6	min

Fig. 9 and Fig. 10 show the tracking error (arc-sec) and the position of the two axes (degrees) as a function of time corresponding to two tracking sessions. The first one corresponds to a Jupiter observation (inertial) and the second to a celestial observation (HD133792) with the Shuttle in LVLH attitude.

The first 35 seconds of the Jupiter tracking session are expanded in Fig. 11: this period corresponds to the catching phase. At the beginning (T_A) the system find the target 0.9 deg from the observing direction. With a mean velocity of 210 arc-sec/s, after 15 seconds (T_B) the target is moved close to the observing direction (110 arc-sec) and the tracking phase starts. After 30 seconds (T_C) the tracking is stable with errors less than 10 arc-sec. A similar rapid catching is present in most of the celestial tracking sessions.

Fig. 12 analyzes the tracking behavior of the F9 (a compact galaxy) observation (MET 4/3:18) during an inversion of the elevation axis (due to a Shuttle roll oscillation) that occurred at time 127 s. Before the inversion the velocity of the elevation axis was –34 arc-sec/s and after the inversion was 17 arc-sec/s. The filter brought the tracking error below 10 arc-sec in approximately 10 s. The tracking updating period was 500 ms, the default value during the mission.
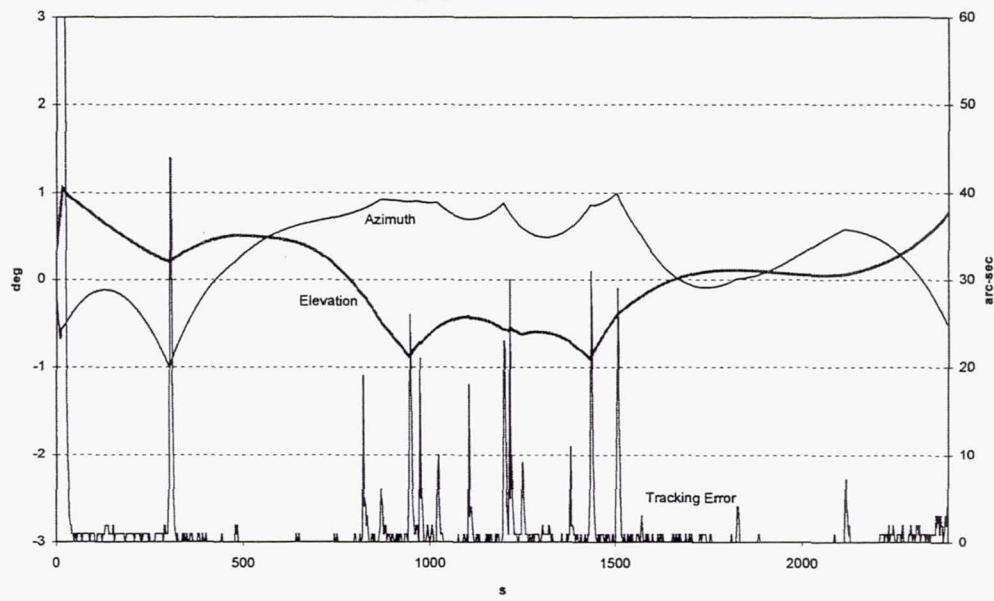
Fig. 9 MET 2:16:08 ; Tracking error curve. Jupiter
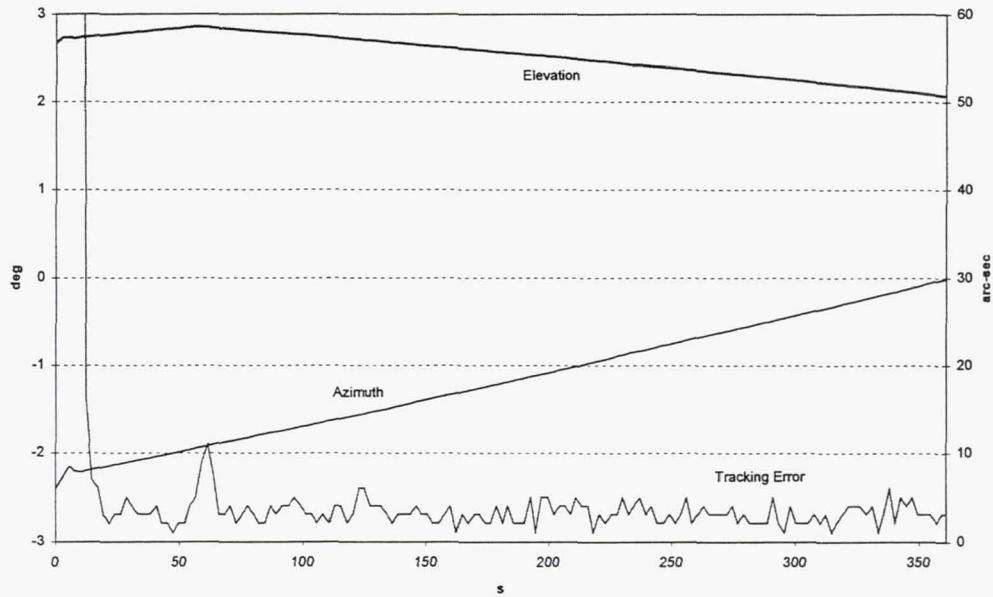
**Fig. 10** MET 4:19:38 ; Tracking error curve. HD 133792
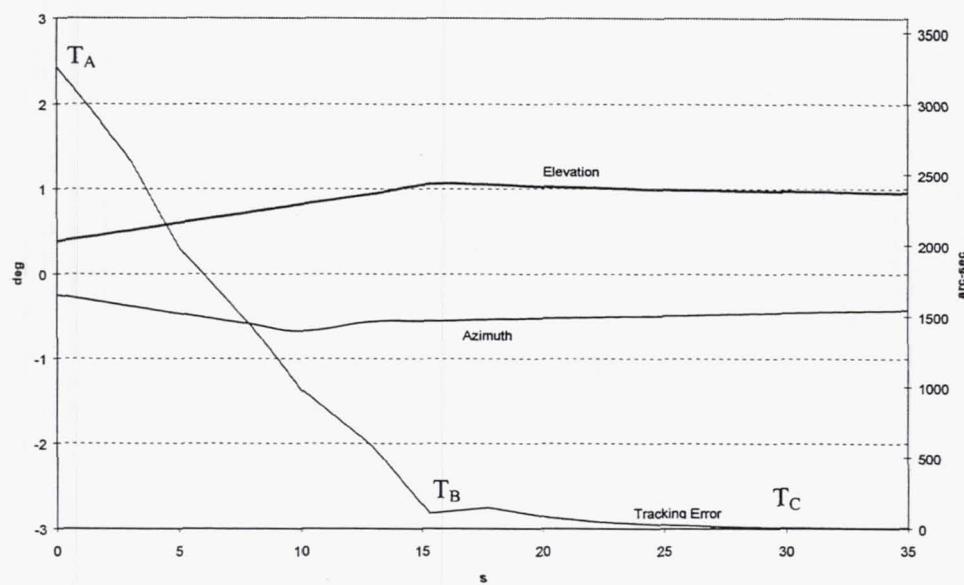
**Fig. 11** End of catching phase and beginning of tracking
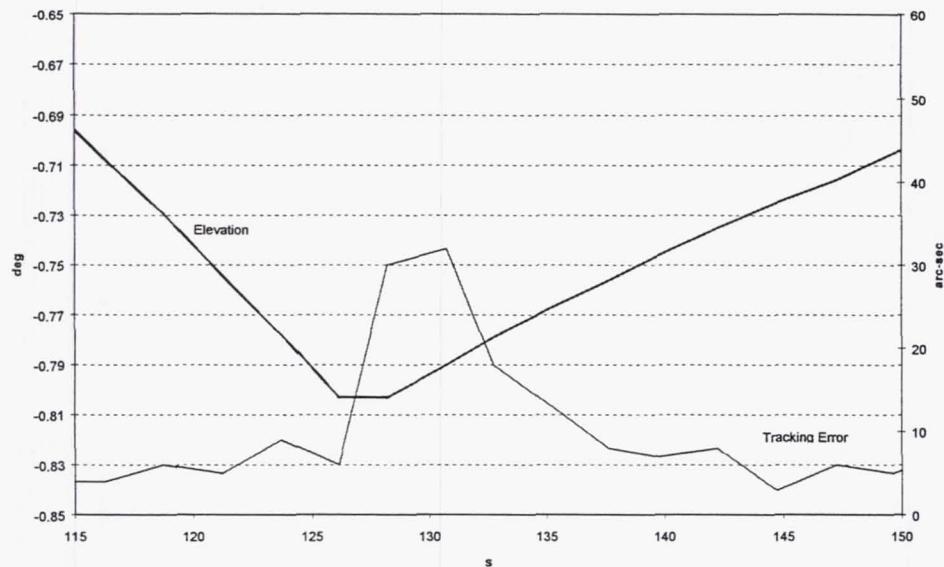
Fig. 12 Tracking curve of the external galaxy F9

CONLUSIONS

The pointing and tracking system of Uvstar based on the wide angle Finder telescope performs quite well under different conditions such as Shuttle inertial and selected LVLH attitudes.

Two upgrades of this system are foreseen both for use on the International Space Station (ISS). The second generation Carso pointing and tracking system will be mounted on the Italian ISS payload UVISS (Ultraviolet Italian Space Surveyor). A modified version of the system, called AMICA (Astro Mapper for Instrument Check of Attitude), will support the Italian mission SPORT. Both UVISS and SPORT will be mounted on the ISS Express Pallet.

REFERENCES

1. R. Stalio, B. R. Sandel, and A.L. Broadfoot, Uvstar, an imaging spectrograph with telescope for the Shuttle Hitchhiker-M platform,1993 Shuttle Small Payloads Symposium

2. B.R. Sandel, L.A. Broadfoot, R. Stalio, UVSTAR, An Imaging Spectrograph With Telescope For The Hitchhicker-M Platform, Optical Engineering, December 1993, Vol 32 Nr 12

3. T.E. Strikwerda and J.L. Junkins, "Star pattern recognition and spacecraft attitude determination", Phase II, U.S. Army Corps of Engineers, Engineer Topographic Laboratory, Report for the period Oct. 1978-Sep.1979

4. F. De Carlo, R. Stalio, P. Trampus, A.L. Broadfoot, B. R. Sandel, and G. Sicuranza, The star identification, pointing and tracking system of Uvstar, an attached payload instrument for the Shuttle Hitchhiker-M platform, 1993 Shuttle Small Payloads Symposium

5. F. De Carlo, R. Stalio, P. Trampus, L. A. Broadfoot, B.R. Sandel, G. Sicuranza, Description And Analysis Of An Algorithm For Star Identification, Pointing, and Tracking Systems, Optical Engineering, August 1994, Vol 33 Nr 8

Page intentionally left blank

THE CONTRIBUTION OF THE SOLCON INSTRUMENT TO THE LONG TERM TOTAL SOLAR IRRADIANCE OBSERVATION

S. Dewitte, A. Joukoff and D. Crommelynck
Royal Meteorological Institute of Belgium

R. B. Lee III
NASA Langley Research Center

R. Helizon
Jet Propulsion Laboratory

ABSTRACT

On century time scales, the variation in the total solar irradiance received by the earth is believed to be a major climate change driver. Therefore accurate and time stable measurements of the total solar irradiance are necessary. We present the latest contribution of the SOLar CONstant (SOLCON) instrument to these measurements, namely its measurements during the International Extreme Ultraviolet Hitchhiker (IEH) 3 space shuttle flight, and its results: the verification of the ageing of the Earth Radiation Budget Satellite (ERBS), and the measurement of the Space Absolute Radiometric Reference (SARR) adjustment coefficients for the Variability of solar IRradiance and Gravity Oscillations (VIRGO) radiometers.

INTRODUCTION

The influx of solar radiative energy is almost exclusively the only energy source for the earthern weather processes. Therefore the long term monitoring of the total solar irradiance is necessary for a correct approach to the "global climate change" question. The monitoring has to be precise in order to measure the solar climate forcing with an error that is at least one order of magnitude lower than the magnitude of the currently studied antropogenic climate forcings.

Making long term total solar irradiance measurements which which remain accurate, is very challenging. Indeed space instruments are subject to ageing, do not necessarily perform overlapping observations, and have limited absolute accuracy compared to the solar irradiance variations that have to be measured..

Therefore a strategy has actually been developed to help to improve this situation. Besides the radiometers operating for long time periods on unretrievable carriers, absolute radiometers have been used periodically for short term space fligths. The measurements of the short term measuring radiometers are used as reference points to verify the ageing of the long term measuring radiometers and to compare their observations.

Very fortunately 6 radiometers made simultaneous solar irradiance measurements during the ATLAS 2 flight period in April 1993. As the dispersion on the observed Total Solar Irradiance (TSI) by single instruments, $S_{instrument}(t)$, was mostly within the range of $\pm$ 0.1 percent, the Space Absolute Radiometric Reference (SARR) (ref. 1) could be defined through a set of instrument adjustment coefficients $a_{instrument}$, so that the adjusted measurements $a_{instrument}S_{instrument}(t)$ provide the same value for the different instruments.

Of these 6 radiometers 4 have been retrieved representing 6 radiometric channels. They can be compared before and after each flight by comparison on ground with absolute radiometers characterised for air and vacuum operation. This allows to control their stability and metrological coherence.

We present the results of the latest space shuttle flight of the SOLar CONstant (SOLCON) radiometer, which is one of the absolute radiometers that was retrieved after the ATLAS 2 space shuttle flight.

SYMBOLS

$S_{instrument}(t)$	time series of the Total Solar Irradiance (TSI) measurement of a single instrument
$a_{instrument}$	the Space Absolute Radiometric Reference (SARR) adjustment coefficient for a single instrument
σ	standard deviation
$S_{SARR}(t)$	SARR TSI time series (eq. 4)

THE SOLCON TYPE RADIOMETER

The SOLCON type radiometer (ref. 2) is a differential absolute solar radiometer developed at the Royal Meteorological Institute of Belgium .

Its radiometric core is formed by two blackened cavities constructed side by side on a common heat sink. In between each cavity and the heat sink a heat flux transducer is mounted. The difference between the two transducers' outputs gives a differential heat measurement, in which the common part of the thermal surrounding radiation seen by the two cavities is eliminated. By the symmetrical construction and good insulation thermal asymmetry is minimised.

Both cavity channels are equipped with a shutter in front of them, by which the sunlight can be kept away from (closed shutter) or allowed into (open shutter) the cavity. In the open shutter phase, solar radiative power flows into the cavity through a precision aperture and is absorbed at the bottom of the cavity.

Besides solar radiative power, electrical resistive power can be dissipated in the cavity. During the design of the cavities, carefull attention has been paid to obtain maximally corresponding spatial locations and distributions for the solar and the electrical power.

Equilibrium between the two cavity heat fluxes is maintained by regulating, using a servo system, the electrical power in one of the two cavities. In the default measurement sequence a constant electrical power is fed into one cavity, the "reference" cavity, while its shutter remains closed. The electrical power in the other cavity, the "measurement" cavity, is regulated continuously, while its shutter sequentially opens and closes (both open and close phases take 90 seconds). When the instrument is pointed to the sun, the equilibrium electrical power in the measurement cavity drops proportional to the absorbed solar power when going from the closed to the open phase.

Accurate electrical power measurements are obtained by separate measurement of the voltage over and the current through both cavity heating resistors. The electrical measurement chains are calibrated continuously using six reference voltages, derived from a single, temperature stabilised, reference voltage. The resistance values of the heating resistors, which were choosen maximally stable with temperature, are used as quality indicators of the electrical measurements.

The basic measurement of the solar radiative flux is the drop in the measurement cavity electrical power divided by the precision aperture area. To this basic quantity corrections have to be applied for the optical characteristics of the cavity (e.g. diffraction around the precision aperture borders, absorption coefficient of the cavity, ...) and for the thermal emission of the shutters. The optical characteristics are part of the parameters determined during the pre-flight characterisation phase. The thermal emission of the shutters is measured in space during deep space pointing. The optical ageing of the instrument is verified in space by

periodic comparison between measurements from both cavities. For this purpose, the total exposure to the sun of the right side cavity is systematically kept much lower than the one of the left side cavity.

Table 1 summarises the space flights of the RMIB radiometers. From these radiometers, SOLCON II and SOVA 1 have the same characteristics, summarised in Table 2.

OBSERVATIONS DURING THE IEH-3 MISSION

The International Extreme ultraviolet Hitchhiker (IEH) 3 payload on the STS-95 shuttle flight is the third of five flights dedicated to sun and earth observations. SOLCON was one of the experiments flown on the IEH-3 pallet from 29/10/1998 to 7/11/1998. The SOLCON timeline included 11 dedicated and 5 non dedicated solar observation periods. Deep space pointing, used by SOLCON for the shutter thermal emission measurement, was obtained before and after most of the solar measurements. With its sun pointing monitor SOLCON continuously measured the high quality of the space shuttle attitude control. During the sun observations mostly a pointing accuracy better than 1 degree was achieved.

The temperature of the base of the radiometer was maintained between 6 and 12 $^\circ$C, the temperature of its top was never lower than 0 and never higher than 20 $^\circ$C.

The thermal emission of the shutters is measured in space during deep space pointing. The temperature of the shutters varied between -25 and 25 $^\circ$C.

One person operated SOLCON at the Goddard Space Flight Center supported by 6 collegues running the Space Remote Operation Centre of the Royal Meteorological Institute of Belgium around the clock. Operations included real time data reception and processing, monitoring of the results and issueing remote commands.

Data and voice communications happened through an ISDN line with internet as a backup for data communication.

DETERMINATION OF THE SARR ADJUSTMENT COEFFICIENTS OF THE VIRGO RADIOMETERS

Coincident with the SOLCON observations during IEH-3, the two types of radiometers which are part of the VIRGO(Variability of IRradiance and Gravity Oscillations)/SOHO(SOlar and Helioseismologic Observatory) package (ref. 3), the DIARAD (DIfferential Absolute RADiometer) and the PMO(Physikalisches-Meteorologisches Observatorium) radiometer types, made continuous measurements of the total solar irradiance.

Figure 1 shows the SARR adjusted SOLCON measurements together with the unadjusted level 1 DIARAD-L and level 2 PMO-VA measurements of the total solar irradiance. For DIARAD-L level 1 data - i.e. **absolute data without any correction defined after launch** - is used, for PMO-VA level 2 data - i.e. data obtained after the post-launch corrections defined in ref. 4 - is used. The SOLCON measurements are given as one mean value with a one sigma error bar for every solar period. The DIARAD-L and PMO-VA are given as hourly mean values.

The SARR coefficients of the VIRGO radiometers are estimated by comparison with the SARR adjusted SOLCON measurements. Since the DIARAD-L measurements have a lower variability than the PMO-VA measurements, in a first step this comparison is done for DIARAD-L.

For every time correspondent level 1 DIARAD-L measurement, $S_{DIARAD-L}(t_i)$, and SARR adjusted SOLCON measurement, $a_{SOLCON-L/RS}SOLCON-L/R(t_i)$ [1], an estimate $a_{SOLCON-L/RS}SOLCON-L/R(t_i) \, S_{DIARAD-L}(t_i)$ of the DIARAD-L SARR adjustment coefficient is obtained.

From n time correspondent measurements, the best estimate of the DIARAD-L SARR adjustment coefficient, $a_{DIARAD-L}$, is the mean value of the individual estimates.

$$a_{DIARAD-L} = \Sigma_{i=1,...,n} \, a_{SOLCON-L/RS}SOLCON-L/R(t_i) \, S_{DIARAD-L}(t_i) \, / \, n = \mathbf{1.000025} \qquad (1)$$

The standard deviation, $\sigma_{DIARAD-L/SOLCON}$, around this mean value is given by equation 2 . This value is indicative of the noise on the comparison of instantaneous DIARAD-L and SOLCON measurements. It is constituted of DIARAD-L and SOLCON instrument noise, as well as coregistration noise.

$$\sigma_{DIARAD-L/SOLCON}^{2} = \Sigma_{i=1,...,n} \left(a_{SOLCON-L/RS}SOLCON-L/R(t_i) \, S_{DIARAD-L}(t_i) \, - \, a_{DIARAD-L} \right)^{2} /n = \mathbf{0.000127}^{2} \qquad (2)$$

The one sigma uncertainty $\sigma_{aDIARAD-L}$ with which $a_{DIARAD-L}$ is determined, is given by equation 3.

$$\sigma_{aDIARAD-L}^{2} = \sigma_{DIARAD-L/SOLCON}^{2} \, / \, n = \mathbf{0.000010}^{2} \qquad (3)$$

Table 3 lists the DIARAD SARR results when only the dedicated solar period measurements are used, when only the non dedicated solar period measurements are used, and when both are used.

The PMO-VA SARR adjustment coefficient is determined trough the mean ratio of DIARAD-L to PMO-VA. This mean ratio can be determined with low uncertainty if a large number of coincident measurements are used. For the eight full days during which SOLCON was active and during which complete DIARAD-L and PMO-VA were available the ratio of the mean TSI value measured by DIARAD-L and of the mean TSI value measured by PMO-VA was **1.000254** . The PMO-VA SARR adjustment, a_{PMO-VA} is determined as 1.000025 * 1.000254 = **1.000279** .

VERIFICATION OF THE ERBS SOLAR RADIOMETER STABILITY

The Earth Radiation Budget Satellite (ERBS) total solar irradiance monitor (ref. 5) has been used for long term solar measurements since 1985. Its SARR adjustment coefficient has been determined in April 1993 during the ATLAS 2 space shuttle flight. By re-comparison with the SARR adjusted SOLCON measurements during the IEH-3 space shuttle flight, it is possible to verify whether the ERBS sun monitor radiometer has been subject to ageing or drifts during the 5 year period between the ATLAS 2 and IEH-3 space shuttle flights. The comparison is done through the VIRGO radiometers for optimal time interpolation of the SARR SOLCON measurements.

Figure 2 shows the SARR adjusted ERBS, level 1 DIARAD-L and level 2 PMO-VA measurements of the total solar irradiance during the IEH-3 mission. The ERBS measurements are given as one mean value with a one sigma errorbar for every observation period. The DIARAD-L and PMO-VA are given as hourly mean values.

---

[1] The notation $a_{SOLCON-L/R}S_{SOLCON-L/R}(t_i)$ for a SARR adjustment SOLCON measurement is used to indicate either a SARR adjusted SOLCON-L measurement, $a_{SOLCON-L}S_{SOLCON-L}(t_i)$, or a SARR adjusted SOLCON-R measurement, $a_{SOLCON-R}S_{SOLCON-R}(t_i)$.

One can see that for all ERBS observation periods in figure 2, except for the first one, the SARR adjusted DIARAD-L and PMO-VA TSI values correspond to the SARR adjusted ERBS TSI values within the one sigma uncertainty interval of the ERBS measurements.

The comparison results are given in Table 4. The ratio of the SARR adjusted ERBS TSI measurements, with SARR coefficient determined in April 1993, to the SARR adjusted VIRGO TSI measurements, with the newly obtained SARR coefficient valid in November 1998, does not differ significantly from one. Thus the ERBS radiometer has not aged significantly from 1993 to 1998. The one sigma uncertainty level is 140 ppm in relative numbers, corresponding to 0.2 Wm^{-2} in absolute numbers.

UPDATED SARR TOTAL SOLAR IRRADIANCE DATA SET

With the newly obtained SARR adjustment coefficients for the VIRGO radiometers, the previously defined SARR total solar irradiance time series (ref. 6,7), can be extended. The daily mean SARR total solar irradiance time series, $S_{SARR}(t)$, is defined as the mean of all avilable daily mean SARR adjusted total solar irradiance measurements.

$$S_{SARR}(t) = \Sigma_{i=1,...,n} \, a_i S_i \, / \, n \qquad (4)$$

Figure show the updated SARR TSI times series, including the VIRGO radiometer measurements SARR adjusted with their newly obtained SARR adjustment coefficients.

CONCLUSIONS

In order to reach the long term total solar irradiance monitoring stability required for climate change studies, a carefull observation strategy has to be implemented. Continuously observing instruments need to be combined with periodically used short term observing instruments.
The latest contributions of the periodically used short term observing SOLCON instrument are:

- The November 1998 level 1 DIARAD-L SARR adjustment coefficient is 1.000025 with a one sigma uncertainty of 10 ppm.
- The November 1998 level 2 PMO-VA SARR adjustment coefficient is 1.000279 with a one sigma uncertainty of 10 ppm.
- The ERBS TSI radiometer has not aged significantly since 1993 within the one sigma uncertainty level of 140 ppm.
- The daily mean SARR TSI time series has been extended until end 1998, using the newly obtained DIARAD-L and PMO-VA SARR coefficients.

As soon as the ACRIM II data will be available the same exercice as done for the ERBS sun monitor will be performed.

REFERENCES

1. D. Crommelynck, A. Fichot, R.B. Lee III and J. Romero, *First realisation of the Space Absolute Radiometric Reference (SARR) during the ATLAS 2 flight period*, Advances in Space Research, vol. 16 no. 8, pp. 17-23, 1995.
2. D. Crommelynck and V. Domingo, Solar irradiance observations, Science, vol. 225, pp. 180-181, 1984.

3. C. Fröhlich, D. Crommelynck, C. Wherli, M. Anklin, S. Dewitte, A. Fichot, W. Finsterle, A. Jimenez, A. Chevalier and H. Roth, *In-flight performance of the VIRGO solar irradiance instruments on SOHO*, Solar Physics, vol. 175, pp. 267-286, 1997.

4. M. Anklin, C. Fröhlich, W. Finsterle, D. Crommelynck and S. Dewitte, *Assesment of the degradation of the VIRGO radiometers onboard SOHO*, Metrologia, 1998.

5. R. B. Lee III, B. R. Barkstrom and R. D. Cess, *Characteristics of the earth radiation budget experiment solar monitors*, Applied Optics, vol. 26, pp. 3090-3096, 1987.

6. D. Crommelynck and S. Dewitte, *Solar constant temporal and frequency characteristics*, Solar Physics, vol. 173, pp. 171-191, 1997.

7. S. Dewitte, D. Crommelynck and A. Joukoff, *Maintenance of a long term solar irradiance data series*, Proceedings of 31st ESLAB conference, 1997.

TABLES

Table 1 : Space flights of the RMIB radiometers. SOVA 1 and SOLCON II are exact copies of each other.

Spacecraft	Date (number of days)	Mission	Instrument
STS-9	28/11/1983 (10)	Spacelab 1 (NASA/ESA)	SOLCON I
STS-45	24/03/1992 (9)	ATLAS 1 (NASA)	SOLCON II
STS-46/57	31/07/1992 - 21/06/1993	EURECA (ESA)	SOVA 1/SOVA
STS-56	07/04/1993 (9)	ATLAS 2 (NASA)	SOLCON II
STS-66	03/11/1994 (10)	ATLAS 3 (NASA)	SOLCON II
Atlas-IIAS	02/12/1995 (continues)	SOHO (ESA/NASA)	DIARAD/VIRGO
STS-85	07/08/1997 (13)	Hitchhiker/TAS-01 (NASA)	SOVA 1
STS-95	29/10/1998 (10)	Hitchhiker/IEH-03 (NASA)	SOLCON II

Table 2 : Characteristics of the SOVA 1 type radiometer (default measurement mode).

Measured quantity	Total irradiance (Wm^{-2})
Number of reference voltages	6
Cavity type	Cylindric, diffuse black
Diameter precision aperture	1 cm
Slope angle	2.5 °
Pointing device	4 quadrant
Solar sampling period	3 minutes
Duty cycle	50 %

Table 3.

Solar periods	n	$a_{DIARAD-L}$	$\sigma_{DIARAD-L/SOLCON}$	$\sigma_{aDIARAD-L}$
Dedicated	126	1.000026	0.000126	0.000011
Non dedicated	36	1.000024	0.000131	0.000022
Combined	162	1.000025	0.000127	0.000010

Table 4.

| Number of observations	Mean ratio SARR ERBS to SARR DIARAD-L	Mean ratio SARR ERBS to SARR PMO-VA	Observed standard deviation	Uncertainty of ratio
13	0.99993	0.99995	0.00047	0.00014
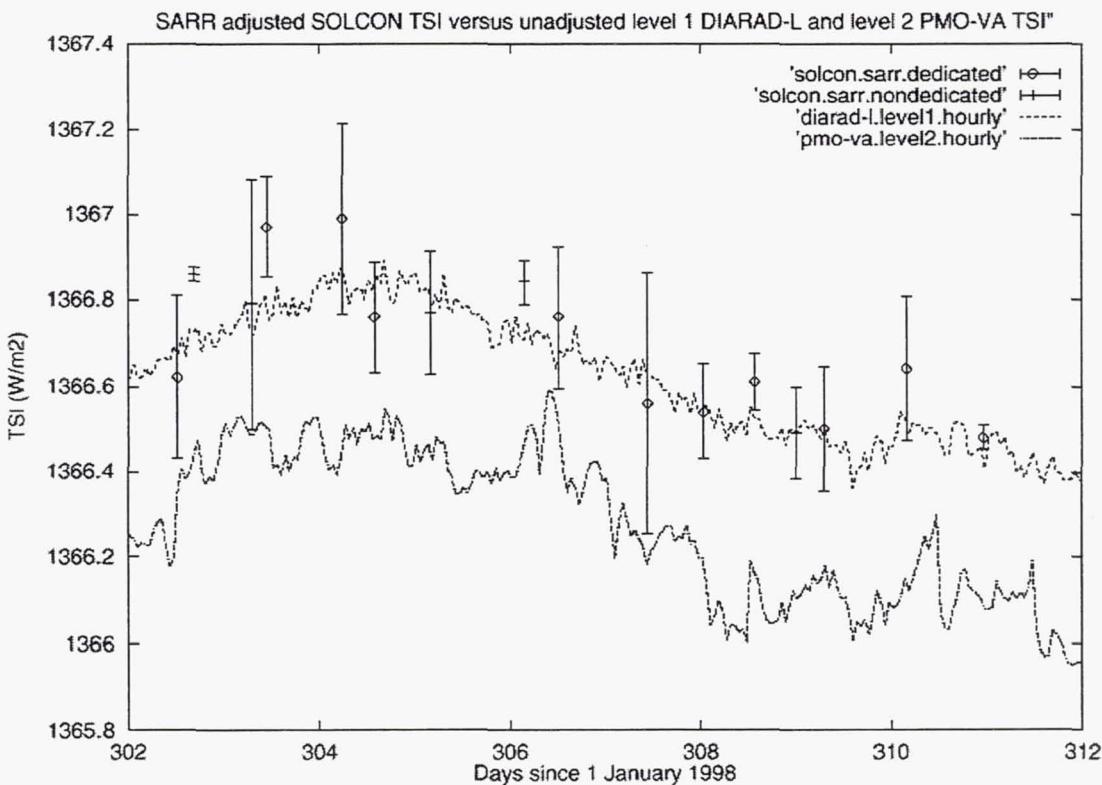
Figure 1 : Correspondent SARR adjusted SOLCON TSI measurements and unadjusted level 1 DIARAD-L and level 2 PMO-VA TSI measurements. The SOLCON measurements are given separately for the 11 dedicated and the 5 non dedicated solar observation periods during the IEH-3 space shuttle flight. During solar periods 2, 6 and 10 (partly) the right channel of SOLCON was used. During the rest of the solar periods the left channel of SOLCON was used. The hourly mean level 1 DIARAD-L measurements are given by the upper continuous curve, the hourly mean level 2 PMO-VA measurements are given by the lower continuous curve.
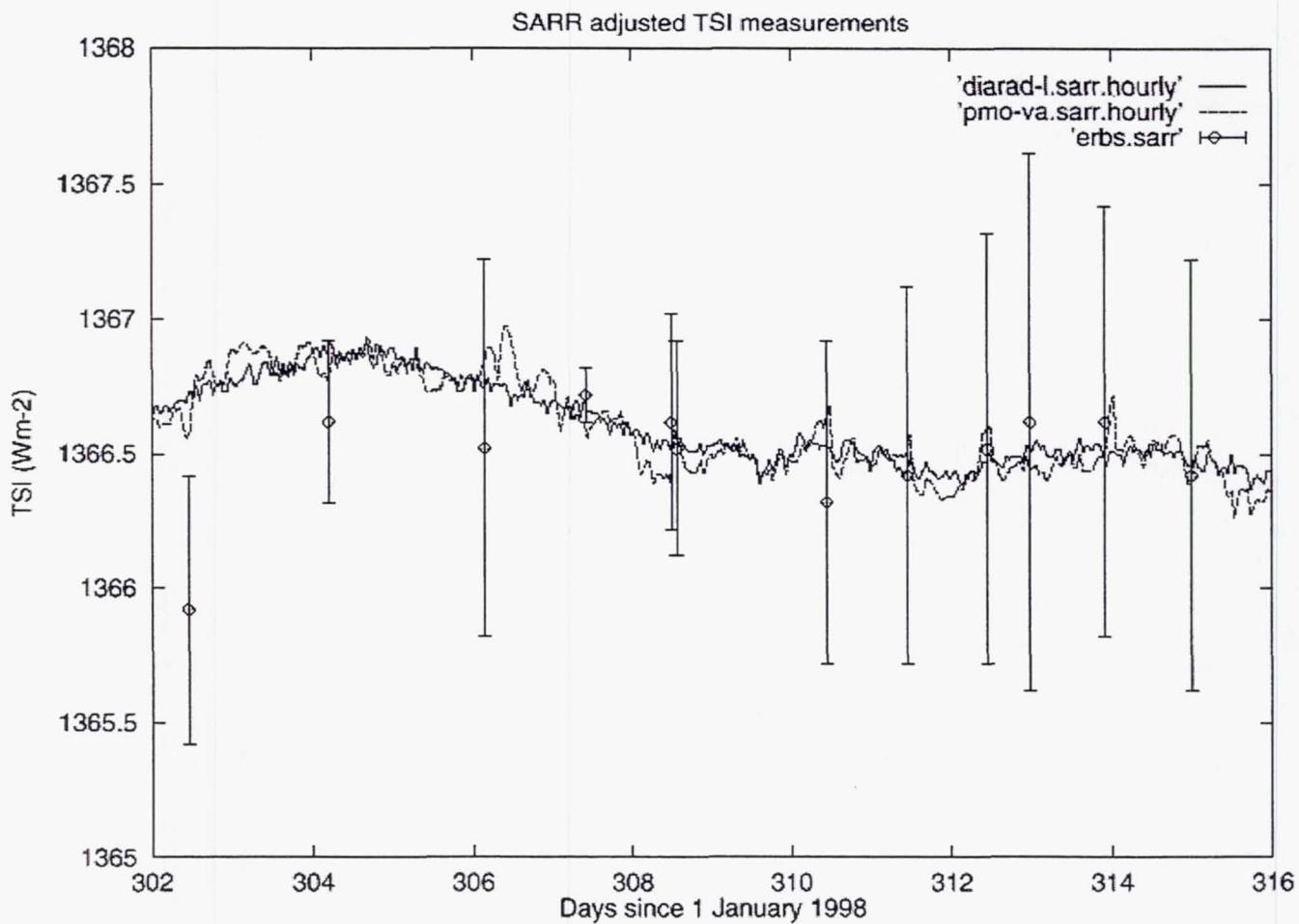
Figure 2 : Correspondent SARR adjusted hourly mean DIARAD-L, PMO-VA and instantaneous ERBS TSI measurements. For the DIARAD-L and PMO-VA radiometers the newly obtained SARR adjustment coefficients have been used. For the ERBS radiometer the SARR adjustment defined during the ATLAS 2 space shuttle flight period (April 1993) has been used.
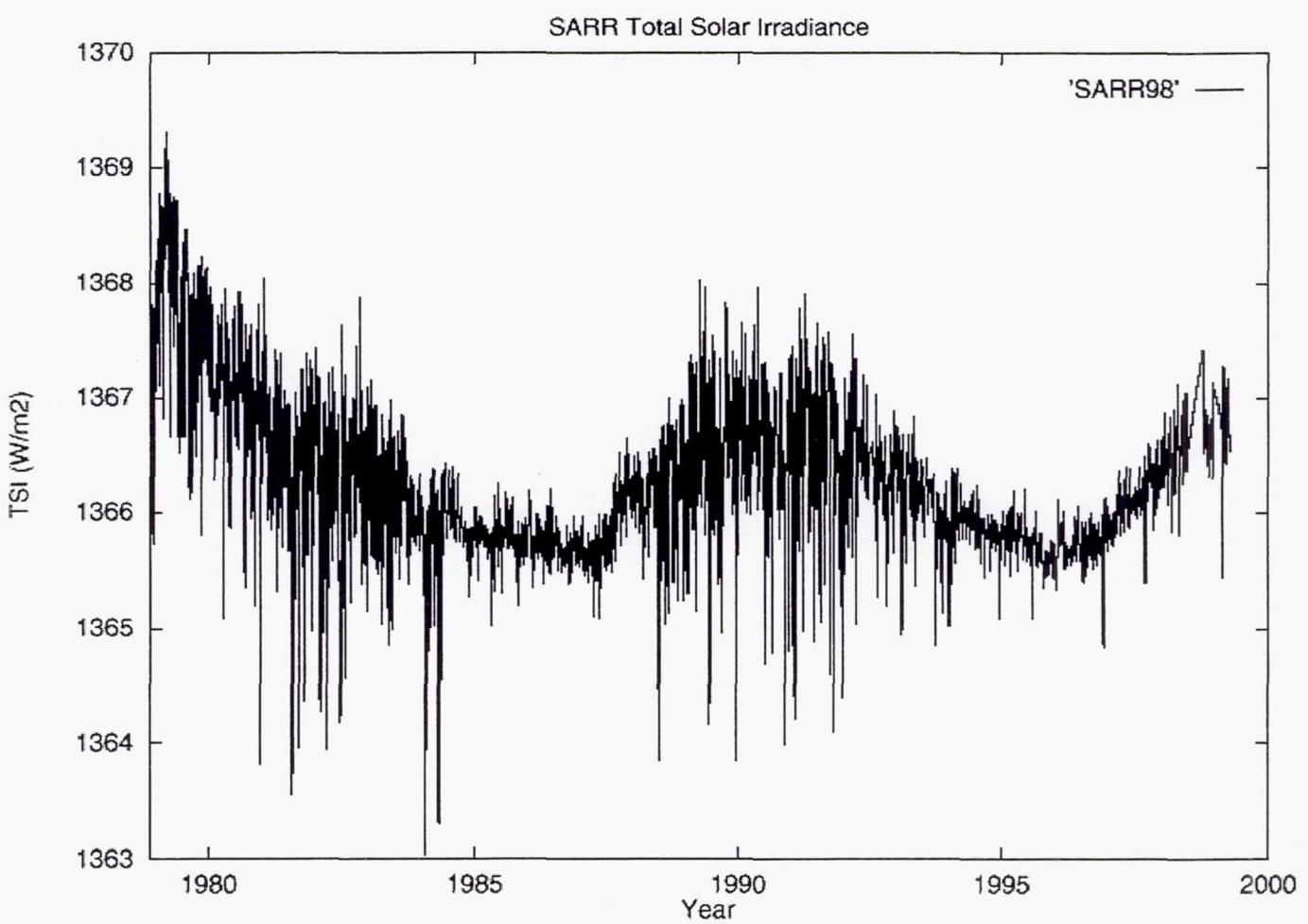
Figure 3 : Updated SARR total solar irradiance series. DIARAD-L and PMO-VA have been added using the newly obtained SARR adjustment coefficients. The data set can be obtained on request at http://estirm2.oma.be.

Page intentionally left blank

PANSAT FUNCTIONAL TESTING SOFTWARE AND SUPPORT HARDWARE

Jim A. Horning
Computer Engineer, Naval Postgraduate School

ABSTRACT

The Petite Amateur Navy Satellite (PANSAT) was successfully launched aboard the STS-95 *Discovery*. PANSAT provides digital store-and-forward communications in a low-Earth orbit, and is a platform for an instructional laboratory. The spacecraft was built and tested at the U.S. Naval Postgraduate School in Monterey, California, by officer students, research staff and faculty. The PANSAT digital hardware was prototyped with various commercial-off-the-shelf (COTS) hardware and software to assist in designing the unique systems which were eventually built and integrated into the spacecraft. This paper presents the hardware and software components used to develop the PANSAT spacecraft. Details of the evolution of design and testing are explained as well as the tools to complete the final functional verification performed during payload integration. The concepts presented are applicable to generic space flight experiments.

INTRODUCTION

PANSAT is a small satellite for digital store-and-forward communications in the amateur frequency band. It features a direct sequence spread spectrum differentially coded, binary phase shift keyed (BPSK) communication system at an operating frequency of 436.5 MHz. The store-and-forward capability will allow NPS and amateur radio operators to send or receive messages during several short communication windows every day.

The PANSAT project began in 1989 as an educational program for students at the Naval Postgraduate School's (NPS) Space Systems Academic Group (SSAG). The project goal is to provide meaningful and realistic research topics for students in the area of space systems engineering and space systems operations. In doing so, the Space Systems Academic Group has prepared students for space related tasks and has developed an infrastructure of facilities and personnel capable of developing space qualified systems.

The entire PANSAT structure weighs approximately 125 pounds, has a diameter of about 19 inches, and was designed to be launched as a secondary payload from the Space Shuttle via the Hitchhiker Program. PANSAT is a 26-sided polyhedron, as shown in Figure 1 with some of the side panels removed in order to show the interior, a configuration chosen to narrow the range of solar flux because the spacecraft tumbles freely. PANSAT is not stabilized and tumbles freely. The satellite uses an omni-directional antenna system consisting of four quarter-wave-length segments to achieve near uniform signal coverage regardless of PANSAT's orientation.

The design, fabrication, testing, and integration of the entire spacecraft were performed at the Space Systems Academic Group at the Naval Postgraduate School. One of the early design objectives was the ability to easily perform functional testing, starting with the prototype subsystems and extending all the way to the system level integration. This was accomplished by reusing many software test components. The support hardware consisted mainly of a general purpose PC and a power supply. Final integration testing performed at NASA Goddard Space Flight Center (GSFC) required only two laptop computers, a power supply, and a brief-case sized RF/Modem unit.
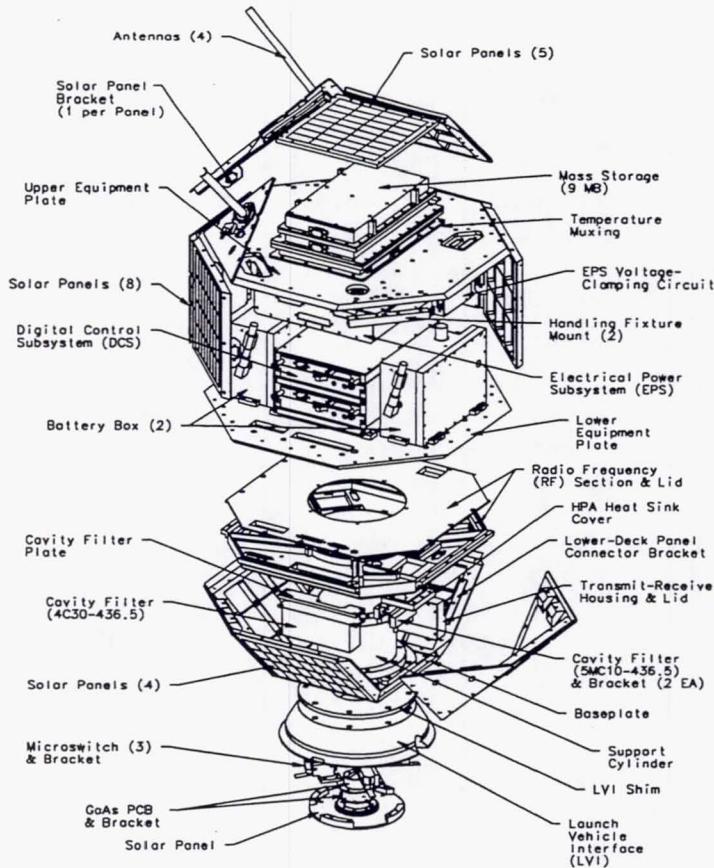
Figure 1. PANSAT Expanded View.

PANSAT ELECTRONIC MODULES ARCHITECTURE

PANSAT electronic modules, as depicted in Figure 2, consist of various subsystems: digital control system (DCS) which includes a computer and the modem, analog temperature multiplexers (TMUX), mass storage (MS) for data and message storage, radio frequency (RF) system for up and down conversion of the communication signals, and the electrical power system (EPS) for the distribution of power on the satellite. Two DCS modules provide a fault tolerant computer and modem pair. Only one DCS is powered and operating at any time.
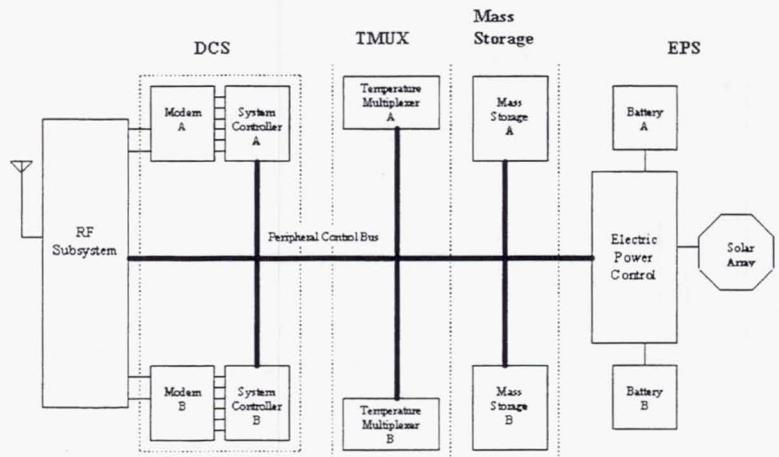

Figure 2. PANSAT Electronic Modules Block Diagram.

Connecting The Electronic Modules Via The Peripheral Control Bus

The PANSAT electronic modules are all interconnected by the peripheral control bus (PCB). The PCB is a power, control, and eight-bit parallel data bus where each module is assigned a particular address. The PCB is controlled by the digital control system (DCS) which is operational (only one DCS is powered up at any time). The active DCS is responsible for asserting the address, data, and control lines of the PCB to perform read and write functions on the electronic modules which are attached to the PCB. The PCB distributes all power control and digital interfaces on the spacecraft. The PCB is implemented with programmable peripheral interfaces (PPI, also known as an 8255); however, analog signals from the TMUX and EPS are sent from those modules directly to an analog input port on the DCS for A/D conversion.

PROTOTYPE HARDWARE AND SUPPORT SOFTWARE

Some early prototypes of PANSAT electronic modules were developed before the DCS existed. These modules were the temperature multiplexing system (TMUX), mass storage unit (MSU), and the electrical power system (EPS). These prototypes began as wire-wrapped modules with the appropriate PCB hardware to allow a common interface which was functionally identical to the final design. Early PCB control was implemented using a National Instruments ATMIO-16 A/D and digital control card available for a PC.

The ATMIO-16 card is capable of accepting multiple analog inputs (for A/D conversion) and has four programmable digital lines which can be used for input and output. Analog data from the TMUX and EPS were connected to this board and allowed simple A/D conversion using National Instrument's LabVIEW® programming system. The digital I/O was used to control the PCB. A special circuit was implemented to allow the ATMIO-16 digital I/O bus to emulate controlling the PCB. Software within LabVIEW was created to allow PCB read and write operations. Power for these modules was provided with a programmable power supply which was connected to the General Purpose Interface Bus (GPIB). The PC with the ATMIO-16 also had a GPIB controller. LabVIEW interfaces were used to control the Hewlett Packard 6653A system DC programmable power supply. The first PANSAT prototype was controlled and tested via a PC running LabVIEW with simple Virtual Instruments (VI) allowing discrete PCB write and read operations, conversion and display of A/D, and the ability to turn on and off the modules via the power supply. This configuration is demonstrated with Figure 3.
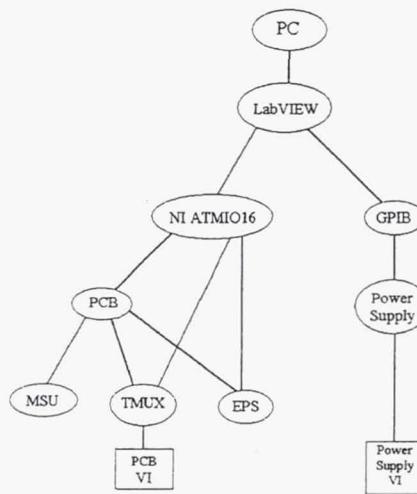

Figure 3. Prototype Support Hierarchy.

LabVIEW was chosen because it is an easy to use and powerful programming tool. It uses a graphical programming language in the form of block diagrams to depict the programming of a system. In addition, LabVIEW offers a rich set of building blocks which makes it very easy to build graphical user interfaces without dealing with the issues of programming these interfaces (Ref. 1). Such a program is called a Virtual Instrument (VI) which consists of a graphical front panel (i.e. the front panel of an instrument which is the interface for a user) and a block diagram (i.e. the internals of the instrument). Although most of the programming was performed by the author, LabVIEW allowed other engineers to comprehend more easily the structure of the algorithms that controlled the PANSAT modules. Thus, the translation from the engineer's need for control and the implementation were similar and allowed more interaction between the computer programmer and the engineers. In addition, once the algorithms were developed, because the LabVIEW VIs documented clearly the design of the program to control the electronic modules, porting of the VIs to the C programming language on the embedded system of the spacecraft was simplified.

PROTOTYPE SOFTWARE

The prototype hardware described above was exercised and tested using the simple PCB VI which allowed only read and write operations on the PCB. This was an awkward interface for the user because most logical commands or response read-back from the electronic modules require multiple write and read operations on the PCB. This lead naturally to the development of a middle layer of VIs which allowed subsystem commands and display of results to occur within a logical VI for each module.

A mass storage unit VI was created which, using the PCB VI, allowed an address (or a range of addresses) to be specified, the ability to specify read or write, and either the data to write to or a display with the results of reading back data. Thus, writing single bytes, blocks of bytes, or even downloading a file from the PC to the MSU became a very simple operation. Furthermore, automated read and write tests were developed which ran exhaustive tests on the storage units over many days.

Similarly a temperature multiplexing (TMUX) VI was created to allow a thermistor to be specified for conversion and display of its temperature. The selected thermistor caused the TMUX to send an analog signal to the ATMIO-16 A/D board which handled the conversion. Additionally, multiple temperature channels could be selected and displayed on a graph. Testing of the TMUX was simplified by running temperature acquisition over long periods of time in parallel with other laboratory temperature acquisition systems so that comparisons could be made.

The VI for the electrical power system (EPS) allowed the individual power lines of all the electronic modules to be controlled. An interface for the prototype batteries was also developed which allowed the control of the battery switches (trickle charge, full charge, online, and discharge). As PANSAT has two batteries, the battery control was duplicated to allow both batteries to be evaluated. Feedback from the power system (e.g. battery temperatures, voltages, and currents) was controlled via the PCB; the analog results were sent to the ATMIO-16 analog inputs. The direction of battery currents (i.e. *to* or *from* the battery) was encoded by reading a single bit back from the PCB (i.e. the analog signal is only a magnitude).

PROTOTYPE SOFTWARE EVOLUTION

The middle layer VIs described above simplified the control of each individual electronic module of the spacecraft. However, in order to implement actual spacecraft algorithms to perform automated control of the spacecraft subsystems, additional VIs were created.

PANSAT requires continuous power system control. This control is now implemented in ROM on the digital computer on board the spacecraft. However, the first battery control algorithms were developed before the spacecraft existed. These algorithms were created as VIs. The algorithm which correctly decides which battery needs charging and which battery is able to supply online power to the spacecraft is known as the Battery Charge Monitor (BCM). The BCM is a non-trivial algorithm since it must keep track of charge state history of each battery, modify charging and discharging depending on

voltages and temperatures of battery cells, and always make sure the preferred battery is online in sunlight and eclipse (Ref. 2). As many anomalies can occur and are only fully identified through testing, implementation of the first BCM was simplified using LabVIEW.

Thorough testing of the batteries and the power system required a more sophisticated power system user interface. Since the solar panels for PANSAT had not yet been acquired, nor was it practical to have the solar panels on the test bench, solar input was simulated using a programmable power supply. An additional VI was created which controlled the power supply while attempting to simulate the orbit of the spacecraft. The solar simulator VI incorporates many variables: the tumbling of the spacecraft (which creates a variable power source since the solar panels produce different energy levels depending on their orientation with the Sun), orbit time, and Sun versus eclipse times. The front panel of the simulator VI is shown in Figure 4.
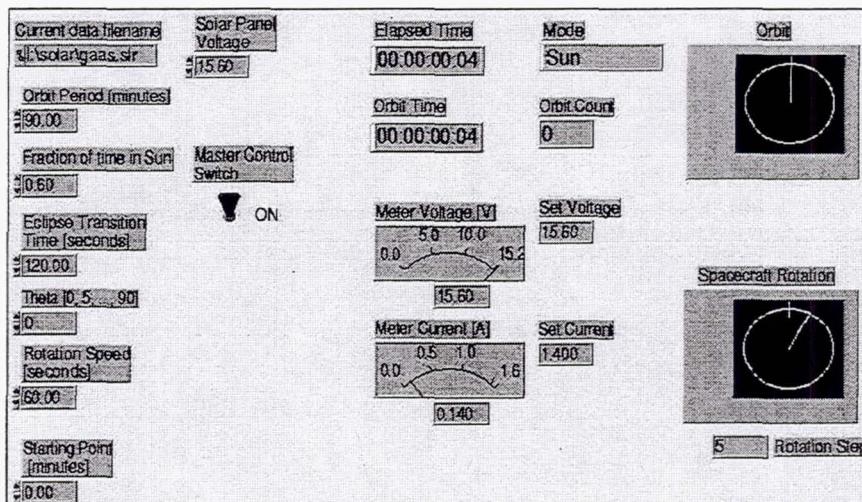

Figure 4. Solar Simulator VI.

With the development of the BCM and Solar Simulator, detailed testing of the PANSAT power system was possible. During this time a power system deficiency was identified. It was discovered that the solar panels would not be able to provide enough power to fully charge the batteries since a higher solar panel voltage (above that of the charging batteries) is required. The batteries were redesigned with one less cell so that over charging of the cells could occur. Figure 5 shows the hardware and software VI hierarchy that existed during this portion of PANSAT's development.
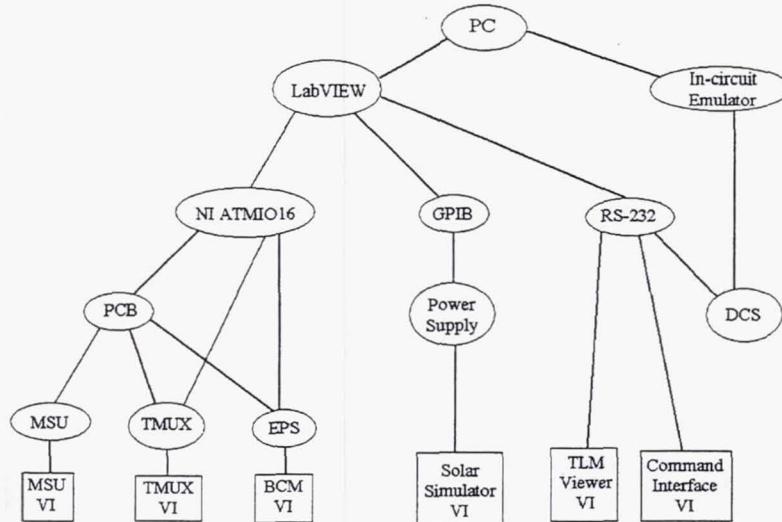
Figure 5. Battery Charge Monitor Support Hierarchy.

SPACECRAFT HARDWARE

The prototype TMUX, MSU, and EPS electronics were implemented as spacecraft flight hardware and environmental testing was performed on these modules. During this time the prototype digital computer, modem, and RF systems were created and tested. The digital computer and the communications hardware were developed with an in-circuit emulator (ICE box) and RF equipment, separate from the infrastructure used to develop the TMUX, MSU, and EPS.

Eventually, the digital computer replaced the ATMIO-16 A/D and digital I/O board. The DCS has a PPI which is used to control the PCB. In addition, the DCS has an A/D converter which receives signals from the TMUX and EPS. The newly developed DCS was added to the other electronic modules on the test bench in order to test the spacecraft's flight hardware.

SPACECRAFT SOFTWARE

In order to take advantage of the VIs developed during the prototype hardware stage, a software interface was created which allowed the DCS to communicate to a PC using a RS-232 port. Thus, command and control to the spacecraft from the PC was implemented by passing commands and data over a serial port. On the PC, the LabVIEW VIs were modified to allow the PCB operations and A/D conversion to occur on the spacecraft's computer, the DCS. The LabVIEW VIs were modified into modules which displayed data. For the PC to command the spacecraft, another VI was developed which allowed controls to be given on the PC and sent via the serial port to the spacecraft computer.

Because the BCM algorithm was mature when the DCS was created, porting of this algorithm from a LabVIEW VI on the PC to a C program on the spacecraft computer was a straightforward task. Thus, the DCS now automated the spacecraft power system control and the PC was used to monitor the data. Figure 6 shows these hardware and software systems.
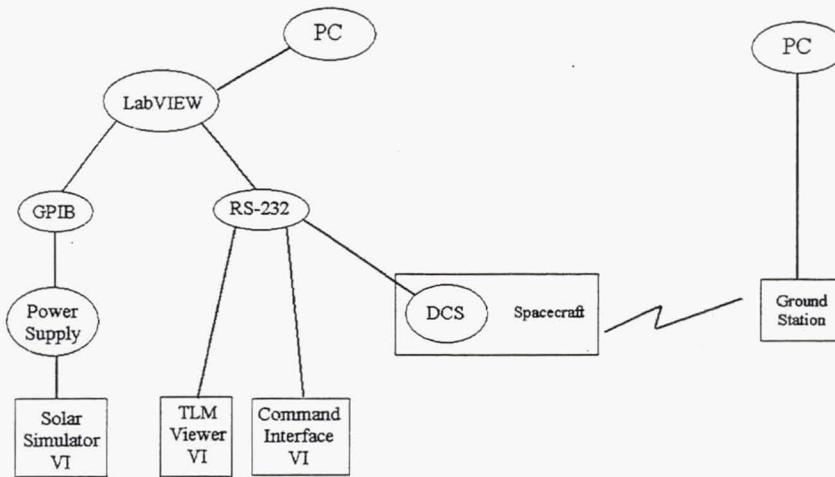
Figure 6. Integration Support Hierarchy.

SPACECRAFT INTEGRATION

At the time of spacecraft integration, all of the electronic modules had been functionally tested independently to insure operation with respect to reliability and workmanship. In addition, module level testing was performed to insure verification of compliance with Shuttle safety requirements (this included random vibration and thermal cycling). A detailed description of the testing requirements is given by Overstreet (Ref. 3).

The ground support hardware used to perform the integration testing at NASA/GSFC consisted of two laptop computers, a Hewlett Packard 6653A DC programmable power supply, and a brief-case sized RF/Modem unit. Using the spacecraft test port interface (STPI) the laptops could exercise each test required to ensure that PANSAT was functioning correctly. The tests performed were as follows.

First a spacecraft computer was powered on. ROM-based software completed an automated hardware check of the computer board to insure all of the hardware peripherals were reset and responded correctly to initialization commands. All of the computer's RAM were checked using moving ones write and read tests (Ref. 4). Then, the peripherals were powered on and subsystem tests were performed. This required about 15 seconds. The power system was then tested by toggling every solid state switch on the electrical power subsystem. Responses of the switch settings were verified by checking the power supply outputs (voltage and current) and also by viewing the LabVIEW Monitor VI, Figure 7, which shows battery voltages, currents, and temperatures. The power system tests took about two minutes to complete. The mass storage tests, using moving ones write and read techniques, required the most time (about 50 minutes); together, the two memory systems contain 9 Megabytes of random access memory. The temperature multiplexing systems were checked in about one minute using a special command which displayed all thermistor readings on one window. Finally, the communications systems (modem and RF) were tested. The communications systems were designed with certain redundancy such that for each operating computer there are eight unique RF states. The separate RF/Modem unit allowed wireless testing of the spacecraft in the lowest RF power mode at the integration site. The eight communication states were tested in about five minutes. An entire spacecraft system level suite of tests was performed in about one hour. This allowed regular testing to be performed throughout the entire integration process.

Test data were filed after each test. All the graphical windows displaying results of various tests were printed to disk. All command and response data were converted into ASCII-readable output and saved to disk.
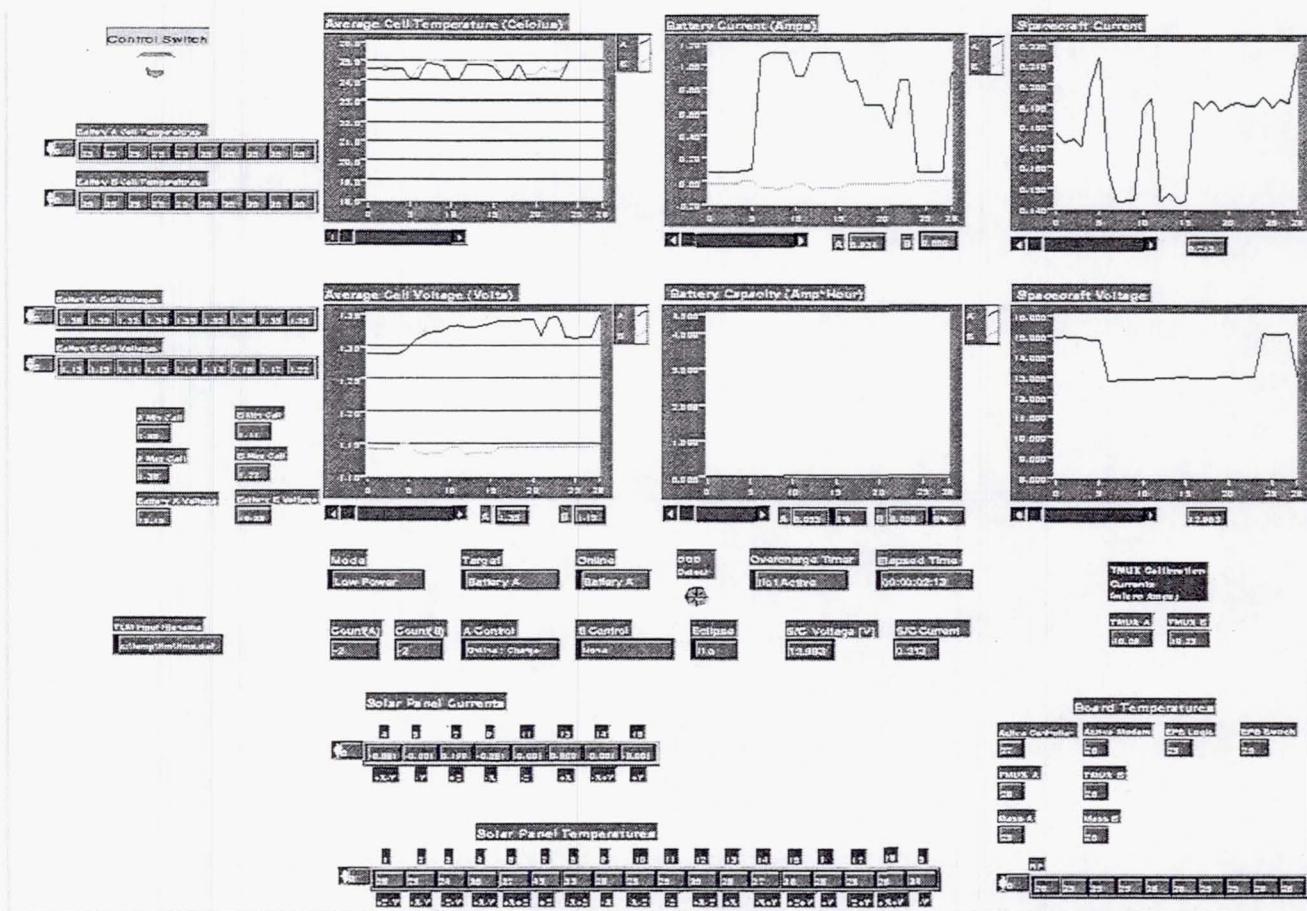
Figure 7. Power System Integration VI.

CONCLUSION

The launch and operation of PANSAT was the effort of several years of work by officer students, staff, and faculty at the Naval Postgraduate School. Successful completion of testing, integrating, and operating an autonomous spacecraft can be accomplished with reusable software modules using a PC, LabVIEW, and some custom programming. The software tools are simple to learn and are appropriate for student instruction.

REFERENCES

1.   *LabVIEW User Manual*, Part Number 32099A-01, National Instruments, January 1996.

2.   *PANSAT Prototype Batteries And Test Results*, Frank H. Strewinsky, Research Report, Naval Postgraduate School, Monterey, CA, 1996.

3.   *Environmental Testing of the Petite Amateur Navy Satellite (PANSAT)*, Paul J. Overstreet, Master's Thesis, Naval Postgraduate School, Monterey, California, December 1997.

4.   *Programming Embedded Systems in C and C++*, Michael Barr, O'Reilly and Associates, January 1999.

10 Gbps Shuttle-to-Ground Adjunct Communication Link Capability Experiment[1]

J.M. Ceniceros, J. V. Sandusky and H. Hemmati
Jet Propulsion Laboratory
California Institute of Technology

ABSTRACT

A 1.2 Gbps space-to-ground laser communication experiment being developed for use on an EXpedite the PRocessing of Experiments to the Space Station (EXPRESS) Pallet Adapter can be adapted to fit the Hitchhiker cross-bay-carrier pallet and upgraded to data rates exceeding 10 Gbps. So modified, this instrument would enable both real-time data delivery and increased data volume for payloads using the Space Shuttle. Applications such as synthetic aperture radar and multispectral imaging collect large data volumes at a high rate and would benefit from the capability for real-time data delivery and from increased data downlink volume. Current shuttle downlink capability is limited to 50 Mbps, forcing such instruments to store large amounts of data for later analysis. While the technology is not yet sufficiently proven to be relied on as the primary communication link, when in view of the ground station it would increase the shuttle downlink rate capability 200 times, with typical total daily downlinks of 200 GB - as much data as the shuttle could downlink if it were able to maintain its maximum data rate continuously for one day.

The lasercomm experiment, the Optical Communication Demonstration and High-Rate Link Facility (OCDHRLF), is being developed by the Jet Propulsion Laboratory's (JPL) Optical Communication Group through support from the International Space Station Engineering Research and Technology Development program. It is designed to work in conjunction with the Optical Communication Telescope Laboratory (OCTL) NASA's first optical communication ground station, which is under construction at JPL's Table Mountain Facility near Wrightwood, California. This paper discusses the modifications to the preliminary design of the flight system that would be necessary to adapt it to fit the Hitchhiker Cross-Bay Carrier. It also discusses orbit geometries which are favorable to the OCTL and potential non-NASA ground stations, anticipated burst-error-rates and bit-error-rates, and requirements for data collection on the ground.

INTRODUCTION

The optical communications system designed for use on an EXPRESS Pallet Adapter (ExPA) as part of the International Space Station Engineering Research and Technology Development (ISSERT) program has a maximum downlink data rate of 2.5 Gbps into the 1 meter OCTL receiver. This paper will discuss the necessary modifications to upgrade the flight terminal to 10 Gbps and interface it to a shuttle Hitchhiker double bay pallet. Modifications to the flight terminal include laser power, mast size, thermal design, electrical interface, and data interface. Modifications in the ground terminal include the detection process and the storage medium.

SPACECRAFT TERMINAL MODIFICATIONS

Transmitter

A wavelength division multiplexing (WDM) scheme will be used to increase the data rate. Four wavelengths, each transmitting 2.5 Gbps, would achieve a 10 Gbps aggregate downlink data rate. This enhancement involves adding three master oscillator lasers to the laser transmitter assembly (LTA) and

---

upgrading its power amplifier to 800 mW; 200 mW for each of the four WDM channels. This design retains the per-channel power and involves only the LTA; the design of the rest of the flight terminal would remain unchanged.

Thermal

The difference in orbit inclination between the shuttle and International Space Station results in different temperature ranges. The largest temperature swing for the EXPRESS pallet is from -110°C to +40°C [1], whereas the cargo bay of the shuttle swings from -160°C to +95°C while on orbit with the doors open [2]. These changes in thermal environment plus increased thermal load from the three master oscillators and a more powerful amplifier will require a change in the thermal design specified for the ISSERT mission. The thermal design for the ISSERT mission uses blankets and heaters to keep the telescope optical assembly (TOA) in the preferred operating range of +10 to +30°C. All other electronics are placed on a radiator with louvers attached to a mirror radiator surface for the hot case, and a heater for the cold case. The changes to this thermal design necessary to support a shuttle mission depend strongly on the shuttle orbit of interest.

Interfaces

Interfaces for the Shuttle Hitchhiker Carrier and the ISS EXPRESS pallet adapter share few similarities, although both provide two 28 VDC power supplies. The Hitchhiker can provide 10 Amps and up to 1600 Watts of simultaneous total customer power, while the ExPA has a configurable current supply, which can be 5, 10, 15, or 20 Amps and is limited to 1000 Watts. In any case the power capability is ample compared to the estimated 135 W total power for the ISSERT mission.

The payload envelopes of the ExPA and the Hitchhiker double bay pallet are similar. The ExPA can accommodate a payload weight of 227 kg and size 86.4x116.8x124.5 cm [1] , and a double bay pallet Hitchhiker carrier can accommodate a payload up to 272 kg with a size of 83.8x139.7 cm [2]. The height of the shuttle payload is limited by a center of gravity that must not exceed 38.1 cm in height [2]. The approximate size of the telescope optical assembly and gimbal is 54x33x31 cm. The estimated volume and mass of 62 kg would easily be accommodated by either platform.

Data interfaces for the ISS EXPRESS pallet adapter and the Shuttle Hitchhiker are a point of dissimilarity. While the EXPRESS pallet uses a MIL-STD-1553B command and control data bus, the Shuttle Hitchhiker uses a RS 422 asynchronous interface. A complete redesign of the data interface would be necessary to modify the ISSERT design for interface to the shuttle.

RECEIVER MODIFICATIONS

The receiver telescope focuses the downlink signal onto the data detectors. To accommodate the four wavelength channel, the receiver telescope design must be modified to separate the four wavelength channels using either prisms, gratings or specially designed long-pass filters. The spatially separated wavelengths would then each be focused on their own data detector receiver, requiring the addition of three data detector channels and data recorders.

ORBIT GEOMETRIES

Obits which have a long contact time with one of the potential ground station sites are favorable. Potential ground stations include the OCTL at the JPL Table Mountain Facility near Wrightwood, CA, the Air Force Maui Optical Station (AMOS) in Maui, HI, the ESA station in the Canary Islands, and the NASDA station in Tokyo, Japan. The ESA and AMOS ground stations are favorable for the normal 26

degree inclination orbit. While the other locations would not have contact times for this orbit, they would be favorable for orbits at 35 degrees or more.

ERROR RATES

Atmospheric fades dominate the error rate in optical communication channels, typically lasting 8-10 ms. The burst-error-rate depends on the elevation of the shuttle above the horizon, the ground wind speed, and the degree of turbulence in the atmosphere. The burst-error-rate is estimated to be typically $< 10^{-5}$ when the shuttle is only 20 degrees above the horizon and reduces to $< 10^{-8}$ when more than 30 degrees above the horizon. When fades are not present, the bit error rate is expected to be 10^{-9}.

REFERENCES

[1] Expedite the Processing of Experiments to Space Station (EXPRESS) Pallet Payloads Interface Definition Document, SSP 52000-IDD-EPP Working Draft, NASA, March 8, 1999.
[2] Hitchhiker Customer Accommodations & Requirements Specifications (CARS) document, HHG-730-1503-07, Goddard Space Flight Center, Greenbelt Maryland, 1994.

Page intentionally left blank

GE◉CAM II

Studying a Changing Earth from a Generation Long Viewpoint
(Proposal for a HH/ISS Experiment)

Authors:
James H. Nicholson, CAN DO Project Principal Investigator - Medical University of South Carolina
Thomas J. O'Brien, CAN DO Project Chief Engineer - Medical University of South Carolina
Carol A. Tempel, CAN DO Project Coordinator - Charleston County School District
Kathy Rackley, EarthKAM Lead Teacher – Mason Preparatory School
Eve Katuna, EarthKAM Lead Teacher – Drayton Hall Middle School

BACKGROUND

At the 1992 Shuttle Small Payloads Symposium, the CAN DO Project described a Gas payload called GeoCam which was designed to obtain the first ever high resolution images of the Earth taken by an educational experiment. The project team, in consultation with the National Geographic Society, had specifically designed the camera system to exactly match the optical and spectral characteristics of the NASA Skylab EREP (Earth Resource Experiment Package) camera system. The goal was to produce images that could be directly compared to the Skylab images taken two decades before. The Skylab EREP produced the first comprehensive and systematic image survey of the earth from space. These 36,000 high-resolution multispectral images represent a priceless treasure as one of the earliest possible baselines from which to evaluate the environmental changes undergone by our beleaguered planet.

The GeoCam payload (G324) did fly on STS-57 in June 1993 and produced spectacular high quality images of the Earth. The cameras were controlled by the orbiter crew based on instructions received from the first ever student operated mission control room. The GeoCam project received national attention and was the subject of a nineteen-page article in the August, 1994 National Geographic Magazine.

Figure 1. GeoCam POCC (1993)

GeoCam has to be considered a great success. Unfortunately, not a single target was obtained that matched a Skylab EREP target area. This was a result of several factors including a 28.5° orbital inclination as opposed to Skylab's 50° inclination, and a change in launch dates which put the Western Hemisphere (where most EREP targets are located) in darkness. More to the point, it clearly demonstrated that the space shuttle is not a suitable platform for highly specific targeting. The short mission duration does not allow for the required confluence of exact orbital track, sun angle, shuttle orientation, and clear weather. The International Space Station, on the other hand, is a perfect platform with an orbital inclination nearly identical to Skylab and the long timeline necessary to systematically duplicate the EREP images. The concept is as valid today as it was in 1992, but now there is a real opportunity to produce images of great educational and scientific value. The EREP images are now over a quarter of a century old, and differences will be all the more observable, and important. They can serve as a means to better understand and measure environmental degradation. The long baseline will more clearly separate long term changes from transient or short-term cyclical events. Historical examinations of change often look far back into Earth's history to determine the rate and degree of natural changes. The rapid growth of human population presents fundamentally different pressures on the Earth's ecosystem. To gain new insight on

human-induced changes, earth scientists focus on the changes that have occurred over a shorter time span (25 years). During this time, natural and human induced changes on the surface of the earth have been photographed from space. Comparison between photos past and present enables documentation of profound changes to the Earth. One of the largest early data sets of earth observing photographs comes from the Skylab archives. These photographs covered much of the Earth's surface, and are an important baseline with which to compare present and future photographs. It is the major goal of the GeoCam II project to provide a direct link to this resource.

The Skylab Legacy

Figure 2. Skylab over the Amazon

One human generation (25 years) has passed since the United States' ambitious Skylab program. A major component of those missions was the acquisition of earth photography using a six camera, multispectral camera system. The first multispectral photography done from space was on the 1968 Apollo 9 mission. Four mounted Hasselblad cameras were aimed at the same target point and their shutters triggered simultaneously. A significant advance in Earth imaging technology resulted from subdividing spectral ranges of radiation into bands (intervals of continuous wavelengths), allowing acquisition of multispectral images. Especially important was the addition of infrared bands. Black and white infrared film was developed in Germany in the early 1900's. The film emulsion differed from regular film in that it was sensitive to wavelengths of energy longer than red light and just beyond the range of the human eye. By 1930, black and white IR (infrared) films were being used for landform studies, and from 1930 to 1932 the National Geographic Society sponsored a series of IR photographs taken from hot air balloons. The infrared bands are often used to emphasize healthy vegetation in which light in the range of 700 - 1100 nm is strongly reflected from the internal cells of plants. A false color composite can demonstrate stressed or unhealthy vegetation and more clearly differentiate barren areas. The use of false color infrared imaging can be especially useful for monitoring change such as the deforestation of rain forests. The value of multispectral photography was not lost on scientists, such as geologists, hydrologists, agronomists, foresters, and those concerned with environmental monitoring and land use assessment. It quickly became a major scientific tool.

The success of this experiment lead directly to the Skylab system as well as the Landsat series of satellites. By the late 1960s, the first unmanned satellite specifically dedicated to multispectral remote sensing entered the planning stages that led to the launch of ERTS-1 (Earth Resources Technology Satellite) in 1972. Renamed Landsat, this series of earth-observing satellites has continuously covered most of the Earth's surface since then, with Landsat-5 and Landsat-7 currently in operation.

Three separate crews worked on Skylab in 1973-74 and participated in the Earth photography experiments. The purpose of the Earth Resource Experiment Package (EREP) was to determine what kind, and how much, photographic data could be acquired of the broad variety of Earth features witnessed on the mission's ground track. This activity was underwritten by intensive training before lift-off, real-time scientific mission planning and on-board procedural support. This focus elevated Earth Imaging from an opportunistic sideline to a major mission goal.

The Skylab spacecraft was launched on May 14, 1973 into a nearly circular orbit at an altitude of 435 km above the Earth. The launch azimuth

Figure 3. Skylab EREP image of southern Louisiana

inclined the orbital plane 50° with respect to the Equator and allowed observations of the Earth between latitudes 50°N and 50°S. It orbited the Earth every 93 minutes and repeated the ground track every five days.

The photographic return from the Earth Resources Experiment Package (EREP) was as follows:

MISSION	DATES	DAYS	PASSES	TOTAL PHOTOS
Skylab2	5/25/73-6/22/73	28	13	5,275
Skylab3	7/28/73-9/25/73	59	48	13,429
Skylab4	11/16/73-2/8/74	84	49	17,000
TOTAL		**171**	**110**	**35,704**

The EREP system included two major instruments:
The S190A Multispectral Camera System consisted of six bore-sighted 70mm cameras equipped with 152mm focal length lenses. Each photograph covered a square image area of 163 km on a side. Each camera was equipped with filters to cover a specific wavelength on a combination of color, black-and-white, color infrared and black-and-white infrared film. The cameras were mounted in a frame that provided programmable camera rotation to compensate for the forward motion of the spacecraft.
S190B Earth Terrain Camera was a single 127mm camera equipped with a 457mm lens. Each photograph covered an area of 109 km square. Film could be selected from a choice of color, black-and-white or color infrared emulsions with an appropriate filter. An internal motion compensator corrected for the forward motion of the spacecraft.
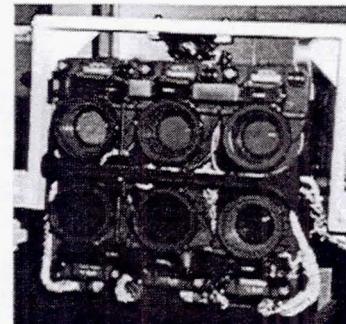

Figure 4. S190A camera system

The GeoCam II Experimental Design
The primary goal for the design of the GeoCam II optical and imaging systems is to match as closely as possible the results of the Skylab S190A and S190B camera systems. This includes the selection of a focal length of lens to match the photographic "footprint" of the S190A cameras and CCD sensors and filters to duplicate the six spectral bands. The collection of 36,000 photos produced by EREP, in six registered wavelengths, represents the most complete multispectral film coverage of the planet ever undertaken. Despite this, the EREP collection remains tragically unused. GeoCam II intends to operationally re-visit what is a considerable national asset, and to contribute a comparative update to this remarkable inventory of planetary data. Because the multispectral bands pioneered on Skylab are very similar to the first four bands of Landsat, the GeoCam II system becomes a capable research instrument in its own right. It will give students a powerful system with which to explore the multispectral images and image processing which is so fundamental to modern remote sensing.
The recent proliferation of relatively inexpensive high resolution CCD chips with
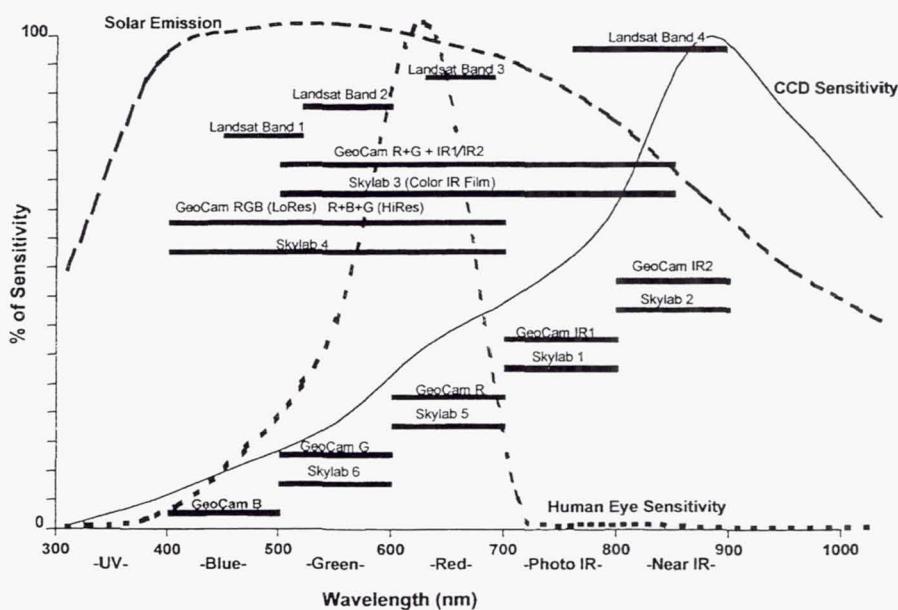

Figure 5. Sensor bands for GeoCam II, Skylab and Landsat

299

color, monochrome and infrared capability makes it possible to design an affordable camera system which will exactly duplicate the optical and spectral properties of the six-camera S190A Skylab multispectral camera system. The high sensitivity of silicon in the infrared means that a CCD-based camera can make an excellent sensor for the near infrared wavelength range of 750 nm to 1000 nm which present a difficult problem for film. Six separate digital sensors will simultaneously capture an image, which will then be downloaded to a central processor using an IEEE 1394 high-speed interface. The inherently small size of the CCDs will allow the lens/camera systems to utilize relatively small optical windows. The use of dichoric beam splitters could reduce the size even more by allowing for multiple wavelengths to be captured through a single lens system. Such a system could be built now with off-the shelf equipment, and the rapid development of the digital image field will allow better performance at an even lower cost in the near future. High-speed architecture and mass storage media will be required to handle the large amount of data produced and to store it pending downlink opportunities. Each multispectral image set will produce between 6MB (1k x 1k at 8bit grayscale) and 32MB (2K x 2K at 12 bits grayscale) of data. Image compression may be used to reduce the data load, but it is well within the reach of current system capabilities. The KidSat and EarthKAM programs have demonstrated the practicality of downloading large digital image files. The control interface could be modeled on NASA's EarthKAM project, which provides a working structure for using high-resolution digital Earth images in education. The multispectral system can serve as a natural extension of the EarthKAM program by allowing the students to conduct a more advanced research project through the comparative study of twenty-five years of environmental change. Access to true multispectral images will allow for a richer learning experience and a chance to explore imagery as a quantitative scientific tool rather than just for color documentation of geographic morphometry.

Payload Design

This concept payload study assumes the use of standard Hitchhiker/GAS hardware and specifications whenever possible. The Hitchhiker canister, with its avionics and adapter ring, possibly mounted on a JEM-EF (Japanese Experiment Module - Exposed Facility) or EXPRESS pallet with an attachment interface for the ISS could conceivably mount at either the JEM, S3 or P3 PAS (Payload Attach System) mounting sites.

The camera system itself is built around a Hitchhiker/GAS five cubic foot canister mated to a motorized door assembly, which is fitted with a fused silica window. Construction is based on four circular plates separated and supported by three equally spaced struts attached on the circumference. The cameras will be mounted behind the first, a 16mm (5/8") 6061-T6 aluminum plate that acts as a containment shield and structural stabilizer, fitted with a thin glass epoxy light baffle to reduce reflected glare in the optical system.
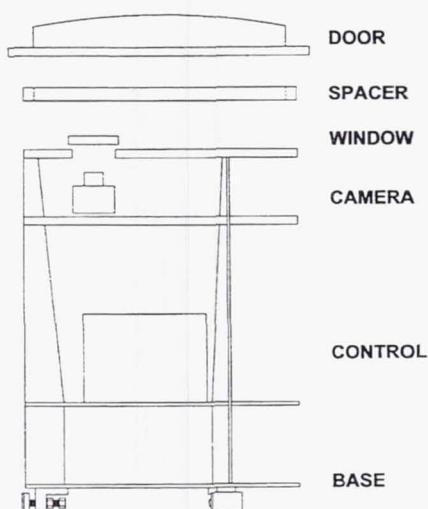

Figure 6. System structure
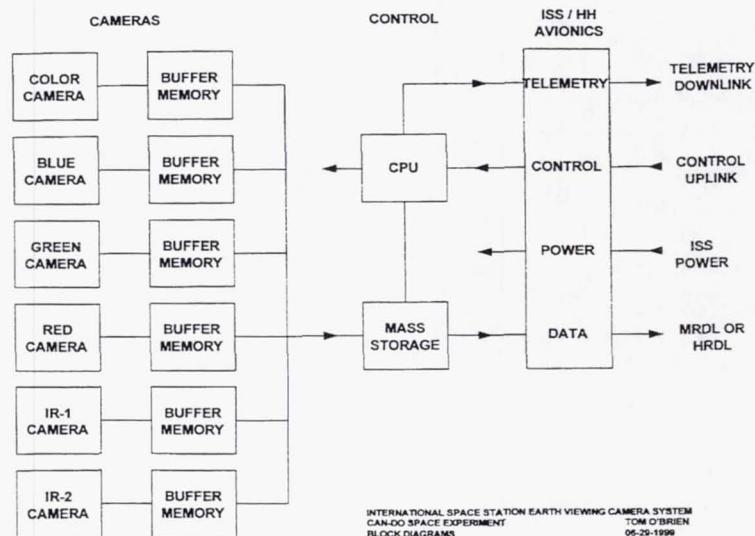
Figure 7. GeoCam II control system

Six digital cameras operating in different portions of the light spectrum from ultraviolet to infrared are aligned and mounted on the second plate located near the containment shield. Below the camera mounting plate is the third of four internal plates. This plate supports the camera electronics and any ancillary electronics packages needed to interface with the ISS Hitchhiker avionics package. Below this is the fourth or bottom structural plate, which provides support and rigidity through the three base bumpers that provide a mechanical interface with the flight hardware.

Each camera optical path is chosen to match its Skylab equivalent in both spectral range and subject footprint size as closely as practical. With improvements in exposure speed allowed by advances in digital technology, the payload will be able to do away with the cumbersome mechanical rotating mechanism used to stabilize the Skylab camera platform, which was necessary to compensate for orbital motion and extended film exposure times. All six cameras will be fired simultaneously, and the pictures transferred to each camera's four picture buffer memory. The picture data files will then be sequentially transferred to a mass storage unit which will compress and warehouse the data until it can be downloaded through either the ISS MRDL (Medium Rate Data Link) or the HRDL (High Rate Data Link) as may be available. Camera control will be uplinked through the Hitchhiker control uplink, which is at present an RS-422 serial format (1200 baud) channel. While in operation, the computer will continually monitor all cameras, electronics, payload environment, and its own health, and return the system status by way of the Hitchhiker downlink, which also runs at 1200 baud. Operational power will be derived from the ISS through the Hitchhiker avionics package, and further regulated for the payload requirements.

THE VIEW FROM SPACE

Photographic analyses of land use practices give insight into changes. Linear functions can be used to project the rate of future change. As growing human population requires an ever-increasing share of the Earth's surface on which to live, human activities change the distribution of plants and animals, alter drainage patterns, and modify natural boundaries. In doing so, mankind changes either the reflective or emissive properties of the surface. Such changes are detectable from space. Human actions that change the reflectance or color of the Earth's surface can be recorded with space photography. Activities include:

- **DEFORESTATION**. Forests are optically dense, green areas. The cutting of the trees produces a more reflective surface and exposes a different color. Deforestation scars are seen in the rain forests throughout the world. Forests are often cleared by setting fire to the vegetation, and smoke from these fires is visible from space.
- **URBANIZATION**. Urban areas are delineated by highly reflective paved surfaces. Because the growth of cities is at the expense of vegetated surfaces, the increase in reflectivity can be measured.
- **FLUVIAL SEDIMENT LOADS**. Clear cut forestry practices in many tropical countries have altered the sedimentary load of the rivers that drain the forest. Rivers loaded with sediment have a different color than "clean" rivers that drain forested areas. Sediment laden rivers, such as the Betsiboka River of Madagascar, are now red-brown when seen from space.
- **DESERTIFICATION**. The reflective surface of deserts and eolian sediment patterns are also visible from space. The encroachment of deserts over once vegetated surfaces will register a shift in the optical and textural character.
- **COASTAL EROSION**. Analysis of the position of the coastal features can be used to determine the rate and location of large-scale coastal changes. Dramatic rates of erosion can be seen on the edge of the Nile and Ganges river deltas.
- **LAKE LEVELS**. Changes in boundary relations can detect variation in water levels in lakes (e. g., Lake Chad) or inland seas (e.g., Aral Sea).
- **WETLANDS**. The delineation of wetlands is sometimes difficult. Changes in vegetation color and the sea land boundary are sometimes needed to detect loss.

Figure 8. East Coast Hurricane

EARTH OBSERVATION AND EDUCATION

Image comparisons are powerful teaching tools, particularly to show change over time. By comparing transformation that has been documented in remote images, changes that have occurred in our lifetimes can be observed. It is hoped that such documentation of global change will make this issue more immediate and real. There is an additional benefit in the lessons that they teach us.

According to Charles F. Kennel, Associate Administrator for Mission to Planet Earth, "The ultimate product of Mission to Planet Earth is education it its broadest form. Our vision is a sustainable Earth system science education program rooted in strong principles and objectives. NASA's Mission to Planet Earth (MTPE) Enterprise provides long-term studies of the Earth system needed to answer critical questions about how the global environment will affect us now and in the future. The unique vantage point of space provides the global perspective needed to better understand how all of the parts of the Earth's environment- air, water, land, and life-interact and make life possible."

NASA has defined specific objectives for its Earth Science Enterprise Education Program. The first are to:

❑ Train the next generation of scientists to use an interdisciplinary Earth system science approach
❑ Continue to educate and train educators as research evolves and capabilities change

An important goal of the CAN DO GeoCam II mission is to provide a vehicle for stimulating hands-on experiences for students so that they can better interpret the global environmental changes that will determine the quality of the world that they will inherit. Specific program goals include:

❑ Provide an educational vehicle to support serious student research in environmental change
❑ Provide training to teachers and students in the use of multispectral imaging and digital image processing
❑ Provide high quality matched images to evaluate geomorphologic change over time
❑ Provide students the opportunity to interact with ISS and leading scientists while conducting real-life research of their own design and under their control.
❑ Provide a vehicle to support advanced technology skill training of teachers

GeoCam II Educational Design

Charleston Can Do teachers and students have consistently demonstrated the use of cutting edge technology in teacher education, student projects, and teacher/student presentations at regional, national, and international conferences. Throughout the GeoCam, KidSat, and EarthKAM projects, NASA has drawn on Charleston educators for leadership roles in all of these projects.

The GeoCam project was the creative development of the Charleston County School District Can Do Project supported by its education partnerships with the Medical University of South Carolina and the College of Charleston. There were many lessons learned from that project and later expanded in the NASA sponsored KidSat and EarthKAM projects. GeoCam II will apply these experiences and build on them. Charleston Can Do teachers have benefited from their ongoing involvement in every one of these missions.

GeoCam developed the concept of a student-run mission control room. This idea evolved and grew more as the teachers and students built a team approach. The central idea that GeoCam promoted was that students would be running the mission operations center using sophisticated (pre-Internet) technology and teachers would support them as advisors and mentors. The idea that students in middle and high school would be running an active control room interacting with the Shuttle crew was an original and innovative idea in educational methodology. Learning to work cohesively with students from other schools and regions was another challenge to overcome.

Figure 9. Student teacher team

Developing job descriptions for the various positions and training students in the job assignments solved the problem. Variations on this model have been used for all student mission control rooms that followed. Major technology changes, especially the development of the Internet, have changed the operational patterns and allowed for the near real-time delivery of the images. The primary personnel functions have remained constant. The decision to have a central student mission control room with students from participating schools

assuming specific responsibilities for a specified shift was one of the early innovations. The specialist positions have been adapted at every subsequent student mission control room. This model allowed for more than 180 students to be active in the mission control room over a period of eight days in groups of 20 to 30. Parents and teachers have been both surprised and pleased by the level of activity and the good order in which students have been able to perform useful targeting in a limited amount of time. It was found that advanced teacher education and practice mission simulations were essential to build the confidence of everyone and test the model before the mission. This process is now part of all student mission control rooms. Teachers and students shared input about how to improve the control room and changes were made as needed. Many students wrote in journals about the positive feelings from the mission control room. A student from Buist Academy wrote that this was real and whatever target was selected was their own responsibility. Students felt very empowered and as a consequence, carefully prepared for and thoughtfully executed their mission responsibilities. In this atmosphere, students often performed at levels beyond their teachers', their parents', and even their own expectations. They left the experience with not only new skills but with a vastly improved self-confidence and self image.

The NASA KidSat project selected Can Do teachers to participate as lead teachers to both write and pilot the project for three years. The idea of individual mission control rooms using the latest computer technology, the new Internet in 1994, was tried in schools. The push to get schools connected to the Internet (almost all were not) was considered innovative at the time. These schools were on the leading edge of image technology use in the classroom. Some schools liked the control they had over the image selection and the event atmosphere that an active mission created in the whole school. But in other schools, because not all students in a school were involved in the project, some teachers and principals found it disruptive. KidSat demonstrated a need to develop a model that fits the school district technology resources and individual principals' comfort zones. As a result, the follow-up EarthKAM project has been experimenting with a consolidated regional control room. GeoCam II suggests a flexible model that will use a central control room and partner schools working together. Individual schools that wish to have a control room site could use the Internet to send requests to the regional control center. This multi-layered model will allow schools and district to choose the form of participation that best meets their individual needs.

The most educationally important outcome has been the use of Earth image technology by students to try to answer science related questions. Lessons were developed from the original GeoCam images that became the models for future lessons in the KidSat and EarthKAM projects. Lessons were developed by Charleston County educators to teach other teachers and students how to relate images, maps, and science questions. As an example, students in the first KidSat project used images to study the Rio Xingu, a river in Brazil. These student-scientists used the 1996 KidSat mission images, 1976 maps, and computer technology to demonstrate river changes. Teachers and students presented these findings at national and international conferences. Other project included exploration of small islands in the Pacific Ocean, changes in the size of the Dead Sea, exploration of coastal changes, and many other examples. Teachers have taught students to look beyond their books and library. They have presented an opportunity for students to take personal interest in areas of science that they choose to explore and to teach them to use new tools to achieve their personal research goals. The role of education in the GeoCam II project is one that will be felt in classes across the country. The placing of the GeoCam II cameras on the International Space Station will offer the chance for multispectral images to be selected and used by students in every classroom. The GeoCam II project will continue to offer students the opportunity to participate in science in a very real way while still having fun.

Main Portion of the Rio Xingu

☐ map of river from 1977

▨ image of river from 1996

12.5 km
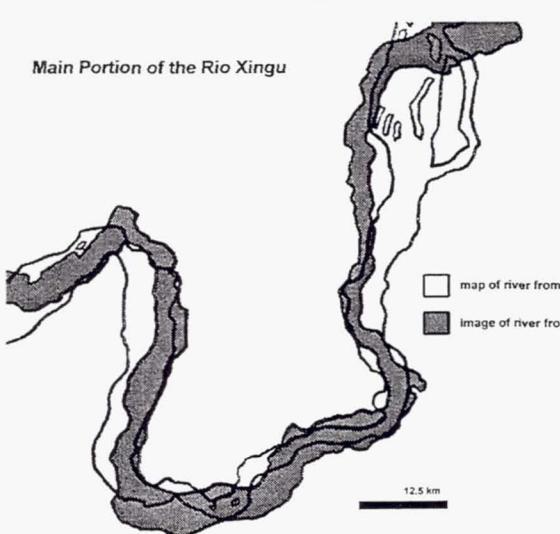
Figure10. River change on the Rio Xingu

Geomorphology and the Analysis of Change

Over a span of time, there is a dramatic change in the geomorphology of the earth's surface. When viewed from above, it is very clear that the Earth's surface has changed dynamically because of natural forces and because of man's intervention into natural geologic processes.

Image comparison over a significant span of time will allow teacher and student to view the environmental impact that man has had on an area. The deforestation of the Amazon rainforest and the on-going change in the course of the sediment-laden streams are clearly defined through image comparison. Deforestation involves the cutting down, burning and damaging of forests. Most of the clearing is for agricultural purposes and commercial logging. The world's population has increased causing a real need for survival. However, at what cost? Students will be able to compare the change in the landscape through time and research the reasons why the deforestation occurred and its profound effects on global climate and the possible loss of unidentified species. A brainstorming for solutions to this and other problems will allow students to problem solve and realize that their environment is influenced by the decisions made by others. Students will have the capability to do an in-depth image comparison over time and enter activities like the NASA Student Involvement Program.
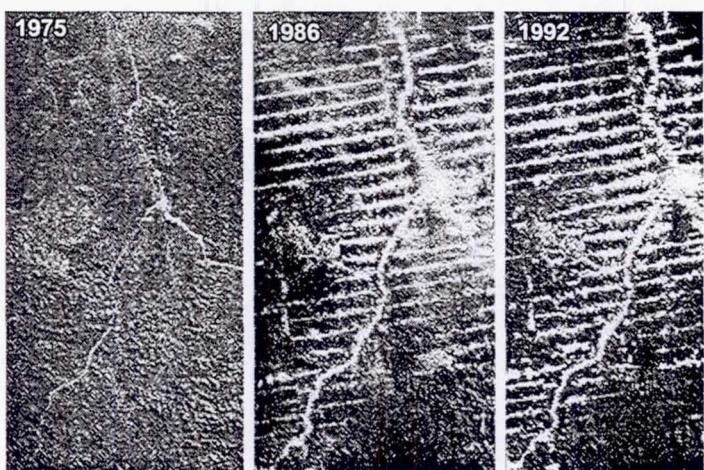

Figure 11. Deforestation in the Amazon

Students might choose to hypothesize as to what effect the burning and clearing technique has on the topsoil. Rainwater carries away the topsoil, which goes into the river system. The turbidity or clarity of river water is an indicator of the amount of sediment that is being transported. If too much sediment is transported and the velocity of the river decreases the sediment is deposited in lobes. These will cause the river to change its' course and become braided. This is evident in satellite imagery. The change in the color of the vegetation and the addition of sediment to the rivers will be evident in images taken by Skylab and by the GeoCam II cameras. A decline in vegetation and an increase in sediment load of rivers clearly points to a future environmental or agricultural problem.

Rivers, deltas, and other natural fluvial and coastal systems change through time. The formation of oxbow lakes, a changing flood plain, the development or erosion of a beach or offshore island could be investigated with a sequence of images that span several years. The tremendous diversity of fluvial systems and its relationship to the accompanying geology of the area on a global scale could be investigated by collaborative groups of students. Projects involving images taken by a camera onboard the space shuttle have engaged the students into comparisons and annotations of images from different geographic areas.

Students might choose to study the development of urban area and the transportation patterns (highways, roads and airports). This will be another feature that will be evident when images of the same area are reviewed over a span of time. The positive or negative impact of urban planning will clearly show up in images. The students' understanding and willingness to investigate a problem of their choice has lead in the past to the development of excellent student projects. For example, students have compared London to Charleston. These projects serve as models as they represent excellence. Students do not limit themselves when given the freedom to expound. Presentations in my classroom, though scientific in nature, are sometimes presented in different methods such as prose. Students are given the opportunity to explore and present in a manner of their choice.

A dramatic change in the geology of an area will prompt students to investigate the cause. The dramatic impact that a volcanic eruption has on the landscape will be best observed by a sequence of images taken over time. It will allow the teacher and students to view the total impact of the volcanic eruption on the landscape and to investigate how the environment recovers from such an event. To evaluate a change requires images of the same area over a span of time. The color images which will be taken by the GeoCam II cameras onboard the International Space Station, covering163km per side, will be ideal for this type of study. The first step will be to

identify those factors that have changed after matching up the latitude and longitude of the area. The students will be able to speculate as to what forces (wind, volcanic, influence of water) caused the changes that they see. They will be able to identify the type of change, cite evidence as taken from the images and speculate as to the cause or causes of the change. This should lead them into an in-depth study as they investigate and even hypothesize as to what will happen to this particular geological area in the future if factors remain the same. Can Do teachers have involved their students in short-range research projects in the past. These were an effective learning tool. If students were able to evaluate and to actually see the geomorphic changes that areas undergo over time, they will engage in active learning and problem solving. This will provide them with a visualization of the changing face of the Earth through time.

Technology Skills

One of the most valuable aspects of the KidSat and EarthKAM programs has been the effective way in which they allow teachers and students to utilize technology skills in an educational setting. Instruction on the use of the Internet and digital cameras serves as a useful method to teach fundamental technology skills. Previous participants have acquired the skills to qualitatively identify, annotate and interpret natural color images of the Earth from space. The KidSat and EarthKAM programs have only used natural color (red, green, blue) images while the GeoCam mission did take a single infrared band as well. Unfortunately, camera orientation limited the usefulness of the GeoCam photographic infrared images. So far multispectral, infrared and false color imagery has not been fully utilized in an educational setting. Its use will make information gathered by remote sensing a more valuable tool that will enhance and enrich the Earth Science

Figure 12. Technology skills for educators

curriculum. The GeoCam II multispectral approach will serve as an ideal instrument to address this need since the selection of spectral bands and digital image processing lie at the very heart of the technique. The inclusion of a separate natural color CCD will provide a more familiar image to users who are not yet advanced enough to take full advantage of the system's capability. These separate true color images will also provide useful reference and catalog images. They will be suitable images to compare to previous KidSat and EarthKAM images which share a similar scale. They will also be useful for comparison to the huge pre-existing library of Space Shuttle handheld pictures that are taken on every flight.

Team Building

To construct such an ambitious undertaking will require a team of educators and scientists coupled with the

active support of NASA, equipment manufacturers and institutions such as the National Geographic Society. Successful projects like GeoCam, KidSat, EarthKAM and the Jason Project have developed the model for this type of teamwork. The International Space Station will provide a new vehicle for such a joint effort to produce a scientific and educational tool of real and lasting value. Since the watershed pictures taken by Apollo 8 showed us a small blue planet hanging in a black void, we have realized just how truly majestic yet fragile our only home is. It is our generation's responsibility to teach the next generation to appreciate and better understand the many diverse but also interdependent systems that exist on this
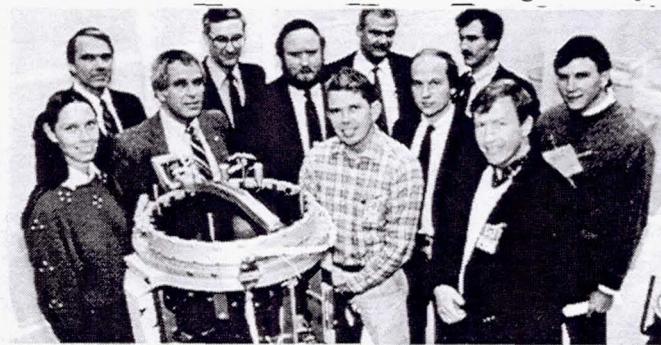
Figure 13. The 1992 GeoCam team representing the astronauts, four NASA centers, the National Geographic Society and the Can Do Project.

planet we call Earth. It is just this appreciation of our fragile planet and the interdependence of one environment on another that may prove to be the key to our survival as a species.

305

Relevant Publications

Nicholson JH: **Students With a Mission, NASA Puts the Can Do Project in Orbit**. National Geographic Magazine Vol. 186, No.2:54-69, August 1994

Nicholson JH, O'Brien TJ, Colgan M, Truluck RA, Frysinger J, Tempel CA: **Earth Observation Photography, Looking Back 20 Years After Skylab**. 1992 Shuttle Small Payload Symposium, NASA Conference Publication 3171:54-56, 1992

NASA -JSC: **Skylab EREP Investigation Summary**, NASA SP-399, prepared by NASA Lyndon B. Johnson Space Center, Washington D.C., 1978

STUDY OF DESERT AEROSOLS IN THE MEDITERRANEAN AREA – AN ISRAELI HITCHHIKER EXPERIMENT (MEIDEX)

Zev Levin, Joachim Joseph, Yuri Mekler, Yoav yair,
Adam Devir, Eliezer Ganor, Peter Israelevich, Edmund Klodz, Tamir Reisin,

Department of Geophysics and Planetary Sciences,
Tel- Aviv University, Tel- Aviv 69978, Israel.

ABSTRACT

The Mediterranean Israeli Dust Experiment (MEIDEX) will be carried out on a future flight of a space shuttle in fall 2000 or spring 2001. The aim is the inter-calibration of the primary current methods for the remote investigation of desert aerosols. The results of this experiment will contribute significantly to current and future investigations of the geographical variation of the optical, physical and chemical properties of desert aerosol properties, including the location and temporal variation of its sinks, sources and transport. This will in turn lead to the possibility to integrate in the future all available sources of information of aerosols into one data base. The idea is to simulate the TOMS and MODIS satellite experiments in one shuttle borne instrument, observing a single atmospheric volume, containing desert aerosols. The observation of this volume by our instrument will simulate TOMS and MODIS experiments as if they were conducted simultaneously. These remote observations will be supplemented from airborne and surface platforms for the purpose of absolute calibration. The prime region of interest for the experiment is the Mediterranean area and its immediate surroundings.

The MEIDEX experiment on the space shuttle includes measurements of light scattering by desert aerosol in six different wavelength intervals from the near UV to the Solar IR. The wavelengths include two used by the TOMS instruments as well as four of those installed on MODIS. The payload consists of a gimbal-mounted CCD radiometric camera. The supporting groundbased and airborne measurements both include measurement of solar spectral irradiation as well as direct sampling of aerosol size spectra and sampling for chemical analysis. A wide-angle white light video camera will make possible the observation of a large area around the instrument field of view and the identification of the presence of a desert aerosol plume and its movements.

Numerical simulations of dust transport clouds will be conducted to forecast dust plume occurrences as well as to determine the evolution of the dust plume trajectories and to understand the atmosphere-aerosol interactions. The co-location and simultaneity of shuttle, aircraft and groundbased-correlated data will make possible the validation of each remotely observed sequence of measurements.

INTRODUCTION

In the last two decades, an understanding has emerged on the extreme importance of the atmospheric aerosols for climatology, weather forecasting and biogeochemical cycling. The effect of aerosols is twofold: (a) the change of radiative balance of the atmosphere due to extinction of the solar radiation, and (b) the change of physico-chemical properties of the atmosphere itself in the presence of aerosol particles (e.g. stimulation of condensation in clouds with further precipitation etc.) For this reason, systematic studies are undertaken now in order to retrieve global distributions of the aerosols. However, well known difficulties in obtaining dust particles characteristics via remote sensing methods (refs. 1, 2) demand also correlated (groundbased, airborne, and space) observations in dedicated campaigns in specific regions (e.g. ACE 1,2, TarFox, Scar A/B/C, ACE-Asia). Such comprehensive studies and specific campaigns, along with the information on the events, will improve the methods of aerosol parameter retrieval, and enable mutual calibration and validation of data sets. In this context, the Mediterranean is a convenient focus for investigation of desert dust properties and its influence on the climate in the region.

The main source for the dust in the Mediterranean region is Sahara desert (see Figure 1). Saharan dust is transported from its sources over land and sea to regions like Europe, the Middle East and even as far as to Mexico City. This transport is effected by spectacular storm-like events, when the cloud of the desert aerosol takes the shape of a giant plume that may span the North- South extent of the Mediterranean and extend more than one thousand km from the source (see Figure 2). The average width of a plume is of the order of 200 km and its total optical depth in the visible solar spectrum may reach as much as 6. Many of the plumes have a SW- NE major axis orientation, with a large variability in direction. The appearance of these plumes does not derive from the average atmospheric circulation that has predominant wind directions from W and NW. The observed dust events are associated with the northward components of winds produced by depressions. The identification of the main zones of cyclogenesis in Mediterranean (ref. 3) enabled reference 4 to identify three major situations responsible for Saharan dust transport over Mediterranean sea. In the spring, these are Sharav cyclones (ref. 5) which move eastward along the North African cost and cross the eastern Mediterranean. In summer, high pressure over Libya (ref. 6) prevents further eastward propagation of these cyclones, and the associated dust transport occurs in the central Mediterranean. At the end of the summer, low pressures near the Balearic Islands result in dust transport mainly to the western Mediterranean. The best estimate for the maximal number of dust events in a two weeks period is 3 – (see refs. 4, 7). Figure 3 shows the seasonal dependence of the average aerosol optical depth (ref. 4) in the Eastern, Central and Western Mediterranean. However, this is only a simple localized statistic, and in order to study Mediterranean weather and climate one needs higher spatial-temporal resolution of the dust transport dynamics and of the aerosol type as well as their spatial and temporal correlations. The work of Levin et al. (ref. 8) illustrates the importance of the size and composition of the dust particles to the formation of clouds and precipitation in the Mediterranean. They showed that mixing of air masses containing pollution from Europe with desert particles produces giant CCN particles that can enhance precipitation and shorten the lifetime of

the clouds. Recent calculations by Feingold et al. (ref. 9) demonstrated that such giant CCN could enhance the drizzle formation in stratocumulus clouds, reduce its lifetime and its albedo.

MISSION DESCRIPTION

The main objective of MEIDEX experiment is the investigation of desert aerosol physical properties (optical, chemical etc.), the temporal variations of its sources, sinks and transportation. Applications to the effect on the energy balance and chemistry of the ambient atmosphere, to weather prediction and climate simulation will also be attempted. These activities include remote as well as in situ measurements of light scattering by desert aerosol particles in different wavelengths starting from the near UV to the solar infrared wavelengths. The selected wavelengths include two wavelengths used by TOMS instrument for determination of aerosol properties, as well as four of those used by MODIS. The supporting ground-based and air-borne measurements both consist of optical observations as well as direct sampling of dust particles. The airborne measurements will be planned so as to fly preferably under contemporaneous shuttle orbits. The co-location, correlation and simultaneity of shuttle, aircraft and ground-based data will make possible the validation of the remote spaceborne observations. The roles of the astronaut will be to observe the underlying terrain and identify dust plumes, their location and their extent. They will carry out the measurement sequence when they will fly over dust plumes, over the locations of the airplane or the ground observation networks or over locations where dust plumes were forecast by the model.

The payload consists of a radiometric camera, functioning in the 300-830nm spectral range. The camera has a field of view, FOV, of about 160. It is boresighted with a wide FOV (600) video camera and will be mounted in a special adjustable truss, located in a GAS canister. This truss can be tilted in the canister in such a way that the swath angle (the angle normal to the footprint line at the nadir for an earth viewing -ZLV attitude) of the FOV of the cameras can be adjusted by remote control in a range of about ±300 (or more) by steps of 50. The GAS canister is equipped with a 16" quartz window. It is pressurized and temperature stabilized by heating tapes and thermistors located in it. The radiometric camera is a Xybion model IMC-201 and it is equipped with six narrow-band filters with respective CW of 340nm, 380nm (TOMS wavelengths), 470nm, 555nm, 660nm and 860nm (MODIS wavelengths). The respective FWHM of these filters is 4nm, 4nm, 30nm, 30nm, 50nm and 40nm.

The radiometric camera will observe a volume of atmosphere containing desert aerosol with a footprint of 100 x 100 km over land sea that is illuminated by solar radiation. The observation of this volume of air by our instrument will simulate simultaneously parts of both the TOMS and MODIS experiments. The wide FOV of the video camera will make possible the observation of a large area around the narrow FOV of the radiometric camera. The astronaut and/or our ground control will identify the presence of a desert aerosol plume and will decide whether to record it on any given overpass. Currently we prefer to record aerosol and dust plumes over the general area of

the Mediterranean and its immediate surroundings (the Atlantic Sahara). On approaching the Mediterranean area (or the Atlantic Sahara region) on any given orbit the instrumentation will be switched on and tested. The astronaut using the wide FOV video camera, for the presence of dust will scan the area below the shuttle orbit and will carry out slant visibility observations. Authorization for starting a measurement sequence will also be based on predictions of dust density and plume trajectories carried out by a mesoscale model and will be transmitted to the astronaut from the ground. Part of the dust experiment is to scan, concurrently, the areas of interest with a specially equipped airplane that will sample the dust, in situ, for analysis of its physical (size distribution) and chemical (composition) properties.

The airplane will cross the dust cloud at different altitudes in order to resolve the vertical variations in dust characteristics. For this purpose the airplane will be equipped with aerosol optical counters (a modified PMS-FSSP-100 [now called SPP100-modified by DMT] and a modified PMS-PCASP [now called SPP-200]), with isokinetic inlets for aerosol sampling and an albedometer for measuring the optical depth of the aerosols above and below the penetration altitude (see Figure 4). Special attention is given to the efficient collection of the giant dust particles. Their low concentrations in the atmosphere and the difficulty in transporting them through long tubes into the cabin, makes the design of the sampling inlet that much more critical. The airplane will also carry GPS and temperature and humidity sensors. Communication between the airplane crew and the ground control scientist will allow some coordination between the shuttle and airplane position.

Additional measurements will be conducted at ground level. Some sampling of mineral dust particles will take place in Israel. These will supplement the measurements taken on the airplane in those cases when the dust storms pass the Israeli coastline. One important input to the project will be the data collected by the AERONET (ref. 10) around the Mediterranean Sea. AERONET (AErosol RObotic NETwork) is an optical ground based aerosol monitoring network and data archive supported by NASA's Earth Observing System and expanded by federation with many non-NASA institutions. The network hardware consists of identical automatic sun-sky scanning spectral radiometers. Data from this collaboration provides globally distributed near real time observations of aerosol spectral optical depths, aerosol size distributions, and precipitable water. There are a number of such instruments around the Mediterranean Sea such as in Israel, Turkey, Italy, Spain, and others.

Radiometric data will always be recorded when the airplane is underneath the shuttle. When the airplane is not on site, data will be recorded only whenever dust is either detected by the astronaut, predicted by the model forecast or both. This will constrain the data flow and storage needs to reasonable values. The instrument calibration will be performed both on-ground and in-flight. The latter is necessary since the radiometric output of the cameras can change as a result of temperature variations in the canister, window optical properties changes or other factors. The primary light source for on- board calibration is the Moon. The possibility of using earth surface regions with well-known and stable albedo and bidirectional reflectance distribution function (BRDF) for absolute and flat field calibrations is examined as well. Necessary data on surface

reflecting properties and aerosol vertical profiles will be also provided by means of the aibedometer installed on the airplane.

DATA HANDLING AND ANALYSIS

All retrieved MEIDEX data will be subdivided in three major data sets: spaceborne data set which will include the results of measurements performed aboard the shuttle, in situ data set which will include the results of airborne and groundbased measurements related to MEIDEX, and calibration data set which will include the data on the instrument calibration (laboratory and in flight) (Figure. 5).

Spaceborne data set will include several levels corresponding to the stages of data analysis. At level 0, raw data obtained during scientific experiment will be converted into digital format and stored for further analysis. Most of the raw data are expected to be the camera's continuous video recordings. These data for each frame will be converted into digital 2D distributions of the registered signal for each spectral channel. This way a 0a set will be prepared and stored for possible future references. At the next step, the raw signal will be converted in physical parameters (radiance) by use of calibration data set, orbital parameters, and technical data (technical data set describes the operation of the instrument and is included in level 0) resulting in 0b set. The 0b set will include 2D distributions of radiance for each frame and for each spectral channel. Sets in level 0 are reference data that will not be modified later.

The basic part of level 1 is 1a data set. 1a set consists of two-dimensional distributions of radiance in each of the spectral channels corresponding to a frame. This set is similar to the 0b set, however it can be modified in further analysis if the need in calibration corrections will be revealed during the further analysis. 2D distribution of radiance for each frame actually is a single snapshot (picture) made by a camera. Each file should contain one picture and its description. The description will include: number of rows in the picture, number of elements in one row, date, time, and frame number, number of spectral channel, geographical coordinates (latitude and longitude) and altitude of the shuttle, shuttle velocity vector, Euler angles of the camera with respect to the local vertical, geographical coordinates of the center of the picture and its corners.

Set 1b at level 1 results from the scientific analysis of set 1a. The measured radiance will be used in order to obtain physical parameters of desert aerosol, i.e. optical depth and parameters characterizing size distribution function. These physical parameters will be stored in the same form of 2D distributions corresponding to each single picture from set 1a. Since the aerosol parameters may be obtained by different procedures, set 1b will consist of several subsets. One of the main tasks of MEIDEX is to perform inter-calibration between the TOMS type and MODIS type measurements of the desert aerosol, we will apply to the MEIDEX data procedures of data analysis similar to those used in TOMS and MODIS experiments (e.g. refs. 11, 12).

The results of MODIS type analysis of set 1a data will be stored in 1-M subset. It is

assumed that the aerosol size distribution is described by two-mode log-normal function:

$$n(r)=\frac{dN(r)}{dr}=\sum_{i=1}^{2}\frac{N_i}{(2\pi)^{1/2}\sigma_i 2.3r}exp\left[-\frac{1}{2\sigma_i^2}\left(\frac{\ln r-\ln R_i}{\ln(10)}\right)^2\right]$$

Here N is the number density, r is the radius of the particles, R is the mean radius, and σ is the standard deviation. Such a simplified model may be applied if one suggests that the observed light is scattered by large (>1 μm) particles originated from the Earth's surface (coarse mode) and by smaller (0.04÷0.5 μm) particles resulting from coagulation (accumulation mode). The library of distributions for both modes will be prepared for our application.

The total radiance detected by the camera can be written (for each channel) as

$$L^C = \eta L^S + (1-\eta)L^L$$

where L^S, L^L are the radiance of the accumulation and coarse modes respectively. L depends on solar zenith, zenith view and azimuth view angles. In order to retrieve the ratio between the modes η and to select the parameters of each mode (R and σ), the following procedure will be applied to the data.

The radiance L^S, L^L will be computed for each of library models for the set of values of aerosol optical thickness (0, 0.2, 0.5, 1.0, and 2.0) at 550 nm. Then, it is possible to calculate the total radiance for specified optical thickness and any value of η.

From the measured radiance at 550 nm, the optical thickness is derived by linear interpolation between these five optical thickness values of each small and large mode combinations.

The fitting parameter for MODIS-type procedure is

$$\varepsilon = \sqrt{\frac{1}{n}\sum_{j=1}^{n}\left(\frac{L_j^m - L_j^c}{L_j^m + 0.01}\right)^2}$$

Where superscripts m and c refer to measured and calculated radiance, respectively, and the sum is taken over all channels.

For each small and large mode combination and each value of η, optical thickness in all channels are derived and the quantity ε is calculated. The two modes that give the smallest ε constitute the aerosol model (the 'best' solution). Along with the 'best' solution, an 'averaged' solution is to be obtained. The procedure will be applied to MODIS library

312

of models, as well as to the library, which will be constructed at TAU. As a result of the procedure, optical thickness in all channels will be obtained along with the parameters of optimal bi-mode log-normal distribution of particle size. The two-dimensional distributions of these quantities will be stored in digital form as 1-M data subset.

The results of the TOMS type analysis will be stored in *1-T* subset. The TOMS type procedure is based on the effect of aerosols on the spectral contrast between 340 nm and 380 nm backscattered radiance. The spectral contrast I_{340}/I_{380} is reduced by the presence of aerosols because of weak wavelength dependence of Mie scattering as compared with that for molecular scattering. Moreover, it becomes possible to discriminate between the UV absorbing (desert dust) and non-absorbing (sulfates) aerosols by comparison of spectral contrast with absolute backscattered radiance in 380 nm, since for the given value I_{380} the spectral contrast strongly depends on the absorption optical thickness.

Subset *1-O* will include the physical parameters obtained by other methods. This will include, in particular, detailed comparison between the remote spaceborne and in situ airborne and groundbased measurements. Also, the in situ data will be used in order to construct size and height distributions of aerosols which can be used as an input for direct radiation transfer calculations the results of which may be used for validation of remote sensing data.

Level 2 will include data averaged over several snapshots. The basis for such an averaging is provided by the fact that each point of the Earth's surface will be photographed ~50 times since the displacement of the camera VOF footprint between two successive snapshots in the same spectral channels is much smaller than the footprint size. As a result, an averaged 2D distribution of radiance will be obtained for each session (and for each spectral channel). These averaged pictures will be stored in the 2a set. The information header to each file will be the same as for the 1a set. Also, each averaged picture will be accompanied by 2D distribution of geographical coordinates of the picture.

The averaged distribution has the following advantages as compared to single picture: (a) It enables to increase the signal/noise ratio by the factor of 6. (b) The averaging procedure enables one to perform in-flight flat field calibration of the camera, since the radiance from the same region of the surface will be registered by different pixels of CCD. Using this procedure, the in-flight flat field calibration parameters will be stored in flat-field b subset of the Calibration data set. In its turn, the flat-field b set may be used for correction of 1a set data. It should be noted that the main disadvantage of the averaging is the loss of information on angular dependence of the scattered radiance.

Averaged distributions of measured radiance will be used for obtaining physical parameters of aerosol distribution similarly to Level 1. The results will be stored in the 2b set which will again include three subsets (2-M – MODIS type analysis, 2-T – TOMS type analysis, and 2-O – TAU analysis).

The Calibration data set will include the data on the instrument calibration

(laboratory and in-flight). Laboratory set will include absolute and flat field calibration results obtained before and after the flight. In-flight set will include the results of absolute calibration (using the Moon observations) and two sets of in-flight flat field calibration (observations of uniform surfaces and results of averaging procedure).

In situ data set will include the results of airborne and groundbased measurements related to MEIDEX. In particular, the albedometer data from this data set will be included in spaceborne data analysis as early as at levels.

SUMMARY

The MEIDEX will provide an important link in the production of future global data sets on desert aerosols.

The TOMS aerosol index – indicative of aerosols above about two kilometers – will be calibrated under conditions of dust transport to the MODIS optical depth in a common atmospheric volume over sea. This might make it possible to convert the TOMS index to an optical depth over both land and sea as well as to use MODIS data over land.

The shuttle measurements may be useful to other planned contemporaneous experiments. They will be supported over the Mediterranean area by airplane based information on aerosol vertical profiles and composition. Moreover, similar data from a ground-based network in the region of interest. Therefore, the remotely sensed information by the shuttle instrument will be absolutely calibrated. All data will be made available to the scientific community.

REFERENCES

1. Kaufman Y.J., D. Tanre, H.R. Gordon, T. Nakajima, J. Lenoble, R. Frouin, H. Grassl, B.M. Herman, M.D. King, and P.M. Teillet, Passive Remote Sensing of Tropospheric Aerosol and Atmospheric Correction for the Aerosol Effect. J. Geophys. Res., 102, 16,815, 1997.

2. Kaufman, Y.J., P.V. Hobbs, V.W.J.H. Kirchhoff, P. Artaxo, L.A. Remer, B.N. Holben, M.D. King, D.E. Ward, E.M. Prins, K.M. Longo, L.F. Mattos, C.A. Nobre, J.D. Spinhirne, Q. Ji, A.M. Thompson, J.F. Gleason, S.A. Christopher, and S.-C.Tsay, Smoke, Clouds, and Radiation – Brazil (SCAR-B) experiment. J. Geophys. Res., 103, 31,783, 1998.

3. Alpert P., B.U. Neeman, and Y. Shay-el. Climatological analysis of Mediterranean cyclones using ECMWF data. Tellus, Ser. A, 42, 65, 1990.

4. Moulin C., C.E. Lambert, U. Dayan, V. Masson, M. Ramonet, P. Bousquet, M. Legrand, Y.J. Balkanski, W. Guelle, B. Marticorena, G. Bergametti, and F. Dulac,

Satellite Climatology of African Dust Transport in Mediterranean Atmosphere. J. Geophys. Res., 103, 13,137, 1998.

5. P. Alpert and B. Ziv, The Sharav Cyclone - Observation and some Theoretical Considerations. J. Geophys. Res., 94, 18,495, 1989.

6. Bergametti G., A.-L. Dutot, P. Buat-Menard, R. Losno, and E. Remoudaki, Seasonal Variability of the Elemental Composition of Atmospheric Aerosol over the Northwestern Mediterranean, Tellus, Ser. B, 41, 353, 1989.

7. Ganor E. and H.A. Foner, The Mineralogical and Chemical Properties and the Behaviour of Aeolian Saharan Dust over Israel, in The Impact of Desert Dust Across the Mediterranean, ed. by S. Guerzoni and R. Chester, p. 163, 1996.

8. Levin, Z., E. Ganor and V. Gladstein, The effect of desert particles coated with sulfate on rain formation in the eastern Mediterranean. J. Apply. Meteor. 35, 1511-1523, 1996.

9. Feingold, G., W.R. Cotton, S.M. Kreidenweis and J.T. Davis, The impact of giant cloud condensation nuclei on drizzle formation in the stratocumulus: Implications for cloud radiative properties. J. Atmos. Sci. In Press, 1999.

10. Holben, B.N., T.F.Eck, I.Slutsker, D.Tanre, J.P.Buis, A.Setzer, E.Vermote, J.A.Reagan, Y.J.Kaufman, T.Nakajima, F.Lavenu, I.Jankowiak, A.Smirnov. AERONET - A federated instrument network and data archive for aerosol characterization. - Remote Sens. Environ. 66, 1-16, 1998.

11. Tanre D., Kaufman Y.J., M. Herman, and S. Mattoo, Remote Sensing of Aerosol Properties over Oceans using MODIS/EOS Spectral Radiances. J. Geophys. Res., 102, 16,971, 1997.

12. Herman J.R., P.K. Bhartia, O. Torres, C. Hsu, C. Seftor, and E. Celarier, Global Distribution of UV-absorbing Aerosols from Nimbus 7/TOMS data. J. Geophys. Res., 102, 16,911, 1997.
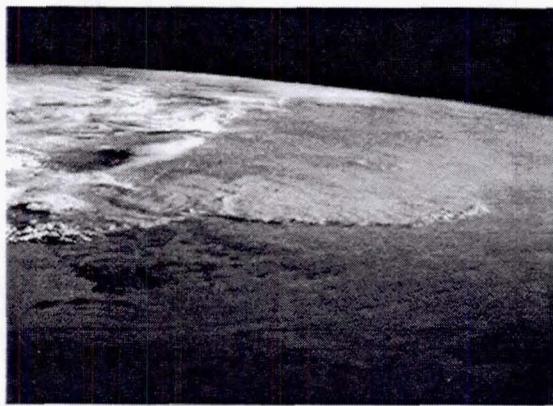
Figure 1. Dust storm in Sahara.


Figure 2. Plumes of desert aerosol.
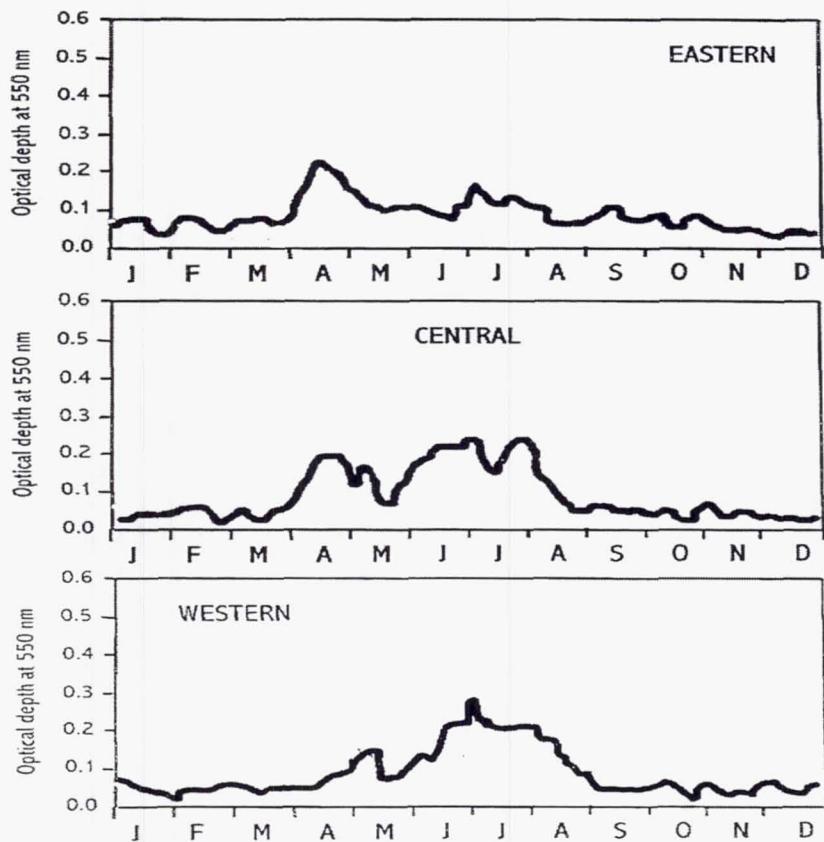
Figure 3. Seasonal dependence of aerosol optical depth in the Eastern (top), Central (center), and Western (bottom) Mediterranean.
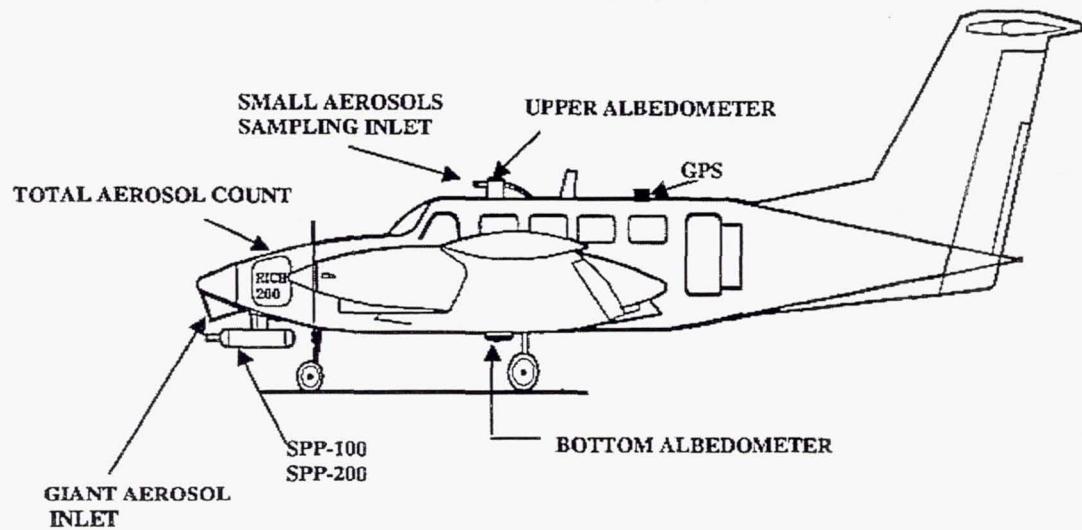
Figure 4. Schematic representation of the instruments' installation on the Cheyenne III airplane.

Data handling
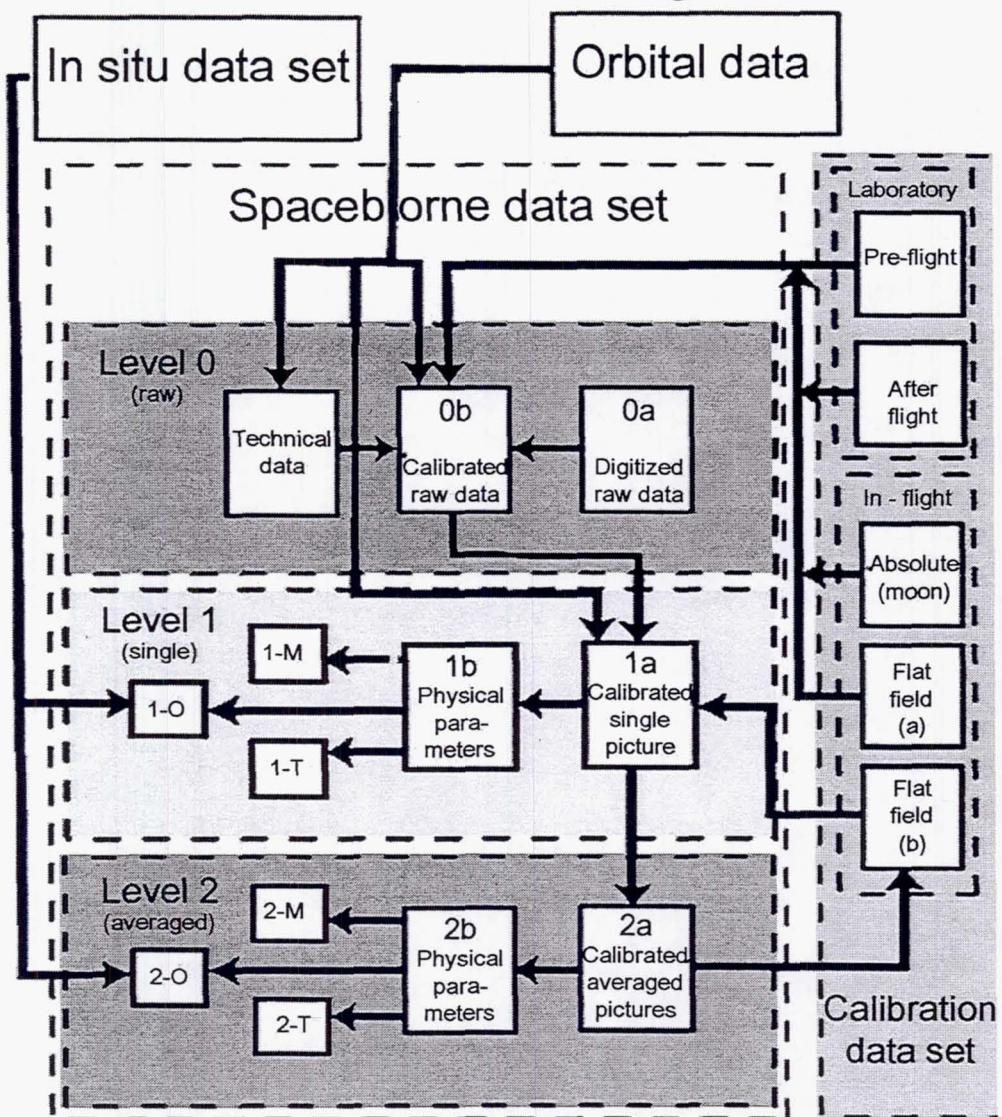
Figure 5. Flowchart of MEIDEX data processing.

CONCEPTUAL DESIGN OF THE RETROREFLECTOR, PHOTODETECTOR, AND OPTICAL BEACON PAYLOADS FOR THE PHOTON TARGET SATELLITE[*]

R. Glenn Sellar[**], Ronald L. Phillips, Larry. C. Andrews, Cynthia Y. Hopen, Derek M. Shannon,
Jennifer J. Huddle, Annabel Marcos, Jason Bachelor, Kit Van
Florida Space Institute
12424 Research Parkway, Suite 400, Orlando, FL 32826

ABSTRACT

The *Photon* microsatellite is a dedicated optical target spacecraft funded by the Ballistic Missile Defense Organization (BMDO), and planned for launch by the Shuttle Hitchhiker Ejection System. This 68 kg spacecraft will carry a 27 cm retroreflector, a photodetector, and an optical beacon; and can be used for research and testing in the fields of laser radar, optical tracking, orbital prediction, atmospheric propagation, differential absorption lidar, geodesy, and optical communications. The conceptual design of the payloads is presented, and planned experiments in atmospheric propagation are described.

INTRODUCTION

Small retroreflectors have been included on many satellites as secondary payloads, and a few satellites carry an array of retroreflectors as their primary payload. A listing of spacecraft known to be carrying retroreflectors is given Table 1. These retroreflectors are employed for a wide range of research and testing in the fields of: laser radar, optical tracking, orbital prediction, atmospheric propagation, differential absorption lidar, geodesy, and optical communications. As a spacecraft entirely dedicated to these applications, Photon is designed with five features that maximize its utility:

1) The use of a retroreflector allows two-way propagation experiments to situate their expensive and complex transmitter and receiver equipment on the ground, and allows for a wide range of experiments to be conducted by investigators in different fields, based at different ground sites.

2) Photon will carry a *single* retroreflector, rather than an array of smaller retroreflectors, thus avoiding the interference effects exhibited by arrays.

3) The effective cross-section of the retroreflector will exceed that of any others currently in orbit, or known to be in development.

4) A photodetector will be included to provide independent data for the uplink path only.

5) An optical beacon will be incorporated to both facilitate acquisition, and to provide independent information on the downlink path only. The combination of a retroreflector, photodetector, and beacon will enable researchers to separate the uplink effects from downlink effects in their experiments.

Table 1: Comparison of Spaceborne Retroreflectors

Satellite	Minimum Range [km]	Effective Diameter [cm]	Figure of Merit D^2/R^4 [1/m^2]	Number of Retro's	Beacon	Detector
LAGEOS-1,-2	5860	24	2 E-28	426	NO	NO
ADEOS	797	50	1 E-24	1	NO	NO
AJSAT	1490	215	4 E-25	1436	NO	NO
STARLETTE	812	24	6 E-25	60	NO	NO
STELLA	800	24	6 E-25	60	NO	NO
ERS-1,-2	780	18	5 E-25	9	NO	NO
TOPEX/POSEIDON	1340	150	5 E-25	192	NO	NO
METEOR-3	1180	28	1 E-25	24	NO	NO
GFZ-1	396	20	8 E-24	60	NO	NO
TIPS	1022	?	?	18	NO	NO
GPS-35,-36	20200	24	1 E-30	?	NO	NO
ETALON-1	19120	129	1 E-29	2134	NO	NO
GLONASS	19140	120	9 E-30	396	NO	NO
FIZEAU	931	15	2 E-25	3	NO	NO
RESURS-01	678	15	7 E-25	1	NO	NO
MSTI-II	431	18	5 E-24	9	NO	NO
BE-C	940	?	?	? (multiple)	NO	NO
PHOTON	350	27	1.8 E-23	1	YES	YES

SYSTEMS DESIGN

Photon is intended for launch by the Hitchhiker Ejection System[1] (HES), and this forms the basis for most of the constraints on the spacecraft design[2], shown in Table 2. The design process is primarily constraints-driven, or 'bottom-up'; the selection of launch vehicle constrains the capabilities of the spacecraft bus, which in turn constrains the payload design, which ultimately limits the science capabilities. In this design approach, the area of the retroreflector, and the intensity of the beacon are both maximized within the constraints that originated from the selection of launch vehicle.

Table 2: Spacecraft Requirements and Constraints

Payload	Maximize retroreflector size Maximize beacon intensity
Pointing	±5° nadir pointing Yaw control during active mode
Communication	2 way at elevation >20°

Telemetry	Commands – 7 Kbps
	Science data - 80 Kbps active
	  mode (2MB / 5min)
	Health - 36 hour history, 64 ch., 8
	  bits, 1 sample/min

Orbit	352 km, 28.5° or 407 km, 51.6°
Design Lifetime	1 year
HES constraints	Max. 68 kg Max. 482 mm dia., 520 mm height Max CG 266 mm axial, 12 mm radial Marmon ring launch adapter NASA safety requirements

The spacecraft structure, as shown in Figure 1a, is an octagonal cylinder, designed to maximize the area of the body-mounted solar arrays, while fitting within the allowed envelope for the HES.

(a)   (b)
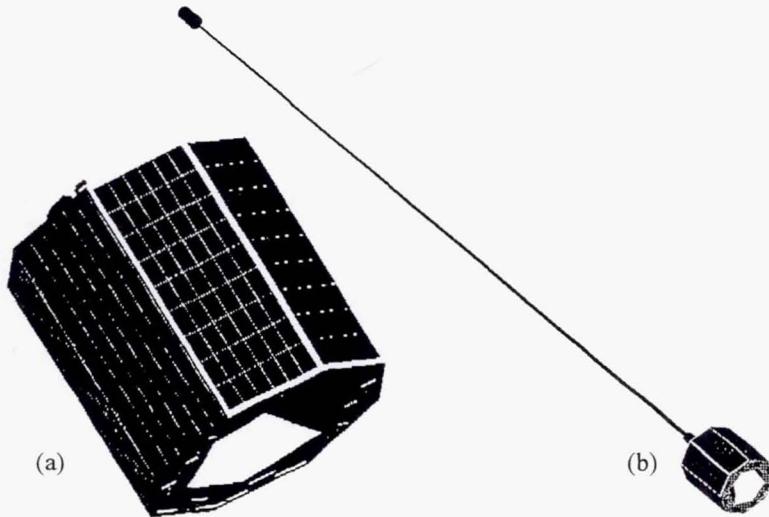
Figure 1: Photon satellite (a) with boom stowed, (b) with boom deployed (different scales).

Attitude is controlled by gravity gradient stabilization with active magnetic damping, which is expected to provide nadir pointing within ±5°. A 6 m long boom, with a 2 kg tip mass, utilizes the gravity gradient, while a set of magnetic torque rods is used to dampen librations. A single, fixed-speed momentum wheel will also be incorporated, to provide stability in the yaw axis. The spacecraft is shown with the boom deployed in Figure 1b.

A three-axis control approach was considered, but was determined to increase the cost and risk substantially, with only a modest improvement in science capabilities. Three-axis control would have enabled the retroreflector to be oriented perpendicular to the line-of-sight to the ground station. It was noted however, that the maximum reflected flux is reached when the ground station is at the nadir of the spacecraft (minimum range), so the *maximum* flux would not be improved by three-axis pointing. The reflected flux is proportional to the projected area of the retroreflector (which is a function of the incident angle θ), and inversely proportional to the fourth power of the slant range. Relative flux is plotted as function of the zenith angle of the spacecraft as seen from the ground station, in Figure 2.
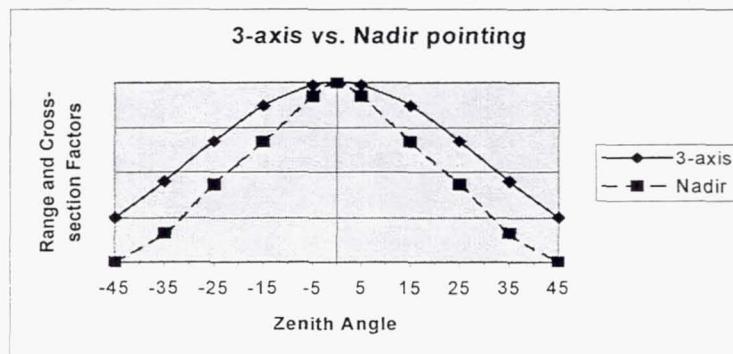

Figure 2: Relative flux versus zenith angle.

Nadir-pointing does add a requirement to the optical beacon, however. In order to maximize the intensity, the beam divergence must be small, and this requires that the beacon be actively pointed at the ground station. A small gimbal designed to meet this requirement is less costly than a three-axis control system for the spacecraft, as discussed later.

Mission Analysis

While maximizing the returned flux will maximize the quality of the data collected, the quantity of data is also an important parameter. Orbital analyses have been completed that show the expected number of passes for a ground station at a latitude of 28°. Analyses for two orbits are presented in Table 3: the Shuttle's 'default' orbit of ~350 km altitude at 28.45° inclination, and the International Space Station orbit of ~407 km altitude at 51.6° inclination. The altitude affects primarily the lifetime of the mission, while the inclination affects the number of passes. A 'pass' as defined here is any orbit when the satellite will reach an elevation of > 45° as seen from the ground station.

Table 3: Predicted number of passes reaching elevation > 45° for a ground station at 28° latitude.

Orbit	Columbia	Space Station
Nominal Lifetime [days]	162	474
95% Prob. Lifetime [days]	85	241
Passes/year	706	177
Nominal Passes	**313**	**230**
95% Prob. Passes	164	117

Of course, weather conditions – particularly cloud cover – will prevent some number of these passes from being used for experiments. For example, for a ground station at Kennedy Space Center, clear or scattered cloud cover is reported 40% of the time, while conditions are broken or overcast the other 60% of the time.

RETROREFLECTOR PAYLOAD

The most practical form of retroreflector is the 'cube-corner' retroreflector. This consists of three planar mirrors, mutually orthogonal to one another. An incident ray of light reflects from each of the three mirrors, and emerges in a direction exactly opposite to the direction of entry. This retroreflecting property greatly relaxes the pointing requirements on the spacecraft. Since the angle of reflection is independent of the orientation of the retroreflector. The retroreflector can be constructed either as a single solid prism, with three internal mirror surfaces; or hollow, comprised of three separate first-surface mirrors. Solid cube-corner retroreflectors are less expensive, but they are more massive, affect the polarization, and are restricted to wavelengths at which the material is transparent. The design for Photon is the hollow version.

To obtain a large reflecting area, arrays of smaller retroreflectors are often used (see Table 1), since these can be less massive, less costly, and require a smaller volume compared to a single retroreflector with the same area. But when reflecting coherent radiation, each element in an array will act as a separate source, thus producing an interference pattern in the return beam. This pattern will move across the ground station as the spacecraft moves along its orbit, which causes additional complications for many experiments. Other projects, such as the Retroreflector in Space[3] (RIS) on the Advanced Earth Observation

Satellite (ADEOS), avoid this problem by employing a single large retroreflector, and the Photon project also takes this approach.

Size constraints

In the Photon conceptual design, the retroreflector (and the other payload elements) are placed at the end of the spacecraft opposite the gravity gradient boom and nearest to the earth. The payload module is shown here in Figure 4:
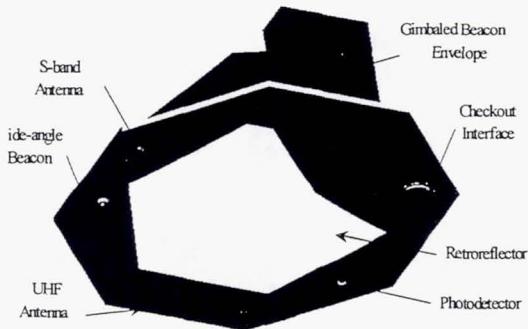

Figure 4: Payload Module

Following the 'bottom-up' design approach, a primary requirement is to maximize the area of the retroreflector, within the constraints imposed by the HES. There are four constraints on the size of the retroreflector: the maximum allowable diameter of the spacecraft, the maximum allowable length of the spacecraft, the maximum allowable mass, and the maximum distance allowed between the center-of-gravity of the spacecraft and the marmon clamp interface with the HES. Which constraint first limits the size of the retroreflector depends upon the shape of the retroreflector facets, and the material used for the mirrors.

If the material for the retroreflector mirrors is glass or fused silica, then as the size of the retroreflector is increased, the first constraint encountered is the maximum allowable distance between the C-of-G and the marmon plate interface. Fortunately, recent advances in composite technology now allow imaging-quality mirrors to be produced on composite substrates, reducing the mass per unit area by roughly an order of magnitude.

For a composite retroreflector, the first constraint encountered is either the maximum length or the maximum diameter, depending on the shape of the facets. Cube-corner retroreflectors commonly have either facets that are right-angle triangles, or facets that are square, as shown in Figure 5a and 5b respectively. The volume encompassed by a retroreflector with triangular facets is a triangle based prism, while the volume occupied by a retroreflector with square facets is a cube.

For a square-faceted retroreflector, the first constraint is on the apex height. The stowage for the gravity gradient boom occupies almost half of the available length along the centerline of the spacecraft, and the apex height of the retroreflector is limited to the remaining length.

A triangular-faceted retroreflector has a smaller apex height compared to a square-faceted retro with the sides of the same length. But with triangular facets, the corners of the triangular aperture are not

effective, since rays that are incident in the corners will miss the third mirror, and thus are reflected in a direction other than back along the incident direction[4].

The retroreflector for Photon is an innovative third configuration. It has the form of a triangular-faceted retroreflector with the corners removed. This produces facets that are actually irregular pentagons, as shown in Figure 5c:
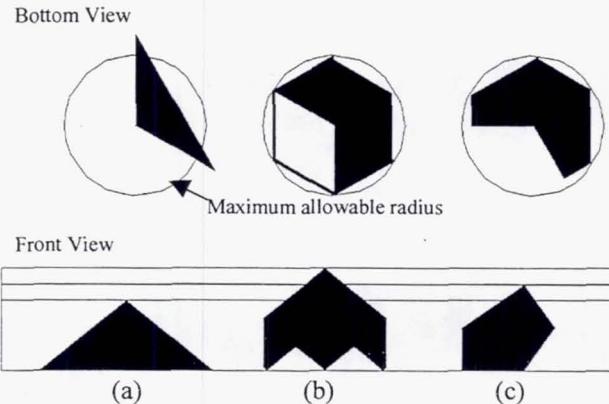

Figure 5: Retroreflector configurations, (a) triangular-faceted,
(b) square-faceted, (c) pentagonal-faceted.

This maximizes the effective area of the retroreflector, while maintaining the apex height within the constraints. As can be seen in Figure 4, the envelope allocated for the retroreflector now fills all of the surface area of the nadir face except for the small area required for other components.

The most important science requirement is to maximize the flux received by the ground station. This flux is proportional to the second power of the diameter of the retroreflector, and the inverse fourth power of the range. Table 1 compares this figure-of-merit (D^2/R^4) for other orbiting retroreflectors. The range factor is highly important, due to the fourth power dependence. Thus, while the retroreflector on Photon will be smaller than the RIS on ADEOS, the returned flux will be a factor of 18 larger due to the lower orbit.

Velocity aberration

An interesting effect that occurs when using a moving retroreflector is known as the *velocity aberration*. This term originates in the field of astrometry, where it is used to designate the difference between the true angle to a star and the observed angle to a star, induced by the relative velocity between the observer and the star. In the context of an orbiting retroreflector, another term for this effect might be *point-behind error*. It is fairly intuitive to expect that in order to hit a moving target one must point slightly ahead of the target along its trajectory. This is the case when aiming a laser beam at a satellite in low earth orbit, where the spacecraft is orbiting at a velocity on the order of 7 km/s. This *point-ahead error* can be incorporated in the control system that points the ground station's beam director. It is perhaps less intuitive that, in the *spacecraft's* frame of reference, it is the ground station that is moving at 7 km/s in the opposite direction. Thus, in order to hit the ground station, the spacecraft should point the reflected beam 'ahead' of the ground station (i.e. in a direction opposite that of the spacecraft's velocity – in that sense *behind* the ground station). But the property of a retroreflector is that it will reflect the beam back in exactly the same

direction that it entered, so this *point-behind error* is not accommodated. Thus, by the time the beam reaches the ground station, it arrives slightly in front of the ground station, as illustrated in Figure 6:
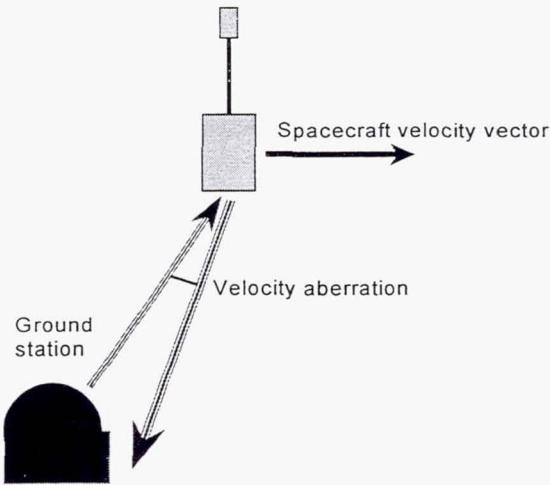

Figure 6: Velocity aberration

The angle of the velocity aberration θ is given by[3]:

$$\theta = \frac{2v \sin\phi}{c} \tag{1}$$

Where v is the tangential velocity, ϕ is the elevation angle of the beam from the ground station, and c is the speed of light. For a satellite in a 400 km altitude orbit, the return beam will be centered on a point about 19 m from the optical transmitter. One solution to this problem would be to locate the ground receiver at this offset location. But each orbital pass visible from the ground station may have different ground tracks, so the direction of this offset may be different for each orbit.

A more practical solution in most cases is to diverge the return beam such that the optical receiver is included within the beam. For a small retroreflector ($< \sim 2$ cm) diffraction will diverge the beam sufficiently. In the case of a larger retroreflector, the retroreflector should be deliberately 'spoiled'.

The retroreflectors for the Relay Mirror Experiment[5] (RME), had vertex angles slightly different from the nominal 90°, and incorporated a cylindrical lens. The RIS experiment[3] on ADEOS also spoiled the angles, but curved one of the mirrors rather than adding a cylindrical lens. The Photon retroreflector design will be similar to that used for the RIS.

These techniques can be used to tailor the beam pattern to some extent. When the angles are spoiled, the beam splits into 4 or 6 separate beams, arranged in pairs on opposite sides of the center of the pattern. By curving one or more of the mirrors, or adding a lens, the divergence of these beams can be increased. Unfortunately, the symmetry properties do not allow the centroid of the beam pattern to be offset, and much of the return flux will still miss the ground station. But it is possible to make the beam pattern roughly elliptical, and to control the radial distribution of flux to some extent, which can be more efficient

than simply expanding a circular beam pattern to include the ground station. An elliptical return beam, however, adds a requirement for yaw control on the spacecraft; and this is the reason for the incorporation of the single, fixed-speed momentum wheel in the attitude control system for Photon.

Link Model

A comprehensive link model has been developed to predict the flux that will be returned to a receiver at the ground station. This model incorporates transmitter power, diameter and wavelength, various retroreflector configurations, the orbital geometry, atmospheric turbulence ('seeing' conditions), atmospheric attenuation, and the design of the receiver. As an example, for a laser transmitting 7 W at 1.5 μm, under moderate atmospheric conditions, the photon irradiance at the ground station is expected to be on the order of 1×10^6 photons/s/cm^2.

BEACON PAYLOAD

The optical beacon on Photon has two functions: it is a source for one-way downlink experiments, and it aids acquisition of the spacecraft by the ground station, particularly when the spacecraft is eclipsed. Since the spacecraft is nadir pointing, there were two options for the beacon design, a fixed beacon with a very wide angle beam, or a gimbaled beacon that is actively pointed at the ground station. An actively pointed beacon could have a beam with low divergence, and therefore higher intensity. The limit on the divergence of the beam is based on the stability of the attitude control system. For this design, the expected stability is ±5°, which enables a beam with an intensity roughly 200 times that for a fixed beacon with a nearly hemispherical beam divergence. The advantage of a fixed beacon, on the other hand, is higher reliability. Photon will carry *both* a gimbaled beacon and a fixed beacon. The fixed beacon is primarily a backup in case of a failure in the gimbal mechanism.

Both beacons will be high power laser diodes with center wavelengths in the 800-900 nm range. Each requires 25 W of electrical power to output ~3 W of optical flux. The 25 W requirement may seem high for a small satellite, but a beacon will be operational only during an experiment. With a maximum of 3 experiments of 10 minutes duration each per 24 hr period, the duty cycle is <2%. The gimballed beacon will be coupled to an optical fiber terminated with a small collimator lens (3 mm diameter, 20 mm focal length). The far-field divergence angle of the beam will be set at 5° half-angle, so the expected irradiance at the ground station will be on the order of 1 nW/m^2.

It is this collimator that will be pointed by the gimbal system. The gimbal system has two degrees of freedom, provided by two nested gimbal mechanisms. Any tracking system based on nested gimbals has a blind-spot, or 'keyhole' in directions near the axis of the outer gimbal. The angular velocity at which a gimbal mechanism can track is limited, but when as the object approaches the axis of the outer gimbal, the required angular velocity of the outer gimbal approaches infinity.

In our design, the axis of the outer gimbal is oriented in the cross-track direction (along the pitch axis of the spacecraft). As illustrated in Figure 2, the returned flux drops to zero when the ground station (as seen from the spacecraft) is >45° from the nadir. Therefore experiments will only be performed only on passes when the spacecraft will reach elevation angles above 45° (as seen from the ground station); and the mechanism will never be required to point near the axis of the outer gimbal. The required angular ranges for the gimbals result from the geometry of the orbit, and the >45° elevation constraint, as shown in Figure 7:
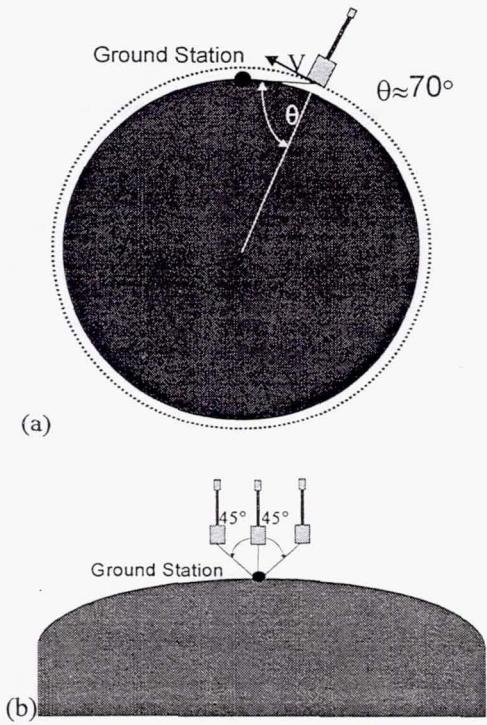
Figure 7: Gimbal ranges: (a) pitch range - viewed perpendicular to plane of orbit,
(b) roll range - viewed along spacecraft velocity vector

The outer (pitch) gimbal has a range of $\pm 70°$, and the inner (roll) gimbal has a range of $\pm 45°$. The gimbal design is shown here in Figure 8:
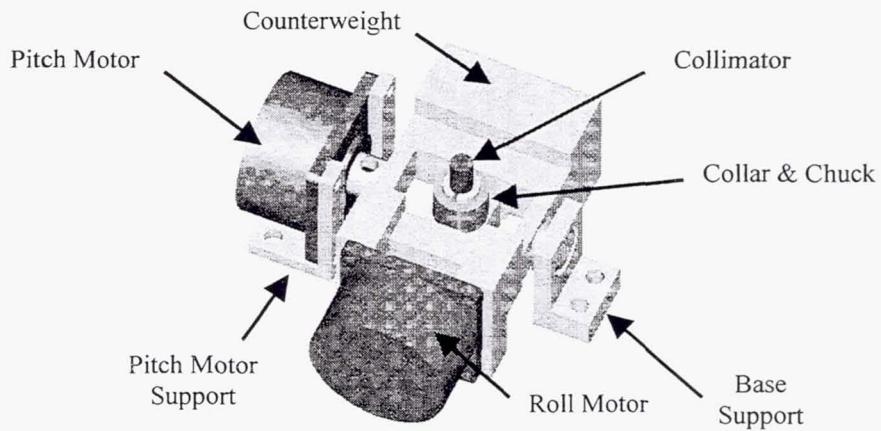

Figure 8: Gimbaled Beacon

The entire assembly shown in Figure 8 fits within a 50 mm x 50 mm x 50 mm envelope.

DETECTOR PAYLOAD

A photodetector will be included to provide a measure of the one-way uplink flux and scintillation. The design of this payload element is currently less advanced than the other payload elements. The science requirements for the co-phased array experiment put the following requirements on the detector, shown in Table 4:

Table 4: Requirements for the Detector Payload

Desired Field-of-view	30° half angle
Expected range of irradiance	1 nW/cm^2 to 1 μW/cm^2
Desired resolution	12-bit; or 8-bit with selectable gain
Sampling rate	10 kHz
Bandpass filter(s)	(to be determined)

CO-PHASED ARRAY EXPERIMENT

The Co-Phased Array Experiment is one example of an investigation that will use the Photon spacecraft. This experiment has two primary objectives: to provide tractable, validated models of propagation of laser beams through the atmosphere[6]; and to demonstrate techniques for mitigation of atmospheric turbulence in laser communications and laser radar from ground to space.

Laser communications techniques are currently being seriously developed by many organizations for inter-satellite communications. But the effects of optical turbulence (refractive index variations) in the atmosphere present challenges for optical communications from space-to-ground or space-to-aircraft. Techniques have been developed to mitigate these effects by employing an array of small apertures, and optically co-phasing the signals from the individual apertures before summing the signals together[7]. This is essentially an application of adaptive optics techniques – which have been successful in imaging applications – to the fields of optical communication and laser radar. Adaptive techniques are particularly well-suited to optical communications since one has *a priori* knowledge that the source is a point source. The co-phased array technique is illustrated in Figures 9 and 10, which shows a four element array:
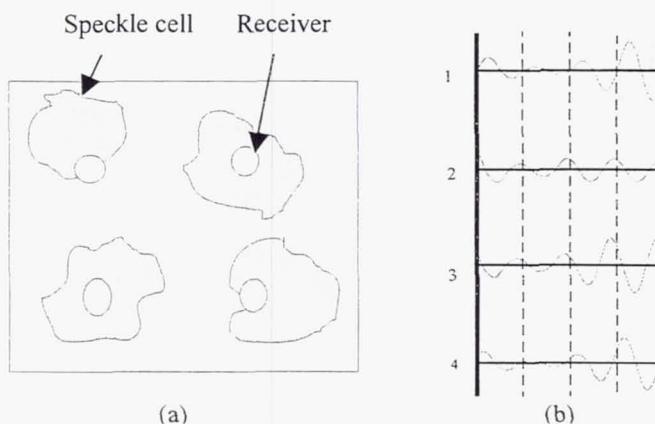

Figure 9. Speckle pattern: (a) speckle cells, and (b) individual signal amplitude characteristics.
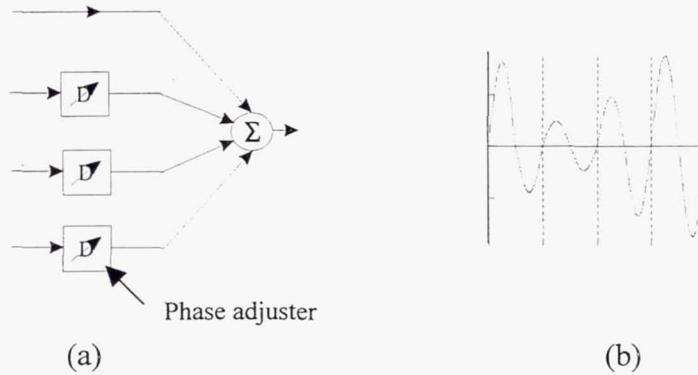
Figure 10. In-phase addition of optical signals: (a) co-phasing signals, and (b) composite output.

The speckle cells in Figure 9 can be thought of as portions of the wavefront that have effectively uniform phase.

This co-phased array technique has been successfully demonstrated on a 1 km horizontal path. The Photon spacecraft will allow tests of a similar system designed to demonstrate this technique in a space-to-ground application. In this experiment, three-frequency heterodyne techniques will be used to compensate for the large doppler shift induced by the spacecraft's high velocity[8,9].

CONCLUSION

The conceptual design of the Photon spacecraft has shown that a spacecraft designed within the constraints of the Hitchhiker Ejection System can serve as a capable target for a wide range of investigations. Photon will carry a single retroreflector with an effective cross-section larger than any other orbiting retroreflector. The inclusion of a high-intensity laser beacon, and an onboard photodetector provide additional data for experiments in laser radar, optical tracking, orbital prediction, atmospheric propagation, differential absorption lidar, geodesy, and optical communications. Experiments in optical communications and laser radar are currently in development, and additional experiments in these and other fields are invited to participate.

REFERENCES

[1] *Hitchhiker Customer Accommodations & Requirements Specification*, HHG-730-1503-07, Goddard Space Flight Center, 1994.

[2] Shannon, D. M., Singh-Derewa, C., Jayaram, S., "The Florida Space Institute's Photon Satellite Bus," *Proceedings of the Thirteenth Annual AIAA/USU Conference on Small Satellites*, Utah State University, September 1999 (submitted).

[3] Minato, A., Sugimoto, N., Sasano, Y., "Optical design of cube-corner retroreflectors having curved mirror surfaces," *Applied Optics*, vol. 31, October 1992, pp. 6015-6020.

[4] Arnold, D. A., *Method of Calculating Retroreflector-Array Transfer Functions*, Special Report Series, Smithsonian Astrophysical Observatory, Cambridge, MA.

[5] Dierks, J. S., Ross, S. E., Brodsky, A., Kervin, P. W., Holm, R. W., "Relay Mirror Experiment overview: a GBL pointing and tracking demonstration," - *Acquisition, Tracking, and Pointing V*, Proceedings of the SPIE vol. 1482, August 1991, p. 146-158.

[6] Andrews, L. C., Phillips, R. L., and Yu, P. T., "Optical scintillations and fade statistics for a satellite-communication system," *Applied Optics*, vol. 34, 1995, p. 7742.

[7] Weeks, A. R., Xu, J., Phillips, R. L., Andrews, L. C., Stickley, C. M., Sellar, R. G., Stryjewski, J. S., Harvey, J., "Experimental verification and theory for an eight-element multiple-aperture equal-gain coherent laser receiver for laser communications," *Applied Optics*, vol. 37, 1998, pp. 4782-4788.

[8] Teich, M. C., Yen, R. Y., "Three-Frequency Nonlinear Heterodyne Detection", *Applied Optics*, vol. 14, 1975, pp. 666-688.

[9] Xu, J., Phillips, R. L., Andrews, L. C., "New scheme of coherent array detection to cancel out phase fluctuations and Doppler frequency shift due to atmospheric turbulence and target movement for laser communications," *Free-Space Laser Communication Technology XI*, Proceedings of the SPIE vol. 3615, 1999, pp. 325-330.

THE HITCHHIKER'S GUIDE TO I&T

Michael R. Wright
NASA Goddard Space Flight Center

ABSTRACT

With over two dozen missions since the first in 1986, the Hitchhiker project has a reputation for providing quick-reaction, low-cost flight services for Shuttle Small Payloads Project (SSPP) customers. Despite the successes, several potential improvements in customer payload integration and test (I&T) deserve consideration.

This paper presents suggestions to Hitchhiker customers on how to help make the I&T process run smoother. Included are: customer requirements and interface definition, pre-integration test and evaluation, configuration management, I&T overview and planning, problem mitigation, and organizational communication.

In this era of limited flight opportunities and new ISO-based requirements, issues such as these have become more important than ever.

HITCHHIKER'S HEROIC, YET HUMBLE, HISTORY

The Hitchhiker program was created in 1984 to provide quick-reaction, low-cost opportunities for small payload customers on the shuttle (ref. 1). The Hitchhiker system was designed with standard, basic payload-to-orbiter interfaces and user-friendly customer-to-carrier interfaces. By minimizing payload-unique design and integration requirements, as well as reuse of flight hardware, development time and recurring costs are reduced. Further, "in-house" development, operations, and management at Goddard Space Flight Center (GSFC) has helped to make the Hitchhiker program an extremely cost-effective means of flying payloads on the shuttle (ref. 2).

The first Hitchhiker flight in 1986 was the start of what has been a 13-year history of successful "faster, cheaper, better" service, long before this phrase was even coined. Since then, over two dozen Hitchhiker missions have been flown, involving over 50 instruments. This flight rate has made Hitchhiker indisputably one of the "frequent fliers" of the U.S. manned spaceflight program.

Despite its successes, Hitchhiker has also seen some challenges. While some of these issues are related to the carrier system, others stem from the customer instruments themselves. Many of the customer-related difficulties encountered over the years could have been mitigated with the proper planning, coordination, and implementation.

HINDSIGHT IS 16-28

From the very start of their requests for flight, Hitchhiker customers must consider what special interfaces, services, integration, test and operations requirements will be needed. The more specific and complete the information provided in the beginning, the better prepared the Hitchhiker I&T team will be to "meet or exceed our customer's requirements," as stated in GSFC's new policies based on ISO-9001 (ref. 3).

This means identifying, well in advance, the requirements for:

- Electrical interfaces, such as command, telemetry, recording, and video;
- Mechanical interfaces, like mounting locations, orientation, and handling;
- Thermal interfaces, including heaters, blankets, and mission thermal modeling;
- Ground support equipment (GSE), such as "customer GSE" (CGSE), slings, and containers;
- Instrument servicing, for example, purging, battery charging, and associated accessibility;
- Safety, including hazardous materials and operations, the requirements of which can be found in the STS safety documents (refs. 4, 5, 6);
- Other I&T issues, such as cleanliness, tethering, temperature, and humidity.

These requirements are defined in the Customer Payload Requirements (CPR) document and in detail in the carrier-to-experiment Interface Control Document (ICD).

TO T&E OR NOT TO T&E . . .

To be qualified for flight, customer hardware must meet the qualification and interface test requirements in areas such as vibration, thermal-vacuum, and electromagnetic compatibility (EMC). In the past, some customers have requested that Goddard perform pre-integration test and evaluation (T&E) activities as an optional service. Although GSFC has done its best to accommodate such requests, this practice is generally discouraged due to the limited resources available to Hitchhiker, both in manpower and facilities. Therefore, it is strongly recommended that customers complete all T&E activities (including EMC testing) prior to arrival at GSFC for final flight integration.

Of course, in order for customers to complete a T&E program adequately, the proper verification requirements must be understood. For example, vibration test requirements are generally contained in the GEVS (ref. 7). For EMC, the requirements are defined in the Orbiter/Cargo "Core" ICD (ref. 8). Environmental test specifications may be driven by mission-unique requirements which would be included in the payload ICD.

Besides the usual qualification and acceptance testing, pre-integration testing with the carrier is also recommended. Pre-integration testing provides customers an opportunity to verify function of both flight and ground system interfaces to Hitchhiker. It is usually performed early enough to allow time to make any modifications, if necessary, prior to final delivery. Tests can be performed using prototype or flight hardware (or software) in development, as well as customer ground support equipment (CGSE).

Pre-integration fit-checking of new flight hardware is also a good idea to verify mechanical interfaces to the Hitchhiker carrier hardware. History has shown that, despite the best drawings, actual hardware may not always fit properly. Pre-integration operations also provide an opportunity to verify the accuracy of I&T procedures prior to final delivery.

CM (DON'T SKIP OVER THIS SECTION)

With the introduction of GSFC's new policies based on ISO-9001, configuration management (CM) has become the buzz-word of the day. As mentioned earlier, one of the overarching goals of the new Goddard policies is to "meet or exceed our customer's requirements."

In the case of payloads, this means flying the customer's hardware and completing the mission objectives. To do that, the SSPP needs to fulfill JSC's safety requirements and GSFC's documentation requirements; and to do that, the detailed instrument "as-built" configuration and certification data are needed. More than one customer has discovered that, if their documentation is incomplete, they won't fly. This is because payload design details are required to support flight and ground hazard analyses, as well as provide proof of flight qualification and traceability. In fact, Hitchhiker is now requiring complete flight cert and safety data before integration activities can commence.

Further, a CM program involving complete and organized documentation lends credibility, not only to the payload customer community, but to the Hitchhiker program itself. That is, it inspires a certain level of confidence that the payload integrity has been maintained through a tracking discipline (ref. 9). It also provides an invaluable source of information if troubleshooting becomes necessary. Besides these concrete, real-world issues, lack of payload CM does not meet the new requirements based on ISO-9001.

For these reasons, experiment developers should keep logs and drawings showing the as-built configuration of the instrument. This documentation can help ensure that the payload safety review process, as well as I&T itself, proceeds smoothly. Documentation which is useful to maintain during instrument development includes:

- Test and assembly logs, including records of any anomalies and modifications;
- Certificates of compliance for materials and components, including those provided by vendors;
- Record of Mandatory Inspection Points (MIP's) to verify safety items and as-built configuration;
- Up-to-date mechanical drawings and electrical schematics, including fuse and wire sizes;
- Parts and materials lists, with MSDS's for hazardous materials;
- Fastener certifications and logs, including torque levels;
- Summary of open items, if any, to be addressed following delivery to GSFC.

Upon delivery to Goddard, customers should have this information available for review, along with a summary of any open items or problems which need to be addressed. Examples of archived documentation such as cert logs, problem records, certificates of compliance, and safety verification tracking logs can be provided by the Hitchhiker project upon request.

In an effort to help define customer documentation requirements, the new revision of the Hitchhiker CARS document (ref. 10) includes a list of customer deliverables. Besides supporting safety verifications, deliverables such as a complete set of interface schematics and procedures (both planned and contingency) can help the Hitchhiker I&T team be better prepared to support customer operations.

YOU'RE NOT IN KANSAS ANYMORE

Upon final delivery to Goddard for preflight integration, approximately eight months prior to launch, the customer performs a post-ship stand-alone functional test. This is usually conducted in a class 100,000 cleanroom facility which supports Hitchhiker integration. Throughout preflight operations, the customer's flight hardware may be accommodated with optional services, such as a dry-nitrogen purge. Again, these services would be predefined in the CPR and payload-to-carrier ICD.

Integration of the experiment with the Hitchhiker carrier begins with mechanical integration, such as into a canister, or onto a plate or pallet. All experiment hardware is then electrically integrated with the Hitchhiker carrier, which includes continuity and isolation resistance measurements. After all electrical connections are made, functional tests are performed with the Hitchhiker flight hardware, Advance Carrier Customer Equipment Support System (ACCESS), and CGSE. To help verify command and telemetry interfaces between the ACCESS and CGSE, it is recommended that customers utilize the command status and link status packets provided by ACCESS (ref. 11).

Once all payload components are integrated and thermal blankets installed, the entire payload is moved to the EMC facility for electromagnetic compatibility testing. Usually around this time, telemetry is also recorded for later use during mission simulations. Since these mission sims are usually scheduled in parallel with I&T, customers should plan to deliver two sets of CGSE to Goddard. Following the EMC test, the payload and GSE are prepared for shipment to the Kennedy Space Center (KSC) launch site.

PREPARING FOR THE STORM

Before the payload is shipped, several important areas must be addressed well in advance. First, arranging the transport of some payloads must begin as early as one-year prior to shipment. This is primarily due to strict Department of Transportation (DOT) regulations for shipping hazardous materials. Customers must keep in mind that any hazardous material or item must be identified early enough for GSFC to obtain the necessary DOT approvals, which can take several months to process.

Second, prior to payload arrival at KSC, all planned and contingency procedures should be already approved by GSFC and KSC weeks in advance. In particular, hazardous operations must be submitted to GSFC 75 days before first use. These include everything from lifting and ordnance operations, to use of lasers and high-pressure gases. The deadline is necessary to allow Goddard enough time to review and submit procedures to KSC for final safety approval.

The last "big hitter" in preparation for KSC operations is training and badging. All payload personnel, NASA and non-NASA, must be properly trained and badged to enter and work in facilities at KSC. Two types of badging are in force at Kennedy: one to allow access onto government property, and another to allow entry into designated areas and facilities. The latter requires training for each individual area or facility, and can be either "escorted" or "unescorted."

Since most Hitchhiker customers are one-time visitors, the escorted badging is usually sufficient and does not require any special training. However, if any customer plans to visit KSC several times or for long periods, then an unescorted badge is recommended. Since a constant escort is not required with this badge, it allows more freedom to conduct payload operations in secure facilities. Customers should plan to submit requests for unescorted badging at least a year prior to need.

THE MAIN EVENT

The payload is shipped via an environmentally controlled vehicle to KSC. Following arrival, the payload is transferred to a payload processing facility (PPF), typically a class 100,000 cleanroom. The payload is then tested and prepared for orbiter integration. This includes functional tests of each instrument using the ACCESS and CGSE, as well as a simulated orbiter interface verification test (IVT). Other optional prelaunch operations, such as alignment or instrument servicing, are also performed at this time.

After all "off-line" operations are complete, the payload is typically transferred to the orbiter integration facility via KSC's payload transport canister (for bridge payloads) or by van (for side-mounted payloads). Orbiter integration is accomplished either horizontally in the Orbiter Processing Facility (OPF) or vertically at the pad, depending on schedule and access requirements.

Following orbiter electrical connections, the payload-to-orbiter IVT is conducted. The purpose of this test is to perform the minimum testing required to verify copper path interfaces between the payload and orbiter; it is not considered a functional test. During the IVT, commands are sent to Hitchhiker by KSC from the Launch Control Center (LCC) and monitored by Hitchhiker and customer personnel at the PPF. Command bit patterns are predefined months in advance; therefore, any experiment-specific command patterns should remain unchanged following submission to Hitchhiker.

After the IVT and prior to final payload-bay door closure, close-out operations are performed. These include removing any purge or trickle-charge lines, removing any non-flight covers, and taking payload close-out photographs. Typically, no customer operations are performed in the orbiter unless previously agreed upon as an optional service.

Following the mission, nominal landing is at KSC. The payload is removed from the orbiter at the OPF and is transferred via transport canister or van to the PPF. Usually, no post-flight testing or experiment deintegration is conducted at KSC.

The payload is then shipped back to GSFC for carrier and experiment deintegration, at which time the hardware is returned to the customer. This occurs no earlier than one month after a landing at KSC. Contingency post-flight testing may also be performed at Goddard, if necessary.

"GREENBELT, WE HAVE A PROBLEM."

Any aerospace program can experience technical problems, whether it be a large project involving hundreds of individuals or a smaller one made up of only a couple of dozen. In the latter case, such as Hitchhiker, the efforts of each individual can have an even greater influence on overall mission success and safety. Each team member must help ensure that integrity is maintained and requirements are fulfilled. For customers, this means making sure that their instruments meet all carrier interface and safety requirements.

For example, electrical problems frequently stem from incorrect or inadequate grounding, isolation, shielding or filtering. Consideration of these design issues is particularly important if the experiment hardware includes pumps or power supplies which may induce noise. These issues can be mitigated through adherence to the customer-to-carrier interface requirements specified in the CARS, as well as the EMC requirements of the orbiter ICD. In addition, full functional testing of the instrument and support hardware prior to delivery can help the I&T process run smoother.

Mechanical problems during integration can arise when there is a misinterpretation, or simply a dearth, of interface drawings and dimensional data. For example, interface drawings for a satellite which used the Hitchhiker Ejection System did not clearly show the clocking required for mounting the satellite to the ejection pedestal. This resulted in having to reorient the satellite after integration on the ejection system -- a dangerous task since ordnance had already been installed. Therefore, clear and complete interface schematics are imperative, particularly if no fit checks are performed between the customer and carrier flight hardware.

In addition, parts and materials must be flight-approved with associated certification. History has seen several payloads entirely disassembled to replace fasteners which were discovered to be non-flight. The process involved in obtaining approval to fly hardware with known defects (such as fractures) is usually a more formidable task than simply replacing the hardware itself.

334

In short, comprehensive definition of requirements and interfaces can help minimize problems and facilitate the I&T process. To this end, Hitchhiker has improved the definition of carrier interfaces with its new revision of the CARS document.

CUSTOMERS ARE FROM MARS, HITCHHIKER FOLKS ARE FROM VENUS

Among all the technical and programmatic issues, by far the most important yet most difficult to achieve is good communication between organizations. It goes without saying that Goddard, like any major institution, has its own share of internal breakdowns in communication. However, the communication between Hitchhiker and the customer is important to address within the scope of this paper.

One area of communication which is critical to successful I&T is the customer informing Hitchhiker ahead of time about planned or unplanned work. While previously approved procedures are important, it is equally crucial for the Hitchhiker team to be cognizant of all payload activities following instrument delivery. Specifically, the I&T manager is considered the single-point contact for all integration and test activities at both GSFC and KSC. The I&T manager must be kept informed of all carrier and experiment plans and activities. This will help ensure availability of resources, proper operational sequencing, and safe implementation.

In the case of KSC operations, good communication about planned activities is especially important to help minimize modifications to documented requirements and approved procedures. Also, since the I&T manager acts as the communication interface between the payload and launch site, customers are requested to go through the I&T manager for special requests to KSC. This approach helps to minimize multiple requests to KSC personnel and helps keep the I&T manager informed about customer operations.

Another aspect of communication which must be addressed is in the area of customer hardware and software configuration management. Besides the as-built configuration and cert data mentioned earlier, post-delivery configuration management of the instruments is also important. For example, customer hardware or software is sometimes modified following delivery in order to effect enhancements or correct problems. Such changes must be brought to the attention of Hitchhiker personnel to ensure that even seemingly benign modifications will not compromise flight safety or mission success.

In the case of the Hitchhiker carrier, hardware and software is controlled via the SSPP configuration management process. Since it does not maintain configuration of customer hardware or software, the SSPP has instituted a process by which modifications by the customer can have greater visibility and review for potential impacts. Following delivery to GSFC, customers are requested to complete and submit a Customer Configuration Change Request (CCCR) for any changes to hardware or software from that originally approved for use. Since the CCCR is used simply as a communication tool, it imposes no new CM requirements on the customer.

Needless to say, the use of CCCR's by the customer can be minimized if the instrument and GSE is delivered to Goddard fully assembled and functional. Since Hitchhikers have, by design, relatively short integration and test schedules, it behooves customers to deliver their instruments and GSE complete and in proper working order. If any "open items" remain to be completed, such as installation of flight batteries or a gas top-off, these should be identified with approved procedures in place prior to integration.

Finally, as part of its commitment to customer satisfaction, the SSPP has introduced a "SSPP Customer Survey" form. This form was designed to provide customers a standardized means of communicating their impressions of Hitchhiker services. Customers are encouraged to submit the survey anytime after deintegration.

IT'S NOT THE SIZE OF THE CARRIER, BUT WHAT YOU DO WITH IT

Despite all the issues presented here, Hitchhiker is still one of the "fastest, cheapest, and best" means to fly shuttle payloads. Although there have been recent increases in documentation and CM requirements, the Hitchhiker I&T process is still relatively streamlined compared to larger payload projects. This allows Hitchhiker customers shorter time between experiment conception and launch, as well as quick return of data.

Customers can help the Hitchhiker team in its continuing effort to improve the I&T process. Examples mentioned include clear definition of requirements and interfaces, pre-integration testing and evaluation, configuration management, adequate planning, and good communication. These efforts can help take Hitchhiker into the 21st Century.

REFERENCES

1. *Hitchhiker-G and Shuttle Payload of Opportunity Carrier (SPOC) Capabilities.* 730-1501-03, NASA/GSFC, n.d.

2. Wright, Michael R., "Shuttle Small Payloads: How to Fly Shuttle in the 'Faster, Cheaper, Better' World," *1996 IEEE Aerospace Applications Conference*, Institute of Electronics and Electrical Engineers, 1996.

3. *The GSFC Quality Manual.* GPG-8730.3A, NASA/GSFC, February 1999.

4. *Safety Policy and Requirements For Payloads Using the Space Transportation System.* NSTS-1700.7B, NASA/JSC, January 1989.

5. *Interpretations of NSTS/ISS Payload Safety Requirements.* NSTS/ISS-18798B, NASA/JSC, September 1997.

6. *Space Shuttle Payload Ground Safety Handbook.* KHB-1700.7 Rev. B, NASA/KSC, September 1992.

7. *General Environmental Verification Specification for STS & ELV Payloads, Subsystems, and Components.* GEVS-SE Rev. A, NASA/GSFC, June 1996.

8. *Shuttle Orbiter/Cargo Standard Interfaces (CORE).* ICD-2-19001 Rev. L + CPN-70, United Space Alliance, July 1999.

9. Carson, Maggie, "Helpful Hints to Painless Payload Processing," *1995 Shuttle Small Payloads Conference*, CP-3310, NASA/GSFC, September 1995.

10. *Hitchhiker Customer Accommodations and Requirements Specifications.* 740-SPEC-008, NASA/GSFC, 1999.

11. Kizhner, Semion and Del Jenstrom, "On the Hitchhiker Robot Operated Materials Processing System Experiment Data System," *1995 Shuttle Small Payloads Conference*, CP-3310, NASA/GSFC, September 1995.

SHUTTLE LASER ALTIMETER

Mission Results & Pathfinder Accomplishments

Jack L. Bufton, David J. Harding, James B. Garvin
Laboratory for Terrestrial Physics
Goddard Space Flight Center
Greenbelt, MD

INTRODUCTION

The Shuttle Laser Altimeter (SLA) is a Hitchhiker experiment that has flown twice; first on STS-72 in January 1996 and then on STS-85 in August 1997 [1]. Both missions produced successful laser altimetry and surface lidar data products from approximately 80 hours per mission of SLA data operations. A total of four Shuttle missions are planned for the SLA series. This paper documents SLA mission results and explains SLA pathfinder accomplishments at the mid-point in this series of Hitchhiker missions.

The overall objective of the SLA mission series is the transition of the Goddard Space Flight Center airborne laser altimeter and lidar technology [2, 3] to low Earth orbit as a pathfinder for NASA operational space-based laser remote sensing devices. Future laser altimeter sensors will utilize systems and approaches being tested with SLA, including the Multi-Beam Laser Altimeter (MBLA) and the Geoscience Laser Altimeter System (GLAS). MBLA is the land and vegetation laser sensor for the NASA Earth System Sciences Pathfinder Vegetation Canopy Lidar (VCL) Mission, and GLAS is the Earth Observing System facility instrument on the Ice, Cloud, and Land Elevation Satellite (ICESat). The Mars Orbiting Laser Altimeter, now well into a multi-year mapping mission at the red planet [4], is also directly benefiting from SLA data analysis methods, just as SLA benefited from MOLA spare parts and instrument technology experience [5] during SLA construction in the early 1990s.

The SLA instrument measures distance by timing the two-way propagation of short (~ 10 nsec) laser pulses over the roundtrip path between the Space Shuttle and the Earth's surface. Laser pulses at 1064 nm wavelength are generated in the SLA laser transmitter and are detected by a telescope equipped with a silicon avalanche photodiode detector. Both transmitter and receiver are located in one Hitchhiker canister referred to as the Laser Altimeter Canister (LAC). They view the Earth through a large 0.38 m diameter window that is located in the upper-end plate of the LAC. The laser transmits through a 40 mm hole in the periphery of the telescope mirror. The LAC sensor is protected in non-operating times by a motorized door assembly that is part of the Hitchhiker canister. The SLA instrument computer and all the command and telemetry interfaces to Hitchhiker are located in a second canister referred to as the Altimeter Support Canister (ASC). The SLA data system makes the pulse time interval measurement to a precision of 10 nsec and also records the temporal shape of the laser echo (i.e., waveform) from the Earth's surface enabling interpretation of the surface height distribution within the 100 m diameter laser footprint. The operational concept of SLA, its implementation as a dual-canister Hitchhiker bridge-mounted payload, and details of its instrument configuration were presented at the 1995 Shuttle Small Payloads Symposium [6]. SLA sensor parameters are summarized here and illustrations of its implementation as a Hitchhiker payload are presented.

The SLA pathfinder contributions presented in this paper are grouped into 3 main areas: (1) laser altimetry measurements from Earth orbit; (2) space-based laser altimeter data processing; and (3) surface lidar. The SLA-01 and SLA-02 mission operations and subsequent data analysis resulted in significant pathfinder accomplishments in each of these three areas. Sensor performance on orbit ran close to predicted in terms of successful acquisition of Earth surface pulse echoes. Statistics are given and explained as are example records of pulse echoes. A major effort was expended and is still continuing to obtain the maximum science benefit from the SLA data. This involves computations of range, waveform, orbit, and pointing angles applicable to each pulse and georeferencing which incorporates all the measurements into a computation of surface elevation and location for each laser footprint. Data sets from both missions are now available on the World Wide Web at the address given below. As we look forward to SLA-03 and SLA-04 missions which are intended to complete the SLA pathfinder objective, we envision a transition to smaller laser footprints on the Earth's surface, higher pulse-rates and thus higher-resolution data sets, scanning laser sensors, and extended periods of observation leading to eventual operation of SLA on the International Space Station.

INSTRUMENT DESCRIPTION

A detailed description of the SLA instrument and its Hitchhiker interface are reported in our pre-flight paper [6]. The SLA works by generation of short laser pulses at 1064 nm optical wavelength on the Space Shuttle and reception of the weak backscattered laser radiation from the Earth. The pulsed laser source is a solid-state, diode-pumped, Nd:YAG device that pulses at a fixed, continuous rate of 10 pps. The optical receiver of SLA collects the near-infrared (i.e. 1064 nm) pulse backscatter from the Earth's surface and converts it to an electronic pulse that traces the time-history, or echo, of the optical reflection from the 100 m diameter laser footprint. Analog electronic signals (i.e. pulse waveforms) from the START and STOP detectors of the LAC are presented to the SLA data system for digital measurements of the START-to-STOP time interval, yielding the range to the first surface intercepted (cloud top, ocean surface, vegetation

canopy top, or bare ground). Furthermore, the shape of the pulse echo is converted into digital samples with a resolution of 2 to 10 nsec. Digitizer sampling rate and averaging are parameters that can be commanded in flight to optimize waveform resolution. Digital timing and waveform data are formatted into packets on-board SLA in the ASC flight computer and are sent by Hitchhiker low and medium rate telemetry to the HH Payloads Operations Center at GSFC as well as recorded on board SLA in hard drives.

The as-flown configuration of SLA is illustrated in Figure 1 in block diagram form. Note that the START signal is generated from a small optical sample of the output laser beam. The nominal duration of the START pulse and the impulse response of the STOP pulse circuitry was found by pre-launch measurements to be approximately 15 to 20 nsec nsec full-width-at-half-maximum. A 15 nsec pulsewidth is nominal when the laser transmitter is operating at full power and has an optimum temperature interface of approximately 0 to 10 C. The pulse broadens to about 20 nsec as the laser pump-diodes heat up in the Nd:YAG laser head to 25 to 35 C. There is a corresponding reduction in pulse energy from a maximum of about 35 mJ per pulse at the lower
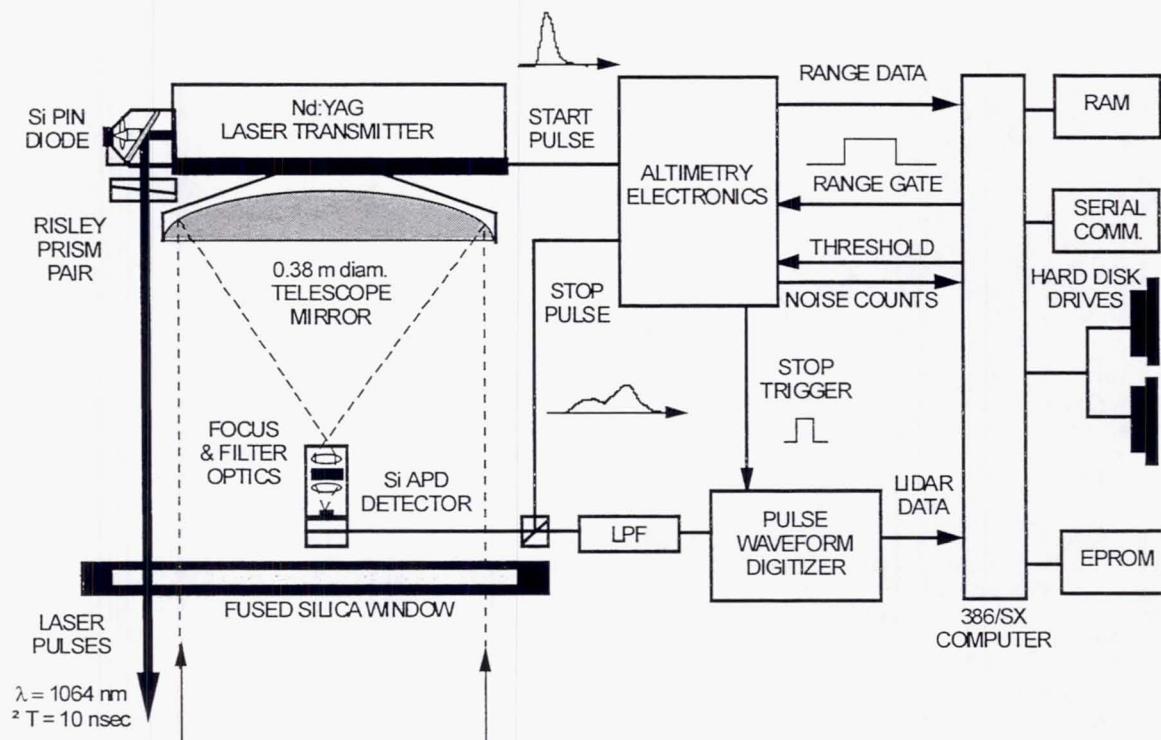

Figure 1. Instrument configuration of the Shuttle Laser Altimeter for the SLA-01 and SLA-02 Missions

temperatures to about 20 mJ at the higher temperatures. These and other as-flown sensor parameters for SLA are documented in quantitative form in Table 1. The STOP signal, broadened and distorted in time by interaction with the reflecting surface, appears as a single- or multi-peaked waveform that typically extends several tens to hundreds of nsec. There is an autonomous digital tracking loop in the SLA data system that facilitates data acquisition by adjusting an electronic threshold based on number of noise counts that appear over a 1 sec average of the detector noise level. This compensates for changes in background noise counts from the detector-noise-limited operations at night to the solar-backscatter-limited operations during daytime. The purpose of this loop is maintenance of the lowest-possible electronic threshold for detection of weak pulse echoes for a given false-alarm ratio of about 1 part in 10^5. The serial communication port for the SLA 386SX computer that is illustrated in Figure 1 is for RS-422 up-link commands and down-link telemetry as relayed by the HH ACCESS payload control system. We also store all data on board on the dual hard drives for post- mission retrieval of a complete flight data record.

SLA INSTRUMENT SPECIFICATION	Minimum	Maximum
SENSOR:		
energy per pulse (mJoule)	20	40
pulse width (nsec, full-width-at-half-maximum)	10 minimum at 40mJ (0-10C) 20 maximum at 20mJ (25-35C)	
pulse repetition rate (pps)	10	
beam divergence (mrad, $1/e^2$)	0.35	
beam far field pattern	multi-mode	
receiver throughput (%)	50	60
bandpass filter width (nm)	2	2.2
detector field-of-view (mrad)	0.75	
detection sensitivity (nWatt)	0.5	2
ALTIMETRY ELECTRONICS:		
time interval range (counts)	0	65536
time interval resolution (nsec/count)	10 with interpolation bit to 5	
clock timebase (MHz)	100	
matched filter bandwidths (MHz)	16.6, 5.5, 1.8, 0.6	32, 16.6, 5.5
noise counter range (counts/sec)	1	16384
threshold setting range (mV)	10	2550
post-detection gain		
system impulse response (nsec, 1 sigma)	20, 60, 180, 540	10, 20, 60
false alarm ratio	1×10^{-5}	1×10^{-4}
PULSE DIGITIZER:		
digitizer input low pass filter (MHz)	15	32
sampling rate range (Megasamples/sec)	100	500
waveform amplitude resolution (bits)	8	
number of waveform samples per pulse	100	120
COMPUTER:		
clock frequency (MHz)	25	
random access memory (Mbyte)	1	
Erasable-prog.-read-only-memory (Kbyte)	256	
flight software size (Kbyte)	150	180
hard drive storage volume (Mbyte)	340	540
downlink data rates (kbps)		
low-rate / medium rate	0.12 / 19.2	

Table 1. Shuttle Laser Altimeter Instrument specifications for the SLA-01 and SLA-02 Missions

Photographs of the completed LAC and ASC payload components of SLA-01 prior to their insertion in the HH canisters are shown in Figures 2 and 3. In the LAC photograph the diode-pumped, Nd:YAG laser transmitter can be seen mounted above the receiver telescope on a circular interface plate. The cylindrical section below the laser with the three reinforcing rings is the telescope tube. The 0.38 m diameter mirror and silicon APD are packaged on the centerline inside that tube. The LAC is mounted to an annular ring (bottom of the photograph) which bolts to the upper end plate of the HH canister. Refer to [6] for more details and a three-dimensional view of the LAC and ASC. In the ASC photograph of Figure 3 it is possible to see the space-frame construction of vertical supports (2) and cross-braces that hold the electronic boxes of power supplies, computer, digitizer, and timing circuits. The hard drives are mounted at the base of the ASC on a thin plate that mounts to the upper end plate of the HH canister. The SLA payload computer is mounted in a tray that also serves as the lower cross-brace. The computer cover is removed in this photograph revealing the copper heat sinks for computer chips.
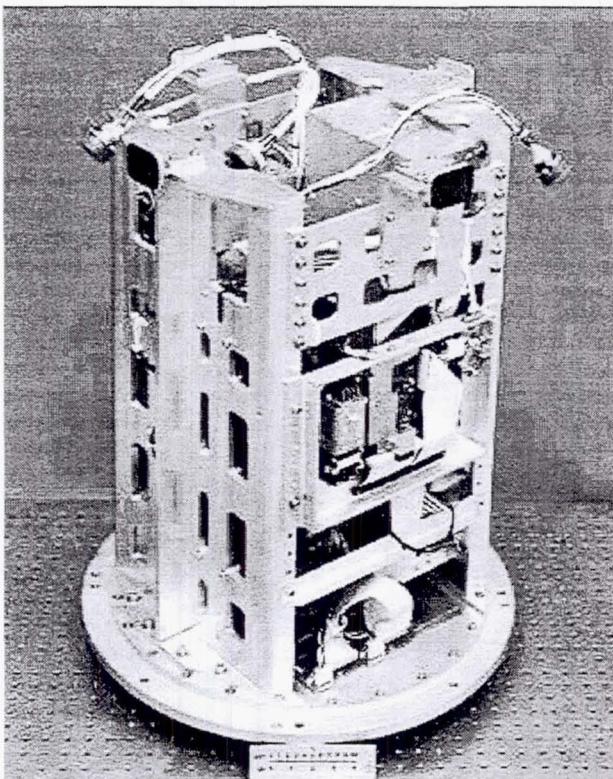
Figure 2. Laser Altimeter Canister (LAC)   Figure 3. Altimeter Support Canister (ASC)

SLA ON-ORBIT OPERATIONS

Both SLA-01 and SLA-02 payload operations followed the same general scenario summarized as follows. Prior to activation of the SLA payload Hitchhiker power is applied to the LAC and ASC only for purposes of replacement heater operation. This permits both canisters to achieve their operational temperture set points between 5 and 20 C. The first step in activation occurs when the ASC canister is powered on and two-way communication (i.e. telemetry & command) is established with the ASC payload computer. After the laser power is enabled and switched on by the crew (using the Standard Switch Panel) the LAC is ready for activation. At this point, the Hitchhiker motorized door assembly (HMDA) for the Laser Altimeter Canister (LAC) is opened. Then, the power-on (activation) command is sent to the LAC in order to initiate SLA operation. Separate commands are used to activate the ASC, activate the LAC, and control laser transmitter operation inside the LAC. Laser activation is a potential eye safety hazard to crew operations, thus the LAC is deactivated and the HMDA door closed during all periods of EVA. Furthermore, SLA operations require that the Shuttle Z axis be controlled to within ± 1° of nadir in an Earth-viewing orientation (-ZLV). Activation of the LAC canister is permitted only when the HMDA is fully open and is controlled by the following: (1) an electrical interlock on the HMDA door; (2) computer commands sent from the ground; and (3) crew procedures.

All ASC and LAC payload operations commence on receipt of uplink commands to the ASC. During operations the laser transmitter pulses at 10 pps, pulse data from laser radiation backscattered by the Earth's surface are collected and processed, and the altimetry and housekeeping data are formatted and recorded. The ASC payload data system computer program operates the laser altimeter instrument in the LAC continuously until the standby or power-off commands are issued. Laser altimeter data are acquired and stored on the hard disk drives and a summary of laser altimeter ranging data and housekeeping data are sent over the HH 1200 baud low rate telemetry channel. The complete data set recorded on the twin hard drives is sent via the HH medium rate data channel at ~ 10 to 50 kbps when the channel is available. The operational cycles for the SLA are contiguous or segmented as required by Shuttle operations and priorities. The nominal minimum operational cycle length is about two orbits (about 3hrs), but shorter periods of operations are implemented if necessary to obtain data over high-priority targets. Maximum operational periods normally extend to about 10 hours, typically during crew sleep cycles. After laser transmitter operation is secured and SLA payload power is removed, the HMDA door on the LAC is closed to complete payload operations.

SHUTTLE MISSION REPORTS

SLA-01: The first on-orbit test of The Shuttle Laser Altimeter, the flight of SLA-01, occurred on the Endeavour Space Shuttle vehicle in a 310 km altitude, 28.45° inclination orbit during the STS-72 mission of January 11-20, 1996. The SLA-01 payload operated successfully for 83 hours in space and logged 3 million laser pulse measurements, more than 90% of which resulted in valid measurements of Earth system phenomena, including landforms, ocean surfaces, and clouds. On

orbit operations of SLA-01 produced a series of laser pulse echo measurements with 100 m diameter sensor footprints spaced at regular 100 msec intervals along the nadir track of the Space Shuttle, yielding a nominal 700 m spacing between footprints. While primarily designed as a laser altimeter that measured distance to the Earth surface by time-of-flight pulse ranging, the laser pulse digitizer in SLA-01 produced detailed pulse shape measurements of each laser echo and enabled both a surface lidar mode of operation and a conventional atmospheric lidar mode of operation. SLA-01 operations were conducted almost exclusively during crew sleep periods. Thus, land observations were biased to a particular pattern leading to intense coverage of Africa, southern Asia, and central South America in a band between 28° north and south latitudes. Further details on the results of the SLA-01 mission are reported in [1].

SLA-02: The space flight of SLA-02 occurred aboard the Discovery orbiter as part of STS-85, during the period August 1-14, 1997. It concluded successfully, with nearly all mission science and engineering objectives achieved. The prime mission of the SLA-02 experiment was to demonstrate, by virtue of its role as a combined engineering/science pathfinder for orbital surface lidar, robust ranging and echo recovery from all major Earth surface types from which a near-global sampling of land-cover vertical characteristics could be derived. Due to the 57° orbital inclination on the STS-85 mission and the attention of the mission planners to the Earth-viewing (at nadir) requirements of the SLA-02 investigation, excellent coverage of all major land-cover classes was achieved. SLA-02 was intended to improve upon the successful SLA-01 experiment by enabling more flexibility in echo recovery operations, as well as higher vertical resolution of land and ocean within-footrpint height distributions. SLA-02 incorporated a Variable Gain Amplifier (VGA) system in the altimeter receiver electronics package that permitted the instrument operators on Earth to control the gain of the Si:APD detector. In addition, a solar rejection filter was installed to reduce background noise during daylight conditions.

SLA-02 operated for ~ 81 hours in Earth orbit in its required nadir-viewing geometry as part of the STS-85 mission. The data were acquired during 21 primary observation periods, mostly of short duration (less than 1 to 3 orbits) but with the final two periods each extending for 8 orbits. Most of SLA-02's data acquisition periods were interspersed with other payload operations and communications attitudes which were not Earth viewing and thus not acceptable for SLA operations. All of the observational data acquired during its 81 hours of data acquisition was recorded within the SLA-02 instrument on two hard disk drives. Only a fraction of this complete dataset was directly transmitted to the Earth during limited Medium Rate downlink times facilitated by TDRSS. By commanding gain adjustments using the VGA to account for large variations in backscatter signal level, SLA-02 echo peak amplitudes were normally kept below detector saturation levels, eliminating an echo saturation problem that affected a significant fraction of the SLA-01 data. SLA-02 fired its laser transmitter approximately 2.92 million times during its 80+ hours of operations in Earth orbit. The laser transmitter and associated altimeter receiver electronics performed essentially as anticipated (nominally), with the exception of an echo "jitter" affecting the position of the backscatter signal within the waveform data record. Waveform resolution was reduced after this anomaly began in order to compensate for the jitter.

As a part of the SLA-02 data processing, each shot is categorized as over ocean or land, and as a return from a cloud top, the Earth's surface, noise, or as shots for which no return was detected. Table 2 summarizes the percentage of shots in each category for SLA-02. The method for defining surface returns uses a maximum difference between the geolocated laser footprint elevation compared to sea level, for the ocean, and to a 10 km resolution gridded elevation model, for the land. The method probably underestimates the ocean surface percentage and overestimates the land surface percentage. Many of the no return shots likely intercepted thin clouds which yielded low-amplitude backscatter energy below the background-defined instrument detection threshold.

	No Return	Noise	Cloud	Surface	Total
Land	6.2	0.9	4.2	14.5	25.8
Ocean	18.5	3.0	25.2	27.5	74.2
Land & Ocean	24.7	3.9	29.4	42.0	100.0

Table 2. Classification of SLA-02 laser shots, as percent of processed returns.

DATA DISTRIBUTION
Data sets from the first two flights of SLA are publicly available from the project web site at: http://denali.gsfc.nasa.gov/lapf. Not all acquired altimetry data could be fully processed due to problems associated with merging the altimetry, attitude, and orbit data records. Ground tracks for the processed data are depicted in Figure 5. Data products for SLA-01 consist of the position (latitude, longitude, and elevation) of the highest detected feature within each laser footprint, enabling topographic profiles of very high vertical accuracy to be constructed after filtering out cloud returns. For SLA-02, a comprehensive data structure is provided which includes, for each laser shot, the geolocation results, return classification type, a geoid correction to convert from an ellipsoidal vertical datum to mean sea level, engineering parameters, the raw backscatter echo, and numerous characterizations of the echo shape. SLA-02 processing methods and the data set parameters are described in detail in documentation available from the web site.

PATHFINDER ACCOMPLISHMENT: SENSOR DEMONSTRATION OF LASER ALTIMETRY FROM ORBIT
Prior to SLA-01, laser altimetry from space was confined to brief episodes of (1) the Apollo Laser Altimeter and its measurements of Lunar topography during the 1970s; (2) Soviet operation of a series of geodetic spacecraft that included laser range data with boresighted photography during the 1980s [7]; and (3) the return to the Moon with the Clementine

Laser Altimeter in 1994 [8]. All of these missions produced sparse data at pulse rates of a few pulses per minute with the first generation of pulsed, solid-state laser technology. The flights of SLA-01 and SLA-02, using second-generation diode-pumped Nd:YAG lasers, represented the first substantive data set that has become publicly available for the Earth surface from orbit. It is also a data set that achieves sub-meter precision and sub-10 m accuracy in determination of surface elevations and does so at the modest pulse rate of 10pps.
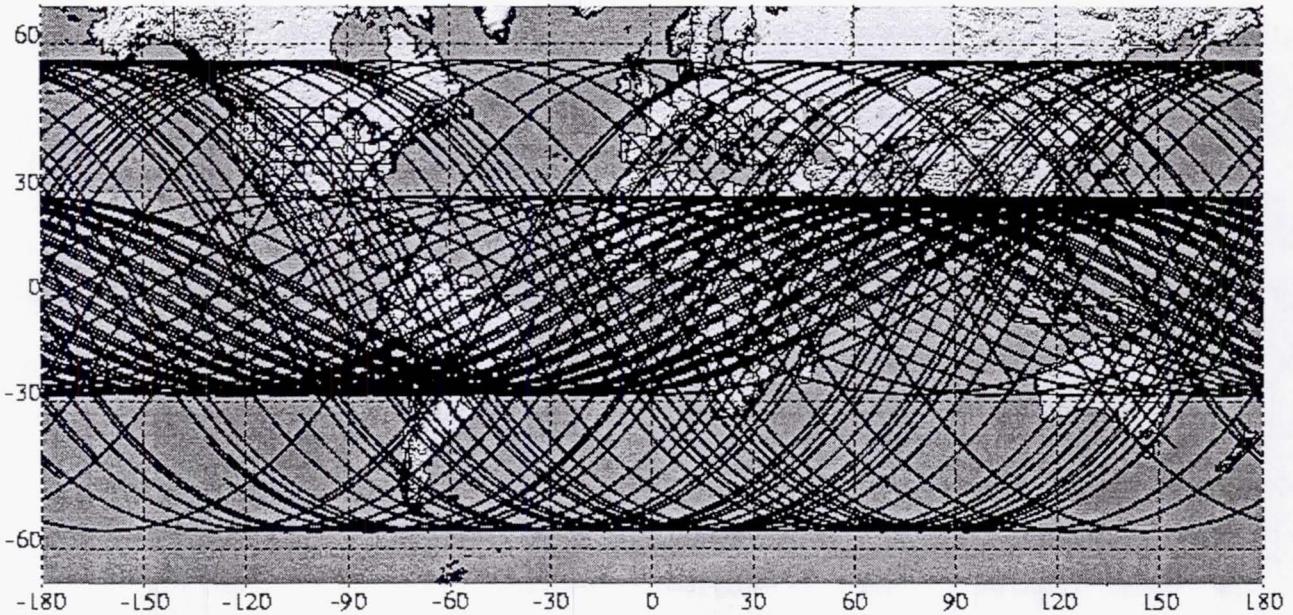

Figure 5. Ground tracks for fully processed observations from SLA-01 (28.5° inclination) and SLA-02 (57° inclination)

SLA data depend on unique determination of each laser footprint elevation. There is no averaging to boost detection signal-to-noise. As a result the design and performance of laser pulse ranging to the Earth's surface in the presence of an interfering atmosphere is a major pathfinder accomplishment of the SLA mission series. The following link analysis and table of results provide design points that were verified in on-orbit operations and are thus available to guide the development of future down-looking laser sensors.

The pulse energy, E_R, received by the SLA telescope in the LAC can be computed from the following formula:

$$E_R = E_T \, A_R \, T_O \, T_A^2 \, R_S / \pi \, Z^2$$

where E_T = transmitted pulse energy (~30mJ), A_R = telescope area (0.1m^2), T_O = optics transmission (0.6), and Z = orbital altitude (300km). Furthermore, at 1064nm wavelength the vertical-path atmospheric transmission, under good conditions of clear to light haze, is approximately $T_A = 0.7$ and the approximate values of diffuse reflection for the Earth's surface are given by, R_S = 0.2, 0.2, 0.4, 0.7, and 0.9 for soil, ocean waves, vegetation, snow, and sand. Experimental values of E_R from SLA data can be computed from: $E_R = W_R \, \Delta T$ where $W_R = V_R / (R \cdot G)$, W_R = pulse peak power (W) received, V_R = pulse peak voltage (V) received, ΔT = impulse response of detector (20nsec for SLA-01, 10nsec for SLA-02), R = detector responsivity (7.7x10^{5}V/W) and G = post detection gain (242 for SLA-01, and 0.5 to 250 for the variable gain amplifier in SLA-02). The results for these computations over vegetated land are listed in Table 3 where fJ is fempto-Joules (10^{-15}J).

	E_R Computed (fJ)	ΔT (nsec)	Post detection gain	V_R Measured (V)	E_R Measured (fJ)	S/N Computed	S/N Measured
SLA-01	1.25	20	242	1 -to- 4	0.32	19	13
SLA-02	1.25	10	75 –to– 150	0.5 –to– 2	0.17	19	8.6

Table 3. Computed and measured signal detection values for the SLA missions.

Results in Table 3 show order-of-magnitude correspondence between computed and measured pulse energies for both SLA missions, but show less signal than expected. This may be due to atmospheric losses. The signal-to-noise ratio S/N computations that are listed in Table 3 follow the approximate formula:

$$S/N = N_R / [F . (N_R + N_B) + N_D]1/2$$

where the received number of photoelectrons for signal (N_R), optical background (N_B), and detector dark current (N_D) follow from the standard deviation of pulse energies, e.g. $N_R = n . E_R / h\nu$, where n = silicon avalanche photodiode quantum efficiency (0.35), F = detector noise factor (3), and hν = energy per photon at 1064nm wavelength (1.87×10^{-19}J). Background S/N was estimated at ~ 130 photoelectrons during the daytime for land observation and detector noise (dark current) photoelectrons are ~ 26. This latter noise source is the effective noise limit for SLA observations of the Earth's surface in eclipse. Note that use of the variable gain amplifier did not appreciably alter measured S/N, but had the considerable advantage of permitting us to adjust the post-detection gain during the mission to maintain the optimum voltage range for digitization of pulse waveforms.

PATHFINDER ACCOMPLISHMENT: GEOREFERENCING OF LASER SPOT LOCATIONS ON THE EARTH'S SURFACE

Analysis of SLA data involves the combination of laser altimeter range to the surface measurements with Shuttle pointing data and a precision orbit for the Shuttle center of mass. The SLA experiment only measured the range data and depended on Shuttle inertial reference units (IRUs) for the precision pointing angle knowledge. Pointing data accessed on the MEWS Shuttle data server in post-mission analysis is thought to be accurate to somewhat better than the 0.01° total angle. Shuttle IRUs are updated with start tracker calibrations when their drift approaches 0.01°. Orbits were computed by the SLA data analysis team at Raytheon (formerly Hughes) STX from TDRSS range and range-rate tracking data [9]. They achieved better than 5 meter radial accuracy in determination of the Shuttle orbit, which is an independent, unprecedented achievement. They also exploited the large sensitivity of laser range measurement to laser beam pointing angle biases by applying a range residual analysis in order to determine and improve upon Shuttle laser beam pointing angle and range biases. This was accomplished by minimizing the residuals between SLA elevation results and a reference surface defined by mean sea level for areas of open ocean. Surface elevations for the open ocean are known, through measurement and modeling, to the 12 cm (1-sigma) level, providing a reference surface with global access throughout the missions. The basis of the range-residual technique is a Bayesian least-squares estimation and batch processing approach. A rigorous measurement model is employed where the various parameters of the model (e.g. laser altimeter pointing and range parameters, and orbit tracking measurement model and force model parameters) are estimated to minimize the range residuals. The methodology and computational model for the range-residual calibration technique are provided in [10]. The methodology utilizes GEODYN, a state-of-the-art orbit determination and geodetic parameter estimation software suite developed at Goddard Space Flight Center. Modifications to GEODYN have been implemented to include a rigorous laser altimeter range measurement model and a new cross-over algorithm [11]. The range-residual analysis was actually used for simultaneous estimation of orbit biases, pointing biases, and range biases. The net result of this analysis for SLA-01 and –02 data was orbit knowledge improvement, range bias determination, and pointing angle calibration to yield SLA surface elevation knowledge at the sub-10m level and georeferencing of the horizontal location of SLA footprints to better than several hundred meters. The GEODYN laser altimeter capabilities initially developed for SLA form the basis of the geolocation methods to be utilized by the upcoming VCL mission, and will serve as a calibration/validation technique for the ICESat mission.

The SLA Data Analysis Team also pioneered the use of "dynamic" cross-over analysis through their use of SLA data crossing points in the open ocean. Residual analysis was applied to verification of the topographic information contained in these orbital track crossover points. The approach of [11] constructs constraint equations which are formulated in terms of a minimum distance between two curves of geolocated altimeter bounce points, instead of a height discrepancy between the curves at a predetermined point as is typically done for radar altimeters. As with range-residual analysis, crossover residual analysis made use of the GEODYN software suite. This crossover residual analysis approach was developed to exploit the small footprint capability of laser altimetry and also to take into account the effect of attitude parameters. This requires that each crossover constraint equation takes into account a series of laser altimeter ranges from each of the two altimeter passes (ascending and descending) that surround the open ocean location where a conventional (height discrepancy) cross-over occurs. The cross-over analysis methodology developed with SLA has been used extensively (and recently) for detailed analysis and dramatic improvement of the Mars Orbiting Laser Altimeter (MOLA) data. The success with MOLA illustrates the success of SLA as a pathfinder investigation. It should be pointed out that the success of the SLA data analysis is due in large part to the strong need to improve Shuttle pointing and orbit determination to match the data quality of the sub-meter ranging data available from the altimeter instrumentation.

PATHFINDER ACCOMPLISHMENT: SURFACE LIDAR PULSE WAVEFORM ANALYSIS

SLA also served as an orbital pathfinder for establishing surface lidar methods that characterize the height distribution of the Earth's surface within individual laser footprints by evaluating the backscatter waveform [1]. The broadening in time of the echo, as compared to the transmit pulse, provides information on ground slope and roughness, and the height of vegetation and/or buildings. The SLA waveform processing algorithms parameterize the return signal resulting from the interaction of the transmitted laser pulse with the intercepted surface on the ground, and identify the response from the multiple targets encountered within the footprint. Returns are modeled as a single Gaussian function or as the sum of several Gaussians when multiple, discrete peaks are present in the echo. In this manner, the vertical extent and

343

approximate height distribution of intercepted surfaces can be derived. Most of the waveforms are single peaked and can be fit by a single Gaussian function, characterized by its maximum amplitude, location of this maximum amplitude in time with respect to the ranging electronics trigger time, and its half width. When complex surfaces are intercepted within the footprint (as with the presence of cloud layers, complex topographic relief, vegetation, or buildings) multi-Gaussian functions are summed to model the resulting multi-peaked waveforms (Figure 6). Gaussian functions are fit to the backscatter echo using a constrained, least-squares residual minimization technique that is initialized with initial estimates for peak position, amplitude, and half-width obtained from the first and second derivative of the echo signal. This waveform fitting methodology developed for SLA has been adapted for use in the planned ICESat data processing system, demonstrating another of the pathfinder aspects of the SLA experiment.

SLA FUTURE MISSIONS

The direction of the future SLA-03 and -04 missions and the instrument complement to be flown in them is being defined from lessons learned in SLA-01 and -02 and the requirements for future free-flyer instruments. Planned improvements are in laser pulse rate, beam quality, pulsewidth, and laser divergence. The eventual goal is a device capable of at least 30 mJ per pulse energy at 1064 nm wavelength, 10 mJ per pulse energy at 532 nm wavelength with a sub-10 nsec pulsewidth, and an increase in laser repetition-rate to approximately 100 pps in a single mode (Gaussian) far-field pattern with 0.1 mrad divergence. The green wavelength will be used in conjunction with the ISIR Hitchhiker payload and its Atmospheric Lidar Module to accomplish sensitive, photon-counting of atmospheric clouds and aerosols. The one-order-of-magnitude increase in laser pulse-rate to 100 pps and the decrease in laser divergence to 0.1 mrad is driven by the desire to produce near-contiguous measurements of Earth surface topography with ~ 30 m diameter sensor footprints. Contiguous profile data avoids potential aliasing of topographic relief and vegetation cover characteristics, enables more rigorous cross-over analyses, and achieves better synergy with space-based radar interferometry and stereoscopic imagery used for topographic mapping. The ultimate goal is across-track measurements and along-track measurements that have this same level-of- performance in a true multi-beam laser altimeter/surface lidar. The direction of the SLA Program beyond the -03 and -04 missions is toward a one-year observation period using a continuation of the familiar Hitchhiker interface implemented on the International Space Station.
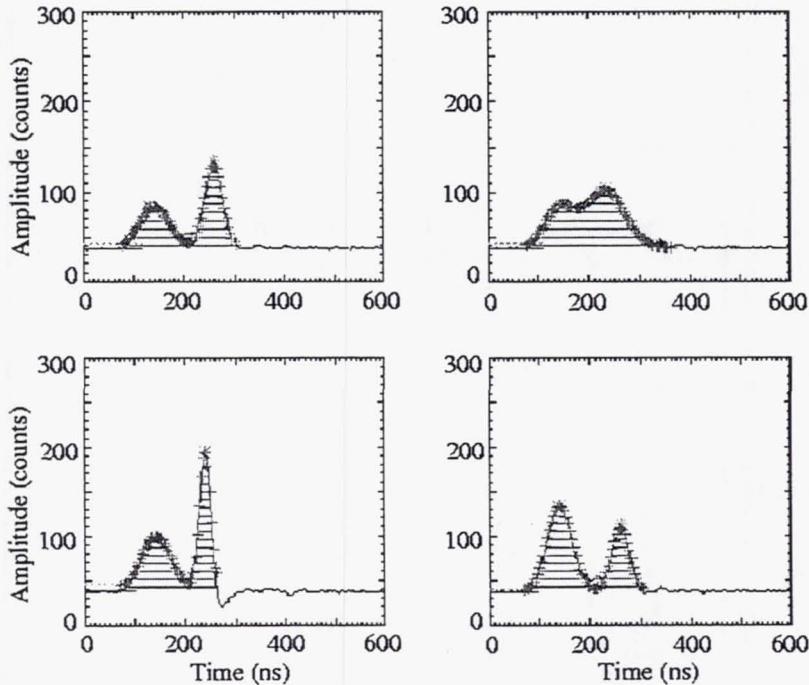

Figure 6. Representative SLA-02 waveforms showing multi-Gaussian fits, with the earlier peak most likely a return from a vegetation canopy and the later peak a return from the underlying ground.

REFERENCES
[1] Garvin, J., Bufton, J., Blair, J., Harding, D., Luthcke, S., Frawley, J., and Rowlands, D., 1998, Observations of the Earth's topography from the Shuttle Laser Altimeter (SLA): laser-pulse echo-recovery measurements of terrestrial surfaces, *Physics and Chemistry of the Earth*, 23: 1053-1068.

[2] Bufton, J.L., 1989, Laser altimetry measurements from aircraft and spacecraft, *Proc. IEEE*, 77: 463-477.

[3] Garvin, J.B., 1993, Mapping new and old worlds with laser altimetry, *Photonics Spectra*, 37: 89-94.

[4] Smith, D.E., et al., 1999, The global topography of Mars and implications for surface evolution, *Science*, 284: 1495-1503.

[5] Zuber, M.T., Smith, D.E., Solomon, S.C., Muhleman, D.O., Head, J.W., Garvin, J.B., Abshire, J.B., and Bufton, J.L., 1992, The Mars Observer laser altimeter investigation, *J. Geophys. Res.*, 97(E5): 7781-7797.

[6] Bufton, J.L., Blair, J.B., Cavanaugh, J., Garvin, J.B., Harding, D., Hopf, D., Kirks, K., Rabine, D., and Walsh, N., 1995, Shuttle Laser Altimeter (SLA): a pathfinder for space-based laser altimetry and lidar, *Proc. 1995 Shuttle Small Payloads Symposium*, NASA CR-3310, 83-91.

[7] Kokhaneko, G.P., G.G. Matvienko, V.S. Shamanaev, Yu.N. Grachev, and I.V. Znamenskii, 1995, Atmospheric Optics, 7, 967.

[8] Smith, D.E., Zuber, M.T., Nuemann, G.A., and Lemoine, F.G., 1997, Topography of the Moon from the Clementine LIDAR, *J. Geophys. Res.*, 102(E1): 1591-1611.

[9] Rowlands, D.D., Luthcke, S.B., Marshall, J.A., Cox, C.M., Williamson, R.G., and Rowton, S.C., 1997, Space Shuttle precision orbit determination in support of SLA-01 using TDRSS and GPS tracking data, *J. Astronautical Sci.*, 46(1): 113-129.

[10] Lutchke, S.B., McCarthy, J., Stoneking, E., Rowlands, D.D., and Pavlis, D.E., in review, Spaceborne laser altimeter pointing bias calibration from range residual analysis, *J. Spacecraft and Rockets*.

[11] Rowlands, D.D., Pavlis, D.E., Lemoine, F.G., Nuemann, G.A., and Luthcke, S.B., 1999, The use of laser altimetry in the orbit and attitude determination of Mars Global Surveyor, *Geophys. Res. Letters*, 26(9): 1191-1194.

Page intentionally left blank

BREAKAGE OF FIBER AT INTEGRATION OF PAYLOAD G-449 COULD HAVE BEEN AVOIDED BY USE OF SMA'S AND HARD MOUNTING OF DECK TO DECK SYSTEM

MIKE MUCKERHEIDE-PAYLOAD MANAGER G-449
EXPERIMENTERS
ELLET DRAKE-PAYLOAD TEAM MEMBER
R. THOMAS MOREHEAD-PAYLOAD TEAM MEMBER
THOMAS OLSEN-PAYLOAD TEAM MEMBER

ABSTRACT

At the time of integration of G-449 a fused silica fiber that was designed to feed optical data from a blood typing experiment to an 8mm-movie camera broke. The break occurred as the decks of the payload were being repositioned after integration.

The fiber had been fed through an access port from the deck on which the He Ne Laser (632nm), the power supply, control module, and a one megawatt peak power Q-switched Nd YAG laser were located. Because of the small orifice and tight configuration of the compartments, a shear condition existed when re-assembly was initiated.

Failure to relocate the laser deck exactly above the port when the payload was being reassembled, and the resulting torque which brought the laser plate against the fiber caused the shear fracture.

The fracture could have been avoided had SMA (Standard Military Adapters) been used as an interface between decks. Polished ends of the fibers would have completed the match with the SMA connections. Because of the rigidity of the fiber, added stress was evident upon re-assembly following integration (The fracture turning radius was approximately 3 centimeters). Because of non-availability of a replacement fiber at the time, the data link was dropped, as part of the experiment.

The lesson learned is that it is better to have small segments of fiberoptic linkage connected by SMA's than to run continuous optical fiber for data links in tightly configured instrumentation. The downside of this approach, however, is the difficulty of making proper polished junctions for the SMA's, considering the wide temperature swings in space, and severe launch vibration.

INTRODUCTION

Payload G-449 utilized an 8mm camera, which was activated by a timer and solenoid switch. The linkage of the 8mm camera with the data access point, which was a liquid column (irradiated by a He Ne laser beam) in a blood typing experiment, was a fused silica fiber.

INSTRUMENTATION

A fused silica fiber transmitted a HeNe 632nm laser beam across the liquid column into a receptor at the continuation of the fused silica fiber. After the intercept, by the receptor, the fiber terminated at a Brewster angle into the camera's optical access.

LABORATORY PRE-INTEGRATION TESTS

In the laboratory the decks of the payload had been removed and re-attached several times. A dry run in the laboratory, of the deck mounting procedure (anticipating the integration operation) had perhaps stressed the fiber optic excessively. The actual NASA payload integration at the Kennedy Space Center may have further stressed the fiber, which resulted in shearing.

INTEGRATION

Unfortunately the disassembly procedure at NASA integration was not properly anticipated or SMA's (standard military adapters) would have been implemented. Additional NASA Safety procedures would have been implemented in the phases of the safety package had a segmented, SMA junctioned, fiber been used.

CONCLUSTION

A disconnect at the deck junction using SMA's back to back would have maintained the optical integrity, plus provided the system mobility required by integration inspection.

REPORT DOCUMENTATION PAGE

Form Approved
OMB No. 0704-0188

1. AGENCY USE ONLY *(Leave blank)*	2. REPORT DATE September 1999	3. REPORT TYPE AND DATES COVERED Conference Publication

4. TITLE AND SUBTITLE
1999 Shuttle Small Payloads Symposium

5. FUNDING NUMBERS
Code 870

6. AUTHOR(S)
Gerard Daelemans and Frances L. Mosier, Editors

7. PERFORMING ORGANIZATION NAME(S) AND ADDRESS (ES)
Goddard Space Flight Center
Greenbelt, Maryland 20771

8. PEFORMING ORGANIZATION REPORT NUMBER
99A01574

9. SPONSORING / MONITORING AGENCY NAME(S) AND ADDRESS (ES)
National Aeronautics and Space Administration
Washington, DC 20546-0001

10. SPONSORING / MONITORING AGENCY REPORT NUMBER
NASA/CP-1999-209476

11. SUPPLEMENTARY NOTES
Frances L. Mosier: Swales Aerospace, Beltsville, Maryland 20705

12a. DISTRIBUTION / AVAILABILITY STATEMENT
Unclassified–Unlimited
Subject Category: 12
Report available from the NASA Center for AeroSpace Information,
7121 Standard Drive, Hanover, MD 21076-1320. (301) 621-0390.

12b. DISTRIBUTION CODE

13. ABSTRACT *(Maximum 200 words)*

The 1999 Shuttle Small Payloads Symposium is a combined symposia of the Get Away Special (GAS), Space Experiment Module (SEM), and Hitchhiker programs, and is proposed to continue as an annual conference. The focus of this conference is to educate potential Space Shuttle Payload Bay users as to the types of carrier systems provided and for current users to share experiment concepts.

14. SUBJECT TERMS
Space Shuttle Small Payloads, Carrier Systems and Experiments—
Past, Present, and Future

15. NUMBER OF PAGES
348

16. PRICE CODE

17. SECURITY CLASSIFICATION OF REPORT Unclassified	18. SECURITY CLASSIFICATION OF THIS PAGE Unclassified	19. SECURITY CLASSIFICATION OF ABSTRACT Unclassified	20. LIMITATION OF ABSTRACT UL

NSN 7540-01-280-5500

Standard Form 298 (Rev. 2-89)